

DOCTORAL RESEARCH THESIS - 2018

UPPER CRETACEOUS NEOSELACHIANS

from the Basque-Cantabrian Region (Northern Spain)

JOSÉ CARMELO CORRAL ARROYO

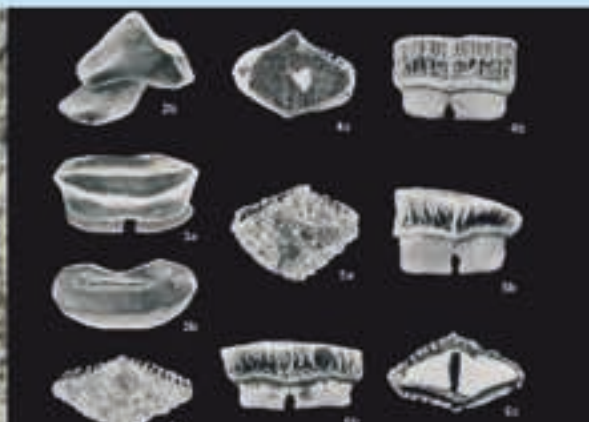


Universidad
del País Vasco

Euskal Herriko
Unibertsitatea

FACULTY
OF SCIENCE
AND TECHNOLOGY
UNIVERSITY
OF THE BASQUE
COUNTRY

Departamento de Estratigrafía y Paleontología - Estratigrafía eta Paleontologia Saila



Upper Cretaceous neoselachians
from the Basque-Cantabrian Region (Northern Spain)



“Shark teeth are the most commonly collected vertebrata fossil.

They appear on beaches, prairies, mountaintops, and deserts, as well as in riverbeds. They have also been found in the Antarctic and the deepest part of the ocean. In the living shark, teeth are constantly produced and shed; a typical carcharhinid, such as the lemon shark *Negaprion brevirostris*, may produce 20,000 teeth in its first 25 years, and may live as long as 50 years.”

Gordon Hubbell, 1996

DOCTORAL RESEARCH THESIS

UPPER CRETACEOUS NEOSELACHIANS

from the Basque-Cantabrian Region (Northern Spain)

Thesis submitted by

José Carmelo Corral Arroyo

for the degree of

Doctor in Geology

within the

Department of Stratigraphy and Palaeontology

Universidad del País Vasco / Euskal Herriko Unibertsitatea / University of the Basque Country

2018



FACULTY
OF SCIENCE
AND TECHNOLOGY
UNIVERSITY
OF THE BASQUE
COUNTRY

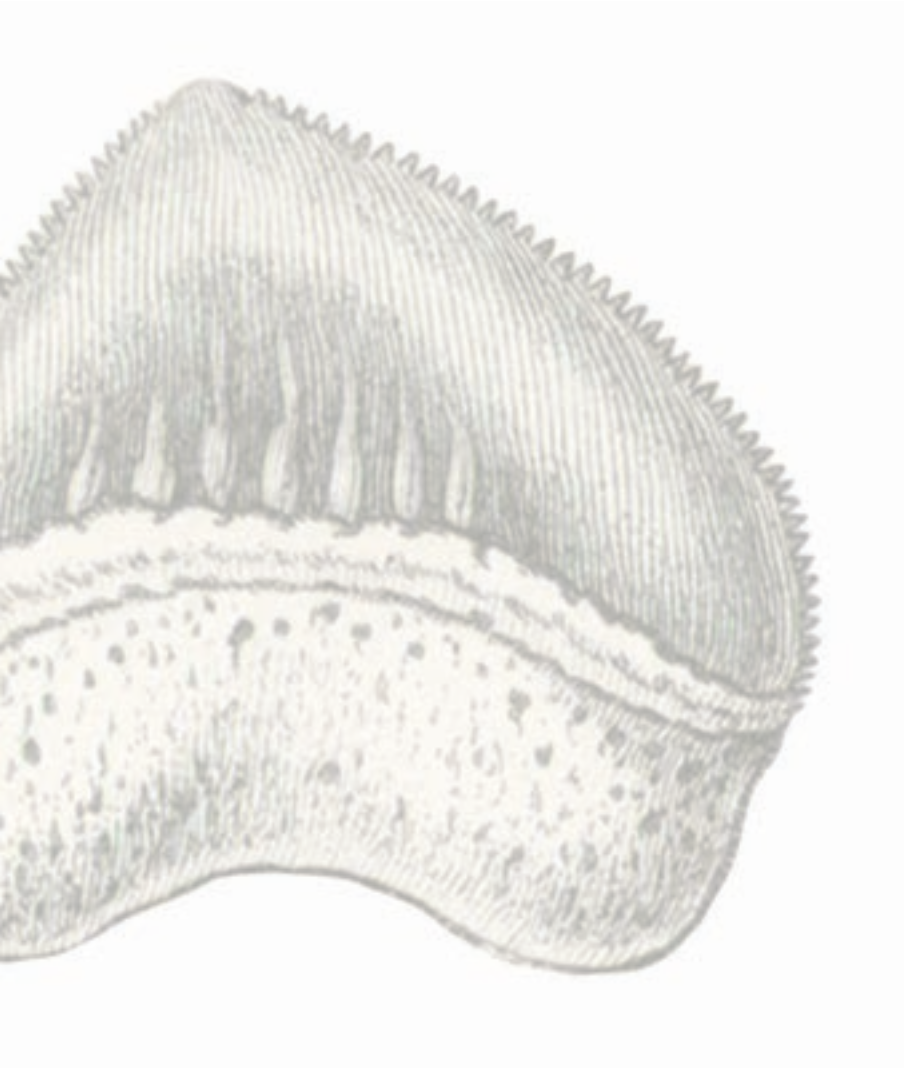
Thesis directors

Dr Javier Murelaga Bereicua | Dr Xabier Pereda-Suberbiola

‘Ad Divisionem piscium priorem pertinent illi dentes Squalorum qui Glossopetrae vulgo appellantur, & qui in nostra quoque formatione cretacea, varii locis & in variis stratis dispersi jacent.’

Sven Nilsson, 1827

*(Petrificata Suecana formationis cretaceae, descripta et iconibus illustrata.
Pars prior, Vertebrata et Mollusca)*



*This thesis is dedicated to my late father, Ernesto, who
fostered mi interest in fossils at an early age, and to my always
encouraging mother, Evangelina.*

Thanks for all your support

CONTENTS

Purpose of investigation and objectives	xxi
Outline of the thesis and Statement on the contribution of others	xxiii
Acknowledgements	xxvii
Abstract	xxix
Resumen extendido	xxxii

INTRODUCTION

Chapter 1

Historical, geographic, and geological settings

1.1 Historical review of fossil neoselachian research in the Basque-Cantabrian Region	3
1.2 Geography of the study area	9
<i>Southwestern region – Plateau of La Lora de la Pata del Cid (Burgos)</i>	9
<i>Central region – Quintanilla Ojada (Burgos)</i>	12
<i>Eastern region (Álava and Treviño County in Burgos)</i>	12
1.3 A brief geological overview of the Basque-Cantabrian Basin	16
<i>Boundaries and structural organization</i>	16
<i>Sedimentary basin fill with particular attention to the study area</i>	18

Chapter 2

Material and methods

2.1 Introduction	33
2.2 General field techniques (specimen collection)	36
2.3 Screen washing	39
2.4 Sorting and picking	41
2.5 Preparation of palaeontological remains	43
<i>Mechanical preparation</i>	47
<i>Chemical preparation techniques</i>	50
<i>Consolidation</i>	54
2.6 Geochemistry methods	55
2.7 Analytical methods for palaeobiogeographical reconstruction	55
2.8 Photography and Illustrations	57
<i>Whitening specimens</i>	59
<i>Infographics and drawings</i>	60
2.9 Management of the elasmobranch collection	61
<i>General considerations</i>	61

<i>Conservation of the specimens discussed in this thesis</i>	61
2.10 Special case: the preparation of a mosasaurid vertebra from Jauregi (Álava)	62
Chapter 3	
An overview of living and fossil elasmobranchs	
3.1 Introduction – What is an elasmobranch?	67
<i>Classification of living elasmobranchs</i>	67
<i>A general overview of the Elasmobranchii fossil record</i>	72
3.2 Endoskeleton	75
<i>Cartilaginous skeleton</i>	77
3.3 Exoskeleton	78
<i>Tooth morphogenesis</i>	78
<i>Tooth histology and composition</i>	80
<i>Dental characters</i>	84
<i>Tooth diversity and orientation</i>	84
<i>Other exoskeletal structures (placoid scales, thorns, tail spines)</i>	89
3.4 Teeth patterns and specialised trophic adaptations	90
3.5 Nomenclature and systematics of elasmobranchs	92
Box 3.1 Most common dental terms (English–Spanish) used to describe shark teeth	96

GEOLOGY AND PALAEOLOGY OF THE STUDIED AREAS

Chapter 4	
Stratigraphy and palaeontology of the Barrio Panizares beds (Nidáguila Formation, Coniacian) from Northern Spain	
4.1 Location and geological setting	101
4.2 Stratigraphy	101
<i>Facies interpretation</i>	103
<i>Stratigraphical position</i>	105
Chapter 5	
Stratigraphy and palaeontology of the upper Campanian Gometxa beds (Vitoria-Gasteiz, Álava)	
5.1 Introduction	111
5.2 Location and geological setting	112
5.3 Stratigraphy	116
<i>Review of the Gomecha Member (GM)</i>	116
5.4 Some general taphonomic features observed on the elasmobranch teeth	128
Chapter 6	
Stratigraphy and palaeontology of the upper Campanian Vitoria Pass beds (Vitoria-Gasteiz, Álava)	
6.1 Introduction	129
6.2 Location and geological setting	130
6.3 Stratigraphy	132
<i>Stratigraphical description</i>	132
<i>Stratigraphical interpretation</i>	138
6.4 Review of the Montes de Vitoria Formation (MVF)	142

<i>Eguileta Member (EM)</i>	143
6.5 Biostratigraphy and age assigned to the Vitoria Pass site	145
<i>The planktonic foraminiferal zones</i>	145
<i>Ammonite zonal scheme</i>	147
<i>Age assigned to the Vitoria Pass beds</i>	151
Chapter 7	
Geology and geochemistry of the Maastrichtian Quintanilla la Ojada beds (Valle de Losa, Burgos)	
7.1 Introduction	153
7.2 Location and geological setting	153
7.3 Stratigraphy	156
<i>Stratigraphical description</i>	156
<i>Stratigraphical interpretation</i>	158
7.4 Geochemistry and Taphonomy	159
<i>Rare Earth Elements analysis</i>	159
<i>Taphonomy</i>	161
7.5 Age of the deposits	164
Chapter 8	
Stratigraphy and palaeontology of the upper Maastrichtian Albaina beds (Treviño County, Burgos)	
8.1 Introduction	167
8.2 Location and geological setting	168
8.3 Stratigraphy	171
<i>Sobrepeña Formation (SPF)</i>	171
<i>Torme Formation (TF)</i>	177
8.4 Taphonomic features of the selachian deposit	191
Chapter 9	
Stratigraphy and palaeontology of the upper Maastrichtian Entzia beds (Urbasa, Álava)	
9.1 Introduction	193
9.2 Location and geological setting	193
9.3 Stratigraphy	194
<i>Puerto de Olazagutía Formation (POF)</i>	194
9.4 Ammonite biostratigraphy	201

NEOSELACHIAN (SHARKS AND RAYS) SYSTEMATICS

Chapter 10	
A rostral spine of the sawfish <i>Onchosaurus</i> (Neoselachii, Sclerorhynchidae) from the Barrio Panizares beds (Northern Spain), with a revision of the genus	
10.1 Introduction	207
10.2 Systematic palaeontology	207
10.3 Redescriptions of the type material of <i>Onchosaurus</i>	212
<i>Onchosaurus radicalis</i> Gervais, 1852	212
<i>Onchosaurus pharao</i> (Dames, 1887a)	212

Chapter 11		
Neoselachians from the Gometxa site (Gomecha Member, upper Campanian)		
11.1	Introduction	215
11.2	Systematic palaeontology	215
Chapter 12		
Neoselachians from the Vitoria Pass site (Eguileta Member, upper Campanian)		
12.1	Introduction	257
12.2	Systematic palaeontology	257
Chapter 13		
Neoselachians from the Quintanilla la Ojada site (Valdenoceda Formation, Maastrichtian)		
13.1	Introduction	279
13.2	Systematic palaeontology	279
Chapter 14		
Neoselachians from the Albaina site (Torre Formation, upper Maastrichtian)		
14.1	Introduction	303
14.2	Systematic palaeontology	303
Chapter 15		
Neoselachians from the Entzia sites (Puerto de Olazagutía Formation, upper Maastrichtian)		
15.1	Introduction	339
15.2	Systematic palaeontology	339

RESEARCH ON THE NEOSELACHIAN PALAEOECOLOGY AND PALAEOBIOGEOGRAPHY

Chapter 16		
Stratigraphical and palaeobiogeographical distribution of the sawfish <i>Onchosaurus</i> (Neoselachii, Sclerorhynchidae)		
16.1	Introduction	349
16.2	Distribution of <i>Onchosaurus</i>	349
	<i>Stratigraphical distribution</i>	349
	<i>Palaeobiogeographical distribution</i>	350
Chapter 17		
Palaeoecology and palaeobiogeography of the Campanian selachians in the Gometxa and Vitoria Pass beds		
17.1	Introduction	355
17.2	Species diversity and faunal affinities	356
	<i>The Gometxa site</i>	356
	<i>The Vitoria Pass site</i>	358
17.3	Palaeoecology and biogeographical faunal patterns	358
17.4	Global patterns in the biogeographical distribution of neoselachians during the Campanian time	366
	<i>Common multivariate ordinations and parsimony analysis</i>	366
	<i>Discussion of the results</i>	370

Chapter 18

Bite marks attributed to a shark on a mosasaurid vertebra (Vitoria Sub-basin, Campanian)

18.1 Introduction	385
18.2 Location and geological setting	386
18.3 Description of the specimen	388
18.4 Discussion	392

Chapter 19

Marine vertebrate predators (Actinopterygii, Chondrichthyes, and Mosasauridae) in the Campanian of the Basque-Cantabrian Basin

19.1 Introduction	397
19.2 Marine vertebrate groups	398
<i>Actinopterygii (Bony Fish)</i>	398
<i>Selachians (Chondrichthyes: Euselachii: Neoselachii)</i>	398
<i>Mosasaurids (Squamata: Mosasauridae)</i>	398
19.3 Selachian ecomorphotypes	401

Chapter 20

Selachian palaeoecology, stratigraphical distribution, and palaeobiogeography of the Maastrichtian assemblages (Quintanilla la Ojada, Albaina, and Entzia)

20.1 Introduction	403
20.2 Palaeoecology	404
20.3 Species diversity, faunal affinities, and palaeobiogeographical implications	408

CONCLUSIONS

Chapter 21

Conclusions

21.1 General conclusions	417
21.2 Conclusions on the Coniacian stratigraphy and associated faunal remains	418
21.3 Conclusions on the Campanian stratigraphy and associated faunal remains	418
21.4 Conclusions on the cut marks on a mosasaurid vertebra from the Campanian of the Vitoria Sub-basin	421
21.5 Conclusions on the marine vertebrate predators (Actinopterygii, Chondrichthyes, and Mosasauridae) in the Campanian of the Basque-Cantabrian Basin (B-CB)	422
21.6 Conclusions on the Maastrichtian stratigraphy and associated faunal remains	422

References	429
------------	-----

Systematic index	471
------------------	-----

It all began with ...



Some of my first findings of shark's teeth discovered (circa 1983) in the Campanian marls of the Vitoria Ranges, near the city of Vitoria-Gasteiz. These specimens are now housed in the Arabako Natur Zientzien Museoa / Museo de Ciencias Naturales de Álava (Basque Country, Spain).

Photography by geologist Agustín Pascual, ca. 1984.

Purpose of investigation and objectives

My interest in fossil shark teeth began in 1983 when I stumbled upon several teeth in an abandoned quarry not far from my birth town, Vitoria-Gasteiz (province of Álava). Soon I became intrigued by the way of these fossils ended in such rock formations, but I never thought that such a find would be the purpose of my doctoral thesis.

Selachian occurrences in the Basque-Cantabrian Region (North Spain) were then considered merely an anecdotal find, but time has shown that Álava and north of Burgos are favourable areas for fossil selachian exploration and an excellent setting for their scientific research. A major discovery of palaeontological interest was made in the late 1980s of the 20th century, while excavating dinosaur fossils in the Laño quarry (Treviño County, province of Burgos). Upwards in the succession – and stratigraphically related to this remarkable site – the marine beds of Albaina (also in the Treviño County) crop out, which have provided, and still do, a major source of fossil elasmobranch teeth. A research team from the University of the Basque Country (UPV/EHU) made another major discovery when founded fossilised remains of selachians in Quintanilla la Ojada (Burgos). This discovery of the 21st century has revealed fossils of equal significance. These fossils and other material not yet published are presented in the form of a doctoral thesis. Much of the geological information related to the sites was obtained from previous authors working in the area, and due reference is made in the thesis itself.

The core objective of this thesis is to investigate the systematics and diversity of Neoselachii (fossil sharks and rays) in the Upper Cretaceous marine deposits from the Basque-Cantabrian Region. The following specific objectives serve to clarify the main research aim:

1. to describe the facies and depositional environments of the sites;
2. to collect fossil samples (vertebrates and invertebrates), which will result in more fossil material being present in a public institution for research and care;
3. to examine the systematics and phylogenetic relationships of all found taxa referred to Neoselachii;
4. to establish the biostratigraphical range of the neoselachian taxa and correlate with regional planktonic foraminiferal and ammonite zonations;
5. to better understand the ecological interactions of these fish with other major fossil groups of the Cretaceous biota; and finally

6. to revise the distribution patterns of the studied taxa in order to investigate possible palaeobiogeographical affinities and possible migration or dispersion routes during the Upper Cretaceous.

Last but not the least, this thesis also presents the opportunity to update the content of the coauthored papers that were published earlier in scientific journals (see next content for details) about this subject, and correct some misconceptions and typos that readers have noticed during this time.

Outline of the thesis and Statement on the contribution of others

This thesis is the result of a mix of sole and coauthored articles published in journals indexed by the International Science Index (ISI), non-ISI listed journals, and original material not previously published. Coauthors also helped with the writing and revision of the manuscript. Due acknowledgement to other authors is given, whenever required, in the text or in the references section.

My supervisors, Drs Javier Murelaga Bereicua and Xabier Pereda-Suberbiola assisted with planning, research projects and proofread of earlier versions of the thesis. I was responsible for most of the field and laboratory work, including fossil collecting and preparation, analysis and interpretation of geological and palaeontological data, and for writing the manuscript. A summary of the coauthors' contribution to this thesis research, and the extent of their contribution, is given by chapters as follows:

Chapter 1. This beginning chapter, which is almost entirely composed of unpublished material, constitutes an introduction to review the historical records about fossil sharks in the Basque-Cantabrian Region, describes the study area, and finally, provides a geological overview of the Basque-Cantabrian Basin in northern Spain. The historical part benefits from a paper published in a journal named *Príncipe de Viana, Suplemento de Ciencias*:

Corral, J.C., 1996. *Squalicorax pristodontus* (Agassiz 1843), selacio citado por M. Ruiz de Gaona en la Sierra de Urbasa (Navarra). Descripción de nuevo material en Álava. *Príncipe de Viana. Suplemento de Ciencias* 14/15, 125–136.

Chapter 2. This unpublished introductory chapter provides information on materials and methods including preparation techniques. Most of the content in this chapter is original and based on personal research work. However, portions of the chapter derive from articles cited below.

Chapter 3. This unpublished chapter is also introductory, and aims to provide an overview of the biology of chondrichthyan fishes (sharks and rays), systematics, and fossilisation processes.

Chapters 4, 10, and 16. Much of the content of these chapters derives from a paper published in the *Journal of Vertebrate Paleontology* in 2012. Drs Xabier Pereda-Suberbiola and Nathalie Bardet are coauthors. Portions of the chapters are revised and updated, including new geological information and figures. Systematics has been also updated.

The paper, of which I am the lead author is:

Corral, J.C., Bardet, N., Pereda-Suberbiola, X., Cappetta, H., 2012. First occurrence of the sawfish *Onchosaurus* from the Late Cretaceous of Spain. *Journal of Vertebrate Paleontology* 32(1), 212–218.

Chapters 5, 6, 11, and 12. These unpublished chapters comprehensively expand the scope of my Master's degree dissertation. Reference, as follows:

Corral Arroyo, J.C., 2009. Selacios (Lamniformes, Neoselachii) del Campaniense de la Cuenca de Vitoria (Cuenca Vasco-Cantábrica). Yacimientos, sistemática y afinidades paleobiogeográficas. Unpublished Master's report, University of Zaragoza, Zaragoza, Spain, 69 pp.

Chapters 7 and 13. The content of these chapters arises from a paper published in the journal *Cretaceous Research* in 2015 (with a few later updates). Drs Ana Berreteaga and Henri Cappetta are coauthors. The geochemical research and the greater part of the geology data are original work of Ana Berreteaga. The paper, of which I am the lead author, is:

Corral, J.C., Berreteaga, A., Cappetta, H., 2015b. Upper Maastrichtian shallow marine environments and neoselachian assemblages in North Iberian palaeomargin (Castilian Ramp, Spain). *Cretaceous Research* 57 (2016), 639–661.

Chapters 8 and 14. Much of the content of these chapters derives from an initial paper by Astibia et al. (1990) and from Cappetta and Corral (1999), published in a special volume of the journal *Estudios del Museo de Ciencias Naturales de Álava*. Continued field work since the publication of these papers allowed to add new information, which has been published in other journals I also coauthored. The content of the chapters have been comprehensively revised and updated to incorporate additional original data relative to the geology, new fossil occurrences, and new figures. References for the chapters:

Astibia, H., Buffetaut, E., Buscalioni, A.D., Cappetta, H., Corral, C., Estes, R., García-Garmilla, F., Jaeger, J.J., Jimenez-Fuentes, E., Le Loeuff, J., Mazin, J.M., Orue-Etxebarria, X., Pereda-Suberbiola, J., Powell, J.E., Rage, J.C., Rodríguez-Lázaro, J., Sanz, J.L., Tong, H., 1990. The fossil vertebrates from Laño (Basque Country, Spain); new evidence on the composition and affinities of the Late Cretaceous continental faunas of Europe. *Terra Nova* 2, 460–466.

Cappetta, H., Corral, J.C., 1999. Upper Maastrichtian selachians from the Condado de Treviño (Basque-Cantabrian Region, Iberian Peninsula). *Estudios del Museo de Ciencias Naturales de Álava* 14 (Número Especial 1), 339–372.

Pereda-Suberbiola, X., Corral, J.C., Astibia, H., Badiola, A., Bardet, N., Berreteaga, A., Buffetaut, E., Buscalioni, A.D., Cappetta, H., Cavin, L., Díez Díaz, V., Gheerbrant, E., Murelaga, X., Ortega, F., Pérez-García, A., Poyato-Ariza, F., Rage, J.-C., Sanz, J.L., Torices, A., 2015. Late Cretaceous continental and marine vertebrate assemblages of the Laño Quarry (Basque-Cantabrian Region, Iberian Peninsula): an update. *Journal of Iberian Geology* 41(1), 101–124.

Corral, J.C., Pueyo, E.L., Berreteaga, A., Rodríguez-Pintó, A., Elisa Sánchez, E., Pereda-Suberbiola, X., 2015a. Magnetostratigraphy and lithostratigraphy of the Laño vertebrate-site: Implications in the uppermost Cretaceous chronostratigraphy of the Basque-Cantabrian Region. *Cretaceous Research* 57 (2016), 473–489.

Chapters 9 and 15. These two chapters also originate from an initial paper published in Spanish in the journal *Príncipe de Viana, Suplemento de Ciencias* in 1996. Contents have been updated with new geological and palaeontological information, and the taxonomic representation of the selachians in the fossil site has been expanded. The key reference for this chapter is Corral (1996), as mentioned earlier.

Chapter 17. This is basically an unpublished discussion chapter, where the findings presented in Chapters 5 through 6 and 11 through 12 are examined and explained.

Chapter 18. Much of this chapter was published in Spanish in the journal *Revista Española de Paleontología*, of which I am the lead author; its contents have been updated and revised to include new information. Reference for the chapter:

Corral, J.C., Pereda Suberbiola, X., Bardet, N., 2004. Marcas de ataque atribuidas a un selacio en una vértebra de mosasaurio del Cretácico Superior de Álava (Región Vasco-Cantábrica). *Revista Española de Paleontología* 19(1), 23–32.

Chapter 19. An earlier version of this chapter appeared in the journal *Paleontologia i evolució* as an extended abstract in Spanish. Here, contents are adapted and updated. Reference for the chapter:

Corral, J.C., Bardet, N., Pereda Suberbiola, X., Arz, J.A., 2011. Depredadores marinos (osteíctios, selacios y mosasaurios) en el Campaniense de la Cuenca Vasco-Cantábrica. XXVII Jornadas Sociedad Española de Paleontología, Sabadell, 5–8 octubre de 2011. *Paleontologia i evolució Memoria especial* 5, 83–87.

Chapter 20. This chapter provides a discussion to the findings presented in Chapters 7 through 9 and 13 through 15. Portions of this chapter are revised and updated from their original versions.

Chapter 21. This chapter is the conclusion to the thesis and draws attention to the major findings and discoveries within the scope of the research project.

Chapter 22. This chapter includes the published sources and references used for the preparation of this PhD thesis.

Acknowledgements

Special thanks and appreciation are due to my supervisors Drs Xabier Murelaga and Xabier Pereda-Suberbiola (Universidad del País Vasco/Euskal Herriko Unibertsitatea, UPV/EHU) for their motivation, encouragement and patience in making this thesis a reality. I would like also to thank Dr David Norman (Department of Earth Sciences, University of Cambridge, UK) and geologist Mr Chris Collins, who were in the Sedgwick Museum (University of Cambridge) in the early 1990s, for professional training and supervision as a geological curator. Sincere thanks are also to the staff of the Restoration Laboratory of the Diputación Foral de Álava/Arabako Foru Aldundia for all the facilities provided, especially to archaeology restorers Ms Paloma López and Ms Isabel Ortiz de Errazti who helped with restoration techniques after returning from my long-term stay in the UK.

My sincere thanks also go to Drs Francisco García-Garmilla and Xabier Orue-Etxebarria (UPV/EHU) who encouraged me to initiate the geological study of this area. I also am grateful to Drs Humberto Astibia and Ana Berreteaga (UPV/EHU) for scientific discussions and advice. I have also appreciated the help and comments that Dr Blanca Guarás has given me in the petrologic analysis of my rock samples from Albaina. Dr Henri Cappelletta (University of Montpellier, France) also deserves a significant note of thanks for his warm and friendly reception in Montpellier, but not less important for the support and guidance throughout the years. I am also indebted to my Master's thesis advisor Dr José Antonio Arz (University of Zaragoza) who identified and dated the planktonic foraminifers collected for my master's thesis and provides many insightful amendments. I like to thank my colleagues and the many people who contributed in many ways to this adventure. Thanks to Drs Juanjo Gómez-Alday (University of Castilla-La Mancha), Mikel López-Horgue (UPV/EHU) and Gregori López (Universitat Autònoma de Barcelona), and geologist Mr Jesús Alonso (Museo de Ciencias Naturales de Álava/Arabako Natur Zientzien Museoa, MCNA) for their assistance, both in collecting fossil teeth and supplying geological information. Amateur collectors, Mr Pedro Eguiluz, Mr Joseba Fernández de Pinedo, Mr José Mari Galbete, Mr Pedro Novella, Mr José Ignacio Sáez Laría, Mr Javier Sáenz and Mr Javier Vigil generously donated fossil specimens to the MCNA, or made available their palaeontological collections. I would also like to thank Mr Gorka Martín for bringing attention to a thin, selachian-rich, fossiliferous bed at Gometxa quarry.

Dr Florian Witzmann (Curator of fossil fishes and amphibians, Museum für Naturkunde, Berlin) provided photographs and valuable information about the type specimens of *Onchosaurus pharao*. Dr Henri Cappetta, Mr L. Datas, Mr J.-Y. Quero and Mr M. Pons supplied photographs of shark teeth which I have used in Chapter 14.

Special thanks to those colleges who helped with useful papers and monographs on recent and fossil sharks (Dr Nathalie Bardet, Mr G.R. Case, Dr David Cicimurri, Dr Ignacio Díaz Martínez, Dr Jacques Herman, Dr Thomas Kuchler, Dr Xabier Perea-Suberbiola, Jürgen Pollerspöck, Dr David R. Schwimmer, Dr Kenshu Shimada, Dr Mikael Siversson), and Lda. Lourdes Sáenz de Castillo and Dipl. Arturo Murga (Library and Documentation Services, UPV/EHU). I also thank Dr Nestor Etxebarria (Department of Analytical Chemistry, UPV/EHU) for assistance with the analysis of rare earth elements (REE), and Drs Ricardo Andrade, Alex Díez and Sergio Fernández from the Advanced Research Facilities (SGIker, UPV/EHU) for the help in obtaining SEM photographs. The help of Dr. Andoni Tarrío (Centro Nacional de Investigación sobre la Evolución Humana, CENIEH, Burgos) with the petrographic images of sedimentary rocks is gratefully appreciated.

I also thank Drs Paul Barrett, Rosa Domènech, Rodolfo Gozalo, Stefanie Klug, Eduardo Koutsoukos, Francisco Poyato and Charlie Underwood, and several anonymous reviewers for their constructive suggestions and criticisms on the various papers that form the core of this thesis.

I would like also to express my deepest gratitude to Dr Ana Rosa Soria (former coordinator of the Master's Programme in Initiation to Research in Geology, University of Zaragoza) for her help and advice regarding the documentation required for the application for "Funding support for student mobility in doctoral studies (Quality Award) for 2008-2009", the evaluators at the University of Zaragoza and the Spanish Ministry of Education, which awarded the funds. Several published papers in the course of the thesis work were partly funded by national and international government bodies such as Ministerio de Ciencia y Tecnología, currently Ministerio de Economía y Competitividad of Spain (CGL2007-64061/BTE, CGL2010-18851/BTE and CGL2013-47521-P), Institut des Sciences de l'Évolution de Montpellier, France (ISEM) (Nos. 2010-150 and 97-018), Gobierno Vasco/Eusko Jaurlaritzza, Spain (GIC07/14-361, IT-320-10, IT834-13 and IT1044-16) and UPV/EHU, Spain (PPG17/5). These research projects were also carried out in accordance with a collaborative agreement among the University of the Basque Country (UPV/EHU), the Museo de Ciencias Naturales de Álava/Arabako Natur Zientzien Museoa (MCNA), the Centre national de la recherche scientifique (CNRS) and the Muséum national d'Histoire naturelle (MNHN) in Paris. Finally, thanks to all those that I forget to mention here, sorry for my fragile memory.

The completion of this doctoral thesis could not have been possible without the support of the staff of the MCNA, a place where I have been lucky to spend most of my professional career helping to create and enlarge its important collections of fossils from the Basque-Cantabrian Region.

Abstract

Historical accounts of fossil sharks in the Basque-Cantabrian Region (northern Spain) were considered rare. Such apparent scarcity was reversed towards the end of the 20th century, when new discoveries of fish-bearing beds in the uppermost Cretaceous of the southern Basque-Cantabrian Basin (B-CB; provinces of Álava and Burgos) provided many teeth of Galeomorphii, Squalomorphii, and Batomorphii fishes. The earliest occurrence of these corresponds to an isolated rostral spine of the rare sawfish *Onchosaurus radicalis* (Rajiformes, Sclerorhynchoidei) from the upper Coniacian of the North Castilian Ramp (Barrio Panizares section, Burgos).

A significant number of teeth have been found in two productive zones of the Vitoria Sub-basin (Navarre-Cantabrian Ramp of the B-CB; Álava) – the Gometxa and Vitoria Pass sites –, and many of the species found there are new records for the Campanian of the Iberian Peninsula. The Gometxa site includes at least 17 taxa of neoselachians, recovered from shelfal and basinal marls with interbedded calcarenite beds of the Gomecha Member of the Vitoria Formation, deposited on unstable mid-ramp to fore slope dominated settings. The stratigraphical age indicated by the planktonic foraminifera is lower upper Campanian age (73.5 Ma). Nearby, in the brick pits of the Vitoria Pass, the glauconitic marl beds of the Eguileta Member of the younger Montes de Vitoria Formation have yielded 8 taxa of neoselachians. The minimum age of these upper Campanian deposits is estimated at 72 Ma, also confirmed by planktonic foraminifera. A mid- to outer ramp setting is interpreted on the basis of lithofacies characteristics and fossil content (e.g. macroinvertebrates and other cooccurring marine vertebrates).

Investigation of shark-tooth marks in a caudal vertebra of Mosasaurinae from the upper Campanian Eguileta Member in the near locality of Jauregi indicates direct trophic interactions between sharks and mosasaurids (either predatory activity or scavenging).

The Quintanilla la Ojada section (Burgos) within the North Castilian Ramp (Valdenoceda Formation) include a mix of semipelagic and bottom-dwellers selachians. Two clearly differentiated vertebrate assemblages – with 16 taxa in total – have been found here. Sedimentological data indicates that this formation was deposited in a nearshore subtidal environment, most possibly, during the early late Maastrichtian based on reasonable lithostratigraphical correlation. Overall, the previous elasmobranch fauna compares with that of the Torme Formation of the eastern Castilian

Ramp in the Albaina site (Treviño County, Burgos). Neoselachians – which includes at least 19 taxa – are the more frequently vertebrate fossils, but the remains of other marine and terrestrial vertebrates have been also found within the same nankin-type calcarenite. This fossiliferous bed represents a transgressive lag deposit formed in a shallow marine inner-ramp environment. The faunal association is original by being a mixture of south-Tethyan and North European taxa. Albaina site, which is unquestionable upper Maastrichtian on the basis of diagnostic selachians and baculitid ammonites, has yielded the most diverse and abundant collection of selachian teeth from this age so far discovered in the Iberian Peninsula.

Also important to complement our understanding of the Upper Cretaceous selachian diversity in southern Europe is the well-dated faunule of semipelagic selachians found in the upper Maastrichtian shallow carbonate strata of the Puerto of Olazagutía Formation (B-CB, Entzia section in Álava), with at least three species.

Resumen extendido

Se estudian seis yacimientos con fósiles de neoselacios (tiburones y rayas) distribuidos por la zona centro meridional de la Región Vasco-Cantábrica (norte de España), dentro de secuencias marinas del Cretácico Superior.

En la parte introductoria se han destacado las escasas referencias históricas sobre dientes de tiburón hallados en esta región, que se remontan a los pasados siglos XIX y XX con la obra general de Adán de Yarza sobre Álava (1885) y de Ruiz de Gaona (1943) sobre el Maastrichtiense de Navarra. A continuación se describe el área de estudio donde se localizan los yacimientos. Esta se divide geográficamente en tres sectores, cuyos rasgos geomorfológicos están condicionados por la litología y la disposición estructural de los estratos. El primer sector corresponde al páramo alto de La Lora de la Pata del Cid (Burgos) —localizado en la región suroccidental—, que se caracteriza por ser una región elevada moldeada por procesos erosivos kársticos. El segundo —en la región central— corresponde a una amplia depresión sinclinal, denominada de Villarcayo-Medina (Burgos), cuyo límite noroeste es una banda de escarpes carbonatados del Cretácico Superior–Paleógeno. Y finalmente, la depresión de Miranda-Treviño y la planicie de Urbasa —en el sector más oriental— que estructuralmente corresponden a un vasto sinclinal y a un sinclinal colgado, respectivamente, enclavadas en la parte central de Álava y el burgalés Condado de Treviño.

La Cuenca Vasco-Cantábrica (CVC) se originó como cuenca sedimentaria entre el margen continental noribérico y la plataforma de las Landas; actualmente corresponde al segmento occidental de la cordillera pirenaica, al oeste de la Falla de Pamplona. La mayoría de las unidades estratigráficas del Cretácico Superior y Paleógeno existentes en el sur y sudeste de esta cuenca representan depósitos de rampa carbonatada, desarrollados durante la etapa de margen continental pasivo. Esta rampa contaría con: (1) una zona externa —denominada Surco Navarro-Cántabro (SNC)— regida por una fuerte subsidencia generalmente compensada por la sedimentación y, (2) una rampa carbonatada interna —denominada Plataforma Norcastellana (PNC)— poco subsidiada y sin depósito en muchos momentos de su historia sedimentaria. Los depósitos cretácicos en estos dos dominios estratigráficos están representados en cuatro ciclos transgresivos-regresivos de larga duración, correspondiendo el último de ellos [C T/R 4 según Floquet (2004); Santoniense a Maastrichtiense superior] a un episodio de regresión generalizada (con fluctuaciones menores). Las condiciones paleoambientales

en el SNC durante el Campaniense superior indican ambientes marinos, observándose series de margas de cuenca y bancos de calciturbiditas derivadas de una plataforma o rampa carbonatada más meridional, correspondientes al Miembro Gomecha de la Formación Vitoria (MG-FV). Esta zona de la cuenca registraría posteriormente depósitos de prodelta-frente deltaico, correspondientes al Miembro Eguileta de la Formación Montes de Vitoria (ME-FMV). También son particularmente interesantes los depósitos de rampa somera de la PNC y el SNC en el Maastrichtiense superior, debido a la presencia de vertebrados marinos. En orden decreciente de edad, estos depósitos están representados por margocalizas dolomitizadas de la Formación Valdenoceda (FV), calizas bioclásticas de la Formación Torme (FT), y finalmente margas y margocalizas de la Formación Puerto de Olazagutía (FPO).

También se incide en las técnicas de campo utilizadas para la recolección de los especímenes (colecta en superficie, extracción, lavado y tamizado de determinados niveles), así como en el proceso de triado de los residuos rocosos en el laboratorio para recuperar los microrrestos fósiles. A su vez, ha sido fundamental la preparación mecánica y química de los especímenes fósiles, tanto para la extracción de la matriz carbonatada como para revelar algunos elementos anatómicos ocultos por roca. Se comentan los equipos y herramientas empleados, y el uso de concentraciones acuosas débiles de los ácidos acético y fórmico. Igualmente se dan algunas indicaciones sobre el uso de la resina acrílica Paraloid B72 como adhesivo y consolidante. En el apartado de documentación gráfica se comentan algunas técnicas fotográficas básicas, incluyendo el blanqueado de especímenes con cloruro de amonio para obtener imágenes más contrastadas, y el tratamiento digital de las imágenes. Todo este trabajo perdería gran parte de su sentido si no se hubieran contemplado medidas para la gestión y conservación de este patrimonio fósil. A este respecto, se ofrecen algunos detalles sobre la integración del material estudiado en la colección paleontológica del Museo de Ciencias Naturales de Álava/ Arabako Natur Zientzien Museoa en Vitoria-Gasteiz.

El último capítulo de la introducción ofrece información básica sobre la biología y clasificación de los elasmobranquios (neoselacios) actuales y fósiles. Estos peces destacan por poseer un endoesqueleto principalmente compuesto de cartílago hialino, cubierto en algunos lugares por placas calcificadas o *tesserae*. También incluyen un exoesqueleto mineralizado formado por escamas placoideas insertadas en la dermis, dientes orales y varios tipos de espinas (i.e., rostrales, cefálicas, apendiculares dorsales y caudales) que tienen un alto potencial de preservación debido a su composición mineral. El hidroxapatito cálcico es la fase mineral predominante de los tejidos duros en los selacios actuales, y el fluorapatito y la francolita en las formas fósiles. En los dientes se distinguen tres tejidos principales en base a su textura y proporción mineral (i.e., vitrodentina, ortodentina y osteodentina). Al final de este capítulo se incluye la sistemática general de los taxones estudiados, así como un listado bilingüe (español-inglés) de términos dentales más comúnmente usados en la parte descriptiva.

El espécimen más antiguo estudiado corresponde a una espina rostral de *Onchosaurus*

radicalis, perteneciente al grupo de peces sierra (Rajiformes, Sclerorhynchoidei) con rostro alargado armado con espinas laterales. Este resto fósil, único en la Península Ibérica, fue hallado en margas de la Formación Nidáguila que afloran en el Sinclinal de Sedano, dentro del dominio de la PNC (norte de Burgos), junto a una variada asociación de ammonites que indicaría una edad mínima Coniaciense superior. El estrato de procedencia de este fósil es interpretado como un depósito de tormenta, sugiriéndose así un transporte desde zonas someras de la rampa carbonatada.

Actualmente se considera que solo las especies *O. radicalis* y *O. pharao* —cuyos tipos han sido revisados y documentados fotográficamente— pueden ser asignadas al género *Onchosaurus*. Con los datos actuales, el género apareció por primera vez en Gondwana, dispersándose luego hacia el norte (sur de Norteamérica y Eurasia) favorecido por los nuevos márgenes de plataforma formados durante el máximo ascenso del nivel del mar del Turoniense. A partir del Campaniense, *Onchosaurus* fue reemplazado progresivamente en ambientes sublitorales marinos por otros esclerorrínquidos, entre los cuales se encontrarían los géneros *Ischyrhiza*, *Ganopristis* y *Dalpiazia*.

Un importante número de dientes de selacios han sido recogidos en el Campaniense superior de la Subcuenca de Vitoria (Rampa Navarro-Cántabra en la CVC). En el yacimiento de Gometxa (GOM), en el municipio de Vitoria-Gasteiz (Álava), afloran niveles de margas y calcarenitas bioclásticas del MG-FV ricos en invertebrados marinos. También se han observado en las calcarenitas trazas fósiles a muro (*Thalassinoides* isp.). Esta unidad corresponde a la base del Campaniense superior (aproximadamente 73.5 Ma, según datación con foraminíferos planctónicos). La presencia de estructuras tipo *slump* en la serie estratigráfica sugiere ambientes inestables de rampa media o parte superior del talud. El yacimiento GOM incluye al menos 17 taxones, habiéndose descrito los siguientes: *Anomotodon hermani*, *Carcharias aasenensis*, *Chiloscyllium* cf. *gaemersi*, *Chiloscyllium* cf. *vulloi*, *Cretolamna borealis*, *Cretolamna sarcoportheta*, *Cretoxyrhina mantelli*, *Hemiscyllium hermani*, *Paranomotodon* cf. *angustidens*, *Parapalaebates pygmaeus*, *Prohaploblepharus riegrafi*, *Ptychotrygon* sp., *Rhinobatos casieri*, *Scapanorhynchus* cf. *texanus*, *Squalicorax* ex gr. *kaupi*, *Squatina* (*Cretascyllium*) *hassei* y *Synechodus* aff. *filipi*. La serie del Campaniense continúa en la Subcuenca de Vitoria con alternancias de caliza-marga, margas glauconíticas y areniscas de la Formación Montes de Vitoria. Esta formación ha sido dividida en tres miembros, aunque sólo el basal ME-FMV, que incluye margas de prodelta depositadas en un ambiente de rampa de media a externa, es particularmente rico en contenido fósil. El yacimiento del Puerto de Vitoria (afloramientos de Gardelegi y Castillo/Gaztelu, Vitoria-Gasteiz, Álava) ha suministrado restos de vertebrados marinos pertenecientes a actinopterigios, selacios y mosasaurios. Junto a estos, equínidos, gasterópodos y ammonites son un componente importante de la asociación fósil. Son numerosos los dientes de selacios que proceden de estas margas del Campaniense superior (con una edad mínima estimada de 72 Ma, según datación bioestratigráfica con foraminíferos planctónicos), aunque debido al sesgo en la recolección superficial únicamente ocho taxones están aquí representados: *Carcharias ad-*

neti, *Cretolamna borealis*, *Cretolamna sarcoportheta*, *Galeorhinus girardoti*, *Protolamna borodini*, *Pseudocorax laevis*, *Serratolamna khderii* y *Squalicorax* ex gr. *kaupi*. El contenido fósil presente en estas facies indica un ambiente nerítico con un cierto grado de profundidad. Además, un análisis preliminar sugiere que la estructura trófica estaba compuesta por invertebrados pelágicos, peces actinoptergios (*Enchodus* y otros miembros del orden Salmoniformes), selacios y finalmente algunos superdepredadores en lo alto de la cadena alimentaria (algunas especies de tiburones y mosasaurios). El estudio de una vértebra caudal de Mososaurinae indet. procedente de la pequeña localidad de Jauregi (Iruraiz-Gauna, Álava), igualmente perteneciente al Campaniense superior margoso del ME-FMV, ha permitido inferir la existencia de interacciones tróficas entre tiburones y mosasaurios a partir del análisis de unas estructuras de bioerosión presentes en ella. Estas marcas son muy parecidas a las características incisiones producidas por selacios con una dentición de tipo cortante (o con una tendencia hacia ese modelo). Y aunque no se puede constatar una asociación directa entre ambos grupos de vertebrados, la presencia de dientes aislados de tiburones lamniformes (e.g., *Squalicorax* ex gr. *kaupi* y *Cretolamna sarcoportheta*) en los mismos niveles permite suponer que algún miembro de estas especies fue el causante de las marcas. Este ejemplo ha representado un nuevo registro europeo de relación trófica (ya sea depredación o carroñeo). Muchos de estos taxones de selacios descubiertos en el Campaniense de Álava, que no habían sido apropiadamente descritos hasta ahora, constituyen además la primera cita para la Península Ibérica. Algunas asociaciones de selacios similares a las aquí consideradas se encuentran en las cuencas Anglo-Parisiense (Francia y el Reino Unido), de Münster (NO de Alemania) y de Kristianstad (Escania, Suecia).

Los fósiles del yacimiento de Quintanilla la Ojada (provincia de Burgos) se encuentran en conglomerados y margas bioturbadas (en su mayor parte dolomitizadas) pertenecientes a la FV de la Rampa Norcastellana. Estos depósitos se formaron en un ambiente submareal cercano a la costa, y corresponden a la base de Maastrichtiense superior; dato este inferido a partir de la correlación estratigráfica debido a la ausencia de fósiles guía. Se han reconocido dos asociaciones fósiles claramente diferenciadas (QLO-1 y QLO-2), cuyo grado de mezcla tafonómica y reelaboración es pequeño o inexistente, basado esto último en el análisis de elementos de tierras raras (REE). Por ello, las diferencias observadas en el grado de conservación de los dientes y mezcla ecológica pueden explicarse mediante procesos biostratinómicos. El contenido agregado de las dos asociaciones fósiles de selacios incluye 16 taxones (distribuidos en 11 géneros): *Carcharias heathi*, *Carcharias* sp., *Coupatezia fallax*, *Cretolamna* sp. aff. *Cretolamna appendiculata*, *Ganopristis leptodon*, *Palaeogaleus faujasi*, *Plicatoscyllium lehneri*, *Rhinobatos echavei*, *Rhinobatos ibericus*, *Rhombodus binkhorsti*, *Rhombodus* sp., *Serratolamna serrata*, *Squalicorax kaupi*, *Squalicorax pristodontus*, *Squalicorax* sp. y *Vascobatis albaitensis*. Este conjunto representa una mezcla de especies locales (i.e., *Rhinobatos echavei* y *Rhinobatos ibericus*) y cosmopolitas (i.e., *Squalicorax pristodontus*, *Serratolamna serrata* y *Rhombodus binkhorsti*), en general moradoras de aguas poco profundas y en menor medida de rampa externa.

El anterior conjunto de neoselacios comparte, en general, grandes similitudes con el descubierto en el yacimiento de Albaina (Condado de Treviño, Burgos) dentro de la Rampa Castellana oriental de la CVC. En esta localidad afloran unas calcarenitas tipo nankin de la FT, que han sido interpretadas como un lag transgresivo producido durante el Maastrichtiense superior en un ambiente costero de rampa interior. La TF en Albaina presenta una variada litología, distinguiéndose tres principales litofacies:

- un término basal (LF-I) formado por areniscas poco fosilíferas —depositadas en ambientes litorales— y conglomerados poligénicos organizados como pequeñas lentes en forma de depósitos residuales,
- un término intermedio (LF-II) constituido por carbonatos formados en aguas poco profundas (calizas bioclásticas), que han proporcionado la mayoría de los restos de vertebrados y algunos macroinvertebrados, y finalmente
- un término siliciclástico (LF-III) formado por sets de areniscas de grano fino, depositadas en un ambiente litoral somero.

Los selacios son los vertebrados fósiles más frecuentes de este yacimiento, pero también hay restos de peces actinopterigios, mosasáuridos, plesiosaurios, tortugas y algunos huesos de dinosaurio. La asociación de selacios de Albaina —con al menos 19 taxones— representa la acumulación de selacios más diversa y abundante del Cretácico tardío en la Península Ibérica, e incluye los siguientes taxones: *Ataktobatis variabilis*, *Carcharias* aff. *gracilis*, *Carcharias heathi*, *Chiloscyllium* sp., *Coupatezia fallax*, *Cretolamna appendiculata*, *Dalpiazia stromeri*, *Ganopristis leptodon*, *Odontaspis bronni*, *Palaeogaleus faujasi*, *Plicatoscyllium lehneri*, *Rhinobatos echavei*, *Rhinobatos ibericus*, *Rhombodus andriesi*, *Rhombodus binkhorsti*, *Serratolamna serrata*, *Squalicorax kaupi*, *Squalicorax pristodontus* y *Vascobatis albaitensis*. Esta asociación fósil es original al contener una mezcla de especies propias del sur del Tetis y el norte de Europa. La edad de estas capas es Maastrichtiense superior no final, debido la presencia de algunos invertebrados significativos desde el punto de vista bioestratigráfico, principalmente ammonites baculítidos, además de las especies *Rhombodus andriesi* y *Odontaspis bronni*.

Por último, se han recogido en superficie unos pocos restos de los selacios *Squalicorax kaupi*, *Squalicorax pristodontus* y *Carcharias heathi* en los yacimientos Entzia-I y Entzia-II (Álava), localizados en flanco norte del sinclinal colgado de Urbasa. Estos especímenes provienen de unos estratos de margas y margocalizas de la FPO con una edad Maastrichtiense superior —según la revisión de los ammonites presentes—, representando un ambiente de rampa carbonatada somera con una gran variedad de equínidos y moluscos fósiles.

Quintanilla la Ojada, Albaina y Entzia se encuentran entre los escasos yacimientos del suroeste de Europa formados al final del Cretácico. Estos lugares de la Región Vasco-Cantábrica (CVC), y particularmente Albaina, han suministrado un rico y diverso conjunto de selacios, contribuyendo así al conocimiento de la diversidad taxonómica, paleoecología y bioestratigrafía de este grupo de peces cartilaginosos que durante el Maastrichtiense habitaron las aguas del sector mediterráneo occidental en el margen norte del mar de Tetis.



INTRODUCTION



YOUNG SHARK: Mammy, Mammy!

SHARK MUM: Again! I have told you a thousand times that we don't have a Tooth Fairy!

Chapter I HISTORICAL, GEOGRAPHIC, AND GEOLOGICAL SETTINGS

1.1 Historical review of fossil neoselachian research in the Basque-Cantabrian Region

Until the late twenty-century, very few references to fossil shark occurrences in the Basque-Cantabrian Region¹ were made, and some of the existing ones are nowadays of questionable taxonomic value. The earliest notice of a selachian remain in the region was made by the nineteenth-century mining engineer Ramón Adán de Yarza (1848–1917), who was involved in various geological exploration works for the ‘*Comisión del Mapa Geológico de España*’ (Fig. 1.1). The ‘*Comisión*’, which was composed mainly of mining engineers, had among its goals the creation of the Spanish geological map, following the path of other European institutions. For those engineers, palaeontology was regarded as a valuable tool for field survey investigations in the context of making geological maps or to solve stratigraphical problems (see Sequeiros, 1988). As a consequence, neither complete description nor figuration of some of these fossil finds was provided.

But going back to the history, Adán de Yarza (1885:69) mentioned the presence of small teeth of a “placoid fish” in the Upper Cretaceous (‘Senonian’) marls, east of the hamlet of Bitoriano² in the province of Álava, when describing the geological cross-section 3, from Mount Gorbea to the Ebro River:

“[...] en un cerro incluido en la zona margosa del Senonense inferior, se han hallado unos diente-cillos de pez placóide que el señor Egozcue no ve medio de distinguir de los del *Lamna elegans*, Agass., por más que esta especie se encuentra representada con profusión en la Arcilla de Londres, la Caliza parisiense y otros depósitos terciarios más recientes, habiéndose citado también por Leymerie en la parte superior de la fauna garúmnica de Marsoulas (Haute-Garonne)”.

The finding of fossil teeth east of Bitoriano was later recorded by Mallada (1904: 77) without adding any new details.

¹ Basque-Cantabrian Region refers to a geographical area in northern Spain. The term Basque-Cantabrian Basin is used to refer to its geological characteristics.

² The official name is nowadays Bitoriano, but it was formerly known as Vitoriano.

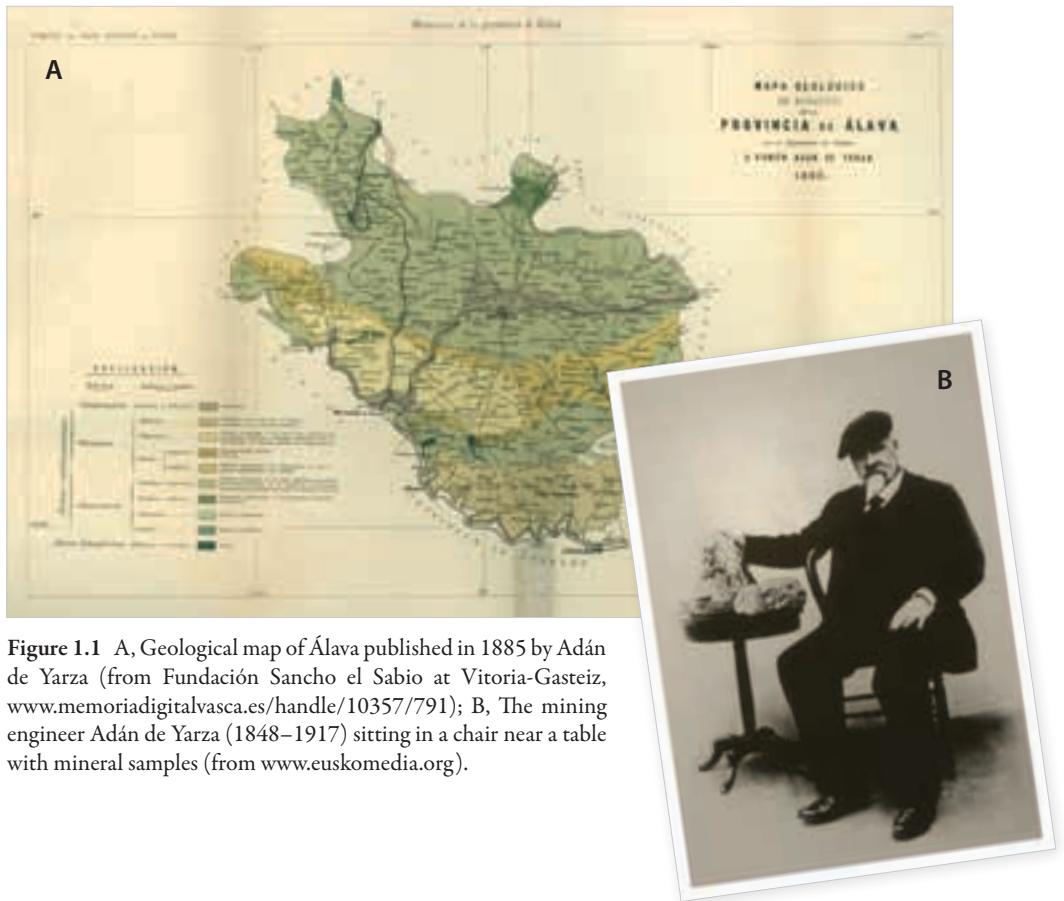


Figure 1.1 A, Geological map of Álava published in 1885 by Adán de Yarza (from Fundación Sancho el Sabio at Vitoria-Gasteiz, www.memoriadigitalvasca.es/handle/10357/791); B, The mining engineer Adán de Yarza (1848–1917) sitting in a chair near a table with mineral samples (from www.euskomedia.org).

The taxonomic attribution of these specimens was made by his colleague Justo Egozcue y Cia (1833–1900), who was professor of geology and palaeontology at the School of Mining Engineering in Madrid (Spain), on the basis of the strong similarities with the Tertiary species to '*Lamna elegans*' described by Agassiz in 1843.

Although '*Lamna elegans*' was initially considered by Agassiz (1843) an Eocene fossil (Fig. 1.2A), its presence in Cretaceous rocks was seen possible at that time, especially after the work of Rutot (1875), who reported the species in the Maastrichtian of Wanzin, near Orp-le-Grand (Brabant, Belgium). Among the taxonomic characters of such specimens is a slender cusp, slightly sigmoidal in lateral view, with sharp edges and two small sharp cusplets, each on either side of the main cusp. Moreover, the lingual face of the cusp is ornamented with fine vertical folds reaching half of the cusp height. Such teeth may reach 4–5 cm in length. Rutot (1875) ended by stating that given his extended stratigraphical range, from Maastrichtian to Oligocene, the species *Lamna elegans* was not suitable for age determination or field correlation.

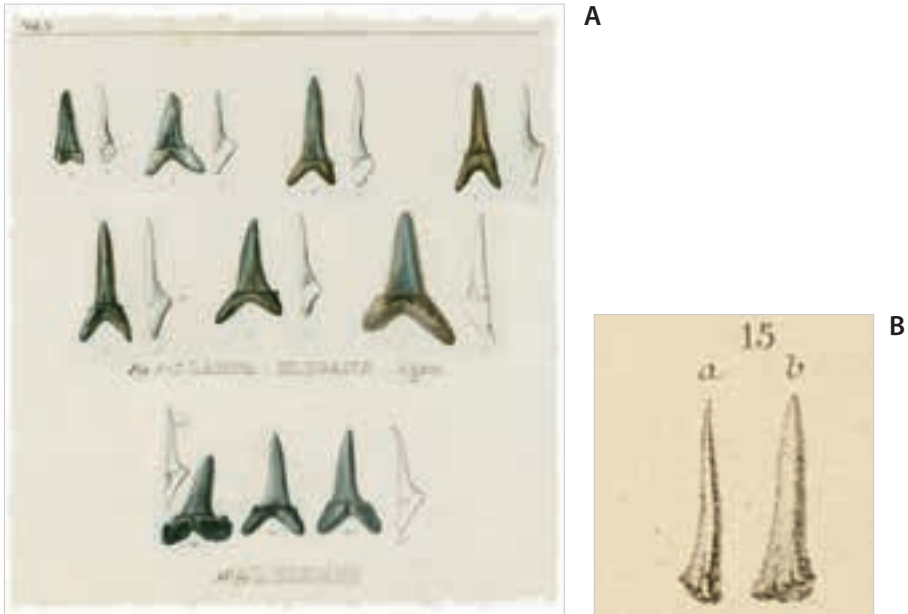


Figure 1.2 A, Figurations of *Lamna elegans* teeth in Agassiz's "Recherches sur les Poissons Fossiles" (1833–1843), Figs. 1–7 from the Lutetian 'calcaire grossier' of Paris, France, and Figs. 58–59 from the Ypresian 'London clay' of Sheppy (UK); B, Incomplete tooth of a shark similar to the Tertiary species *Lamna elegans* from the Maastrichtian Auzas Marls Formation, Marsoulas (Haute-Garonne, France), figured in Leymerie (1878). Sources: A, Jubilotheque (jubilotheque.upmc.fr); B, The Biodiversity Heritage Library (www.biodiversitylibrary.org).

Another occurrence of the same species was documented by the French geologist Alexandre Leymerie (1801–1878), who was professor at the Faculty of Sciences in Toulouse (France) and a specialist in the geology of the Pyrenees. The shark teeth reported by Leymerie (1881: 782)¹, which seemed identical to the '*Lamna elegans*' of the Tertiary limestone of Paris (Fig. 1.2B), were found in a marl bed of the upper Maastrichtian Auzas Marls Formation (overlying a lignite bed at Marsoulas, Haute-Garonne), and studied by the palaeontologist Henri-Émile Sauvage (1842–1917). However, the taxon '*Lamna elegans*' has been nowadays relegated to the synonymy of *Striatolamia macrota* (Agassiz, 1843), a mitsukurinid species from the Lutetian of Sheppey (UK) and the 'calcaire de Veteuil' (equivalent to 'calcaire grossier') from the Basin of Paris, France (Cappetta, 2006).

As axial folds on the lingual face of the crown are among the characteristics of mitsukurinid teeth (Cappetta, 2012), two possible Upper Cretaceous genera of this family

¹ His posthumous book "Description géologique et paléontologique des Pyrénées de la Haute-Garonne" was printed in two volumes. The text volume that was left almost complete at his death in 1878 was published posthumously three years later with the help of Louis Lartet (1840–1899), his successor at the chair of mineralogy and geology. The Atlas volume of the first edition was printed in 1878.

may correspond to the teeth reported by Adán de Yarza (1885), either *Scapanorhynchus* or *Anomotodon*. This problem can only be solved if new fossil teeth are found nearby the original location.

There is no other relevant selachian find until the publication by Ruiz de Gaona (1943) of precursory details on the Maastrichtian stage in Navarre. Máximo Ruiz de Gaona (1902–1971) was a distinguished Navarre-born scientist that balanced his teaching duties with geological research (Fig. 1.3). Although he was well known by its studies on fossil foraminifera from the Basque-Cantabrian Region and adjacent Pyrenean areas, he also collected and gathered along his career many fossil invertebrates in addition to some relevant Quaternary vertebrates (see Astibia et al., 1996). The remarkable geology around the village of Olazti-Olazagutía inspired him to start a passionate geological work that later would extend to other nearby territories. As the geology in that area is covered with dense vegetation, new road cuts in the route Olazti-Olazagutía to Estella (Navarre) was seen as a good opportunity for fossil collecting, and there he discovered for the first time in Navarre the existence of the Maastrichtian stage— then considered the penultimate stage of the Cretaceous —, which had passed unnoticed below the prominent Tertiary limestones of the Urbasa range. The results of this discovery were published in 1943, one of his earliest papers. During the first part of the 20th century, the stratigraphy represented by the Upper Cretaceous in Navarre was based on the scheme given by Palacios (1919) in his book “*Los terrenos mesozoicos de Navarra*”. Palacios adopted the ideas of some 19th century French geologists, such as Hébert (1875b) and Seunes (1890), who in turn had followed the proposals of d’Orbigny (1840a) when classifying the Upper Cretaceous stages. Then, the last two stages of the Upper Cretaceous were the Senonian, which included the sub-stages, Santonian and Campanian, and above it was the Danian that was also subdivided into a lower group called Maastrichtian¹ and the upper strata or ‘Garumnian’².

These fresh outcrops exposed near Olazti-Olazagutía provided Ruiz de Gaona with a “typical Maastrichtian fauna”, and in the outcropping marls he referred the occurrence of shark teeth, one of them assigned to ‘*Corax pristodontus*’ Agassiz, 1843 (Fig. 1.3):

“Poseemos [...] varios dientes de diversas especies de selacios, uno de los cuales, triangular, más ancho que alto, de borde totalmente denticulado, pero al que le falta la raíz refiero al *Corax pristodontus* Agass. (lám. I, núm 56).”

¹ Seunes (1890) also called it ‘Assises Da¹’ with *Pachydiscus jacquoti* and pointed out other different names given: ‘Système maastrichtien de Dumont’; Dordonien by Coquand; Sénonien Supérieur by d’Orbigny and Leymerie. The unit was also named ‘Limestone with *Hemipneustes* and *Orbitoides*’ in the Pyrenees or chalks of Clipy and Maastricht in northern Europe. Moreover, the nankin limestone and marls with *Hemipneustes* of Gensac (Haute-Garonne) and the Monlón beds (Hautes-Pyrénées) with cephalopods, both in southern France, were regarded as equivalent to the Maastricht Chalk by Leymerie (1881).

² Seunes (1890) called it ‘Assises Da²’ with *Nautilus danicus*. Other correlated units are the Garumnien of Leymerie, ‘Calcaire à *Lychmus*’ de Rognac (Provence, France) and ‘Calcaire à *Micraster tericensis*’ in Aquitaine, Pyrenees and Corbières (France).

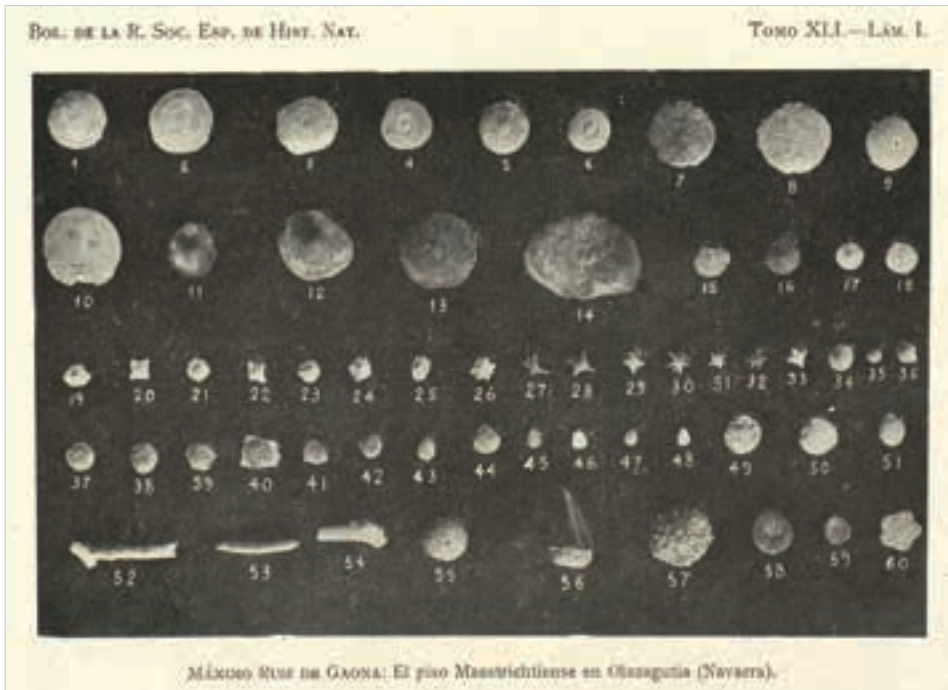
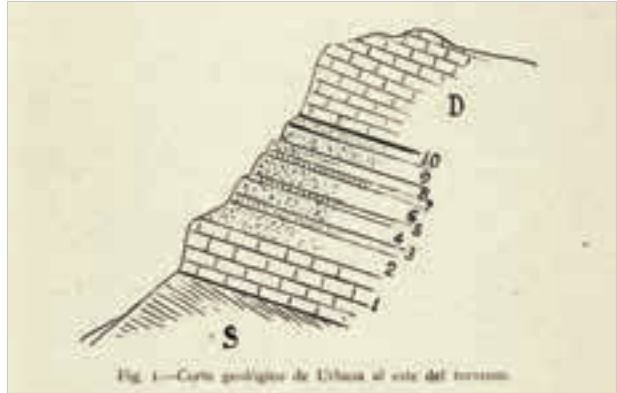
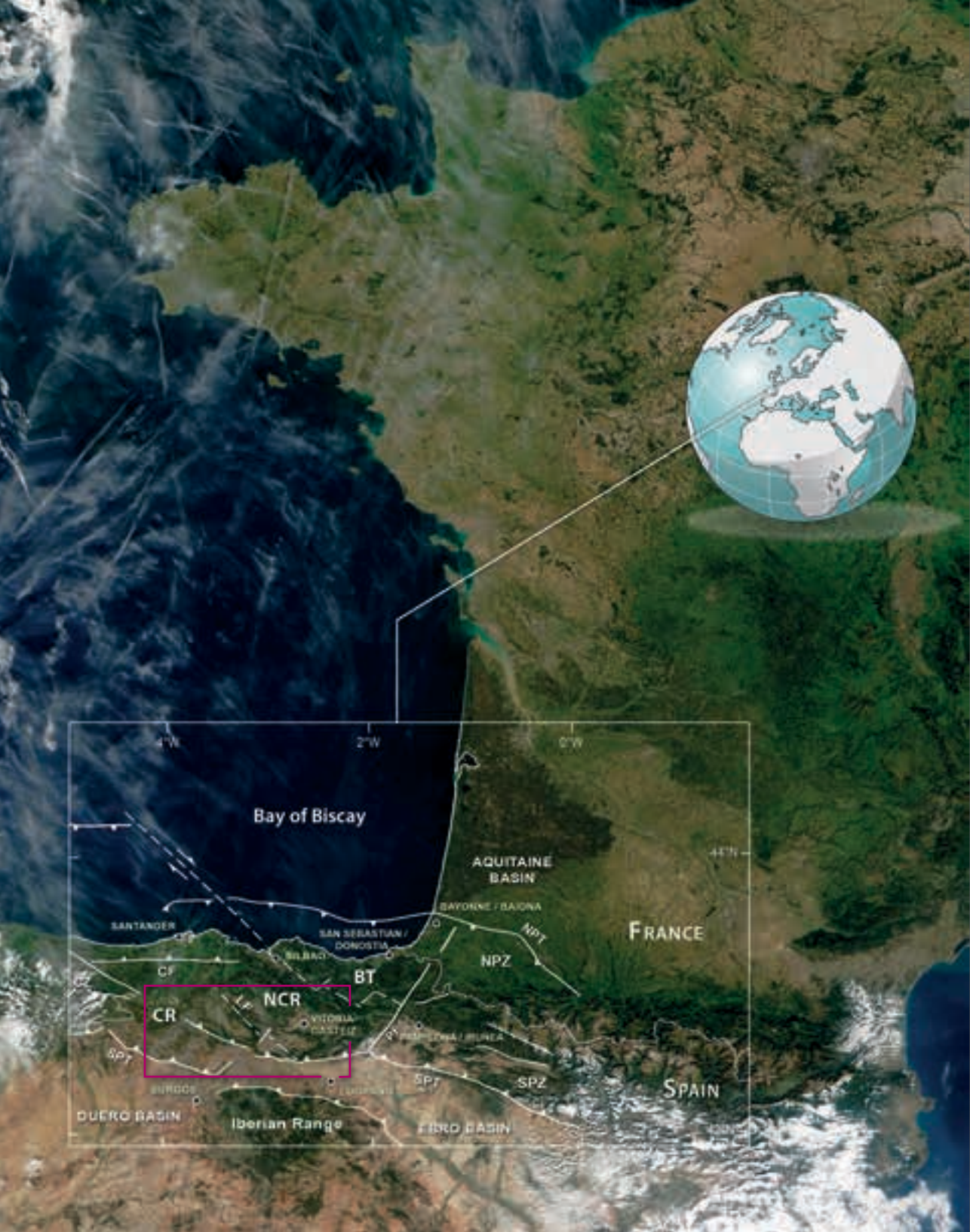


Figure 1.3 Portrait of Máximo Ruiz de Gaona (above left), photo source: Latasa (1996). Geological cross-section of the Urbasa range near Olazagutía (Navarre) (above right) and plate from his paper on the Maastrichtian of Navarre issued in 1943 (below); number 56 depicts an incomplete tooth of *Squalicorax pristodontus* (Agassiz, 1843) (source: Biblioteca Real Jardín Botánico, CSIC; bibdigital.rjb.csic.es).

This citation might have been overlooked – or in a worst case not been valued properly –, among the profuse list of forams and invertebrates included in his paper. But it must be stressed that this taxon was the first mention of the species in Spain and one of the few Cretaceous selachian examples cited in the Spanish palaeontological literature



Bay of Biscay

AQUITAINE BASIN

FRANCE

SANTANDER

SAN SEBASTIAN / DONOSTIA

BAYONNE / BAIONA

CF

BT

NPZ

CR

NCR

VITORIA GASTELU

PREMONTANA / BILBAO

DUERO BASIN

Iberian Range

EBRO BASIN

SPAIN

BURGOS

LEZAMA

SP1

SP2

LEZAMA

LEZAMA

LEZAMA

LEZAMA

LEZAMA

LEZAMA

LEZAMA

LEZAMA

LEZAMA

LEZAMA

LEZAMA

LEZAMA

then, whose Mesozoic faunae were then still poorly known according to Bataller (1960). However, despite his renowned drawing skills, neither a full description and clear figuration nor a precise stratigraphical location for the specimens was provided, perhaps because his primarily palaeontological interest lay in other groups rather than fossil fishes.

It would take 50 years until other palaeontologists made further contributions to this fossil group from this part of the Basque-Cantabrian Region. Bardet et al. (1993) cited a few shark species from the upper Campanian marls nearby the city of Vitoria-Gasteiz, and a few years later Corral (1996) and Cappetta and Corral (1999) gave detailed account on the selachians of late Maastrichtian age from the province of Álava and the Treviño County (Burgos), respectively. Such details are beyond the scope of this introduction and they will be dealt with in detail in subsequent chapters.

1.2 Geography of the study area

The area lies in the Basque-Cantabrian Region (north of the Iberian Peninsula) (Fig. 1.4), which is the continuation of the Pyrenees (one of the Alpine chains of western Europe), and strictly speaking within a hilly area spanning about 150 km from East to West in its southern part, approximately between $4^{\circ}00'$ – $2^{\circ}15'$ longitude west and $42^{\circ}56'$ – $42^{\circ}38'$ latitude north. A number of localities in the provinces of Álava and Burgos, which are respectively situated in the autonomous communities of the Basque Country and Castile and León within northern Spain, have yielded significant selachian assemblages (Fig. 1.5). Details about the precise location of the fossil sites are given in the corresponding chapters.

Southwestern region – Plateau of La Lora de la Pata del Cid (Burgos)

The physiographic region known as La Lora de la Pata del Cid (termed La Lora in short form) is located north of the Burgos province, and is the largest of several folded structures that occur in the southeasternmost sector of the Basque-Cantabrian Region. On geomorphological grounds, the area comprises a flat-topped moorland (plateau) dominated by Upper Cretaceous carbonates with average elevations of about 1000 to 1200 m. These rock formations are the result of uplift, planation, and fluvial

-
- ◀ **Figure 1.4.** NASA's Terra satellite image of the Bay of Biscay in which palaeogeographical domains and tectonic setup of the Basque-Cantabrian Basin are noted (photo credits: Jacques Descloitres, Moderate-Resolution Imaging Spectroradiometer (MODIS) Rapid Response Team, NASA/GSFC, 29 September 2002; <http://visibleearth.nasa.gov/view.php?id=62480>). The purple box indicates the study area within this thesis. Abbreviations: BT, Basque Trough; CF, Cabuérniga Fault; CR, Castilian Ramp; CZ, Cantabrian Zone (Asturian Palaeozoic Massif); LF, Losa Fault; NCR, Navarre-Cantabrian Ramp; NPT, North Pyrenean Thrust; NPZ, North Pyrenean Zone; PF, Pamplona Fault; SPT, South Pyrenean Thrust; SPZ, South Pyrenean Zone (modified from Corral et al., 2015a).

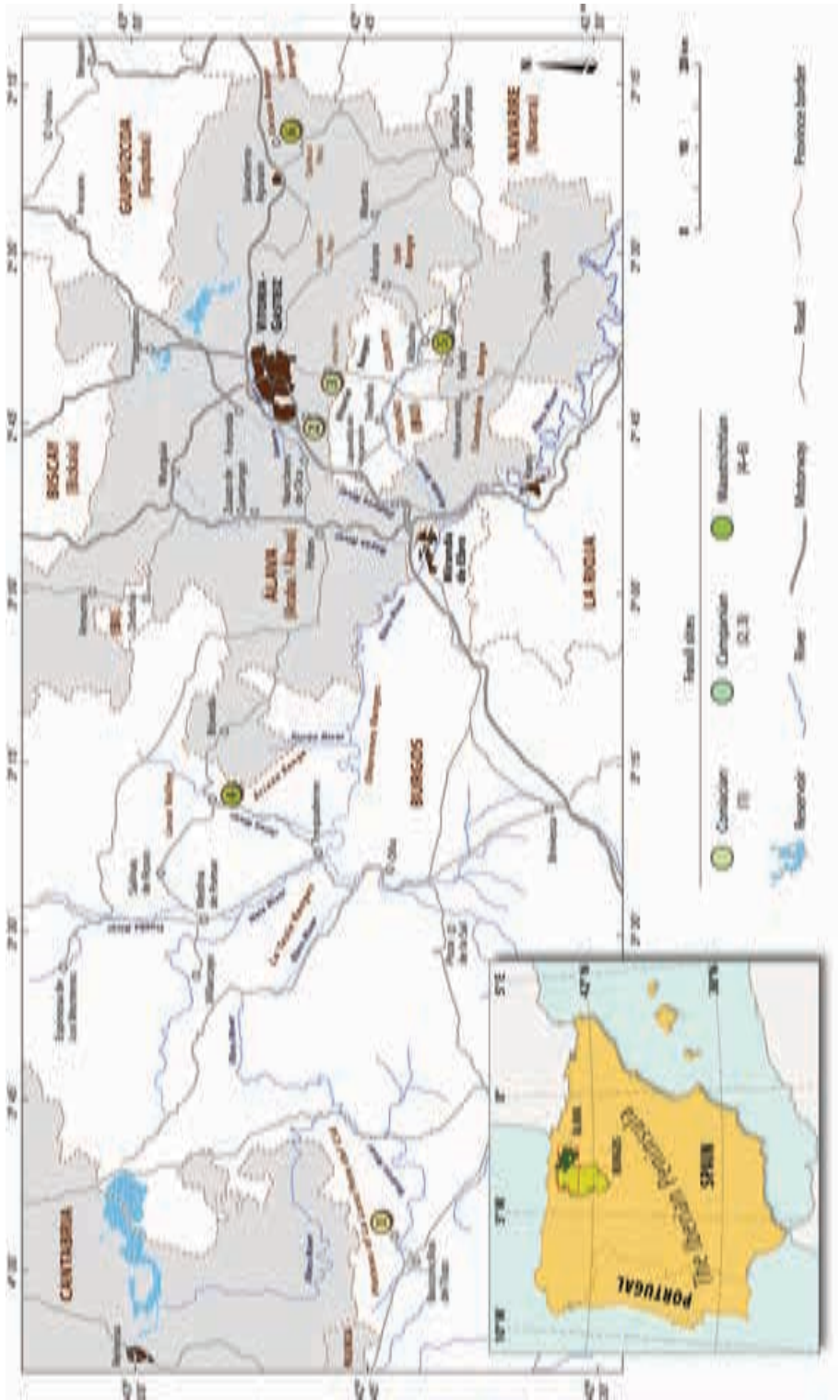




Figure 1.6 Late Cretaceous cuervas formed in the southern limb of the La Lora syncline at Basconillos del Tozo (Burgos). Lower Cretaceous ('Wealden') conglomerates and sandstones crop out in the foreground. Photograph looking northwest.

incision in a large syncline hill characterised by limbs with relatively low dips. Typical landforms include escarpments formed by outcropping beds of resistant Santonian limestones, canyons, hills, cuervas, and badlands on the soft sedimentary rocks (Fig. 1.6, and Fig. 4.3 in Chapter 4). This synclinal structure is bounded on the north by the Ebro River and by the Urbel River on the south, the latter of which runs much along the anticlinal valley of the Tozo. Eastwards, La Lora connects with a large basin formed by the Sedano Syncline.

The region is characterised by an Atlantic climate influenced by the altitude with high annual rainfall and cool and snowy winters, but summers are generally dry and warm. Further south, in the Duero Basin the climate is dryer and hotter, especially in the summer (i.e. continental Mediterranean climate). The rain water drains through permeable rocks into caves or is discharged eastwards by a dendritic drainage network of small streams and rivers on the surface. The Rudrón River (a tributary of the Ebro River) is the main river in the plateau and has significant downcutting power to create steep-walled canyons.

-
- ◀ **Figure 1.5** Map showing the main geographical features of the study area. Circled numbers indicate the studied fossil locations: 1, Barrio Panizares, Coniacian; 2, Gometxa, Campanian; 3, Vitoria Pass (Gardelegi-Castillo), Campanian; 4, Quintanilla la Ojada, Maastrichtian; 5, Albaina, Maastrichtian; and 6, Entzia, Maastrichtian. Inset: location of the study area in a general map of the Iberian Peninsula.

Central region – Quintanilla Ojada (Burgos)

The Villarcayo-Medina depression, together with the Miranda-Treviño depression (see below), represents one of the two main Neogene-aged intramontane basins, dominated by fluviolacustrine deposits formed during the Neogene orogenesis (Robles, 2014). The area, which is approximately 15 km wide and 59 km long in its present outline, is the westernmost sector of a large geological structure known as South Cantabrian Syncline (SCS)¹, trending west-east or NW–SE, across the provinces of Burgos, Álava, and Navarre. Thus, the rhombic-shaped basin of Villarcayo-Medina corresponds to a syncline striking roughly NW–SE. Its NW closure, which exhibits a topographic ridge formed on the erosion-resistant Paleogene carbonates, is marked by a shifting of the fold axis, whereas the western extremity terminates against the anticline valley of Lahoz, trending NW–SE, whose core is formed by rocks of Triassic and Jurassic age. To the NE the flank is bordered by the monoclinical series of the Losa valley, whereas its southwest subvertical strata pinch out against the anticline of La Tesla.

Two narrow bands of uppermost Cretaceous rocks are represented on each limb of the syncline. The band in the vicinity of Quintanilla la Ojada is covered with a dense forest, but outcrops are accessible on the northeastern foothills of the Vienda range (Vienda Mt., 1073 m) and the genetically-related line of escarpments that run southeast. Further to the south, in the northern limb of the anticline of La Tesla², there is also a thin band of Upper Cretaceous–Paleogene rocks, recognised on the geological cartography.

The area is crossed by several water courses, among the most important rivers are the Nela and its tributary the Trueba River, the Jerea, and the Purón, which discharge directly to the Ebro River (Fig. 1.5).

Eastern region (Álava and Treviño County in Burgos)

Broadly, the central and eastern parts of Álava and Treviño County – the latter of which is an enclave of Burgos in Álava –, correspond to the middle sector of the South Cantabrian Syncline (SCS) (Fig. 1.7). This long structure is bounded to the north by a wide valley, named the ‘Llanada Alavesa’ (Álava Plain), which has historically been a wide natural passage to connect the Duero Basin with the Pamplona Basin via the Barranca corridor, and to the south by some narrow intermontane valleys (e.g. Peñacerrada, Bernedo, Maestu, and Arana) that roughly run parallel to the Sierra Cantabria thrust belt.

The SCS is outlined on the north by the successive escarpments of three E–W trending belts, whose crests are mainly composed of Paleogene carbonate rocks. From East to West, they are the Vitoria Mountains³, the Iturrieta Mountains⁴, and the north-

¹ Pajaud and Plaziat (1972) used this name. Also termed South Pyrenean Syncline by Mangin (1958).

² The highest peaks in La Tesla Range are Peña Corva (1332 m), and Alto de Tesla (1172 m).

³ The main peaks of the range are Busto (976 m), Zaldiaran (778 m), Palogan (1029 m), and Capilduy (1176 m).

⁴ The main peaks of the range are Itxogana (1026 m), Santa Elena (1110 m), and Arrigorrista (1143 m).



Figure 1.7 An elevation model created from topographical maps showing the main mountain ranges of southern Álava and Treviño County.

ern escarpment of the Entzia Range¹. The southern flank is broadly outlined by several peaks that lie along the Baroja–Laño valley², the Izkiz Mountains³, and the southern escarpment of the Entzia Range⁴. Mangin (1958) subdivided this middle sector of the SCS into two structural units on the basis of geomorphological criteria, namely, the Miranda-Treviño Basin (corresponding to a wide syncline), and the Plateau of Urbasa (partim) (which corresponds to a long, narrow syncline hill).

The intersection of the higher-level Urbasa Plateau with the lower-level Miranda-Treviño Basin could be established in a transition zone west of the Maestu diapir valley, which is part of a geological boundary within a regional system of tectonic faults (cf. Wiedmann et al., 1983). The Miranda-Treviño depression widens rapidly from there toward the west, due to plunging of the synclinal axis. This has allowed the preservation of a much thicker sedimentary sequence in the Miranda-Treviño Basin.

¹ The main peaks are Baio (1197 m), and Mirutegi (1167 m).

² The main peaks are Txulato (946 m), Moraza (1054 m), and the summits of mounts Peñas de Uriacha (834 m), Goba (773 m), and Krutzia (787 m).

³ The main peaks of the range are Belabia (971 m), San Justi (1024 m), San Cristobal (1057 m).

⁴ The main peaks are Bitigarra (1169 m), San Cristóbal (1145 m), and Marube (1135 m).



Figure 1.8 The Basin of Miranda-Treviño is characterised by a distinctive concave shape. It is apparent the synclinal nature of the basin between the southern slopes of the Vitoria Mountains in the background, on the right, and the gentle slopes of the hills on the left. Photograph taken near Albaina (Treviño County, Burgos) looking west.

The syncline of Miranda-Treviño. Also called the Miranda-Treviño Depression (Riba, 1956; Ramírez del Pozo, 1973; Martín Alafont et al., 1978). This natural drainage area south of the city of Vitoria-Gasteiz is about 45 km long and 20 km wide, having an average elevation of about 800 m above sea level, although it decreases until 500 m in some river beds (Fig. 1.7). This structural depression is connected with the Llanada Alavesa valley by several mountain pass roads through the already mentioned Vitoria Mountains that form the outer north perimeter (e.g. the mountain passes of Zaldiaran, Vitoria, Azáceta, and Opakua). The basin is folded into a syncline with the axis trending in an average WNW–ESE direction (Fig. 1.8). Both flanks are perfectly outlined by limestone and sandstone rocks, which form the mountain crests, although elevations are higher in the northern limb. Gentle slopes dip toward the centre of the basin in both limbs.

The southern flank is broadly outlined by the Izki Mountains and a line of summits formed by the mounts Peñas de Uriacha, at one end, and Krutzia at the other. It is worth noting in the latter the presence of a complex of man-made caves carved in the Early Medieval Period, between the villages of Markinez and Laño, exploiting a Danian soft dolomitic formation (Azkarate, 1988). Among these caves are *Las Gobas*¹, nearby the village of Laño. The dwellings were first occupied in the seventh century AD and used both for living and worship, but at some time in the ninth century AD the caves were used as cem-

¹ *Las Gobas* stands for The Caves in Basque language.



Figure 1.9 *Las Gobas* 4–6 (Laño, Treviño County, Burgos), a complex of caves carved in a Danian-aged dolostone unit, circa VII century (above); ruins of a worship cave (left). Photographs looking north.

etry and finally became abandoned in the eleventh century AD (Azkarate and Solaun, 2008) (Fig. 1.9). The interior of the region is dominated by rocky hills and ridges, following the main axis of the syncline fold. The basin is crossed by the Ebro River and its two main tributaries, namely the Bayas and Zadorra rivers, the latter being fed in its final part by the Ayuda River¹, whose river's source is in the southern slopes of the Vitoria Mountains (eastern part of the basin). At about 40 kilometres in length, the river itself passes through the basin with a typical dendritic drainage pattern. Generally, the Neogene fill of the basin erodes easily, having formed valleys, cuervas, terraces, and badlands. *The Plateau of Urbasa* (partim). Geographically, this sector of the SCS is a plateau with medium altitudes of 1000 metres, being located in the easternmost part of Álava, where

¹ Uda River in Basque language.

is often termed Entzia Plateau. It forms a narrow symmetric syncline (about 18 km long and 5 km wide) with flanks gently inclined (dips about 15–20°). Westwards, the syncline broadens to become the Miranda-Treviño depression. The plateau is clearly outlined on both north and south edges by ridge crests formed by erosion-resistant Paleogene (Lutetian) carbonates. However, these crests have been cut by tranverse streams (i.e. Sabando and Larrondo streams among others) at some particular places. A moist, temperate climate affects the region. Rainwater is drained to the flowing westward Igo-roin stream, or it can contribute to the recharge of aquifers (Fig. 1.7). Karst landforms such as karst valleys, small dolines, and limestone pavements developed occasionally on the plateau. Along the axis of the synclinal, two small patches of Miocene lacustrine and fluvial deposits (formed by lutites and carbonate conglomerates) are present northeast of the Maestu diapir, near the villages of Laminoria and Iturrieta (Carreras Suárez and Ramírez del Pozo, 1978). These low-thickness deposits may be relicts of the Miranda-Treviño intramontane basin (see below).

1.3 A brief geological overview of the Basque-Cantabrian Basin

Boundaries and structural organization

Geologists consider the Basque-Cantabrian Basin (hereafter B-CB) a large geological structure located between the northern continental margin of the Iberian plate (southern Biscay Bay) and the southwest French margin (the Landes Plateau). Strictly speaking, the B-CB occupies the western segment of the Pyrenean System (eastern Cantabrian Mountains), and is bounded to the east by the NE–SW-trending Pamplona Fault and by the central Cantabrian Mountains to the west (Barnolas and Pujalte, 2004). The northernmost area of the basin is delimited by the North Pyrenean Thrust (NPT) in Aquitaine (France) and its offshore continuation on the continental shelf and slope of Capbreton Canyon (Rat, 1988). To the south, the boundary is marked by the line of ranges Sierra Cantabria–Obarenes, regarded as the western exposition of the South Pyrenean Thrust (SPT) (Rat, 1988; Robles, 2014; Robles et al., 2014) (Fig. 1.10).

The geological evolution of the B-CB, recently summarised by Robles (2014), comprises: a) a rift phase associated with the thinning of the continental lithosphere in the Lower–Middle Triassic; b) an inter-rift phase during the Jurassic; c) a rift phase in the uppermost Jurassic–lower Cretaceous, which resulted in the opening of the Bay of Biscay (in the middle Aptian–lower Albian according to Uchupi, 1988); d) a passive-margin phase composed of a variety of transgressive marine carbonate sediments (Cenomanian to upper Santonian); e) an active-margin phase (Campanian to Eocene) that resulted in several transgressive-regressive cycles, including non-marine sedimentation in the southern part of the basin during some intervals; and finally f) a compressive phase that marked the onset of the Pyrenean deformation with development of foreland and intramontane basins.

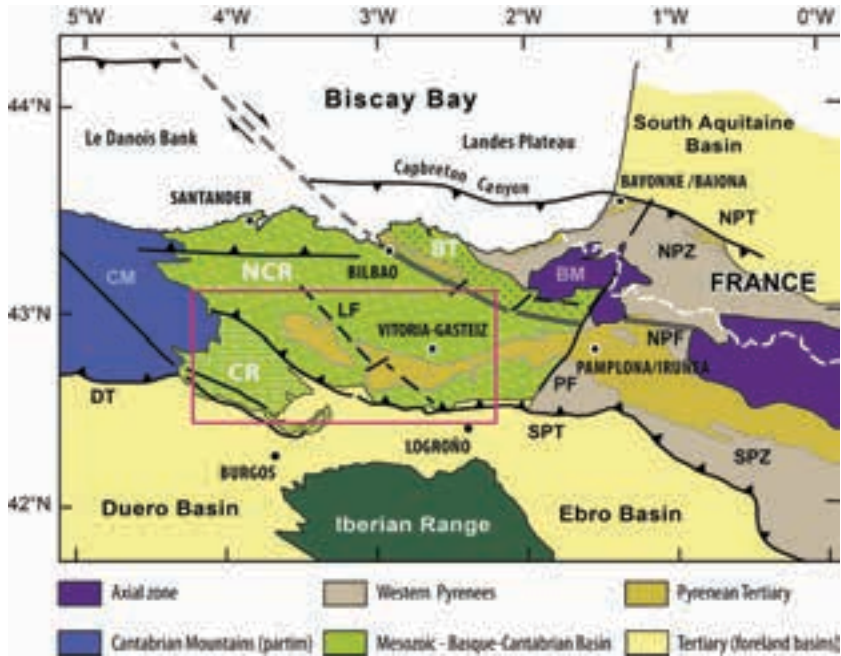


Figure 1.10 Tectono-stratigraphical domains in the Basque-Cantabrian Basin (modified from Barnolas and Pujalte, 2004): Basque Trough (BT); Navarre-Cantabrian Ramp (NCR); and Castilian Ramp (CR). BM, Basque Massif; CM, Cantabrian Mountains (partim); DT, Duero Thrust; LF, Losas Fault; NPF, North Pyrenean Fault; NPT, North Pyrenean Thrust; NPZ, North Pyrenean Zone; PF, Pamplona fault; SPT, South Pyrenean Thrust; and SPZ, South Pyrenean Zone. The red box indicates the study area.

In general terms, the B-CB is divided during the Upper Cretaceous into three tectono-stratigraphical domains¹ with a strong northeastward bathymetric gradient. They are termed: 1) Basque Trough (BT) – the deepest pelagic region –; 2) Navarre-Cantabrian Ramp (NCR)² – an outer carbonate ramp-type shelf, generally with a high subsidence rate in relation to sediment supply (Amiot et al., 1983) –; and 3) Castilian Ramp (CR) – the shallow inner part of a carbonate ramp with a low subsidence rate that failed to keep pace with the sediment input in many moments of its sedimentary history (Amiot et al., 1983; Barnolas and Pujalte, 2004). The boundary between the

¹ Several areas with similar tectonic and depositional histories were first established by Feuillée and Rat (1971), who included the Basque Trough, Periasturian Domain, Ebro-Navarre Block and Navarre-Cantabrian Domain (also called ‘Álava Block’). Later, French geologists (Institut des Sciences de la Terre, 1983) added the Northcastilian Platform (i.e. the CR) to the detriment of the Navarre-Cantabrian Domain. See also Floquet (2004).

² The NCR Domain is also termed Navarre-Cantabrian Domain (Feuillée and Rat, 1971) or ‘Álava Trough’ (Ramírez del Pozo, 1973), although the latter is of smaller extension, and divided into the Vitoria Sub-basin, to the west (Amiot, 1983a), and the Estella Sub-basin, to the east (Wiedmann, et al., 1983).

two ramp-type domains in the basin is attributed to the Losas Fault (LF)¹, which is an inferred NW–SE trending fault that coincides with the alignment of the Villasana de Mena, Salinas de Añana, and Peñacerrada diapirs (Fig. 1.10).

Sedimentary basin fill with particular attention to the study area

The geology of the B-CB is characterised, in great part, by widespread exposures of Upper Cretaceous and Paleogene sedimentary deposits that were formed during the two different passive-and active-margin phases (Fig. 1.11). Much of these deposits are nearly entirely of marine origin, although non-marine sequences were also locally deposited (see Alonso-Zarza et al., 2002; Martin-Chivelet et al., 2002; Gräfe et al., 2002; Floquet, 2004). But returning to the origins of the basin itself, its geological history begins with a Triassic rift stage, where extensive movements caused both stretching and thinning of the continental crust with the consequent deposition of red coloured clastic sediments (Bunt facies), marine carbonates, and evaporites in an arid coastal plain or sabkha (Keuper facies) (Wiedmann et al., 1983; Uchupi, 1988; Robles, 2014; Robles et al., 2014). However, strictly speaking, the B-CB is considered a basin that typically begins with the onset of the Kimmeridgian–Barremian rifting (Rat, 1988), the consequence of which was the opening of the Bay of Biscay in the middle Aptian–lower Albian – with an anti-clockwise rotation of Iberia – and the formation of oceanic crust in its western portion (Uchupi, 1988). This extensional stage resulted in a subsiding rugged palaeo-margin of thinned continental crust with tilted blocks resting along listric faults and typical troughs and highs (Wiedmann et al., 1983), in which three main depositional complexes developed, namely, the ‘Wealden’ in the earliest Cretaceous (deposition of terrestrial clastics), and both the ‘Urgonian’ (rudist-bearing carbonate platforms) and ‘Supra-Urgonian’ (ranging from fluvial to turbidite deposition) in the Aptian–Albian interval (García-Mondéjar, 1990; Robles, 2014; Robles et al., 2014).

The regional distribution of the Upper Cretaceous stratigraphical units shows an almost uninterrupted post-rift marine sedimentation, dominated by fine-grained clastic and carbonate facies, which ended when a thick sequence of synorogenic and postorogenic sedimentary deposits (Oligocene–Neogene) accumulated above it.

A new major depositional episode in the BC basin is associated with the onset of the first large transgressive-regressive (T–R) cycle, which allowed deposition of deep marine successions in some parts of the BC basin, related to the thermal subsidence phase (Floquet, 2004; Robles, 2014; Robles et al., 2014)². The cycle C T/R 1 (uppermost Albian to middle Cenomanian) is the first of four regional T–R cycles recognised by Floquet (2004) in the Upper Cretaceous successions. During the lowermost part of the cycle

¹ This major regional structure was termed “Losas deep fault” by Amiot in Amiot et al. (1983).

² ‘Transgressive sequence’ in Amiot et al. (1983); ‘Megasequence 2 – Maximum transgression’ in Wiedmann et al. (1983).

C T/R 1, a vast transgression occurred over a low-angle ramp margin, and led to the deposition of several sandstone-dominated formations. Coastline moved southward and tidal-flat environments with ostreids – referred by Floquet (1983) as ‘oyster facies’ – developed during middle Cenomanian in vast areas of the Castilian Ramp domain.

The cycle C T/R 2 (upper Cenomanian to lowermost Coniacian) is associated with the onset of a major transgression that was more evident in both CR and NCR domains. A shallow carbonate ramp extended to southernmost areas of the CR domain, producing rock units commonly of a few metres thick. In contrast, submareal conditions in the NCR (including the Vitoria Sub-basin) allowed the deposition of thick series of carbonates (limestones with grainstone/rudstone textures), corresponding to the inner and middle shelf (shallow to mid neritic environments), and sequences of limestone (textures packstone/wackestone: ‘Garate Limestones’) and interbedded marls with ammonites corresponding to outer self, deep neritic environments (Ramírez del Pozo and del Olmo Zamora, 1978; Wiedmann and Kauffman, 1978). The peak of the Turonian transgression is indicated in the CR and NCR regions by ammonite-rich marl and limestone sequences that allow both a regional biozonation to be made and a correlation between the North Temperate and Tethyan Realms (Wiedmann, 1964, 1979; Wiedmann and Kauffman, 1978; Barroso Barcenilla, 2004; Barroso-Barcenilla and Goy, 2007).

The transgressive phase of the cycle C T/R 2 was less evident in the Basque Trough (BT), where sedimentation continued as in the previous cycle (Floquet, 2004). In deeper areas of the continental slope, calcareous turbidites developed (Robles, 2014; Robles et al., 2014). The occurrence of pelagic sedimentation (i.e. siliciclastic flysch or ‘Black Flysch’) during the Cenomanian was limited to two troughs between the North Iberian continental margin and the Landes plateau to the north, namely the St-Jean-de-Luz, and Plentzia troughs to the south (Rat, 1988). Later during the Turonian, the sedimentation was differentiated into two main flysch deposits, a ‘calcareous flysch’ with pelagic fauna in the central part of the basin (Basque Trough or ‘Surco del Flysch’), which also underwent an important underwater volcanic activity, and the ‘silex flysch’ in the North Pyrenean zone (Robles, 2014; Robles et al., 2014). The Upper Cretaceous calcareous flysch is well developed until the Campanian, when is replaced by siliciclastic flysch – now deposited in the Orio trough – covering the sea floor between the Aquitaine platform and the North Iberian margin (see Mathey, 1986).

The post-Turonian gradual filling of the B-CB is arranged into two major depositional cycles (i.e. C T/R 3 and C T/R 4), according to Floquet (2004). A transgression at the base of the Coniacian marks the boundary of the major transgressive–regressive cycle C T/R 3 in the study area¹ (Feuillée and Rat, 1971; Ramírez del Pozo, 1973; Amiot, 1983b; Floquet, 1991, 2004). Thus, the previous sedimentary units were overlain by a thick succession of hemipelagic limestones (wackestone texture) and marls with

¹ ‘Losa Megasequence’ sensu Gräfe (1994), Gräfe et al. (2002); ‘Megasequence 3: 2. Regression and compression phase’ sensu Wiedmann et al. (1983).

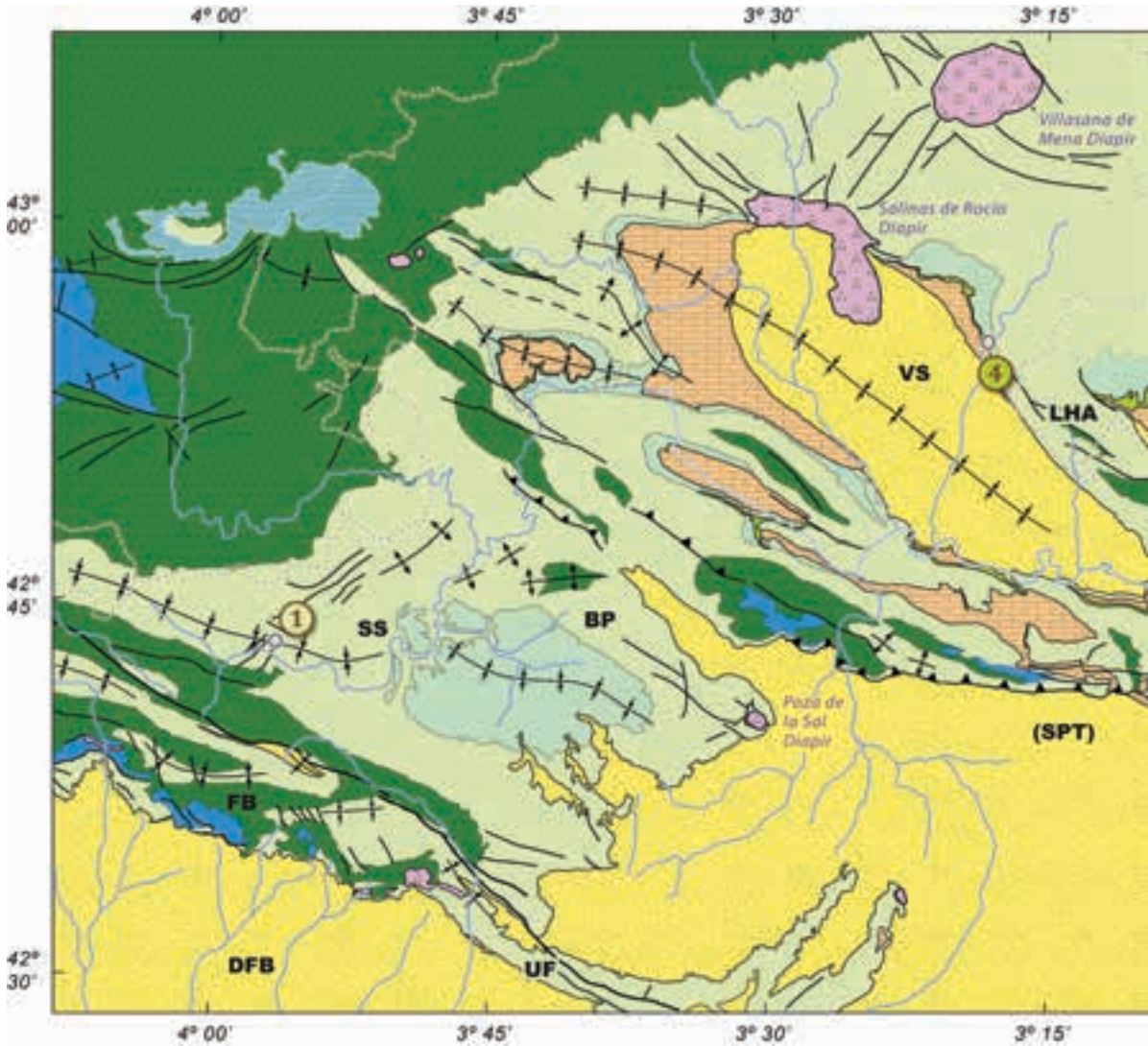
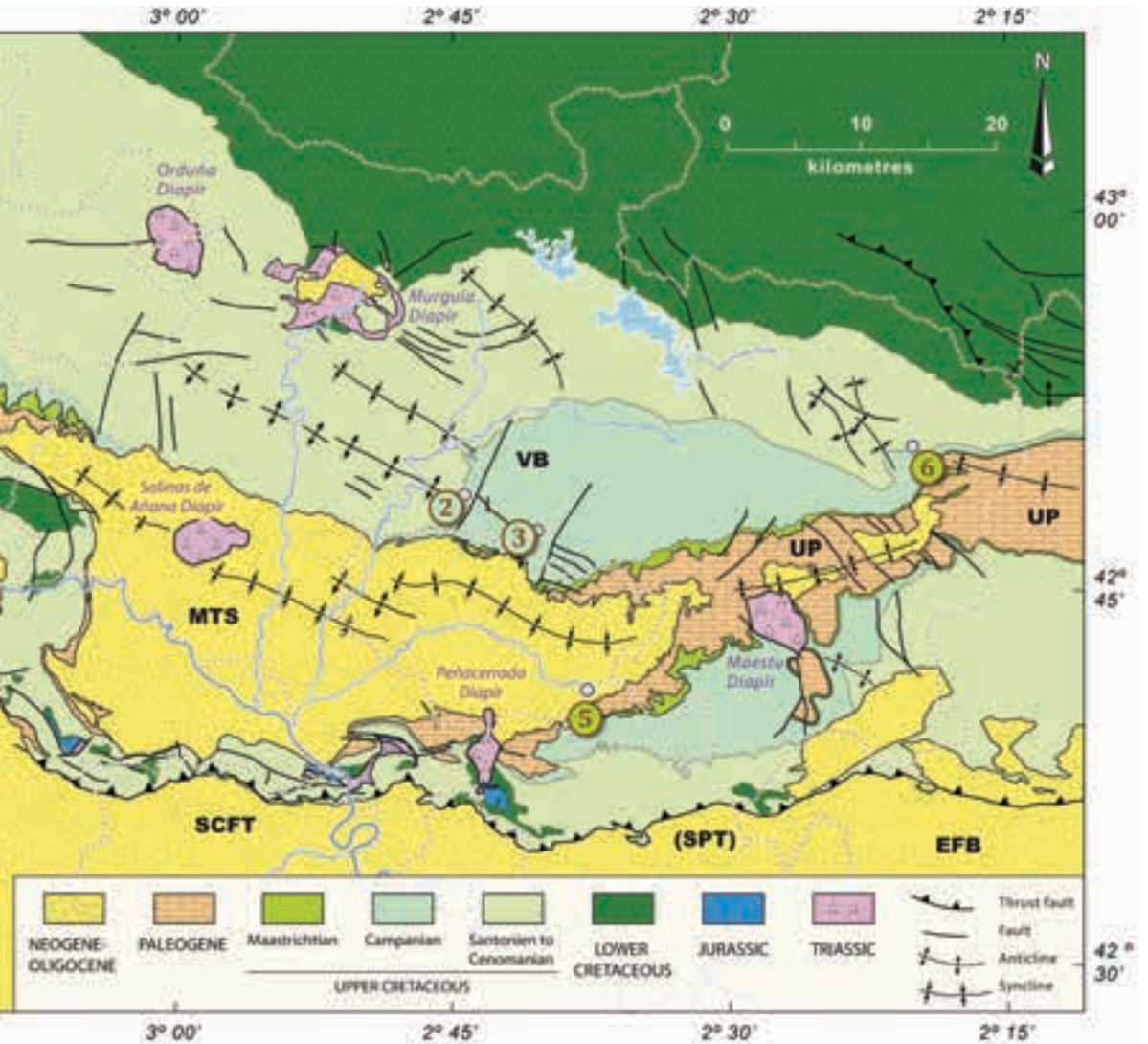


Figure 1.11 Generalised geological map of the study area compiled from several map sheets (scale 1:50.000) of the Spanish National Geological Map (MAGNA, 2nd series) published by the IGME. Circled numbers indicate the studied fossil sites: 1, Barrio Panizares, Coniacian; 2, Gometxa, Campanian; 3, Vitoria Pass (Gardelegi-Castillo), Campanian; 4, Quintanilla la Ojada, Maastrichtian; 5, Albaina, Maastrichtian; and 6, Entzia, Maastrichtian. BP, Burgos Platform; DFB, Duero Foreland Basin; EFB, Ebro Foreland Basin; FB, Folded Band; LHA, La Hoz Anticline; MTS, Miranda-Treño Syncline; SCFT, Sierra Cantabria Frontal Thrust; SPT, South Pyrenean Thrust; SS, Sedano Syncline; UF, Ubierna Fault; UP, Urbasa Plateau; VB, Vitoria Sub-basin; VS, Villarcayo Syncline.



planktonic foraminifera, inoceramids, and ammonites deposited from the middle Coniacian to lower Campanian in vast open-marine shelfal areas (Wiedmann et al., 1983; Gräfe, 1994)¹. The cycle C T/R 3 is also signified by the basinward development of thick successions of echinoid-bearing, hemipelagic marl-limestone alternations (Olazagutía Fm) (Fig. 1.12). Palaeontological and stratigraphical data indicate that such deposits were generated in areas below the wave base, whose depth has been estimated to be 500–1000 m, according to their foraminiferal content (Gräfe, 1994).

¹ See Chapter 4 for an expanded section on this.

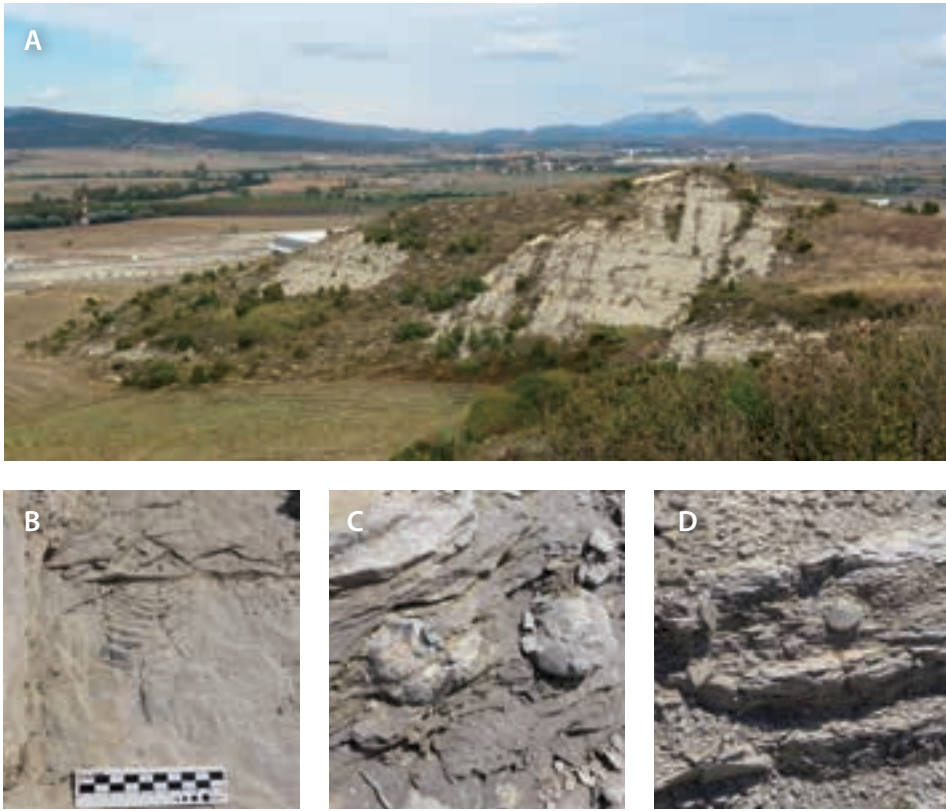


Figure 1.12 Outcrops and invertebrate fossils of the Olazagutía Formation (Santonian) at Ariñez (Álava), west of Vitoria-Gasteiz. A, well-bedded hemipelagic marls in the foreground, photograph looking north; B, Undetermined inoceramid; C, *Micraster* sp., in situ echinoids; D, the bivalve *Spondylus spinosus* (Sowerby, 1814). Fossils in photos C and D are about 5 cm in width.

After a passive-margin period during the first part of the Upper Cretaceous, the North Iberian margin experienced a different tectonic evolution at the Santonian–Campanian boundary, when conditions changed to become an active-margin setting at the onset of convergence between the European and Iberian plates, finally resulting in tectonic inversion and the record of the first compressive stages in the basin (Gischler et al., 1994; Robles, 2014). This tectonic condition significantly affected both the CR and NCR domains of the B-CB, but especially the latter where two separate sub-basins with different evolution have been identified on the basis of rock and facies differences: 1) the Vitoria Sub-basin to the northwest, and 2) the Estella Sub-basin to the southeast (Amiot, 1983a; Wiedmann, 1979). The origin of such stratigraphical differences (e.g. exposures with shallower sedimentation and thinned series adjacent to others in which subsidence allowed a thicker pile of sediments to accumulate) has been often attributed

to the presence of diapirs that controlled the sedimentation across the domain¹ (Wiedmann et al., 1983) (Fig. 1.13). Kind (1967) considered that the effects of salt migration and emergence at the sea floor of some of these diapirs were most evident during the Upper Cretaceous, forming bathymetric highs and lows.

A time of overall regression, with minor fluctuations, is reported from the uppermost Santonian onwards, with calcarenite and terrigenous clastic deposits (Amiot, 1983b; Wiedmann et al., 1983; Floquet, 1991; Gräfe et al., 2002). The rock succession corresponds to the cycle C T/R 4 (in Floquet, 2004), which is subdivided into four minor subcycles, namely C T/R 4.1 to C T/R 4.4. Other authors consider different classifications, using for this the lithological interval ‘Megasequences 3 and 4 [pro-parte]’ (Wiedmann et al., 1983) or the ‘Sedano’ and ‘Urbasa’ megasequences (Gräfe et al., 2002). Besides such discrepancies, the uppermost Cretaceous shallow marine deposits are further subdivided into three short term transgressive-regressive depositional cycles – DC–11 to DC–13 – which were defined by Floquet (1991, 1998) in the Castilian Ramp and extended to southern Álava by Corral et al. (2015a). The subcycle C T/R 4.1 (mostly upper Santonian) is signified by a new marine transgression across much of southern and southwestern parts of the basin, and by the deposition of thick bioclastic limestones, exhibiting grain-supported textures (packstone and grainstone), and interbedded marls. These shallow marine rock sequences of the Tubilla del Agua Formation (Floquet et al., 1982), also termed ‘*Lacazina* limestone’ by Gischler et al. (1994), and the lower part of the Vitoria Formation straddle the Santonian–Campanian boundary.

The lower Campanian minor transgression of subcycle C T/R 4.2 initiated the deposition of the Quintanaloma Formation and the upper part of the Tubilla del Agua Formation in the CR and NCR domains, respectively. Moreover, the NCR reflects a different basin-fill history from north to south during the lower Campanian (basal part of C T/R 4.2)². A general shallowing across the Vitoria Sub-basin is evidenced by the grey marl deposits with varying sand and mica flakes content. The basal part of the upper Campanian, outcropping in the northern flank of the Miranda-Treviño Syncline, was deposited in an external platform environment, and although it shows a progressive enrichment in fine-grained clastics, conditions were still favourable for the presence of macro- and microfossils (Wiedmann et al., 1983; San Martín, 1986; Santamaría Zabala, 1996)³. In addition, several isolated exposures of allochthonous limestones (calcirudites and calcarenites), which are interspersed among the thick succession of hemipelagic marls of the Vitoria Formation, are present in the southern part of the Vitoria Sub-basin. Such outcrops of relatively brief geological duration and

¹ The halokinesis activity in the area, and its influence on stratigraphy, has been recognised since the Albian times (Ramírez del Pozo, 1973).

² See Chapters 5 and 6 for an expanded section on this.

³ See Chapters 5 and 6 for an expanded section on this.

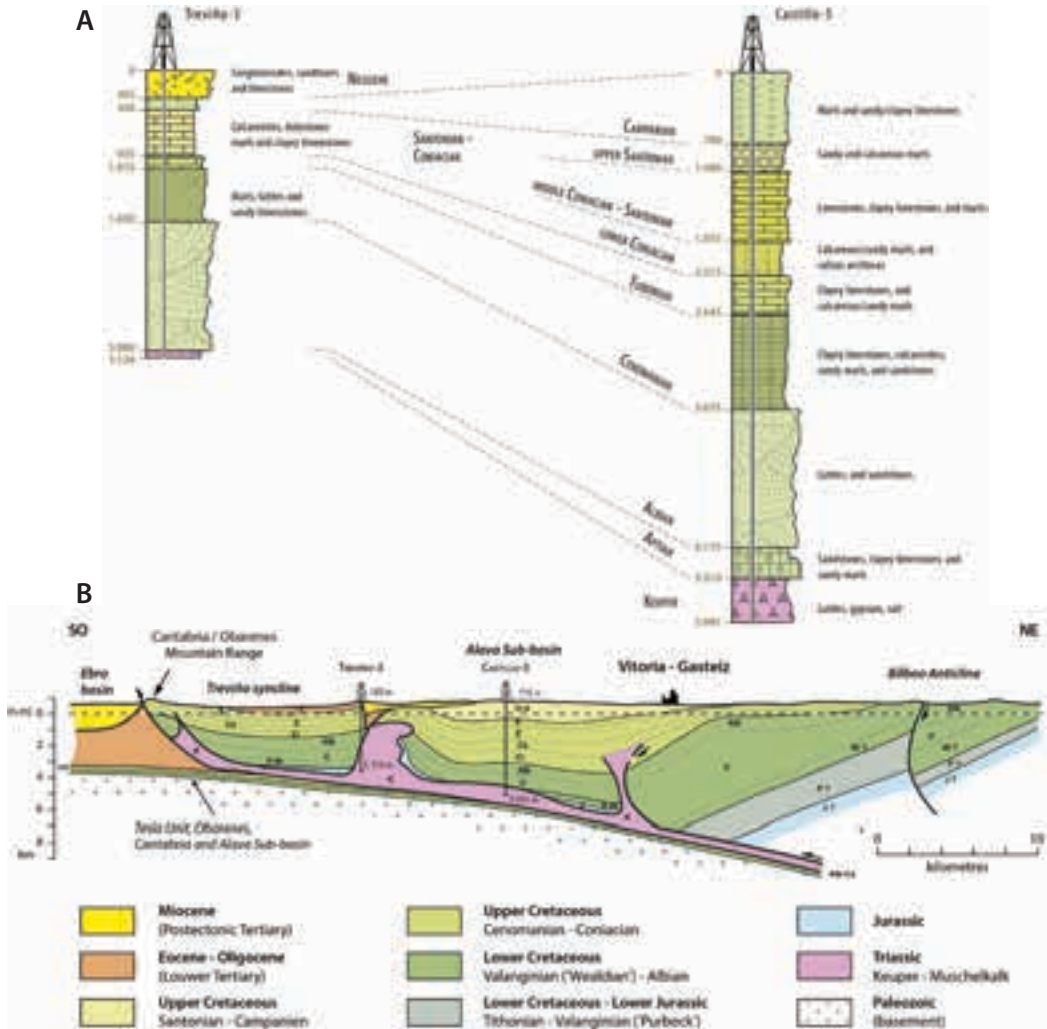


Figure 1.13 A, lithologies and ages from nearby wells (drawn from the data of Martín Alafont et al., 1978); B, schematic cross-section illustrating the generalised structure of the Miranda-Treviño Syncline (adapted from GESSAL, 1990).

of regional extent (essentially restricted to Gomecha¹, Olárizu, Alegría, and Alaiza-Gereñu localities in Álava province) are assigned to different members of the Vitoria Formation and thought to be derived from southwestern carbonate ramps favoured by halokinetic movements (Engeser, 1985; Gräfe, 1994)².

¹ Nowadays, the official name is Gometxa but the former name, Gomecha, is extensively found in the geological literature.

² See Chapter 5 for an expanded section on this.

In contrast to about 1300 m of offshore limestone and marlstone rocks of the Vitoria Formation recorded on northern areas of the NCR domain (Martín Alafont et al., 1978), the sediment-starved easternmost part of the Castilian Ramp (south of Vitoria-Gasteiz) is initially dominated by marlstone and sandy limestone (Tubilla del Agua Fm or ‘Lacazina limestone’), although sedimentation later changed to shallower marine deposits (Moradillo de Sedano and Sedano formations) (see Fig. 7.7 in Chapter 7).

Typical processes of silicification, studied by Gómez-Alday et al. (1994, 2002) and Elorza and Orue-Etxebarria (1985), occur in rocks of the Tubilla del Agua Fm, nearby Laño (south of Vitoria-Gasteiz). These Laño quartz geodes are located in a lithified bioclastic calcarenite (grainstone to packstone textures) with macrofossils, generally echinoderm skeletal parts, sponges, gastropods, brachiopods, bivalves, and bryozoans, which was deposited in a shallow ramp setting (Fig. 1.14). The silicification processes of the geodes (originated from previous anhydrite nodules, according to the authors) and the partial replacement in bivalve shells by silica (particularly shells of the genus *Pycnodonte*) are associated with the percolation of marine brines originated in very shallow facies (from tidal-flat to sabkha) that installed in the region thereafter. According to Gómez-Alday et al. (1994, 2002), the local shallowing of the Laño area was influenced by the nearby diapir of Peñacerrada, which was active during the Campanian, favouring depositional settings suitable for the development of anhydrite nodules. The large accumulation of *Pycnodonte* oysters, preserved in the form of a coquina bed (Fig. 1.15A), is easily identified in the Laño area, and may be considered to represent an event horizon indicative of environmental stress, likely related to an increased terrigenous influx. Another *Pycnodonte* event has been reported in northern Germany by Wilmsen and Voigt (2006). Not far from Laño locality, nearby Loza hamlet, outcrops of Campanian age consist of sandy marlstone and calcarenite with asphalt impregnations (Portero and Ramírez del Pozo, 1979; Marín et al., 2014).

The uppermost Campanian is represented in the Vitoria Sub-basin (within the NCR) by a 420–520 m thick series of deltaic sandstone and sandy siltstone, belonging to the Montes de Vitoria Formation (Engeser, 1985), which is interpreted as lowstand systems tract (LST) deposits, including prodelta, subtidal to intertidal delta-front, and fluvial dominated facies (Gräfe, 1994). This change in sedimentation from the underlying marly Vitoria Formation occurred in response to a regional tectonic uplift event (compressive phase), which is also marked by an unconformity between the Montes de Vitoria and the open-marine Puerto de Olazagutía formations (Portero García et al., 1978; Carreras Suárez and Ramírez del Pozo, 1978; Alonso, 1986; San Martín, 1986).

The above mentioned compressive phase resulted in the uplift of shallower areas of the CR domain in the uppermost Campanian (see Corral et al., 2015a), which is recognised in the upper regressive interval of the subcycle C T/R 4.2 (T–R DC–11 of Floquet, 1998). On the basis of lithological and palaeontological characteristics, fluvial and lacustrine environments (‘Rognacian facies’) are inferred, which appeared to be similar to those in other regions of Europe (see Plaziat, 1970a, 1970b). The stratigraphy of this

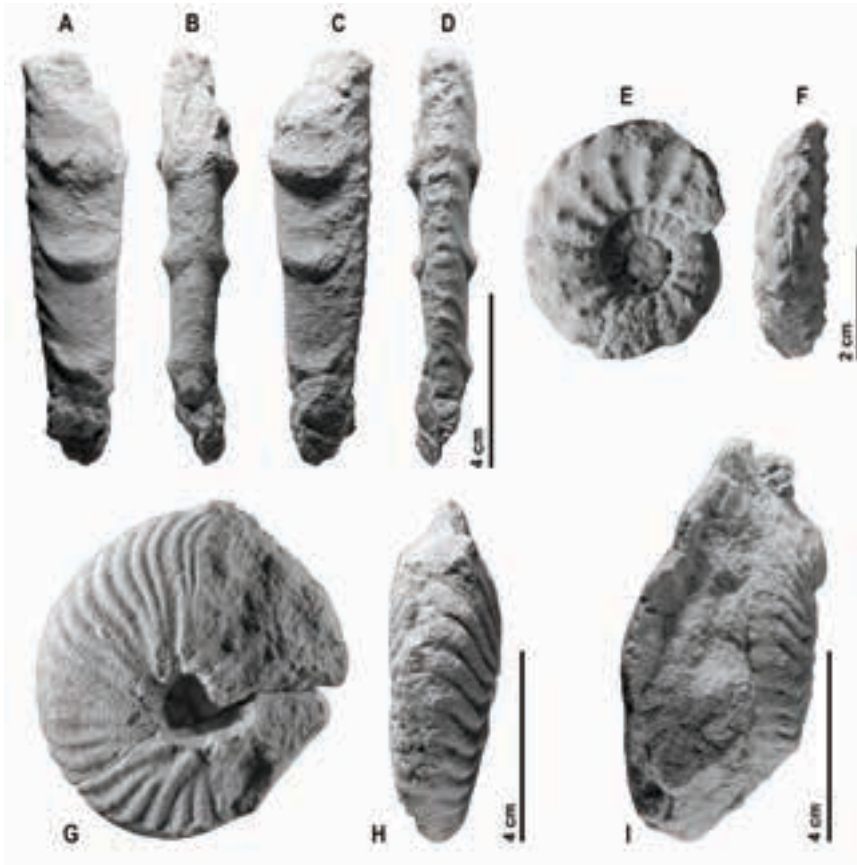


Figure 1.14 Ammonites from the Campanian Tubilla del Agua Formation in Laño (Treviño County) from Corral et al. (2015a). A–D, MCNA 14984 *Baculites vaalsensis* Kennedy and Jagt, 1995, lower Campanian, (A, C) lateral view, (B) dorsal view, (D) ventral view. E–F, MCNA 1835 *Menabites (Bererella)* sp., upper Campanian, (E) lateral view, (F) dorsal view. G–I, *Hoplitoplacenticeras marroti* (Coquand, 1859), upper Campanian: G–H, MCNA 1960, (G) lateral view, (H) posterior view; I, MCNA 1959, posterior view.

period of time is exceptionally well exposed at Laño quarry (see Astibia et al., 1987, 1999a; Pereda-Suberbiola et al., 2015a)¹, where two successive beds of ferruginous sand and silt (L1A and L1B) with continental fossil vertebrates were discovered. Another silt-mudstone bed with fossil vertebrates crops out in the eastern end of Laño quarry (L2), the lower position of which was inferred by stratigraphical correlation. Many fossil bones in Laño are typically characterised by diagenetic alterations in the form of millimetric globular crusts (a goethite and quartz grain mixture) that were formed as a result of seasonal variations in groundwater level (Elorza et al., 1999). Based on stratigraphical correlations, these fossiliferous beds were initially regarded as late Campanian

¹ See also Chapter 8 for an expanded section on this.

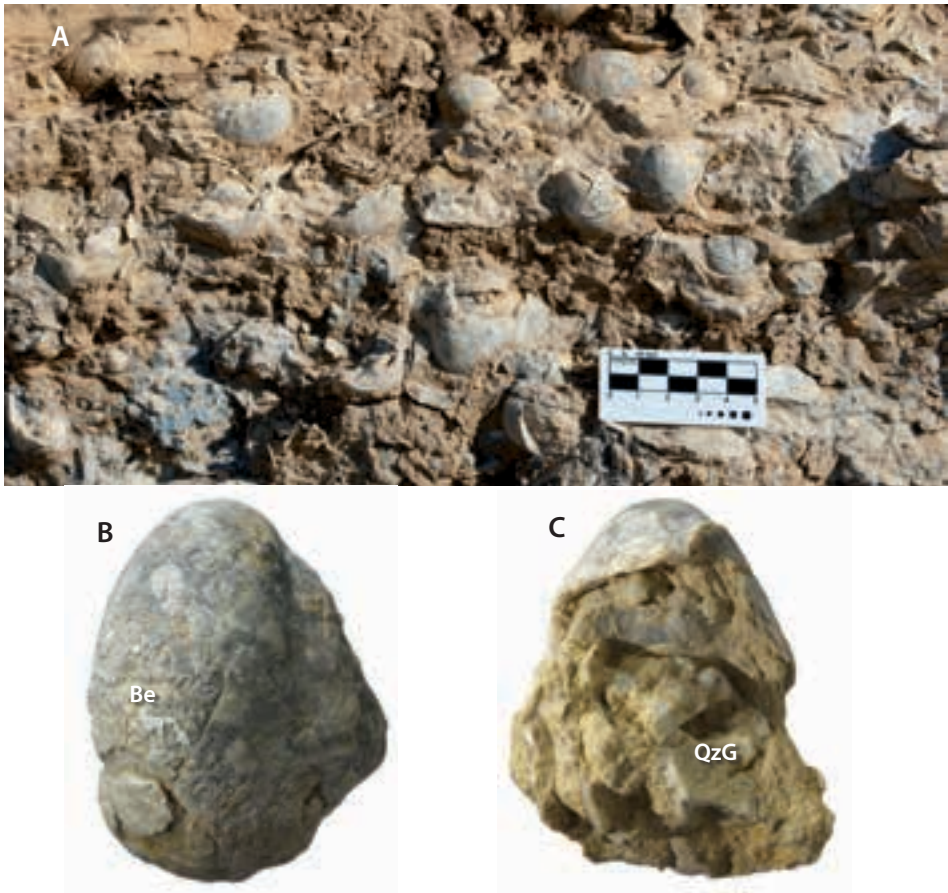


Figure 1.15 A, *Pycnodonte* event, oyster bed interstratified in sandy marlstones and limestones of the Tubilla de Agua Formation at Laño (Treviño County, Burgos); B–C, Fossil shell of *Pycnodonte (P.) vesicularis* (Lamarck, 1806) partially replaced by silica, note the formation of chalcedony on the shell surface in distinctive beekite ring outlines (B) and a quartz geode (C), length 6 cm, Be, beekite, QzG, quartz geode.

to early Maastrichtian in age (Baceta et al., 1999; lateral equivalent to the upper part of Depositional cycle DC–11 sensu Floquet, 1998; see Berreteaga, 2008). The combined lithostratigraphical and magnetostratigraphical analyses made by Corral et al. (2015a) allowed the dating of the continental vertebrate site of Laño (Treviño County, Burgos), which is now considered latest Campanian as the falls within the C32n ($\approx 72\text{--}73.5$ Ma).

An areally-limited lower Maastrichtian deepening event, associated with subcycle C T/R 4.3 (or T–R DC–12 in Floquet, 1998) in the CP domain, initiated the deposition of the Valdenoceda Formation, which is accessible in the northcentral part of the studied area. In Quintanilla la Ojada (Burgos), this formation is mainly composed of bioturbated sandy dolomitised carbonates, arranged in small, shallowing upward se-

quences. These rocks were deposited as carbonate sand and lime mud within a proximal platform (inner to mid ramp) and a nearby shelf lagoon with open circulation (Berreteaga, 2008). Marine fossil vertebrates have been found at this locality in the Valdenoceda Formation, including teeth of elasmobranchs, actinopterygians, and mosasaurians (Berreteaga, 2008; Berreteaga et al., 2011; Corral et al., 2015b)¹.

A widespread regression terminated the T–R subcycle, causing uplift on both CR and NCR domains, and the deposition of alluvial/fluvial deposits and lacustrine/palustrine carbonates of the Sobrepeña and Ircio formations, respectively (Corral et al., 2015a)². The Ircio Formation is represented in the south of Álava by continental lacustrine limestones ('Belabia limestones')³ that contain characteristic land-snail specimens (see Fig 8.12 in Chapter 8) (Mangin, 1958; Plaziat, 1970a, 1970b).

The upper Maastrichtian transgression is associated with subcycle C T/R 4.4 (or T–R DC–13 in Floquet, 1998), and records a new episode of relative sea-level rise in both CR and NCR domains. The base of the subcycle is bounded regionally by a major intra-Maastrichtian unconformity (IMU boundary: Baceta, 1996; Baceta et al., 1999) that is well shown at Laño quarry (south of Vitoria-Gasteiz). Overlying this boundary, there is a thick transgressive succession belonging to the Torme Formation, which represents the infilling of an incised valley and subsequent generalised flooding of the ramp over much of southern Álava during the upper Maastrichtian (Pujalte et al., 2000a, Berreteaga, 2008). The stratigraphy of this unit was initially described by Cappetta and Corral (1999) as a package of dominant limestone (yellowish bioclastic calcarenite) and sandstone beds situated above a lag interval. Most of this calcarenite has been diagenetically decalcified, resulting now in a friable, carbonate rock with moldic and interparticle porosity. In addition to orbitoid tests and mollusc shells that accumulated in these beds, it is remarkable the presence of skeletal remains of marine vertebrates, notably mosasaurids, elasmosaurids, selachians, and actinopterygians (Bardet et al., 1997, 1999, 2013; Cappetta and Corral, 1999; Poyato-Ariza et al., 1999). This fossil-rich succession grades upward into a siliciclastic subunit (i.e. the regressive part of the cycle which disappears basinward) where shark teeth are only occasionally found. The deepening event that marked the beginning of the C T/R 4.4 subcycle in the NCR domain is represented basinward by thicker successions of marl and limestone rocks (Puerto de Olazagutía Formation) that accumulated on a shallow-water carbonate ramp⁴.

¹ See Chapters 7 and 13 for an expanded section on this.

² 'Megasequence 4: 2. Regression and compression phase' sensu Wiedmann et al. (1983). See Chapter 8 for an expanded section on this.

³ Unit S2U1 in Astibia et al. (1987, 1990).

⁴ The Puerto de Olazagutía Formation (Amiot, 1982) in the type section consist of fossiliferous marls (with orbitoidids, macroinvertebrates and selachian remains) and interbedded silty calcarenites (biosparite and biomicrite), as described by Ruiz de Gaona (1943), Ramírez del Pozo (1971), Martín Alafont et al. (1978), Amiot (1982), and Wiedmann et al. (1983). See Chapter 9 for an expanded section on this.

An arid/semiarid period of relative tectonic quiet in the early Paleogene favoured the development of a shallow ramp in the southern part of the B-CB (see Alonso-Zarza et al., 2002; Robles, 2014). Although the correct identification of shallow marine carbonates deposited in such shallow shelfal environments at the beginning of the Paleogene (Danian to Selandian) is difficult – as are affected by dolomitisation (see Plaziat, 1986) –, they represent the onset of a new depositional T–R cycle (DC–14 sensu Floquet, 1998). In any case, the lower portion of this stratigraphical unit is considered to be a light-gray, fine grained, laminated to thick-bedded dolomite containing skeletal elements of molluscs and calcareous algae. The areal distribution of this resistant unit is easily observed either forming the crests of many ridges on the northern limb of the Miranda-Treviño Syncline, or as the ruiniform reliefs of the Fresnedo Formation in the southern limb of this syncline. Although its Danian age cannot be demonstrated with certainty by palaeontological methods, the unit can be correlated eastwards – toward Navarre – with pinkish limestones with globigerinid foraminifera, the age of which is well established (Plaziat, 1970a; Pajaud and Plaziat, 1972).

The temporal platform architecture and the correlation of the shelf strata to time-equivalent deposits on both slope and basin settings have been accomplished by Pujalte et al. (2000b). According to these authors, shallow shelfal areas in the basin were primarily filled with mixed carbonate-siliciclastic sedimentation from the Thanetian to lower Ypresian (Ilerdian). These strata are arranged into four major units with an upward increasing in carbonate content, which reflects a response to more open marine palaeoenvironmental conditions. After a short sea-level fall (marked by the presence of sandy lutites), a subsequent sea level rise occurred during the Selandian causing the deposition of marly limestone (wackestone texture) and bioturbated marlstone on a shallow carbonate ramp (lower part of the Unit A, in Pujalte et al., 2000b). The lower Thanetian shelf (upper part of the Unit A, in Pujalte et al., 2000b) is represented by neritic limestone strata (mostly biomicrite, intrabiomicrite and intrabiosparite) and marly facies with a rich fossil content, which are associated with reefal deposits. Their faunal association consists of large benthic foraminifera (*Discocyclina* and *Operculina*), bryozoans, echinoids (see Plaziat et al., 1975), small brachiopods (see Pajaud and Plaziat, 1972), cnidarians, and encrusting algae (Melobesia), which suggests either a perireef environment or a shelf environment, where corals occurred but without forming real reefal buildups (Pajaud and Plaziat, 1972; Martín Alafont et al., 1978). Southwards (in south Álava) this unit passes into dolomitised white oolitic limestones and alternating marly beds with planktonic foraminifera ('San Justi Beds' in Mangin, 1955). This unit¹ is interpreted to represent a restricted, marine lagoon deposit because of its fossil-barren regular stratification and the lack of current structures (Astibia et al., 1987).

The overlying unit (Unit B in Pujalte et al., 2000b) is a mixed carbonate-siliciclastic succession, the associated fauna of which includes large benthic foraminifera that are

¹ S2U2 Unit in Astibia et al. (1987).

indicative of persistent shallow marine conditions. Unit B grades upward into sandstone bodies of Unit C with a low carbonate content (Pujalte et al., 2000b).

The upper part of the shelf deposits, which displays a coarsening upwards regressive lithofacies, was termed Unit C by Pujalte et al. (2000b). This unit is interpreted to represent a major change in the depositional environment, namely from marine carbonates to siliciclastic-dominated facies, indicative of terrestrial depositional conditions (i.e. cross-bedded, gravelly sands that also contain intercalations of lutite lacking marine fossils). The origin of this formation is related to the hyperthermal event at the Paleocene–Eocene transition (Paleocene–Eocene thermal maximum), when areas receiving heavier rainfall amounts (but with intra-annual rainfall variability) provided an important supply of sediments to the Pyrenean Gulf in a relative sea-level fall (Pujalte et al., 2015). These formations have been regionally targeted for silica sand mining (e.g. Villalain and Laminoria quarries in the Villarcayo and Miranda-Treviño synclines, respectively). Finally, a thick succession of bioclastic limestone (grainstone texture), rich in alveolinids and ostracods (Unit D in Pujalte et al., 2000b), occurs at the uppermost part of the series, and commonly comprise the last carbonate-dominated marine facies in the southern half of the basin – aged lower Ypresian (Ilerdian) to Lutetian – (Ramírez del Pozo, 1973; Portero García et al., 1978; Carreras Suárez and Ramírez del Pozo, 1978). This unit can be correlated eastward with the transgressive *Alveolina* limestone described by Montes Santiago et al. (1989) in the Villarcayo Syncline.

To the north in deeper marine basinal areas, the Paleocene–lower Eocene succession was dominated by toe-of-slope megabreccia deposits and carbonate turbidites eroded from the carbonate shelf-margin (Ermua section), which pinch out basinward into pelagic/hemipelagic limestones and marls (Zumaia section)¹.

Finally, the lower Eocene sedimentation was conditioned by a new pulse of deformation corresponding to a significant compressive phase of the Pyrenean contraction² that caused folding and uplift of internal areas of the B-CB (Pujalte et al., 2000a; 2000b). As a result, continental sedimentation with palustrine carbonates occurred in the southernmost part of the basin (Riba, 1976). However, marine sedimentation continued through the upper Lutetian, and probably younger times in deeper areas of the basin (i.e. the Biscay Synclinorium), but the lack of outcrops precludes the identification, according to Rat (1988). In contrast, the Eocene is represented in the southern part of the B-CB (between Portilla and Peñacerrada, south of Vitoria-Gasteiz) by lacustrine limestone and marl strata that have freshwater molluscs, algal structures, and chert nodules (Portero and Ramírez del Pozo, 1979). In the upper Eocene (Priabonian), a second and more important tectonic phase³ firstly affected the eastern part of the

¹ The reader is referred to Robles (2014) for a summarised view on this.

² ‘Pre-Pyrenean phase’ in the Ypresian (Plaziat, 1986).

³ ‘Pyrenean orogenic phase’ in the Priabonian (Plaziat, 1986); south-vergent compressive phase (Martínez-Torres and Eguiluz, 2014).

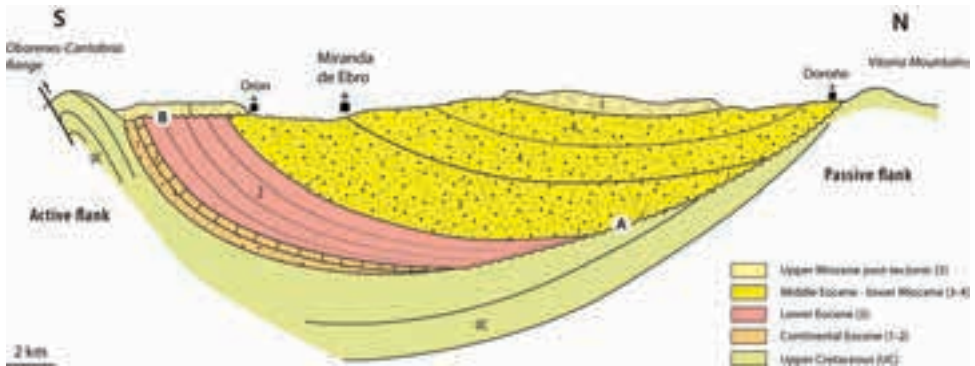


Figure 1.16 Cross section of the asymmetric Miranda-Treviño Basin. A, syntectonic unconformity in the active flank; B, post-tectonic unconformity in the passive flank. Redrawn from Riba (1976) with modifications. Vertical scale is exaggerated.

Basque-Cantabrian Region, but progressively propagated westward¹. Such collisional period produced major folding of the sedimentary fill, salt tectonics, and thrust faulting (such as the South Pyrenean Thrust or SPT), in addition to the uplift and formation of the present-day basin architecture (Riba, 1976; Plaziat, 1986; Megías, 1988; Rat, 1988; Robles, 2014; Robles et al., 2014).

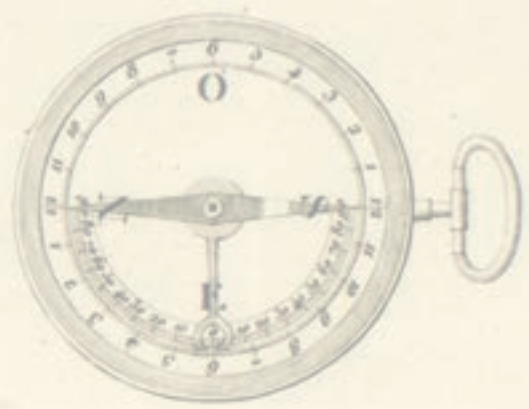
A reactivation pulse in the Miocene, whose consequence was the formation of the intramontane basins of Villarcayo (to the west) and Miranda-Treviño (to the east), represents the last stage in the evolution of the B-CB. The structural evolution of both intramontane basins is similar, according to Robles (2014), being filled during the Miocene times (and probably earlier during the late Oligocene), initially with Paleogene rocks and subsequently with Cretaceous source deposits. Three following main continental groups of facies, which clearly rest unconformably on previous sedimentary complexes, have been recognised by Robles (2014): (1) palustrine carbonates; (2) sandy and clayey facies (distal fan deposits); and finally, (3) conglomerates arranged in coarsening-upward sequences (channel-fill deposits). A particular characteristic observed in the Miranda-Treviño Basin is the northward migration of the folding axis and depocentre (passive flank) during the sedimentation, which was accompanied by a syntectonic unconformity in the passive flank (Riba, 1976) (Fig. 1.16). In sum, this sedimentary basin was deformed during the Neogene orogenic uplift of the region, but diapir tectonics also influenced its sedimentary fill, at least locally (Ramírez del Pozo, 1973) (see Fig. 1.13).

¹ Deep marine facies are preserved until the Oligocene in San Vicente de la Barquera-Cabo de Oyambre (Cantabria, northwestern part of the B-CB), according to Rat (1988) and Robles et al. (2014).

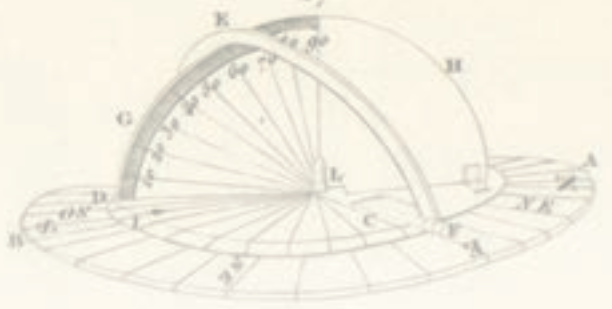
15



14



17



“Tratando de ocuparnos de lo relativo á las expediciones, tócanos fijar sobre todo nuestra atención en lo que respecta á instrumentos del viaje científico á que nos referimos, los cuales deben no ser muy numerosos, tanto por evitar la curiosidad de los campesinos, como por librarnos de objetos que dificulten las marcha.”

Salvador Calderón, 1875

Chapter 2 MATERIAL AND METHODS

2.1 Introduction

Fossil shark remains, on which this thesis is primarily based, come from several localities in the southern part of the Basque-Cantabrian Region, an area well known for its rich record of Upper Cretaceous fossil fishes (Cappetta and Corral, 1999; Corral et al., 2015b, and references therein). The assembled collection of uppermost Cretaceous selachian remains currently contains over 1,600 one thousand specimens, and it mainly consists of isolated teeth and, to a lesser extent, dermal denticles and caudal sting fragments of batoids. The bulk of the collection has been acquired as a result of field collection and disinterested donations by fossil enthusiasts, local geologists and this author. Currently, the Museo de Ciencias Naturales de Álava (MCNA) holds one of the largest collections of fossil shark material from the Basque-Cantabrian Region. Moreover, the Luberri-Oiartzungo Ikasgune Geologiko Museoa, in Oiartzun (Gipuzkoa) also houses a small collection of fossil teeth from this area.

But gathering such large collection has not been easy. The Basque-Cantabrian Region is characterised by a well vegetated landscape that often hampers direct access to the rocks. Although few natural outcrops with selachian content occur, most fossil sites were made available when fresh rock exposures resulted either from excavations during construction of several irrigation reservoirs in the 1990s or from a series of pits along the foothills of the Vitoria and Entzia Mountains. Quarrying operations ended long time ago, but many of the unrestored quarries still become available for fossil collection. The collection of such remains has been the result of long time palaeontological investigation of the fossiliferous beds, visited at irregular intervals over a period of more than 30 years. Collecting techniques have included surface collecting ('crawling on hands and knees'), excavation with hand tools, bulk sampling, and screen washing of the fossil-bearing matrix (Fig. 2.1)

The Albaina fossil locality (Treviño County, Burgos), which is aged Maastrichtian, is regarded by far the most important fossil site of selachian remains in the Basque-



Figure 2.1 Prospecting for fossils at the exposures in the study area. A, searching for fossils at the Ariaza pit (Gardelegi, Álava) with the Mingobaso pit (Castillo/Gaztelu, Álava) in the background (arrowed); B, excavating a rock fall from the quarry face at Albaina (Treviño County, Burgos); C, Exposed portion of the vertebrate-rich beds of the Valdenoceda Formation at Quintanilla la Ojada (Burgos); D, Dr Cappetta and the author prospecting for fossils at Quintanilla la Ojada (Burgos).

Cantabrian Region. Since the late 1980s, this site has continuously produced a large number of selachian remains, exceeding one thousand, and has the most diverse faunal assemblage (Cappetta and Corral, 1999). Here, collecting directly from the productive beds becomes difficult as they are located up above in the quarry face. This impediment was overcome by the occasional occurrence of rockfalls from identifiable strata along the quarry face, which allowed collectors to obtain isolated vertebrate remains and other invertebrate fossils. Collection techniques here included handpicking and screen washing in order to obtain small vertebrate fossils from either friable fossil-bearing rocks or acid treated residues of the more lithified samples.

The initial collection of vertebrate fossils from the Maastrichtian beds at Quintanilla la Ojada (Burgos) started in 1997 when the site was discovered by researchers working in the UPV/EHU (see Berreteaga, 2008). More specimens have been subsequently collected from this locality by the author of this thesis, in total numbering the collection about 180 selachian teeth. These specimens are also held in the MCNA.

The Maastrichtian collection from the Entzia Mountains (Álava) is not as large as those above mentioned, containing scarcely a few surface-collected specimens ($n=18$), but it has a sufficient number of specimens to identify at least four taxa.

The Campanian record of chondrichthyan teeth is apparently less rich in numbers. Fossil occurrences are usually scant and patchy and, as a result, have been considered hitherto less significant than those from the Maastrichtian sites. A consequence of the poor knowledge of the palaeontological resources in the region and the surface collecting techniques used for recovering fossils is that fossil remains from small species of sharks (microteeth) have been until now overlooked. Here, the study has been limited to two localized fossiliferous areas in Vitoria-Gasteiz (Álava), namely the Vitoria Pass (near Gardelegi and Castillo/Gaztelu localities) and the village of Gometxa, where surface collecting during all these years has provided a representative sample of elasmobranch teeth. Both areas represent different stratigraphical horizons and sedimentological settings, thus adding further interest. The Vitoria Pass collection has yielded more than 130 catalogued shark teeth. All of them were surface collected in open pits, where mudstone was mined for the brick and construction industry. The Gometxa collection of selachian remains, with more than 120 catalogued specimens, comes from fossiliferous beds exposed in a small limestone quarry that has supplied stone blocks and construction aggregates. Obviously these figures are, so far, modest and cannot be compared to the exceptional fossil deposit that represents Albaina but they are, by no means, of less taxonomic importance.

This elasmobranch collection, on the whole, represents many years of searching, collecting, curation, and cataloguing each of the fossil remains. The specimens are housed at the MCNA has been documented and integrated in the general palaeontology database built in FileMaker® Pro 13 software (see below). Each record includes information details regarding locality, stratigraphical provenance, taxonomy, skeletal parts, measurements, journals where the fossils have been published, and other rele-

vant information. Currently the entire shark database has 1,631 records including all published specimens. Moreover, many cooccurring fossil invertebrates, collected in the course of this thesis or housed in the MCNA storerooms, have been investigated to gain valuable biostratigraphic information.

Institutional acronyms. MCNA, Museo de Ciencias Naturales de Álava / Arabako Natur Zientzien Museoa, Vitoria-Gasteiz (Álava), Basque Country, Spain; OIGM, Luberri-Oiartzungo Ikasgune Geologiko Museoa, Oiartzun (Gipuzkoa), Basque Country, Spain; MNHN, Muséum national d'Histoire naturelle, Paris, France; MB.f., Museum für Naturkunde, Berlin, Germany.

2.2 General field techniques (specimen collection)

Basically, the working techniques used to gather the fossil material have included:

1. picking up isolated teeth visible to the naked eye;
2. extraction of isolated visible teeth through mechanical methods; and
3. collecting and processing rock samples using screen washing and concentration techniques (for microvertebrates invisible to the naked eye).

During field expeditions, pit slopes and stockpiles were carefully picked for surface accumulation of fossil teeth of sharks, as rain wash and frost weathering continuously provides new specimens (Fig. 2.2). When a fossil tooth occurs in marlstones it is extracted with steel point tools and easily removed by hand or with tweezers. But before lifting a specimen from the surface, it is always advisable to look for open cracks in the fossil. Fossil shark teeth that have been long exposed in the field to chemical weathering caused by rain water often show an alteration in the minerals of the crown, with a waxy lustre and whitish areas on the enameloid surface, in addition to cracking lines along their cusps. When this is the case, and when parts of the tooth became obviously loose, a matrix block is cut and properly packed to prevent further disintegration that would make more difficult the fossil restoration.

The quarrying (excavation and extraction) of shark teeth embedded in well indurated rocks, such as the limestones found at Gometxa quarry, requires the use of mechanical tools including a lump hammer and assorted cold chisels. At the site, it is more convenient to remove the fossils surrounded by an adequate amount of rock (matrix) that will prevent the specimen from damage (Fig. 2.3). In addition to the material found in the quarry debris, shark teeth are also present on the bedding planes of large natural blocks of hard calcarenite that have been wedged out of the rock face, and their extraction without electric machinery requires some degree of expertise. At first, a hand point chisel is used to break the hard rock along a broad path (Fig. 2.3A); this concentrates the hammer blow onto one point. Vibrations should be reduced as teeth are susceptible to cracking from hard blows. After a simple groove is cut out around the fossil, it has to be widened and deepened, alternating between hand and point



Figure 2.2 Tooth of a Maastrichtian *Squalicorax pristodontus* (Agassiz, 1843) from Albaina site (Treviño County, Burgos) that was exposed by weathering and erosion of a fossiliferous bed of a former bioclastic calcarenite/calclrudite. See some hard-wearing lithoclasts at the upper-left side. The specimen measures 9 mm in width.

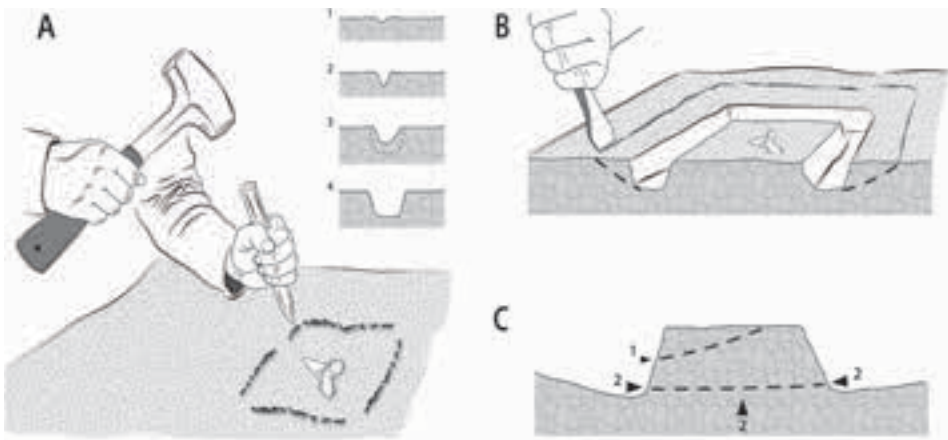


Figure 2.3 Extracting a fossil specimen from the rock exposure. A, making a groove around the fossil with a point chisel and a hammer; B, enlarging a surrounding trench with a flat chisel; C, dashed lines indicate both predicted fracture surfaces according to the blow impact.



Figure 2.4 Final process of removing the hand sample from the calcarenite bed. The arrow indicates the fossil remain.

chisels until a rock prism is carved out (Figs. 2.3B, 2.4). The groove should be deep enough to ensure a safe removal of the sample. To do so, it is necessary to hit horizontally around the base the prism with a wide hand chisel to create a weakness plane that make it eventually to break apart (Figs. 2.3C, 2.4). Obviously, the extraction of the rock sample can be speeded up by using a saw with a diamond blade (more convenient a battery-powered one), but it will require posterior preparation of the sample edges to get a natural aspect (e.g. for exhibition purposes), rather than the unappealing saw cut made by the diamond blade.

When the targeted fossil is near an edge of a rock block, the task becomes easier and just a few blows with the hammer and chisel are necessary to break off a small sample. Subsequent mechanical or chemical removal of the matrix – also called development – can be done more precisely at the laboratory. Trimming in excess the sample edges at the field is not advisable as can result in disaster. Only on rare occasions some of the collected teeth have been completely extracted from the matrix for study (see below).

Finally, the specimens have to be packed carefully using tissue paper, wrapping paper or any suitable packaging material, and brought to the laboratory in ziplock polyethylene bags, plastic vials or plastic storage boxes with several compartments.

When dealing with moderately to poorly indurated fossil-bearing rocks, such as those found in Albaina (Treviño County, Burgos), a minimal preparation of the fossils at the field should be taken into consideration. A large number of these specimens have extremely fragile roots, and whenever possible the teeth should be extracted with

enough matrix (or adhering sediment) to withstand a safe transportation to the laboratory for preparation. Field consolidation is only considered to avoid specimen disintegration (see Madsen, 1996).

Special attention was given to the cracks, so as to decide whether or not to apply a protective layer of consolidant Paraloid B72 (copolymer of ethyl methacrylate and methyl acrylate), or the like. Unless strictly necessary, consolidation in the laboratory was only accomplished after mechanical or chemical preparation.

2.3 Screen washing

In addition to the easily spotted specimens, collected by either surface prospection or excavation, an important number of small specimens resulted from wet sieving. This basic technique for collecting vertebrate microremains is highly effective and allowed to discover tiny fish teeth that were invisible to the naked eye. The working method in the excavations has been barely conditioned by the mineralogical composition or nature of each rock deposit. In general terms, the technique includes transportation of the bags containing the samples to the workplace (either in the field or the laboratory), spreading them to dry well, and little by little continuously passing portions of the fossiliferous matrix through the stacks of sieves. Because initially there was no need to use deflocculants or other chemical pollutants to help disaggregate the sediments, field screen washing was accomplished in nearby natural water sources.

Screen washing is a common procedure in vertebrate palaeontology to recover microvertebrate specimens from rock units that otherwise might have passed unnoticed (McKenna, 1962, 1965; McKenna et al., 1994; Cifelli et al., 1996; Green, 2001). To do that, some samples of soft rocks are mechanically crushed or disaggregated by hand



Figure 2.5 Wet laboratory space with a series of sieves, a graduated cylinder, and the reactive chemical (black plastic container) for extraction of microscopic fossil remains from the rock samples.

and placed on top of a stack of nested sieves in the chosen mesh size. There is no other consideration than thoroughly drying the samples to facilitate the disaggregation of the matrices prior to washing. After that, the sample is manually sieved under a continuous supply of water that removes the thinner sediment and leaves the fossiliferous residue in the sieves. After that, the washed fractions are gathered and put in plastic bags. Back in the laboratory, all fractions of the sieved residue are spread onto a polyethylene-backed absorbent bench paper and allowed to dry at room temperature.

Bulk sampling of rocks and wet-sieving for extraction of microvertebrate remains has been undertaken in only three of the six main fossil sites studied. The fossiliferous beds from Albaina (ALB), Quintanilla la Ojada (QLO-1 and QLO-2) and Gometxa (GOM) locations differ in lithology and fossil content, and form part of different Campanian and Maastrichtian successions.

Albaina site includes a well-lithified orange-yellow calcarenite, rich in orbitoids, and friable sandstone–calcarenite alternations resulted from diagenetic alteration. The author processed about 200 kg of these friable rocks and the disintegrated material was wet screened through three stacked screens with mesh sizes of 2 mm, 1 mm, and 0.5 mm. In addition to field collecting, several blocks of friable calcarenite from the same fossiliferous bed (about 30 kg in total weight) were collected and taken to the palaeontology lab for dissolving and extraction of microscopic teeth (Fig. 2.5). The technique (see explanation below) involved immersing blocks of rock into a plastic lidded container filled with a buffered solution of acetic acid (see Jeppsson et al., 1985). The process required many regular changes of acid along several weeks until total breaking up of the original rock. The insoluble residue was regularly removed from the acid bin for wet sieving. After acid neutralization, it was wet processed in the same way as other residues through a stack of sieves of mesh sizes 2.0 mm, 1.0 mm, 0.5 and 0.25 mm. Given the fragile nature of these particular fish remains, this recovery method increased the risk of breakage of the more delicate fossils, but in return, it yielded an interesting microvertebrate assemblage including four new batoid species (see Chapter 14).

The fossiliferous beds of Quintanilla la Ojada consist of sandy bioturbated dolostones, above which grey clayey dolostones have yielded abundant marine remains of vertebrates, pyritized orbitoids and euhedral pyrite. Only few tooth specimens were collected in situ, being most of them collected by hand picking on quarried rocks from identified strata. At the less productive bed QLO-1 (a transgressive lag deposit in between the 'Rioseco facies' and the Valdenoceda Formation) only a few abraded reddish brown teeth were collected. Upwards, several stacked parasequences of fossil-rich sandy carbonates, deposited above the previous deposit, have yielded larger number of greyish black teeth, either abraded-polished or pristinely preserved. Only a thick bed from the youngest sandy carbonates (QLO-2) was bulk sampled. Totally, 300 kilograms were taken for sieving through 2 mm, 0.7 mm and 0.5 mm meshes by Berreteaga (2008). About 180 elasmobranch teeth were thus obtained, in addition to other fragmentary material.

Many of these teeth also required mechanical preparation and some of them were also treated with a 5% solution of buffered acetic acid to remove carbonate fillings. Those acid-treated were rinsed thoroughly in ambient tap water, dried and finally consolidated with acrylic resins when deemed necessary (see below for details). These preparation techniques allowed to reveal hidden dental characters on the bony tissue (i.e. osteodentine) of the root, such as nutritive grooves and other tiny foramina.

Broken specimens and isolated small bone fragments were not discarded, but kept separately in order to facilitate reassembling in the laboratory. Incomplete fish remains, but still taxonomically identifiable, were kept aside for use in eventual geochemical analysis (Berreteaga, 2008; Corral et al., 2015b).

Finally, a test sample of approximately 35 kg of dark grey bioclastic marls containing fossil invertebrates, glauconite and phosphatic material from Gometxa site (GOM) was wet sieved through a set of sieves with mesh sizes, from top to bottom, of 4, 2, 1, 0.4, and 0.3 mm. Apart from drying in advance, no previous treatment of the sample was required as it washed easily. This preliminary sampling has yielded for the first time a promising set of microfaunal remains of elasmobranchs and apparently unique to the Iberian Peninsula, which offers a valuable insight into the Campanian shark and rays faunae in southern Europe.

2.4 Sorting and picking

Fish remains in the concentrated fossiliferous residues were picked out and identified using a magnifier lamp and stereoscopic microscopes (an Olympus SZ30 stereo microscope mounted on a boom stand for the observation of large size specimens and a Leica Wild M420 macroscope). Most of the work was done by the author at the MCNA, and in collaboration with Dr. Ana Berreteaga for the Maastrichtian microfossils collected at Quintanilla la Ojada (Burgos).

The dry residue of concentrated fossiliferous sediment was spread out on a custom-made picking tray (26 cm long by 18 cm wide) in a uniform and low density of grains. Then, each sample fraction was examined for fossil content under a binocular microscope (Figs. 2.6, 2.7). The tray was fabricated with a sheet of white paperboard (about 200 g/cm²), marked with a 1 cm square grid pattern, which was covered by a clip-frame glass for easy sliding of the residue. The paperboard was mounted to glass with clear double sided tape (see construction details in Fig. 2.8). I founded this tray particularly useful in picking shark teeth because a larger amount of residue can be spread onto the empty tray than using the standard metal picking tray of about 11 by 7 cm in size.

Vertebrate remains (including elasmobranch teeth and actinopterygian fish remains) and other fossil invertebrates included in the residue were sorted using a mounted needle (dissecting pick) and eventually removed with either fine tip tweezers or a slightly moistened fine brush (size #00 or smaller), and organised in micropalaeontology slides.



Figure 2.6 Sorting and picking under a magnifier lamp.

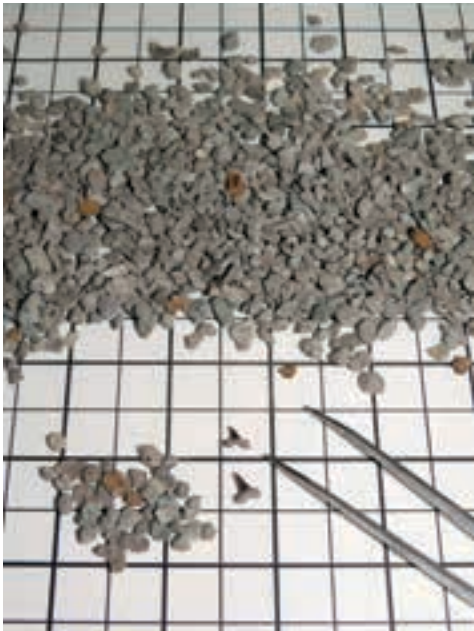


Figure 2.7 Detail of a partially sorted rock residue with two selachian teeth recovered.

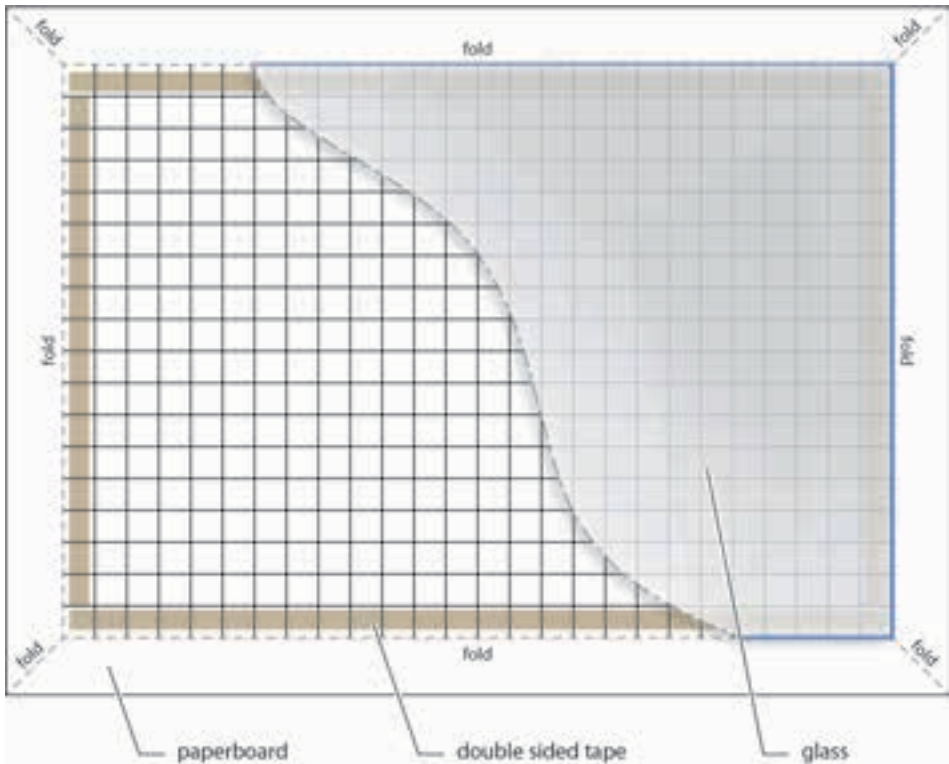


Figure 2.8 Custom-made picking tray.

2.5 Preparation of palaeontological remains

In general, fossil preparation combines manual dexterity, experience and a pinch of anatomical knowledge. The techniques have been discussed in detail by Converse (1989), Chaney (1989), May et al. (1994), and Wilson (1995). Modern restoration and conservation practices advocate to keep any intervention treatment to a minimum, but this general principle is often in conflict with the researchers' needs, since both scientific and cultural values rest upon a good palaeontological preparation.

Quite often, the fossil specimens are weathered by the erosive action of ice and meteoric water in our latitude, or are found fractured with missing parts. And apart from such natural deterioration, fossil specimens may have broken during quarrying or occurred partially covered by matrix. In all cases, fossil cleaning, stabilization, or restoration was required prior to be handled safely for study.

Fossil selachian teeth vary in colour and degree of physical preservation at each fossil locality studied. Each set of teeth recovered from the same fossil horizon have, in broad terms, similar taphonomic characteristics as a result of shared types of min-

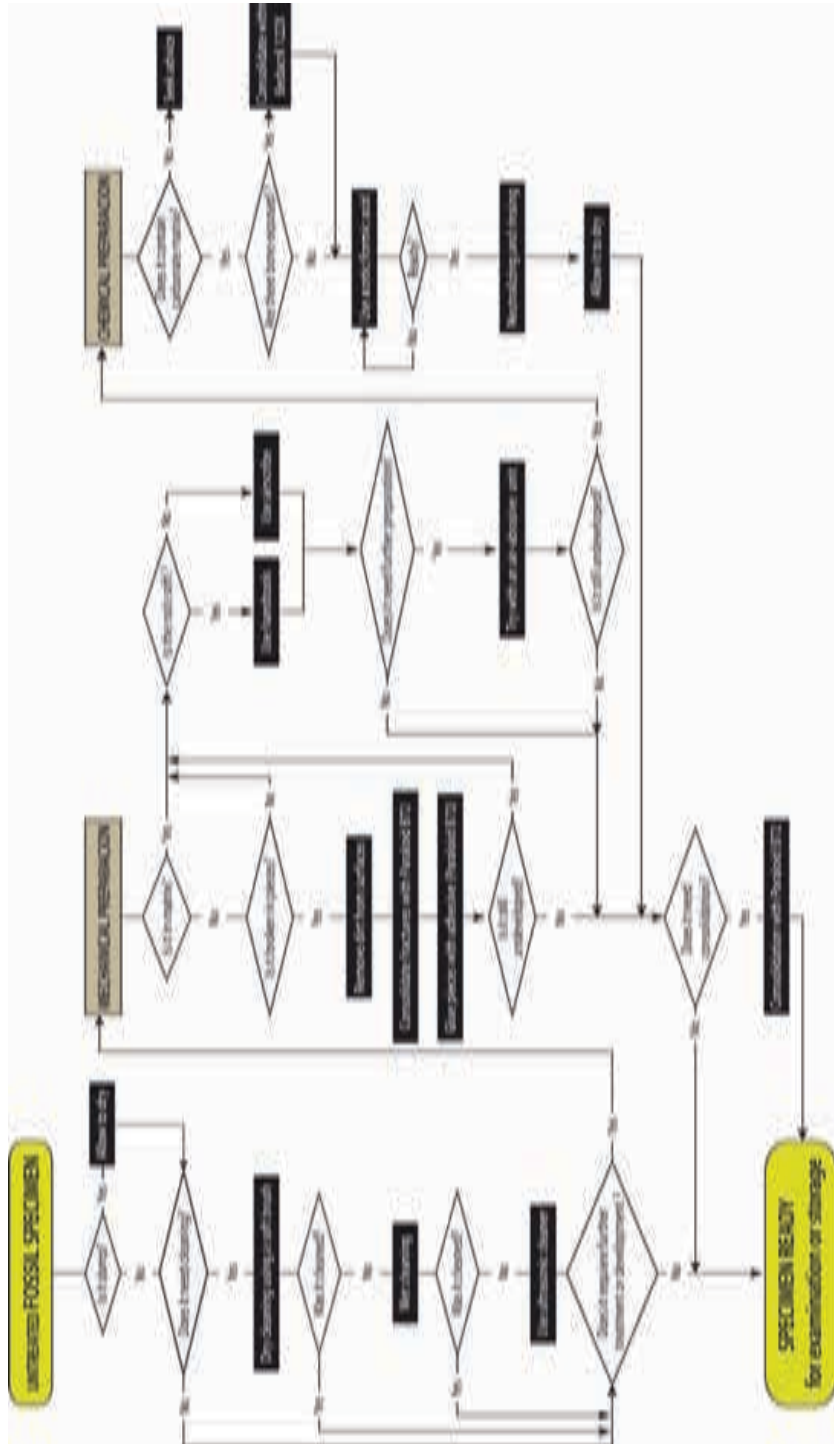


Figure 2.9 Decision flow chart for determining the appropriate procedure for the preparation of fossil specimens. Actions are indicated in black boxes.

eralization after burial and both postburial chemical alterations (fossil diagenesis processes) and physical alterations (i.e. fractures). Some criteria to prepare and conserve the palaeontological specimens are as follows:

1. to further manipulate them safely;
2. to observe anatomical characteristics hidden by matrix;
3. to ensure their long-term structural integrity and conservation; and
4. to withstand eventual environmental conditions existing in exhibition and storage areas.

The type and degree of preparation (or micropreparation) of the fossil teeth has been different in each case, depending upon their state of conservation, but generally mechanical and chemical techniques have been used (see Fig. 2.9). Initially, few tools are needed, and each preparator has his own preferences (Fig. 2.10). Thus, upon arriving at the laboratory, fossils and matrices should be allowed to air dry before cleaning. Much of the sediment, or loosely adherent dirt, can be easily removed with thin needles or by cleaning it with a soft brush. Some fossil specimens just only needed a wash



Figure 2.10 Selected instruments and basic material for fossil micropreparation. A, fine tip curved tweezers; B, 0.5 mm mechanical pencil with a steel needle; C, pin vise; D, scalpel with removable blades; E, fine paint brush with solvent-resistant hair; F, bamboo stick cotton bud; G, cotton pad; H, acetone; I, consolidant Paraloid B72 in acetone at 5–10% weight by volume (w/v) ratio.

with a toothbrush (or a soft artist brush) to remove soil and loose sedimentary debris deposited on their surface, but this procedure had to be done with care since some of them may be very fragile. However, this basic procedure does not work in every case, and other cleaning (or preparation) techniques need to be employed in areas where the sediment is firmly adhered, and only brushing does not remove the dirt.

If the general condition of the specimen is good enough, ingrained dirt can be removed with an ultrasonic cleaner (Pojeta and Balanc, 1989; Green, 2001). Sonication of sounded fossil teeth using an ultrasonic bath serves, moreover, to uncover delicate anatomical features in the root. Cleaning is accomplished because sound waves generated by a transducer, travelling through the medium (generally water), generate microscopic bubbles that collapse or implode (cavitation) on the surface of the object to be cleaned. This action releases powerful energy on a microscopic scale. Specimens are not submerged directly in the bath; instead, they are placed in small glass containers filled with liquid (indirect method). A 50 mm in diameter crystallizing dish (or short test tube) filled with either water or acetone ($\text{CH}_3\text{-CO-CH}_3$) was used to hold the specimen. The container was then placed into the ultrasonic cleaner tank and sonicated for a few seconds. The fact of using acetone in the crystallizer is because the cavitation bubbles are more effective in this medium and, moreover, the preparation can continue without waiting so long for the solvent to evaporate. Ethanol ($\text{CH}_3\text{-CH}_2\text{-OH}$) is other quick evaporating solvent that can be used instead of acetone.

Moreover, field consolidation of specimens (with Paraloid B72, or the like) generally results into fine particles get stuck to the fossil bone, which are difficult to remove solely with swabs soaked in acetone or by brushing them with a solvent-laden fine brush. Ultrasonic baths can be equally effective to remove such traces of consolidant previously applied to the specimen during excavation. In this cases, the consolidant better softens by filling the crystallizer, where the specimen is placed, with a mixture of acetone and water (1:1), which loosens the consolidated sediment out without sticking again.

Very often algae, fungi or lichens grow on stone substrates in wet climates, which may cause either material dissolution on limestones (biocorrosive pitting) or disaggregation of lithified sandstones. Natural or man-made outcrops exposed to damp environmental conditions for long periods of time may form biological patinas both on fossils and the surrounding matrix. An aqueous solution of sodium hypochlorite (NaClO) has long probed to be an efficient chemical to remove organic matter on hard substrates. In recent past, Buckley and McCrea (2009) developed a new application of the technique, taking advantage of that feature, to clean sound consolidated slabs of organic-rich sandstones that contained avian and non-avian theropod tracks obscured by lichen growth. To deal with the problem of biological patinas, when occurred in our materials, cleaning was done by dipping the specimens in a 20% bleach aqueous solution (an unscented household bleach, at concentration of 35 g of chlorine per litre was used) for a few minutes, followed by thorough rinsing in water.

Mechanical preparation

The excess of rock, surrounding a hand specimen, was carefully chipped away with a hammer and a small chisel, in cases when the fossil remains were left embedded in matrix. But when a large amount of rock had to be eliminated it was found more convenient to use a masonry splitter (Fig. 2.11).

Many other specimens have been entirely freed from matrix, as well, in order to observe all their anatomic characteristics. In this case, the removal of matrix has been carried out carefully, little by little, using thermally tempered steel needles (i.e. pin vises and sewing needles) and a few hand instruments (dissecting needles, pin vises and scalpels). However, a Pferd MST engraving pen (pneumatic aircscribe) fitted with a fine tungsten carbide needle gauge was chosen to remove large amount of matrix when necessary. Fine engraving needles are more suitable to chip away hard matrixes and, additionally facilitate a more accurate preparation in closer areas to the fossil surface (see Fig. 2.12). When working with small specimens this task is called micropreparation. Techniques, tools, and procedural matters related to micropreparation have been treated by Amaral (1994), Madsen (1996), and Cavigelli (2009). This particular preparation technique requires a binocular microscope, good lighting provided by cool white LED lamps, a great deal of patience, and steady nerves, because any accidental nick or scrape on the fossil may end in catastrophe.



Figure 2.11 Hand sample being processed in a masonry splitter.

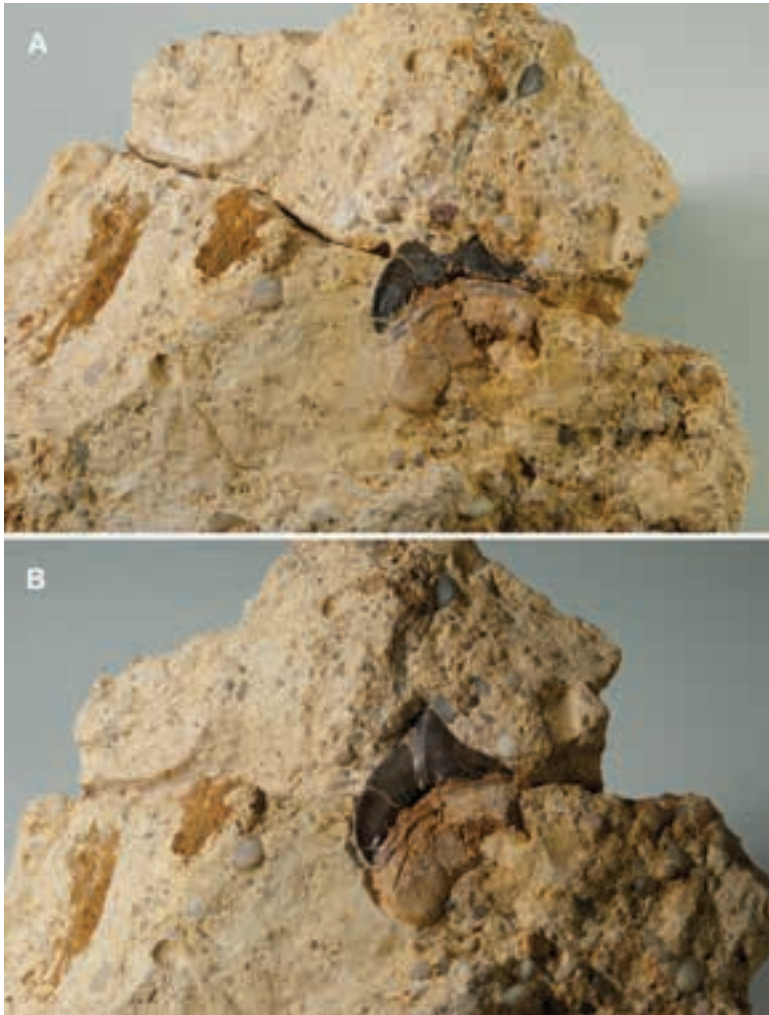


Figure 2.12 Tooth of *Squalicorax pristodontus* (Agassiz, 1843) partly embedded in matrix from the Maastriichtian of Quintanilla la Ojada (Burgos), MCNA 15158. A, notice the open crack running across the tooth crown, existing prior to arrival at the lab; B, the same specimen after restoration.

Before reassembling the fragments of a fossil specimen, it is convenient to remove from the working bench all matrix fragments detached during preparation. This makes an easier location of small fossil parts that may eventually have fallen on top of the working surface during preparation. Thoroughly cleaning of both fracture surfaces prior to bonding has important effects on the quality of the final appearance of the restoration, since any loose sand grain or bone fragment on the bonding surface, how small it might be, will impede a perfect joining.

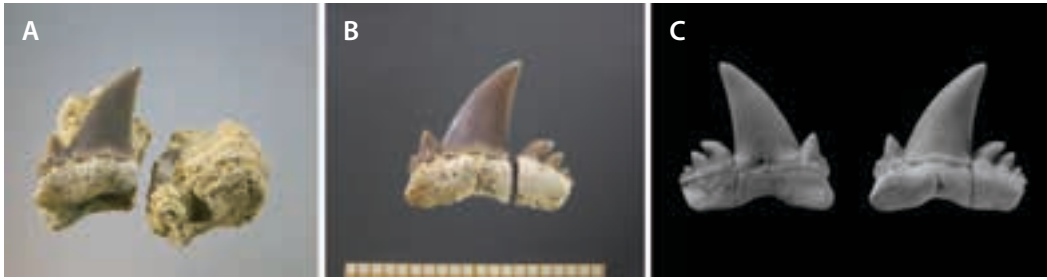


Figure 2.13 Tooth of *Serratolamna serrata* (Agassiz, 1843) from the Maastrichtian of Albaina (Treviño County, Burgos), MCNA 15039. A, the distal lobe of the root was broken off during collection; B, the same specimen freed from the matrix; C, the specimen restored in labial and lingual views respectively. The length of the scale (B) is 20 mm.

During adhesive application it is important that all detached parts (e.g. the main cusp, cusplets or root lobes) are properly confronted on a flat surface. Then, Paraloid B72 adhesive is applied in the correct amount and location on the larger tooth part and, generally, as soon the detached part of the tooth is forced to touch the glue drop, it will be drawn instantly into its original position. Paraloid B72 adhesive was used here because of its mechanical properties and reversibility (see Koob, 1986; Davidson and Brown, 2012). Any excess of adhesive that may eventually come out of the joint can be wiped out immediately using a cotton-tipped swab soaked in acetone, or eliminated once the glue has set up, either mechanically removed or dissolved with just a little acetone dropped on it. If readjustment of a glued fragment is required, it can be done by gently applying force to it with tweezers after a drop of acetone was added to the joint (see Fig. 2.13).

Gluing together fragments of larger vertebrate specimens can be more easily done by spreading a moderately thinned coat to each fracture surfaces, allowing a few seconds to evaporate the solvent, and finally fitting the pieces together. Initially, some pressure has to be applied with the fingers to the reattached fragments, after which the specimen may be left hold balanced on a sand container until the glue sets up.

Consolidation is important for the fish remains collected at Albaina site, and particularly for the shark teeth. Although they exhibit well mineralised crowns, their roots (made up of spongy tissue) are delicate and very often exhibit cracks. Such broken or fragile fossils have been hardened, or consolidated, with a 5 to 10% weight by volume (w/v) solution of Paraloid B72 resin, dissolved either in acetone or toluene, which is able to penetrate well into the fossil bone (see more on consolidation and solvents below).

Slow solvent evaporation inside a plastic zip lock bag prevents the unattractive excess of consolidant accumulating on the surface of the fossil, which may also obscure important anatomical features. Any residue of dry resin (especially in the crown of the teeth) can be easily removed by means of cotton swabs impregnated in acetone.

In other cases, when fragments of limestone matrix needed to be bonded, a stronger two-part epoxy adhesive (resin and hardener) was used. Epoxy resins are durable and strong chemical compounds for joining, to which powder dyes can be added to match any desirable rock hue. Unless using the fast-setting formulation, the adhesive could flow out of joints before it sets. In these cases, a desired thixotropic performance is obtained by adding a few amount fumed silica (Aerosil®) to the epoxy mix.

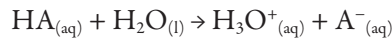
Chemical preparation techniques

A chemical procedure, beyond the use of cleaning solutions above mentioned, may be necessary in those vertebrate fossils found fossilised in marl and limestone rocks, particularly when further development is required either to uncover important fossil details or free the fossils themselves from the matrices.

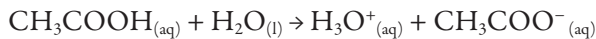
Diluted acetic or formic acids (i.e. aqueous-acidic solutions) are generally utilised in the development of fossil skeletal remains (see Table 2.1). Both acids have long been successfully used to free fossils from carbonate matrices, and therefore are useful reagents to consider in palaeontological laboratories (see Corral, 2012; Jeppsson and Anhus, 1995; Jeppsson et al., 1985, 1999; Lindsay, 1987, 1995; Rixon, 1976; Rutzky et al., 1994; Siverson, 1992; Toombs and Rixon, 1959). However, one of the main concerns when using these acids in fossil preparation rests on preventing uncontrolled acid attack on the matrix and the fossil itself.

Weak aqueous solutions of acetic and formic acids (e.g. in concentrations 5–10% by volume) selectively remove carbonate minerals from the interstices of phosphatic fossil bones, working in areas where mechanical tools cannot access, and uncover in this way intricate anatomical microstructures – hidden by the matrix – that may be of great importance for palaeobiological studies (Lindsay, 1987).

The chemistry involved in this process is based on the fact that weak organic acids partially dissociate in aqueous solutions to yield a hydronium ion (H_3O^+) and a conjugate base, according to the general reaction:



For example, acetic acid dissociates incompletely as follows:



where CH_3COO^- is the conjugate base of the acetic acid because it can take a proton from the hydronium ion to generate the original acid.

The reaction between the acetic acid and calcium carbonate from the matrix produces calcium acetate in aqueous solution and carbon dioxide, which is released as bubbles, in this way (Hellawell and Nicholas, 2012):

Table 2.1 Properties of two organic acids used in fossil preparation.

Reagent	Formula*	Molecular Weight (g/mol)	Specific gravity g/mL	Molarity	Weight (% w/w)**	V (mL)***
Acetic acid (glacial)	C ₂ H ₄ O ₂	60.05	1.049	17.4	99.7	57.4
Formic acid	CH ₂ O ₂	46.03	1.22	25.18	95.0	39.7

* molecular formula;

** weight by weight percent;

*** volume needed to prepare 1 L of solution 1 M.

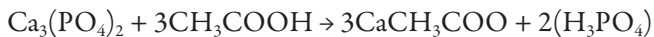
acetic acid + calcite → calcium acetate + carbon dioxide + water



The smaller the extent of dissociation of acetic (or formic) acid, the smaller the solubility of calcium phosphate in fossil teeth and bones, and thus additionally resulting in lowered solubility with the dissolution of the carbonate matrix (Lindsay, 1987, 1995).

The literature indicates that the solubility of calcium phosphate (or hydroxyapatite) is higher in formic acid than in acetic acid, especially when immersion the times are prolonged (Lindsay, 1987; Rixon, 1976; Rutzky et al., 1994). According to Rutzky et al. (1994), weak solutions of formic acid (at a concentration of 5% by volume) have greater dissolving capacity of carbonate matrices, as compare to acetic acid, and emit less pungent gases, but the authors warn that formic acid solutions should be saturated with about 1 g per litre of solution of tricalcium diphosphate [Ca₃(PO₄)₂] to prevent any damage to the fossil.

Acetic acid reacts with tricalcium phosphate as shown in the following reaction:



Brailon (1973) also recommended adding 2.7 g/l of tricalcium diphosphate to acetic acid solutions of 15% by volume. Jeppsson et al. (1985) moved from the classical empirical approach to follow scientific tests when trying to determine the grade of alteration caused by the acidic solutions in phosphatic fossils extracted from carbonate rocks. According to these authors, a range of damage in conodont elements were observed when using unbuffered acidic solutions (i.e. whitening, surface corrosion and destruction of the hyaline matter). They indicate that aqueous acid concentrations of 5%, 10%, and 15% by volume produce inverse amount of corrosion and dissolution (i.e. lower at high concentration). However, by adding calcium carbonate (CaCO₃) to the solution an 'acetic soup' forms that slightly raises the pH and releases Ca⁺⁺ ions preventing the dissolution of bone minerals (e.g. hydroxyapatite s.l.). Actually, when pH is kept above 3.6 it decreases the risk of dissolution of skeletal microstructures (see Fig. 2.14).

Before starting any acid treatment, it is important to check the condition of the specimen and decide how long the specimen will be into the acid bath. Close monitor-

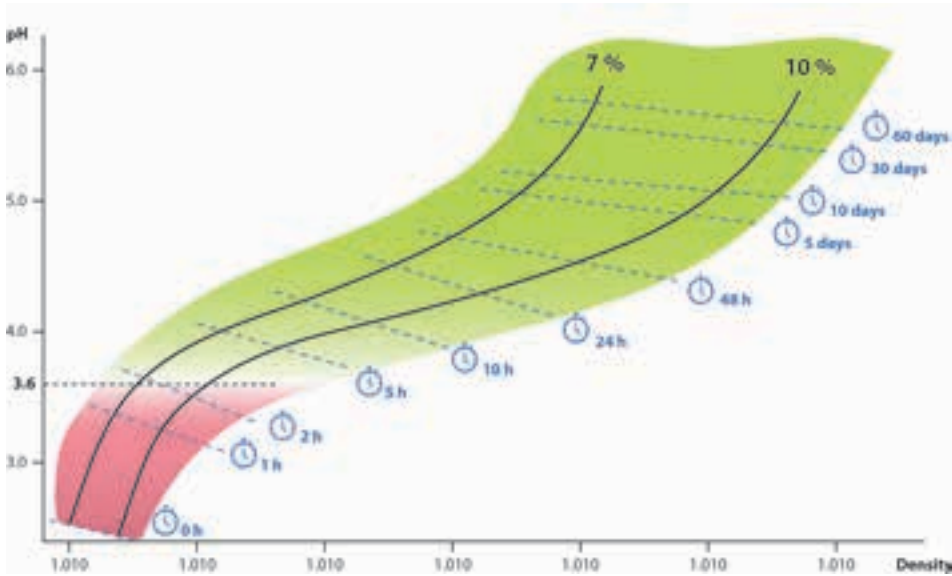


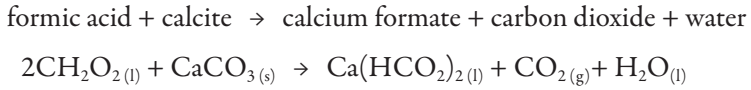
Figure 2.14 The relation between pH and density of 7% and 10% acetic acid solutions as carbonate is dissolved (adapted from Jeppsson et al., 1999). A pH value above 3.6 is considered safe for phosphatic fossils.

ing of the acid treatment is also important to prevent any unwanted reaction. Consequently, specimens immersed in an acid solution should not be left unattended for too long. Fragile areas in the fossils, or the matrix portion that we do not want to be dissolved, are usually sealed with a thick layer of Bedacril® 122X (a methyl methacrylate polymer) to protect them from the acid.

Many elasmobranch specimens studied in this thesis have been treated chemically in the laboratory of the Museo de Ciencias Naturales de Álava. As general rule, the fossil specimens were immersed in a 5% aqueous solution of glacial acetic acid (at a molar concentration of about 0.9 M), and to this solution 0.1% (w/v) tricalcium phosphate ($\text{Ca}_3(\text{PO}_4)_2$) was added. A considerable effervescence is produced when the specimens are immersed in the acid solution, but it normally ceases after a few hours. The reaction also results in an increase in the pH (from 3 to 4 one hour later; measured with pH strips).

A diluted solution of formic acid is also a good choice when the time counts, as above said, or when the dissolution of a large volume of rock is required. Formic acid is typically used to dissolve carbonate matrices at concentrations less than 9–10% (Kalfayan, 2008). The solubility of calcium carbonate depends on pH, but to avoid unwanted damage of biogenic apatite crystals, the acid bath should not be below a pH of 3.6. The procedure involves using double buffered formic associations, by adding 20–30 g of calcium carbonate and about 1 g of tricalcium phosphate to every litre of solution (Green, 2001).

Formic acid reaction with the carbonate is represented as follows:



However, when the preparation project involved the development of a single fossil tooth, which had already being released from the matrix and generally only required a short acid bath, a solution of acetic acid was primarily used. Procedures are similar in both techniques and the choice of acetic or formic acid is mainly determined by the preparator needs.

The standard treatments through an acidic bath usually lasted a few hours, given the size of the samples and specimens treated, and considering that much of the concealing matrix has been already mechanically removed. After that, the specimens were carefully removed from the bath, neutralized with a dilute aqueous solution of ammonium hydroxide 5% volume by volume (v/v) and rinsed in running tap water for at least 30 minutes to remove any residual acid or calcium salts from the aqueous solution. Calcium salts formed during the acid reaction will grow, over time, on cracks or inside the bone pores causing damage the specimens unless a desalination treatment is done. Calcium acetate, $\text{Ca}(\text{HCO}_2)_2$, and calcium formate, $\text{Ca}(\text{C}_2\text{H}_3\text{O}_2)_2 \cdot 2\text{H}_2\text{O}$, are both water-soluble salts that may be removed with a prolonged soak in tap water, or better in deionized water. As a general rule, chemical development by acetic acid was used because the solubility in water of calcium acetate is higher than calcium formate at ordinary laboratory temperature, and the desalination process can thus be easily accomplished. Some examples of chemical preparation of fossil samples are given in Figs. 2.15 and 2.16.

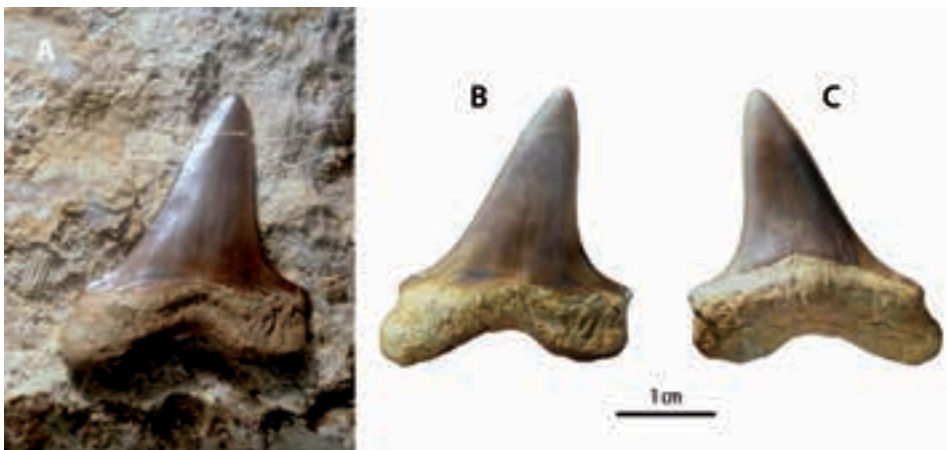


Figure 2.15 Tooth of *Cretoxyrhina mantelli* (Agassiz, 1843) from the Campanian of Gometxa (Álava). A, exposed on an air-weathered limestone surface; B–C, the same specimen in labial (B) and lingual (C) views after freed from the matrix.

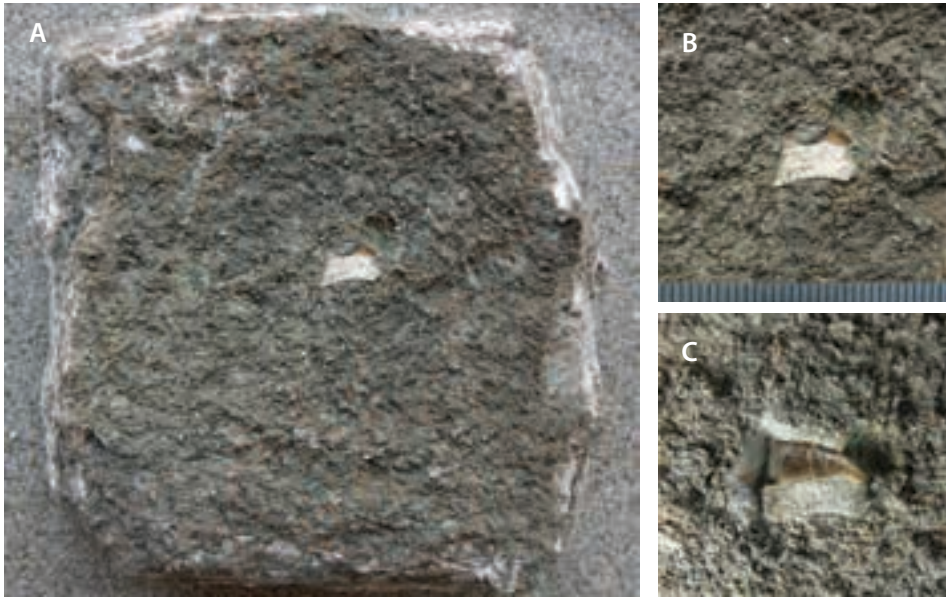


Figure 2.16 Tooth of an anacoracid shark from the Campanian at Gometxa site (Álava), MCNA 15160. A, the unprepared hand sample; B, close up of the fossil tooth in matrix; C, the same tooth with the matrix partially dissolved with a chemical solution of acetic acid. Scale in mm.

Finally, when considering safety laboratory measures, both acetic and formic acids are relatively harmless at low concentrations (< 10% by volume). But at higher ones, they are harmful and highly pungent, and consequently should be handled in very well ventilated areas.

Consolidation

Some conservation treatments to permanently stabilize the specimens were also followed. Acid-treated specimens keep their size but may become fragile (Lindsay, 1987), and the fragility is higher when are still damp, so they must be handled with care before completely dry. Additionally, consolidation is needed to strength and stabilize the specimens. It is therefore important to choose a good consolidant, and among the requirements for any consolidant or adhesive used in conservation are these (Keene, 1987):

1. being not harmful to the specimen;
2. being chemically stable;
3. being non-toxic to the user;
4. having a mechanical strength appropriate to the material treated;
5. having a suitable glass transition temperature (T_g); and
6. being easily reversible.

When dealing with dry fossil specimens, thermoplastic acrylic resins are regarded

the best option (Koob, 1986; Shelton and Chaney, 1994). The above-mentioned copolymer of ethyl methacrylate-methyl acrylate (70:30), which is easily soluble in toluene or acetone (Paraloid B72 and Acryloid B72 are two brand names of the same product), is a very stable resin. By its excellent mechanical qualities, chemical resistance to atmospheric agents, Tg of approximately 40° C, and low tendency to cross-linking (i.e. good reversibility) this resin is widely used in conservation works.

In our case, the fossil specimens were consolidated – when deemed necessary – with a 5% (weight/volume) solution of Paraloid B72 in toluene (C₆H₅CH₃), applied either by brush or immersion. Similarly, any detached small fragment of a particular fossil was consolidated before being bonded to each other with adhesive Paraloid B72 under a stereomicroscope. The fact of applying a chemical strengthener onto the broken surfaces of detached fossil parts greatly improves the bond strength.

2.6 Geochemistry methods

The geochemical composition of rare earth elements (REE) from 13 fossil fragments of assemblage QLO-2 and one sample of the host rock at Quintanilla la Ojada site (Burgos) have been investigated by geochemical analytical procedures (see: Berreteaga, 2008; Corral et al., 2015b). The samples, which were previously acid digested, were filtered through a 0.45 µm Millipore Millex HV filter and conditioned with 1% de HNO₃. Inductively coupled plasma mass spectrometry (ICP-MS) was carried out by Berreteaga (2008) using an Elan 9000 system (Perkin Elmer, USA) spectrometer. Measurement accuracy was guaranteed by taken three value readings from each sample and exactitude was evaluated with the use of USGS rock reference materials (MAG-1, SCO-1 and SGR-1) used in identical analytical procedures. All measured concentrations have been normalized to the values of concentration of Post-Archean Australian Shale (PAAS) proposed by Taylor and McLennan (1985).

2.7 Analytical methods for palaeobiogeographical reconstruction

The palaeobiogeographical distribution of Euselachii genera, occurring during the Campanian (including the assemblages of the Vitoria Sub-basin), has been quantified using multivariate ordination techniques. The findings are based on available data compiled from published literature (see Chapter 17 for references) and unpublished sources (this research). The systematics revision of these genera in accordance with recent handbooks (e.g. Cappetta, 2006; Cappetta, 2012) deemed necessary in order to avoid redundancies and provide more coherent results. Moreover, fossil sites where diversity is reported as having lower than seven taxa have been disregarded, in order to obtain a homogeneous data set. This resulted in a row data matrix of 18 operational geographical units (OGUs sensu Seeling et al., 2004) by 86 columns, the latter representing the genera analysed (Table 17.3).

The number of genera present in each OGU resulted from either a single fossil association deposited in a geological basin or an aggregated association from geologically related sedimentary settings within a geographical area. Genera occurrence is expressed in terms of binary data in a Q-matrix (presence represented by 1 and absence by 0). The choice of a genus as a basic taxonomic unit has been proven convenient according to Seeling et al. (2004). Higher-level taxonomic categories are not contemplated here because of the presumed widespread distribution of selachians in the Campanian oceans.

The basic following ordination techniques and cluster analysis are intended to represent (dis)similarity connections between marine regions during the Campanian, based on multiple variables found within them (i.e. selachian genera are represented in columns in the table). The principal coordinate analysis (PCoA)¹ is used for positioning a multivariate data set for visualization, either in a plane or space, preserving the distance relationships between OGUs. Such points (or areas) are more similar if they are closer to each other. This multivariate method does not enforce any particular union as clustering does (Hammer and Harper, 2006). Non-metric multidimensional scaling (NMDS) is another ordination method that analyses the matrix of (dis)similarities between the OGUs when absolute distances are not of primary importance. The NMDS technique tries to sort the data in the reduced ordination space, as PCoA does, but instead NMDS plots similar points (i.e. OGUs) together by transforming the distances (dissimilarities in their composition) into their ranks, which are compared with those of the Euclidean distances in the ordination plot. The quality of the arranged distances against the original ones is visible in the Shepard plot; ideally, it should produce a diagonal line ($x = y$), and quality is considered to be good when deviation (stress value) is below 0.1, as reported by Hammer and Harper (2006). Cluster analysis, based on the unweighted paired-group average algorithm (UPGMA), has been also used to find hierarchical groupings of the analysed geographical units, and thus obtain dendrograms with distinct palaeobiogeographical patterns. The use of other algorithms such as average linkage or Ward's method has not been tested here since they are more appropriate in ecological and morphometry studies, respectively, according to Hammer and Harper (2006).

PCoA, NMDS, and clustering analysis are based on Jaccard's coefficient of similarity². This index focuses on the presence/absence of a taxon in the samples of comparison. Only binary data of the sample composition is required (1 for presence and 0 for absence), and the calculated coefficient gives values that range from 0 to 1. The closer to 1 they get, the more similar the geographical units (i.e. OGUs) are. Jaccard's coefficient differs from the Simpson's similarity coefficient³ in that it ignores absences in pairwise comparison, and thus the value obtained in samples of highly unequal in size (one of

¹ Also known as metric multidimensional scaling (MDS).

² Defined as follows: $M/(M+N)$, where the number of shared taxa (M) is divided by the total number of taxa (N).

³ Defined as follows: M/S , where S is the lowest number of taxa in each of the two samples compared.

the samples is much larger than the other) will always be smaller (Hammer and Harper, 2006). Within the cluster analyses, both Jaccard and Dice similarity indices have been used and results compared. Dice's index¹ is somewhat less sensitive to differences in sample size than is Jaccard's index and, moreover, it puts more weight on matches than on mismatches (Hammer and Harper, 2006).

Finally, a parsimony analysis of endemism (PAE) was also performed. Considering the selachian taxa of an OGU as analogous to taxonomic characters in a phylogenetic context, shared genera between areas could possibly give us information about their palaeobiogeographical relationships, which are able to be represented in branching hierarchical trees or cladograms (Cecca, 2002; Seeling et al., 2004). Those taxa identified either as being found only in a single OGU (equivalent to autapomorphies) or occurring in all the geographical units (similar to plesiomorphic characters) have been removed for a better result, following recommendations of the mentioned authors. Thus, the genera matrix was reduced to 60 taxa. A sample locality lacking all the taxa (i.e. expressed as 0) was added as outgroup, representing either a locality back in time where none of the taxa in the UGOs had yet evolved or a hypothetical area where ecological factors prevented the occurrence of all taxa (Cecca, 2002). Because of the large number of characters used to calculate a most-parsimonious tree, a heuristic search using a TBR algorithm (tree bisection and reconnection) and Fitch optimization was applied. This allowed to find a limited number of trees in a reasonable computing time.

Raw data processing was carried out using Microsoft Office Excel 2007 and PAST v1.91 software (Hammer et al., 2001).

2.8 Photography and Illustrations

Photography is a very important issue in palaeontology since it serves to: 1) record working processes, 2) give objective documentation, and 3) provide a complementary visual description of the studied specimens. The widespread availability of digital cameras in recent times, combined with powerful photo editing software, has opened an opportunity for amateur photographers to capture inexpensive professional-like imaging for scientific purposes. And palaeontologists too can succeed in this technique by mastering camera controls and a few technical aspects of lighting.

Much of the material studied here was photographically recorded using different imaging techniques, depending on the sample's size. Generally, specimens up to about 10 mm were photographed with DSLR system cameras or compact digital cameras with good macro capabilities that do not compromise the depth of field. Different cameras have been used over time for studio and outdoor shooting, principally the Nikon D60 DSLR (equipped with lenses AF-S Nikkor 18–55 mm, Tamron 70–300 mm, and Micro-Nikkor AF-S 60 mm) and the Panasonic Lumix models DMC-FZ20 and DMC-LX7.

¹ Defined as follows: $2M/(2M+N)$. M (shared taxa); N (total number of taxa).

When doing macro photography for fossil description, the specimens are usually photographed on a flat piece of transparent glass, horizontally raised over the background and adequately lit (Scovil, 1996). This arrangement produces no shadows around the specimen and good contrast between fossil and background, which makes easier subsequent photo editing in the computer. Using a copy stand or a tripod is essential for still photography because it allows to hold the camera steady in long exposures. Alternatively, a clamp tripod attached to lab stand – a cheap alternative to commercial copy stands – can be used.

Another important aspect to consider in photography is lighting. Some good studio photographs can be taken using soft sunlight in the morning hours, provided there is access to a room with east facing windows. This is an interesting technical resource when promptness is a must; however, replacing natural lighting with artificial lamps enables a better control of the light. Traditional incandescent bulbs and halogen lamps have recently given way to LED lights that are also manufactured with daylight/cool white colour temperature of around 5,800° K. Thus, it is easy to get well-lit pictures with natural colour. LED lamps emit low heat emission (infrared radiation), and thus different effects of illumination could be tried to obtain a better shot without dealing with the discomfort of long work hours with incandescent lamps. Light sources may be placed by the side of specimen, and the light is counter balanced with a reflector. Tangential illumination (at low angle) helps to increase shadows and emphasises surface texture (Siveter, 1990). An aspect to consider is to use light diffusers, made of translucent velum paper, because they reduce undesirable glare and render uniform illumination.

Small-sized specimens were photographed by using a DFC228 digital camera fitted to an optical microscope Leica Wild M420 with a stand that allows either bright-field or dark-field illumination. A fibre optic illuminator was also used. Fibre illumination sources, which provide bright and cool illumination, may cause glare on enameloid surfaces (i.e. in the tooth crowns) and therefore the ends of the light pipes were fitted with light diffusers. The incandescent orange light of traditional fibre optic illuminators can be either blue-filtered or corrected with the digital camera's auto white balance to obtain natural tones, but a correct colour temperature is not essential when the final outcome is a monochrome picture.

Chondrichthyan microremains smaller than a few millimeters were selected for observation with a standard SEM microscope (JEOL JSM-6400 operating at an acceleration voltage of 20 kV) located at the Faculty of Science and Technology (University of the Basque Country, UPV/EHU). Such specimens were mounted on a 10 mm diameter specimen holder (metallic stub) and attached to its flat side with double-sided conductive carbon tape. Then, they were sputter coated with a thin layer of gold-palladium (Au/Pt) alloy to make them conductive and thus being able imaged by electron microscopy techniques. High-quality photographs, showing surface topography, were acquired using secondary electrons (SE). Additional pictures of gold-coated selachian specimens from Gometxa (Álava) were photographed at the Leioa

Campus of the University of the Basque Country (Analytical and High-Resolution Microscopy in Biomedicine – SGIker) using a Hitachi S-3400N-II variable pressure SEM microscope (VP-SEM) working at 15 kV, in low-vacuum and secondary electron (SE) imaging modes. Moreover, an uncoated fossil shark tooth from Albaina (Treviño County, Burgos), belonging to the family Triakidae (Fig. 3.7 in Chapter 3) was imaged at the Instituto de Carboquímica (CSIC - Zaragoza, Spain) using a Hitachi S-3400N VP-SEM equipped with an EDS detector, and its elemental composition in both dentine and enameloid surfaces was obtained. The advantage of using a VP-SEM system is that images can be obtained without having made the samples conductive (i.e. non-conductive samples do not need to be sputter coated with conductive films when imaging), and this is very interesting when dealing with scientifically valuable materials that need to be properly managed (e.g. fossil specimens from the type series).

Whitening specimens

When photographing fossil elasmobranch teeth, lighting control is important as the light reflects differently on crowns than it does on roots. Such light interactions are result of crystal structure differences in the bone tissues. Enameloid surfaces, such as those occurring in tooth crowns, reflect light in a specular direction (glossy appearance), whereas root surfaces simply become matt because light is scattered in all di-



Figure 2.17 Basic equipment for whitening fossils prior to photography. A, microscope slide for mounting the specimens; B, rubber hand pump; C, customized test tube with a hole at the end for heating ammonium chloride; D, double-ended spatula and spoon; E, lighter; F, Bunsen burner; G, ammonium chloride reactive.



Figure 2.18 Tooth of the Late Cretaceous batoid *Parapalaecobates pygmaeus* (Quaas, 1902) from Gometxa (Álava) photographed using a DFC228 digital camera and a Leica Wild M420 macroscope. A, untreated specimen; B, the same specimen whitened with ammonium chloride sublimate; C, B image converted to greyscale. Scale in mm.

reactions when hitting a less densely mineralised fossil tissue. To overcome the effects of such physical property, and thereby increase the contrast of morphological details, samples were whitened with ammonium chloride (NH_4Cl) sublimate (see Feldmann, 1989; Green, 2001; Villas and Herrera, 2001). The technique for coating fossils can be easily applied using simple equipment present in any palaeontology laboratory (Fig. 2.17). In the lack of fume hood, respiratory protective equipment (RPE) must be used, and work carried out in a well ventilated room because pungent ammonia and hydrogen chloride gases are released when burning ammonium chloride (Green, 2001).

The whitening procedure involves heating with a Bunsen burner a few grams of the reagent, which is placed in a modified test tube, until the sublimation completes. The ammonium chloride sublimate is projected out of the test tube using a rubber hand pump, coating the specimen surface with a white inert layer of tiny crystals. Specimens must be completely dry to produce a very subtle coating, and thus achieve the best photographic results (Fig. 2.18). Low relative humidity conditions (40–50% of RH) in the lab while taking photographs helps, because it allows more working time prior to the deliquescence of the ammonium sublimate. The coating technique was only used to illustrate specimens for greyscale printing.

Infographics and drawings

Digital photos, and digitised slides taken with a film camera, have been edited with Adobe Photoshop CS5.5, which is a powerful software package for image enhancement and correction. The image processing included, among other things, scaling, resolution setting, colour curve correction, image adjustment levels (and contrast), noise removal, figure rotation, plain background creation, and black and white conversion. Additionally, the Photoshop's lens correction filter was used to fix common optical errors (such as barrel distortion), specially when using the macro mode with a compact digital camera. Infographics and drawings were created with the vector drawing software Adobe Illustrator CS5.5.

2.9 Management of the elasmobranch collection

General considerations

Palaeontological collections are fundamental to our knowledge about the ancient life, and they can also be a potential source for new scientific discoveries. Museums and other public institutions having this type of collections have the legal and moral obligation of caring for them, and making them accessible to scientists. It is well known that the scientific research is based on proposed statements (hypotheses) that need to be tested, and an important matter during this process is the verification by other scientists. Essentially, taxonomic descriptions in the palaeontological literature are supported by the fossil specimens themselves. Without well-preserved specimens, the validation of the original investigation would be difficult or would only rely on printed texts.

Curating a palaeontological collection involves a workflow that begins with accessioning a particular fossil specimen, to which a unique identification number is given. Specimens must also be accompanied by any supporting information, not inherent to them, that will allow to link them to a particular geological horizon and locality. By not doing that, much of the scientific value of the collection may be lost or diminished, with the resulting limitations of its use.

Conservation of the specimens discussed in this thesis

The remains of fossil elasmobranchs and invertebrates collected in the region have been appropriately curated according to the museums standards (see Brunton et al., 1985; Paine, 1993). The purpose of this is to ensure that both specimens and information about them are available for future research. The documentation work included gathering of data not only from source documents (usually field notebooks), but also information about the fossils condition, conservation treatments or taxonomic attribution. All this was eventually keyed into the computer. For many years, the management needs of the palaeontology collection in the Museo de Ciencias Naturales de Álava have been addressed using the FileMaker Pro database platform because of its powerful, easy-to-use, general-purpose. To that end, I have been responsible for the development and maintenance of an easily updatable application program, called 'Paleontoteca*.fm12', to storage and retrieval of both scientific and administrative information (Fig. 2.19). The application is also provided with scripting tools to print file cards, specimen labels, lists, and catalogues, just to name a few (Fig. 2.20).

Good storage practice provides easy access to the collections. Different containers have been provided for that (i.e. specimen trays, plastic and cardboard boxes, and vials) before being stored in metal storage cabinets in the collections storage area. Many specimens have been arranged in lidded, divided polystyrene boxes, and each individual inner compartment was provided with polyethylene foam as bottom padding. Microscopic teeth and other fish remains have been put into small glass vials with cotton wool

The screenshot displays the 'Paleontoteca' application interface, which is a FileMaker Pro 13 tabbed interface. The main header shows 'MCNA - ANZM' and 'Formulario de Documentación de la Colección de Paleontología'. The interface is divided into several sections:

- Top Bar:** Includes navigation icons for 'Catalogo', 'Consultar registro', and 'Centro de Utilización'.
- Form Header:** Contains the specimen ID 'MCNA Caja fuerte' and '8281'. It also displays the specimen name 'Vascobella albatensis' and its location 'Albaina (Castell de Treviño) (Burgos), ESPAÑA'. A 'Holotype Figs. 10' label is present.
- Main Content Area:**
 - Left Panel:** Contains fields for 'Vascobella' and 'albatensis', and a reference to 'Cajavita & Corral, 1988'.
 - Right Panel:** Features a photograph of the fossil specimen, labeled 'A', with a scale bar indicating '1 mm' and '8281a.jpg'.
- Bottom Section:** Includes a 'Descripción' tab with fields for 'Dimensiones - longitud' (3.78 x 2.79 mm), 'Dimensiones - anchura', 'Dimensiones - profundidad', and 'Oriente lateral-anterior'. It also has a 'Material' field with 'Holotipo' and 'Conchales' listed.
- Footer:** Shows the user 'Josep Carmelo Corral' and the date '31/12/2007'.

Figure 2.19 FileMaker Pro 13 tabbed interface of the application 'Paleontoteca' used for managing the palaeontological collection in the Museo de Ciencias Naturales de Álava (MCNA).

stoppers. Those fossil specimens that are still embedded in matrix are kept in cardboard specimen boxes (Fig. 2.21). Type material (holotypes and paratypes) are isolated from the general collection and stored separately in a safe.

2.10 Special case: the preparation of a mosasaurid vertebra from Jauregi (Álava)

This singular fossil, which is extensively described in Chapter 18 of this thesis, was fortuitously discovered in 1995 in the hamlet of Jauregi (formerly known as Jáuregui), when prospecting for invertebrate fossils at the new exposures created during the construction of an irrigation reservoir (Corral et al., 2004).

 Museo de Ciencias Naturales de Álava Arabako Natur Zientzien Museoa Sarrats de Jexú, 28 01501 Vitoria-Gasteiz		Filum: Chordata Clase: Chondrichthyes Orden: Rajiformes Infraorden:	Suborden: Rhinobatoides Superfamilia: Familia: Rhinobatoides incert. Fam. Subfamilia:
Colectión de Paleontología			
Nº de inventario:	Nº Campo / ejemplares anteriores:	Ubicación:	Fecha de documentación:
MCNA 8281		MCNA Caja fuerte	31/12/1997
Estado: Tajado			
Holotipo Vascobatis albatensis CAPPETTA & CORRAL, 1999 Figurado			
Elemento anatóm.: Diente latero-anterior / Parte conservada: Completo Dimens. espesor.: 2,75 x 2,75 mm. Dimens. longitud.: Peso (g):			
Observaciones:	Conservación:	Ministración:	
Bibliografía: Cappetta, H. & Corral, J. C. (1999). Upper Maastrichtian Selachians from the Condado de Treviño (Basque-Cantabrian Basin, Northern Spain). <i>Est. Mus. Cienc. Nat. de Álava</i> 14(Núm. Espec. 1): 329-372 (Pag. 361, Placa 7, figs. 1a-d).			
Estratigrafía: Sistema: CRETACICO SUPERIOR - Piso: Maastrichtiense sup.			
Procedencia: Yacimiento: Albaina (Condado de Treviño) / Topónimo: Cantera de Echave Provincia: Burgos / Autonomía: Castilla y León / País: ESPAÑA			
Adquisición: Fuente: R / J. Carmelo Corral - Fecha de depósito: 25/01/1997 Legit.: J. Carmelo Corral, 25/01/1997			
			Colección: J. Carmelo Corral <small>Este ficha fue impresa el: 18/12/2011</small>



Figure 2.20 Material for documentation produced with the application FileMaker Pro 13 at the Museo de Ciencias Naturales de Álava. Examples of this includes an A-5 sized printed file card (above) with essential information about the sample, and an 45 x 37 mm sized specimen label (below) to be kept in the specimen container.



Figure 2.21 Different materials used to curate the elasmobranch collection (here is depicted a small part of the specimens). Cardboard storage boxes with lid and clear polystyrene boxes were employed. Small-size specimens are placed in either glass vials with cotton wool stoppers or foraminiferal microslides.

The fossil arrived to the lab broken to small pieces after being excavated from a large fossiliferous rock (Fig. 2.22, 2.23A). These fragments were unpacked with care from their parcels, brushed and washed away with a toothbrush, specially the rough contacting surfaces. During the mechanical preparation, most of marly matrix surrounding the bone was carefully removed under microscope using an aircscribe and mounted needles (pin vise). After thoroughly dried in air, the loose fragments were finally piece together with Paraloid B72 adhesive. Then, the remaining matrix was eliminated by immersing the vertebra in a buffered aqueous solution of 5% acetic acid (v/v), following the method indicated above. After repeated washing in deionized water to remove the soluble acetate salts, the specimen was allowed to fully dry and finally consolidated with a solution of 5% Paraloid B72 in toluene (w/v). Epoxy putty was used to strength a several zones in the neural arch that had become structurally weakened when the supporting matrix was dissolved.

During the chemical preparation of the vertebra, some noteworthy longitudinal punctures were revealed on the lateral surface of the centrum, which had pierced through the cortex and reached the spongy bone (partially filled by diagenetic pyrite) (Fig. 2.23B). The use of weak organic acid solutions is common practice for chemical preparation of fossilized bones, and as explained before; the technique gives very good results because the bone microstructure is retained by the selective action of the acid on carbonates.

Except for recent fractures caused during the collection of the specimen, the surface bone tissue was well preserved. Therefore, and as mechanical abrasion caused during the preparation of the fossil was discarded, the occurrence of these marks raised two possibilities: either possible cut marks left by an indeterminate object during the taphonomic reelaboration or a possible evidence of fossil predation. Such puncture damage is considered to have existed prior burial of the vertebra, since there is no evidence of resedimentation and reelaboration (*sensu* Fernández López, 1998) in other cooccurring invertebrate fossils such as ammonites, bivalves, gastropods, and echinoids (see full discussion in Chapter 18).



Figure 2.22 Vertebra of *Mosasaurinae* indet. collected in the Eguileta Member (upper Campanian) at Jauregi (Iruaiz-Gauna, Álava), MCNA 5354. The specimen broken into several pieces, as found. The centrum is indicated by the arrow.

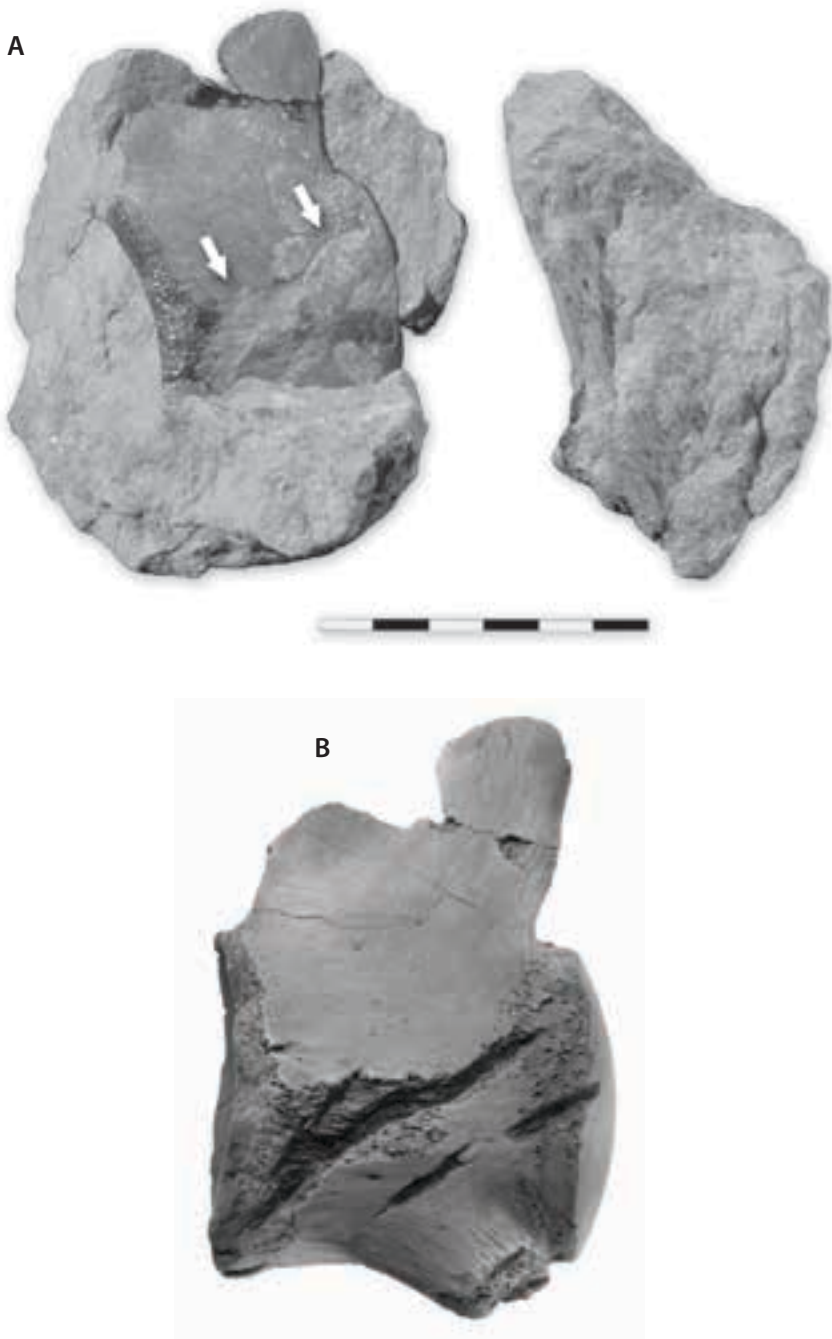


Figure 2.23 Mosasaurid vertebra from Jauregi, MCNA 5354. A, bone parts temporarily reassembled into the matrix before preparation (white arrows show the matrix-filled marks); B, the marks became evident on the bone surface after acid preparation of the specimen. Fossil preparation by the author. Scale in cm.

Chapter 3

AN OVERVIEW OF LIVING AND FOSSIL ELASMOBRANCHS

3.1 Introduction – What is an elasmobranch?

Sharks and their close relatives, the rays, are gnathostome vertebrates that belong to the taxonomic class Chondrichthyes¹ (subclass Elasmobranchii²). As the etymology of the word indicates, the members of this class are characterised by having a skeleton made up primarily of cartilage, which is lighter and more flexible than bone. However, some skeleton parts of them may be mineralised to a notable extent.

Other skeletal characteristics of these particular fishes, as reported by Compagno (1999a), include: (1) simple, boxlike neurocranium; (2) movable jaws, where there are numerous well-developed teeth lined in the upper and lower jaws; (3) differentiated functional and replacement tooth series; (4) hyostylic jaw suspension (in modern elasmobranchs, where jaws are supported only by the hyomandibular cartilage); (5) jointed hyoid and branchial arches; (6) vertebrae with calcified centra but having cartilaginous neural and hemal arches; and (7) placoid scales that form an outer skeleton. Moreover, (a) four to seven gill openings on both sides of the head, or located on the ventral surface; (b) the lack of lungs or swim bladders; (c) paired pectoral and pelvic fins; (d) unpaired dorsal and anal fins; (e) paired claspers (copulatory organs); (f) a caudal fin supported by the vertebral column; (g) preoral snout with nostrils; and (h) spiracles, or openings used in respiration, located just behind the eyes (found in bottom dwelling sharks and rays) are among other major anatomical features (Compagno, 1999a).

Classification of living elasmobranchs

The class Chondrichthyes is represented by the subclasses Elasmobranchii (elasmobranchs: sharks, skates, rays, and sawfishes) and Holocephali (holocephalans: chimaeras or ratfishes) (Fig. 3.1). They all share the presence of prismatically calcified cartilage in

¹ Chondrichthyes from the Greek *khóndros*, cartilage, and *ichthýs*, fish.

² Elasmobranchii from the Latin *elasma*, plate, and the Greek *bránchia*, gills (meaning plate-gilled).

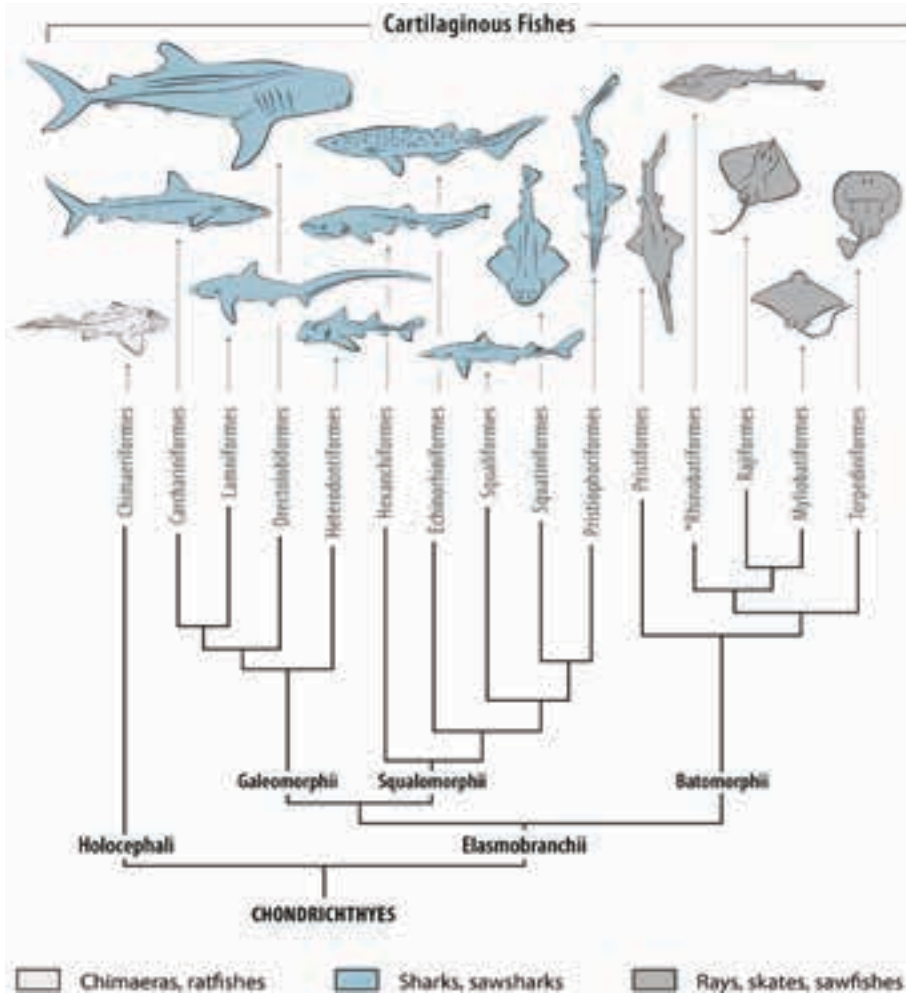


Figure 3.1 Relationships of living chondrichthyans (sharks and rays). Sharks data adapted from Maisey (2012), Maisey et al. (2004); batoid data adapted from Nishida (1990, in Cappetta, 2012). *Guitarfishes and the like are considered to constitute the order Rhinobatiformes in modern batoids, but their fossil taxa are placed in suborder Rhinobatoidei of Rajiformes (see Cappetta, 2012). Silhouettes not to scale.

the endocranium, visceral skeleton, vertebral column, and fin radials (Schultze, 1993). Undoubtedly, chondrichthyans are a diverse, successful group of fishes that occupy a wide array of marine and freshwater habitats, and represent an important component of the living vertebrates, numbering today more than 503 species of sharks, 699 species of rays, and 49 species of chimaeras (Klimley, 2013)¹.

¹ The classification of elasmobranchs is a matter of debate. Phylogenetic results based on molecular evidence and traditional morphological characteristics are not always coincident, not to say highly divergent.

The cohort Euselachii¹ (or true selachians) includes the extinct superorders Xenacanthiformes, Ctenacanthiformes, and Hybodontiformes – all presenting anal fins and two dorsal fins, each of them preceded by a single spine –, and all the elasmobranchs in the subcohort Neoselachii (both extant and immediate fossil relatives) (Guinot, 2011) (Fig. 3.2A). At the same time, Neoselachii is further subdivided into superorders Galeomorphii and Squalomorphii (both of which include the highly diverse group of sharks and its extant representatives), Squatinomorphii, and Batomorphii (which includes all fossil and living ray species and look alike forms).

Sharks of the superorder Galeomorphii, whose fusiform bodies make them good swimmers, are divided into the orders Carcharhiniformes (ground sharks), Lamniformes (mackerel sharks), Orectolobiformes (carpet sharks), and Heterodontiformes (bullhead sharks). The superorder Squalomorphii includes the orders Hexanchiformes (called cow and frilled sharks), Echinorhiniformes (bramble sharks), Squaliformes (dogfish sharks), Squatiniformes (angel sharks), and Pristiophoriformes (called sawsharks). Their anatomical descriptions, below provided, are mainly taken from Compagno (1999a) and Stevens (2005).

The distinctive anatomical features of the order Carcharhiniformes include a cylindrical to moderately depressed body, two dorsal fins, small to large paired pectoral and pelvic fins, one anal fin, and a heterocercal caudal fin (i.e. vertebral axis extending into the upper lobe of the tail). The head, which has five pairs of gill openings on either side, may be either conical or with lateral bladeliike expansions, as in Sphyrnidae (hammerhead sharks), which may help them to improve the sensory capabilities. This group of sharks have eyes with nictitating membranes.

Lamniform sharks have stout, fusiform bodies and conical to broadly round snouts. Mouth is subterminal in most of them. Five lateral gill slits are located on each side of the head. Moreover, two dorsal fins and one anal fin are present in their bodies. Paired pectoral fins vary from small to large and are much larger than the pelvic ones. All have heterocercal tails, whose upper lobe is remarkably long in members of the family Alopiidae (thresher sharks). Lateral keels may be present or absent, depending on the genera, in the area where the tail joins the body (caudal peduncle). The group includes the planktivorous sharks *Megachasma pelagios* Taylor, Compagno and Struhsaker, 1983 (megamouth shark) and *Cetorhinus maximus* (Gunnerus, 1765) (basking shark), which have numerous small teeth and elongated gill rakers.

The order Orectolobiformes includes sharks with a cylindrical to depressed body. They have generally a short mouth that are located in the anterior region of the head. Nostrils are connected to the mouth that may also bear small barbels. Five pairs of large gill openings are on the side of the head, in addition to small to very large spiracles. Two dorsal fins arise in the posterior half of the body. Pectoral fins are small to large, but generally are larger than the pelvic ones. All these sharks have anal fin. The caudal fin may

¹ Euselachii (cartilaginous fish) from the Greek *Eu*, true, good or original, and *selachos*, shark.

be heterocercal, as in many other sharks, or diphyrcercal, being linked to the rest of the body by a caudal peduncle, either keeled or not. The filter-feeder whale shark (*Rhincodon typus* Smith, 1828), which is the largest living fish species in the ocean being able to swallow plankton and small fish whole, is placed in this order.

The order Heterodontiformes includes small sharks that are characterised by a conical and elevated head with crests above the eyes. Mouth is short with labial furrows. They have pavement-like (molariform) posterior teeth that allow them to crush invertebrates. They also have five pairs of gill slits, small spiracles, and a cylindrical trunk that ends in a heterocercal caudal fin by means of a round peduncle. They also have two spined dorsal fins, and moderately large paddle-like paired pectoral fins. All of them possess anal fin.

The major diagnostic features of Hexanchiformes include a cylindrical, or elongated, trunk with a single dorsal fin located posteriorly, paired pectoral and pelvic fins, which are small to moderately large, and an anal fin. The caudal fin is heterocercal with a short ventral lobe. The caudal peduncle does not have ridges. Contrarily to other sharks, the hexanchiforms possess six to seven pairs of gill slits on each side of the head. The snout is short and varies from truncated to round. Spiracles are reduced. Teeth are cuspidate in the upper jaw but compressed, comb-like in the lower jaw.

Echinorhiniform sharks are characterised by having a stout, cylindrical body covered with thorns (i.e. a type of dermal denticles). The depressed head have five gill slits on each side, in addition to minute spiracles located well behind the eyes. These sharks also have two small dorsal fins, very posteriorly placed, but they lack anal fin. The paired pelvic fins are much larger than the pectoral ones. The body is connected to the heterocercal caudal fin by a sort caudal peduncle without lateral keels. Some authors do not recognize this order and prefer to include these rare sharks into the Squaliformes (Compagno, 1999a; Klimley, 2013).

The order Squaliformes includes sharks whose body is cylindrical-shaped with paired, small pelvic and pectoral fins. They also have paired dorsal fins with associated spines, although this characteristic may be secondarily lost in certain families. These sharks have no anal fin. Their caudal fins are heterocercal to diphyrcercal. Other anatomical features are preoral snouts approximately conical in shape but not excessively long, five pairs of gill slits located on each side of the head, and small spiracles.

Sharks of order Squatiniformes are characterised by a flattened, ray-like body with a very short snout and a wide frontal mouth. Teeth are needle-like. Squatiniforms bury themselves in the sand and hunt by ambush, leaping out at unsuspecting preys by snapping their jaws. Other external anatomical features of the group include expanded, paired pectoral fins, two dorsal fins on a stout tail, and a slightly hypocercal caudal fin. They lack anal fin. Moreover, these sharks are also distinguished by five pairs of gill openings, which are situated on their underside, spiracles behind the eyes, and large denticles (or thorns) arranged along the medial line of the body.

The order Pristiophoriformes includes sharks whose cylindrical body has two non-spinate dorsal fins and a barely heterocercal caudal fin. They also lack anal fin. The head

is depressed and possesses an elongated, heavy calcified saw-toothed rostrum, in each side of which a pair of long soft barbels (i.e. sensory organs) are formed. Five to six gill slits are located on each side of the head. These sharks have attached on each side of the rostrum many sharp rostral teeth, which alternate in size and length, being continuously replaced through life when lost.

The superorder Batomorphii¹ is thought to be monophyletic on the basis of highly corroborated synapomorphies (Cappetta, 2012), although there are different opinions among taxonomists with regards to its exact classification. Major living representatives of this group comprise the Pristiformes (sawfishes), Rhinobatiformes (Guitarfishes and shark-rays), Rajiformes (skates), Torpediniformes (electric rays), and Myliobatiformes (stingrays, eagle rays, manta rays), which are treated as orders following the works of Nishida (1990) and Compagno (1999a). However, Cappetta (2012) relegated some of them to a subordinal status within Rajiformes that would thus be represented by Rajoidei, Rhinobatoidei, Pristoidei, and the extinct Sclerorhynchoidei (see Fig. 3.1). The external anatomy of batomorphs differs from other elasmobranchs because of their dorsoventrally flattened body, which results from the fusion of the pectoral fins to the sides of the head. Batomorph fishes also have gill slits ventrally located, spiracles on the dorsal side, and both the wing-like tail and caudal fin are generally reduced.

The depressed body of the skates (order Rajiformes) has paired pectoral fins that expand to form a pectoral disc. Snout is elongate and strong. Some rajiform species may have two round dorsal fins relegated to the end part of the tail. Pelvic fins are divided (bilobate). Their tail is long and slender, being adorned with a dorsal line of denticles and large thorns located in the precaudal part. Caudal fins are small or vestigial. Modern skates are usually found on shallow sandy bottoms of the continental shelf.

The myliobatiform rays (order Myliobatiformes) have the pectoral fins either expanded to form a diamond-shaped body, as in Myliobatidae and Gymnuridae, or fused to the head to form a disc, as in Dasyatidae and Potamotrygonidae. Another anatomical feature is the paired spiracles on the top of the head, posteriorly to the eyes. Members of this order have a slender whip-like tail that may bear one to several barbed venomous stinging spines used for defence. However, tail spines in members of the plankton-feeder Mobulidae (devil rays) are small, and perhaps not functional (Compagno, 1999a).

The pristids (order Pristiformes) are rays with a long, blade-like snout (rostrum) edged on each side with spines (also called rostral teeth), giving it a saw-like appearance. However, the pristids are easily differentiated from sawsharks because the former have the gill slits located entirely on the ventral surface. Moreover, and unlike sawsharks, pristids have rostral teeth, of about similar size and equally spaced, that are firmly implanted in alveoli, where they grow continuously. Members of the extinct suborder Sclerorhynchoidei also had a saw-toothed snout. However, the attachment mechanism of the rostral spines found in these fish differed from that of pristids as the spines were

¹ Batomorphii (= Batoidea Compagno, 1973) from Greek *batis*, a kind of ray fish, and *morphos*, form.

joined by connective tissue to the sides of the rostrum, presenting a continuous replacement through life (Cappetta, 1987; Wüerger et al., 2009).

Guitarfishes and other closely related representatives (order Rhinobatiformes), have a elongated preoral snout (i.e. long flat rostral cartilages) and a flattened trunk covered with denticles or thorns, some of which are lined along the body. The moderate-sized pectoral fins form an angular to round pectoral disc. In addition, they also have two moderate-sized round to angular dorsal fins, depending of the species, confined to the hind part of the body. Pelvic fins are not divided. Their body is followed by a long tail, stouter in the precaudal part, whose caudal fin is weakly heterocercal.

Batoids with paired bioelectric organs involved in self-defence or hunting, which are located between the head and the pectoral fins, are included in the order Torpediniformes. Other additional anatomical features in this order include a thick depressed body, enlarged pectoral fins to form an extended pectoral disc, one or two moderately large round dorsal fins, and pelvic fins separated into anterior and posterior lobes.

A general overview of the Elasmobranchii fossil record

The presence of isolated dermal denticles in chondrichthyans supports the view that they form an ancient lineage dating back to the late Ordovician (Guinot, 2011). However, other hard body parts of these fishes such as the multicusped teeth and skeletons did not occur until later in the geological record, near the Lower Devonian (Botella et al., 2009; Martínez-Pérez et al., 2010, and references therein; Miller et al., 2003).

The long evolutionary history of primitive sharks (Fig. 3.2) has been discussed by Carroll (1988), Benton (2004), and Klimley (2013); a short description is given below. The extinct orders of primitive sharks Cladoselachiformes and Symmoriiformes from the Upper Devonian are among the basal elasmobranchs. *Cladoselache* sharks are characterised by an elongated body with the mouth located at the front of the head – in contrast to a subterminal position in modern sharks – and were well adapted to swallowing small fishes due to this jaw architecture. Cladoselachiform fossils are not found after the Devonian. Two families of Carboniferous spined sharks, stethacanthids and falcathids, are among the symmoriidans. Like cladoselachids, symmoriidans have multicusped teeth (or cladodont type) suitable for grasping and swallowing whole preys. But the most striking feature in Symmoriiformes is a long shelf-like spine located dorsally on the head, whose function is not completely understood.

The members of Xenacanthiformes originated in the Devonian and persisted until their extinction at the end of the Triassic. These fishes are easily recognised by their distinctive teeth consisting of a large base bearing two large and laterally directed cusps, larger than the median little button (termed '*Diplodus*' type; see Carroll, 1988). Moreover, some specimens, such as *Xenacanthus*, have a symmetrical narrow diphyccercal tail. The group is most predominantly freshwater.

Ctenacanthiformes is the most basal order of Euselachii (Carroll, 1988). Mem-

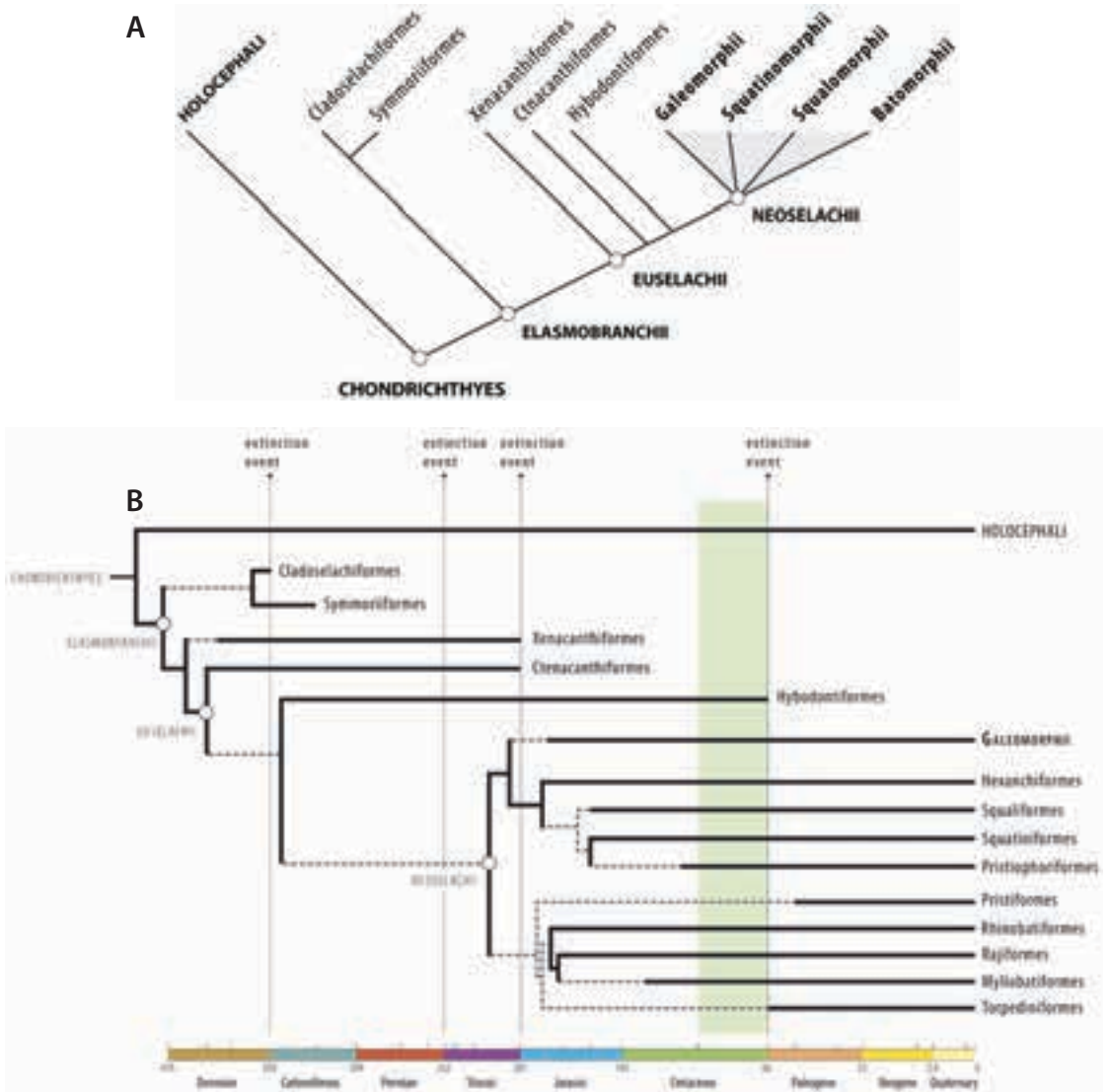


Figure 3.2 A, hypothetical phylogeny of chondrichthyans (redrawn and simplified from Guinot, 2011), neoselachians are highlighted in grey colour; B, cladogram of the evolutionary relationships of the chondrichthyans through geological time (based on data from Benton, 2004 and Cappetta, 2012). Notes: the Upper Cretaceous is highlighted in pale green; the order Echinorhiniformes is not considered here.

bers of this order, which exhibit many characteristics of the modern sharks, were most common at the end of the Carboniferous, but lasted until the end of the Triassic period (Carroll, 1988; Klimley, 2013). They have, like other primitive sharks, a terminal mouth and multicusped teeth (i.e. cladodont-type); but the novelty is the presence of two dorsal fin spines made of dentine and decorated with an outer mantle of enameloid

denticles, which indicate that these spines were exposed superficially (Carroll, 1988). Moreover, these selachians also had the surface of the body covered with dermal denticles, and not only limited to certain parts of it.

Hybodontiformes is an extinct order of fossil sharks considered to be the sister group of all neoselachians (Cappetta, 2012). Hybodontid sharks became common in the Carboniferous and Permian and rapidly diversified in the Triassic, after the Permian extinction. They were the dominant sharks in the seas of the Northern Hemisphere (i.e. Europe and North America) during the Jurassic, and advanced hybodonts survived into the Upper Cretaceous together with the neoselachians (Benton, 2004). Members of this group possess cephalic spines and fin spines of trabecular dentine decorated with denticles (see hard tissues in the next section). The hybodontid heterodont dentition, in which teeth have different functions, evidences some degree of feeding specialization. Their anterior teeth, with which they seized fish, molluscs, and crustaceans, have pointed cusps flanked by smaller cusplets, while the pavement-like posterior teeth were most effective in crushing the aliment (Klimley, 2013). Although Hybodontiformes was essentially a marine group of likely sluggish, demersal swimmers, some species also became adapted to freshwater settings (Benton, 2004). They had a heterocercal tail (like neoselachians), which is thought to produce lift in addition to thrust.

The widening and extension of epicontinental shelves over most of western Europe and North America during the end of the Triassic period (Rhaetian transgression) marked the onset of a major radiation and diversification of the Neoselachii, and also showed their adaptability to fill new empty niches in shelfal, open marine, lagoonal, and freshwater habitats (Cuny and Benton 1999; Klimley, 2013). Neoselachian fishes, which likely originated from Triassic ctenacanths, presented more efficient feeding and locomotion structures and enhanced sensory capabilities, including larger brains, than precedent shark groups (Carroll, 1988). Furthermore, the presence of calcified vertebral centra, which is a derived character of the clade, is an anatomical novelty that improved their swimming abilities for dispersal, also easing the pursue and capture of preys. The teeth of early neoselachians are basically cladodont-type.

Neoselachians have been the dominant elasmobranchs through much of the Mesozoic and Cenozoic until the present time. They are known from as long ago as the lower Triassic (e.g. teeth of *Palidiplospinax* and *Synechodus* of the family Palaeospinacidae), but they were relatively rare until the Early Jurassic times (Underwood, 2006). They diversified rapidly (both taxonomically and geographically) throughout the Jurassic and Cretaceous periods, although their diversity is much better known in the Cretaceous (see Cappetta, 2012). Numerous neoselachian remains have been reported by the end of the Lower Cretaceous, representing many families of squaliforms (e.g. Squalidae), carcharhiniforms (e.g. subfamilies Pteroscylinae and Scyliorhininae and some genera of Scyliorhinidae, Triakidae), lamnids (e.g. Anacoracidae, Cretoxyrinidae, Mitsukurinidae, and Odontaspidae), orectolobiforms (e.g. Ginglymostomatidae), and sclerorhynchiforms (e.g. Sclerorhynchidae).

The first evidence for moderately large lamnid teeth was in the Aptian, and the Albian represents the earliest time period with tooth assemblages recorded from a wide range of palaeoenvironments across several continents (from offshore to marginal marine depositional settings), according to Underwood (2006). The Late Cretaceous was a time of high diversity of neritic sharks occurring in many families of Squaliformes (e.g. Centrophoridae, Dalatiidae, Etmopteridae, Oxynotidae, and Somniosidae), Carcharhiniformes (e.g. *Archaeotriakis*, *Palaeogaleus*, *Paratriakis*, and *Squatigaleus* of the family Triakidae), and several batoids (e.g. Hypsobatidae, Gymnuridae, Myliobatidae, Platyrhinidae, Rajidae, and Rhombodontidae).

It has long been assumed that neoselachians form a monophyletic group falling into five main clades: the galeomorphs, the hexanchiforms, the squaliforms, the squatiniforms, and the batoids (Benton, 2004). In this regard, there is much controversy about the systematic position of batoids (rays and skates). Morphological data suggest that batoids are derived selachians, whereas molecular analyses highlight that they represent the basal sister group of sharks within the Neoselachii clade, as represented in many phylogenetic trees of living neoselachians (Fig. 3.1) (see also Underwood, 2006).

3.2 Endoskeleton

The endoskeleton of elasmobranchs broadly includes the skull, the vertebral column and other hard elements of the appendicular skeleton that support the fins (Compagno, 1999b). Many skeletal parts are composed of hyaline cartilage, although some others may be as densely mineralised as bone tissues in other vertebrates. In the words of Hall (2005: 41) “cartilaginous fishes or elasmobranchs have to do with cartilage what other vertebrates do with bone.”

The neurocranium (or chondrocranium) is the box-shaped portion of the skull that contains the brain and the sense organs (Fig. 3.3). It supports the splanchnocranium (or visceral skeleton), which is the part of the skull that includes the mandibular arch (Fig. 3.4), the hyoid arch, and 5 to 7 branchial arches (Cappetta, 1987). The mandibular arch of elasmobranchs is formed by the paired palatoquadrates, dorsally, and the Meckel’s cartilages, ventrally. The palatoquadrates, or upper jaw, are attached to the neurocranium by ligaments and other connective tissue. They articulate below with the Meckel’s cartilages, or lower jaw, just behind the skull (Klimley, 2013). The anteromedial end of the palatoquadrates, as also does the Meckel’s cartilages, articulate mesially with each other at the midline (symphysis) in most sharks and batoids, but the jaw mobility is lost in those myliobatoids adapted for durophagy (e.g. eagle and cow-nose rays with short, heavy jaws, and massive tooth plates) or to plankton feeding (e.g. devil rays with elongated jaws) (Compagno, 1999b). Elasmobranchs exhibit a hyostylic jaw suspension because the hyomandibula articulates with the palatoquadrate to some degree (Schultze, 1993).

The neurocranium, jaws, and axial skeleton are covered with a layer of calcified plates or *tesserae* to strengthen them. Large predatory species of sharks have developed

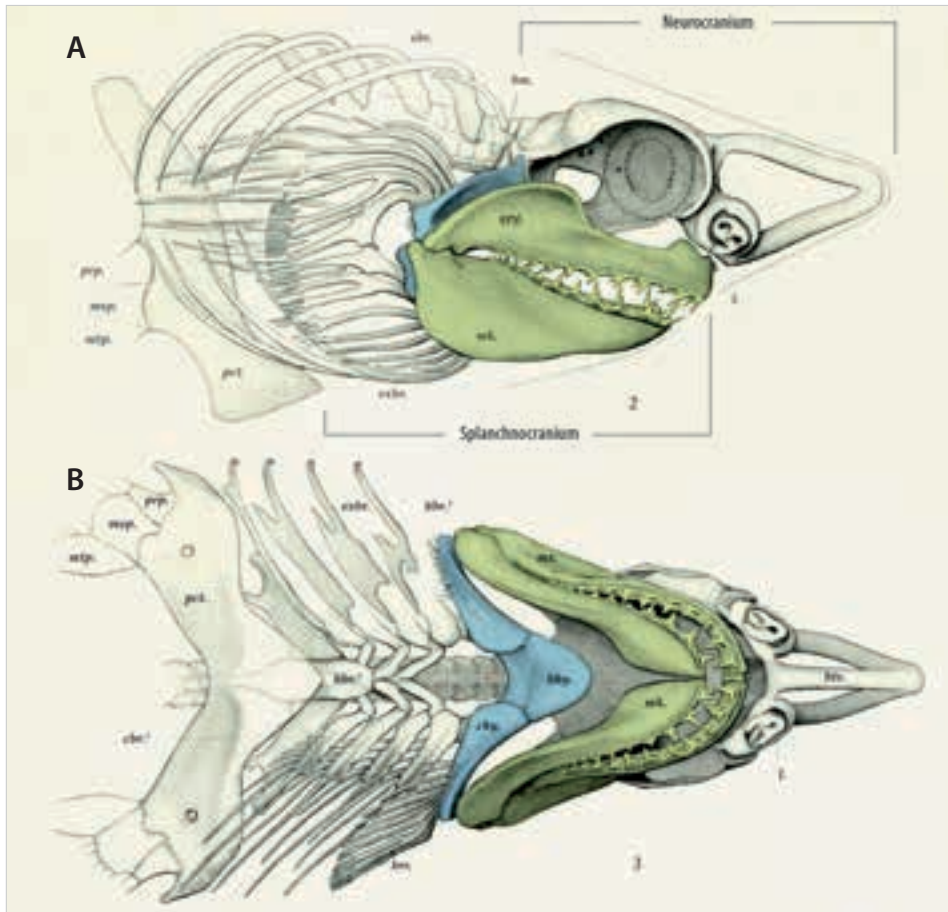


Figure 3.3 Skull, jaws, teeth, branchial cartilages, vertebrae, and shoulder girdle of a Recent porbeagle shark *Lamna nasus* (Bonnaterre, 1788): A, lateral view; B, ventral view (adapted from Garman, 1913; source: www.biodiversitylibrary.org). Mandibular and hyoid arches are highlighted in green and blue colours respectively. Selected abbreviations: bhy; basihyoid; chy, ceratohyoid; hm, hyomandibula; mk, Meckel's cartilage; ppg, palatoquadrate.

several layers of *tesserae* (see below) in the mandibular arch to provide it added support and strength when biting preys' bones, or to deal with the highly demanding adaptations to a durophagous feeding mode (Dean and Summers, 2006; Klimley, 2013). Elongation of the rostral process occurs within different neoselachian groups, namely Mitsukurinidae (Lamniformes) and Rhinobatidae (Rhinobatiformes), but only in sawsharks (Squalimorphii: Pristiophoriformes) and sawfishes (Batomorphii: Pristiformes and the extinct Sclerorhynchoidei within Rajiformes) the rostrum is heavily calcified and armed with spines (also called rostral teeth). The axial skeleton supports the body and is composed of a series of cylindrical vertebrae (Fig. 3.5A, above), which runs in



Figure 3.4 Mandibular arches of the extant long fin mako *Isurus paucus* Guitart, 1966 (left) and the tiger shark *Galeocerdo cuvier* (Peron and Lesueur, in Lesueur, 1822) (right); photograph by the author at the Reef HQ Aquarium, Townsville, Australia.

straight line from the occiput of the neurocranium to the upper lobe of the caudal fin, the appendicular skeleton, and the fins (Cappetta, 1987). Chondrichthyes have amphicelous vertebrae. This means that their vertebral centrum is formed by a calcified double cone named *corpus calcareum*, where the cartilaginous neural (above the centrum) and the hemal (below the centrum) arches are inserted.

Cartilaginous skeleton

Cartilage is a supporting elastic skeletal tissue, much lighter than bone, which may or may not mineralise. It is deposited by cartilage-forming cells (i.e. chondrocytes) in an extracellular matrix (ECM) surrounded by a fibrous membrane called perichondrium (Dean and Summers, 2006). According to these authors there are three types of calcification in supporting tissues: (a) areolar calcification, a compact densely calcified tissue that occurs in the vertebral centra of most cartilaginous fishes; (b) prismatic calcification, which is always perichondrally associated; and (c) globular calcification, formed by minute spherules of hydroxyapatite fused together. Prismatic and globular calcification is produced by deposition of crystallites of calcium phosphate (hydroxyapatite) in the ECM. Dean and Summers (2006) also show that all three calcification types occur in vertebral cartilage in this way: (a) in the areolar cartilage present in the centrum of vertebrae; (b) in neural/hemal arches formed by uncalcified cartilage sheathed with *tesserae* (see below); and (c) on the outer surface of the centra, where globular calcification may also be present. Other skeletal elements of chondrichthyan fishes, except the vertebrae, are mainly composed of hyaline cartilage that is covered with a thin layer of

denser and stiffer prismatic cartilage or calcified tissue called *tesserae* (Klimley, 2013). These are blocks of mineralised tissue arranged in a continuous mosaic between the outer perichondrium and the inner uncalcified core (Dean and Summers, 2006).

3.3 Exoskeleton

The skin of most elasmobranchs is covered with an investiture of non overlapping scales termed placoid scales (Kemp, 1999). In addition to these elements, oral teeth (restricted to the margins of jaw cartilages), fin and cephalic spines, rostral teeth, and tail spines are part of the elasmobranch exoskeleton (Cappetta, 1987) (see some examples in Fig. 3.5). They all are made up of hard, mineralised tissue that preserves well, explaining thus their relative abundance in the fossil record.

Elasmobranchs have a varied dentition, both in size and form, whose distinctive morphological characters are significantly varied to allow species identification. The basic structure of an oral tooth in sharks is a main cusp that may be flanked by other ones of minor size (i.e. cusplets). However, skates and rays have their jaws equipped with modified (flattened) crushing or grinding teeth to feed on hard-shelled invertebrates.

Tooth morphogenesis

It is now believed that oral teeth probably derived from dermal denticles (Cappetta, 1987; Compagno, 1999b) and consequently are part of the exoskeleton. Elasmobranchs have polyphyodont dentition, which means that they can replace the teeth continuously

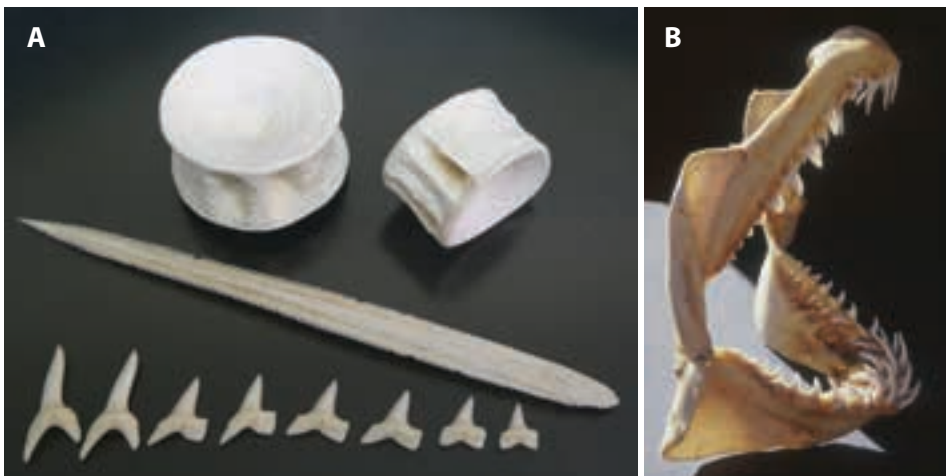


Figure 3.5 A, skeletal elements of some modern elasmobranchs: two vertebrae of an undetermined lamniform (above), a tail spine of a common stingray *Dasyatis pastinaca* (Linnaeus, 1758) (middle), and teeth of a lamniform shark (*Isurus oxyrinchus* Rafinesque, 1810) (below); length of the tail stinger 140 mm. B, mandibular arch of *Isurus oxyrinchus*, note the translucent cartilage of the jaws; the height is 260 mm.

in their life time. The teeth begin to develop along the inner end or the dental lamina, which is an infolding of epithelial tissue derived from the ectoderm on the buccal side of the jaw cartilage (according to Kemp, 1999). The teeth in different developmental stages are anchored in the perichondral connective tissue, which covers the inner (buccal) face of the jaws' cartilages (Kemp, 1999). Non-erect teeth are moved to the edge of the jaw, like a conveyor belt, to replace those shed or lost during feeding and defence (Cappetta,

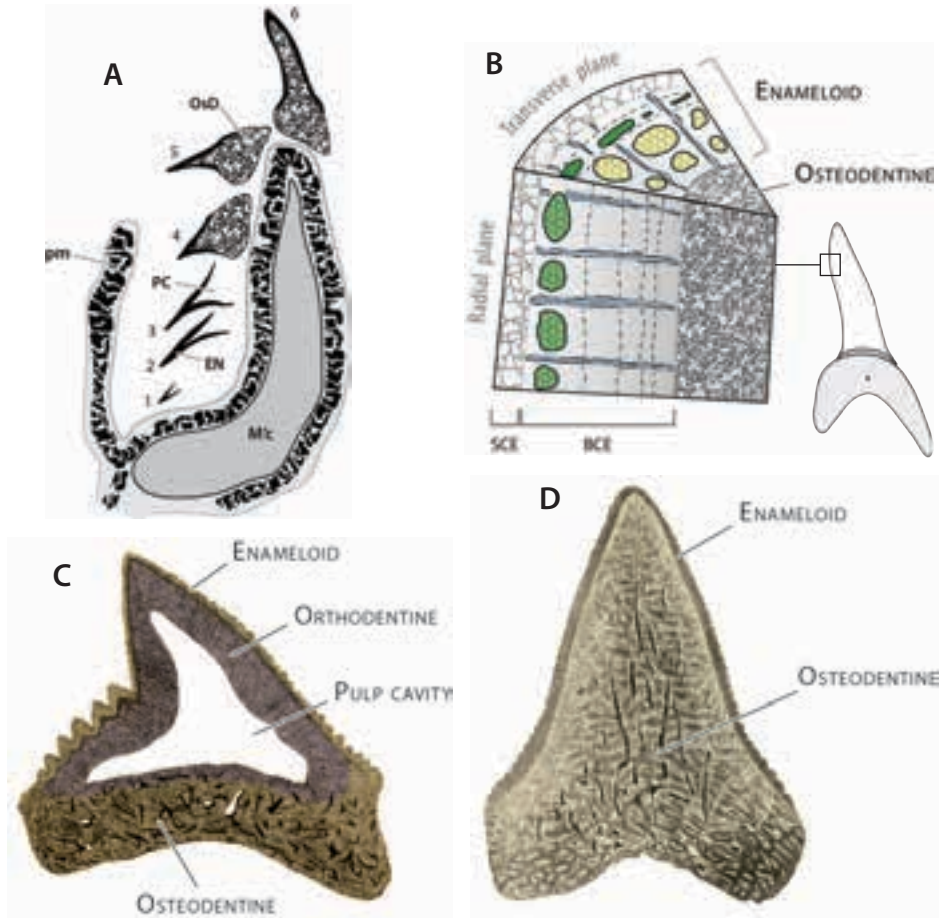


Figure 3.6 A, diagrammatic sagittal section of a shark jaw (*Isurus oxyrinchus* Rafinesque 1810) showing a file of teeth at successive stages of growth, redrawn with changes from Miake et al. (1991); B, diagrammatic section of the crown of an *Isurus oxyrinchus* tooth showing the arrangement of crystallite bundles (based on Enax et al., 2014); C–D, mesiodistal sections showing the general arrangement of hard tissues: orthodont histotype (C) in *Galeocerdo capellini* Lawley, 1876, and osteodont histotype (D) in *Carcharodon carcharias* (Linnaeus, 1758) (adapted from Lawley, 1881; source: www.biodiversitylibrary.org). Abbreviations: 1–6, teeth in different developmental stages; BCE, bundled crystallite enameloid; EN, enameloid; M'c, Meckel's cartilage; OsD, osteodentine; PC, pulp cavity; pm, protective membrane; SCE, single crystallite enameloid.

1987; Schultze, 1993). In other words, such replacement teeth are continuously emerging to reach a terminal functional state (Fig. 3.6A). The duration of the functional dentition varies, and not all the teeth are shed at the same time. This replacement rate appears to be more rapid during early stages of the shark life, caused by ontogenetic growth of the individuals and the need of filling the gaps in a larger growing jaw (Luer et al., 1990).

Tooth histology and composition

Different types of mineralised tissues are observed in fish teeth (Lund et al., 1992; Cappetta, 2012; Enault et al., 2015; Moyer et al., 2015), but only three of them, whose characteristics are presented below, are present in elasmobranchs. These types may be grouped into two basic varieties: (1) the enameloid, the hard outer covering of the tooth; and (2) the dentines (i.e. orthodentine and osteodentine), which form the internal supporting structure of the tooth (Fig. 3.6). Notably, the basic ultrastructure of the teeth in both fossil and living sharks is almost identical (Lübke et al., 2015).

At histological level, there can be two types of mineralised tissue arrangement: (1) orthodont (Fig. 3.6C); and (2) osteodont (Fig. 3.6D) (Cappetta, 1987; Moyer et al., 2015). The orthodont histotype is characterised by retaining a pulp cavity, which is surrounded by thick orthodentine from the earliest stages and throughout the full development of the tooth. On the contrary, the osteodont histotype lacks the hollow pulp cavity, and only osteodentine fills the core of the crown.

Calcium hydroxyapatite (HA) is the dominant phase of biological apatites, with the formula $\text{Ca}_5(\text{PO}_4)_3\text{OH}$ in which Ca^{2+} is partially substituted by Na^+ , Mg^{+2} , Sr^{+2} , K^+ , and some trace elements. Moreover, the partial substitution of F^- for OH^- may also occur. Both enamel and dentine in elasmobranch teeth are formed by fluorapatite (FA) [$\text{Ca}_5(\text{PO}_4)_3\text{F}$], which is deposited as elongated crystallites with different structural organization, according to Lübke et al. (2015). These authors also demonstrated that the fluoride content in both fossil orthodentine and enameloid is high and in similar concentrations, contrarily to what happens in living shark teeth, in which high fluoride values only occur in the enameloid layer. Moreover, the fluorine content in tooth enameloid is considered, a priori, a constituent element of the bioapatite during the formation of the teeth rather than a differential fluoride (F^-) uptake during diagenesis. The EDS analysis (energy-dispersive X-ray spectroscopy) carried out on a triakid shark tooth from Albaina (Treviño County, Burgos) shows values that are consistent with those that might be expected within living sharks (Fig. 3.7, and quantitative results in Tables 3.1 and 3.2). The fluorine values in the enameloid of the crown along with cosubstituted essential trace elements (Na, Mg) are consistent with expected substitutions in pure HA, but further analytical methods are required to discern if the phase mineral in this case is either fluorapatite or a carbonate-rich fluorapatite (i.e. francolite).

Tooth crowns in sharks are very resistant to abrasion. Nanoindentation and Vicker's microhardness tests made by Enax et al. (2012) on teeth of the living species *Isu-*

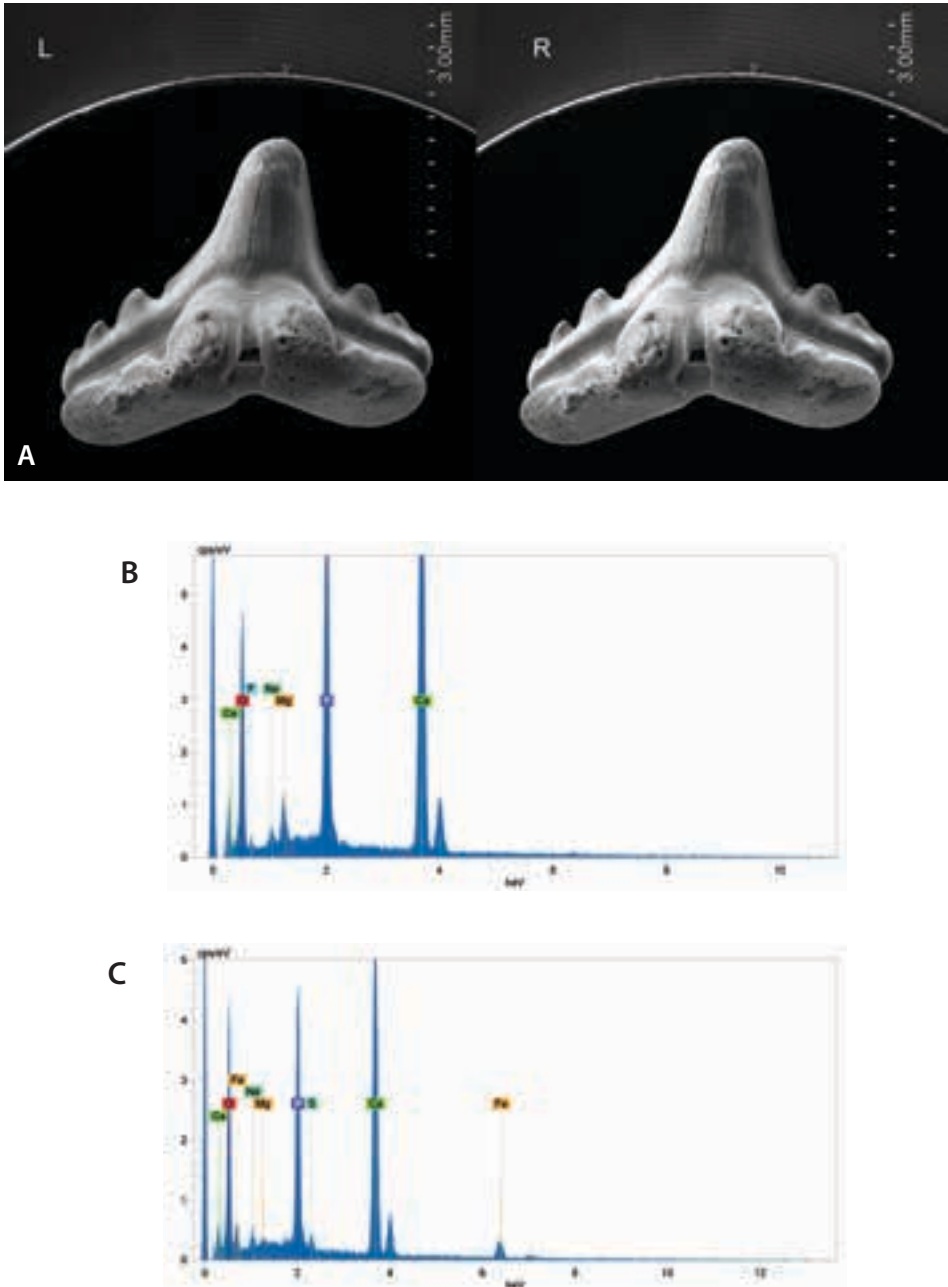


Figure 3.7 A, VP-SEM stereo photo pair in lingual view of a lateral tooth of *Palaeogaleus faujasi* (Geyn, 1937) from the Maastrichtian of Albaina (Treviño County, Burgos), MCNA 14998; B, energy-dispersive X-ray spectroscopy (EDS) results in the same specimen showing the elemental spectrum of the enameloid surface of the crown; C, EDS results in the same specimen showing the elemental spectrum of the osteodentine surface of the root. Note the presence of fluorine (F) in the enameloid tissue.

Table 3.1 Quantitative results in EDS analysis for the principal elements on fossil enameloid (from the specimen in the figure 3.7).

Element	Atomic No.	Series	unn. C [wt. %]	norm. C [wt. %]	Atom. C [at. %]	Error [%]
O	8	K-series	36.92	39.38	55.68	6.8
Ca	20	K-series	32.30	34.46	19.45	3.1
P	15	K-series	11.72	12.51	9.13	1.0
F	9	K-series	10.86	11.59	13.80	7.3
Mg	12	K-series	1.44	1.53	1.43	0.5
Na	11	K-series	0.50	0.53	0.52	0.6

Total: 93.7%

Table 3.2 Quantitative results in EDS analysis for the principal elements on fossil osteodentine (from the specimen in the figure 3.7).

Element	Atomic No.	Series	unn. C [wt. %]	norm. C [wt. %]	Atom. C [at. %]	Error [%]
O	8	K-series	43.45	48.62	69.46	7.9
Ca	20	K-series	29.67	33.20	18.93	3.4
P	15	K-series	9.08	10.16	7.50	0.9
Fe	26	K-series	5.58	6.25	2.56	2.4
Na	11	K-series	0.76	0.85	0.85	0.6
S	16	K-series	0.60	0.67	0.48	0.7
Mg	12	K-series	0.22	0.24	0.23	0.4

Total: 89.4%

Note: **unn. C [wt.%]**, unnormalised concentration in weight percentage of the element; **norm. C [wt.%]**, normalised concentration in weight percentage of the element; **C Atom. [at.%]**, atomic weight percentage.

rus oxyrinchus Rafinesque, 1810 and *Galeocerdo cuvier* (Peron and Lesueur, in Lesueur, 1822) show that enameloid is about six times harder than dentines. This was explained by the different proportion of mineral content and their structural organization.

A brief summary of the principal facts of the dental tissues is provided below:

Enameloid. This is a glossy, highly mineralised tissue that forms the outer surface of the dental and scale crowns. It is known to occur in fossil Agnatha and Gnathostomata (Placodermi, many Chondrichthyes, and Actinopterygii), according to Lund et al. (1992). Many authors consider that enameloid is derived from ectoderm and mesenchyme cells (Cappetta, 2012; Enax et al., 2014; Lübke et al., 2015; Lund et al., 1992; Moyer et al., 2015), and therefore, it differentiates itself from the enamel of higher vertebrates, which is only an ectodermal product. A discussion of the ultrastructure and chemical composition of the enameloid has been given recently by Enault et al. (2015), Enax et al. (2014), and Lübke et al. (2015). In general, the ultrastructure of the enameloid is almost identical in both fossil and recent teeth of sharks.

The fully-formed neoselachian enameloid is shown as having three layers (Enax et al., 2014), which is a synapomorphic feature that differentiates neoselachians from their sister group Hybodontidae and other extinct basal chondrichthyes (Enault et al.,

2015). These layers are, from the outside inward: (1) a very thin surface lamina named shiny-layered enameloid (SLE); (2) a parallel-bundled enameloid (PBE); and (3) a tangled-bundled enameloid (TBE). However, in structural terms, only two layers may be considered: (1) an outer shiny layer with a random structure, called single crystallite enameloid (SCE); and (2) an inner bundled crystallite enameloid layer (BCE) formed by axially oriented bundles that are interlocked by other perpendicular ribbon-shaped radial bundles, the latter normally oriented to the crown surface (Enax et al., 2014; Enault et al., 2015) (Fig. 3.6B).

In sharks, the overall tooth size is limited by the enameloid layer, which always mineralises before the dentine is formed (Lund et al., 1992; Moyer et al., 2015) (see Fig. 3.6A). After mineralization, the enameloid is not remodelled and the tooth only increases in thickness by adding orthodentine at the expense of the soft tissue of the pulp cavity (Kemp, 1999).

Enameloid studies among batomorph taxa are, however, still in their infancy, but it seems that the triple-layered enameloid structure is lacking (Enault et al., 2015).

Similar arrangement of the enameloid layers occurs in orthodont and osteodont histotypes, according to Moyer et al. (2015), but the differences in the dentine–enameloid junction (DEJ) are significant. Thus, a sharp DEJ is observed in the orthodont *Prionace*, but the junction is less regular in the osteodont histotype [as seen in *Carcharodon carcharias* (Linnaeus, 1758) and other lamniforms], with extensions of osteodentine entering into the inner TBE layer.

Batomorph teeth are microstructurally more complex than previously assumed. Most of their tooth crowns are adapted for crushing and grinding (as in *Rhombodus* spp.), displaying a single SCE unit over a well-developed dentine, which is in coincidence with the traditional idea of enameloid microstructure (Enault et al., 2015).

Orthodentine. This is a bone-like mineralised tissue that occurs bordering the hollow intracoronal pulp cavity of the tooth, being usually capped by a hypermineralised layer of enameloid (Cappetta, 1986; Kemp, 1999). During its formation, the pulp cavity decreases as needle-like crystals of hydroxyapatite are deposited within an organic matrix containing collagen fibres (Kemp, 1999). This dental tissue is considerably softer than the enameloid. The transition from orthodentine to root osteodentine (OsD, read below) is apparent due to differences in texture (Moyer et al., 2015). These authors also noted that orthodentine (as seen in sharks of the genus *Prionace*) shows circumferential lines around the pulp cavity, called ‘*lines of Owen*’, which arise from oscillations on dentinal deposition in the teeth (Moyer et al., 2015).

Osteodentine. The root of the teeth and the basal plates in dermal denticles consist of this spongy-like dentine (OsD), which has been also called trabecular dentine (Cappetta, 2012). This dentinal tissue contains numerous coarse canals that are either divergently branched or traverse to the long axis, and they also anastomose reticularly (Lund et al., 1992). During the development of a osteodont-type tooth, OsD fills the already formed

enameloid crown (from the apex towards the root that is lacking in the early stages of the tooth development), as stated in Moyer et al. (2015). The tooth is ready to erupt through the oral mucosa when mineralization completes to form a single mass. OsD in orthodont-type teeth (e.g. as in *Prionace*) is basically relegated to the root, and it starts to appear simultaneously with the formation of the enameloid crown (Moyer et al., 2015).

Dental characters

The taxonomic classification of isolated elasmobranch teeth is largely based on their dental characters (Fig. 3.8). Firstly, a tooth has a bony base (root) and a crown, the latter being covered by enameloid. When the crown is pointed, as in sharks, it is named cusp and very often it become the more durable component of the tooth. The cusp can be slender with an acute apex, or flattened into a blade-like shape. The surface of the cusp can be smooth in the selachian teeth, but it may also bears folds and vertical ridges, either on the lingual side or the labial side, or in both. The cusp itself has two cutting edges, called mesial and distal, which are arched to some extent. Several types of cutting edges may occur in the cusp, namely continuous, crenate, sinuate, irregular dentate or any variant of them (Fig. 3.9). Moreover, small accessory cusplets, whose number and shape varies among particular groups (e.g. fang-like appearance in odontaspids or triangular shaped in otodontids) can occur on each side of the main cusp. Exception is used to describe the serrated crowns of hexanchid teeth. Thus, the primary cusp is termed acrocone and conules is used instead smaller, accessory cusps. Many batomorph teeth are characterised by presenting pavement-like cusps (see *Rhombodus* tooth in Fig. 3.8), a feature associated with a particular feeding habit.

The root is the portion of the tooth – opposite to the crown – that is attached to the jaw cartilage by connective tissue. The constricted band between the crown and the root in shark teeth is usually termed neck. Important diagnostic characters in the root for species-level identification are the presence (or absence) of foramina, lingual protuberances (also called median boss), nutritive grooves, and the shape of the root lobes itself.

Shark teeth are organised in files and rows (following the terminology of Cappetta, 2012; Moyer et al., 2015). A row includes a series of teeth in the same stage of growth with different positions in the jaw from the symphysis to the commissure (i.e. they are mesiodistally arranged). A file includes all the teeth in different stages of formation and calcification that have the same position across the jaw cartilage, varying from a non-functional (replacement teeth) to a functional condition (see Fig. 3.10).

Tooth diversity and orientation

Elasmobranch teeth exhibit different shapes depending on their position in the jaws, what is known as heterodont dentition (Cappetta, 1986, 1987; Welton and Farish, 1993). Gradual differences in tooth morphology (monognathic heterodonty) can occur along the dental rows (series), which as mentioned above is the sequence of all the

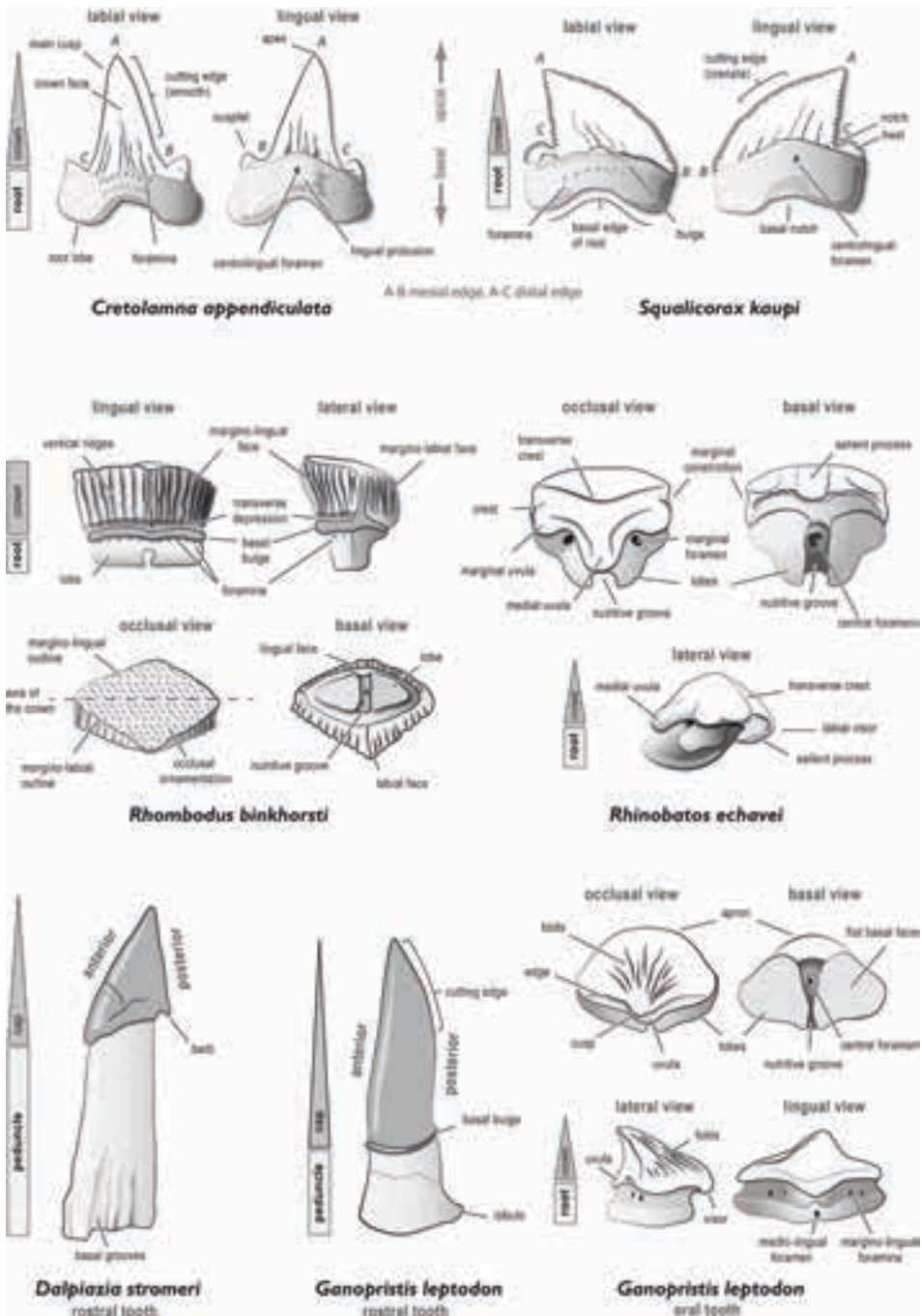


Figure 3.8 Terminology used in the description of neoselachian tooth morphology.

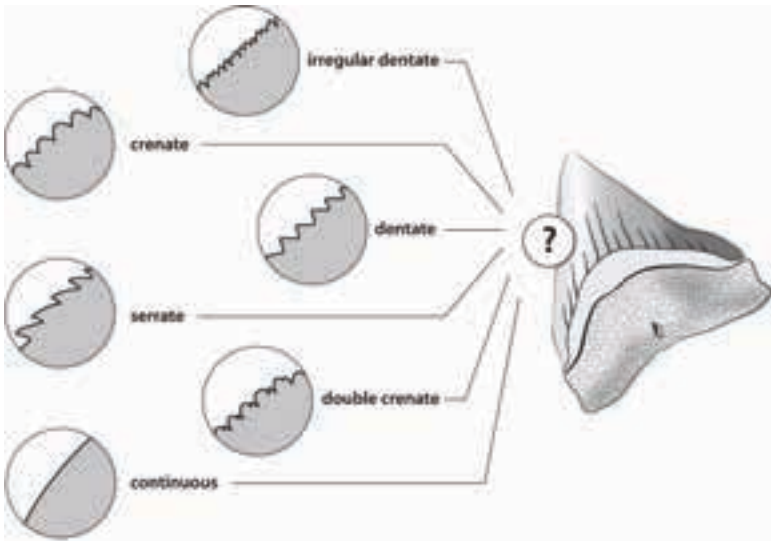


Figure 3.9 Margin variability (cutting edge shape) in shark teeth: continuous (e.g. *Isurus oxyrinchus* Rafinesque, 1810), serrate [e.g. *Hemipristis serra* (Agassiz, 1843)], crenate [e.g. *Squalicorax pristodontus* (Agassiz, 1843)], double crenate [e.g. *Squalicorax yangaensis* (Dartevelle and Casier, 1943)], dentate (e.g. *Carcharodon carcharias*), and irregular dentate [e.g. *Palaeocarcharodon orientalis* (Sinzow, 1899)].

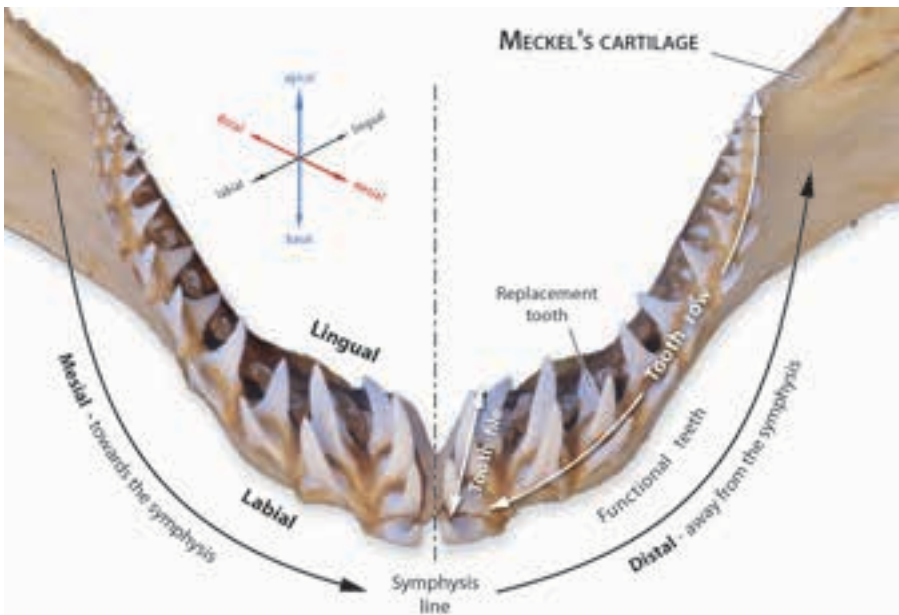


Figure 3.10 Application of the dental nomenclature in the anterior portion of the jaw (occlusal view) of a shortfin mako shark (*Isurus oxyrinchus*). The teeth and parts of them may be described as being away from the symphysis (distal) or towards the middle (mesial). Tooth labial and lingual faces apply to the exterior and interior, respectively.

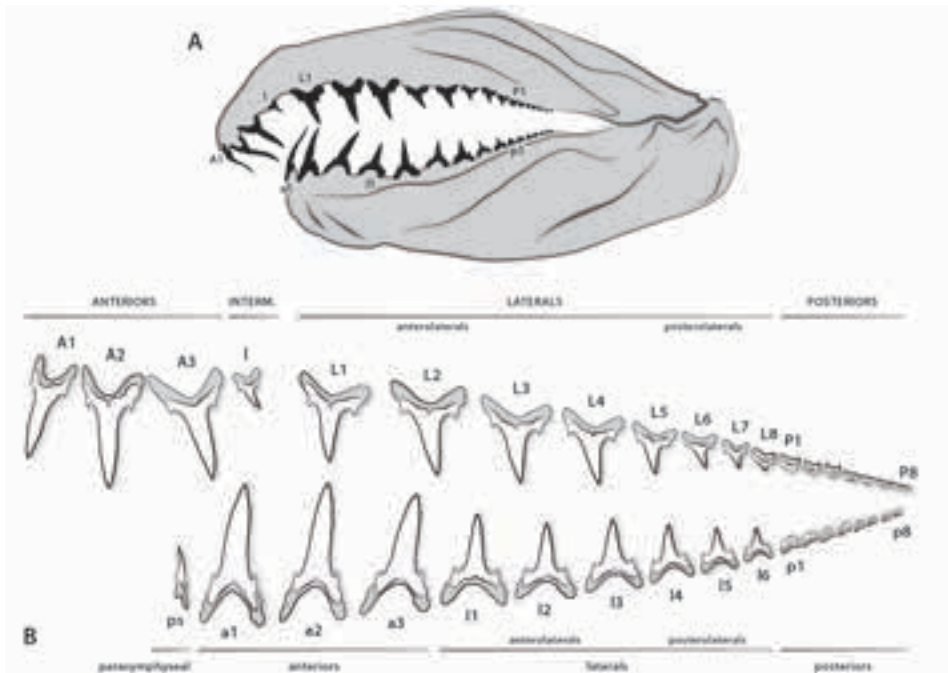


Figure 3.11 Dentition of an extant sand tiger shark *Carcharias taurus* (Rafinesque, 1810); A, lateral (left) view of the jaws and teeth; B, labial view of upper and lower functional series with types of teeth identified (left side of the jaw). Redrawn from a jaw and a study tooth set given by Cunningham (2000).

teeth from the symphyseal region towards the distal corner of the jaw, known as commissure (Fig. 3.11). There is dignathic heterodonty when the tooth shape is different in an equivalent upper and lower position, such as occurs in Hexanchidae sharks. In addition to the above changes in dentition, the shape of a same positioned tooth may also vary as individuals grow (i.e. ontogenetic heterodonty), or between males and females (i.e. sexually dimorphic dentition called gynandric heterodonty), as in batoids.

Sharks, in general, have the following types of teeth: (1) symphyseals, the paired teeth that are near the juncture, or symphysis, of the jaws; (2) parasymphyseals; (3) anterior, those that occur at the front of the jaws; (4) laterals, those that are towards the side; and (5) posterior, which are smaller and placed towards the commissure of the jaws (see their positions in Figs. 3.11B, 3.12–13). Sometimes, very posteriorly situated teeth are called commissurals.

Some authors have given the description of fossil selachian teeth arranged in the form of a dental formula (Applegate, 1965; Applegate and Espinosa-Arrubarrena, 1996), but this notation is not generalised among most of palaeontologists. Each tooth within this dental scheme is represented by the initial letter in its name (i.e. ps for parasymphyseal, s for symphyseal, a for anterior, I for intermediate, l for lateral, and p for

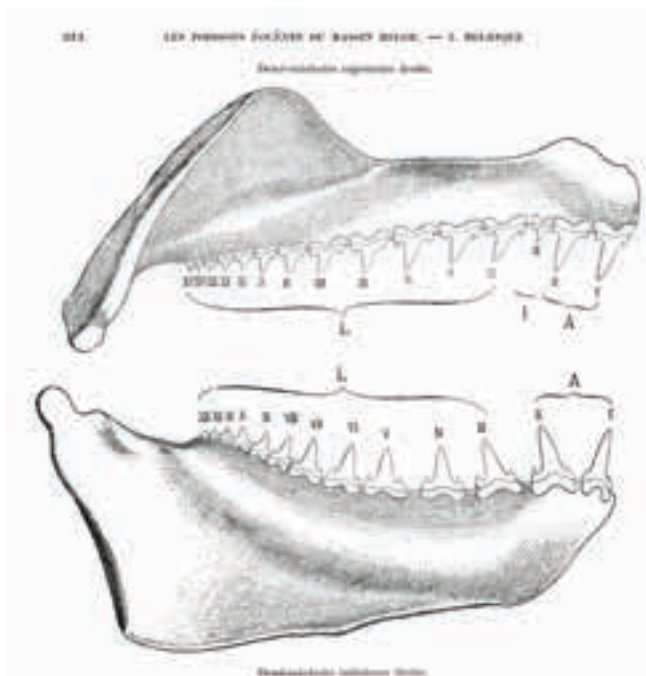


Figure 3.12 Dentition of an extant porbeagle shark *Lamna nasus* (Bonnaterre, 1788); A, anterior teeth I, intermediate tooth; L, lateral teeth (after Leriche, 1905).

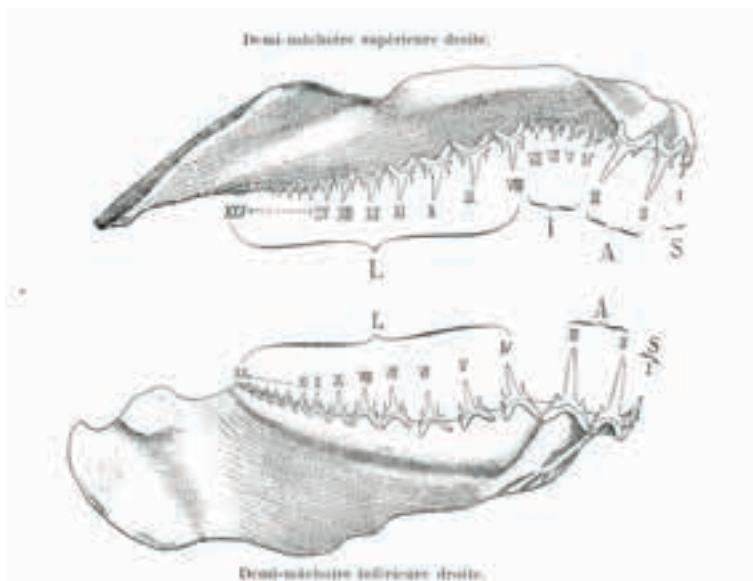


Figure 3.13 Dentition of an extant smalltooth sand tiger shark *Odontaspis ferox* (Risso, 1810); S, parasymphyseal teeth; A, anterior teeth I, intermediate teeth; L, lateral teeth (after Leriche, 1905).

posterior) followed by a number, being arranged in an increasing order. Letters a, l, and p may be either capitalised or not, referring to the upper and lower jaws respectively, and numbers denote position from the symphysis. Dental formulae are useful when dealing with living sharks, or in the rare case of having preserved a natural fossil tooth set. But in most cases, the correct assignment of a isolated fossil tooth is impossible, and therefore terms such as anterolateral and posterolateral are used to help descriptions. Associated tooth sets assigned to a species from some rich fossil assemblages can be built by comparing with natural tooth sets of modern analogous (see several examples in Welton and Farish, 1993).

The terminology related to the tooth orientation indicates place or direction. A tooth is divided into surfaces that are named in relation to other anatomical structures. Such terms include: apical (to the top), basal (to the bottom), mesial (toward the median line or symphysis), distal (away from the symphysis), labial (facing toward margin of the mouth, outer face), lingual (facing toward the interior of the mouth, inner face) and occlusal (masticating surface) (Fig. 3.10).

Other exoskeletal structures (placoid scales, thorns, tail spines)

The most common elasmobranch skeletal elements that are represented in the fossil record are the teeth, but other calcified structures of in the body of these fishes are also prone to fossilisation. Normal covering placoid scales (and specialised derivatives of them, such as thorns), fin spines, rostral saw teeth, and stings are considered here – although not all of them are present at the same time in each shark or batoid fish (Cappetta, 1987; Compagno, 1999b).

Placoid scales. They are described by Kemp (1999) as flat, not overlapping minute tooth-like units, which form alternate rows and are distributed over the head, trunk, tail, fins, and the orobranchial cavity in elasmobranchs. These units are also called dermal denticles because they are embedded in the skin. Morphologically, a placoid scale consists of a basal plate, composed of vascular orthodontine, which is embedded in the dermis, and an enameloid cap that forms the outer tip. The shape of the denticles is very variable according to the region of the body where are located, and therefore one species may bear more than one scale morphotype (Cappetta, 2012). Noteworthy is that the shape and disposition of the denticles, some of which are backwards curved and decorated with longitudinal ridges, play an essential role in reducing the hydrodynamic drag force (e.g. in nectic and pelagic forms of the Lamniformes and Carcharhinidae groups) (Cappetta, 2012).

Thorns. Some shark members of Echinorhinidae and batomorphs within the order Rajiformes have enlarged bony denticles that are either irregularly arranged dorsally or extended in lines, reaching areas of the precaudal tail, as in many skates (Compagno, 1999a). Thorns are considered to represent defensive structures for benthopelagic batoids, which live near or on the bottom, or for elasmobranchs that are not fast swimmers (Cappetta, 2012).

Protective spines (anterior to dorsal fins). Single, stout spines with triangular cross-section are present on the front margin of each of the two dorsal fins in two living orders of sharks (i.e. Squaliformes: Squalidae; Heterodontiformes: Heterodontidae), in addition to fossil representatives of the orders Ctenacanthiformes and Hybodontiformes. These sharp spines, which are supported by a basal cartilage and connected to poison-producing glands, are made of an orthodontine-like tissue capped anteriorly by an enameloid layer in the extant sharks, and may occur severely abraded in mature selachians (Kemp, 1999). These spines grow continuously throughout life, and are regarded as unique hypertrophied dermal scales (Lebrun, 2001). Comparable fossil examples may be either smooth or decorated with enameloid tubercles or ribs (Cappetta, 1987).

Rostral spines. These tooth-like structures are distributed along the lateral margins of the expanded anterior rostrum found developed in the head of sawsharks (e.g. in the order Pristiophoriformes) and sawfishes (e.g. in the batoid order Pristiformes and the exclusively fossil family Sclerorhynchidae within the suborder Sclerorhynchoidei) (Cappetta, 1987; Wueringer et al., 2009). For this reason, these hard structures are also named rostral teeth. The spines have a short peduncle and a long cap of either smooth or folded enameloid. Pristiophorids have rostral teeth of unequal size, not implanted in sockets but attached to the rostrum by connective tissue, also reflecting different growth stages. Sclerorhynchids also have the rostral teeth attached to the rostrum via connective tissue, being replaced with new ones when being lost. The shape and ornamentation of the rostral spines – specially the enameloid part – vary among species, but generally they are formed by an expanded peduncle with a basal face and an enameloid cap, whose core can be formed by either orthodontine or osteodontine. Pristids possess a different mode of rostral tooth attachment comparing to that of the sclerorhynchids. In this group of batoids, all the pointed teeth are of about equal size and deeply embedded in sockets of the rostral cartilage. Spines grow continuously – as they are worn – by osteodontine addition from their bases to the proximal ends and peripheries (Compagno, 1999a).

Tail spines. Most stingrays (suborder Myliobatoidei) have bone-like spines – also called caudal stings – rooted in the dorsomedial surface of the tail, and they may be used for self-defence against predators or when disturbed (Compagno, 1999b). The spine is composed of hard bone-like material, and consists of a long, flattened sting with backward-pointing barbs along the edges (Fig. 3.5A). Stingrays usually possess a single spine, which is shed periodically, on the caudal peduncle, although, two or more spines inserted at the same time in the tail are not infrequent (Halstead, 1971). Moreover, these spines are covered with venom secretory cells and enclosed in a thin layer of integumentary sheath of skin (Halstead, 1971).

3.4 Teeth patterns and specialised trophic adaptations

The function of the teeth in elasmobranchs is to grab, hold, tear, cut, and grind the food before it is ingested. There is a large number of tooth morphologies, but the dental ar-

rangements are limited to a few models, which are related to trophic specializations, as argued by Cappetta (1986, 1987, 2012). This categorization may be summarised as follows:

Clutching type. The teeth in this category are usually small, sharp with slender cusps and lateral cusplets, which facilitate catching and holding bite-sized fishes and cephalopods before swallowing them whole. Many sharks that live on or above the sea bottom have this kind of dentition. These are most typically members of the orders Squatiniformes, Orectolobiformes, and Carcharhiniformes (Scyliorhinidae and Proscylliidae families). Moreover, male batoids also have this tooth pattern. Although the clutching type dentition does occur in recent planktivorous sharks, such category is not the only pattern among planktivorous rays.

Tearing type. Sharks with this type of dentition inhabit varied, marine environments, from mesotrophic littoral zones (e.g. *Carcharias* spp.) to epipelagic or deeper bathypelagic zones (e.g. odontaspids, lamnids, and mitsukurinids). These sharks all have in common the presence of several functional teeth, whose cusps are narrow in the anterior files but somewhat enlarged in the lateral rows. These inward-leaning teeth are used for piercing (impaling) preys that have to be swallowed whole, and the enlarged lateral teeth may have a special function for cutting flesh (i.e. they show a tendency towards the cutting type). Batoids lack this type of dentition.

Cutting type. Sharks with this dental model are characterised by having labio-lingually flattened teeth with cusps generally slanted distally. Usually there is just one functional row, forming an almost continuous sharp blade (except for the genus *Carcharodon* and *Otodus*). This type of dentition occurs in different families, such as Carcharhinidae, Isuridae, and Anacoracidae, and can also be found in the least advanced sharks of the order Squaliformes and in members of the order Echinorhiniformes. The acquisition of serrations (*sensu lato*) along the crown cutting edges, which occur in nearly all the forms, considerably enhances the functional effectiveness of the teeth, meaning that these sharks are able to kill and dismember prey larger than themselves. This dental arrangement occurs in large predatory sharks, such as the extant tiger shark (*Galeocerdo cuvier*), whose teeth are heavily serrated in both jaws. The *cutting-clutching combination* represents an advance for large predatory sharks. In this category a strong dignathic heterodonty is observed, in addition to the gradual monognathic heterodonty. Teeth in one of the jaws become wider and flatter in labio-lingual direction (i.e. cutting function), whereas the opposite ones have narrow cusps (i.e. clutching function), at least for those teeth placed in anterior and anterolateral positions. The cutting teeth may be fixed either to the palatoquadrate (e.g. Carcharhinidae and Hemigaleidae) or to the Meckel's cartilage (e.g. Dalatiidae and Hexanchidae). The *cutting-clutching combination* seems to be a significant improvement, since the flattened, serrated teeth act as knives that can remove large pieces of flesh while cuspidate teeth, often unserrated or weakly serrated, enable the predator to hold the prey in place. The dental replacement – driven by tooth wear or failure – drifts the newly formed teeth to the margins of the jaws, and

sometimes the older ones also remain attached on the outer side. However, only one tooth row becomes functional.

Crushing type. Many batoids, and even a few sharks of the family Triakidae (e.g. genera *Scylliogaleus* and *Mustelus*), have developed this dental type. Usually, the enameloid crown of the teeth is bulged and often bears a transverse keel. The individual jaws are provided with several functional rows of rather narrow, imbricate teeth to form an effective tool for either crushing shellfish hard shells or eating cephalopods and small fishes. Sexual heterodonty in Rajoidei and Dasyatoidei has been related to behavioural traits (i.e. courtship) rather than feeding (Cappetta, 1987). Thus, mature males often have clutching-type dentition, whereas females have crushing-type dentition. The crushing type dentition is mainly found in living and fossil (e.g. genus *Rhinobatos*) elasmobranchs with a benthic or nektobenthic mode of life.

Grinding type. Rays (Batoidea) with benthic habits have their teeth adapted for a durophagous diet (i.e. feeding on sea urchins, shelled molluscs, and crustaceans). Their robust flattened teeth, whose crowns show a polygonal outline, are arranged in a pavement-like dentition, forming thus a single dental plate with a nearly plane surface that is suitable for grinding hard benthic preys. There are many fossil and living species with this type of dentition, and among them the myliobatid stingrays. This dentition pattern is also shared by the Mesozoic hybodonts (i.e. *Asteracanthus*, *Acrodus*, and *Ptychodus*).

Clutching–grinding combination. This specialised dentition occurs exclusively in bullhead sharks (i.e. Heterodontidae), which are benthopelagic, mostly confined to rocky and sandy bottoms in the continental shelves. Teeth in these sharks are used to grab and crush preys, mainly sea urchins, shelled molluscs, and fishes. *Heterodontus* species have cuspidate anterior teeth (clutching type), whereas lateral teeth are provided with a thick layer of enameloid (grinding type). Moreover, ontogenetic differences in dentition may occur coinciding with a dietary change (i.e. dentition in juvenile bullhead sharks is essentially of clutching type).

Cutting–grinding combination. This dentition only occurs in the Cretaceous anacoracid genus *Ptychocorax*. However, the teeth of the living bonnethead sharks [*Sphyrna tiburo* (Linnaeus, 1758)] recall such type dentition, allowing them to have an alternative source of food not exploited by other species of sharks.

Crushing–grinding combination. This type is only observed in batoids such as the living genus *Pastinachus*. They mainly have a grinding-type dentition on both (right and left) sides of the upper jaw, in addition to some crushing-type files of teeth along the symphysis area. This pattern is also observed in a few Upper Cretaceous batoids from the genus *Youssoubatis*, according to Cappetta (2012).

3.5 Nomenclature and systematics of elasmobranchs

Nomenclature and descriptive terminology for selachian remains principally conform

to that of Cappetta (1987, 2012), and the taxonomic scheme follows those of Cappetta (2006, 2012) and Noubhani and Cappetta (1997). Some common dental terms that are used throughout this doctoral thesis are presented in Box 3.1, at the end of the chapter. The selected English terms are listed with their respective translations into Spanish.

Finally, the taxonomic list of the Upper Cretaceous neoselachians that have been studied here from the Basque-Cantabrian Region is given in Table 3.3.

Table 3.3 Taxonomic list of the Upper Cretaceous neoselachians from the Basque-Cantabrian Region here studied. The dagger (†) after a taxonomic group, at any rank above the species level, denotes extinct.

CLASS CHONDRICHTHYES

Subclass Elasmobranchii

Superorder Galeomorphii

Order Carcharhiniformes

Family Scyliorhinidae

Genus *Prohaploblepharus* †

Prohaploblepharus riegrafi (Müller, 1989)

Family Triakidae

Genus *Galeorhinus* †

Galeorhinus girardoti Herman, 1977

Genus *Palaeogaleus* †

Palaeogaleus faujasi (Geyn, 1937)

Order Lamniformes

Family Anacoracidae †

Genus *Squalicorax* †

Squalicorax kaupi (Agassiz, 1843)

Squalicorax ex gr. *kaupi* (Agassiz, 1843)

Squalicorax pristodontus (Agassiz, 1843)

Family Cretoxyrhinidae †

Genus *Cretoxyrhina* †

Cretoxyrhina mantelli (Agassiz, 1843)

Family Mitsukurinidae

Genus *Anomotodon* †

Anomotodon hermani Siverson, 1992

Genus *Scapanorhynchus* †

Scapanorhynchus cf. *texanus* (Roemer, 1849)

Family Odontaspidae

Genus *Carcharias*

Carcharias aasenensis Siverson, 1992

Carcharias adneti Vullo, 2005

Carcharias aff. *gracilis* (Davis, 1890)

Carcharias heathi Case and Cappetta, 1997

Genus *Odontaspis*

Odontaspis bronni (Agassiz, 1843)

Table 3.3 (cont.)

Family Otodontidae †
Genus <i>Cretolamna</i> †
<i>Cretolamna appendiculata</i> (Agassiz, 1843)
<i>Cretolamna borealis</i> (Priem, 1897)
<i>Cretolamna sarcophortheta</i> Siversson et al., 2015
Family Pseudocoracidae †
Genus <i>Pseudocorax</i> †
<i>Pseudocorax laevis</i> (Leriche, 1906)
Family Pseudoscapanorhynchidae †
Genus <i>Protolamna</i> †
<i>Protolamna borodini</i> (Cappetta and Case, 1975b)
Family Serratolamnidae †
Genus <i>Serratolamna</i> †
<i>Serratolamna kbderii</i> (Zalmout and Mustafa, 2001)
<i>Serratolamna serrata</i> (Agassiz, 1843)
Lamniformes incert. fam.
Genus <i>Paranomotodon</i> †
<i>Paranomotodon</i> cf. <i>angustidens</i> (Reuss, 1845)
Order Orectolobiformes
Family Ginglymostomatidae
Genus <i>Plicatoscyllium</i> †
<i>Plicatoscyllium lehneri</i> (Leriche, 1938)
Family Hemiscylliidae
Genus <i>Hemiscyllium</i>
<i>Hemiscyllium hermani</i> Müller 1989
Genus <i>Chiloscyllium</i>
<i>Chiloscyllium</i> cf. <i>gaemersi</i> Müller, 1989
<i>Chiloscyllium</i> cf. <i>vulloi</i> Guinot et al., 2013
<i>Chiloscyllium</i> sp.
Order Synechodontiformes †
Family Palaeospinacidae †
Genus <i>Synechodus</i> †
<i>Synechodus</i> aff. <i>S. filipi</i> Siversson et al., 2016
Superorder Squalomorphii
Order Squatiniformes
Family Squatinidae
Genus <i>Squatina</i>
<i>Squatina</i> (<i>Cretascyllium</i>) <i>hassei</i> Leriche, 1929
Superorder Batomorphii
Order Rajiformes
Suborder Rhinobatoidei
Family Parapalaeobatidae †
Genus <i>Parapalaeobates</i> †
<i>Parapalaeobates pygmaeus</i> (Quaas, 1902)

Table 3.3 (cont.)

Family Rhinobatidae
Genus <i>Rhinobatos</i>
<i>Rhinobatos casieri</i> Herman, in Cappetta and Case 1975b
<i>Rhinobatos echavei</i> Cappetta and Corral, 1999
<i>Rhinobatos ibericus</i> Cappetta and Corral, 1999
Rhinobatoidei incert. fam.
Genus <i>Ataktobatis</i> †
<i>Ataktobatis variabilis</i> Cappetta and Corral, 1999
Genus <i>Vascobatis</i> †
<i>Vascobatis albaitensis</i> Cappetta and Corral, 1999
Suborder Sclerorhynchoidei
Family Ptychotrygonidae †
Genus <i>Ptychotrygon</i> †
<i>Ptychotrygon</i> sp.
Family Sclerorhynchidae †
Genus <i>Dalpiazia</i> †
<i>Dalpiazia stromeri</i> Checchia-Rispoli, 1933
Genus <i>Ganopristis</i> †
<i>Ganopristis leptodon</i> Arambourg, 1935
Genus <i>Onchosaurus</i> †
<i>Onchosaurus radicalis</i> Gervais, 1852
Order Myliobatiformes
Superfamily Dasyatoidea
Dasyatoidea incert. fam.
Genus <i>Coupatezia</i> †
<i>Coupatezia fallax</i> (Arambourg, 1952)
Superfamily Myliobatoidea
Family Rhombodontidae †
Genus <i>Rhombodus</i> †
<i>Rhombodus andriesi</i> Noubhani and Cappetta, 1994
<i>Rhombodus binkhorsti</i> Dames, 1881
<i>Rhombodus</i> sp.

Box 3.1 Most common dental terms (English–Spanish) used to describe shark teeth
(n: name, adj: adjective, *syn.*: synonym, Esp.: Spanish)

A

anterior [adj]. Esp., anterior.
apex [n] (*syn.* crown tip). Esp., ápice.
apical [adj]. Esp., apical.
apron [n]. Esp., faldón, mandil.

B

barb [n]. Esp., barba.
basal [adj]. Esp., basal.
basal bulge [n]. Esp., anillo basal.
basal face [n]. Esp., cara basal.
basal groove [n]. Esp., surco basal.
basal notch [n]. Esp., escotadura basal.
basal plate [n] (*syn.* root). Esp., placa basal, raíz.
bilobate [adj]. Esp., bilobulado/a.
bulge [n] (*syn.* cingulum). Esp., burlete.

C

cap [n] (*syn.* enameloid cap). Esp., funda de vitrodentina.
caudal sting [n] (*syn.* tail spine). Esp., aguijón, espina caudal.
centrolingual foramen [n] (*syn.* central foramen). Esp., foramen centrolingual.
collar [n] (*syn.* neck, lingual furrow). Esp., cuello, banda lingual.
constriction [n]. Esp., constricción.
crown [n]. Esp., corona.
crown tongue [n]. Esp., lengüeta.
cuspl [n]. Esp., cúspide.
cuspidate [adj]. Esp., cuspidado
cusplet [n] (*syn.* “lateral cuspl”). Esp., cuspidilla.
cutting edge [n]. Esp., filo, arista cortante.
continuous — [n]. Esp., filo liso.
crenate — [n]. Esp., filo crenado.
dentate — [n]. Esp., filo dentado.
serrate — [n]. Esp., filo serrado.
sinuate — [n]. Esp., filo sinuado.
smooth — [n]. Esp., filo liso.

D

dental tissue [n]. Esp., tejido dental.
enameloid [n]. Esp., vitrodentina.
orthodontine [n]. Esp., ortodentina.
osteodontine [n] (*syn.* trabecular dentine). Esp., osteodentina.
denticle [n] (*syn.* dermal thorn). Esp., escama placoidea, denticulo.
dentition [n] (*syn.* teeth). Esp., dentición.
dermal denticle [n]. Esp., denticulo dérmico.
dermal thorn [n] (*syn.* denticle). Esp., espina dérmica.
distal [adj] (*syn.* commissural). Esp., distal.

E

enameloid [n] (*syn.* vitrodentine), *see* dental tissue.
enameloid cap [n] (*syn.* cap). Esp., funda de vitrodentina.

F

file [n]. Esp., fila.
fold [n]. Esp., pliegue.
foramen [n]. Esp., foramen.
foramina [n, pl]. Esp., forámenes.
furrow [n]. Esp., surco

G

groove [n]. Esp., surco.

H

heel [n] (*syn.* shoulder). Esp., talón.

L

labial [adj]. Esp., labial.
labial face [n]. Esp., cara labial (cara externa).
lateral [adj]. Esp., lateral.
lateral cusplet [n] (*syn.* cusplet). Esp., cuspidilla lateral.
lingual [adj]. Esp., lingual.
lingual bulge [n]. Esp., anillo lingual.

lingual face [n]. Esp., cara lingual (cara interna).
lingual furrow [n] (*syn.* neck, collar). Esp., cuello, banda lingual.
lingual protuberance (of the root) [n] (*syn.* protusion). Esp., protuberancia lingual (de la raíz).
lobe (of the root) [n] (*syn.* branch). Esp., lóbulo.

M

main cusp [n]. Esp., cúspide principal.
marginal face [n]. Esp., cara marginal.
medial [adj]. Esp., media.
mesial [adj]. Esp., mesial.

N

neck [n] (*syn.* collar, lingual furrow, lingual groove). Esp., cuello, banda lingual.
notch [n]. Esp., escotadura, hendidura.
nutritive foramen [n]. Esp., foramen nutricional.
nutritive groove [n] (*syn.* transverse groove, central furrow). Esp., surco nutricional.

O

occlusal face [n]. Esp., cara oclusal.
oral tooth [n]. Esp., diente oral.
orthodontine [n], *see* dental tissue.
osteodontine [n], *see* dental tissue.

P

peduncle [n]. Esp., pedúnculo.
process [n]. Esp., proceso.
protusion [n] (*syn.* lingual protuberance). Esp., protuberancia lingual de la raíz.

R

root [n] (*syn.* basal plate). Esp., raíz, placa basal.
root lobe [n] (*syn.* root branch). Esp., rama basal.
rostral tooth [n] (*syn.* “lateral tooth”). Esp., diente rostral.
rostrum [n]. Esp., rostro.
row [n] (*syn.* tooth set). Esp., línea.

S

series [n] (*syn.* tooth set, row). Esp., serie, línea, hilada.
serrations [pl]. Esp., crenulaciones, puntas serradas.
symphyseal, symphyisial [adj]. esp., sínfisario.
symphysis [n]. Esp., sínfisis.

T

tail spine [n] (*syn.* caudal sting). Esp., aguijón, espina caudal.
thorn [n]. Esp., púa, espina.
tooth [n]. Esp., diente
 anterior — [n]. Esp., diente anterior.
 commissural — [n]. Esp., diente comisural.
 intermediate — [n]. Esp., diente intermedio.
 lateral — [n]. Esp., diente lateral.
 posterior — [n]. Esp., diente posterior.
 symphyseal — [n]. Esp., diente sínfisario.
tooth set [n]. Esp., serie dental.
transverse crest [n] (*syn.* transverse keel). Esp., cresta transversal.
transverse depression [n]. Esp., depresión transversal.
transverse groove [n] (*syn.* nutritive groove). Esp., surco transverso.
trabecular dentine [n] (*syn.* osteodontine), *see* dental tissue.

U

uvula [n]. Esp., úvula.
 lingual marginal — [n]. Esp., úvula marginal lingual.

V

vertical ridges [n] (*syn.* vertical wrinkles). Esp., crestas verticales.
vertical wrinkles [n] (*syn.* vertical ridges). Esp., arrugas verticales.
visor [n]. Esp., visera.



GEOLOGY AND PALAEOLOGY OF THE STUDIED AREAS

Un día cualquiera de la familia *Liramosaurus astibiae*
pasando por el Cretácico Superior de Laño (Comitao de Treviño)



A typical day of the *Liramosaurus astibiae* family walking around Laño
(Treviño County) in the Upper Cretaceous...

DINO DAD: If the Upper Cretaceous ends, what do you prefer, to fossilise in a sandy delta
or to become burnt black by a meteorite?

DINO MUM: Fossilisation is better! ... and to become discovered by a palaeontologist

YOUNG DINO: Hey, fossilisation hurts?

Chapter 4

STRATIGRAPHY AND PALAEOONTOLOGY OF THE BARRIO PANIZARES BEDS (NIDÁGUILA FORMATION, CONIACIAN) FROM NORTHERN SPAIN

4.1 Location and geological setting

The tectonostratigraphical domain known as Castilian Ramp (CR), as defined by Floquet (1991, 2004), is located in the southwestern part of the Basque-Cantabrian Basin (B-CB), and spreads over much of the provinces of Palencia, Cantabria, and Burgos in Northern Spain. It represents the inner or proximal part of a ramp developed along the northern palaeomargin of the Iberian Peninsula, being a transition area towards an outer neritic zone with higher subsidence rates named the Navarre-Cantabrian Ramp.

Good outcrop conditions coupled with ammonite-rich rocks have made this region a target for detailed geological and palaeontological investigation by Floquet (1991), Santamaría-Zabala (1992), Santamaría (1995), and Gallemí et al. (2007) among others. But, contrary to its abundant fossil invertebrates, marine vertebrate remains are rare. A reputed scapular bone from a marine reptile and a sawfish rostral tooth of *Onchosaurus radicalis* Gervais, 1852 are the only vertebrate remains collected from a unit named as the upper marls ('Marnes superieures') at the top of the Nidáguila Formation (Floquet, 1991), near the small village of Barrio Panizares (Basconcillos del Tozo, Burgos province) (Fig. 4.1).

4.2 Stratigraphy

The stratigraphical characteristics of the Barrio Panizares section (Figs. 4.2, 4.3) do not differ much from those observed in the type locality where the Nidáguila Formation was first established in 1991 by Floquet. Subsidence in this part of the B-CB was moderate during the Upper Cretaceous, reaching its maximum deepening at the middle Coniacian, when clayey carbonates of the Nidáguila Formation were deposited (Floquet, 2004). In ascending stratigraphical order – and over a major basal discontinuity – a set of bioclastic limestones, which have not here studied (Member of Ribera Alta,

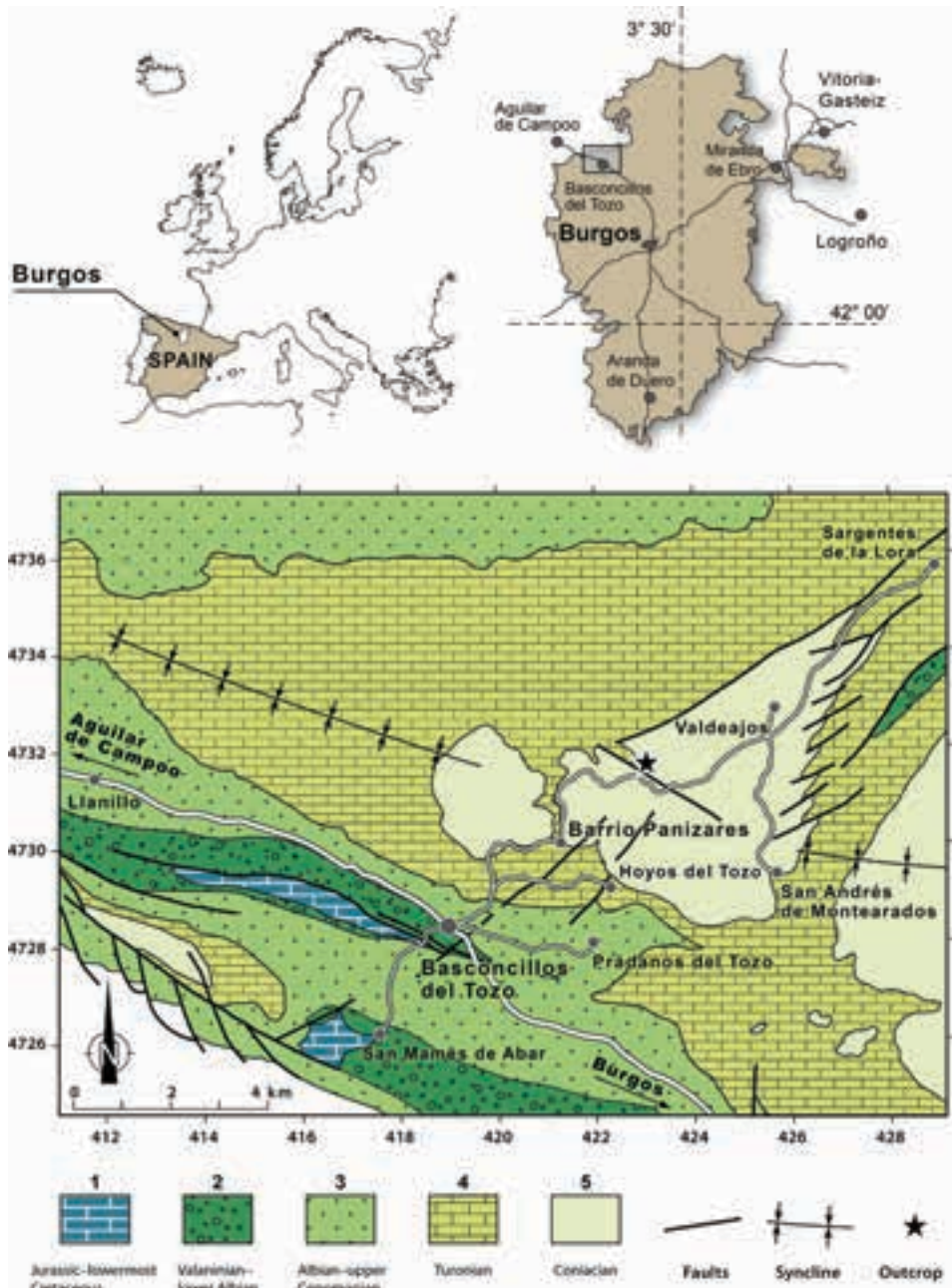


Figure 4.1 Geographical location and simplified geological map of the Basconillos del Tozo area showing the fossil location (modified from Corral et al., 2012). **Key:** 1, conglomerates and micritic limestones, Jurassic–lowermost Cretaceous; 2, microconglomerate sandstones, Valanginian–lower Albian; 3, quartz conglomerates, kaolinite-rich sandstones, and mudstones, upper Albian–upper Cenomanian; 4, marls and limestones, Turonian; 5, marlstones and limestones, Coniacian.

sensu Floquet, 1991), give pace to an alternating limestone–marl succession that occasionally contain *Pycnodonte* sp. bivalves. This basal unit is overlain by a 4.5 m thick succession of nodular to wavy, thick-bedded grey packstone-grainstone, separated by thin beds of mudstone. These bioclastic limestones, which are continuously exposed, contain inoceramid shell fragments, pyrite crystals and glauconite, and have supplied some ammonites [e.g. *Metatissotia ewaldi* (von Buch, 1847), *Tissotioides haplophyllus* (Redtenbacher, 1873), and *Peroniceras* sp.] (Fig. 4.4). At the base of one of the more indurated beds sub-horizontal feeding burrows are visible.

Upwards the profile follows with marly limestones and marls (mudstone–wackestone) rich in macrofossils. The total thickness is about 13 m, and internal stratification is observed as being alternating layers of marly limestones and marls, representing different carbonate content. These have yielded bivalves [with large specimens of *Plagiosotoma gigantea* (Sowerby, 1814), cardids, and elements of *Pterotrigonina* (*Scabrotrigonina*) *scabra* (Lamarck, 1819)], gastropods (with the genera *Tylostoma* and *Leptomaria*), ostreids [e.g. *Pycnodonte* sp. and *Ceratostreon pliciferum* (Dujardin, 1837)], several species of ammonites, including *Prionocycloceras iberiense* (Basse, 1947), *Prionocycloceras turzoi* (Karrenberg, 1935), *Protexanites bourgeoisianus* (d'Orbigny, 1850), and *Forresteria* (*Harleites*) aff. *nicklesi* (Grossouvre, 1894) (Fig. 4.4), and a reputed incomplete shoulder bone from a marine turtle (Fig. 4.5). The upper part of the unit passes into soft yellowish marlstones, where the sawfish rostral tooth was collected. This bed also contains a mixture of complete invertebrates including molluscs, echinoids, and brachiopods, and fossil skeletal parts of them (i.e. interambulacral plates and spines of echinoids, inoceramid prisms, and shell fragments, disarticulated valves of ostreids, and fragments of bryozoans). Up-section this bed passes gradually into poorly exposed marls (about 28 m thick) where occasionally Tisseritidae ammonites (*Hemitissotia* sp.) are found. The section is capped by wavy thick bedded beige limestones (grainstone texture) with some internal moulds of macrofossils (i.e. gastropods and bivalves). In the Barrio Panizares section, the sub-horizontal limestone strata of the uppermost unit are easily observed as they crop out as resistant cap-rocks, forming low-angle cuestas.

Facies interpretation

Several Upper Cretaceous carbonate units have been described from several areas of the CR. There, Floquet (1991, 1998) has recognised thirteen regional T–R cycles organised in four long term depositional megacycles (LTC) related to sea-level fluctuations in a shallow epicontinental sea (dominated by proximal and distal ramp deposits). The series of the CR considered to represent the Nidáguila Formation forms part of the Coniacian carbonate-dominated marine ramp sequence and is a constituent formation of the depositional cycle DC 8 (included in the depositional megacycle LTC 3), which began in early–middle Coniacian times. The sparsely fossiliferous lowermost unit ('Marnes inférieures') is bounded below by an unconformity which truncates the

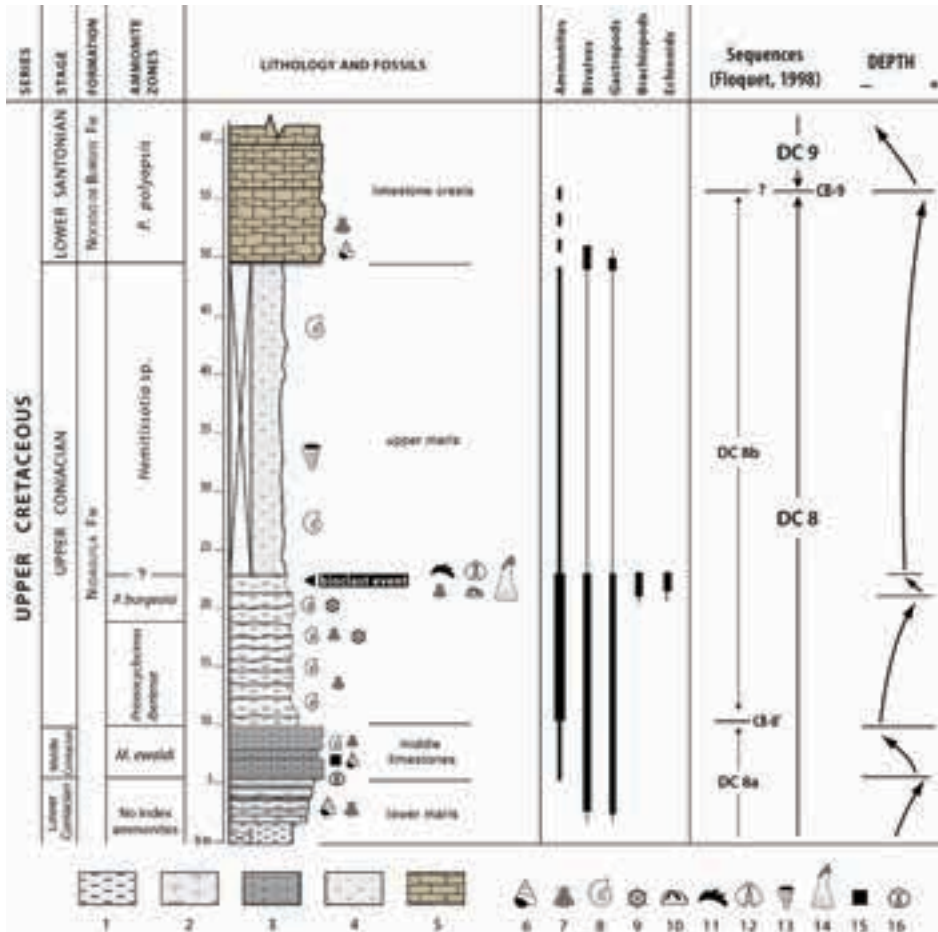


Figure 4.2 Stratigraphical column of the fossil site; Key: 1, mudstones and marls; 2, marls and clayey limestones; 3, bioclastic limestones; 4, marls; 5, limestones (grainstone); 6, gastropods; 7, bivalves; 8, ammonites; 9, solitary corals; 10, echinoids; 11, ostreids; 12, brachiopods; 13, rudists; 14, *Onchosaurus* tooth; 15, pyrite, and 16, glauconite (modified from Corral et al., 2012).

underlying upper Turonian–lower Coniacian limestones (cycle boundary CB-8), according to Floquet (1998). This is the result of a general and progressive deepening of the ramp with respect to the underlying carbonate series, later on interrupted by a weak somerization trend during the middle Coniacian (‘Calcaires intermédiaires’ of Floquet, 1991), designated as T–R subcycle DC 8a. This fact is inferred by the occurrence of bioclastic limestones that would indicate shallow conditions. The glauconite pellets here probably originated from alteration of organic matter in an environment with low sedimentation rate (see Burst, 1958). The organic matter also favoured the uptake of sulphate ions from the sea water to form pyrite.



Figure 4.3 Stratigraphy of the Nidáguila Formation, north of Barrio Panizares (La Lora, Burgos); Key: lC, lower Coniacian; mC, middle Coniacian; uC, upper Coniacian; IS, lower Santonian. Photograph taken looking south.

A shift in the sedimentation, above a recognised minor discontinuity (cycle boundary CB-8'), marks the onset of the T–R subcycle DC 8b. The overlying upper marlstones represent an open marine deeper circalittoral zone with a dominance of sessile organisms (such as oysters and mobile molluscs) and nektonic ammonites. The bioclast-rich event at the middle of the unit (see Fig. 4.2) appears to indicate a storm bed event in a shallow-water ramp. The circalittoral zone extends upwards the section, but it was probably shallower. The final part of the section includes some limestone strata (texture grainstone) that belong to the Nocado de Burgos Formation. These carbonates represent the infralittoral zone, namely a shallower environment owed to the prograding infill, although still permanently submerged.

According to the stratigraphy, this *Onchosaurus* specimen from the CR comes from a rock sequence deposited in an open-marine, inner neritic sea, apparently far away from the natural dwelling preferences of the extant sawfishes. As indicated above, a storm episode could have transported and deposited basinward such skeletal element, although, a semipelagic lifestyle for the fossil sawfish is not completely ruled out.

Stratigraphical position

Biostratigraphical subdivision of the Coniacian was based on the rich ammonite assemblages found in the north of the CR. Above an upper Turonian rudistid carbonate

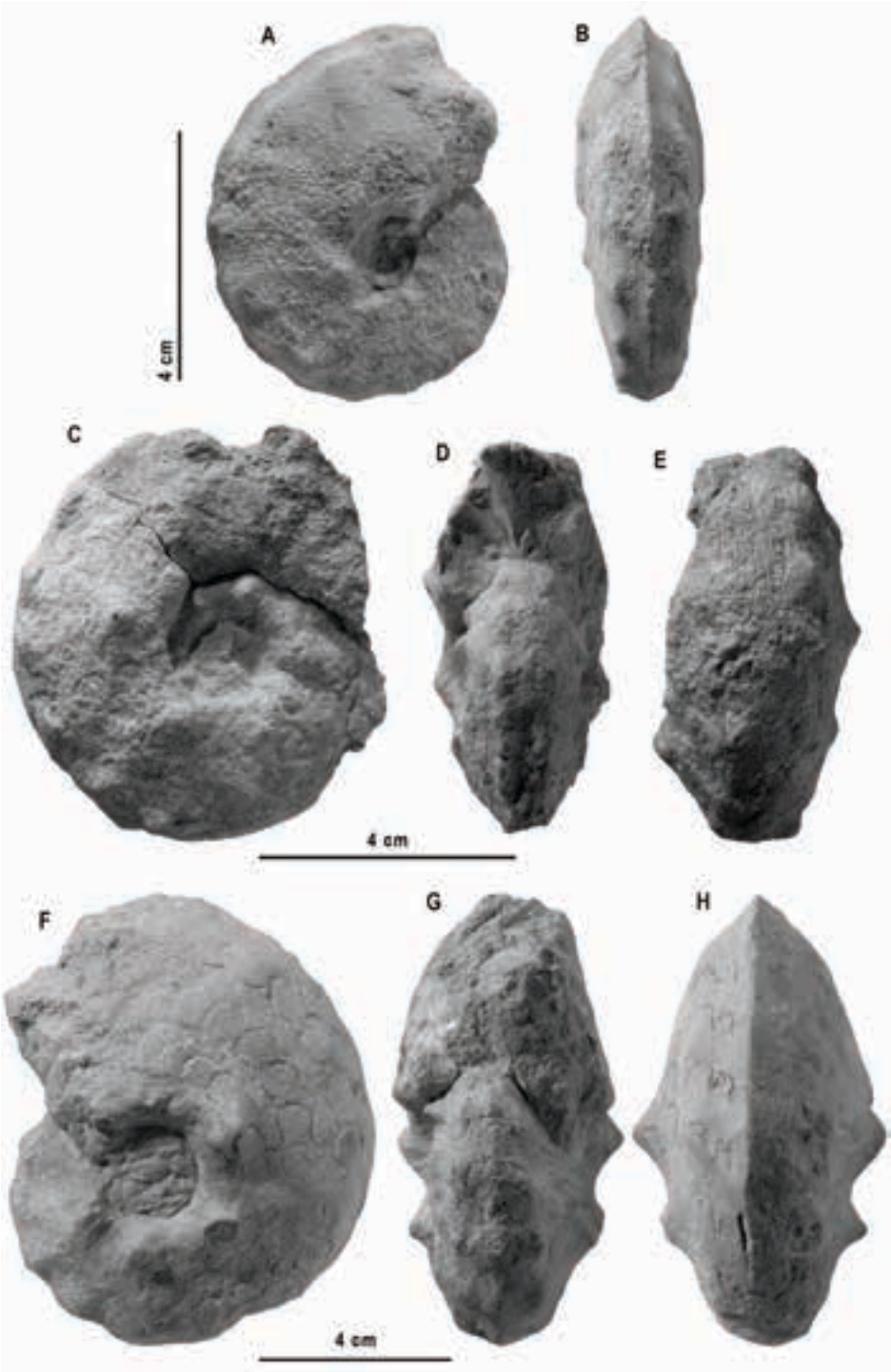
bank, distinguished in the Floquet's (1991) depositional cycle DC 7 and that is not considered in this chapter, ammonite faunae recovered again, representing a diversified mixture of cosmopolitan and endemic elements. Some characteristic ammonoids of the Barrio Panizares site are illustrated in Figure 4.4. Field data and fossil evidence have permitted to identify the fourfold subdivision of the Coniacian that was formalised by Santamaría-Zabala (1992) for the Basque-Cantabrian Region (Fig. 4.6). This ammonite zonal and subzonal scheme, which was built on the basis of previous works made by Karrenberg (1935), Ciry (1939), Wiedmann (1960), and Wiedmann and Kauffman (1978), has been subsequently used by Martínez et al. (1996) and Gallemí et al. (2007).

In the Tethyan realm of Western Europe, the base of the Coniacian stage is marked by the first occurrence (FO) of *Forresteria* (*Harleites*) *petrocoriensis* (Coquand, 1859) according to the revision of the French Coniacian by Kennedy (1984). But, contrary to nearby regions in Southern France, no ammonites have been found in the CR from the lower Coniacian substage. Thus, the ammonite zones proposed by Santamaría-Zabala (1992) overlie a basal interval apparently devoid of ammonites (to be correlated eastwards to the Ribera Alta Member at the base of the Nidáguila Formation), which is considered early Coniacian in age (Floquet, 1991). Typical Coniacian marine faunae occur stratigraphically above these beds. In terms of ammonoids, the lowest identified zone in the area is the *Metatissotia ewaldi* interval biozone, which indicates a middle Coniacian age. Associated ammonites include the cosmopolitan *Tissotioides haplophyllus*, *Peroniceras* cf. *tridorsatum* (Schlüter, 1867), and the endemic *Tissotioides hispanicus* Wiedmann, 1960. The *Metatissotia ewaldi* zone is replaced, when visible, by the *Gauthiericeras margae*¹ subzone or, usually, by the *Prionocycloceras iberiense* interval biozone (named by the FO of this endemic taxon), where the stronger ornamented form *Prionocycloceras turzoi* is also an important taxon. The twofold subdivision of the *Prionocycloceras iberiense* zone represents the lower upper Coniacian.

The overlying interval biozone is named for the FO of the moderately ornamented *Protexanites bourgeoisianus*. The zonal species cooccur with *Paratexanites serratomarginatus* (Redtenbacher, 1873), *Texasia* sp., *Gauthiericeras vascogoticum* Wiedmann, 1964, and *Forresteria* (*Harleites*) aff. *nicklesi* (Grossouvre, 1894), among others.

¹ Named after *Gauthiericeras margae* (Schlüter, 1867).

Figure 4.4 Ammonites from the Coniacian Nidáguila Formation of Barrio Panizares (Burgos). A–B, *Metatissotia ewaldi* (von Buch, 1847), MCNA 2224; C–E, *Tissotioides haplophyllus* (Redtenbacher, 1873), MCNA 15423; F–H, *Tissotioides hispanicus* Wiedmann, 1960, MCNA 15424; I–J, *Gauthiericeras vascogoticum* Wiedmann, 1964, MCNA 15425; K–L, *Prionocycloceras turzoi* (Karrenberg, 1935), MCNA 15426; M–N, *Protexanites bourgeoisianus* (d'Orbigny, 1850), MCNA 15427; O–P, *Forresteria* (*Harleites*) aff. *nicklesi* (Grossouvre, 1894), MCNA 15428; Q–R, *Hemitissotia turzoi* Karrenberg, 1935, MCNA 2222; S–T, *Hemitissotia lenticeratiformis* Wiedmann, in Wiedmann and Kauffman, 1978, MCNA 15429. ►



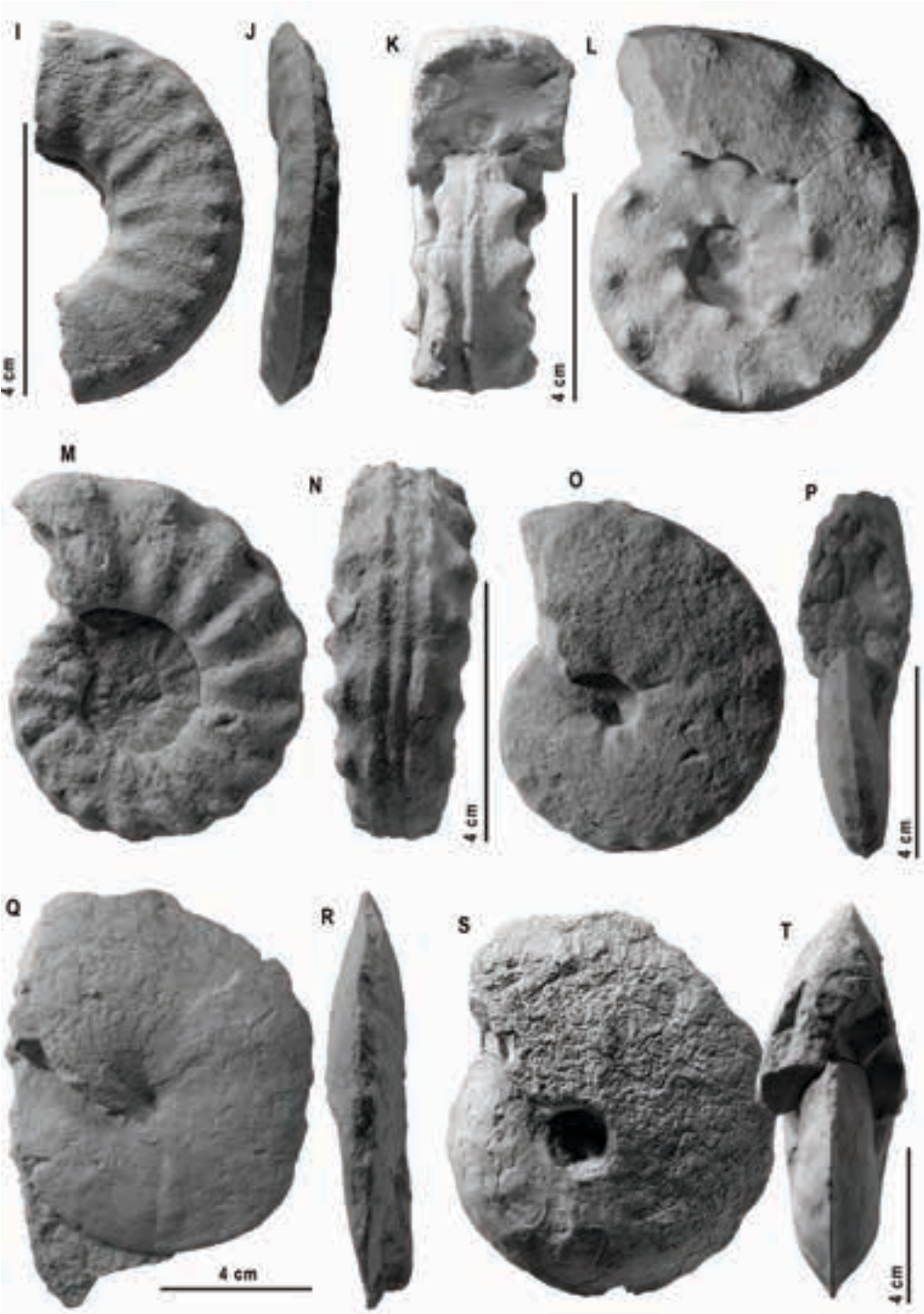


Figure 4.4 (cont.)



Figure 4.5 Reputed shoulder bone from a marine turtle, Barrio Panizares (Burgos) in various lateral (A–D) and proximal (E) views, Coniacian, MCNA 15159. Arrows indicate predation marks.

		Europe	North Castilian Domain (Spain)		
		Kennedy (1984)	Wiedmann (1960), Wiedmann and Kauffman (1978)		Santamaría-Zabala (1992)
86.1 Ma	Upper	<i>Panotoceras serratum/argutum</i>	CO V	<i>Hemitosia leucostriatiformis</i>	<i>Hemitosia</i> sp.
			CO IV	<i>Hemitosia turtos</i>	
	Middle	<i>Gastrioceras margin</i>	CO III	<i>Prionocycloceras turtos</i>	<i>Ferretaria (H.) aff. sublaia</i> sp.
					<i>Prionocycloceras iberiense</i>
Lower	<i>Ferretaria (H.) petrosariensis</i>	CO II	<i>Tinosioides hispanicus</i>	<i>Meratinosia eraldi</i>	
		CO I	<i>Tinosioides heplephyllus</i>		
89.8 Ma				No record	

Figure 4.6 Ammonite zonations for the Coniacian of France (Kennedy, 1984) and the North Castilian Domain (northern Spain). The zonal scheme proposed by Wiedmann (1960) and Wiedmann and Kauffman (1978) has been standardised by Santamaría-Zabala (1992). Sz., subzone.

Santamaría-Zabala (1992) promoted to the rank of subzone the occurrence of *Forresteria* (*Harleites*) aff. *nicklesi* at the younger part of the *P. bourgeoisianus* zone. The boundary with the overlying biozone (*Hemitissotia* sp. zone of Santamaría-Zabala, 1992) is recognised by a shift in the lithology and the FO of hemitissotid forms, among which are *Hemitissotia turzoi* Karrenberg, 1935 and *Hemitissotia lenticeratiformis* Wiedmann, in Wiedmann and Kauffman, 1978. It is worth noting that the ornamented species, representatives of older biozones, are replaced by oxicone forms in the uppermost Coniacian.

The age of the Barrio Panizares sequence (within the Nidáguila Formation) is ascertained on the basis of Tethyan ammonites and endemic ammonite species occurring in the Basque-Cantabrian Region. A late Coniacian age to this new *Onchosaurus radicalis* tooth is assigned because the fossil was collected in a bed well above the FO of *Protexanites bourgeoisianus* but before the first specimens of the species *Hemitissotia turzoi* appear in the stratigraphical section (corresponding to the *Hemitissotia* spp. zone).

Chapter 5

STRATIGRAPHY AND PALAEONTOLOGY OF THE UPPER CAMPANIAN GOMETXA BEDS (VITORIA-GASTEIZ, ÁLAVA)

5.1 Introduction

Despite that the Upper Cretaceous in the central part of the B-CB comprises an about 4500-m-thick succession of alternating marine limestone and marl (Martín Alafont et al., 1978), only few localities with shark teeth are reported, and those known lie primarily within the uppermost Cretaceous. This may be in part explained to the lack of favourable facies during most of the Upper Cretaceous period for the accumulation of fish bones and teeth (i.e. condensed beds of low net sedimentation rates, glauconitic clays deposited in inner neritic environments, or lag deposits).

In the course of researching this thesis, it became evident that the existing knowledge of Campanian selachians in the study area was far too incomplete to reflect their diversity. Two prominent fossil-rich sites of Campanian age in central Álava, which have been known for a long time, are considered for study comparisons (Fig. 5.1), namely Gometxa site (see also Chapters 11 and 17) and Vitoria Pass section (see Chapters 6, 12, and 17).

Selachian teeth from the Campanian have been known in Western Europe for decades, yet comprehensive study benefited much from the work of Herman (1977), and more recently from those of Cappetta and Odin (2001), Guinot (2013a, 2013b), Guinot et al. (2012a, 2012b), Guinot et al. (2013), Hübner and Müller (2010), Müller (1989, 1991, 2014), Müller and Diedrich (1991), Müller and Schöllmann (1989), Siverson (1989, 1992), Siverson et al. (2015, 2016), Thies and Müller (1993), and Vullo (2005). Most of these records are related to assemblages living in the Cretaceous temperate (boreal) marine zone, but other occurrences reported from southwestern France (the Aquitaine Basin: Cappetta and Odin, 2001; Charentes: Vullo, 2005) and the scanty material from the northern Iberian continental margin previously considered (Bardet et al., 1993; Corral et al., 2004, 2011) occupied a mid-latitude position (palaeolatitude above 34°N).

The Gometxa beds have already received stratigraphical and micropalaeontological attention (Ramírez del Pozo, 1971; Gräfe, 1994). However, no special consideration has been given with respect to their fossil macroinvertebrate and selachian content. Having said all that, the primary purpose of this chapter is to provide a short geological overview of the Gomecha Member, followed by a brief review of its fossil content. To date, no selachian assemblages from the Campanian have been systematically described in other sedimentary basins of the Iberian Peninsula to compare with. Thereby the description and systematic position of such selachian species will provide new insights into the distribution of this fishes, as will be seen in following chapters.

5.2 Location and geological setting

Gometxa quarry is located about 2 km south the Gometxa village¹, southwest of the capital city of Vitoria-Gasteiz, Álava province (Fig. 5.2). The site is a small, abandoned limestone quarry that is cut into the Peña Eskibel hill (UTM 30T 521878 : 4740308 E/N). The targeted resistant calcarenite-calcirudite strata have formed a prominent escarpment or flatiron in the topography (Fig. 5.3), together with soft marls, make up the main fossiliferous beds. This is one of the few remaining sites still producing Campanian fish vertebrates in Álava. However, highly unstable quarry faces make this location dangerous for fossil collecting. Rock discontinuities (e.g. joints) and other structural weakness (i.e. dip running into quarry), in addition to the extremely fractured material, produce frequent rock falls that accumulate at the toe of the highwall (i.e. rock mass failure) (Fig. 5.4). This pit is also important for showing a section of the Gomecha Member (within the Vitoria Formation).

Several transgressive–regressive short-term cycles (C T/R 4.2 to C T/R 4.4; Floquet, 2004) are recognised for the Campanian–Maastrichtian interval in this southern region of the B-CB. They are represented, in ascending order, by the Vitoria, Montes de Vitoria, and Puerto de Olazagutía formations. The geological outline of the region has already been discussed in section 1.3 of Chapter 1, so I shall not expand on it here.

The largest and best exposures of Campanian strata in Álava (central part of the NCR) occur along the northern foothills of the Vitoria and Iturrieta mountain ranges (Figs. 5.1, 5.5B). The site of Gometxa is located within the Vitoria Sub-basin of the southern B-CB. During most of the Campanian, open-marine sedimentation of the Vitoria Formation² extended throughout this sub-basin. A thick sequence of alternating clayey limestone (wackestone texture) and grey marl containing important associations of planktonic and benthic foraminifera, lithistid sponges, endobenthic echinoids, inoceramids, and ammonites characterises its lower part (Wiedmann et al., 1983; San Martín, 1986). During the upper Campanian the series becomes enriched in clastics

¹ The official name is now Gometxa, but Gomecha can also be found in previous works.

² See Chapter 6 for more information on this lithostratigraphical unit.

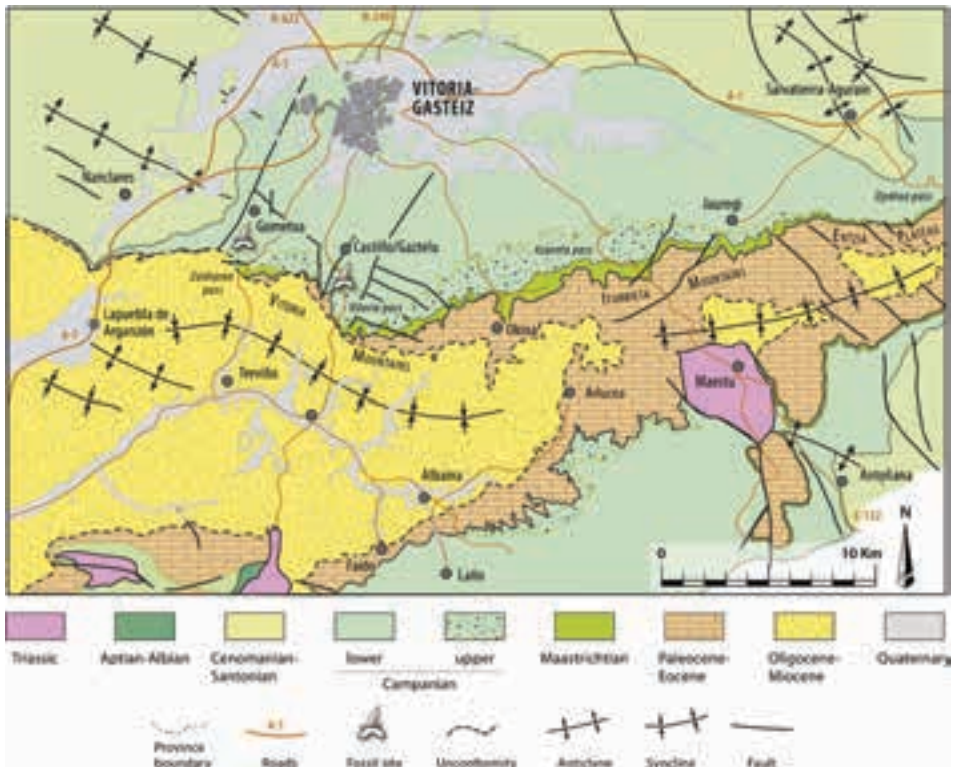


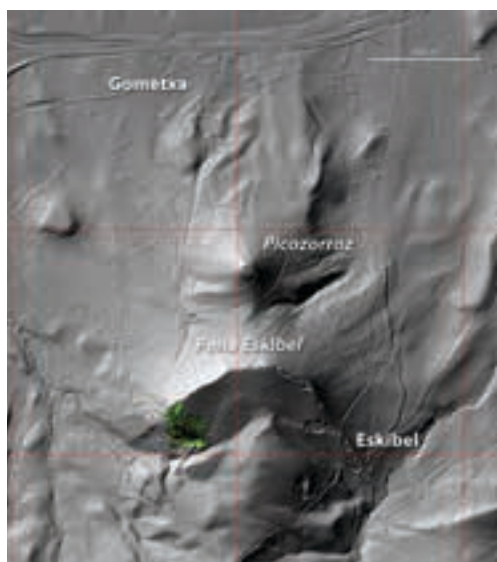
Figure 5.1 Generalised geological map of the central part of Álava showing the location of the two Campanian fossil localities studied in this thesis (compiled from Martín Alafont et al., 1978; Ramírez del Pozo and del Olmo Zamora, 1978; Portero García et al., 1978; Carreras Suárez and Ramírez del Pozo, 1978).

(mainly in fine-grained sand and small flakes of muscovite) with the sedimentation of prodelta silty marls, but marine conditions still prevailed across the sub-basin as indicated by the presence of ammonites and inoceramids (Santamaría Zabala, 1996; Santamaría and López, 1996). Several isolated interbeds of grey calciturbidites (not exceeding 30 m in thickness), which do not persist laterally, occur in the uppermost part of the Vitoria Formation. Engeser (1985) established several named rock units or members for each of these outcrops based on their lithological and genetic features. They are easily identifiable as small hills aligned from east to west in the Álava Plain (i.e. Gometxa, Olarizu, Alegría-Dulantzi, and Alaiza-Gereñu) and are regarded as derived from a carbonate platform, or ramp, which developed further south (Engeser, 1985).

The uppermost Campanian–lower Maastrichtian interval in this area is represented by the terrigenous clastic rocks of the Montes de Vitoria Formation (named by Engeser, 1985). These rocks are yellowish poorly cemented sandstone and carbonate-matrix sandstone with interbeds of silty marls, which are generally fossil-barren with the exception of some microfossil-rich beds, formed by coarse calcarenites (biosparite)



▲ **Figure 5.2** Northeastward panoramic view of the Vitoria Plain showing the quarry pit excavated in the scarp of the Eskibel hill (Peña Eskibel). The photograph was taken from the Vitoria Mountains.



◀ **Figure 5.3** LIDAR image revealing former limestone quarrying in the Peña Eskibel; Gometxa site is shaded in green (source: GeoEuskadi - The Spatial Data Infrastructure of Euskadi; <http://www.geo.euskadi.eus>).

containing benthic foraminifera, ostreids [i.e. *Pycnodonte vesicularis* (Lamarck, 1806)], and echinoid plates (Ramírez del Pozo, 1971; Martín Alafont et al., 1978). These deposits are interpreted by Engeser (1985) to have been deposited in both prodelta and subtidal to intertidal deltaic front environments, indicating sea-level regression. Farther to the south, continental sedimentation continued through upper Campanian and lower Maastrichtian, being represented by terrigenous deposits of the Moradillo de Sedano, Sedano, and Sobrepeña formations (see Corral et al., 2015a; see also Floquet, 1991; Berreteaga, 2008).

The earliest phase of the Alpine orogeny (first tectonic pulses) can be initially identified in this area by a regional unconformity and a hiatus spanning the Campanian



Figure 5.4 Significant rock falls from ‘the pinnacle’ of Gometxa quarry, which occurred at the end of 2013. The pinnacle is about 18 m high and was left by the quarrying operations, note the strata dip running into quarry. Photograph taken on 7 March 2014, view to the northwest. The inset is an aerial orthophoto of the quarry taken in 2015, spatial resolution of 0.25 m (source: GeoEuskadi, www.geo.euskadi.net).

and the Maastrichtian (Alonso, 1986; San Martín, 1986)¹. Fully marine conditions returned in the Maastrichtian, resulting in the deposition of the Puerto de Olazagutía Formation (named by Amiot, 1982) exposed in central and southeast Álava and western Navarre². This formation is predominantly carbonate (sandy fossiliferous limestone and marl sequences) with orbitoidids, brachiopods, molluscs, and large irregular echinoids deposited in shallow marine environments, as observed from exposures in its type locality and other nearby localities (Wiedmann et al., 1983)³.

¹ See Chapter 8 for an expanded section on this.

² Other Maastrichtian outcrops in southern Álava have been correlated with this formation, but are assigned to the Torme Formation as is discussed in Chapter 8 of this thesis.

³ See Chapter 9 for an expanded section on this.

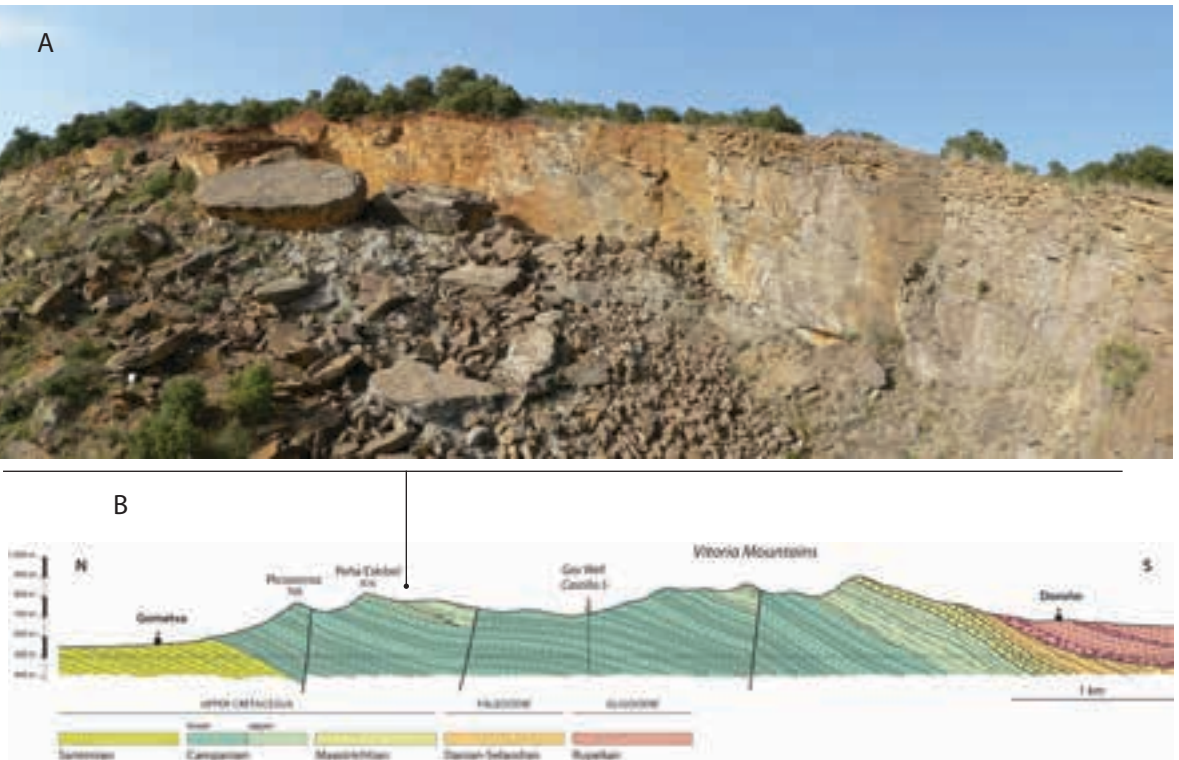


Figure 5.5 A, northward panoramic view of the limestone quarry at Gometxa, Vitoria-Gasteiz; B, cross-section through the northern limb of the Miranda-Treviño synclinal showing the approximate location of the quarry (modified from EVE cartography, 1:25.000).

5.3 Stratigraphy

Review of the Gomecha Member (GM)

Original author. This is one of the several calcirudite–calcarenite units distributed in the E–W direction within the marly upper part of the Vitoria Formation (Vitoria Sub-basin, Basque-Cantabrian Region) that Engeser (1985: 152) clearly distinguished on the basis of lithology and sedimentology.

Type locality. A good exposure of this lithological unit occurs in the abandoned limestone quarry in Gometxa, 8 km southwest of Vitoria-Gasteiz (Álava).

Boundaries. The lower contact is conformably placed at the lowest bioclastic marls, over the marls with siliceous sponges and echinoids (*Micraster* sp.) of the Vitoria Formation (*sensu lato*). Presumably, the upper contact of the member is conformably overstepped by the upper part of the Vitoria Formation, but bad exposures do not allow any further comment on that.

Thickness. The measured section at Gometxa pit is up to 11 m thick.

Lithology. The stratigraphical succession studied is sub-divided into two distinct lithofacies: (1) a lower interval of marl with interbedded parallel-laminated calcarenites, and (2) an upper calcarenite interval arranged in compact beds, usually from 5–10 cm up to 1 m thick. The contact between the two units is commonly sharp planar. A sedimentary log of the lowermost 11 m of the Gomecha Member is shown in Fig. 5.6.

In general, the basal subunit (lithofacies-1) consists of about 2 m of bluish grey marls and alternating marly limestones (wackestone), some of which with gravitational slump flow structures (Fig. 5.7A). These strata contain planktonic foraminifers and a rich assemblage of autochthonous and allochthonous macrofossils (see below). In this lithofacies, benthic foraminifers and internal casts (steinkerns) of gastropods are fre-

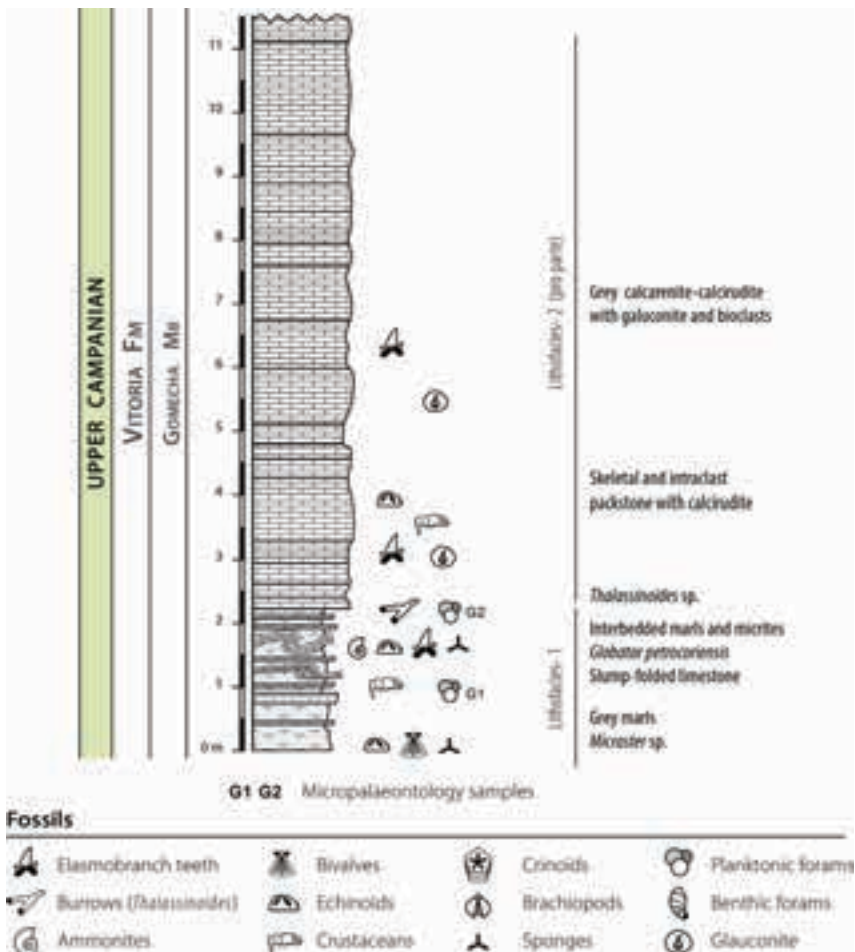


Figure 5.6 Stratigraphical column of the succession exposed at the Gometxa quarry, Vitoria-Gasteiz, with the position of the different fossiliferous beds.

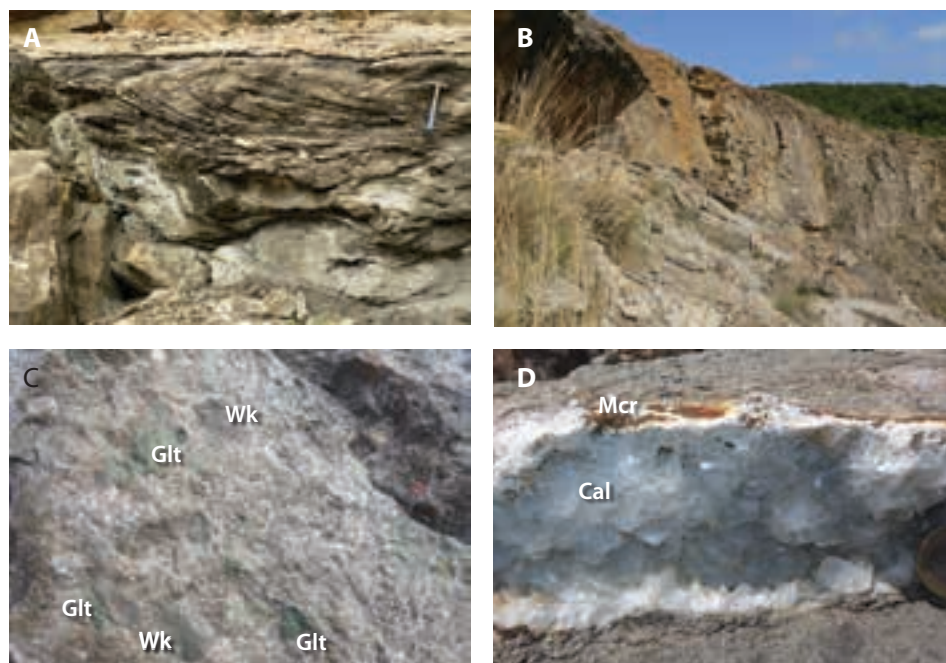


Figure 5.7 Gometxa quarry site, Vitoria-Gasteiz, lowermost upper Campanian. (A) small-scale slide (slump-folded limestone) within the lower lithofacies-1; (B) northeastern face of the quarry (note the medium- and thick-bedded calcarenite over marl beds; the lowermost marly levels are hidden by large size blocks blasted from the quarry face); (C) hand specimen of Gometxa limestone showing a calcirudite texture, Wk (wackestone clasts), Glt (glauconite); (D) druse of white flattened rhombs of calcite crystals on a matrix of limestone, Cal (calcite), Mcr (marcasite).

quently pyritised. Moreover, very small grains of retinite and authigenic red quartz crystals¹ (either sharp-edged or abraded) have been recovered in the residue from bulk sieving elasmobranch remains. The overlying interval (lithofacies-2) is at least 9 m thick, as seen in the quarry wall, and consists of thickly bedded, glauconite-rich packstone calcarenite–calcirudite showing parallel to wavy lamination (Fig. 5.7B) (Tarrío and Corral, unpublished data). Fresh limestone surfaces are greenish grey due to the glauconite content, but weathered surfaces are light grey or brownish-grey.

The Gometxa rock is an arenaceous bioclastic limestone (intrabiosparite and intrabiosparrudite), mostly with a packstone to rudstone texture (Fig. 5.8). The characteristic components of this rock are bioclasts and intraclasts (i.e. monocryalline quartz grains, authigenic crystals of quartz, muscovite flakes, glauconite, and medium grey intraclasts of micritic limestone) in a micrite–microsparite matrix. The most distinc-

¹ Named 'Jacintos de Compostela' in Spanish.

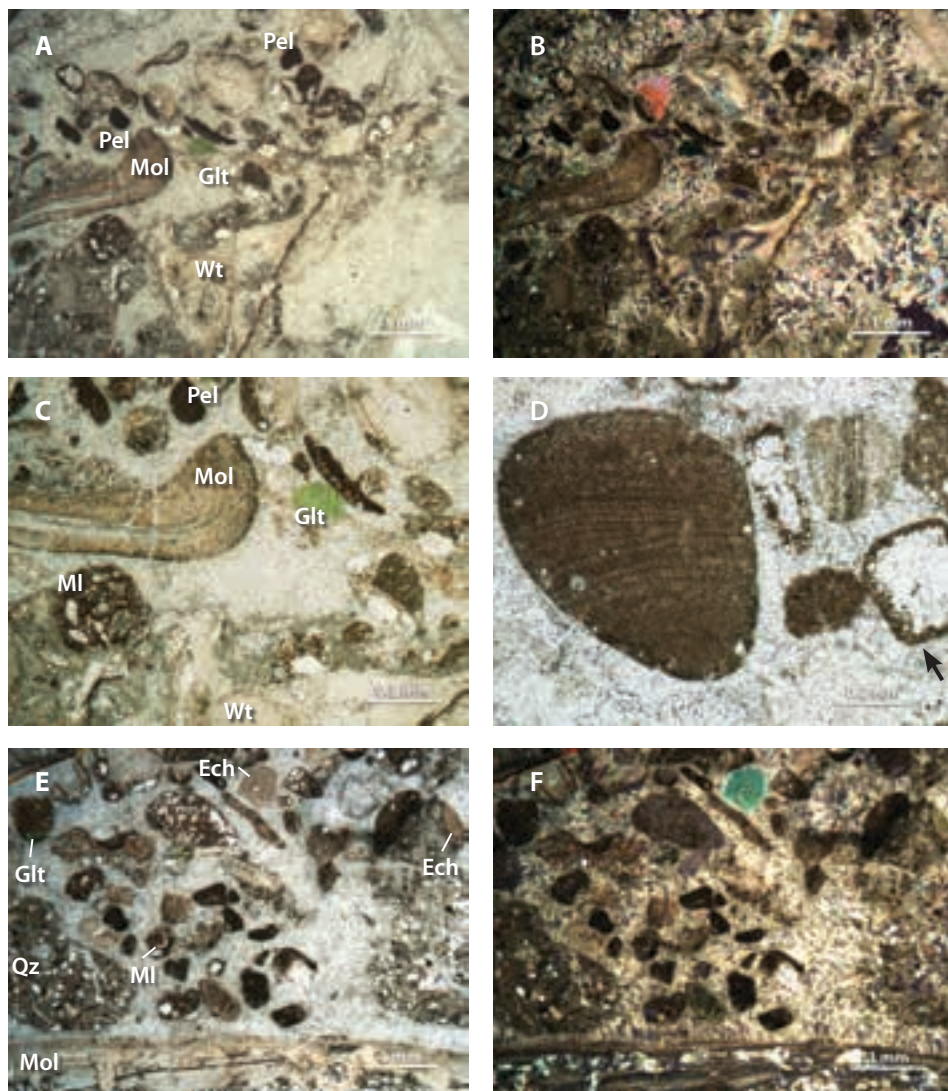


Figure 5.8 Photomicrographs of microfacies in the calcarenite/calcuridite of the Gomecha Member at Gometxa, Vitoria-Gasteiz. A–B, thin section of a packstone–rudstone (intrabioparite to intrabioparrudite) containing faecal pellets, miliolid foraminifers, broken mollusc fragments, and well preserved worm tubes showing their layer microstructure; bio- and lithoclast either in microsparite matrix or cemented by blocky sparite; glauconite and fine sand grains are also present; C, close-up of the central left portion of A; D, coralline algal fragment on the left side (probably *Lithothamnion* sp.) from the same thin section sample, arrow is pointing to the micritised crust on a lithoclast; clasts are cemented by blocky sparite; arrow is pointing a lithoclast; E–F, another thin section of the same sample showing a large mollusc fragment, probably of an oyster, (bottom), a miliolid foraminifer, an echinoderm columnal (left) and echinoid spine (right). Key: Ech (echinoid part), Glt (glauconite), MI (miliolid), Mol (mollusc fragment), Pel (peloids), Qz (quartz), Wt (calcareous worm tubes). A, C, D, and E taken under plane-polarised light (PPL); B, as A but under crossed polars (XPL); F, as E but under XPL.

tive macroscopic bioclasts are fragments of oysters, echinoid plates and spines, serpulid tubes, and occasional fish teeth. Miliolid and other benthonic foraminifers, minute fish faecal pellets, and broken fragments of corallinean algae (*Lithothamnion* sp.) are the most important microbioclasts (Fig. 5.8D). Shelter, mouldic and fracture porosities are observed. Diagenetic alteration of micrite to microsparite and patches of spar calcite occurs. Other diagenetic signatures include calcite druses (Fig. 5.7D), pressure solution surfaces (i.e. stylolites), and some scattered small marcasite crystals. Horizontal burrows, mainly of *Thalassinoides* type, are common at the bottom of some particular calcarenite beds (Fig. 5.9).

Palaeontological content and age. The most remarkable feature of lithofacies-1 is its fossil content. Although it remains to be studied in detail, the representative fauna comprises

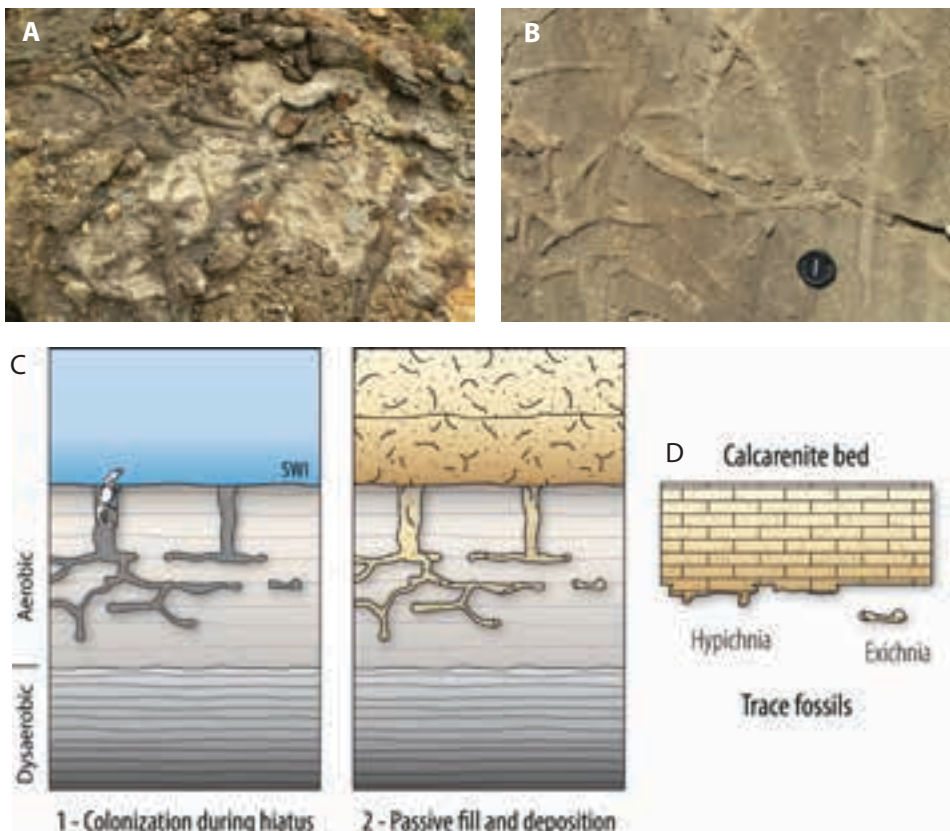


Figure 5.9 A–B, bedding-plane exposure with horizontal networks of burrows, regularly branching, assigned to *Thalassinoides* isp. (calcarene beds of the Gomecha Member, Gometxa quarry); C, schematic drawings of burrows excavated and subsequent filled by carbonate sand (inspired on modern burrow types made by marine benthic ghost shrimps: Decapoda, Callianassidae); D, terminology of the trace fossils observed at the site. Lens cap is 6 cm in diameter; SWI, sediment-water interface.

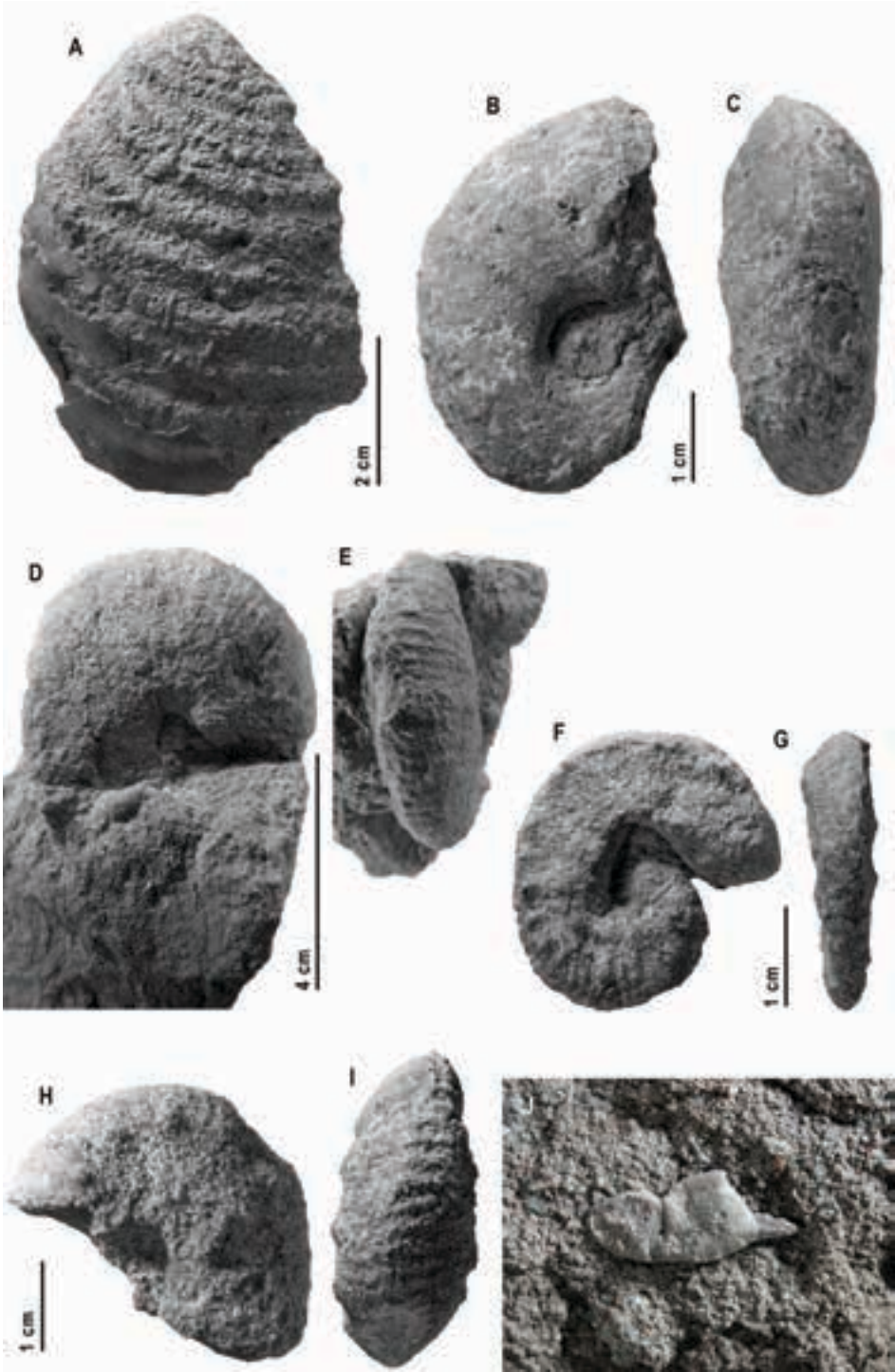
foraminifers, sponges, molluscs (bivalves, ammonites, and gastropods), brachiopods, echinoderms, loose calcareous worm tubes, and crustaceans coexisting with actinopterygian and elasmobranch fishes. The assemblage includes autochthonous–parautochthonous representatives of epifaunal and semi-infaunal species and allochthonous benthic components.

Planktonic foraminiferal fauna has been recorded in samples G1 and G2, though no exhaustive study has been carried out. At the base of lithofacies-1 (G1 association), marls contain a high density of planktonic foraminifers (J.A. Arz, pers. comm.), namely *Heterohelix globulosa* (Ehrenberg, 1840), *H. labellosa* Nederbragt, 1991, *Pseudotextularia nuttalli* (Voorwijk, 1937), *Planoglobulina carseyae* (Plummer, 1931), *Hedbergella holmdelensis* Olsson, 1964, *H. monmouthensis* (Olsson, 1960), *Globotruncanella havanensis* (Voorwijk, 1937), *Rugoglobigerina rugosa* (Plummer, 1926), *Archaeoglobigerina cretacea* (d'Orbigny, 1840b), *Globotruncana arca* (Cushman, 1926), *G. mariei* Banner and Blow, 1960, *G. orientalis* El-Naggar, 1966, *G. bulloides* (Vogler, 1941), *G. aegyptiaca* Nakkady, 1950, *G. linneiana* (d'Orbigny, 1839), and *Contusotruncana plummerae* (Gandolfi, 1955). The upper beds of this unit (G2 association) yielded the following planktonic foraminifera species (J.A. Arz, pers. comm.): *Heterohelix globulosa*, *H. planata* (Cushman, 1938), *Globigerinelloides prairiehillensis* (Pessagno, 1967), *Rugoglobigerina rugosa*, *Globotruncana arca*, *G. mariei*, *G. bulloides*, *G. aegyptiaca*, *G. linneiana*, *Globotruncanita insignis* (Gandolfi, 1955), and *Contusotruncana fornicata* (Plummer, 1931).

Among the various types of macroinvertebrate fossils that colonised this offshore habitat are the sponges. An initial look at the collected material shows that the sponge assemblage is characterised by lithistid representatives of the order Tetractinellida [i.e. *Amphilectella piriformis* Schrammen, 1901, *Homalodoriana ficus* (Schrammen, 1910), and *Homalodoriana ramosa* (Mantell, 1822)]. Modern lithistids live mainly in shallow water extending through the photic zone of the ocean, but epibathyal species also exist (Świerczewska-Gładysz, 2006, and references therein).

A few number of fairly small specimens referred to *Neithea* (*Neithea*) *regularis* (von Schlotheim, 1813) have been collected from the marly spoil heap of the member, but oysters constitute the most important group of the bivalves. The most frequent species among these include *Amphydonte* (*Ceratostreon*) *pliciferum* (Dujardin, 1837), *Pycnodonte* (*Phygraea*) *vesicularis* (Lamarck, 1806), *Hyostissa semiplana* (Sowerby, 1825), and *Gryphaeostrea vomer* (Morton, 1828). Oysters, being sessile filter feeders, prefer low sedimentation rates and adequate water movement to survive. Other stratigraphically important fossil found here is the inoceramid cf. *Cataceramus balticus* (Böhm, 1907), considered to be an epifaunal suspension feeder (Fig. 5.10A).

Ammonites, although uncommon, occur particularly preserved as calcarenite steinkerns within the marly lithofacies-1. Only two taxa have been identified, the heteromorph *Scaphites* (*Scaphites*) *gibbus* Schlüter, 1872 (Figs. 5.10D–I), and a fragmentary specimen referred to *Pachydiscus* sp. (Figs. 5.10B–C).



Many microbrachiopod specimens belonging to the Terebratulida and Craniida orders were recovered from the marly lithofacies-1 as well. Identified species include *Argyrotheca hirundo* (von Hagenow, 1842), *Terebratulina chrysalis* von Schlotheim, 1813, and *Isocrania campaniensis* Ernst, 1984. The specimens, which are comparable to those described by Simon (2000) from the Mons Basin (province of Hainaut, Belgium) and by Bitner and Pisera (1979) from the chalk of Mielnik (eastern Poland), are benthic epifaunal suspension feeders, capturing food particles from bottom currents.

A few skeletal elements of stalked crinoids (i.e. disarticulated ossicles of *Bourgueticrinus* sp. and small pentastellate columnals resembling to *Isocrinus* sp.) and a large number of starfish ossicles belonging to the Goniasteridae were collected from the sieved sediment samples of lithofacies-1. Post-mortem disarticulation of asteroids and crinoids occurs quickly after death and decay of the soft tissue; and when this occurs in shallow-water agitated environments many fragmented, abraded skeletal parts are produced. Many of specimens from Gometxa present considerable signs of abrasion and, thus, an eventual transport to the marly depositional setting was most likely.

Echinoids constitute another important group of fossils. Regular echinoids include complete but usually abraded phymosomatid tests. The matrix inside them is calcarenite. Moreover, dissociated interambulacral plates and both long slender and club-shaped primary spines of the cidarid *Tylocidaris* sp. are frequently found. Among the irregular echinoids are the conulids *Globator petrocoriensis* (Desmoulin, 1837) and *Conulus douvillei* (Cotteau and Gauthier, 1895), juvenile specimens of the micrasterid *Micraster* sp., and undetermined Holecypidae individuals.

The most distinctive forms of calcareous worm tubes are represented by the serpulids *Neovermilia ampullacea* (Sowerby, 1829), *Rotularia (Rotularia) hisingeri* (Lundgren, 1891), *Rotularia (Praerotularia) saxonica* Müller, 1966, and *Placostegus* sp., and the sabellid *Glomerula gordialis* (von Schlotheim, 1820). With regard to lifestyle, tubicolous polychaetes depend on water movement for feeding purposes (sessile filter feeders). Observations indicate that bryozoan colonies and large bioclasts (e.g. inoceramid shell fragments) have been used by many of the above taxa as relatively stable substrate. However, other specimens show no evidence of being fixed to a hard substrate, suggesting that they encrusted some biological structures not preserved as fossils to cope with soft bottom marine regimes.

◀ **Figure 5.10** Selected macrofossils from lowermost upper Campanian at Gometxa quarry (Vitoria-Gasteiz). A, cf. *Cataceramus balticus* (Böhm, 1907), MCNA 15520; B–C, *Pachydiscus* sp. in lateral and ventral views, MCNA 15526. D–I, *Scaphites (Scaphites) gibbus* Schlüter, 1872, (D–E) partial shaft and curved hook of a macroconch in lateral and ventral views, MCNA 15542; (F–G) laterally crushed microconch in lateral and ventral views, MCNA 15540; (H–I) partial shaft and curved hook in lateral and ventral views, MCNA 15527. J, undetermined Brachyura, left chela with carpus in ventral view, length 2 cm, MCNA 15519.

Decapod remains are uncommon but occur, specially isolated chelipeds or detached parts of them (e.g. propodus and dactylus) (Fig. 5.10J). Moreover, trace fossils assigned to decapod activity occur as hyporeliefs (e.g. hypichnia and exichnia) at the bottom of strata in the calcarenite–calcirudite subunit (lithofacies-2) (Fig. 5.9) and are dominated by large horizontal branching-shaped burrows and tunnel systems (e.g. *Thalassinoides* isp.).

From the above evidences, the invertebrate faunae of Gometxa share strong similarities with those of the Hannover area (Germany), the Vistula and Nida sections (south-east Poland), the Mons Basin (Belgium), and the southern Limburg (Netherlands).

Elasmobranch remains constitute another important group within the Gomecha Member. Many well-preserved teeth of selachians, ranging from coastal marine to oceanic and deep water, have been recovered from the basinal lithofacies-1 and the shallow-derived lithofacies-2. They will be further dealt with in Chapters 11 and 17.

The age of the Gomecha Member can be bracketed by the rich microfossil associations of the marls of the Vitoria Formation, beneath, and the silty marls and sandstones included in the Montes de Vitoria Formation, above (Ramírez del Pozo, 1971: 183). Therefore, the Gomecha limestone was considered to be lower middle Campanian (Ramírez del Pozo, 1971; Engeser, 1985) and correlated with the genetically related Olárizu Member, whose age is lower-middle Campanian on the basis of their microfossil content, according to Martín Alafont et al. (1978). However, in terms of the twofold division of the Campanian used for the European formations, the middle Campanian should be considered the lower part of the upper Campanian (Kennedy and Cobban, 2001).

The dating of Gometxa beds is supported by the occurrence of the scaphitid ammonites *Scaphites* (*Scaphites*) *gibbus*. In Germany, this species ranges from the uppermost lower Campanian to the lowermost upper Campanian, and in Poland the species occurs in the lower upper Campanian (Machalski et al., 2004). Küchler (2000b) described the species *Scaphites hippocrepis* (De Kay, 1828) IV, a variant form of the taxon *Scaphites hippocrepis* (De Kay, 1828) III, noticing that the taxon is restricted to the basal upper Campanian of the Navarre-Cantabrian Domain of the B-CB. However, such specimens seem to be more closely related to *Scaphites* (*Scaphites*) *gibbus*, according to Machalski et al. (2004). The species of microbrachiopods and calcareous polychaetes found in the Gometxa beds have been reported in coeval deposits from Belgium (Simon, 2000) and Poland (Bitner and Pisera, 1979; Radwanska, 1996). Identifiable sponges from the lower marly unit of the Gometxa succession may be also compared with those of the uppermost lower Campanian described by Schrammen (1901, 1910) in Germany and others of the lower to lowermost upper Campanian from Poland (see Bieda, 1933; Hurcewicz, 1966; Świerczewska-Gładysz, 2006, 2016). The echinoid faunae may also be compared with the species known from the lower upper Campanian (=middle Campanian) of northern Cantabria in the northeastern of the B-CB, which have been reported by Schluter et al. (2004) and Wilmsen et al. (1996). However, the

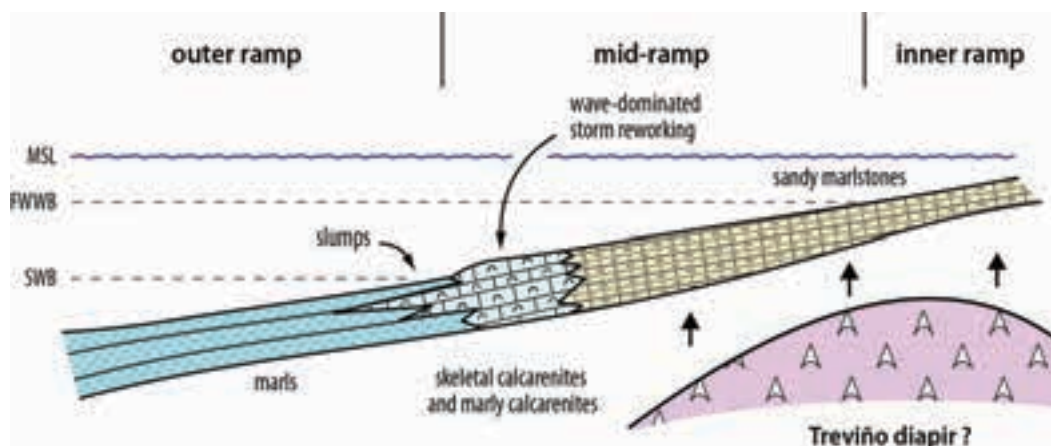


Figure 5.11 General facies for the Gometxa ramp, during the upper Campanian. Key: MSL, mean sea level; FWWB, fairweather wave base; SWB, storm wave base.

micropalaeontological study of the samples collected in the Gometxa beds indicates a younger age, specifically a late Campanian age of deposition according to the Arz and Molina (2002) calibration. The two samples (G1 and G2) have a foraminifer association that characterises the *G. aegyptiaca* zone (*G. aegyptiaca* subzone), with an approximate age of 73.5 Ma (J.A. Arz, pers. comm.) (see Fig. 6.11 in Chapter 6). This value is interesting because the overlying calcarenites (lithofacies-2) had been regarded in regional studies as the base of the middle Campanian (Engeser, 1985; Gräfe, 1994).

Depositional environment. The GM represents a local shift in the depositional area from the normal open marine conditions of the Vitoria Formation (e.g. a marly carbonate ramp with echinoids and siliceous sponges) to mid-ramp to fore slope settings represented by calcarenite–calcirudite and marl–wackestone interbeds, respectively.

The lower interval of the GM (lithofacies-1) is characterised by prevailing marine mudstone deposition (mainly marl with abundant fossil bioclasts, many of them derived from the upper part of the ramp). The presence of scaphitid ammonites may imply neritic waters within the continental shelf, although there is also the possibility of a post-mortem transport for those shells to deeper deposits. The planktonic foraminifers suggest mainly basinal depositional conditions. Ramírez del Pozo (1971) suggested an outer ramp (or upper slope) depositional setting on the basis of the analysis of benthic and planktonic foraminifers, whose sea depth were most likely from 80 to 400 m and deepening eastward. Engeser (1985) suggests a lower shelf depositional setting (below 100–150 m water depth). The abraded, disarticulated skeletal parts of macroinvertebrates are thought to be derived likely from shallower areas of the carbonate ramp, and the slump-folded limestones suggest a distal steepening palaeoenvironment located near the mid- and outer ramp boundary. According to the biostratigraphic features observed in the echinoids, it is considered that the disarticulated skeletal parts of

cidarids resulted in shallow high-energy environments after the death of the individuals, being eventually transported basinward by physical processes. Moreover, Schluter et al. (2004) have indicated that globular echinoids of the family Conulidae, which are considered to be epifaunal grazers and deposit feeders, predominantly occur on coarse-grained substrates in shallow waters. This all would indicate that many of the echinoderms have derived from shallower areas of the carbonate ramp.

The cooccurrence of autochthonous-parautochthonous and allochthonous faunal components is thought to be due to material washing into deeper water settings by storm-induced flows. The slump morphologies may also be explained by downslope movement of semi-consolidated sediment, triggered by seismic activity during halokinesis (Engeser, 1985) (Fig. 5.11).

As suggested by a sharp bed contact with the overlying subunit (lithofacies-2), the period of pelagic marl deposition with burrowing in normal calm conditions was interrupted by an episode of carbonate deposition that rapidly infilled the *Thalassinoides* burrow makers (Fig. 5.9). The grain-supported limestone (packstone to rudstone textures) in this lithofacies is essentially interpreted to represent a deposit of distal calciturbidites derived from one of the several structural highs located in the central part of the Vitoria Sub-basin. Both the fossil content (i.e. epifaunal oysters, disarticulated skeletal elements of echinoids and reworked shell detritus) and the presence of glauconite suggest, for the origin of the sediment, a relatively shallow agitated depositional environment under the influence of currents or storms-waves that, in turn, were not great enough to completely winnow the carbonate mud. Among the most common extraclasts in this limestone are millimetric red authigenic quartz grains and red mudstone clasts derived from an exposed diapir (Wiedmann et al., 1983). It is thought that salt tectonics in this part of the Vitoria Sub-basin (probably related to the non-outcropping Treviño diapir) led to instabilities that presumably triggered slumping and turbidity currents on distal parts of the ramp (Engeser, 1985).

In sum, the depositional site was relatively deep (below storm wave base), where coarse material (e.g. calcarenitic sand) derived from salt diapir highs was transported downward and interfingered with basinal sediment (Engeser, 1985). Keuper-derived red clayey intraclasts and abraded red quartz crystals in the calcarenites indicate a significant influence by a diapir (Engeser, 1985). The calcarenite–calcirudite facies passes upward into alternations of grey silty marls with sponges, which represents a return to a most typical ramp deposition within the NCR domain of the B-CB.

Stratigraphical relationships and correlations. The major lithostratigraphical divisions for the Campanian in the Vitoria Sub-basin are shown in Fig. 6.10 (in Chapter 6). The GM interfingers with the marly ramp facies of the Vitoria Formation and passes upward into the main body of this formation. This lithological unit has been correlated eastward with similar calcarenite lithosomes, named Olárizu-Member, Alegría-Member, and Alaiza/Gereñu-Member (Engeser, 1985; Gräfe, 1994), which crop out in a west–east-trending direction along the northern slopes of the Vitoria and Iturrieta ranges.

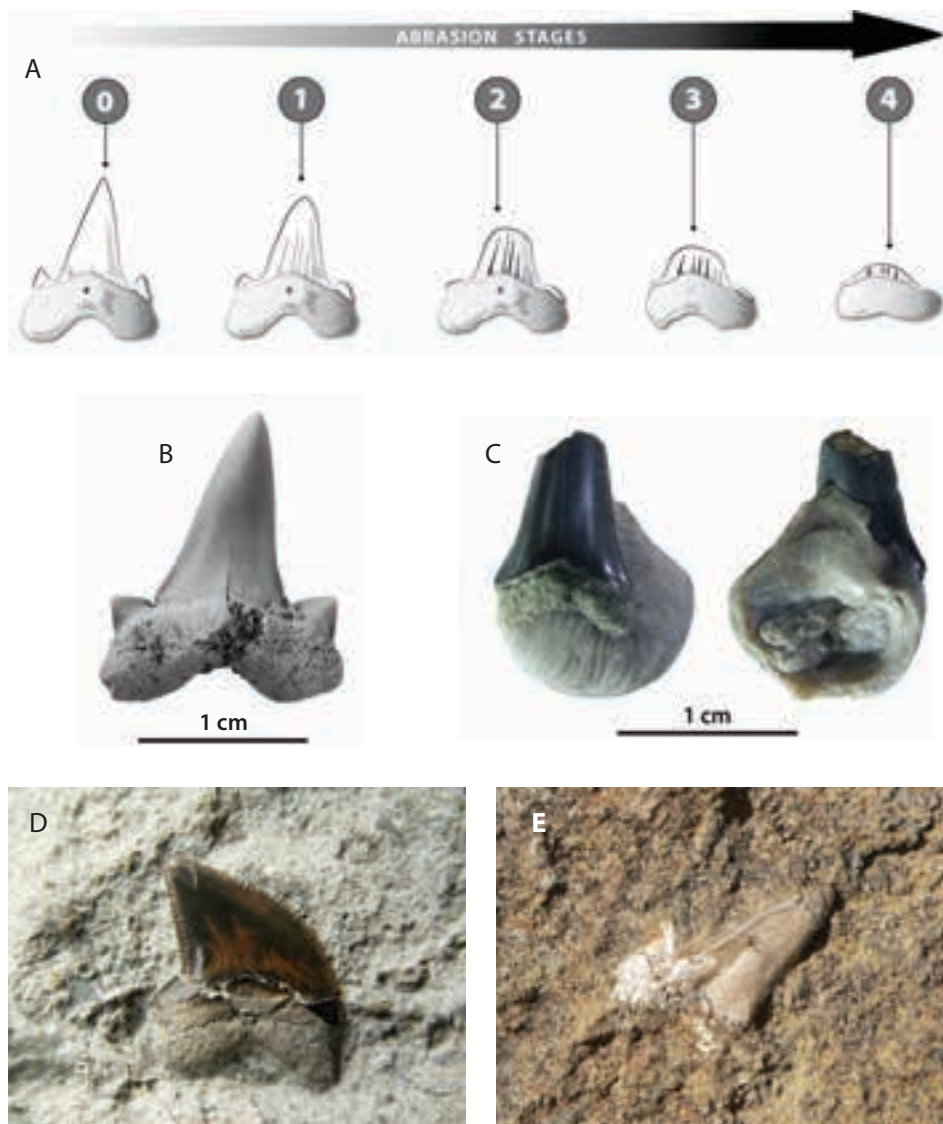


Figure 5.12 Taphonomic features in selachian teeth from the Gomecha Member. A, abrasion stages of a shark tooth (based on Benton, 2015). B–C, specimens from the marly lithofacies-1: (B) *Cretolamna* sp., tooth well preserved (grade 0); (C) *Cretolamna* sp., abraded, rootless tooth (grade 3) to which is firmly cemented an isolated oyster shell [*Gryphaeostrea vomer* (Morton, 1828)] in lingual and labial views, MCNA 15516. D–E, combined effect of abrasion damage by biostratinomy and mechanical compaction produced during diagenesis from the grain-supported limestone lithofacies-2: (D) *Squalicorax* ex gr. *kaupi* (Agassiz, 1843), slightly abraded tooth (grade 1) in calcarenite matrix showing fractures across the crown that originated by compaction after burial (acid-prepared specimen, note the splintering or feeding-related damage in the apex of the crown; tooth width 1.5 cm); (E) *Cretolamna* sp., collapsed tooth (grade 2) in calcarenite matrix severely damaged by burial compaction (note the brown insoluble clayey residue left during stylolitization; tooth length 1.5 cm).

5.4 Some general taphonomic features observed on the elasmobranch teeth

Because elasmobranch fishes are continuously losing and shedding their teeth in a lifetime, the chances of preservation of such hard skeletal elements are high. In the Gomecha Member, elasmobranch teeth occur as loose specimens, as they do in many other fossil sites all over the world.

The recognized taphonomic features of these elements include encrustation and abrasion. Different grades of abrasion (Fig. 5.12A), which are related to the sedimentary facies from which they came, characterise the teeth assemblages. In general, those teeth from the marly lithofacies-1 are well preserved, ranging from grade 0 (unabraded; Fig. 5.12B) to grade 1 (slightly abraded) after Benton's classification (see Benton, 2015). Occasionally, there may be cases with grade 3 as shown in Fig. 5.12C. In general terms, abrasion is usually higher in those teeth from the calcarenite unit (lithofacies-2), ranging from grade 1 (slightly abraded; Fig. 5.12D) to grade 3 (rootless and heavily abraded).

A remarkable taphonomic feature is the encrustation of a selachian tooth by a *Gryphaeostrea vomer* shell (Fig. 5.12C). As the oyster has grown on an abraded, loose shark tooth, this is an exclusively post-shed process. Furthermore, the presence in the marly lithofacies-1 of such oyster specimen, distinctive inhabitant of nearshore and shallow subtidal settings, would indicate downslope reworking, disarticulation and redistribution by currents and sediment gravity flows across the depositional setting.

Cracking and implosion are other observed post-burial taphonomic features in the selachian teeth. They were resulting from sediment loading in coarse-grained deposits (i.e. calcarenite strata of lithofacies-2), having caused several fractures along the cusp and other elements of the crown (Fig. 5.12E).

Chapter 6
STRATIGRAPHY AND PALAEOLOGY OF THE UPPER CAMPANIAN
VITORIA PASS BEDS (VITORIA-GASTEIZ, ÁLAVA)

6.1 Introduction

Rock exposures of the Eguileta Member (EM) have yielded a well-preserved marine vertebrate fauna, particularly notable for their fish (osteichthyes and elasmobranchs) and mosasaur remains (Bardet et al., 1993, 2006; Corral et al., 2004, 2011). The importance of elasmobranch occurrences in Campanian formations has been anticipated in previous chapters, and it is for this reason that I will therefore not expand further on it here —just a reminder that their presence in other parts of the Basque-Cantabrian Basin (B-CB) is rather scarce. Many of these fossils come from a series of small pits excavated along the northern foothills of the Vitoria Mountains in Álava province, which once supplied material for brick making. Notable among these are the Vitoria Pass¹ quarry pits, embracing the territory of the Gardelegi² and Castillo villages in the Vitoria-Gasteiz municipality. The open pits have long been regarded among amateur palaeontologists as a classic area for fossil collecting soon after the abandonment of the pits in the 80's of the 20th century. Unfortunately, most collecting areas are no longer accessible because some of the no longer active pits became disposal sites for the excess material removed during construction of an improved pass road on the existing route A-2124/BU-750, and some other rock exposures became restored over a decade ago. Thus, much of the content of this chapter is based primarily on unpublished geological data from my own field work and that of others, and on fossil specimens collected at that time when the fossiliferous strata were available. Apart from elasmobranchs, invertebrate fossils such as ammonites, bivalves, gastropods, irregular echinoids and decapods are the most common type of fossils found at the sites, some of them of great value for correlation with other Campanian successions in northern Europe.

¹ Puerto de Vitoria in Spanish.

² The locality was erroneously given as Lasarte (Vitoria-Gasteiz) in previous articles.



Figure 6.1 Map of the former clay quarries, Ariaza pit and Mingobaso pit at Vitoria Pass, Vitoria-Gasteiz, showing the position of the fossil sites.

6.2 Location and geological setting

The Vitoria Pass quarrying area (Fig. 6.1) is situated about 8 km south of the capital city of Vitoria-Gasteiz and comprises two adjoining partially infilled quarry pits: the Ariaza pit (also called the Farm) on the west side of the A-2124 (UTM 30T 525784 : 4736892 E/N) (Fig. 6.2), and an small pit named Mingobaso, now backfilled, to the east (UTM 30T 526652 : 4736636 E/N) (Fig. 6.3).

Geologically, the area belongs to the shallow-marine Navarre-Cantabrian Ramp (NCR) of the B-CB, developed at the northern passive continental margin of the Iberian plate. The relevant aspects of the site was briefly described by Bardet et al. (1993) and some general information on the regional geology and stratigraphy has been already covered in Corral et al. (2015a) and preceding chapters. Previously, other authors such as Ramírez del Pozo (1971), Martín Alafont et al. (1978), Wiedmann et al. (1983), and Engeser (1985) provided valuable geological and biostratigraphical information that



Figure 6.2 Southwestern panoramic view of the Ariaza pit quarry at Gardelegi, Vitoria-Gasteiz. Arrows represent the fossiliferous strata: 1, clayey marls with fish fossils; 2, glauconitic marls with ammonites. Ariaza Mount is in the background. Photograph taken circa 1989.



Figure 6.3 The Mingobaso pit quarry at Castillo, Vitoria-Gasteiz. Photograph taken in 1993, view to the northeast.

have effectively contributed to a better understanding of the area. Here I will continue to focus on the Eguileta Member (within the Montes de Vitoria Formation), which define shallow-marine settings developed south of the NCR, and that are particularly well accessible in the northern slopes of the Vitoria Mountains (Vitoria-Gasteiz, central part of the Basque Cantabrian Region) (see Fig. 5.1 in Chapter 5).

A phase of shallow-marine carbonate sedimentation developed in the Vitoria Sub-basin during the lower to lowermost upper Campanian (Vitoria Formation). This marly sequence (up to 1000 m thick) includes smooth shelled ostracods and planktonic foraminifera accounting for up to 50%, which would correspond to an outer shelf environment (Engeser, 1985). This depositional period was followed by a regressive phase – included in the large scale cycle C–T 4 recognised by Floquet (2004) –, which is represented successively by silty marls with ammonites and siliceous sponges, and the series of marl and siltstone with sandstone interbeds of the Montes de Vitoria Formation (Engeser, 1985). Martin Alafont et al. (1978) noticed that these silty marl beds of the upper Campanian were fossil-rich, mainly with benthic foraminifera and oysters (*Pycnodonte* sp.), while the mostly friable sandstone strata of the upper part of the sequence (both friable sandstone and well cemented sandstone with a carbonate matrix) were almost barren of fossils. Farther south, in southern parts of the Vitoria Sub-basin, compressive pulses caused uplift and subaerial exposure, producing rich deposits of continental vertebrates of late Campanian age (Astibia et al., 1990, 1999a; Corral et al., 2015a; Pereda-Suberbiola et al., 2015a). The continued regression observed in the south central part of the B-CB corresponds to the time of compression between the Iberian and European plates (Pyrenean compression of the Alpine phase), when thick fluvio-deltaic deposits accumulated (Robles, 2014).

An important stratigraphical discontinuity existing between the Campanian and the upper Maastrichtian is interpreted as the result of these above mentioned compressive tectonic pulses (Baceta, 1996). The upper Maastrichtian transgression initiated a carbonate platform with expansive shallow hemipelagic deposits of marl and clayey limestone (Wiedmann et al., 1983; Baceta, 1996; Robles, 2014). Such strata contain abundant orbitoidids, molluscs, including ammonites, and irregular echinoids in eastern Álava (see Chapter 9) and in the type locality of the Puerto de Olazagutía Formation (named by Amiot, 1982). However, this formation in the higher part of the Vitoria Pass section is almost entirely comprised of bioclastic limestone, the age of which was determined as Maastrichtian using benthic foraminifera (Ramírez del Pozo, 1971).

6.3 Stratigraphy

The Vitoria Pass succession has permitted the recognition of distinct Campanian–Maastrichtian facies that are shown on the generalised stratigraphical column in Fig. 6.4.

Stratigraphical description

The lower Campanian of the Vitoria Sub-basin is composed mostly of grey micrite or biomicrite (wackestone texture) with interbeds of marl that correspond in part to the Vitoria Formation. The faunal content is scarce throughout this part of the series, but some echinoids of the genus *Micraster* and *Echinocorys*, and lithistids sponges have been reported (Bardet et al., 1993). These rocks are overlain by blue-gray clayey marl

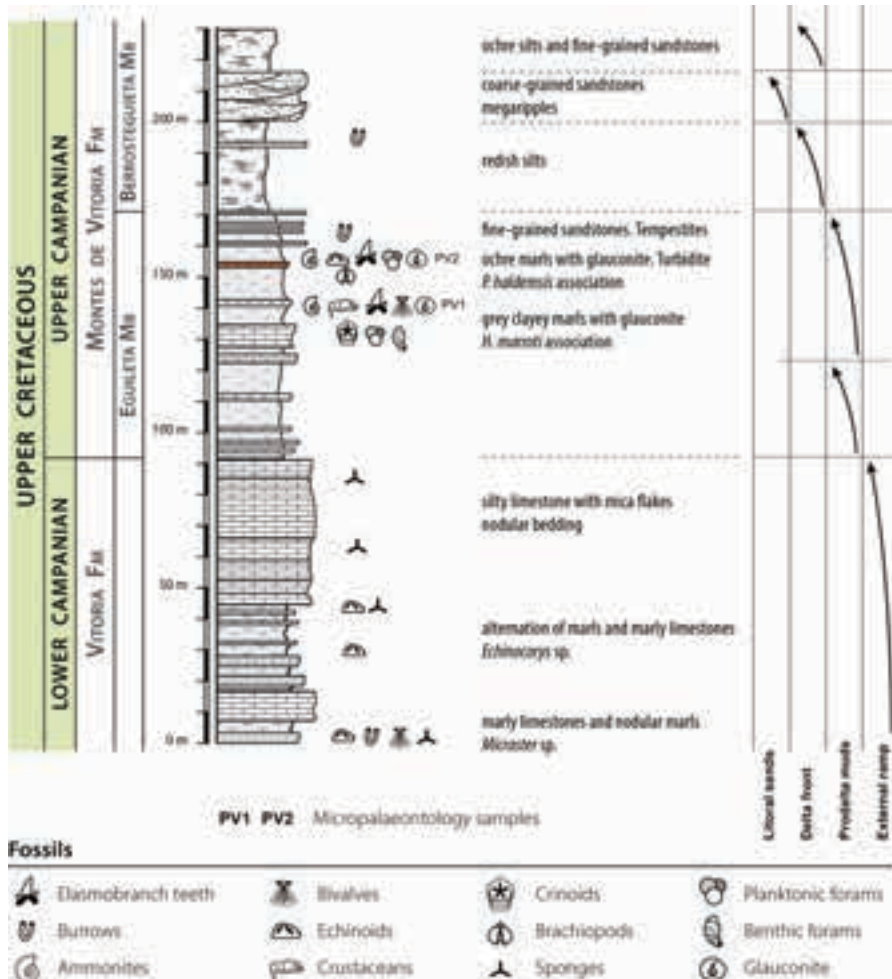


Figure 6.4 Generalised stratigraphical column representing the rocks exposed at Vitoria Pass showing the position of main fossiliferous beds (modified from Bardet et al., 1993).

and siltstone rocks of the Eguleta Member (EM), which is the basal member of the Montes de Vitoria Formation (named by Engeser, 1985). Lithologically, the EM consists of 35–40 m thick dark-grey to bluish-grey clayey marl beds with some interbeds of sandy marlstone and fine-grained sandstone (Fig. 6.5). It is difficult to identify directly the sedimentary contact between the underlying Vitoria Formation and the Montes de Vitoria Formation, but the basal EM of the latter seems to rest conformably on the underlying lower Campanian strata.

The main part of the EM consists of a thick succession of soft, grey marls with glauconite grains and framboid aggregates of pyrite–marcasite (Figs. 6.6A–B). The base of the section was better exposed on the western part of the Ariaza pit, but unfortunately,



Figure 6.5 A view of the Ariaza clay pit in the Puerto de Vitoria site, Vitoria-Gasteiz (Álava), showing the clayey marls of the upper Campanian (Eguileta Member). Note the geologists prospecting for fossils along the outcrop (now inaccessible). Photograph taken ca. 1986 looking south. Author unknown.

most part of the section is now covered by dumped material and overgrown by vegetation. Phosphatic concretions (crab balls) also occur sporadically at some stratigraphical levels, some of them include isolated carapaces of the raninid crabs of the genus *Cretacorantina*. Numerous other fossil invertebrates are concentrated on some horizons within this succession. Especially frequent among them are echinoids of the species *Echinocorys subglobosa* (Goldfuss, 1826), which are very often deformed by compactation, and bioclasts derived from other echinoderms (i.e. plates and spines of cidarids, stems parts of the crinoid *Bourgueticrinus* sp., and isolated ossicles of asteroids). Moreover, bryozoans, small solitary corals, small gastropods, and bivalves also occur (some components of this fauna occur as pyritised casts). As reported by Santamaría Zabala (1996), the common ammonites of this part of the succession are *Baculites* sp. and *Hoplitoplacenticeras marroti* (Coquand, 1859), also occurring as pyritised cast, to which is added *Lewyites elegans* (Moberg, 1885) (Fig. 6.7). The vertebrate fossils include remains of teleosteans (teeth and vertebrae) and especially loose teeth of shark and marine reptiles, which are concentrated in some horizons within this succession (Bardet et al., 1993, 2006; Corral et al., 2004, 2011; see also Chapters 12 and 17 in this thesis).

Two samples taken from the Ariaza pit have yielded planktonic foraminifers (J.A. Arz, pers. comm.) (see Fig. 6.4 with respect to their position in the stratigraphical log). The older sample analysed contains the following planktonic foraminifers (PV1 association): *Heterohelix globulosa* (Ehrenberg, 1840), *H. planata* (Cushman, 1938),

H. navarroensis Loeblich, 1951, *Pseudotextularia nuttalli* (Voorwijk, 1937), *Globigerinelloides prairiebillensis* (Pessagno, 1967), *Hedbergella holmdelensis* Olsson, 1964, *H. monmouthensis* (Olsson, 1960), *Rugoglobigerina rugosa* (Plummer, 1926), *Archaeoglobigerina cretacea* (d'Orbigny, 1840b), *Gansserina gansseri* (Bolli, 1951), *G. wiedenmayeri* (Gandolfi, 1955), *Globotruncana arca* (Cushman, 1926), *G. mariei* Banner and Blow, 1960, *G. bulloides* (Vogler, 1941), *G. aegyptiaca* Nakkady, 1950, *G. rosetta* (Carsey, 1926), *G. linneiana* (d'Orbigny, 1839), *Globotruncanita angulata* (Tilev, 1951), *G. insignis* (Gandolfi, 1955), *Contusotruncana patelliformis* (Gandolfi, 1955), *C. fornicata* (Plummer, 1931), and *C. plummerae* (Gandolfi, 1955). The younger sample has yielded the following planktonic foraminifera species (PV2 association): *Laeviheterohelix glabrans* (Cushman, 1938), *Heterohelix globulosa*, *H. planata*, *Pseudotextularia nuttalli*, *Globigerinelloides multispina* (Lalicker, 1948), *Rugoglobigerina rugosa*, *R. hexacamerata* Brönnimann, 1952, *R. milamensis* Smith y Pessagno, 1973, *R. rotundata* Brönnimann, 1952, *Archaeoglobigerina cretacea*, *Gansserina gansseri*, *G. wiedenmayeri*, *Globotruncana arca*, *G. mariei*, *G. bulloides*, *G. aegyptiaca*, *G. ventricosa* White, 1928, *Globotruncanita stuartiformis* (Dalbiez, 1955), *Contusotruncana fornicata*, and *C. plummerae*.

Above the monotonous marly succession there is a 0.5–0.75 m thick layer of compact grey – or usually ochre-brown due to the oxidation – marlstone with parallel laminations that contains oxide-coated glauconite, siderite grains, and detrital quartz (Figs. 6.6C–D). This layer also contains many macroinvertebrates, including ammonites, being relatively large the size of some of them (up to 35 cm in diameter). This is the layer called by Santamaría Zabala (1996) 'Association with *Pachydiscus haldemsi*' in which ammonites are frequent. The ammonite list includes *Baculites* cf. *texanus* Kennedy and Cobban, 1999, *Gaudryceras* cf. *kayei* (Forbes, 1846), *Pachydiscus* (*P.*) *oldhami* (Sharpe, 1855), *Pachydiscus* (*P.*) *haldemsi* (Schlüter, 1867), *Pseudophyllites indra* (Forbes, 1846), and *Trachyscaphites spiniger porchi* (Adkins, 1929) (Fig. 6.9). This bed also contains undetermined nautiloids, large specimens, very often deformed, of the echinoid *Echinocorys subglobosa* (Goldfuss, 1826), the rhynchonellid *Owenirhynchia* aff. *rubra* Calzada, in Calzada and Poci, 1980, and the bivalves *Spondylus truncatus* (Lamarck, 1819), *Amphydonte* (*Ceratostreon*) sp., *Corbicula* sp., *Neithea* (*Neithea*) *sexcostata* (Woodward, 1833), and *Panopaea* sp. (G. López, 1996, pers. comm.).

Further upsection, and intercalated within a 10 m thick monotonous marly succession, there are some decimetre-thick layers of grey, fine-grained sandstone. This rock is characterised by detrital mica, fine carbonaceous material, pyrite nodules and undetermined epichnia traces (Figs. 6.6E–F).

The remaining upper part of the Vitoria Pass succession comprises the siliciclastic-dominated unit (thickness up to 280 m, partly shown in Fig. 6.4) of the Berrosteguieta Member. It consists of reddish siltstone beds and yellow, coarse-grained to microconglomeratic sandstone (subarkose) with varying degrees of cementation, dominated by sub-angular and well sorted quartz grains with mica flakes (Bardet et al., 1993). Occasionally, they contain interbeds of biosparite and silty marl with benthic foraminifera

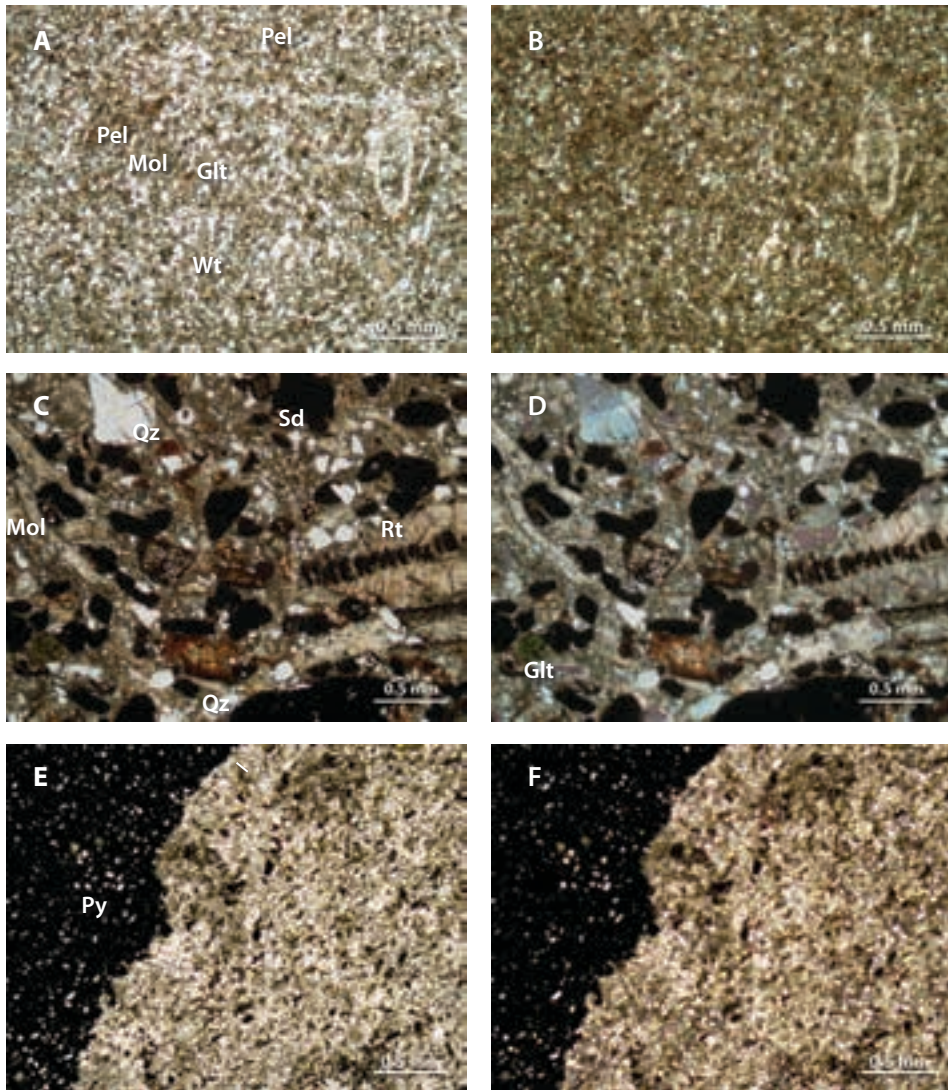


Figure 6.6 Representative microfacies of the Eguileta Member at Vitoria Pass, Vitoria-Gasteiz (Álava). A–B, mudstone containing silt-sized quartz grains in clay-dominated matrix from the clayey subunit; C–D, bioclastic mudstone from the turbiditic subunit containing glauconite and greater abundance of siderite grains; E–F, fine-grained sandstone with pyrite nodules. Key: Bf (benthic foram), Glt (glauconite), Mol (mollusc fragment), Qz (quartz), Rt (Rotaliina), Sd (siderite). A, C, and E taken under plane-polarised light (PPL), B, D, and F as A, C, and E respectively, but taken under crossed polarised light (XPL).

Figure 6.7 Selected ammonites from the clayey marl facies of the Eguileta Member, brick pits of the Vitoria Pass, Vitoria-Gasteiz (Álava). A–C, *Hoplitoplacenticeras marroti* (Coquand, 1859) in ventral (A), side (B), and apertural (C) views; D–F, *Lewyites elegans* (Moberg, 1885) in side (D), ventral (E), and dorsal (F) views, MCNA 15510; G–I, *Baculites* sp. 1 in side (G), dorsal (H), and ventral (I) views, MCNA 15512; J–L, *Baculites* sp. 2 in side (J), dorsal (K), and ventral (L) views; MCNA 15511. ▶

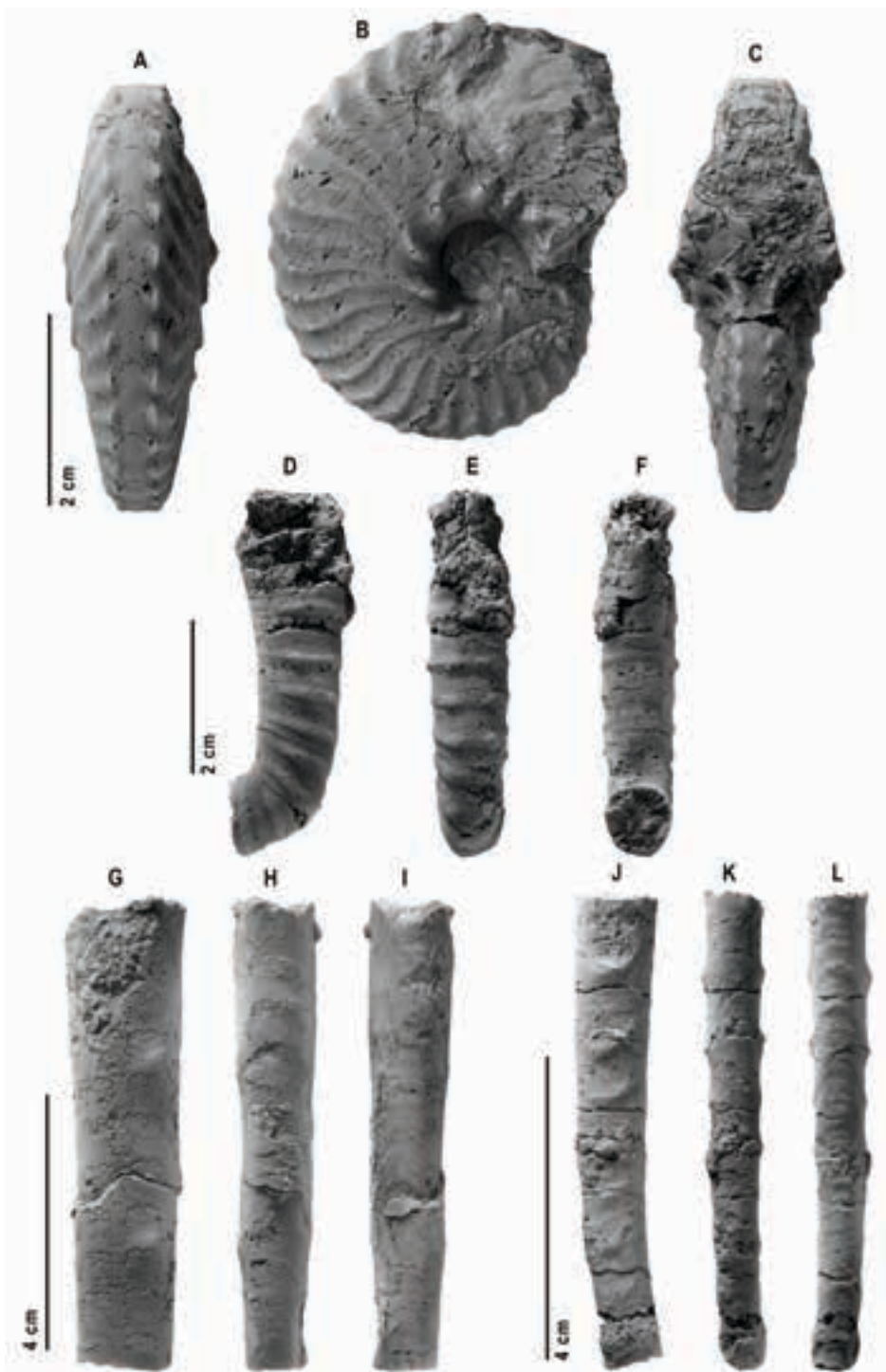




Figure 6.8 Cross-stratified sandstone channel incised into yellow to red-brown very fine silty sandstones (shallow subtidal and intertidal facies) of the upper Campanian Berrostequieta Member. Upper part of the Puerto de Vitoria site (Vitoria-Gasteiz, Álava). Photograph taken in 1993 looking north.

(Ramírez del Pozo, 1971; Wiedmann et al., 1983; San Martín, 1986; personal observation). Sandstone units are arranged in cross-sets. Large-scale, planar cross-stratification is the dominant internal structure as seen in two small outcrops at the top of the Vitoria Pass (Fig. 6.8). No macrofossils are present in these rocks, apart from burrows assigned to the ichnotaxon *Rhizocorallium* isp. (Engeser, 1985). This siliciclastic interval is capped by prominent limestone strata of the Maastrichtian Puerto de Olazagutía Formation.

Stratigraphical interpretation

The carbonate facies and foraminifera in the Vitoria Sub-basin during the lower Campanian suggest deposition in an open-marine, mid to outer ramp with water depth more than 50 m and temperate, well oxygenated waters (San Martín, 1986). However, an epi-

Figure 6.9 Selected ammonites from the turbiditic facies of the Eguileta Member, brick pits of the Vitoria Pass, Vitoria-Gasteiz (Álava). A–C, *Gaudryceras* cf. *kayei* (Forbes, 1846) in side (A), ventral (B), and apertural (C) views; D–F, *Pseudophyllites indra* (Forbes, 1846) in side (D), ventral (E), and apertural (F) views, MCNA 1438; G–I, *Baculites* cf. *texanus* Kennedy and Cobban, 1999, in side (G), dorsal (H), and ventral (I) views; J–K, *Trachyscaphites spiniger porchi* (Adkins, 1929), partial shaft and curved hook in side (J), and ventral (K) views, MCNA 1632; L–N, *Pachydiscus* (*P.*) *haldensis* (Schlüter, 1867) in side (L), ventral (M), and apertural (N) views, MCNA 10078; O–Q, *Pachydiscus* (*P.*) *oldhami* (Sharpe, 1855) in side (O), ventral (P), and apertural (Q) views, MCNA 10103. ▶▶

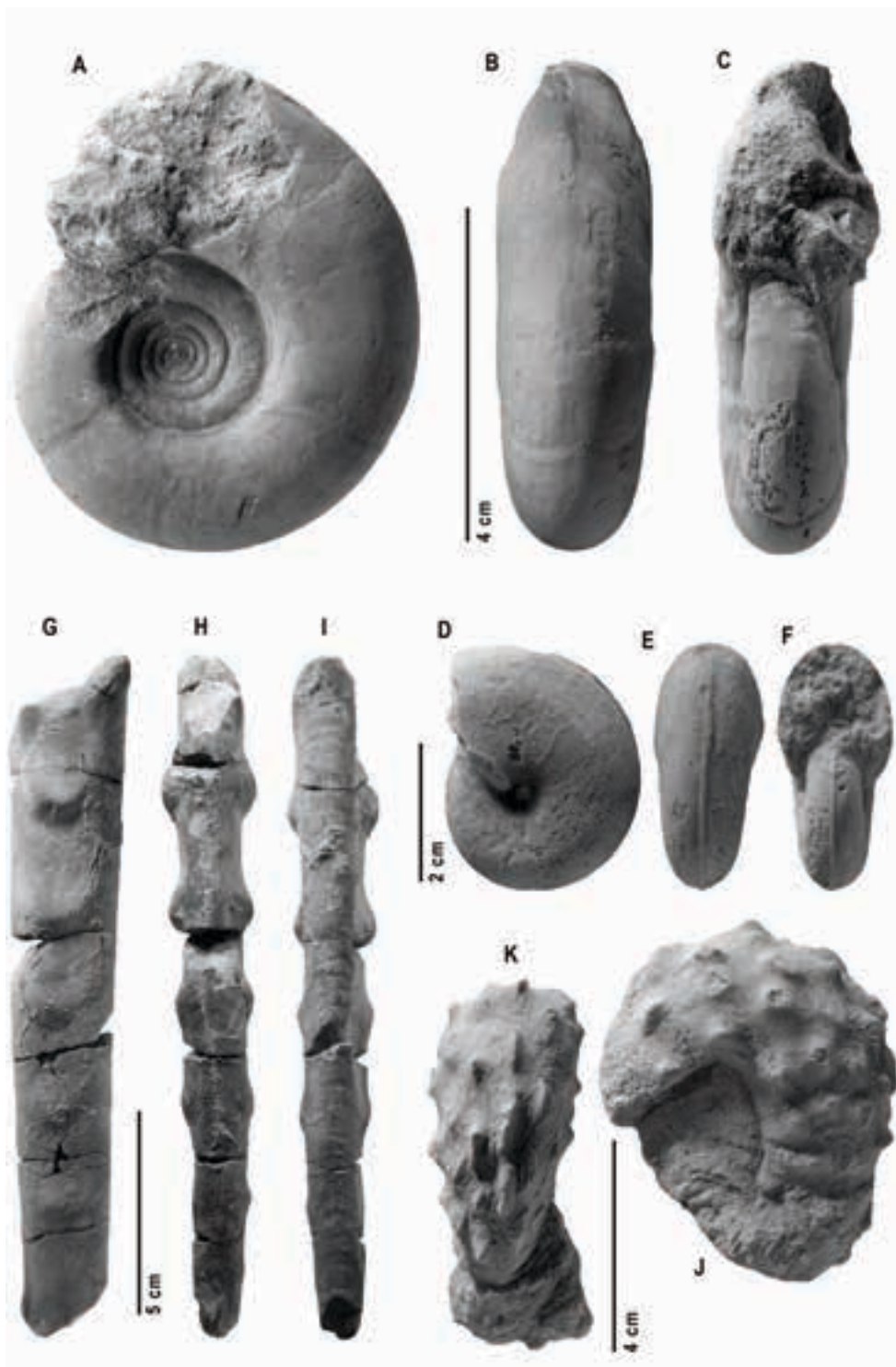




Figure 6.9 (cont.).

sode of siliciclastic progradation occurred in the Vitoria Sub-basin (central-southern part of the NCR Domain) during the upper Campanian, the resulting sedimentary complex is well exposed in the central part of the Vitoria Mountains (Wiedmann et al., 1983; Engeser, 1985; Martins, 1989).

The deposition of the basal marly sub-unit occurred in muddy, moderate deep environments. Authigenic glauconite occurs disseminated as sand-sized granules in individual beds throughout this unit, which can also give some clues about the deposit formation. Normal salinity and slightly reducing conditions in sea water in addition to the presence of phosphorus, iron sulphide and decaying organic matter are favourable conditions for the formation of present-day glauconite (Haq, 1991). Glauconization occurs in fine-grained muds near the sediment-water interface (Einsele, 1992) in present-day passive continental margins at depths between 60 and 500 m, with the optimal genesis at about 200 m depth, as for example in the western margin of the Atlantic Ocean (Odin and Morton, 1988; Haq, 1991). Although glauconite has been reported in deepwater sediments (at depths greater than 500 m), it is likely that such glauconite grains are of allochthonous origin (Odin and Morton, 1988).

Iron sulfides cooccur with glauconite. They are in the form of pyrite–marcasite and were formed diagenetically. Early diagenetic pyrite is commonly formed by sulfate-reducing bacteria in iron- and sulfate-rich sediments deposited in front of rivers entering the sea under anoxic conditions, usually enhanced by abundant organic matter dispersed in the sediments, when a dysoxic–anoxic condition in the sediment-pore waters is commonly reached once the sediment became buried to a depth (see Bridge and Demicco, 2008). Such dysoxic–anoxic conditions may have existed below the seafloor during the deposition of the EM, as both irregular, granular masses and fossil casts are considered representations of diagenetic pyrite (or the dimorph marcasite), and not syngenetic pyrite precipitated from euxinic waters. This is corroborated by the presence in the same layers of numerous epifaunal and infaunal benthic communities that were able to live in such sea floor conditions.

Ammonites, isolated corals and marine vertebrates are commonly collected fossils within the EM, which indicates that these deposits were formed in open-marine environments, and probably in water depths greater than 100 m. Concentration of phosphatic vertebrate remains on the sea floor is commonly interpreted as representing low sedimentation rates, which is also ideal for glauconite formation, and the resulting layers represent the deepest water deposits of the transgression (Bridge and Demicco, 2008).

The clayey marl facies of the EM represents a prodelta deposit formed by fine-grained sediments settling from suspension farther offshore and distributed laterally (from W to E) by longshore currents, as corroborated in nearby outcrops (Engeser, 1985). Temporally, the slow deposition rate was interrupted by deposition of bioclastic marlstone layers (with a detrital clayey matrix) that have been interpreted as downslope turbiditic processes (Engeser, 1985). Moreover, some layers of fine-grained sandstone that occur intercalated in the upper part of the soft unit are interpreted as result of storms currents reaching the seawardmost area of the subaqueous delta (tempestite deposits).

The regressive siliciclastic unit of the Berrosteguieta Member gradationally progrades over muddy prodelta deposits of the EM. Lithological and sedimentological

features, such as channelised sands with current ripples, flaser and wavy bedding and characteristic trace fossils (i.e. *Rhizocorallium* isp.), suggest that such facies represents shallow subtidal to intertidal zones of the delta front (Engeser, 1985). Inter-distributary areas not directly influenced by sandy sediments of the delta system crop out in nearby eastern sections, and show characteristic faunal associations including large benthic foraminifers, bryozoans, echinoids, oysters and other bivalves, ammonites, and crab remains (Engeser, 1985).

Finally, the overlying limestones of the Puerto de Olazagutía Formation indicate that shallow open-marine conditions returned in the upper Maastrichtian.

6.4 Review of the Montes de Vitoria Formation (MVF)

Engeser (1985) presented an improvement to the original lithostratigraphical scheme of Amiot (1982) for the uppermost Cretaceous rocks in the NCR Domain of the B-CB. Thus, according to Engeser (1985), the Campanian stratigraphical interval is represented in the central part of the Vitoria Sub-basin, in ascending order, by the Vitoria Formation (VF) and the Montes de Vitoria Formation (MVF). The VF is characterised by alternating clayey biomicrite (wackestone) and grey marl interbeds with rich associations of planktonic and benthic foraminifera, siliceous sponges, endobenthic echinoids, inoceramids, and ammonites deposited on an external ramp depositional setting (Ramírez del Pozo, 1971; Amiot, 1982; Wiedmann et al., 1983, San Martín, 1986; López, 1993a, 1996; Santamaría Zabala, 1996).

In short, the MVF was named by Engeser (1985: 164–181) for a regressive, predominantly sandy–silty sequence deposited in the Vitoria and Estella sub-basins, in the central-southern part of the NCR Domain, during the major cycle TR-4 of Floquet (2004). The MVF is about 500 m thick and records a shallowing-upward deltaic marine sequence developed over a mid-outer carbonate ramp represented by the underlying VF. Good exposures along the northern slopes of the Vitoria Mountains (south of Vitoria-Gasteiz) were originally designed as the composite type locality to best represent the lithology and genesis of the MVF. The formation was divided into four members (Mbr) in order to characterise the main depositional facies in the delta and, from younger to older, are: Eguileta Mbr (prodelta facies), Oro Mbr (carbonate reef build-up northwest of the delta system that is not present in the Vitoria Mountains), Berrosteguieta Mbr (subtidal to intertidal delta front), and Oquina Mbr (fluvial dominated facies association not observed in the Vitoria Pass section). According to Engeser (1985), the delta system extended laterally at least 20–30 km and up to 10 km, but probably more basinward. The age of the MVF is considered to be upper Campanian to (?) lower Maastrichtian as reported by Engeser (1985). For the scope of this thesis only the fossiliferous basal Eguileta Mbr, which has produced the fossil selachian remains, will be discussed in detail.

Eguileta Member (EM)

Original author. Engeser (1985: 166) defined this lowermost member of the MVF.

Type locality. It was located at the old brick pit west of the Eguileta village¹ (Alegría-Dulantzi, Álava). However, the original section is no longer available after restoration of the abandoned mining pit. The Eguileta member is still relatively accessible at the Ariaza pit, Gardelegi (Vitoria-Gasteiz, Álava), although most of the pit slopes have been flattened and obscured by landfill.

Boundaries. The Eguileta Member (EM) overlies diachronically the marls and carbonate mudstones of the Vitoria Formation, with younger deposits occurring eastward of the type locality (aged late Campanian, *Nostoceras (Bostrychoceras) polyplocum* zone). The unit is overlain by a sparsely fossiliferous sequence (Berrosteguieta Mbr) of yellow to red-brown very fine silty sandstones (corresponding to the subaqueous delta front facies).

Thickness. The maximum thickness of the EM was estimated to be ca. 100 m at the type section, although its thickness may vary laterally, being only 10 m in the Berrosteguieta section (Engeser, 1985). The thickness of the unit is estimated to be 35–40 m at Vitoria Pass site.

Lithology. The member is dominantly represented by bluish-grey fossil-rich, glauconitic marls of commonly homogenous appearance. The highly plastic condition of the clayey marl allows it suitable for brick making. Occasional marcasite nodules and pyritised fossil casts may occur. Engeser (1985) noted that these basal strata are overlain in the Vitoria Pass section by a thick bed, ranging in thickness from 0.5 to 1 m, of grey to ochre-brown, iron-rich, glauconitic marlstone (Fig. 6.5). Other rocks in the upper part of the member are grey, fine-grained sandstones interbedded within the clayey marls.

Palaeontological content and age. The marly beds of the EM have yielded rich assemblages of ammonites, infaunal and epifaunal bivalves, gastropods, crabs, echinoderms, and trace fossils (Engeser, 1985). In addition, solitary corals, brachiopods, and vertebrate remains can also be found. A brief review is given below.

The Foraminifera were significantly present for most of the clayey marls of the unit (San Martín, 1986), but the percentage of planktonic forms in the foraminiferal assemblages is low, around 5%, according to Engeser (1985). Two associations of planktonic foraminifers (PV1 and PV2) are above-mentioned from the Ariaza pit in the Vitoria Pass section, allowing comparison with the planktonic foraminiferal zonation of the upper Campanian (see planktonic foraminifera biozones below). Other groups such as echinoderms are still poorly known taxonomically, but crinoids, asteroids and echinoids occur. Among the latter, large specimens of the genus *Echinocorys* and cidarid skeletal parts are included. Santamaría Zabala (1996) identified three ammonite assemblages of different age within the Campanian in Álava, but the two representing

¹ The official name is now Eguileta, but Eguileta can also be found in past geological works.

the EM were erroneously assigned to the Vitoria Formation. These assemblages are as follow (from older to younger):

1. *Baculites alonsoi* Santamaría Zabala, 1996, *Hoplitoplacenticerias marroti* (Coquand, 1859), *Pseudoxybeloceras* (*Parasolenoceras*) *phaleratum* (Griepenkerl, 1889), and *Scaphites* (*S.*) *gibbus* Schlüter, 1872; and
2. *Baculites* sp., *Pachydiscus* (*P.*) *oldhami* (Sharpe, 1855), *Pachydiscus* (*P.*) *haldemisi* (Schlüter, 1867), *Phylloceras* (*Hypophylloceras*) sp., and *Pseudophyllites* sp.

Additional ammonite taxa have been referred previously within the stratigraphical description of Vitoria Pass site. In addition to the ammonites, Santamaría and López (1996) listed several inoceramids and other fossil macroinvertebrates recovered from the EM, although erroneously described them as belonging to the marl and clayey limestone strata of the Vitoria Formation. Phosphatic concretions (crab balls) occur sporadically at some stratigraphical levels. Van Bakel et al. (2012) identified the rarinid crab *Cretacorantina schloenbachi* (Schlüter, 1879) in the marly sequence of the Vitoria Pass (Álava). Besides, elasmobranch teeth were also recorded throughout the lower marly sub-unit of the member, along with actinopterygian fishes and mosasaurid remains (Bardet et al., 1993, 1997, 2006; Corral et al., 2004, 2011). Moreover, spiral-shaped coprolites produced by undetermined elasmobranchs have also been collected.

The EM was assigned a late Campanian age by the ammonites discovered in the former clay pit of Egileta (Wiedmann determination in Engeser, 1985). Apart from the type locality, the EM contains useful ammonoid-bearing beds for the dating and correlation in the Jauregi¹ and Vitoria Pass sections, being represented the *H. marroti* zone and part of the younger *Nostoceras* (*B.*) *polyplocum* zone (Santamaría Zabala, 1996). On the basis of the ammonites present in the member, both historical and new discoveries, and on the planktonic foraminifera found in the Vitoria Pass section during the present study, this age is confirmed (see discussion below).

Depositional environment. Based on the above data, the EM represents the subaqueous and lower energy part of the delta, which is referred to as the prodelta (Engeser, 1985). These facies are characterised by gray, highly plastic, clay-derived rocks, either massive or partially laminated, that were deposited from suspension and in which fossil remains are common. Moreover, interbeds of graded mudstone with glauconite grains, often associated with ferric oxide crusts, may have been carried from shallower zones of the carbonate ramp by slow turbidity currents over a flat prodelta environment (Engeser, 1985). All this is compatible with a well-oxygenated environment, as proposed by San Martín (1986) for the lower to lowermost upper Campanian, typically with water depths greater than 50 m. The high diversity of marine invertebrate fossils supports this interpretation.

¹ This is more fully discussed in Chapter 18.

A characteristic feature of the argillaceous facies is the presence of abundant glauconite pellets and pyritised fossil casts. Phosphorite concretions also occur, although they are less frequent. They may have been formed during diagenesis in organic-rich muds, associated with deeper water, low-energy areas located seaward of the delta front (see Sheldon, 1981). Authigenic glauconite, in addition to phosphate and pyrite, has been regarded as a reliable marker in distinguishing condensed sections caused by very low net deposition in passive-margin, marine sequences (Banerjee et al., 2016, and references therein). Condensed sections are also characterised by mixed accumulation of different age fossils in relatively thin layers due to the slow accumulation of sediment. It is generally assumed that condensed beds represent a maximum flooding surface (MFS) during a transgressive episode.

The distinction between allochthonous and autochthonous glauconite is of great relevance for the interpretation of stratigraphical sequences. Thus, the sedimentology and palaeontological data are compatible with an authigenic origin for the clayey lithofacies of the EM. However, it seems likely that the origin of the turbidite-related glauconite found in the Vitoria Pass section was allochthonous, but this will be finally elucidated after further determination of the glauconite analysis. The presence of fine-grained sandstone beds in the upper part of the EM suggests sediment deposition associated with storm events (tempestites), according to Engeser (1985).

Stratigraphical relationships and correlations. The marly EM conformably overlies the uppermost Santonian to lower upper Campanian Vitoria Formation, below, and is conformably overlain by subtidal to intertidal siliciclastic strata, almost barren of fossils, of the Berrostequieta Mbr of the MVF, above (Fig. 6.10). The EM is exposed in the northern flank of the Vitoria Mountains, south of Vitoria-Gasteiz, which are part of the east- to west-trending strike ridges of the Miranda-Treviño Syncline (south of the B-CB). Beyond the type locality, the EM tapers to a narrow strip both westward and eastward. The lower part of the member is easily correlated with the upper part of the Vitoria Formation by the presence in both units of the zonal ammonite *Hoplitoplacenticeras marroti* (Coquand, 1859).

6.5 Biostratigraphy and age assigned to the Vitoria Pass site

The planktonic foraminiferal zones

The planktonic foraminiferal biostratigraphy of the Campanian–Maastrichtian interval in the Vitoria Sub-basin has been investigated in detail by Ramírez del Pozo (1971), San Martín (1986, 1987), and Alonso (1987). The revision and updating of the scales by them provided, following the ideas of Arz and Molina (2002), in parallel with ammonite-based zonations (see below), enables a better stratigraphical understanding of the local rock successions.

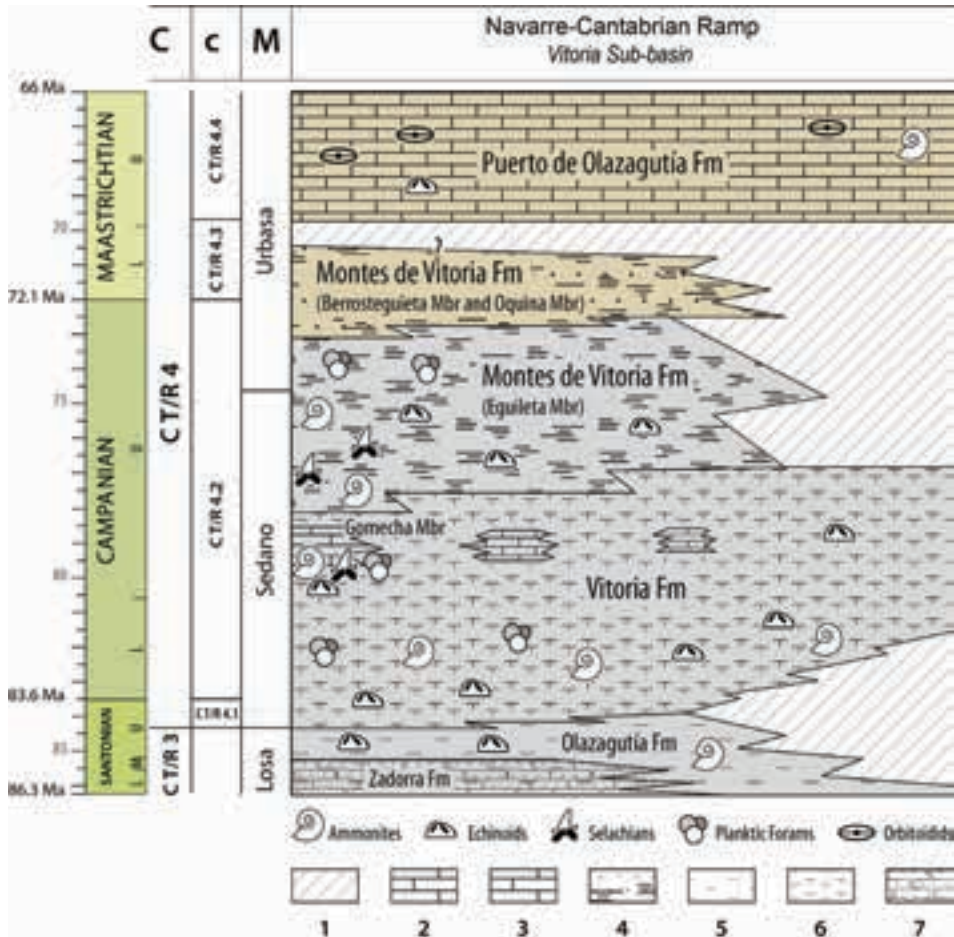


Figure 6.10 Lithostratigraphical units of the Vitoria Sub-basin (modified from Gräfe, 1994). Legend: 1, hiatus; 2, limestone with orbitolids; 3, sandy marl and silt; 4, limestone and silty marl; 5, marls, clayey marl and lutite; 6, marl with echinoids; 7, calciturbidite. Abbreviations: C, large-scale T–R cycle; c, small-scale T–R cycle; Fm, formation; M, megasequence; Mbr, member (cycles and sequences after Floquet, 2004).

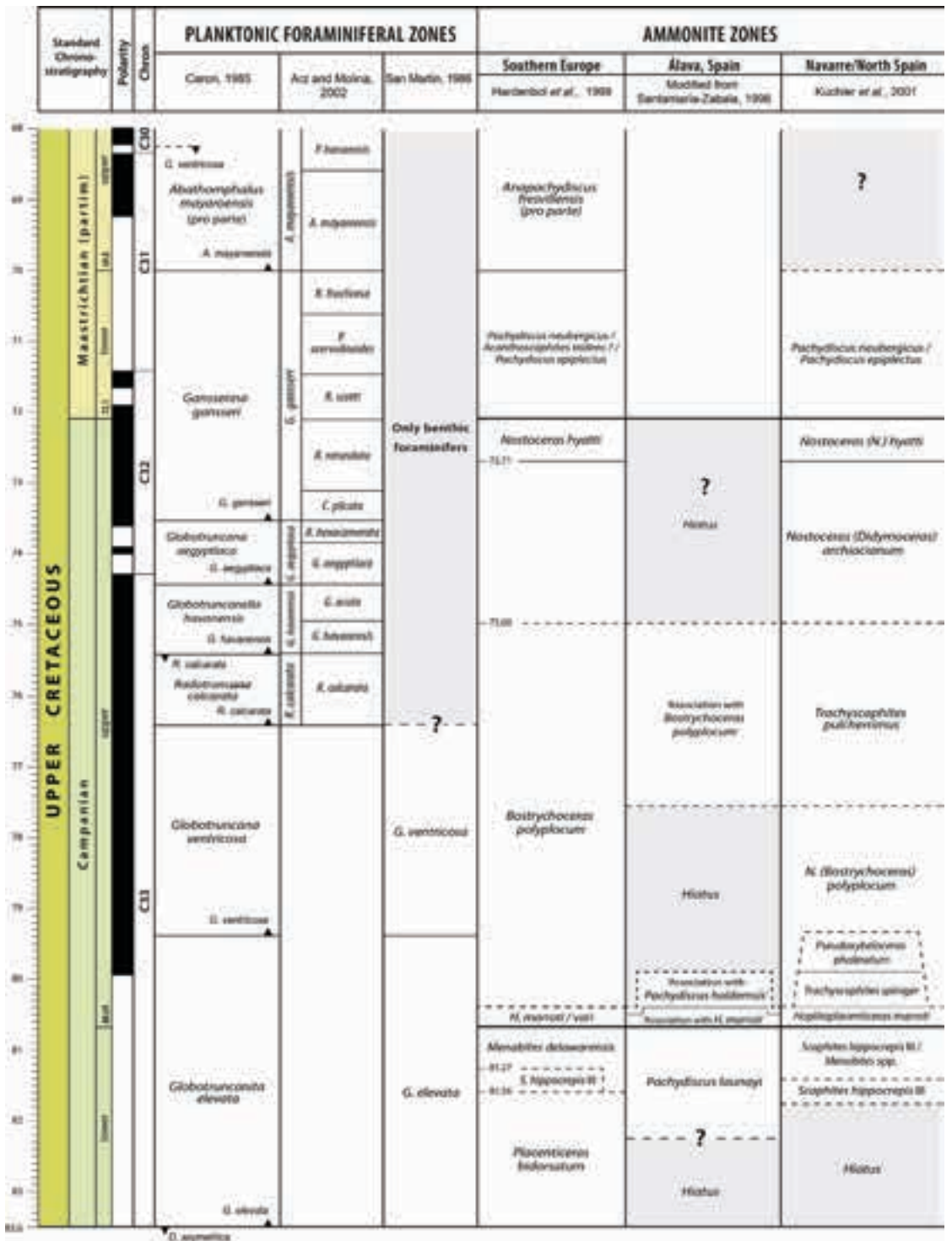
Caron (1985) proposed the division of the Campanian in the western Tethys area into three successive biozones (from older to younger): (1) *Globotruncanita elevata* zone (interval zone); (2) *Globotruncana ventricosa* zone (interval zone); and (3) *Radotruncana calcarata* zone (taxon range zone). This scheme was followed in the Vitoria Sub-basin by San Martín (1986), who identified the *G. elevata* and *G. ventricosa* zones, but as the author indicated the planktonic foraminifera quickly declined in the upper Campanian and, therefore, the younger *R. calcarata* zone was not identified. In consonance with this, Gräfe (1994) pointed out that the planktonic foraminifera biozones of Caron (1985) should apply with high reliability only to the eastern and northern parts of the B-CB, because the southernmost areas were affected by regressive episodes.

An amelioration of the Caron's (1985) standard zonal scheme for the upper Campanian and Maastrichtian was proposed by Arz and Molina (2002) based on a detailed review of Upper Cretaceous sections in the Bay of Biscay (France and Spain). In this new zonal scheme (see Fig. 6.11), the authors erected 12 sub-biozones (from older to younger): (1) *Globotruncanita calcarata* (total range sub-biozone) within the *Globotruncanita calcarata* zone; (2) *Globotruncanella havanensis* (interval sub-biozone) and (3) *Gublerina acuta* (interval sub-biozone) within the *Globotruncanella havanensis* zone; (4) *Globotruncana aegyptiaca* (interval sub-biozone) and (5) *Rugoglobigerina hexacamerata* (interval sub-biozone) within the *Globotruncana aegyptiaca* zone; two upper Campanian sub-biozones, namely (6) *Contusotruncana plicata* (interval sub-biozone) and (7) *Rugoglobigerina rotundata* (interval sub-biozone); three lower Maastrichtian sub-biozones, namely (8) *Rugoglobigerina scotti* (interval sub-biozone), (9) *Planoglobulina acervulinoides* (interval sub-biozone) and (10) *Racemiguembelina fructifera* (interval sub-biozone) within the *Gansserina gansseri* zone; and finally (11) *Abathomphalus mayaroensis* (interval sub-biozone) and (12) *Pseudoguembelina hariaensis* (interval sub-biozone) within the upper Maastrichtian *Abathomphalus mayaroensis* zone.

Ammonite zonal scheme

Ammonites are widely used in biostratigraphy as they usually provide high-resolution temporal data. However, their use is not without limitations, derived from the provincialism and endemism that some species present. Considering the duration of the Campanian stage (about 12 Ma), the global zonation scales do not offer good resolution to solve the stratigraphical problems, apart from those developed in the western interior of the USA and Madagascar (Hancock, 1991). The scarcity of ammonites in the type area of the Aquitaine region, southwestern France, is reflected in the classic divisions and the zonal scheme proposed by Kennedy (1986), which consisted of two zones for the lower Campanian (*Placenticerias bidorsatum* zone¹ and *Menabites delawarensis* zone) and two other zones for the upper Campanian [*Hoplitoplacenticerias marroti* zone and *Nostoceras (B.) polyplacum* zone]. Hardenbol et al. (1998) developed a further biostratigraphical scheme for the Campanian in southern Europe, in which the suggested zones are (from older to younger occurrences) *P. bidorsatum* (Roemer, 1841), *S. hippocrepis* (DeKay, 1828) III, and *M. delawarensis* (Morton, 1830), for the lower substage, *H. marroti* and *N. (B.) polyplacum*, for the upper Campanian, and finally *Nostoceras (N.) hyatti* Stephenson, 1941 for the uppermost part of the stage (Fig. 6.11).

¹ The first occurrence (FO) of the ammonoid *Placenticerias bidorsatum* (Roemer, 1841) has been considered to be the base of the Campanian stage, for some time now, but currently the Santonian–Campanian boundary is placed at the last occurrence (LO) of the pelagic crinoid *Marsupites testudinarius* (von Schlotheim, 1820) (Ogg and Hinnov, 2012). However, the last taxon is unknown in the B-CB.



The lower Campanian strata of the Tubilla del Agua Formation (also called ‘*Lacazina* limestone’ by some authors) in the eastern part of the Castilian Ramp (CR) of the B-CB, which is correlated with lower part of the Vitoria Formation (see Fig. 7.7 in Chapter 7), have yielded ammonites at scattered localities in northern Burgos and western Álava (Wiedmann in Gischler et al., 1994). The list includes two specific assemblages of temporally restricted species: (1) *Bevahites subquadratus* Collignon, 1948 and *Submortonicerias tenuicostulatum* Collignon, 1948 for the lowermost Campanian; and (2) *Scaphites hippocrepis* (DeKay, 1828), *Pachydiscus* (*Pachydiscus*) cf. *basae* (Collignon, 1932), and *Neocrioceras* (*Schlueterella*) *riosi* Wiedmann, 1962 for the upper lower Campanian. Other lower Campanian species that also are present in this formation are *Pachydiscus* (*Pachydiscus*) *praecolligatus* (Collignon, 1955), *Eupachydiscus grossouvrei* (Kossmat, 1897), and *Eupachydiscus levyi* (Grossouvre, 1894). Gräfe (2005) has proposed two ammonite zones for the lower Campanian of the B-CB, namely *Bevahites subquadratus* zone (lowermost Campanian), which is equivalent to the lower part of *Placenticerias bidorsatum* zone in northern Europe, and *Scaphites hippocrepis*/*Neocrioceras* (*Schlueterella*) *riosi* zone (upper lower Campanian).

The northwestern part of the Navarre-Cantabrian Ramp (NCR) of the B-CB formed the less subsiding Santander Sub-basin (Gräfe et al., 2002) where Campanian ammonites have also been found (Wiese et al., 1996). The outcrops near Santander have yielded above a stratigraphical hiatus the following taxa: *Scaphites hippocrepis* (DeKay, 1828) III, *Glyptoxoceras* cf. *retrorsum* (Schlüter, 1872), *Bevahites subquadratus* Collignon, 1948, *Cirroceras* sp., and *Placenticerias* sp. Other ammonites also present are the species *Menabites* (*Delawarella*) *delawarensis* (Morton, 1830) and *Pseudophyllites* cf. *indra* (Forbes, 1846). Finally, *Submortonicerias tenuicostulatum* Collignon, 1948, and *Scaphites* (*S.*) *gibbus* Schlüter, 1872 occur higher up the section, corresponding to the upper part of the *Scaphites hippocrepis* zone or upper lower Campanian (Wiese et al., 1996).

In his zonal scheme, Santamaría Zabala (1996) reported the presence of *Pachydiscus* (*P.*) *launayi* Grossouvre, 1894, and *Baculites* sp. in the lower Campanian (Vitoria Formation, pro parte) of the Vitoria Mountains (southcentral part of Álava), but the scarcity of ammonite fossils limited him to go further in giving a zonation for this part of the substage. Küchler et al. (2001) proposed two ammonite zones for the lower Campanian of northcentral Spain, on the basis of a rich and diverse Campanian ammonite association collected in northern Navarre (i.e. La Barranca and Erro successions), but again the lowermost part of the Campanian stage is misrepresented by the existence of a significant stratigraphical hiatus.

◀ **Figure 6.11** Correlation of uppermost Cretaceous planktonic foraminiferal zones with ammonite zones in southern Europe. General scales (Caron, 1985; Arz and Molina, 2002; Hardenbol et al., 1998), regional scales (Küchler et al., 2001), and local scales (San Martín, 1986; Santamaría Zabala, 1996) are compared. Uncertain stratigraphical positions for zonal boundaries are shown in dash lines. The lower and upper boundaries of the Campanian are 83.6 and 72.1 Ma respectively, following Ogg and Hinnov (2012).

There is a general consensus that the base of the upper Campanian for southern Europe, in terms of the European twofold division, is placed at the base of the *Hoplitoplacenticeras marroti* zone (Kennedy, 1986; Hardenbol et al., 1998). In general terms, both the *marroti* (older) and *polyplacum* zones (younger) have been recognised in the successions of the Navarre-Cantabrian Ramp (NCR) by Wiese et al. (1996) and Santamaría Zabala (1996). With reference to the proposed division of Santamaría Zabala (1996), this author refers to three successive ammonite associations as follows: (1) first appearing an ‘Association with *Hoplitoplacenticeras marroti*’ represented by the species *Hoplitoplacenticeras marroti* (Coquand, 1859), *Menabites* (*Bererella*) sp., *Scaphites* (*S.*) *gibbus* Schlüter, 1872, *Scaphites* cf. *gibbus* Schlüter, 1872, *Pseudoxybeloceras* (*Parasolenoceras*) *phaleratum* (Griepenkerl, 1889) and *Baculites alonsoi* Santamaría Zabala, 1996; then (2) an ‘Association with *Pachydiscus haldemsi*’ represented by *Trachyscaphites spiniger porchi* (Adkins, 1929), *Pachydiscus haldemsi* (Schlüter, 1867), *Pachydiscus* (*P.*) sp., *Phylloceras* (*Hypophylloceras*) sp., *Pseudophyllites* sp. and *Baculites* sp.; and finally (3) an ‘Association with *Bostrychoceras polyplacum*’ represented by the taxa *Nostoceras* (*B.*) *polyplacum* (Roemer, 1841), *Baculites alavensis* Santamaría Zabala, 1996, and *Trachyscaphites spiniger porchi* (Adkins, 1929). Both the *Hoplitoplacenticeras marroti* and *Pachydiscus haldemsi* ammonite associations are present in the Vitoria Pass site (see Fig. 6.5), but the youngest ‘Association with *Bostrychoceras polyplacum*’ has only been described in the easternmost Azazeta and Jauregi sections¹ in the Álava province (Santamaría Zabala, 1996). On the other hand, the first appearance of the subspecies *Trachyscaphites spiniger spiniger* (Schlüter, 1872) is a good indicative of the lower, but not lowermost, upper Campanian, and the less ornamented subspecies *Trachyscaphites spiniger porchi* would be the final form in terms of an evolutionary progress over time of the species (Cobban and Kennedy, 1992).

Although the upper Campanian in the NCR has produced a relatively large collection of ammonites, in terms of abundance and taxonomic variety, a complete ammonite-based biozonation was not properly established due to problems in correlating the stratigraphical sections. A diverse, rich fauna of ammonites found in western Navarre has enabled the most precise zonation until now for the upper Campanian, being of regional value for northern Spain, according to KÜchler et al. (2001). Seven biozones were proposed to span a period of about 9.5 Ma; from older to younger are the zones *marroti*, *spiniger*, *phaleratum*, *polyplacum*, *pulcherrimus*, *archiacianum*, and *hyatti*. Moreover, KÜchler et al. (2001) indicated that the introduced *archiacianum* zone is equivalent to the *donezianum*² zone established by Błaszczewicz (1980) for the boreal northwestern Europe. In sum, the zonal scheme given by KÜchler et al. (2001), besides expanding the zonal scheme of Hardenbol et al. (1998), enables a correlation with oth-

¹ The current official names are Azazeta and Jauregi, but they are also found written Azáceta and Jáuregi in previous geological works.

² Named after *Didymoceras donezianum* (Mikhailov, 1951).

er successions not only in the Aquitaine region, southwestern France (Kennedy, 1986), but also in other northern Europe sections, such as those in Germany (Hancock, 1991) and the Vistula Valley, Poland (Błaszkiwicz, 1980).

Age assigned to the Vitoria Pass beds

The micropalaeontological content observed at Vitoria Pass section (samples PV1 and PV2) indicates a late Campanian age, with the foraminiferal association being characteristic of the *G. gansseri* zone (*Rugoglobigerina rotundata* subzone) (J.A. Arz, pers. comm.). Thus, the age is estimated to be 72 Ma, according to the planktonic foraminiferal scheme proposed by Arz and Molina (2002). However, the maximum concentration of fossil elasmobranchs from this section occurs with the pyritised ammonites *Hoplitoplacenticerias marroti*, which is lowermost upper Campanian in Aquitaine, France (see Kennedy, 1986) and Álava (see Santamaría Zabala, 1996) and Navarre (see Kuchler, 2000c) in Spain. Few vertebrate remains appear above this bed, and when they do, they are found within or immediately above the turbiditic bed, where the ammonite species *Pachydiscus haldemsi* and *Trachyscaphites spiniger* cooccur. This would date the elasmobranch assemblage as lower upper Campanian in terms of the twofold division used for the Campanian European formations (see Kuchler, 2000c), and therefore an age of about 80 Ma (see Fig. 6.11).

A further study of the biostratigraphical scheme deems necessary to solve the age discrepancy between ammonite and planktonic foraminifera markers extracted from the Vitoria Pass elasmobranch beds, which are thought to represent condensation deposits as different-aged fossil accumulation and the presence of glauconite may suggest.

Chapter 7

GEOLOGY AND GEOCHEMISTRY OF THE MAASTRICHTIAN QUINTANILLA LA OJADA BEDS (VALLE DE LOSA, BURGOS)

7.1 Introduction

Prior to the discovery of this fossil site much of the knowledge on fossil elasmobranchs in the Basque-Cantabrian Region (northern Spain) was based on some other Late Cretaceous occurrences (Bardet et al., 1993; Corral, 1996; and chiefly Cappetta and Corral, 1999). Uppermost Cretaceous rocks (lower Campanian to upper Maastrichtian) crop out almost continuously in the central part of the Basque-Cantabrian Region, from the eastern Urbasa Mountains to the Anderejo–Vienda Mountains at the western end, across the provinces of Navarre, Álava and Burgos. The initial investigations about the fossil content in this locality were carried out by Berreteaga (2008), who preliminarily described a new discovery of marine vertebrates in her doctoral research thesis. Subsequent fieldwork in the region has produced a relatively large collection of vertebrate fossils, the principal of which are selachian teeth, but actinopterygian microfossils and a few mosasaur teeth also occur (Berreteaga et al., 2010; Berreteaga et al., 2011). The following describes the geology of the region where the fossil site is, with an emphasis on his a particular taphonomic and geochemical history.

7.2 Location and geological setting

The material was collected from two sand pits situated on the northern flank of the Vienda Mountain Range, in the vicinity of Quintanilla la Ojada (Burgos province, northern Spain; UTM coordinates: 30T 475337.8 4749958.1 and 30T 475570.5 4749464.2) (Fig. 7.1). Quarrying has targeted a bed of silica sand that outcrops along this hilly region within the Rioseco Member (see Stratigraphy description, below) (Fig. 7.2). The region, which is geologically found in the North Castilian Ramp domain, or Castilian Ramp (CR) in a simple form, contains several Upper Cretaceous series of clayey carbonate and limestone that are rich in pelagic fossils (Floquet 1991, 2004).

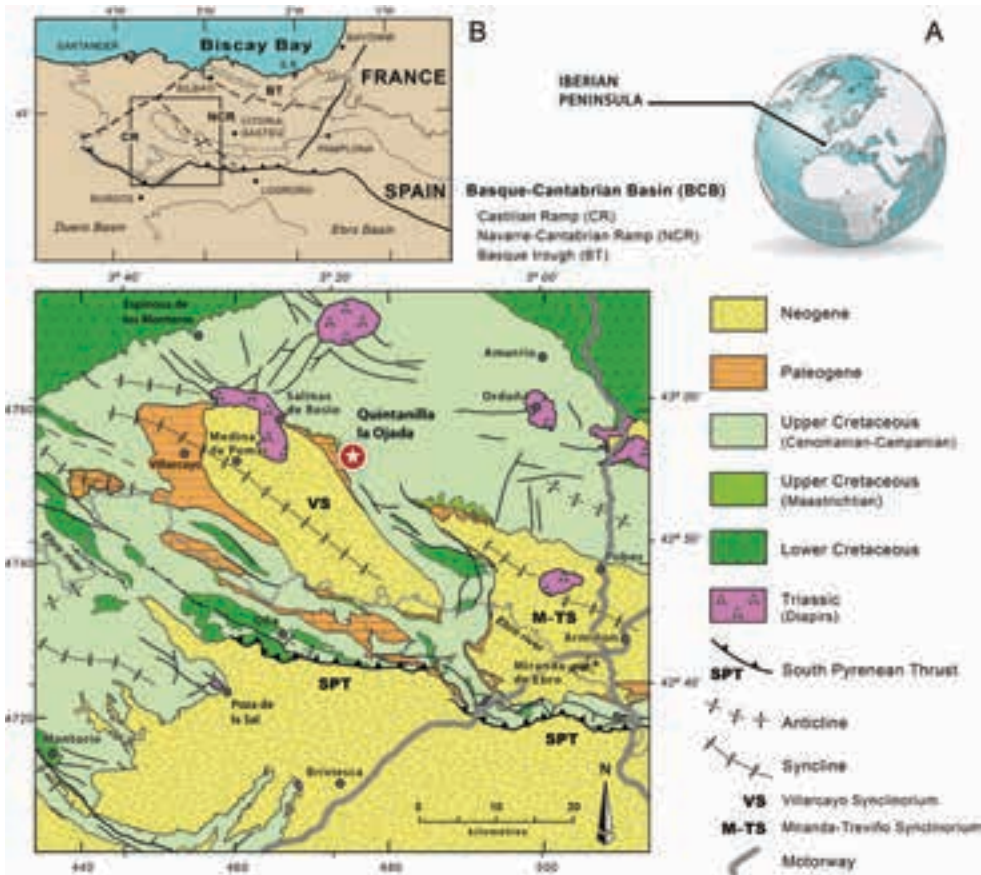


Figure 7.1 A and B, general location maps of the study area; C, simplified geological map in the Villarcayo Syncline area (Navarre-Cantabrian Ramp of the B-CB), showing the location of the vertebrate fossil site (based on photomosaic maps, MAGNA E 1:50000, IGME, Spain). Redrawn from Corral et al., 2015b.

This domain broadly represents the distal part of a ramp-like platform developed within the Basque-Cantabrian Basin (B-CB) (northern continental palaeomargin of the Iberian plate). Throughout the latest Cretaceous and early Paleogene, shallow depositional settings developed in the southwestern part of the B-CB, ranging from inner shelf to coastal and even continental environments (Floquet, 1991; Pluchery, 1995).

The northernmost palaeogeographical area of the Castilian Ramp comprises thick deposits (900–1000 m) of siliciclastic and shallow marine carbonates arranged in transgressive-regressive cycles (Floquet, 1991, 1998; Berreteaga, 2008). Fossil-rich Maastrichtian outcrops are, for the time being, limited to the northern limb of the Villarcayo Syncline (abbreviated as VS in Fig. 7.1), which forms the western end of the South Cantabrian Synclinorium. Similar uppermost Cretaceous materials have also

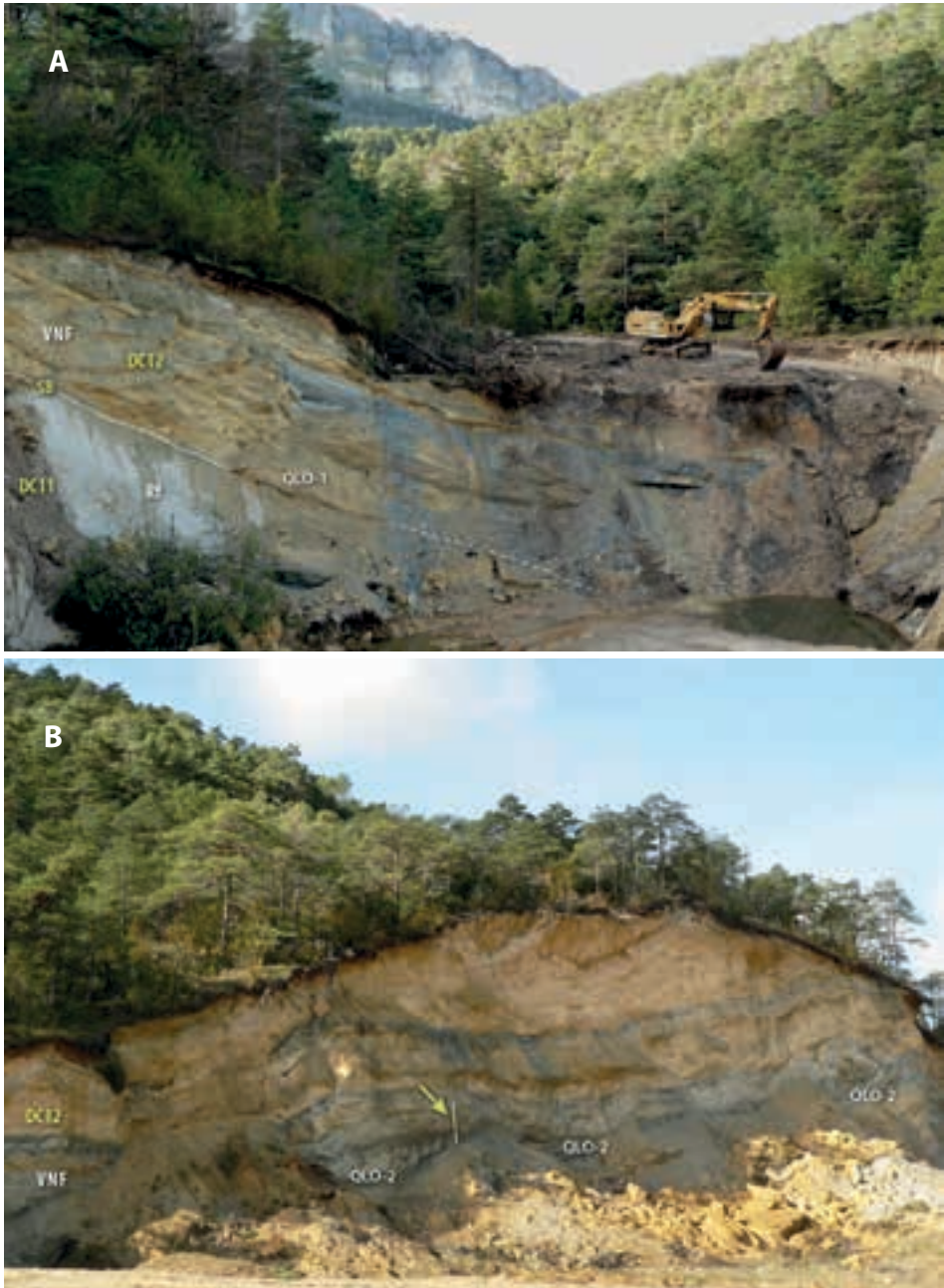


Figure 7.2 Sedimentology and facies associations. (A) Pit exposure showing the cross-bedded sandstone of the ‘Rioseco facies’ (Rf) that is overlain by a basal lag deposit (QLO-1) and several stacked parasequences of sandy carbonates included within the Valdenoceda Formation (VNF); (B) Metre-scale carbonate parasequences within the basal part of the VNF, including the one containing the fossil-rich deposit QLO-2. SB: sequence boundary; scale bar (arrowed) is 2 metres long. Photos taken in 2010.

been arranged in time equivalent transgressive-regressive cycles in the nearby Miranda-Treviño Syncline (abbreviated as M-TS in Fig. 7.1) (Baceta, 1996; Baceta et al., 1999), where the comparable fossil site of Albaina is located (see Chapter 8).

7.3 Stratigraphy

Stratigraphical description

The Quintanilla la Ojada section (Fig. 7.3) is represented by marine bioclastic calcarenites in its lower part, corresponding to the top of the Tubilla del Agua Formation (defined by Floquet et al., 1982). Age-assessment of this unit was late Santonian to probably early Campanian on the basis of its ammonite and foraminiferal content (Floquet, 1991, 1998; Gräfe, 2005). The upper part of the Tubilla del Agua Formation gradually passes to non-marine rocks within the overlying 'Rioseco facies' described by Floquet (1991). Although the basal beds of the latter informal unit are not easily recognised, they are composed of well-rounded quartz conglomerates and sandstones, arranged in metre-scale tabular sets with trough cross-stratification, and interbedded with very thin laminated greenish siltstones (cm-thick beds). This siliciclastic unit, which is up to 60 m thick, shows noticeable thickness variations across the northern limb of the Villarcayo Syncline, decreasing its thickness northwestwards and southwards. Thus, the Quintanilla la Ojada section and the Rioseco section, located in the northern and southern limbs respectively, record the maximum thickness of the unit. The 'Rioseco Member', which represents deposits of the Rioseco coastal system, is a lateral equivalent of the Moradillo de Sedano, Quintanaloma, and Sedano formations, ranging in age from Campanian to lower Maastrichtian (Floquet et al., 1982; Floquet, 1991, 1998; Berreteaga, 2008).

The Rioseco rocks are irregularly overlain by mudstones and coarse gravel-sized conglomerates (named QLO-1 bed) containing vertebrate fossils (Fig. 7.4A). Both lithologies, which do not exceed 50 cm, are overlain by sandy dolomites and organic-matter-rich clays organised in metre-scale upward thinning sequences, one of them also containing fossil vertebrates (named QLO-2 bed) (Fig. 7.4B). Scattered vertebrate fossils, pyritised orbitoids, and euhedral pyrite occur within the two first metres of bioturbated dolomitised carbonates that crop out in the lower part of the formation, immediately above and closely related to the unconformable boundary between the 'Rioseco Member' and the Valdenoceda Formation (VNF) (Berreteaga et al., 2008b). A massive dolomite body (30–40 m thick) overlies these parasequences. Both basal parasequences and the overlying dolomite body are regarded by its sequence architecture as being laterally equivalent deposits of the VNF, the age of which is thought to be late early Maastrichtian or early late Maastrichtian (Floquet et al., 1982; Floquet, 1991; Berreteaga, 2008; Berreteaga et al., 2010). Dolomite beds gradually increase upwards in clay content, passing into nearly 30 m of variegated clays, assigned to the Sobrepeña

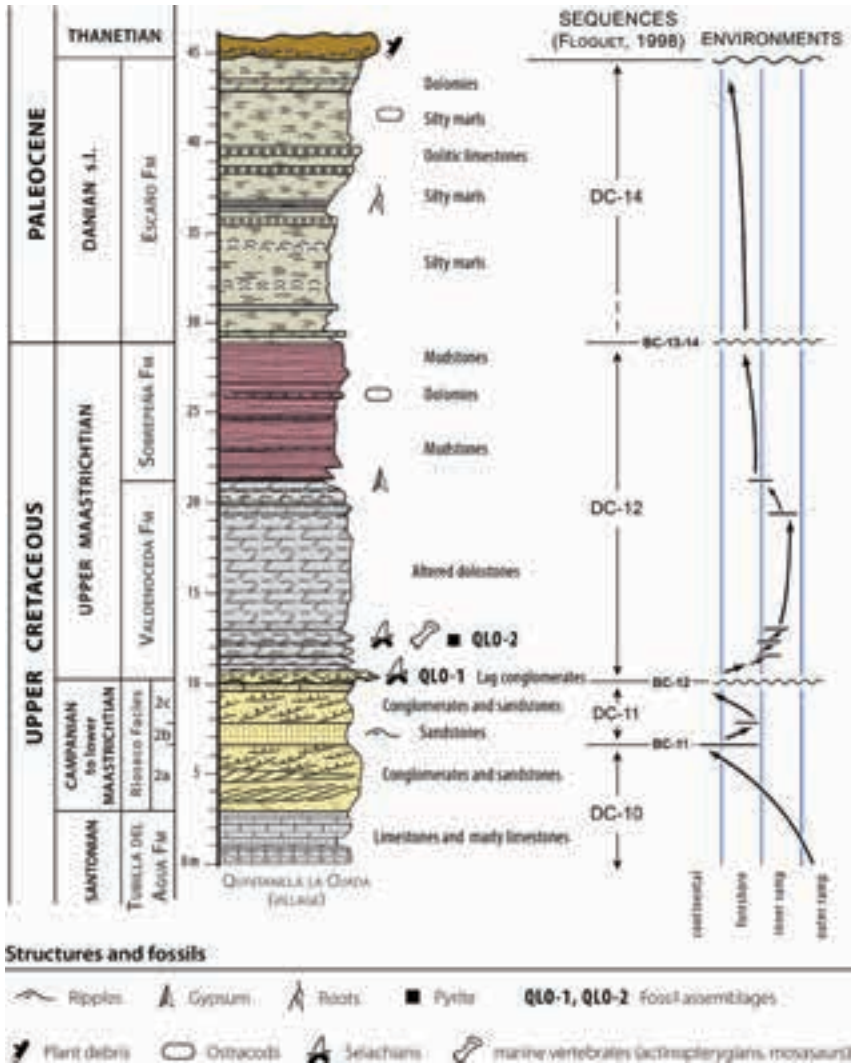


Figure 7.3 Synthetic stratigraphical column of Quintanilla La Ojada (Burgos, Spain) with the lithostratigraphical units and interpreted changes in depositional environments. Explanation for the Rioseco facies: 2a, Moradillo de Sedano Formation; 2b, equivalent to the Quintanaloma Formation; 2c, equivalent to the Sedano Formation (modified from Berreteaga, 2008).

Formation and considered to be upper Maastrichtian based on charophytes (Floquet, 1991; Berreteaga et al., 2008a). Upwards, this unit is overlain by a series of characteristic whitish dolomitic marlstones with oolites and stromatolites, considered Danian on account of the stratigraphical framework, which are assigned to the Esaño Formation (named by Pluchery, 1995).



Figure 7.4 (A) basal polygenic conglomerate, formed as a transgressive lag above an erosional base (basal lag deposit QLO-1). Note the fractures and displacement within the root of an *Squalicorax pristodontus* (Agassiz, 1843) tooth; (B) dolomitised bioturbated marlstone with a *Squalicorax pristodontus* (Agassiz, 1843) tooth (from QLO-2 bed).

Stratigraphical interpretation

The Valdenoceda Formation (VNF) is unconformably bounded below by the ‘Rioseco Member’, which is interpreted as an eastward progradational deltaic system (Floquet, 1991; Berreteaga, 2008). This basal discontinuity, upon which the above mentioned fossiliferous conglomeratic lag deposit occurs, is a transgressive ravinement surface that can be correlated with the basal boundary of the depositional T–R cycle DC-12 (one of the many T–R cycles defined by Floquet in 1998), within the Castilian Ramp. On the other hand, the shallow marine beds at the base of the VNF represent an increasing influence of marine conditions in the system (i.e. the transgressive phase of T–R cycle DC-12). Time-equivalent transgressive-regressive cycles were also recognised in the Miranda-Treviño Syncline (Floquet, 1991; Pluchery, 1995), however, the marine vertebrate fossils found there (Albaina site) are not apparently related to the T–R cycle DC-12, but to the cycle DC-13. Albaina’s fossils occur within a sedimentary unit basally marked by a major transgressive surface (named intra-Maastrichtian unconformity, or IMU, by Baceta et al., 1999) that can be confidently correlated with the regional cycle

boundary CB-13 (*sensu* Floquet, 1998). The shallow marine fossil-rich calcarenites and sandstones of Albaina correlate westward to the Torme Formation (named by Floquet et al., 1982), and are regarded as upper Maastrichtian by Baceta et al. (1999). It is noteworthy to mention that the T–R cycle DC-13 is poorly represented across the northern limb of the Villarcayo Syncline due to local palaeogeographical conditions (Floquet, 1991; Pluchery, 1995; Berreteaga, 2008).

7.4 Geochemistry and Taphonomy

Rare Earth Elements analysis

The distribution of rare earth elements (REE) in vertebrate fossils is especially used in taphonomic studies to assess the degree and type of diagenetic alteration (Lécuyer et al., 2003), in addition to identify fossil reworking prior to final burial (Trueman et al., 2006). Bone apatite crystals incorporate REE traces at high concentrations shortly after having been buried under sediment, even just in tens of years (either after the death of the animal or, in the case of selachian teeth, after being shed naturally), and therefore REE traces are used as geochemical indicators to know whether a bone remain and its enclosing current sediment, or rock, shared a similar diagenetic environment (Plummer et al., 1994; Trueman and Benton, 1997) and, if applicable, the extent of reworking in bone accumulations (Trueman et al., 2003, 2005; Metzger et al., 2004). Trace-element uptake, which is limited by its availability, supply, and filling effectiveness in post-mortem and early diagenetic processes ends when recrystallization closes a bone porosity initially occupied by collagen. Therefore, differences in the relative concentration of REE in fossil bones reflect the local variations in the pore-water chemistry (Trueman, 1999; Trueman and Tuross, 2002).

Bone mineral is relatively reactive for taking rare earth elements directly from pore waters (Koeppenkastrup and De Carlo, 1992; Reynard et al., 1999; Hodson et al., 2001). The total concentration of REE in fresh bones is about 100 ppb (parts per billion), while fossil bones are typically enriched by increase of two to five orders of magnitude (Trueman and Tuross, 2002), and hence large amounts of REE traces are incorporated into bone post-mortem. The average REE concentration of about 500 ppm in fossil remains from the Quintanilla la Ojada fossil site contrasts with the average concentration of 7.3 ppm found in the host rock (see Table 7.1), but the total amount of REE incorporated into the fossil samples is well comparable to other REE deposits cited in literature (Hubert et al., 1996; Samoilov and Benjamini, 1996; Trueman and Benton, 1997; Elorza et al., 1999; Samoilov et al., 2001; Trueman et al., 2006).

The REE abundances measured in selachian teeth (in both dentine and enameloid), one actinopterygian tooth, an indeterminate bone element, and the host rock show three different REE patterns (Figs. 7.5). The graphs of the selachian dentine (Fig. 7.5A), the actinopterygian fish tooth, and the undetermined bone fragment (Fig. 7.5B)

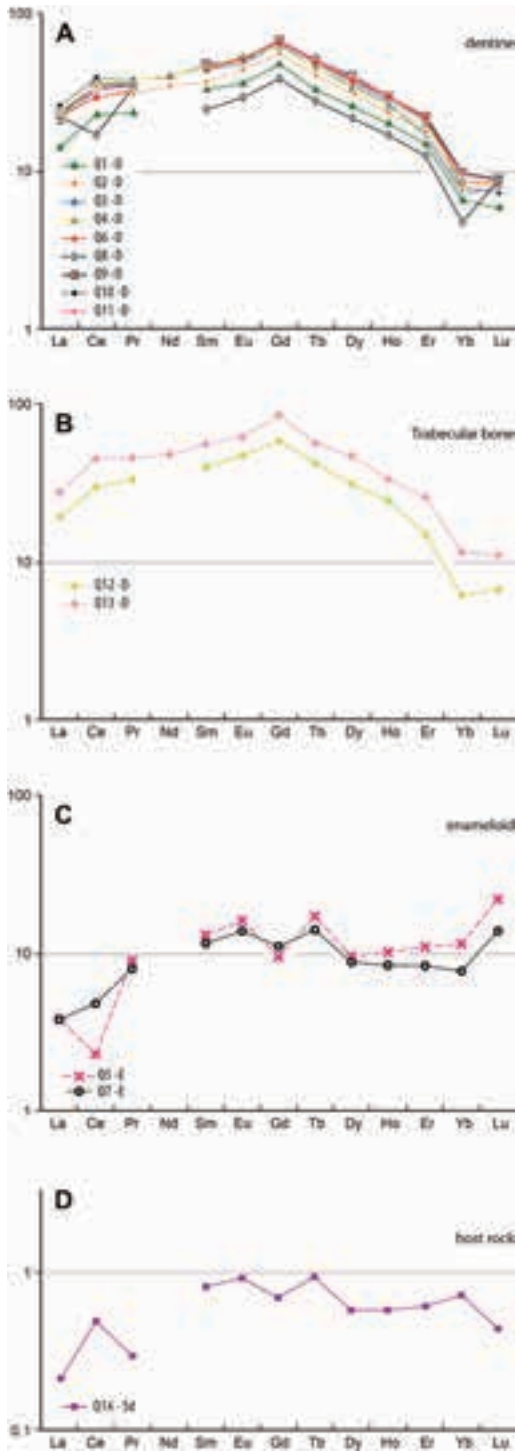


Figure 7.5 REE patterns for Late Cretaceous vertebrate remains and deposits from Quintanilla la Ojada (Burgos, Spain). A–B, selachians and fish tooth display similar ‘semi-flat’ patterns with low MREE enrichments and Yb depletion; (A) dentine, (B) trabecular bone; C, enameloid patterns in shark teeth display minor MREE enrichments; D, REE pattern from the hosting rock clearly differs from those obtained in the fossils. Note that the tissue microstructure of fossils plays important role in element incorporation during post-mortem and early diagenesis (see sample details in Table 1). Taken from Corral et al., 2015b.

record a 'dome-shaped' pattern where a clear Gd-enrichment, and a strong Yb-anomaly occur. The only two REE patterns measured for selachian enameloid (Fig. 7.5C) record a clearly different pattern with lower summation trace-element enrichment (136.1 ppm and 114.91 ppm) than in dentine samples. This is typical, as fresh enameloid contains less collagen than dentine or bone, and therefore the post-mortem destruction of soft collagen tissue results in a lower porosity, and consequently will incorporate less REE into its structure during diagenetic recrystallization (Kohn et al., 1999). A lower trace uptake into initial biogenic apatite occurs because there is less contact surface between bone and pore waters saturated in REE. Unlike biogenic apatite, where the closure of the porosity during recrystallization prevent late REE uptake, trace exchange between the sediment particles and pore water is prolonged in time, and thus the REE pattern of host rock is clearly different (Q14-Sd sample, plotted in Fig. 7.5D). Apart from the Ytterbium anomaly in dentine, REE patterns in the Quintanilla la Ojada material are quite flat, which indicate that samples have not undergone significant modification in late diagenesis, according to the conclusions of Reynard et al. (1999). Figure 7.6 plots concentration (ppm) ratios of La/Sm versus La/Yb as proposed by Reynard et al. (1999). In this bivariate plot, fossil vertebrate samples fall into two separate groups (dentine and enameloid), clearly showing again that the absorption of REE is different in diverse apatite tissues. This kind of diagram, which was also used in the study of the diagenetic history of rock formations (Reynard et al., 1999; Picard et al., 2002; Lécuyer et al., 2003; Berreteaga et al., 2004; Trueman et al., 2006; among others), is used here to reflect a low influence in the fossils in the final composition of REE of late diagenetic processes. Trueman et al. (2006) categorised four main groups of relative abundance of REE patterns through compilation of 1,691 analyses on terrestrial and marine fossil bones, ranging in age from the Silurian to the Pleistocene. Group 2 [i.e. samples with high $(La/Yb)_N$ values >1 , which they explained by the release of REE to pore waters from light REE-enriched sediments and subsequent incorporation into the bone mineral crystals], mainly corresponded to bones recovered from either coastal or shelf marine environments, or terrestrial environments with a significant aeolian input. The dentine values in the Quintanilla la Ojada fossils (Fig. 7.6) lie within group 2, and therefore reinforce the idea of shelf marine settings as the source of the fossil-rich rocks, using the model proposed by Trueman et al. (2006).

Taphonomy

The vertebrate fossil concentrations exhibit mixed preservation states, ranging from pristine to polished, abraded, or broken teeth. Effects of physical abrasion are more evident in roots than in cusps due to higher toughness of the latter. Different grades of functional breakage, later obliterated by mechanical rounding, are also observed in tooth crowns. Weathering artefacts due to a prolonged surface exposure, for instance enameloid exfoliation, are minimal as quarrying works regularly supply new material.

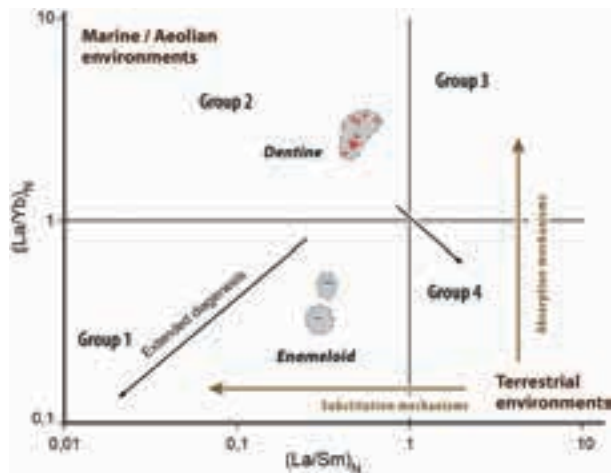


Figure 7.6 Normalised La/Yb ratios versus La/Sm ratios for vertebrate remains from Quintanilla la Ojada (Burgos, Spain) reported in the bivariate diagram proposed by Reynard et al. (1999). See discussion in text. Taken from Corral et al., 2015b.

However, root lobes or single cusplets in some large lamniform teeth may appear broken off due to mechanical damage during wet sieving.

Two fossil assemblages are thought to occur in the locality (see Fig. 7.3). The oldest assemblage (QLO-1) is found in conglomerates of the basal lag and contains few taxa [i.e. *Squalicorax pristodontus* (Agassiz, 1843), *Carcharias heathi* Case and Cappetta, 1997, and *Serratolamna serrata* (Agassiz, 1843)]. The total number of individuals is low because specimens were exclusively handpicked since the rock is not suitable for wet screen-washing. These teeth are easily identified because oxidation process has yielded them a reddish brown hue, and because they also exhibit severe mechanical abrasion and faceting, that in some cases have led to severe root wearing. This assemblage could be referred as grade three of abrasion of the five-grade classification established by Vullo (2005), namely incomplete teeth lacking part of the root elements.

The younger assemblage (QLO-2) is richer, both in number of recovered elements and taxonomic diversity. It occurs well above the transgressive surface (boundary cycle BC-12), and is associated to small fining upward sequences inside the tidally-influenced depositional cycle DC-12 at the base of the VNF. Polish is developed all over these greyish black teeth, and abrasion is also frequent although in a slightly lesser extension than in assemblage QLO-1. In some cases, most of these elasmobranch remains exhibit a sort of physical abrasion, and therefore could be referred as grades two and three according to classification proposed by Vullo (2005), namely a mixture of generally complete and incomplete teeth. There is no apparent size sorting, as both large and microscopic teeth occur together.

The oldest assemblage (QLO-1), occurring above the basal discontinuity of the DC-12 depositional cycle, corresponds to a lag concentration sensu Kidwell (1991). It

Table 7.1 Rare earth element (REE) concentrations in bone and host rock (ppm) from the Quintanilla la Ojada site (Burgos, Spain). Normalised to Post-Archean Australian Shale, PAAS (Taylor and McLennan, 1985).

Sample	Description	La	Ce	Pr	Nd	Sm	Eu	Gd	Tb	Dy	Ho	Er	Yb	Lu	La/Sm	La/Yb	Dy/Yb	Total REE
Q1	Tooth -D (L)	14.2	23.0	23.7	—	33.4	36.5	48.4	33.2	26.1	20.3	14.9	6.6	5.9	0.4	2.2	4.0	286.1
Q2	Tooth -D (S)	24.1	35.1	31.5	35.1	37.4	44.7	56.3	41.2	31.3	23.7	18.1	7.7	7.9	0.6	3.1	4.1	359.0
Q3	Tooth -D (Sk)	22.4	32.7	36.6	—	44.4	48.6	65.5	46.1	35.3	27.1	16.9	7.3	7.9	0.5	3.1	4.8	390.7
Q4	Tooth -D (Sr)	21.0	36.3	37.9	40.7	46.1	54.2	62.8	46.5	34.1	25.6	19.7	8.7	8.5	0.5	2.4	3.9	401.4
Q5	Tooth -E (Sr)	3.8	2.3	9.1	—	13.2	16.3	9.5	17.4	9.6	10.2	11.0	11.5	22.2	0.3	0.3	0.8	136.2
Q6	Tooth -D (L)	22.4	29.9	32.5	—	45.2	52.4	67.0	50.2	38.1	30.0	22.3	8.6	8.4	0.5	2.6	4.4	406.9
Q7	Tooth -E (Od)	3.8	4.8	8.0	—	11.6	14.0	11.1	14.2	8.8	8.5	8.4	7.7	13.9	0.3	0.5	1.1	114.9
Q8	Tooth -D (Od)	22.5	17.2	34.2	—	24.9	29.6	39.0	28.1	21.9	17.0	12.5	4.8	8.8	0.9	4.7	4.6	260.7
Q9	Tooth -D (Rh)	23.3	35.8	36.0	—	48.5	50.9	68.4	51.2	40.8	30.2	22.5	9.8	9.0	0.5	2.4	4.1	426.5
Q10	Tooth -D (Rh)	26.2	39.5	38.3	40.0	47.4	52.3	69.2	48.8	37.2	28.5	21.2	8.0	7.3	0.6	3.3	4.7	423.8
Q11	Tooth -D (Rh)	22.2	34.0	35.2	—	47.4	52.8	68.3	51.3	40.0	30.0	21.6	9.7	8.7	0.5	2.3	4.1	421.2
Q12	Bone -Trab (IV)	19.5	30.1	33.7	—	40.9	48.1	59.5	42.8	31.5	24.7	15.1	6.2	6.7	0.5	3.1	5.1	358.9
Q13	Tooth -D (En)	27.9	45.7	46.3	48.5	56.4	62.9	86.7	57.2	47.7	33.8	26.0	11.6	11.0	0.5	2.4	4.1	513.2
Q14	Sediment (Sd)	0.2	0.5	0.3	—	0.8	0.9	0.7	1.0	0.6	0.6	0.6	0.7	0.4	0.3	0.3	0.8	7.3

Abbreviations: En= *Enchodus*, IS= Indeterminate shark, IV= Indeterminate vertebrate, L= Lamniform indet., Od= Odontaspidae, Rh= *Rhombodus*, Sk= *Squalicorax kaupi*, Sr= *Serratolamna*. D= dentine, E= enameloid, Trab= trabecular bone, Sd= host rock (sandy dolomite).

is characterised by eroded fossil elements, but other well preserved ones, which purportedly were supplied through exhumation and erosional resedimentation of laterally deposited sediments, may occur. The younger assemblage (QLO-2) seems to correspond to a 'within-habitat time-averaged assemblage' (Kidwell, 1998), as accumulations of this kind include mixed representatives from a single persistent community. Small teeth belonging to nektobenthic sharks and rays (including the families *Ginglymostomatidae*, *Triakidae*, *Rhinobatidae*, *Sclerorhynchidae*, and *Rhombodontidae*), large teeth of pelagic sharks (including the families *Anacoracidae*, *Serratolamnidae*, and *Odontaspidae*) plus benthic foraminifera occur in the lower two metres of stratum QLO-2. Moreover, the taphonomic signature of this deposit is dominated by a mixture of well-preserved and variably abraded selachian teeth. Post-mortem damage in teeth includes longitudinal cracks (showing rounding edges), blunted cutting-edges, rounding, and polish. Authigenic pyrite, which appears within the porous tissue and on surface of the fossil teeth, formed later by precipitation after burial and compaction of sediment.

When considering the roundness and abraded shape of some *Rhombodus* specimens, which are frequent elements in the younger assemblage QLO-2, it may be assumed a prolonged exposure on the seabed of these dense apatite elements, and that rounding was induced by bottom currents prior to final burial. On the other hand, polish on surfaces is only formed on permineralised material that underwent an initial burial episode and early diagenesis followed by exhumation, either occasional or gradual. Rogers and Kidwell (2000) stated that this stage is a "prerequisite for abrasion to result in polishing rather than rounding alone." Hiatal or condensed concentration is suggested for the younger assemblage QLO-2. According to Kidwell (1991) such deposits are thinner to coeval deposits and can form by either sediment starvation (non deposition in an area of passing sediment) or by alternating processes of thin deposition and erosion (dynamic bypassing). As the thickness of the VNF in the quarry section of Quintanilla la Ojada is smaller than in its type section (Berreteaga, 2008), this would indicate a condensed concentration with lower net accumulation of sediment. Thus, teeth from the marine fishes and their enclosing sediment were contemporaneous, being deposited in a low sedimentation rate environment. Local geological conditions at the site coupled with halokinetic uplift related to nearby diapire of Salinas de Rosio probably resulted in formation of palaeoheights within shallow-marine environments, which would have favoured condensation episodes.

7.5 Age of the deposits

The selachian assemblages QLO-1 and QLO-2 at Quintanilla la Ojada derive from the lower part of the VNF, a unit which is regarded lower Maastrichtian to lower upper Maastrichtian on the basis of its rudist content (Floquet, 1991). However, a refined dating can be obtained by using biostratigraphically calibrated Maastrichtian selachian faunas from the phosphatic successions of Benguéir and other Moroccan exposures,

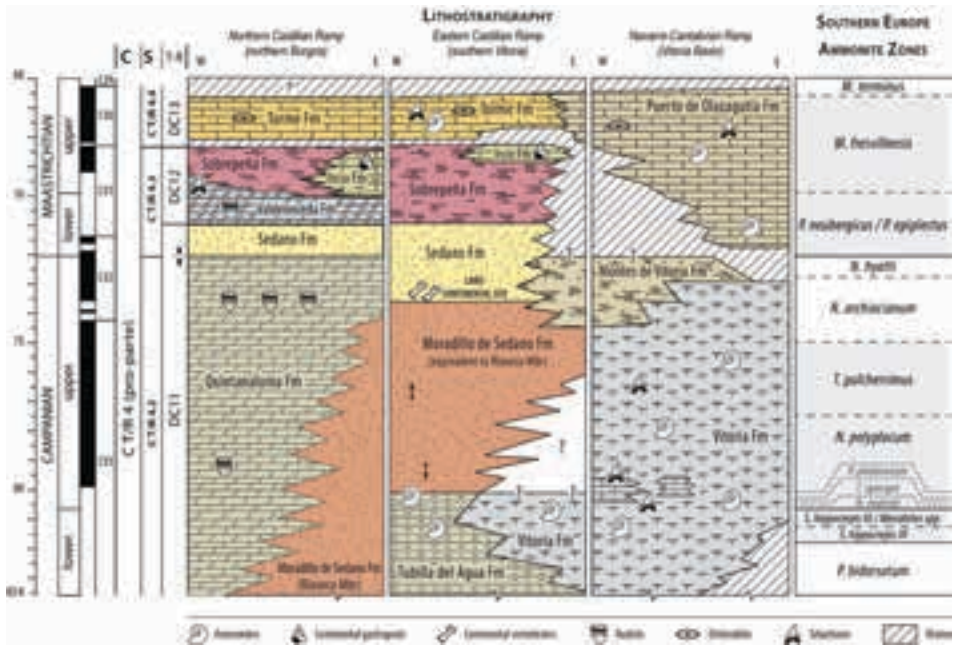


Figure 7.7 Chronostratigraphical summary of the uppermost Cretaceous lithostratigraphical units in the outer proximal Castilian Ramp and the relationship to the Navarre-Cantabrian Ramp (Vitoria Sub-basin). Stage boundaries of formations in the CR based on Floquet (1991). Key: C, major depositional cycles; Fm, formation; Mbr, member; S, minor depositional sequences; T–R, depositional cycles after Floquet (1998). Ammonite biostratigraphy for Southern Europe based on Hardenbol et al. (1998), Santamaría Zabala (1996) and Küchler et al. (2001). Identified biozones in Álava and Navarre provinces are shown in grey shade; hiatuses are marked by diagonally ruled lines (modified from Corral et al., 2015a).

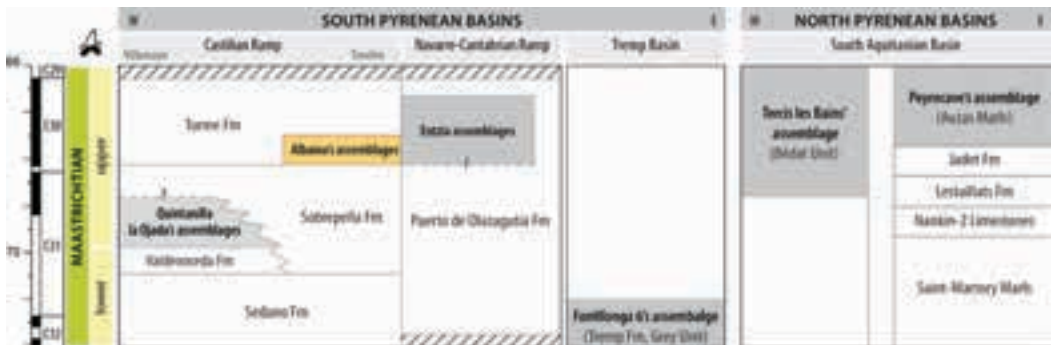


Figure 7.8 Scheme of stratigraphical positions of Maastrichtian localities with selachian remains in south-western Europe (adopted from Gheerbrant et al., 1997; Cappetta and Corral, 1999; Laurent et al., 1999; Cappetta and Odin, 2001; Kriwet et al., 2007; and this chapter). The exact chronostratigraphical range of some lithostratigraphical units is still a matter of debate (modified from Corral et al., 2015b).

which are remarkably useful for their completeness and abundance of marine vertebrate remains (see Cappetta et al., 2014b). Quintanilla la Ojada has yielded the age-diagnostic species *Serratolamna serrata* (Agassiz, 1843), *Carcharias heathi* Case and Cappetta, 1997, *Plicatoscyllium lehneri* (Leriche, 1938), *Coupatezia fallax* (Arambourg, 1952), and large teeth of *Rhombodus binkhorsti* Dames, 1881, regarded as late Maastrichtian in age by Cappetta et al. (2014b). The species *Squalicorax pristodontus* (Agassiz, 1843) is known to range through Maastrichtian successions worldwide, but variations in the size and form of the teeth may also shed light on the age of the deposit. According to observations made by Cappetta et al. (2014b), the contour of the crown of this species varies in a continuous manner along the Benguérir section: the early Maastrichtian forms from levels L6 and L5 exhibit a notch in the distal cutting edge of the crown, which results in the formation of a distal heel, whereas scant latest Maastrichtian forms from level L2 show symmetrical crowns in labial/lingual views. The teeth of *Squalicorax pristodontus* (Agassiz, 1843) from Quintanilla la Ojada do not match the characteristics of the uppermost Maastrichtian forms because they do not have symmetrical crowns, and their distal cutting edges are slightly concave (see Fig. 13.11–Q in Chapter 13). These contour shape differences are therefore in favour of a relatively older age of the Quintanilla la Ojada specimens, with regard to the tooth morphologies occurring in the uppermost Maastrichtian of Benguérir (level L2). As indicated earlier, Quintanilla la Ojada and Albaina sites have strong faunal similarities, although the two deposits correspond to different aged formations (see Figs. 7.7 and 7.8).

The recent magnetostratigraphical calibration of the underlying Sobrepeña Formation at Laño quarry (Treviño County, Burgos), a few metres eastwards from the Albaina section, indicates an early late Maastrichtian age for the upper part of the formation (Corral et al., 2015a; see Chapter 8), which is consistent with the known biostratigraphical age of the overlying marine Torme Formation unit.

Using lithostratigraphical data and other cooccurring taxa, it is possible to give a lower upper Maastrichtian for the youngest selachian assemblage (QLO-2) of Quintanilla la Ojada. However, the cooccurrence of *Carcharias heathi* Case and Cappetta, 1997, *Coupatezia fallax* (Arambourg, 1952), *Plicatoscyllium lehneri* (Leriche, 1938) and *Rhombodus binkhorsti* Dames, 1881, which is indicative of a latest Maastrichtian age (Cappetta et al., 2014b), would give a younger age for at least a part of the Valdenoceda Formation. This is at the moment inconsistent with the known lithostratigraphical dating of this unit. What it seems clear is that the Quintanilla la Ojada assemblages are relatively older than those of the Albaina's beds on the basis of their stratigraphical position within the Valdenoceda Formation, as this unit lies directly below the Sobrepeña Formation (see Figs. 7.3, 7.7). In this regard, it may be recalled that final depositional cycle DC-13 is absent in the Quintanilla la Ojada section. Therefore, the Quintanilla la Ojada assemblages should be assigned to the lower upper Maastrichtian, although the exact age of such assemblages remains to be verified by further palaeontological studies or other means such as magnetostratigraphy.

Chapter 8 STRATIGRAPHY AND PALAEONTOLOGY OF THE UPPER MAASTRICHTIAN ALBAINA BEDS (TREVÍÑO COUNTY, BURGOS)

8.1 Introduction

The Albaina-Laño section in the southcentral part of the Basque-Cantabrian Region provides a remarkable exposure of the uppermost Cretaceous–early Paleogene formations. The series, which is represented by three consecutive transgressive–regressive cycles, typically comprises: (1) marine carbonates passing up into marine littoral sandstones; (2) continental deposits; and again (3) marine carbonate and siliciclastic strata at the top. The rock sequence records a regionally regressive episode with subaerial exposure of the area and, finally, a renewed flooding of the ramp margin.

The section was first described by Astibia et al. (1987), but subsequently a large number of studies have focused on the geology (to name a few: Gómez-Alday et al., 1994; Pujalte et al., 1993; Floquet, 1991; Baceta et al., 1999; Gómez-Alday, 1999; Berreteaga, 2008; and Corral et al., 2015a) and, especially, on the palaeontology of the continental unit (Astibia et al., 1990, 1999a and references therein; Pereda-Suberbiola et al., 2000, 2015a, 2015b).

Maastrichtian strata crop out as a thin strip that extends a few kilometres eastwards along the southern flank of the Miranda-Treviño Syncline, overlying a thick series of terrigenous siliciclastic rocks. Albaina beds are known for their extraordinary abundance and diversity of selachian teeth, which are the conspicuous fossil elements, with at least 19 species of sharks and rays (Corral and Cappetta, 1999). However, a diverse record of actinopterygians (Poyato-Ariza et al., 1999), marine reptiles (mosasaurs and elasmosaurids) (Bardet et al., 1997, 1999, 2013), and continental vertebrates (Pereda-Suberbiola et al., 2015b) have also been reported in the same rocks, which makes these area the source of the most complete marine vertebrate assemblages, known to date, from the Cretaceous in the Basque-Cantabrian Region.

Invertebrate fossils have not received adequate attention so far, but several heteromorph ammonites, gastropods, few bivalves, a single inoceramid, a rudist mould,

and body parts of decapod crustaceans, in addition to large benthic foraminifera (e.g. orbitoidids) are among the found ones.

The Maastrichtian Albaina fossil site represents the most eastern location of the Torne Formation (TF), in addition to being the southernmost exposures yielding a typical upper Maastrichtian mollusc assemblage in the Basque-Cantabrian Basin (B-CB). The purpose of this chapter is to clarify the biostratigraphy of the uppermost Cretaceous (Campanian and Maastrichtian) sequences by integrating some newly-discovered Maastrichtian fossil molluscs and to correlate these units with nearby sequences of similar age occurring in the B-CB.

8.2 Location and geological setting

Albaina section is located halfway between the villages of Albaina and Laño in Treviño County (Burgos province), about 30 km to the south of the capital city of Vitoria-Gasteiz (Fig. 8.1) on the southcentral part of the Basque-Cantabrian Region. Its study was made possible thanks to the presence of the abandoned Albaina-Laño quarry, which exploited high-quality silica sand especially for the glass and foundry industries. The quarry extends over 1.5 km in an E–W direction (Fig. 8.2), having a west face of about 460 m along the hill (referred to as west pit, or Albaina site) (Fig. 8.3) and an east face of about 1 km on the southern slope of the ‘Castilletes hill’ (referred to as east pit, or Laño site) (Figs. 8.4, 8.5).

Different stratigraphical schemes, which are broadly similar, have been established for the region by Wiedmann et al. (1983), Floquet (1991), Pujalte et al. (1993), and Gräfe et al. (2002). According to those authors, the depositional history was controlled by phases of overall regression, with minor fluctuations, caused by compression and uplift during the Campanian and Maastrichtian [megasequences 3 and 4 (pro-parte) according to Wiedmann et al. (1983); megasequences Sedano and Urbasa according to Gräfe et al. (2002)]. Wiedmann et al. (1983) reported two successive compression–regression episodes in this area, the older one during the upper Campanian, when a deltaic complex settled nearby Vitoria-Gasteiz and fluvial sediments with vertebrate fossils accumulated southwards (cf. Astibia et al., 1999a). Both environments replaced a shallow carbonate setting with sedimentation of silty limestones and marls containing ammonoids (as seen in Chapters 5 and 6). As a result of a subsequent second compression–regression episode, most of the lower Maastrichtian was removed or preserved only as thin sequences (López, 1996), revealing a mappable intra-Maastrichtian unconformity.

Farther west in the Castilian Ramp, uppermost Cretaceous shallow sedimentation is recorded by three short term transgressive–regressive depositional cycles DC-11 to DC-13, named by Floquet (1998), ranging in age from upper Campanian to Danian (see Corral et al., 2015a). This well-known stratigraphical framework can be confidently extended within the study area (southern Álava, B-CB), which lies approximately 90 km southeast of the Castilian outcrops (Floquet, 1991).

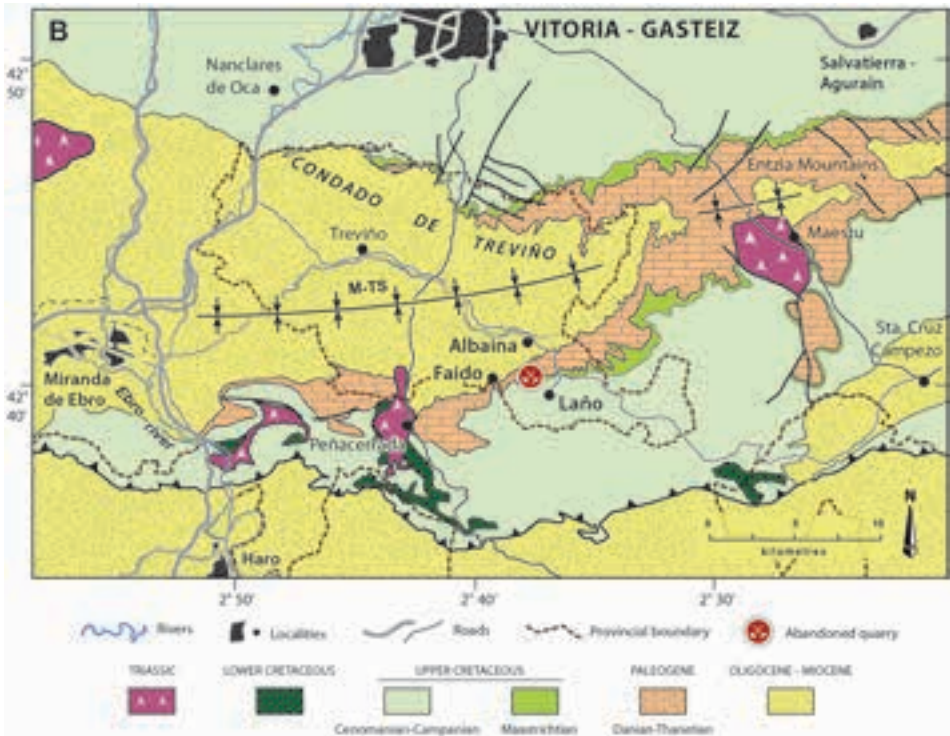


Figure 8.1 Simplified geological map of the southern central part of the Basque-Cantabrian Basin showing the distribution of the major units and the location of the abandoned Albaina/Laño quarry. M-TS, Miranda-Treviño Syncline.



Figure 8.2 General view of the Albaina-Laño quarry (Basque-Cantabrian Region) with the Treviño basin (TB) and the Vitoria Mountains (VM) at the horizon; wp, western pit; ep, eastern pit. Picture taken toward the northwest (photo by the author, modified from Astibia et al., 1999b).



Figure 8.3 A view of the western face of the Albaina-Laño quarry (Albaina site) looking west.



Figure 8.4 A view of the eastern face of the Albaina-Laño quarry (L1 site) looking east.



Figure 8.5 A view of the eastern face of the Albaina-Laño quarry (L2 site) looking west. The Albaina site is in the background.

The palaeogeography of this region during the Upper Cretaceous was inferred to be a subsiding low-gradient marine ramp placed on the northern margin of the Iberian plate. Both inner and outer shelf zones are enclosed into the Navarre-Cantabrian Ramp domain, whereas the nearshore zone, and occasionally inner platform, corresponds to the Castilian Ramp domain of the B-CB.

8.3 Stratigraphy

The uppermost Cretaceous sedimentary succession in the Albaina-Laño area includes, from older to younger, the Moradillo de Sedano, Sedano, Sobrepeña, and Torme formations (Figs. 8.6, 8.7) (see also Corral et al., 2015a). This proposed lithostratigraphy is mostly based on previous works of Floquet et al. (1982) and Floquet (1991) but also incorporates the work of Cappetta and Corral (1999) and new descriptive information on their palaeontology and stratigraphical relationships. Despite the fact that this lithostratigraphical framework was proposed for the Cretaceous rock record of the proximal Castilian Ramp domain in the eastern part of the B-CB, it can be confidently adopted for this southcentral part of the B-CB. Only the upper Maastrichtian rock units will be considered here (Figs. 8.8, 8.9).

Sobrepeña Formation (SPF)

Original authors. Floquet et al. (1982) with additional information in Floquet (1991).

Type locality. It is located east of the village of Sobrepeña (Burgos province) in the western part of the Villarcayo Syncline, but the formation best crops out at the Km 5 marker, in the route between the villages of Torme and Cornejo, also in the province of Burgos.

Boundaries. The Sobrepeña Formation (SPF) disconformably overlies dolomitised, limestone-mudstone interbedded strata of the Valdenoceda Formation (VNF), and is disconformably overlain by the Torme Formation (TF) in the type area. However, the VNF has not been recorded in the Albaina-Laño area, where is underlain disconformably by the Sedano Formation (Figs. 8.6, 8.7, 8.9). The upper boundary is a major regional unconformity (named IMU), involving a short hiatus in relation to the overlying TF.

Thickness. According to the authors, the SPF shows a minimum and maximum thickness of 60 and 100 m respectively in the type area. However the thickness of this unit is only about 21 m at Albaina/Laño quarry.

Lithology. In general the unit is basically terrigenous. Major lithologies are variegated mudstone, but interbedded dolomicritic deposits and intermixed sandstone may occur within the formation. The formation at Laño quarry is mainly composed of variegated mudstones (green to grey), streaks of microconglomerate layers, and silty clays (Fig. 8.10). The base of the formation begins with a thin bed of greenish mudstone above the IMU. This is followed by alternating beds of dark grey terrigenous and carbonaceous



Figure 8.6 Photograph showing the lithological units observed in the west face of the Albaina quarry (Treviño County). The detail of the formations is given in the text. View looking west.



Figure 8.7 Photograph showing the lithological units observed in the east face of the Albaina quarry (Treviño County). Descriptions and geologic age range are given in the text. View looking north.

mudstone (CM1) that contains strings of lignite, nodules of pyrite, scattered granules of amber, and few undetermined vertebrate bones (Fig. 8.10). This mudstone is overlain by a dolomitic breccia interval (about 6 m thick), in whose matrix voids calcite and thin white barite crystals occur. Above the carbonate lithofacies, a terrigenous unit (about 14 m thick) of reddish pebbly mudstones, along with interbedded layers of gyp-

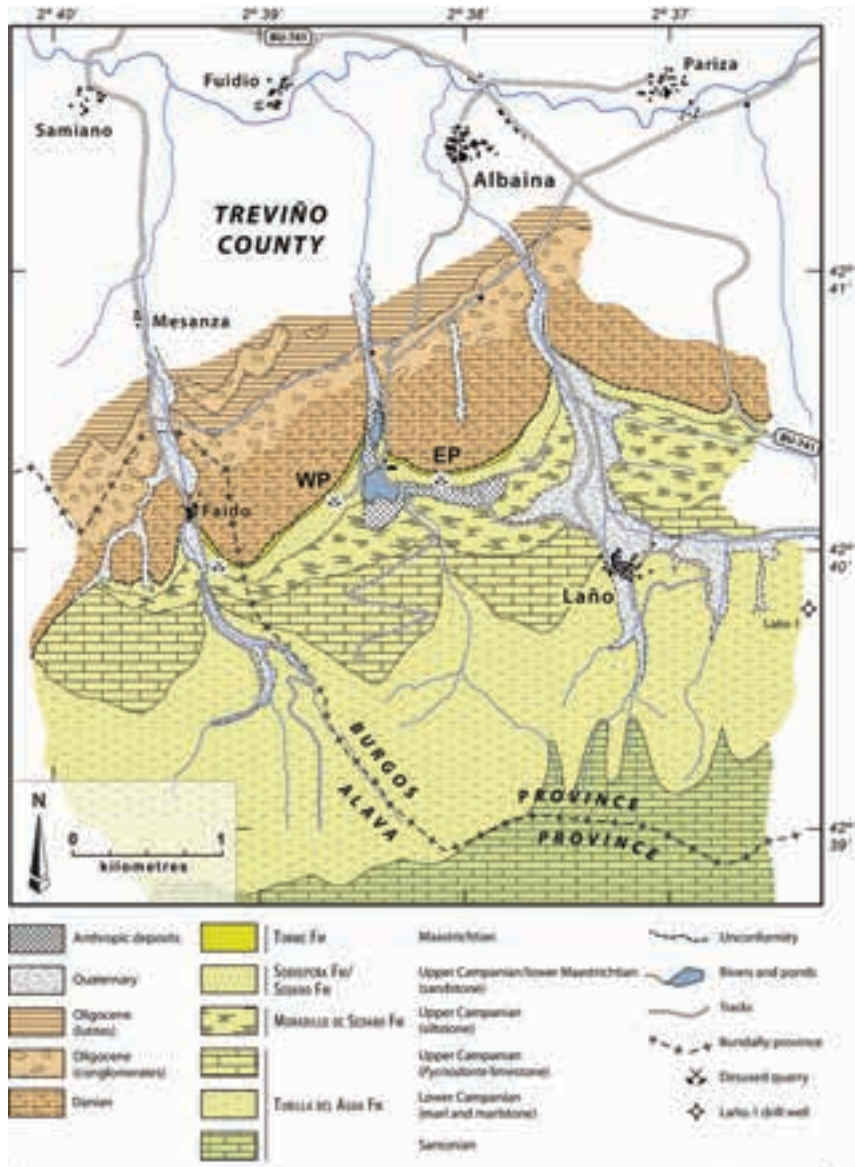


Figure 8.8 Geological map of the Laño area (Basque-Cantabrian Region, B-CB) showing the silica sand quarries. The terms WP and EP stand for the western and east pits of the Albaina-Laño quarry.

sum, is identified (Fig. 8.11). The sequence continues upwards with a 2 m thick bed of matrix-supported brown conglomerate devoid of structures and a second carbonaceous mudstone layer (CM2) with iron sulphides (probably marcasite).

Palaeontological content and age. Fossils are scarce in the type area but a non-marine microfossil assemblage of charophytes and ostracods has been recorded. Floquet (1991)

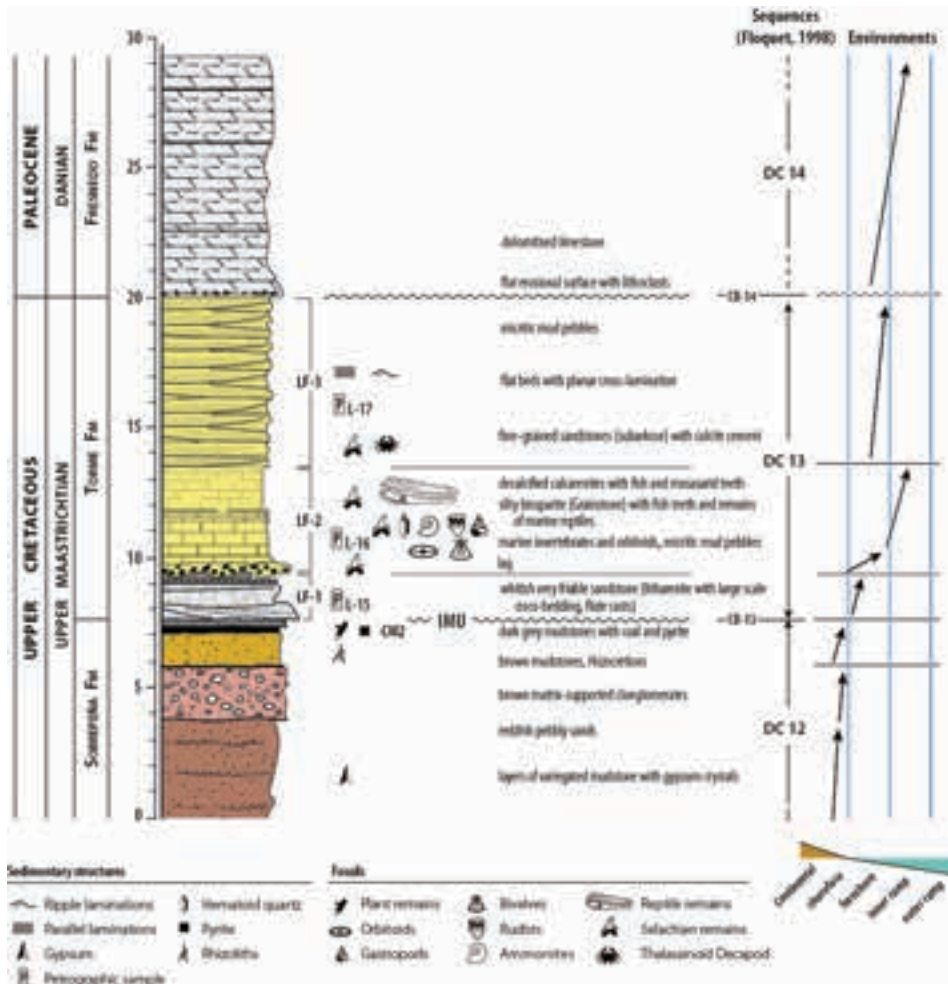


Figure 8.9 Stratigraphical column of the Upper Cretaceous cropping out at Albaina/Laño quarry (modified from Cappetta and Corral, 1999). CB, cycle boundary; CM, carbonaceous mudstone; DC, depositional cycle; IMU, intra-Maastrichtian unconformity; LF, lithofacies association.

reported the following charophytes: *Platychara caudata* Grambast, 1971, *Platychara turbinata* Grambast and Gutiérrez 1977, *Retusochara macrocarpa* Grambast, 1971, and *Dughiella* aff. *obtusa* Grambast and Gutiérrez 1977, in addition to some bivalves and gastropods typical of garumnian facies. The presence of charophytes and the lithostratigraphical position of the SPF, between the Valdenoceda and Torme formations, indicate an early late to latest Maastrichtian age in the type area (Floquet, 1991).

In the Laño exposure, the formation has also yielded plant remains and a few undetermined bone fragments related to the black grey subunit CM1. Nuñez-Betelu (1999) tentatively indicated a late Campanian age for the carbonaceous mudstones

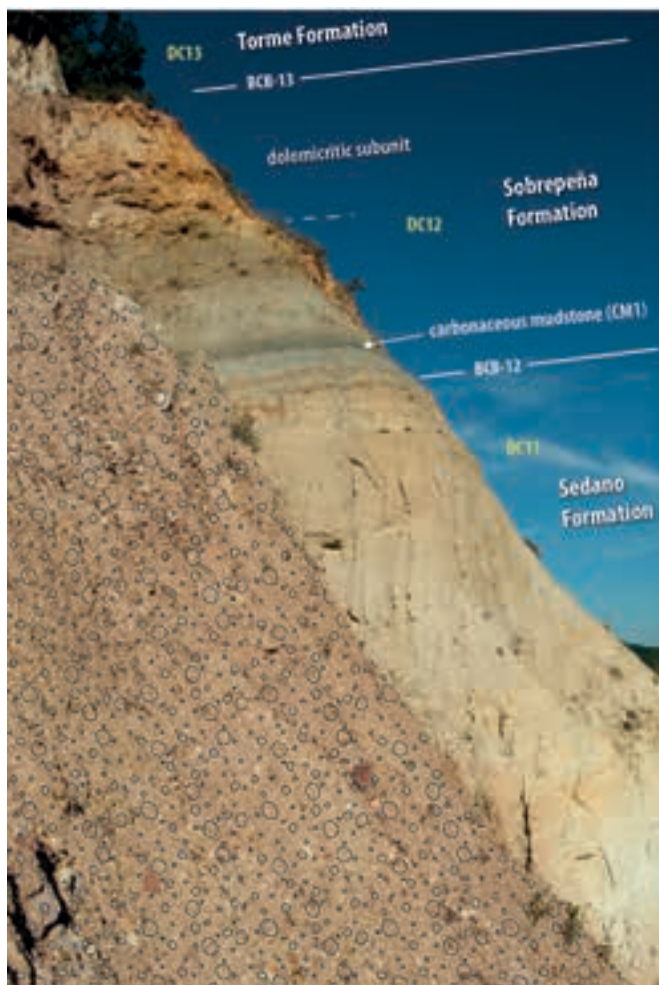


Figure 8.10 Detail section showing the lithology of the lower part of the Sobrepeña Formation in the Laño quarry (looking east). The upper variegated mudstones with gypsum do not crop out in the photograph but are visible as a small alluvial cone (patterned on the left side of the photograph).

determined from their palynological content (*Extratropopollenites* sp., *Tetraporites* sp., *Tricolpoporopollenites* sp., *Cicatricosisporites aratus*, *Interulobites triangularis*, and *Matonisporites* sp.; see references therein). Such dating had to be constrained by either the small number of diagnostic taxa found on the samples or the considered position of the Campanian–Maastrichtian boundary at the time of the publication of the Nuñez-Betelu's (1999) paper, or both. In the absence of reliable palaeontological data, an early Maastrichtian age could be ascertained by stratigraphical correlation (J.I. Baceta, com. pers., 1996). Recently the Laño section was sampled for magnetostratigraphy (Corral et al., 2015a), the results of which provide a late early to early late Maastrichtian age.



Figure 8.11 Idiomorphic crystals of gypsum embedded into a yellow-red-dish mudstone matrix of the Sobrepeña Formation. Field of view is about 1.5 metre.

Depositional environment. The SPF reflect a variety of depositional settings including alluvial–fluvial floodplains subject to periodic flooding with extended periods of hypoxia and/or anoxia (CM1 and CM2 facies), shallow palustrine water depths where carbonates formed, and arid supratidal sabkha or playa lakes where arid conditions led to iron oxidation and precipitation of gypsum in ephemeral ponds.

Cycle framework. The SPF was deposited during the T–R cycle DC-12. The lower contact of the cycle is found merged disconformly with a sandy sequence of the Sedano Formation, reportedly to contain a rich continental vertebrate assemblage (Astibia et al., 1999a; Pereda-Suñerbiola et al., 2015a). The basal part is composed of quartz microconglomerate sandstones that gradually pass upwards to sandy mudstone and lacustrine facies. They underlie reddish conglomerate sandstones and variegated mudstones deposited during the regressive phase of the cycle. The upper boundary results in an important unconformity (IMU) that has long been recognised in the regional geological cartography and is linked to an initial uplift of the basin (Pujalte et al., 1993; Baceta, 1996).

Stratigraphical relationships and correlations. The SPF unit, named and described as DS-1 by Pujalte et al. (1993), is a tilted and truncated sequence of mainly terrigenous rocks, whose upper part gradually disappears westwards, probably due to synsedimentary activity generated by diapiric uplift (Gómez-Alday et al., 1994). The dolomicrites in the middle part should not be mistaken for the carbonate facies of the Ircio Formation (Floquet et al., 1982) that crops out not far from the Albaina-Laño site and was informally named ‘Belabia limestones’¹ by Mangin (1958), because the latter has typical Garumnian freshwater gastropods such as *Palaeostoa hispanica* Oppenheim, 1895 and those of the genus *Lychnus* (Fig. 8.12).

¹ Plaziat (1970b) listed the following gastropods in these strata: *Lychnus giganteus* Repelin and Parent, 1920, *Palaeostoa hispanica* Oppenheim, 1895, ‘*Viviparus*’ *cingulata* (Matheron, 1842), *Clausilia* cf. *matheroni* Oppenheim, 1895, and *Dissostoma* sp.

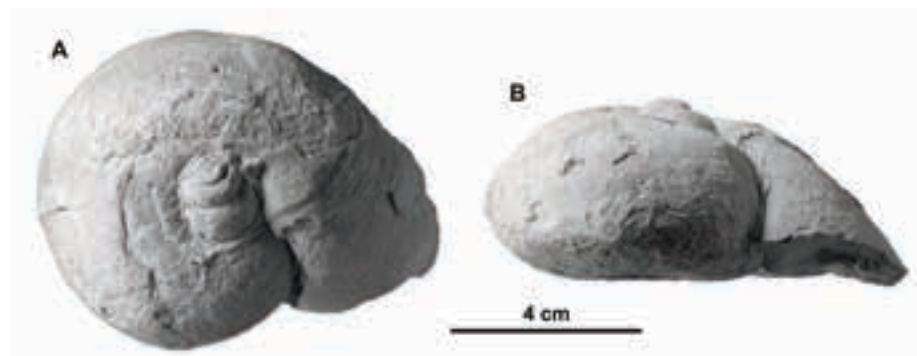


Figure 8.12 *Lychnus ellipticus* Matheron, 1832, internal mould with part of the shell preserved from the upper Maastrichtian ‘Belabia limestones’, Urarte (Álava province); MCNA 10120, (A) dorsal view, (B) apertural view.

Torme Formation (TF)

Original authors. Floquet et al. (1982) with additional information in Floquet (1991).

Type locality. The section is exposed in a road cut north of the village of Torme, which is located near Villarcayo in the northern part of the province of Burgos.

Boundaries. The Torme Formation (TF) rests unconformably on mudstone of the SPF and is disconformably overlain by the Danian Fresnedo Formation in the type area. However, in the Laño area the lower contact lies unconformably on either a thick quartz sandstone body of the Sedano Formation or the terrigenous SPF, whereas the upper boundary is disconformable with the overlying Fresnedo Formation, the base of which is often associated with a basal conglomerate lag (Floquet, 1991).

Thickness. According to the author, the maximum thickness of the TM is about 58 m in the type area. The unit reaches about 13 m in thickness in Albaina.

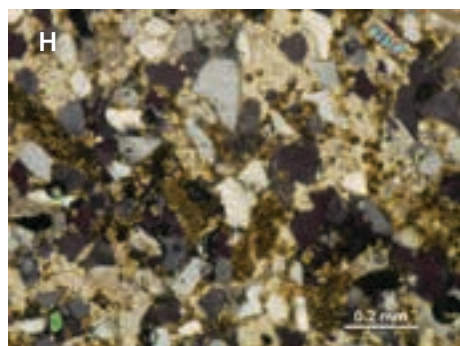
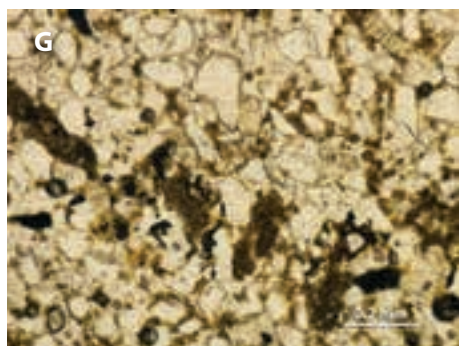
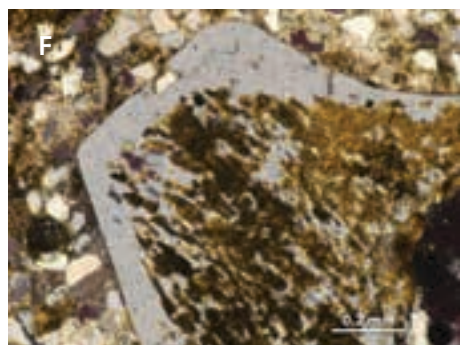
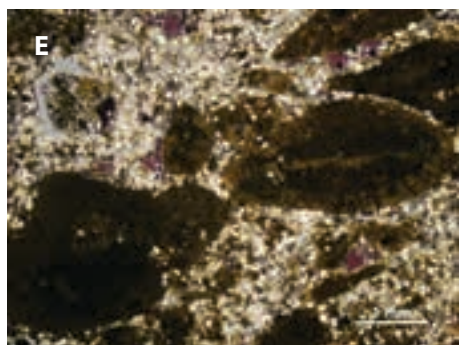
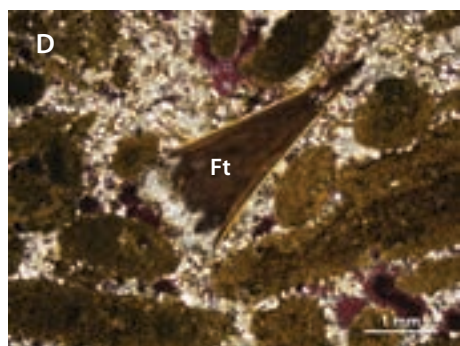
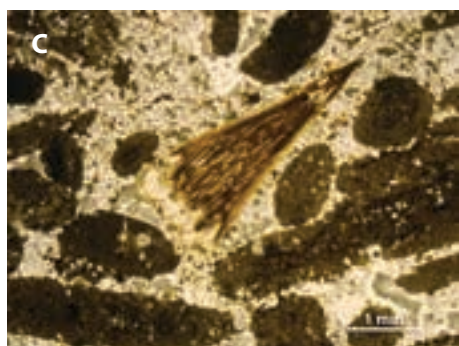
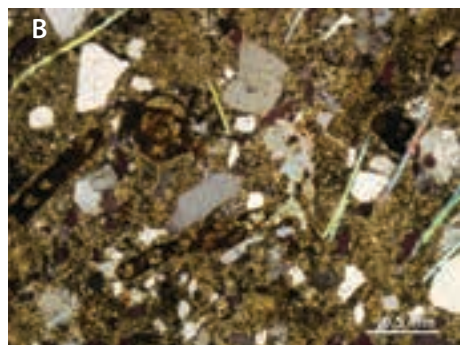
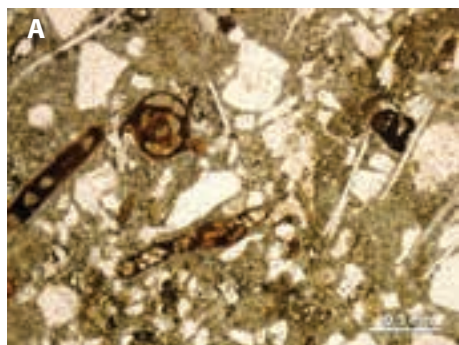
Lithology. This writing expands, with minor emendations, on the description given by Cappetta and Corral (1999) and Corral et al. (2015a). Based on field observations and thin section examination, three depositional facies are recognised in Albaina, above a thin discontinuous layer of black carbonaceous mudstone (CM2) that marks the lower boundary. In ascending order they are (Fig. 8.9):

A nearshore lithofacies (LF-I) consisting of a basal part of weakly cemented white to light grey sandstone (litharenite) and irregular discontinuous layers of microsparite and spar-cemented sandstone with benthic foraminifera, echinoid plates and peloids (Figs. 8.13A–B). This subunit is underlain by occasional polygenic conglomerate arranged in high-angle cross-laminated beds (Fig. 8.14A). Flute casts, originated during the transgressive episode, occur on the lower bedding surface of the initial stratum. According to principal components, the unaltered rock of LF-I is classified as a litharenite, since it contains a high proportion of benthic foraminifera (miliolids and rotaliids), algal fragments, echinoderm plates, and peloids. There is also present a remarkable

amount of muscovite flakes. In addition, mono and polycrystalline quartz and alkaline feldspars occur, but not in a very high proportion (up to 35%). These medium to fine size grains are subrounded to subangular. Some grains of quartz show undulose extinction. Calcitic cement (both microsparite and spar textures) occurs but in low quantity, which explain the friable condition of the lithofacies. Microsparite cement is more abundant and it is interpreted as being the recrystallization of former carbonate mud that constituted the matrix. The test of calcareous organisms (predominantly benthic foraminifera) have been completely replaced by a cryptocrystalline red-brown iron-rich mineral, though whether it is oxidised glauconite or a phosphate mineral cannot be ascertained by petrographic microscopy. Finally, as a result of cement dissolution processes, secondary porosity is estimated to be about 3%.

The overlying offshore/lower shoreface lithofacies (LF-II) mostly comprises friable silty bioclastic limestone with intercalations of more indurated horizons. This subunit is about 3.8 m thick. It abruptly starts with an irregular bed of matrix-supported conglomerate with erosive base which has been interpreted as a ravinement surface (Pujalte et al., 1993). The dominant lithology of this basal lag is constituted by poorly sorted quartzite pebbles and intraclasts floating in a sandy matrix. Unidentified bone fragments up to 15 cm long have been collected in it. Upward, the unit gradually pass into a yellowish teeth-bearing friable silty calcarenite strata. These are wavy bedded and their thicknesses are generally in the range of 1 m. An interbedded minor sequence made up firstly of greenish laminated mudstone, and then of very friable calcareous sandstone and clastic limestone, occurs again. Major components present in the calcarenite are skeletal particles, including orbitoid foraminifera, but miliolids and rovaliids are in smallest proportion (Figs. 8.13 C–E, 8.14C–D). Peloids and intraclasts, which may incorporate silt-sized quartz grains, are also present. Detrital euhedral authigenic grains of coarse sand-size quartz (hyaline and red varieties) are occasionally incorporated, but angular to sub-angular grains of silt-size quartz are most prevalent in the matrix of the rock (Figs. 8.13 E–F). Overburden pressure before cementation have given rise to both brittle fracture of skeletal fragments and pressure-solution at the contact points of some grains, leaving an insoluble red-dark opaque residue in between. Primary intragranular (i.e. inside the foraminifera chambers) and shelter porosity nearby platy benthic foraminifera can occur. Subsequent dissolution in the subsurface of pre-existing cements

Figure 8.13 Photomicrographs of selected lithofacies from the Tome Formation in Albaina. A–B, litharenite from LF-I showing detrital quartz, muscovite, benthic foraminifera and calcite cement (the red-brown colour of the microfossils may be some form of cryptocrystalline iron-rich mineral). C–F, bioclastic limestone from LF-II: C–D, phosphate grains and phosphatised microfossils sowing a fish tooth (Ft); E, phosphatised microfossils and euhedral authigenic quartz, porosity is shown as purple-black areas under crossed polars; F, euhedral authigenic quartz in E at higher magnification showing tiny crystals of anhydrite. G–H, fine-grained subarkose from (LF-III) showing grains of quartz, alkaline feldspar, zircon cemented by microsparite/spar calcite. A, C, and G taken under plane-polarised light (PPL); B, as A but under crossed polars (XPL); D, as C but under XPL; E–F, under XPL; H, as G but under XPL. ►



has generated secondary porosity as well. The fine spar calcite cement is poikilitic and includes small quartz grains of the matrix. Small foraminifera have chambers filled with microsparite. This burial cementation filled the pore spaces, making the rock a skeletal grainstone with coarse silt contamination. Peloids and large skeletal particles are pervasively micritized. As these rocks have the usual, brown isotropic cryptocrystalline aspect of phosphatic minerals (e.g. collophane) under crossed-nicols, they may have undergone a phosphomicritization process. Micritization also has caused earthy roots in many selachian teeth, which are readily removed leaving only cusps with rounded bases. Towards the top of the subunit, the calcarenite become more decalcified, resulting in very friable packstone with moldic and interparticle porosity. Although numerous marine vertebrate teeth and bones can be found across this calcarenite unit, they especially occur within a 25 cm thick basal bed as a result of a concentration process (Fig. 8.14B). Up to the unit, the series grades upward into a siliciclastic succession (see below), where shark teeth have been occasionally found, but not intensive sieving was made to define their biostratigraphical framework.

The shoreface lithofacies (LF-III) consist of whitish very fine-grained subarkose strata (Figs. 8.13G–H). These rocks are composed principally of very-fine grains of mono and polycrystalline quartz and alkaline feldspar. Accessory minerals include amphiboles, zircon, tourmaline, biotite, and grains of opaque iron oxides. Texturally, it is a mature sandstone, but little matrix content of clay minerals occurs. Although cement formed both as microsparite and spar calcite, the latter prevails with blocky and poikilitic textures. It does not fill completely the pore spaces of the rock, yielding lastly a friable rock. Bedding remains fairly constant throughout the unit and beds mainly contain planar cross-bedding and ripple lamination. Furthermore, in some places convolute lamination and burrowing also occur. This subunit is about 6.5 m thick.

Palaeontological content and age. Ciry (1939) observed that the Maastrichtian rocks in Torme contained fossils of similar composition to that of the ‘*calcaire nankin*’ (nankin limestone¹) from the Petites Pyrenees of Ariège and Haute-Garonne (France). He listed in the type locality of the formation the following taxa: teeth of a lamniform shark (as ‘*Lamna* sp.’), a nautilid cephalopod (as ‘*Nautilus* sp.’), the bivalves *Neithea* (*Neithea*) cf. *quadricostata* (Sowerby, 1814) (as ‘*Neithea* cf. *geinitzii*’), possibly *Amphydonte* (*Amphydonte*) *pyrenaicum* (Leymerie, 1851) (as ‘*Pycnodonta uncinella*’), *Agerostrea ungulata* (von Schlotheim, 1813) (as ‘*Alectryonia larva*’), possibly *Otostoma retzii* (Nilsson, 1827) (as ‘*Desmiera tchihatcheffi*’), the brachiopod *Thecidea papillata* (von Schlotheim, 1813) (as ‘*Thecidea radiata*’), the large holasteroid echinoid *Hemipneustes*

¹ Leymerie (1877, 1881) introduced in the geological literature the term ‘*calcaire nankin*’ to describe a yellowish limestone with typical Maastrichtian fossils from the Upper Cretaceous (‘Senonian’) of the Petites Pyrenees (Haute-Garonne, France). The etymology of the word nankin derives from the characteristic yellow colour invented by Chinese artisans in the XIX century to dye fabrics, which were imported to Europe from the city of Nanjing (China).



Figure 8.14 Different microfacies and fossils observed in the Torme Formation at Albaina/Laño quarry. A, conglomerate and nearshore sandstone; B, teeth of actinopterygian and selachian fishes on sandstone matrix: aulopiform *Enchodus* sp. (En) and lamniform *Carcharias* sp. (Ch); C, orbitoid-rich packstone layer; D, bioclastic packstone, lithoclasts (lt), orbitoid foraminifera (or) and a bivalve steinkern (bv); E, large gastropod steinkern in a bioclastic rock; F, longitudinal section of a large gastropod shell and smaller bioclasts of bivalves (coarse bioclastic fabrics). A, from lithofacies LF-I, B-F, from lithofacies LF-II.

cf. *pyrenaicus* Hébert, 1875a, and the orbitoidids *Orbitoides apiculata* Schlumberger, 1901 (as ‘*Orbitella apiculata*’), *Orbitoides gensacicus* (Leymerie, 1851) (as ‘*Simplorbites gensacicus*’) and *Omphalocyclus macroporus* (Lamarck, 1816) (as ‘*Omphalocyclus macropora*’). It is worth to note in this list the presence of orbitoidids, and in particular the species *Omphalocyclus macroporus*, which according to Özcan (2007) is considered to occur at the beginning of the *Abathomphalus mayaroensis* zone (= upper Maastrichtian).

Continuous search during the 30 years that the Albaina site has been known has allowed to gather a rich collection of marine vertebrate skeletal components, notably of actinopterygians (Poyato-Ariza et al., 1999), selachians (see Cappetta and Corral, 1999, and Chapter 14 of this thesis), mosasaurids and elasmosaurids (Bardet et al., 1997, 2013), along with scant turtle and dinosaur bones (Pereda-Suberbiola et al., 2015b). The greatest majority of the fossils came from the calcarenitic middle part of the formation (LF-II), but thin layers of the underlying sandstone LF-I show benthic foraminifera that are also indicative of marine settings. Nothing else can be said here about them since their study goes beyond the scope of this thesis.

Other important invertebrate fossil in the LF-II include large benthic foraminifera (e.g. orbitoids), forming occasionally layers of densely stacked test parallel to the bedding plane (Figs. 8.14C–D), and a scarce but remarkable collection of invertebrates (see Figs. 8.14), most of them slightly lithified. Contrarily to the vertebrate remains, where both hard dental tissue and porous internal microstructure are perfectly preserved, the preservation of these molluscs is generally poor being the specimens friable due to late diagenetic processes. Although they are internal moulds (i.e. steinkerns), except for a gastropod specimen that had also preserved the external mould of the apical zone (Fig. 8.16.P), most of the specimens keep enough characters to allow their identification. Included among the invertebrate macrofossils are the inoceramid *Cataceramus? glendivensis* Walaszczyk, Cobban and Harries, 2001 (Fig. 8.15A) (G. López, pers. comm.), a veneroid clam (Lucinidae genus indet.) (Figs. 8.15B–D), an undetermined Radiolitiidae showing a trapezoidal shell outline (Figs. 8.15E–I), the gastropods *Otostoma retzii* (Nilsson, 1827) and *Otostoma ponticum* d’Archiac, 1859 (Fig. 8.16), among others, a few baculitid ammonites (Fig. 8.17) including *Baculites anceps* Lamarck, 1801 and *Eubaculites cf. vagina* (Forbes, 1846), the echinoid *Hemipneustes striatoradiatus* (Leske, 1778) (Fig. 8.18), and a few decapod remains (Fig. 8.19).

Most Cretaceous biostratigraphical zonation is based on ammonites but inoceramid bivalves, which are facies independent, have also been proved useful index fossils. As said before, macrofossils are rare along the Albaina profile, but despite this, some biostratigraphical important molluscs have been found in rocks of the middle calcarenitic subunit (LF-II). The inoceramid specimen, which is referrable to *Cataceramus? glendivensis* Walaszczyk, Cobban and Harries, 2001 (Fig. 8.15A), is of medium size and have valves ornamented by subregularly spaced, round folds with interspaces increasing ventrally. According to Walaszczyk et al. (2009), *C.? glendivensis* was originally re-

ported from the lower Maastrichtian (*Endocostea typica*¹ and *Trochoceras radius*² zones) of the Western Interior of North America, where is known to occur in the upper part of the ammonite *Baculites baculus*³ zone and *Baculites grandis*⁴ zone (lower Maastrichtian). Moreover, the species possibly occurs in the lower Maastrichtian of Madagascar (Walaszczyk et al., 2009: 63). The authors also indicate that in Europe (France, Austria, and the type Maastrichtian area) *C.?* *glendivensis* occurs below the '*Inoceramus*' *ianjonaensis*⁵ zone (= upper Maastrichtian), but the taxon ranges from the upper lower Maastrichtian to the lower upper Maastrichtian in South Africa (*Trochoceras radius* and '*Inoceramus*' *ianjonaensis* zones), however. The latter is consistent with the results observed at Albaina section.

The ammonites *Baculites anceps* Lamarck, 1801 (Figs. 8.17A–G) and *Eubaculites* cf. *vagina* (Forbes, 1846) (Figs. 8.17H–K) are also among the stratigraphically important fossils from Albaina. All specimens occur as internal moulds with septal suture poorly preserved. In the description of the species *Baculites anceps*, Kennedy (1986) says that individuals have a shell straight with ovoid whorl section, rounded dorsum and convex flanks converging to an acute venter. Shell ornament varies from growth striae and reticulate lirae to weak ribs projected towards the venter. Dorsolateral nodes may also be present in some specimens. Three specimens collected from Albaina match the diagnosis of this taxon, including one individual that has the flank ornamented with fine ribs ending in marginal nodes (Fig. 8.17A), and another one with a fine ribbed flank and a very weakly ribbed venter (Figs. 8.17F–G). The taxon *Baculites anceps* is restricted to the lower Maastrichtian in the deep-water Maastrichtian successions of the Biscay Region (Ward and Kennedy, 1993) and the upper Maastrichtian shallow ramp deposits of the Puerto de Olazagutía Formation (Santamaría and López, 1996). This species is an important faunal element of the Maastrichtian with a Western European and former USSR distribution (Kennedy, 1986).

On the other hand, members of the *Eubaculites* genus are characterised by having a compressed pear-shaped section with fastigate or tabulate venter and a flattened dorsum. Some species are smooth but other are laterally ribbed or ornamented with dorsolateral tubercles (Kennedy and Henderson, 1992b; Klinger and Kennedy, 1993). Both the specimens from Albaina (Fig. 8.17D–G) belong to bituberculate forms that have a tabulate to slightly convex dorsum, so they could be referred either to *Eubaculites vagina* (Forbes, 1846) or *E. ootacodensis* (Stoliczka, 1866). They are distinguishable from each other by the shape of the ventral regions, with distinctly fastigate venter in the latter species. For this reason our specimens are referred provisionally to *E. cf. vagina*.

¹ Named after *Endocostea typica* Whitfield, 1877.

² Named after *Trochoceras radius* (Quaas, 1902).

³ Named after *Baculites baculus* Meek and Hayden, 1861.

⁴ Named after *Baculites grandis* Hall and Meek, 1855.

⁵ Named after '*Inoceramus*' *ianjonaensis* Sornay, 1973.

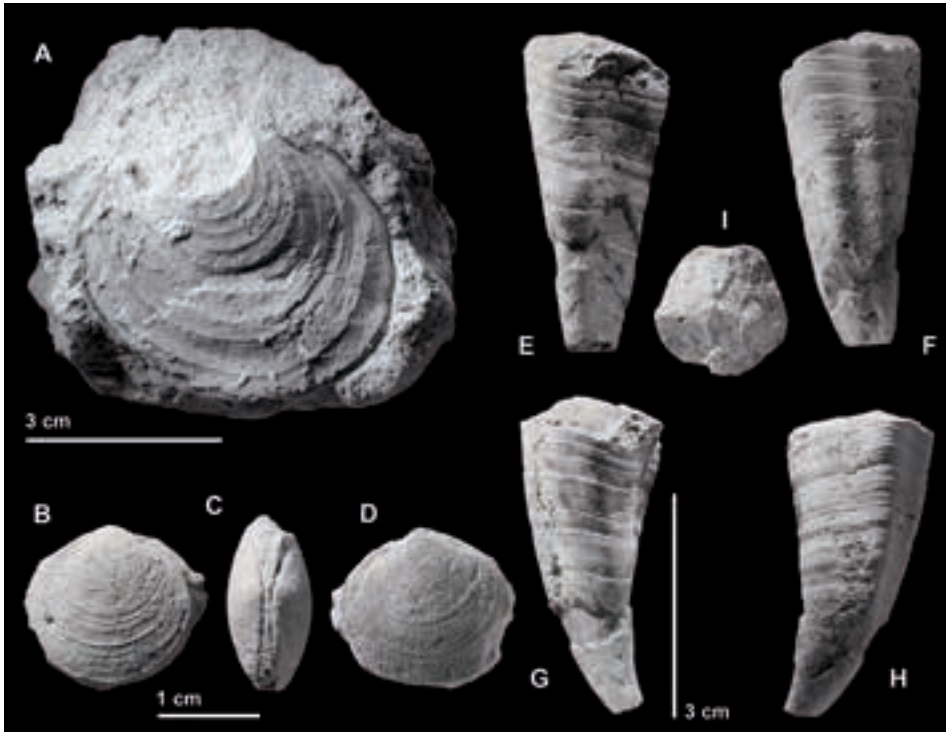
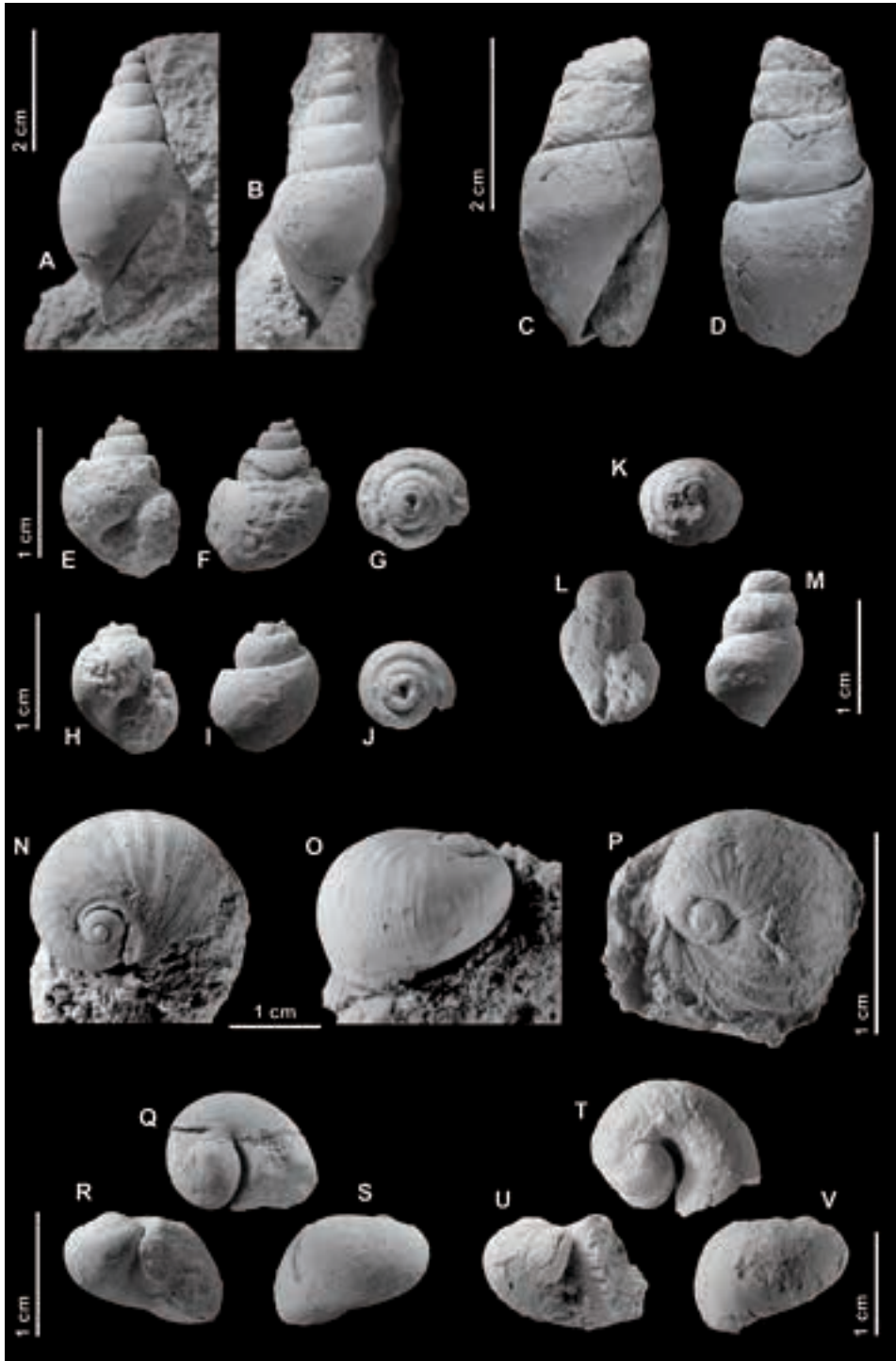
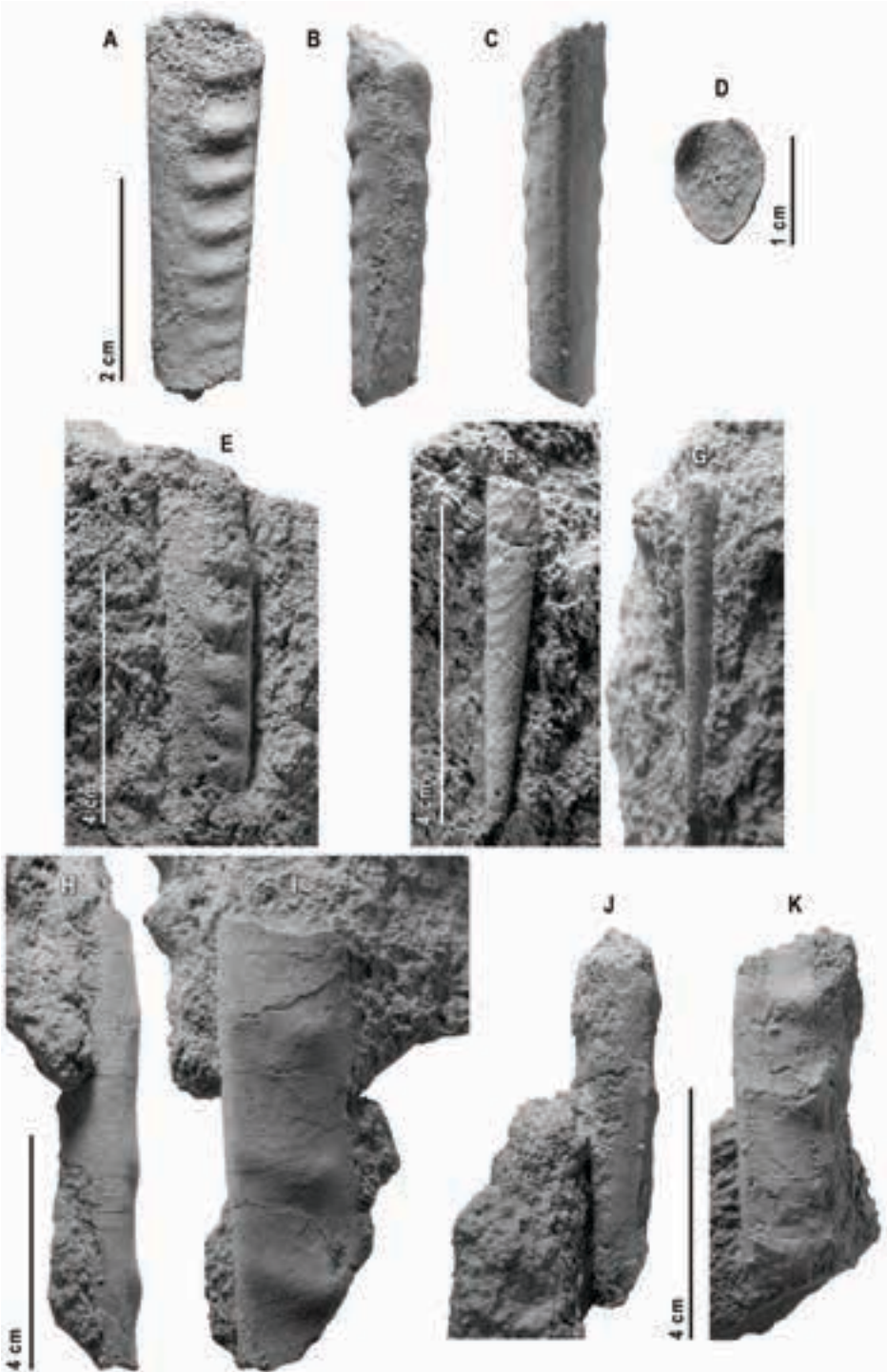


Figure 8.15 Bivalves from the Maastrichtian Torme Formation of Albaina (Treviño County, Burgos). A, *Cataceramus? glendivensis* Walaszcyk, Cobban and Harries, 2001, left valve, MCNA 14243. B–D, Lucinidae genus indet., internal mould of conjoined valves of a veneroid clam, (B) right valve with a gastropod boring on the left-hand side, (C) dorsal view, (D) left valve, MCNA 15417. E–I, Radiolitidae indeterminate, inner cast of the right valve in (E) ventral, (F) dorsal, (G) anterior, (H) posterior, and (I) apertural views, MCNA 14634.

Figure 8.16 Gastropods from the Maastrichtian Torme Formation in Albaina (Treviño County, Burgos). A–D, Rostellariidae (*Rostellaria* sp.), A–B, MCNA 10834, (A) apertural view, (B) side view, C–D, MCNA 14627, (C) apertural view, (D) abapertural view. E–J, Naticidae (cf. *Euspira* sp.), E–G, MCNA 10839, (E) apertural view, (F) abapertural view, (G) apical view; H–J, MCNA 14630, (H) apertural view, (I) abapertural view, (J) apical view. K–M, Volutidae (*Rostellana* sp.), MCNA 14629, (K) apertural view, (L) abapertural view, (M) apical view. N–P, *Ostostoma ponticum* d'Archiac, 1859, MCNA 15034, (N) dorsal view, (O) abapertural view, (P) silicone cast of the external mould in apical side view. Q–V, *Ostostoma retzii* (Nilsson, 1827), Q–S, MCNA 14631, (Q) dorsal view, (R) apertural view, (S) abapertural view; T–V, MCNA 15161, (T) dorsal view, (U) apertural view, (V) abapertural view. ►





According to Kennedy (1986), *Baculites anceps* Lamarck, 1801 ranges into the upper Maastrichtian (*Menuites fresvillensis*¹ zone). Numerous specimens of *E. vagina* (Forbes, 1846) occur in the Valudavur Formation (Pondicherry, southeast India) from beds probably belonging to the lower part of the *A. mayaroensis* zone of the upper Maastrichtian (Kennedy and Henderson, 1992a). Similarly, other species in the genus *Eubaculites* have been reported nearby in the coastal outcrops of the Biscay Region (France and Spain), specially the species *Eubaculites carinatus* (Morton, 1834) from Hendaye and Bidart (France), which seems also to be confined to the upper Maastrichtian *A. mayaroensis* zone (Ward and Kennedy, 1993). In this way, the ammonite taxa recorded from Albaina would confirm a late Maastrichtian age for the middle calcarenitic subunit (LF-II) of the TF. Moreover, the cooccurrence of the ammonite *Baculites anceps* and the gastropods *Otostoma* spp. also indicates a late Maastrichtian age.

Complete echinoids are rare at Albaina site and only the figured specimen has been found so far (Fig. 8.18). This specimen is a poorly preserved internal cast (the external calcite test has been dissolved), but the overall shape allows one to confidently assign the specimen to *H. striatoradiatus*. It is a juvenile specimen, judged from its size, with an oval test slightly larger than wide, and dome-shaped in lateral view. The remnants of flexed ambulacra, the frontal groove, and a large peristome area are also characteristics of the species. In Spain, this taxon has been recorded from the Maastrichtian in Navarre and probably from similarly aged rocks in Cantabria (Smith et al., 1999). The genus has been previously cited in the type area of the TF in Burgos by Ciry (1939) and the Puerto de Olazagutía Formation in Álava (Corral, 1996), both sites Maastrichtian in age.

The subunit LF-III is fossil-poor but has yielded a fossil callianassid in addition to a few selachian teeth. The discovery of a claw of the callianassid ghost shrimp (Thalassinidea) *Mesostylus faujasi* (Desmarest, 1822) (Fig. 8.19) is illustrative since it provides useful information regarding the depositional setting. Modern species of *Callianassa* possess large calcified chelipeds in accordance with their burrowing lifestyle. They inhabit marine habitats, burrowing in soft substrate of sand and mud, being usually confined within the mesolittoral zone or in very shallow sublittoral muddy sand or pure sandy bottoms to a depth of up to 6 metres (Holthuis, 1991; Ngoc-Ho 2003). The callianassid burrower *Mesostylus faujasi* is the most frequent genus among fossil decapods in the Maastrichtian type area according to Swen et al. (2001), where it occurs associated with other fossil bivalves and ammonite species of the genus *Baculites*.

¹ Named after *Menuites fresvillensis* (Seunes, 1890)

◀ **Figure 8.17** Ammonites from the Maastrichtian Torme Formation in Albaina (Treviño County, Burgos). A–G, *Baculites anceps* Lamarck, 1801; A–D, MCNA 15418, (A) lateral view, (B) dorsal view, (C) ventral view, (D) whorl section; E, MCNA 15156, lateral view; F–G, MCNA 15157, (F) lateral view, (G) ventral view. H–K, *Eubaculites* cf. *vagina* (Forbes, 1846), H–I, MCNA 15031, (H) dorsal view, (I) lateral view; J–K, MCNA 15030, (J) dorsal view, (K) lateral view.

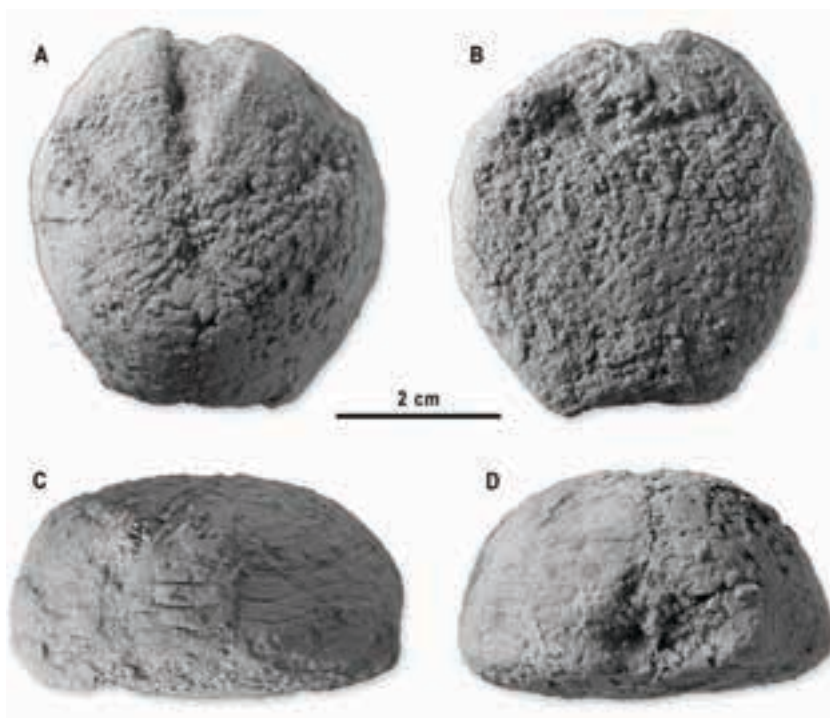


Figure 8.18 *Hemipneustes striatoradiatus* (Leske, 1778), inner cast in apical (A), oral (B), lateral (C), and posterior (D) views, MCNA 15420 from the Torme Formation, Albaina (Treviño County, Burgos).

A late Maastrichtian age is given to the TF in the type area on the basis of orbitoids (Radig, 1963) and macroinvertebrate fauna (Ciry, 1939; Floquet, 1991), but no ammonites were found there. The TF is considered to be upper Maastrichtian on stratigraphical grounds because it comes to represent the T–R cycle DC-13 (Floquet, 1991, 1998; Berreteaga, 2008).

The Albaina mollusc faunule is clearly upper Maastrichtian. Ammonite and inoceramid zones are correlated to the established Maastrichtian planktonic foraminiferal zonation (see Figure 9.7 in Chapter 9). Moreover, the presence of a rich selachian assemblage in the middle calcarenitic subunit (LF-II) also provides a narrow biostratigraphical constraint. The Albaina assemblage contains typical Maastrichtian elasmobranchs [i.e. *Squalicorax pristodontus* (Agassiz, 1843), *Odontaspis bronni* (Agassiz, 1843), *Serratolamna serrata* (Agassiz, 1843), *Plicatoscyllium lehneri* (Leriche, 1938), *Palaeogaleus faujasi* (Geyn, 1937), *Dalpiazia stromeri* Checchia-Rispoli, 1933, *Ganopristis leptodon* Arambourg, 1935, *Coupatanzia fallax* (Arambourg, 1952), *Rhombodus binkhorsti* Dames, 1881, and *Rhombodus andriesi* Noubhani and Cappetta, 1994], which strongly supports a late but not latest Maastrichtian age for the TF in Albaina



Figure 8.19 Callianassidae claw. *Mesostylus faujasi* (Desmarest, 1822), P1 propodus, MCNA 15242 from the Torme Formation, Albaina (Treviño County, Burgos). Scale in mm.

(Cappetta and Corral, 1999). Moreover, the occurrence of *Rhombodus andriesi* is also in favour of an upper Maastrichtian, as established by Noubhani and Cappetta (1994) for the Maastrichtian phosphate deposits of Morocco.

Not far from Albaina site, in the Entzia-Urbsa mountain range in Álava, an ammonite assemblage has been correlated with the upper Maastrichtian (see Chapter 9) and, further to the east, the analogue formation ‘nankin limestones’ from the Petites-Pyrénées (southern France) contains large benthic foraminifera in addition to other macroinvertebrates, as above explained, although ammonites are not common in the formation (Kennedy et al., 1986).

Depositional environment. In addition to lithology, microfacies and fossil content, the presence of channel deposits, large scale cross-bedding lamination and other sedimentary structures suggest a shallow marine inner-ramp environment for the TF in the Albaina area. The nearshore litharenite (LF-I) was deposited in channel systems over the underlying terrigenous deposits as a result of a Maastrichtian marine transgression that flooded a vast transitional (estuarine) sedimentary environment. After an episode of truncation and tilting, sedimentation continued again with a mixed carbonate–siliciclastic depositional sequence deposited above an erosional surface (named IMU). According to Seilacher (1990), phosphatic vertebrate fragments, often abraded and concentrated in clastic strata (bone beds), commonly occur at the beginning of a

transgression. Consequently the basal conglomerate and sandstone lag of lithofacies LF-II would represent a transgressive deposit. After this transgressive pulse the area transformed into an offshore or lower shoreface depositional setting. This was a period of basin deepening where storm wave currents were effective to periodically rework and concentrate carbonate sands and marine biota, although calm conditions occurred over a long enough period to allow clasts' micritization to occur, as observed in thin sections. Moreover, an important amount of silt-size terrigenous grains were supplied from the hinterland. The calcarenite rocks are interpreted to be derived from bioclastic carbonate sand shoals with the accumulation of large benthic foraminifers, echinoids, bivalves, gastropods and ammonites (Figs. 8.15–18), and the removal of carbonate mud through winnowing. The exclusive presence of baculitid ammonites (as above indicated) would indicate an ecologically favourable zone to these straight-shelled cephalopods, but the fact they were drifted by ocean currents after death (i.e. necrotic distribution) cannot be ruled out. The overlaying succession of fine-grained sandstone with ripples (subunit LF-III), which accumulated in a shoreface setting, is the result of a decrease in the subsidence rate of the basin and the progradation of the littoral conditions (a sand shoal deposit). This shallowing-upward sequence represents the transition from subtidal nearshore to an upper shoreface environment. Daily tidal and wave currents were not strong enough to have hindered some crustaceans to live in such sandy environments (Fig. 8.19). The shallowness of the depositional environment reversed upwards into an offshore open platform, where primary precipitates of calcium deposited (Fresnedo Formation). The base of this new depositional sequence occurs as a 'nearly plane erosional surface' with some terrigenous clasts (Floquet, 1991; Pujalte et al., 1993). These very thick massive beds of pink-whitish diagenetic dolomicrite with foraminifer ghosts (Baceta, 1996) are easily recognised in the field because they resembled a ruined landscape as result of the weathering (Fig. 8.5). The age of the Fresnedo Formation, named '*Calcaires de San Miguel*' by Mangin (1955), has been traditionally established as Danian on the basis of regional correlation.

Cycle framework. The Torme Formation (TF) was deposited during T–R cycle DC-13 of Floquet (1998). It is bounded below by a major intra-Maastrichtian unconformity (IMU boundary: Baceta, 1996; Baceta et al., 1999), which is best shown in the western pit of the Albaina/Laño quarry (Albaina site) (see Fig. 8.6). In the transgressive phase of the DC-13 cycle, incised valleys were drowned and filled by a marine-influenced sandy deposit, mainly accumulated at a shallow depth, marginal marine system (Pujalte et al., 1993; Berreteaga, 2008). These beds are much thinner or absent in the western pit (Albaina site) but when present they connect to yellow microvertebrate-rich calcarenites containing vertebrate skeletal remains and other marine fossils by means of a lag that occasionally includes vertebrate remains.

The presence of planar cross-bedded and ripple-bedded sandstone beds (lithofacies LT-III) corresponds to the regressive phase of the T–R cycle DC-13. Such stage is recorded by wave-influenced sandstone strata that display planar and ripple lami-

nation. The sequence is truncated at the top by an erosion surface, which marks the boundary to the overlying Fresnedo Formation. This lithological unit, mainly made of dolomitised carbonate, is bounded below by a conglomerate layer, representing the transgressive phase of T–R cycle DC-14 *sensu* Floquet (1998).

Stratigraphical relationships and correlations. The major lithostratigraphical divisions for the Maastrichtian in the study area are shown in Figure 7.7 (in Chapter 7). The TF in Albaina-Laño also shows the three-fold division observed in the type area (terrigenous, carbonate, and terrigenous facies again), but in the Laño area this unit unconformably overlies both the Sobrepeña and Sedano formations, as a result of uplift and tilting of the sedimentary area, coupled with a regional sea transgression. As indicated by Floquet (1991) and corroborated by personal observations, the TF is stratigraphically correlated northeastward with the Puerto de Olazagutía Formation (designated by Amiot, 1982), which is characterised by coarse-grained bioclastic grainstone–packstone limestone strata interbedded with fossiliferous sandy marl beds that were deposited on an outer marine ramp. This fact has been confirmed on the basis of showing both macrofaunal (Ciry, 1939; Santamaría and López, 1996) and microfaunal similarities (Ciry, 1939; Radig, 1963; Ramírez del Pozo, 1971).

8.4 Taphonomic features of the selachian deposit

Elasmobranch teeth are hard skeletal elements, made up of phosphatic mineral, that are joined by cartilaginous tissue to upper and lower jaws (palatoquadrate and Meckel's cartilage respectively). As previously discussed (Chapter 3), the selachian dentition is continuously renewed throughout the life of the individual, as teeth are worn or broken during feeding. Thus, teeth are continuously scattered on the sea bottom, being exposed to sedimentological processes of a marine environment. Teeth also suffer disarticulation after the death of the individual by biochemical tissues breakdown, being incorporated to the sediment.

The large number of teeth found in the subunit LF-II, in relation to both the whole marine sequence of Albaina-Laño quarry and other Maastrichtian deposits of the Miranda-Treviño Syncline, allows us to think that a concentration process occurred. Due to their phosphatic nature both teeth and other fish remains are denser than sedimentary lithoclasts, and hence in the course of time they were gathered by storm and strong tidal currents on the sea bottom. This accumulation seems to be a stratiform concentration deposit (*sensu* Seilacher, 1990).

The fact that teeth with a pristine conservation are accumulated in the same layer together with other ones showing evident signs of abrasion, such as physical grinding-polishing and surface detail lost, suggests that the latter have remained in a nearshore energetic environment for a long time before being definitely buried.

The abrasion features are evidenced by roundness in the cusp edges of teeth (cutting edges) and by the different stage of erosion in the root lobes (made up of osteodentine),

which eventually can lead to a completely worn out root. In some cases, by example, the teeth of the myliobatoid ray *Rhombodus* are so highly eroded that few characters remain to identify them. Only the phosphatic nature and microstructure differentiate them from lithoclasts. Some teeth also are broken off with matrix-filled cracks. This is due to differential matrix-tooth behaviour during mechanical compaction in the early stages of diagenesis.

A different kind of abrasion is noticeable at the apex of some well preserved teeth. This part of the cusp may be splintered with sharp edges, while other times it is smooth-rounded with inner less mineralised tissue arising in both cases. These characteristic features may have happened by worn use or were due to tooth damage during feeding.

Chapter 9
STRATIGRAPHY AND PALAEOLOGY
OF THE UPPER MAASTRICHTIAN ENTZIA BEDS (URBASA, ÁLAVA)

9.1 Introduction

The Entzia profile provides one of the best exposed Maastrichtian successions deposited in a shallow ramp environment in the southern part of the Basque-Cantabrian Basin (B-CB). The rock exposures contain a rich assemblage of macroinvertebrates dominated primarily by echinoids, oysters and ammonites, although occasionally selachian teeth are found. This part of the basin has been extensively studied by López (1993a, 1993b, 1996) and Santamaría and López (1996). Numerous species of bivalves and ammonites were reported as a result of that research, which allowed the subdivision of the depositional sequence. But while the lower part of the Maastrichtian was tentatively recognised in the area, the upper Maastrichtian strata are well distinguished by its richer content of fossil macroinvertebrates, including the zonal ammonites *Menuites fresvillensis* (Seunes, 1890) in association with *Pachydiscus jacquoti* Seunes, 1890, *Pseudophyllites indra* (Forbes, 1846), *Hoploscaphites constrictus* (Sowerby, 1818), and *Baculites anceps* Lamarck, 1801 (see Santamaría and López, 1996).

9.2 Location and geological setting

These outcrops are located nearby the villages of Vicuña (Entzia-I site) and Andoin (Entzia-II site), southeast of Salvatierra-Agurain (Álava province), in the northern slopes of the Urbasa Mountain Range¹ (Fig. 9.1). This range is, from the geological point of view, a syncline occupying the central sector of the Navarre-Cantabrian Ramp domain. Natural outcrops and man-made exposures (road cuttings) have yielded an almost continuous sequence through the Maastrichtian and Paleocene, which is exposed running parallel along the foothills of the mountain range (Fig. 9.2).

¹ Often referred to as Entzia Mountain Range in the Álava province.

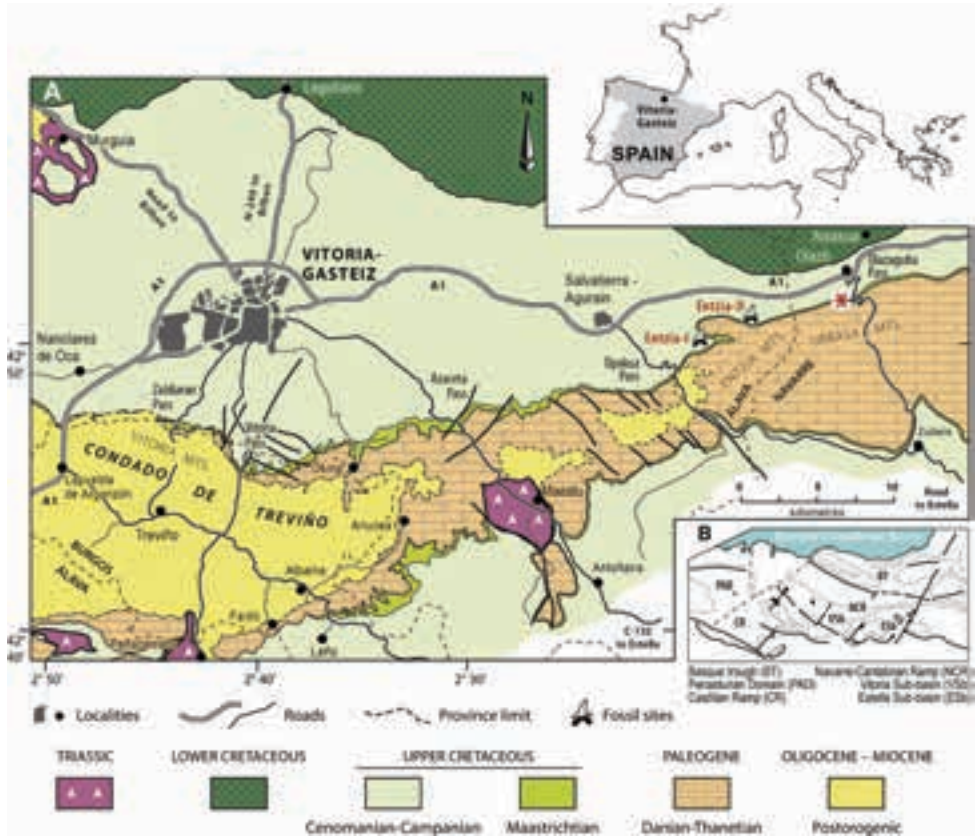


Figure 9.1 Geological sketch map of the study area. (A) Geographical and geological details and location of the fossil sites. (B) Palaeogeographical domains in the Basque-Cantabrian Basin. The asterisk marks the type section of the Puerto de Olazagutía Formation.

9.3 Stratigraphy

The Maastrichtian depositional episode (over 100 m-thick) of the Puerto de Olazagutía Formation (POF), described below, expands the information given in Corral (1996).

Puerto de Olazagutía Formation (POF)

Original author. The formation was named by Amiot (1982: 109). Ruiz de Gaona (1943) first described the section and noticed its interesting micropalaeontological content, especially in orbitoidid Foraminifera. Ramírez del Pozo (1971) provided a list of the microfossils found in the same exposures.

Type locality. The type section is located on the northern flank of the Urbasa plateau south of Olazti-Olazagutía (Navarre). It is exposed along the Puerto de Olazagutía pass, a heavily forested road that cut the Urbasa Mountains.

Boundaries. At the type area, the lower boundary of the POF rests unconformable on



Figure 9.2 Exposures of the uppermost Cretaceous and Paleogene strata outcropping at the Vicuña locality (Entzia Mountains, Álava) looking northeast. POF: Puerto de Olazagutía Formation; DC12–DC14: depositional cycles after Floquet (1998).

the marine marlstones of the Vitoria Formation (western Navarre), but on the upper Campanian sandstones of the Montes de Vitoria Formation in the westernmost part (eastern Álava). Possibly, the formation is disconformably succeeded in all its extension by Tertiary dolostones. The unconformable lower boundary of the formation, which is recognised at regional scale, is placed in the lower–upper Maastrichtian according to Baceta (1996) and López-Horgue et al. (1996). However, the occurrence of some lower Maastrichtian invertebrate macrofossils in the nearby Vicuña beds (Santamaría and Lopez, 1996) seems to question this dating.

Thickness. According to Ramírez del Pozo (1971) the POF shows a maximum thickness of 190 m in the type area, but the total thickness is lowered to 150 m by López-Horgue et al. (1996). In either case, the thickness of the unit is gradually decreasing westward, reaching 90–95 m in the Berrostequieta section (or Zaldiaran Pass exposures) (Ramírez del Pozo, 1971; Martín Alafont et al., 1978).

Lithology. The POF mainly consists of alternating marl–limestone beds. The sequence includes basal bioclastic calcarenite beds (packstone, grainstone, and rudstone textures), fossiliferous bioturbated marls with calcarenite interbeds (textures mudstone/wackestone), and finally a younger unit of marls, marly limestones with orbitoidid foraminifera, and indurated calcareous silt–sandstones (López-Horgue et al., 1996, and own observations in the Álava outcrops) (Fig. 9.3).

Palaeontological content and age. When Ramírez del Pozo (1971) and López-Horgue et al. (1996) described the section at its type locality gave a list of dating benthic macro-

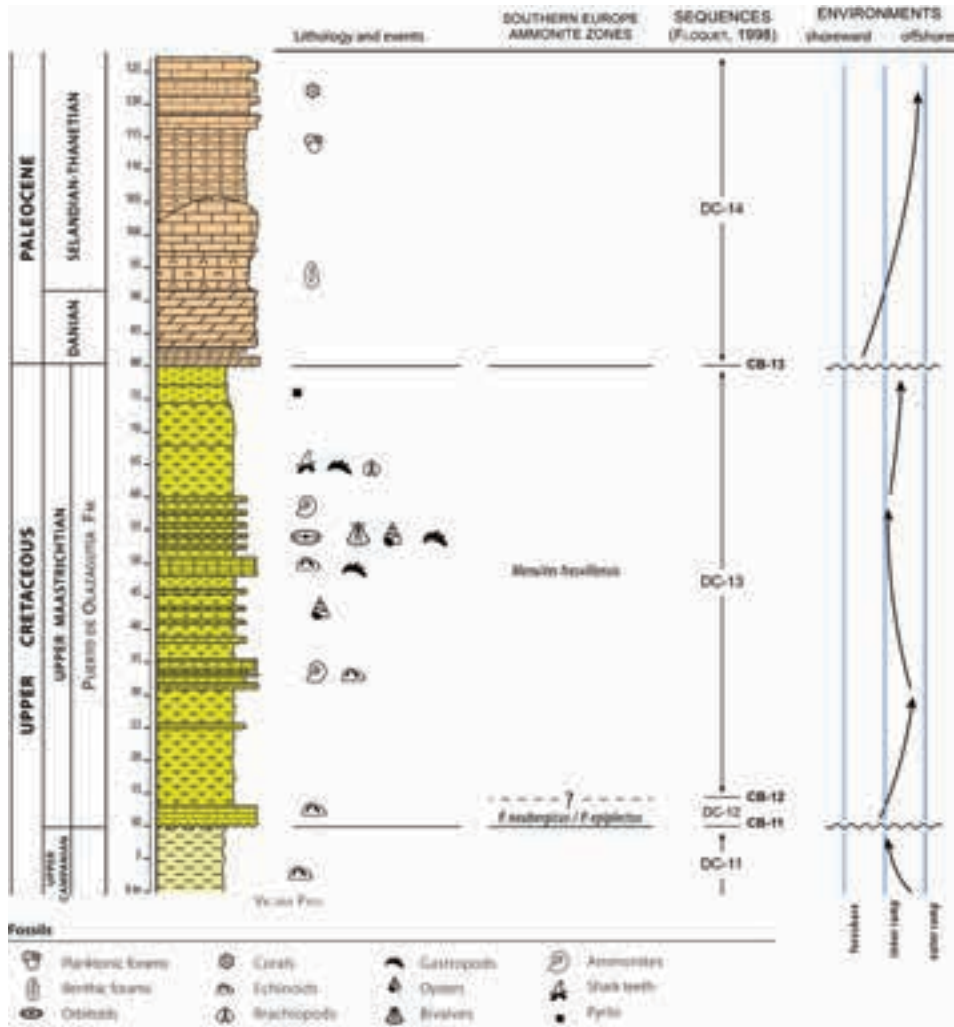


Figure 9.3 Stratigraphical column of the Entzia-1 section showing lithostratigraphical units, ages, fossil content and characteristic lithologies. CB, cycle boundary; DC, depositional cycle.

foraminifera and planktonic foraminifera. The latter authors assigned a late Maastrichtian age to the unit, stating that there is a substantial hiatus spanning the upper Campanian and lower Maastrichtian. López (1993a, 1993b, 1996) and Santamaría and López (1994, 1996), whose systematic and biostratigraphical research focused on the Upper Cretaceous in Álava and Navarre, inferred the presence of the lower and upper Maastrichtian on the basis of the ammonoids and inoceramids collected along the Entzia exposures (Fig. 9.2). Thus, the latter authors reported the presence of *Pachydiscus neubergicus* (von Hauer, 1858) and *Endocostea* aff. *impressus* (d’Orbigny, 1845), which



Figure 9.4 Overview of marlstones and limestones of the Puerto de Olazagutía Formation at the Vicuña locality topped by Paleogene limestones.

would indicate a early Maastrichtian age for the lower part of the formation. The overlying series (Figs. 9.4, 9.5) is similar to that defined in the type section of the POF, consisting largely of alternations of calcarenite and ochre marl that become increasingly terrigenous, with abundant orbitoidid foraminifera and the echinoids including *Hemipneustes pyrenaicus* Hébert, 1875a, *H. striatoradiatus* (Leske, 1778) and *Conulus gigas* (Cotteau, in Leymerie and Cotteau, 1856). Overall, these beds are highly fossiliferous having other marine neritic macroinvertebrates such as cidaroid spines, bivalves, gastropods, and ammonites (Fig. 9.6). In sum, the upper Maastrichtian fossil assemblage is characterised by the occurrence of the ammonoids *Menuites fresvillensis* (Seunes, 1890), *Pseudophyllites indra* (Forbes, 1846), *Hoploscaphites constrictus* (Sowerby, 1818) and *Baculites anceps* Lamarck, 1801, the bivalves *Agerostrea ungulata* (von Schlotheim, 1813), *Rastellum (F.) macropterum* (Sowerby, 1825), *Neithea (Neithea) striatocostata* (Goldfuss, 1836), *Exogyra (E.) overwegi* (von Buch, 1852) and *Amphydonte (A.) pyrenaicum* (Leymerie, 1851), and the gastropod *Otostoma retzii* (Nilsson, 1827) (= *Otostoma rugosa*). Finally, the uppermost part of the POF becomes clayey and is poor in macrofossil content.

Lamniform shark teeth of *Squalicorax kaupi* (Agassiz, 1843), *Squalicorax pristodontus* (Agassiz, 1843) and *Carcharias beathi* Case and Cappetta, 1997 are limited to the upper part of formation in the fossil site Entzia-I, which correlate with the “third upper zone” of the Olazagutía Pass section given by Ruiz de Gaona (1943). Selachi-

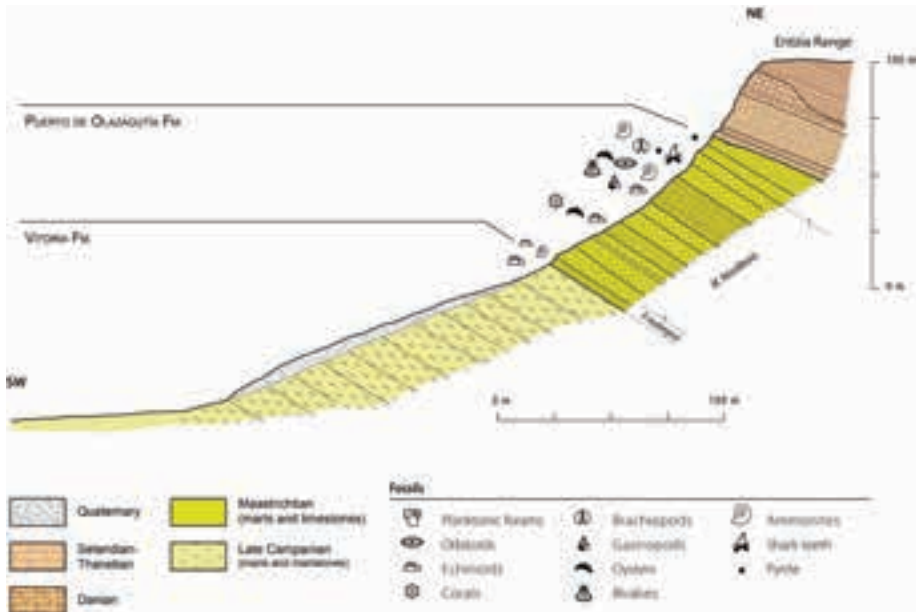


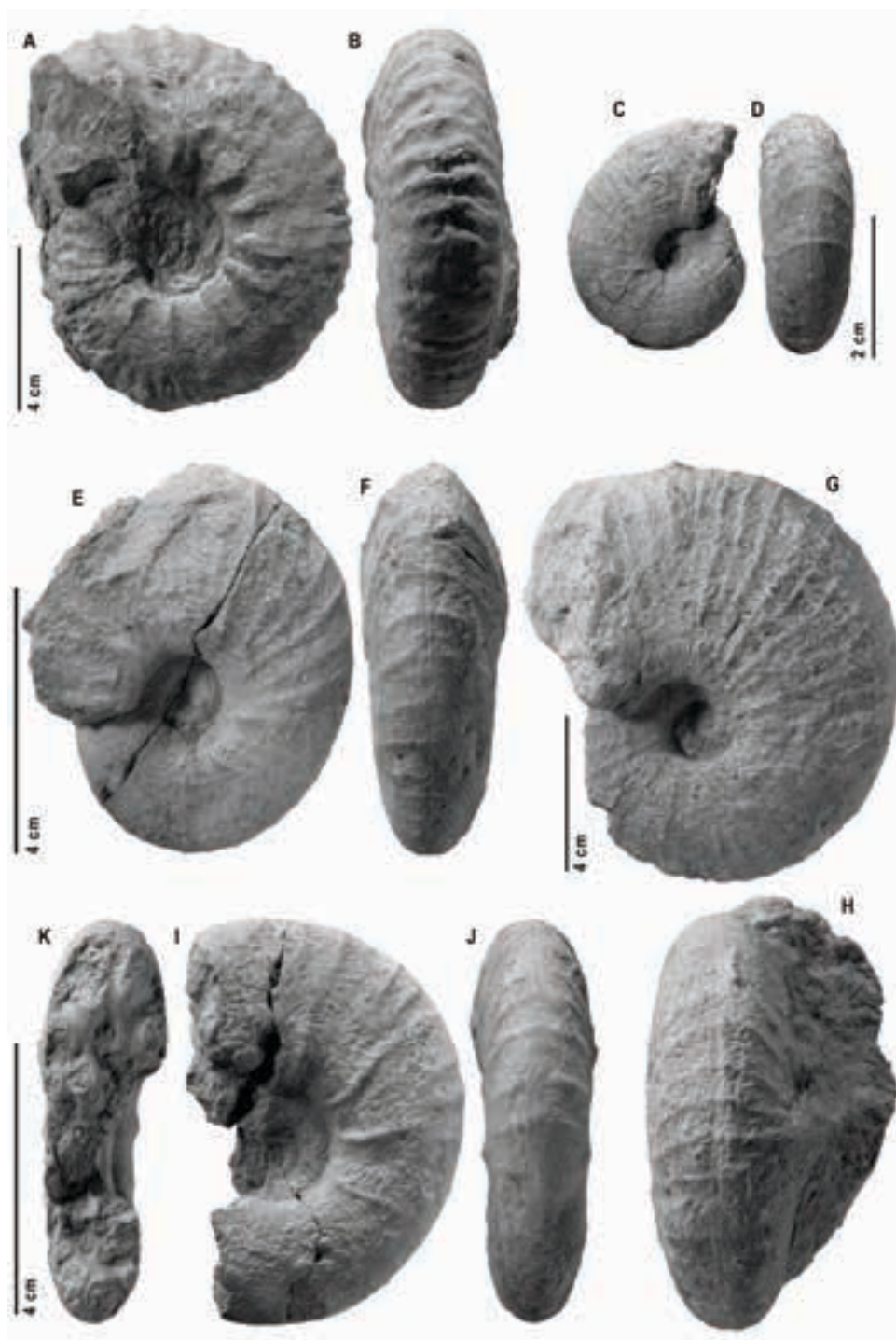
Figure 9.5 Stratigraphical section measured at Vicuña (Entzia-1 site).

ans are associated to spines of the cidaroid sea urchin *Tylocidaris ramondi* (Leymerie, 1851). In contrast, the Entzia-II site has only yielded, so far, a single tooth of *Squalicorax pristodontus*.

Depositional environment. These successions are thought to represent distal marine ramp environments associated with intervals of deeper depositional facies (Amiot, 1982; Wiedmann et al., 1983; López-Horgue et al., 1996).

Stratigraphical relationships and correlations. The principal outcrops of the POF in the province of Álava are in the Entzia Mountains, where the Maastrichtian acquires its maximum development (Fig. 9.5). Westwards, other Maastrichtian outcrops of the Puerto de Olazagutía Formation and the marine Tertiary units are progressively overlapped by a thick cover of Neogene detrital series of the Miranda-Treviño Syn-

Figure 9.6 Ammonites from the Maastrichtian of the Puerto de Olazagutía Formation, Entzia Mountains, southern B-CB. A–B, *Pachydiscus* (*P.*) *neubergicus* (von Hauer, 1858), MCNA 1285; C–H, *Menuites fresvillensis* (Seunes, 1890), (C–D) MCNA 1104, (E–F) MCNA 1262, (G–H), MCNA 1631; I–K, *Pachydiscus* (*P.*) *jacquoti* Seunes, 1890, MCNA 5291; L–N, *Pseudophyllitesindra* (Forbes, 1846), MCNA 1103; O–P, *Saghalinites?* sp., distorted steinkern, MCNA 1953; Q–T, *Hoploscaphites constrictus* (Sowerby, 1818), (Q–R) MCNA 1439, (S–T) MCNA 14878; U–Z, *Baculites anceps* Lamarck, 1801, (U–W) MCNA 15422, (X–Z) MCNA 15421. All specimens from Vicuña (Entzia-I site), except the labelled MCNA 14878 (S–T) which is from Andoin (Entzia-II site). ▶



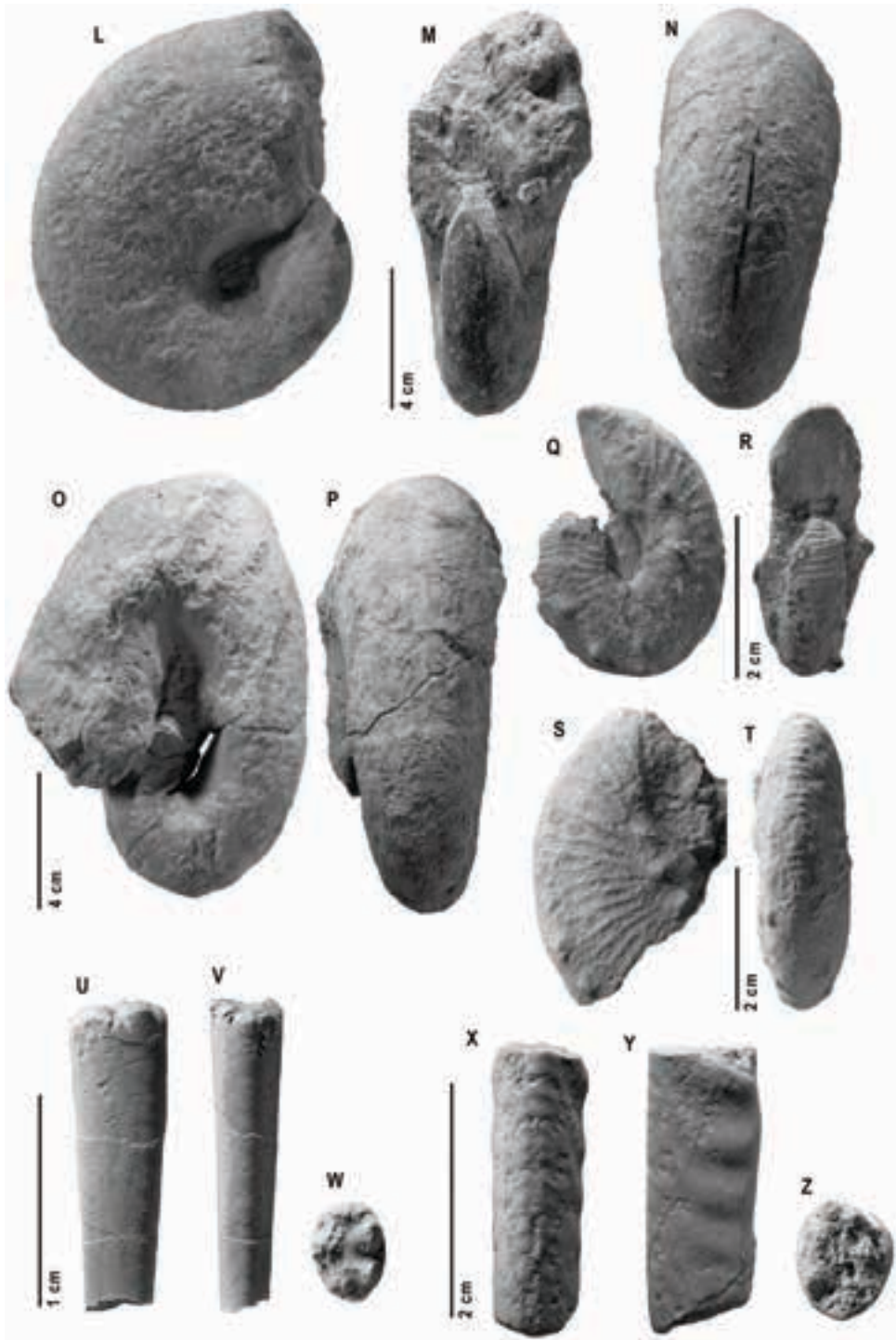


Figure 9.6 (cont.)

cline. Wiedmann et al. (1983) differentiate during the Late Cretaceous times two megasequences (transgressive–regressive) in the area, whose characteristics are outlined as follows:

- i. *Megasequence 3 – regression and compression* (from Coniacian to Campanian). Basal Coniacian strata include biopelsparite rocks, interpreted to record outer ramp sedimentation (Institut des Sciences de la Terre, 1983). Upwards, Campanian facies evinces a clear shallowing-upward depositional trend, with the shallowest environments occurring in the western part of the Vitoria Subbasin, as inferred by the deposition of terrigenous sedimentation, with no sedimentation and erosion episodes. According to Wiedmann et al. (1983), a Gilbert-type delta installed in what we now refer to as Vitoria Mountains, the result of which was the silt and unconsolidated subarkosic sandstone deposits with megaripple structures of the Montes de Vitoria Formation (MVF). A marine-influenced setting is still evident on account of the occurrence of vertical burrows and miliolid benthic foraminifera. Further eastward, in Iturrieta and Entzia mountains, the upper Campanian is lacking of zonal planktonic foraminifera (Alonso, 1986).
- ii. *Megasequence 4 – regression and compression*. Carbonate-dominated strata encompassing this megasequence were deposited from the Maastrichtian through the Palaeocene (Wiedmann et al., 1983). A siliceous-carbonate breccia above an erosional unconformity is recognised on lower Campanian materials in the Opacua pass (Alonso, 1986), and it would mark the base of the sequence.

In general, the upper Maastrichtian would be represented in the Sierra de Entzia (and Urbasa) by marine fossil-rich carbonate beds, which are indicative of protected inner-ramp settings. Active salt tectonics (diapirism) played an important role in the area throughout the Upper Cretaceous. It was an important control in the generation of sediments of the POF, causing also local shallowing and local disturbance in the related series (Wiedmann et al., 1983). The upper part of the series increasingly shows restricted environmental conditions due to the input of terrigenous content. Planktonic foraminifera are scarce, but a concentration of fossil macroinvertebrates, particularly large oysters, occurs. The upper part of the POF formation passes into the Torne Formation to the south of Álava and the westernmost part of the B-CB (see Fig. 7.7 in Chapter 7, and Chapter 8). Eastwards, the unit gradually passes into a succession of basinal facies of the Cía Marls Formation (Amiot, 1982).

9.4 Ammonite biostratigraphy

Deep-water Maastrichtian successions formed by flysch and limestone–marl rhythmites occur along the Bay of Biscay coast in Spain and France (Sopelana, Zumaya, Hendaye and Bidart localities in a West–East direction), many of which are ammonite-rich,

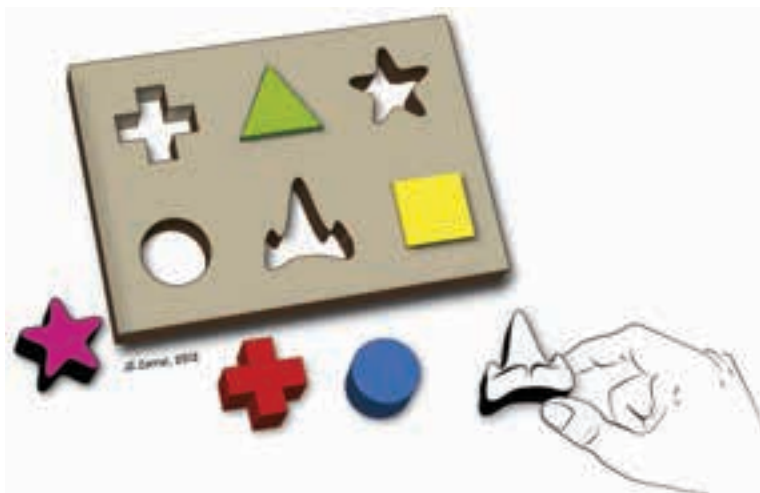
and therefore suitable for detailed zonation. First ammonite zonations were made by Wiedmann (1988a, 1988b) in the context of fossil distribution and mass extinction at the K–Pg boundary event observed at the easily accessible Basque coastal exposures. However, his fivefold subdivision for most of the upper Maastrichtian strata above the *Pachydiscus* (*P.*) *neubergicus* zone was later simplified to a single zone [i.e. *Menuites fresvillensis* (Seunes, 1890)] by Ward and Kennedy (1993) due to problems in fossil identification (Fig. 9.7). Based on their findings (32 species in 21 genera) the latter authors proposed a revised ammonite zonation for the Maastrichtian of Western Europe. This zonal scheme has been kept more or less similarly since then, even in the platform environments of the B–CB where the presence of ammonites is more limited.

As indicated above, López (1993a, 1993b, 1996), and Santamaría and López (1996) documented the Upper Cretaceous invertebrate-rich successions in the southern part of the B–CB, upon which a regional ammonite biostratigraphy was developed for the upper Campanian and Maastrichtian. The Entzia area (Vicuña site) includes one of the best known successions of marl and interbedded limestone strata of the POF in the southern part of the B–CB with ammonites and other mollusc faunas. Here, the lower Maastrichtian was tentatively recognised by the *ex situ* occurrence of the zonal ammonites *Pachydiscus* (*P.*) *neubergicus* (von Hauer, 1858) and the inoceramid *Endocostea* aff. *impressus* (d'Orbigny, 1845) (Santamaría and López, 1996). In contrast, the upper Maastrichtian resulted richer in fossil macroinvertebrates, and included the zonal ammonites *Menuites fresvillensis* (Seunes, 1890) in association with *Pachydiscus* (*P.*) *jacquoti* Seunes, 1890, *Pseudophyllites indra* (Forbes, 1846), *Hoploscaphites constrictus* (Sowerby, 1818) and *Baculites anceps* Lamarck, 1801, cited previously by Santamaría and López (1996). The *Menuites terminus*¹ zone was introduced by Ward and Kennedy (1993) to characterise the youngest part of the Maastrichtian. This index species was initially found at the Hendaye section (France), but later was seen that it also occurred in other sections of the Bay of Biscay together with the diagnostic species *Pachydiscus* (*P.*) *armenicus* Atabekian and Akopian, 1969, and *Pachydiscus* (*P.*) *jacquoti* Seunes, 1890, so the authors confirmed its validity. For the time being, this ammonite zone has not been documented in the carbonate ramp environments of the Entzia–Urbasa sections by previous authors or by our own research.

¹ Named after *Menuites terminus* (Ward and Kennedy, 1993)



NEOSELACHIAN (SHARKS AND RAYS) SYSTEMATICS



Systematics: It's all a matter of sorting out the pieces.

Chapter 10

A ROSTRAL SPINE OF THE SAWFISH *ONCHOSAURUS* (NEOSELACHII, SCLERORHYNCHIDAE) FROM THE BARRIO PANIZARES BEDS (NORTHERN SPAIN), WITH A REVISION OF THE GENUS

10.1 Introduction

Onchosaurus (Batomorphii, Sclerorhynchidae) is an Upper Cretaceous cosmopolitan genus of sawfish-like batoids. The sclerorhynchids are highly modified rays that possess a long snout (rostrum) with hard spines anteroposteriorly fastened to its lateral margins. Such spines are also named rostral teeth. On the contrary to extant pristids, whose rostral teeth are firmly held in socket-like structures and are not replaced when lost (Slaughter and Springer, 1968; Wueringer et al., 2009), representatives of the extinct family Sclerorhynchidae had the spines attached by connective tissue to the lateral margins of the rostrum as in the rostra of pristiphorids (Cappetta, 1987). It seems therefore that this convergent form of tooth attachment allowed sclerorhynchids to continually replace their rostral teeth in essentially the same way as living pristiphorid sawsharks do (Slaughter and Springer, 1968).

Sclerorhynchids, whose phylogenetic relationships will be explained below, are regarded to be bottom-dwellers with similar habitus and benthic lifestyle to that of modern sawfishes (Pristidae). Their armed rostrum could be used either for feeding purposes (namely mud grubbing and prey immobilization) or for self-defence against predators, as extant sawfishes do (Breder, 1952; Wueringer et al., 2009).

A new specimen of *Onchosaurus* from the North Castilian Platform of the B-CB is described here, and then the validity of the so far two nominal species is considered.

10.2 Systematic palaeontology

The systematic position and relationships of sclerorhynchids is a matter for debate. Although Kriwet (2004) and Kriwet and Klug (2012) has proposed the order Sclerorhynchiformes, here the opinion of Cappetta (2012) is followed in retaining Rajiformes (sensu Cappetta 1980a, 1987) as the order for the sclerorhynchid sawfishes.

Class CHONDRICHTHYES Huxley, 1880
 Subclass ELASMOBRANCHII Bonaparte, 1838
 Superorder BATHOMORPHII Cappetta, 1980a
 Infraclass NEOSELACHII Compagno, 1977
 Order RAJIFORMES Berg, 1940
 Suborder SCLERORHYNCHOIDEI Cappetta, 1980a
 Family SCLERORHYNCHIDAE Cappetta, 1974

Genus *ONCHOSAURUS* Gervais, 1852

- 1852 *Onchosaurus* Gervais; 262, figs. 26–27 (original description).
 1852 *Anchosaurus* Gervais; pl. LIX, figs. 26–27 (*lapsus calami*).
 1887a *Titanichthys* Dames; 70 (preoccupied by *Titanichthys* Newberry, 1885, a placoderm).
 1887b *Gigantichthys* Dames; 137.

Type Species. *Onchosaurus radicalis* Gervais, 1852; Campanian of Meudon, near Paris, France, MNHN F-CTE-196 (Fig. 10.4).

Elongated rostral spines having a pointed enameloid cap, whose anterior edge is longer than the posterior one. The peduncle, which is very high and sub-rectangular in basal view, widens proximally. The basal surface of the peduncle is hollow with raised ridges. An anterior furrow and a longer and better developed posterior one undercut the contour of the base. Some furrows and many folds develop at the basal end in the lateral faces. The boundary between enameloid and peduncle is sharply defined (oblique concave to its tip). The emended diagnosis of the genus is provided by (Kriwet and Klug, 2012).

Onchosaurus radicalis Gervais, 1852

Figs. 10.1A–E

- 1852 *Onchosaurus radicalis* Gervais; 262, vol. 1, pl. LIX, figs. 26–27 (original description).
 1908 *Onchosaurus radicalis* Gervais; Priem, p. 61, fig. 24.
 1940 *Onchosaurus radicalis* Gervais; Arambourg, p. 147, pl. 3, fig. 1.
 1951 *Onchosaurus* cf. *radicalis* Gervais; Dunkle, p. 345, fig. 1.
 1989 *Onchosaurus radicalis* Gervais; Lehman, p. 534, fig. 2.
 2006 *Onchosaurus radicalis* Gervais; Spielmann and Lucas, p. 218 (name only).

Material. MCNA 5463, a rostral tooth.

Locality and Horizon. Barrio Panizares, Burgos, Spain; Nidaguila Formation, *Protexanites bourgeoisianus* zone, upper Coniacian, Upper Cretaceous.

Description. The specimen is an incomplete rostral tooth, whose length measures 39.4 mm. It is slightly abraded. The tooth has a slight distal curvature and lacks most of the enameloid cap, but still preserves part of its anterior edge, which forms a sharp keel overhanging the anterior face of the peduncle. The cap is devoid of pointed barbs. The

basal enameloid boundary is sharp and forms a wide arch. The peduncle, which broadens towards its base, is dorsoventrally compressed. It possesses four lateral faces, being both the dorsal/ventral faces approximately flat (Figs. 10.1A–B). The anterior face (Fig. 10.1C) is convex, with a notch at its base, whereas the posterior one is distally flat but mainly concave by the presence of a deep straight furrow (Fig. 10.1D). The dorsal/ventral faces of the peduncle proximally bear a band of weak incisions, measuring approximately 3 mm wide, which is cut by two and four deep furrows respectively (Figs. 10.1A–B). These extend distally halfway the length of the peduncle. On the whole, the basal shape is roughly rectangular (Fig. 10.1E), despite the fact that one of the long sides is slightly convex, and both anterior and posterior sides are indented. The basal face measures 24.6 by 13.1 mm, bearing a marked medial notch which deepens ventrally.

Discussion. The genus *Onchosaurus* is represented so far by the species *O. radicalis* Gervais, 1852 and *O. pharao* (Dames, 1887a). Rostral teeth of the two species are rather similar to such extent, and shared much the same stratigraphical range, that doubts have arisen over the validity of the two nominal species (Lehman, 1989; Antunes and Capetta, 2002). However, due to distinctive morphological features, as indicated below, it is considered wise to keep both species *O. radicalis* and *O. pharao* as valid (Fig. 10.2).

Described rostral teeth of *O. radicalis* are usually smaller than those of *O. pharao*, although this may not be a valid character in fossil sawfish-like batoids because differences in size would only reflect a different ontogenetic stage of tooth development, as seen in the sclerorhynchid *Onchopristsis numidus* (Slaughter and Springer, 1968). The restoration of a nearly complete specimen of *O. radicalis* figured by Arambourg (1940) would give a tooth length of about 47 mm. This measurement is clearly smaller than

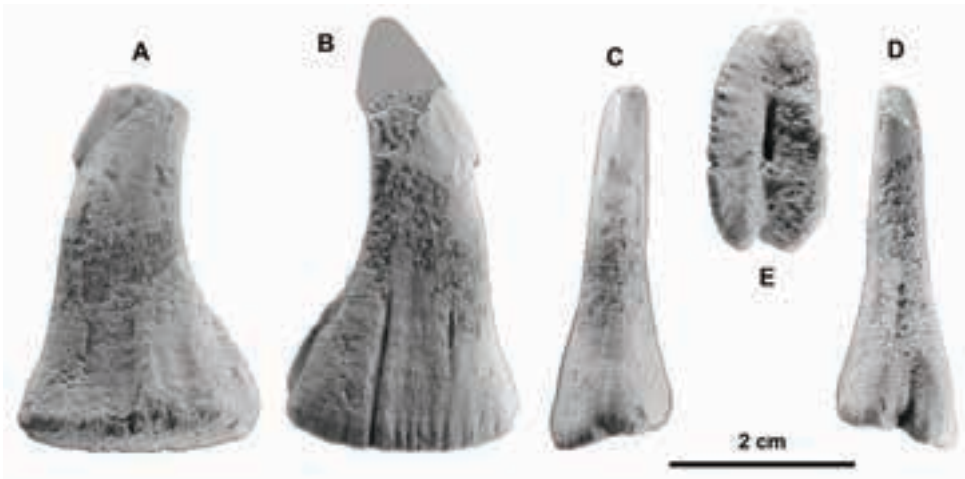


Figure 10.1 A–E, *Onchosaurus radicalis* Gervais, 1852, rostral tooth, Barrio Panizares, Burgos, Spain, MCNA 5463, (A) lateral view, (B) lateral view the putative shape of the cap restored in grey-shade, (C) anterior view, (D) posterior view, (E) basal view.

the average length of *O. pharao* (Cappetta, 1987; Lehman, 1989) but similar to the holotype tooth of *O. radicalis* figured by Gervais (1852).

In general shape, the teeth of *O. radicalis* are more distally curved than those of *O. pharao*. Indeed, both anterior and posterior edges of the peduncle are less curved in *O. pharao* than in *O. radicalis*, whose posterior face is deeply concave. As a result, *O. pharao* has a nearly straight peduncle, quite different from that of *O. radicalis*. The teeth of *O. pharao* are also more dorsoventrally compressed and apparently more robust, comparing to those of *O. radicalis*, which show a slender and longer peduncle root upwards.

Further differences between *O. radicalis* and *O. pharao* are the shape of the enameloid cap in addition to the boundary line between the cap and the peduncle. *Oncho-*

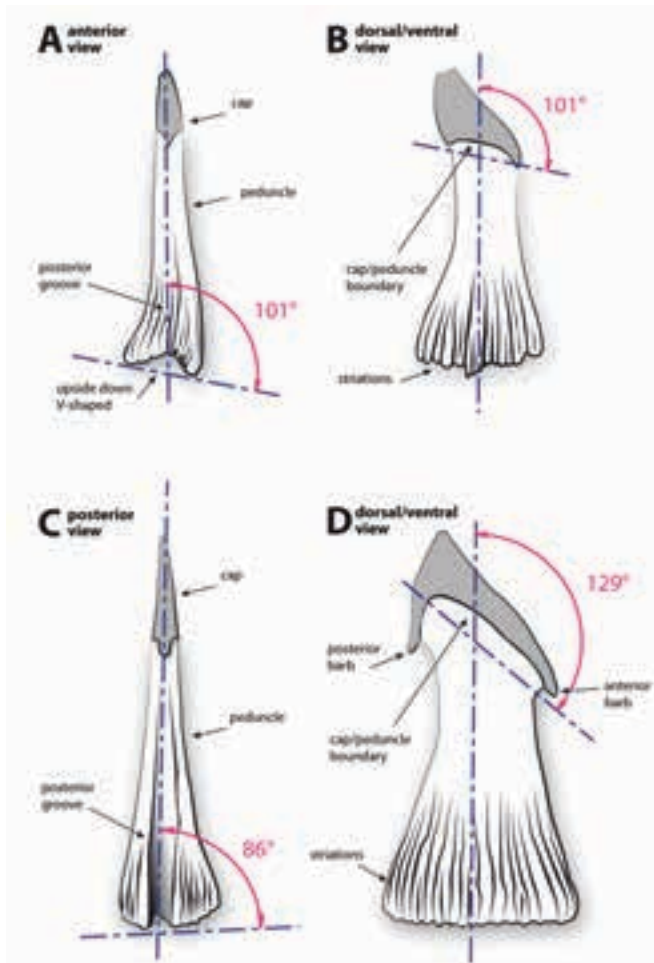


Figure 10.2 Descriptive features and angular measurements in *Onchosarus*. A–B, *Onchosaurus radicalis*; C–D, *Onchosaurus pharao*.

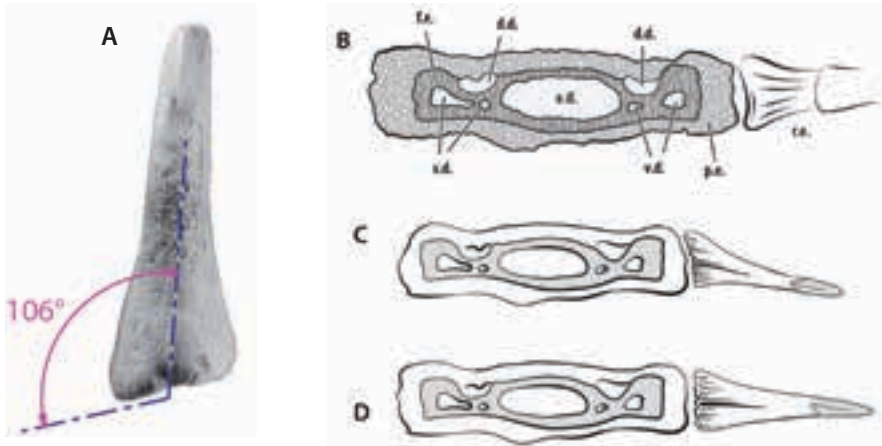


Figure 10.3 A, Attachment angle in the rostral tooth of *Onchosaurus radicalis* from Barrio Panizares, Burgos (MCNA 5463, anterior view); B, transverse cross section through the rostrum of the sclerorhynchid *Onchopristis numidus* (redrawn from Werner, 1989), abbreviations: a.d., axial duct; d.d., dorsal ducts; f.e., cone-shaped fibrous prismatic structure; p.e., irregularly undulating, finely laminated, porous structure; r.e., rostral spine; v.d., ventral ducts; C–D, a hypothesis about the basal attachment of the rostral spines in *Onchosaurus radicalis* (C) and *Onchosaurus pharao* (D).

saurus radicalis presents a rounded triangular cap, whose basal boundary forms a wide arch backwards pointing, whereas in *O. pharao* the basal boundary of the arrowhead cap forms an acute arch also pointing backwards. Moreover, the enameloid cap of *O. pharao* has two narrow barbs pointing downwards, whereas the cap of *O. radicalis* is devoid of barbs or only possesses a blunt or poorly developed anterior boss. In the Barrio Panizares specimen, the enameloid cap is posteriorly rounded and devoid of any barb like the holotype of *O. radicalis*.

Only minor differences can be appreciated with respect to the decoration in the dorsal/ventral surface of the peduncle; both species bear fine longitudinal striations separated by few longer furrows. These crenulations are more irregular at the base of the peduncle in *O. pharao*. On these aspects, the specimen from Spain looks much like *O. radicalis*. Differences also arise in the basal face of the tooth. The basal contour in *O. radicalis* is subrectangular to nearly ovoid, whereas in *O. pharao* it is rectangular. The ratio between the length (L) and width (W) of the basal face is 1.9–2.0 in *O. pharao* and 1.6–1.7 in *O. radicalis*, which produces a longer basal rectangle in the former. The basal section of the Barrio Panizares specimen is roughly ovoid in shape like in *O. radicalis* although much elongated; its L/W ratio being 1.9 is much like in *O. pharao*.

Additionally, another feature that apparently distinguishes the species *O. radicalis* is the inclination of the basal plane with respect to the peduncle plane (Figs. 10.2A, 10.2C, 10.3). This angle is about 101° in the holotype, and therefore it would indicate either an upward or downward flexure in relation to the horizontal plane of the

rostrum or the inclination of the lateral side of the rostrum where teeth are attached. Both planes meet nearly orthogonally (about 86°) in the teeth of *O. pharao*, apart from a single specimen of the species described by Antunes and Cappetta (2002). This angle is about 106° in the Spanish specimen (Fig. 10.3A).

10.3 Redescriptions of the type material of *Onchosaurus*

Onchosaurus is a cosmopolitan genus that is currently only known from rostral teeth (Cappetta, 2006, 2012). The data obtained from fossil findings indicate that the range of the genus is Turonian to upper Campanian. The genus is represented by two valid species as detailed below.

Onchosaurus radicalis Gervais, 1852

The holotype of *Onchosaurus radicalis* (MNHN F-CTE-196) is an isolated rostral tooth from the lower upper Campanian (*Belemnitella mucronata* zone) of Meudon, near Paris (France), that was initially identified as belonging to an animal close to a mosasaurid, but different from *Mosasaurus* and *Leiodon* (Gervais, 1852: 262) (Fig. 10.4). The tooth is 48 mm in length but lacks the apex of the crown (estimated length of 50 mm). The asymmetric enameloid cap is smooth having cutting edges, and is devoid of anterior and posterior pointed barbs. The peduncle is slender, slightly curved posteriorly, having a neck with rounded anterior and posterior faces. Both the dorsal and the ventral faces bear fine folds running halfway the length of the peduncle. The posterior face bears a curved furrow. The basal face is concave and sub-rectangular in contour. There is another specimen with catalogue number MNHN 1891-6 from the Senonian of Chemillé-sur-Indre near Tour (western France) that was first illustrated by Priem (1908) and later by Arambourg (1940, pl. III, fig. 1) as *O. radicalis*. This specimen is 12% longer than the holotype (estimated length of 56 mm) and differs from it by the basal face that is regularly oval in profile. The specimen reported by Dunkle (1951) from the Turonian of Ecuador shows in the anterior edge of the cap that a basal end overhangs the peduncle. Although eroded, this feature may perhaps indicate a bulge or rounded projection. The posterior edge is devoid of any barb.

Onchosaurus radicalis is known from the Turonian to the lower upper Campanian of Europe, North and South America (see Table 16.1, Fig. 16.1 in Chapter 16).

Onchosaurus pharao (Dames, 1887a)

The two syntypes of *Onchosaurus pharao* are isolated rostral teeth from the Santonian that were located 10 km west to the Gizah pyramids in Cairo, Egypt (MB.f.11217a-c and MB.f.11223) (Fig. 10.5). The remains were initially considered fish teeth related to the enchodontid genus *Titanichthys* (Dames, 1887a: 69-70, figs. 1-2), but as *Titanichthys* Newberry, 1885 was preoccupied by a placoderm fish, they were reassigned to

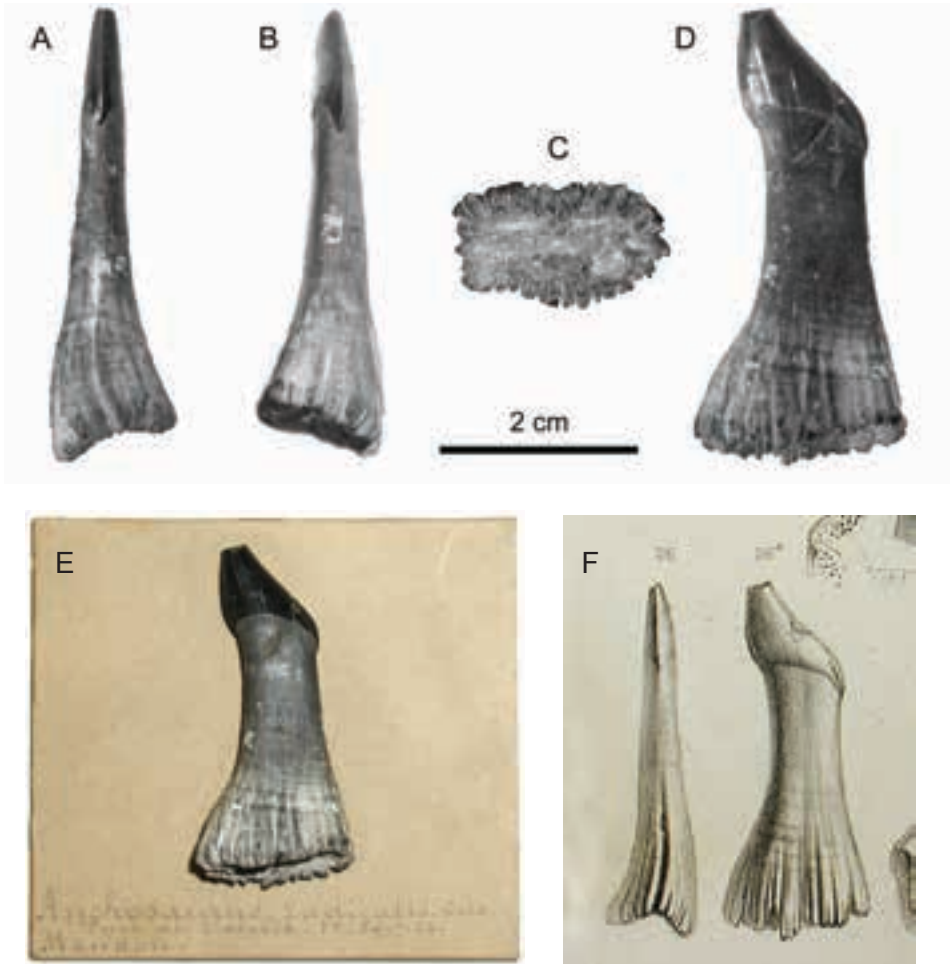


Figure 10.4 *Onchosaurus radicalis* Gervais, 1852, rostral tooth from Meudon, France, holotype MNHN F-CTE-196. A, posterior view, B, anterior view, C, basal view, D, lateral view, E, photograph of the specimen mount, F, reproduction of the original figuration by Gervais, 1852; notice that the posterior view (Fig. 26) is a mirror image of the original. Photographs A–E by Nathalie Bardet.

genus *Gigantichthys* (Dames, 1887b: 137). *Gigantichthys* was then synonymised with *Onchosaurus* (Eastman, 1904; Priem, 1914), an opinion later confirmed by Arambourg (1940). One incomplete syntype is 51 mm high (Fig. 10.5A) and shows as well preserved arrow-shape cap, the other one is 53.5 mm high and only conserves a pointing barb on the anterior edge of the cap (Fig. 10.5B). Both fragments would allow the reconstruction of the entire tooth. The basal enameloid boundary forms a pointed arch on the cap. The peduncle is triangular with nearly straight anterior and posterior edges. Fine longitudinal striations extend to both dorsal and ventral faces in the distal

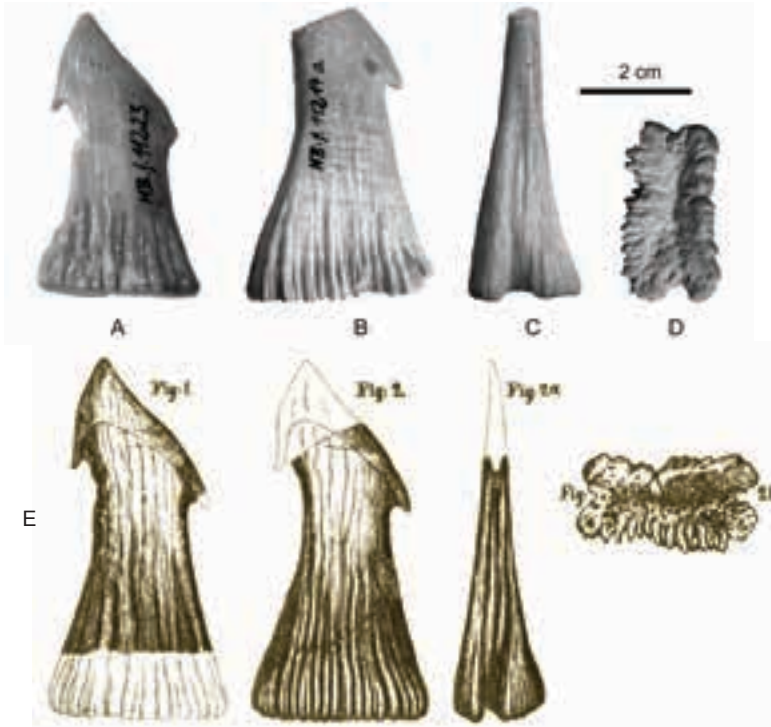


Figure 10.5 *Onchosaurus pharao* (Dames, 1887a), rostral teeth from the Santonian of Gizah, Egypt. A, lateral view of syntype MB.f.11223; B–D, lateral, posterior and basal views of syntype MB.f.11217; E, original figuration of the specimens by Dames (1887a). A–D, photographs by Florian Witzmann.

end. The characteristic notch in the posterior face is larger and straight in this taxon (Fig. 10.5C). The basal face (measuring 32 mm long by 17 mm wide) is rectangular in contour, with a long depression medially placed. Though the restored specimen from Egypt would be 65.5 mm high, some specimens from Texas referred to *O. pharao* might have reached up to 90 mm (Lehman, 1989).

The taxon *Ischyrbiza iwakiensis* Uyeno and Hasegawa, 1986, which was erected for an incomplete rostral tooth from the lower Santonian of Iwaki (Fukushima Prefecture, Japan), is considered as a junior synonym of *Onchosaurus pharao*, according to Cappetta (2006), because of its general appearance and especially its peduncle shape. The species *Onchosaurus pharao* is known from the Turonian to the middle Campanian of South America and North America, Africa, Middle-East, and Western Asia (see occurrences in Antunes and Cappetta, 2002; also Table 16.1 and Fig. 16.1 in Chapter 16).



Chapter 11 NEOSELACHIANS FROM THE GOMETXA SITE (GOMECHA MEMBER, UPPER CAMPANIAN)

11.1 Introduction

The present chapter gives the systematic description of some isolated selachian teeth collected at an abandoned limestone quarry on the western slope of Peña Eskibel, near the locality of Gometxa (Vitoria-Gasteiz, Álava). This Campanian fossil site (dated with planktonic foraminifera) has yielded the most diverse selachian fauna in the Iberian Peninsula known to date from beds of this age, and have a significant place among other important sites in Western Europe. The specimens have been collected by surface prospecting of the marly (lithofacies-1) and calcarenite (lithofacies-2) sub-units that occur in the Gomecha Member. Moreover, for this study approximately 35 kg of matrix from the marly subunit was bulk sampled for wet-screening (see details in Chapter 2).

Despite the long known existence of selachian remains in the Campanian deposits of the Vitoria Sub-basin (Navarre-Cantabrian Domain of the B-CB), this is the first comprehensive study of the group, which includes specimens large enough to be seen by the naked eye in addition to microselachian teeth. Non-dental remains (mainly placoid scales) were not considered here, and would be examined in future research. The fossils here described are curated at the Arabako Natur Zientzien Museoa/Museo de Ciencias Naturales de Álava (MCNA) and the Luberri-Oiartzungo Ikasgune Geologiko Museoa (OIGM).

11.2 Systematic palaeontology

- Class CHONDRICHTHYES Huxley, 1880
- Subclass ELASMOBRANCHII Bonaparte, 1838
- Cohort EUSELACHII Hay, 1902
- Subcohort NEOSELACHII Compagno, 1977
- Superorder GALEOMORPHII Compagno, 1973

Order LAMNIFORMES Berg, 1958
 Family ANACORACIDAE Casier, 1947
 Genus *SQUALICORAX* Whitley, 1939

Type species. *Corax pristodontus* Agassiz, 1843; Maastrichtian of Maastricht, Netherlands.

Squalicorax ex gr. *kaupi* (Agassiz, 1843)
 Fig. 11.1

For the synonymy see Cappetta and Case (1975b), Siverson (1992), Antunes and Cappetta (2002), and Vullo (2005).

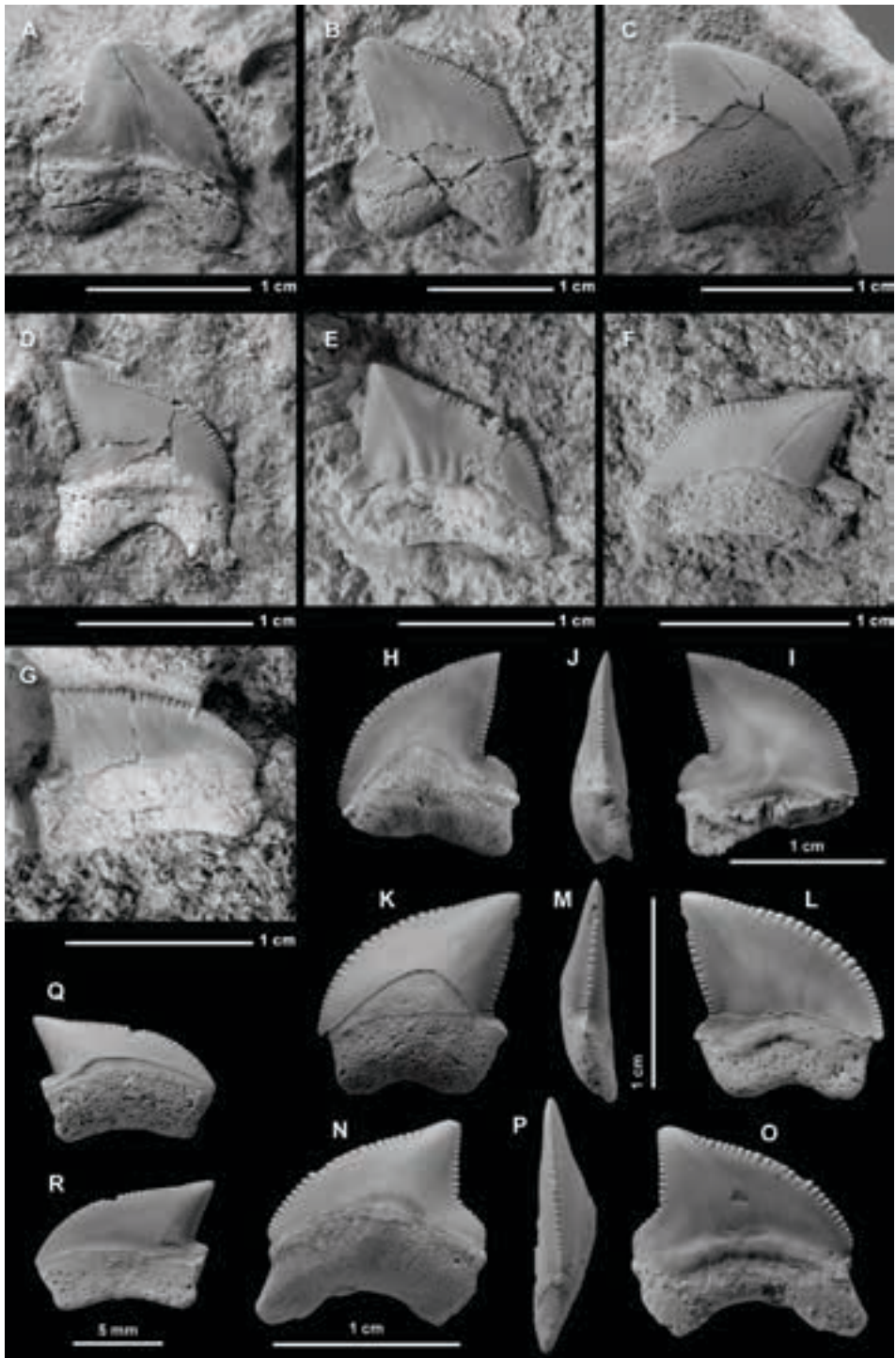
Material. Fifteen teeth, MCNA 10496, MCNA 10498, MCNA 10500, MCNA 14666, and three other catalogued specimens from lithofacies-1; OIGM-GM11, MCNA 5452, MCNA 5658, MCNA 5659, MCNA 6493, MCNA 14665, MCNA 15160, and another catalogued specimen from lithofacies-2.

Locality. Gometxa in Vitoria-Gasteiz municipality, Álava (Basque Country, Spain).

Age. Lower upper Campanian (*G. aegyptiaca* zone).

Description. Typically of small to medium size; the teeth of this species barely exceed one centimetre in width. Much of the crown is formed by a broad pointed triangular, acute cusp that progressively inclines downward in lateral and posterior teeth. The labial face is flat to slightly convex, whereas the lingual face is convex. Both faces are smooth, except in one specimen, where a few folds occur on the basal one-third of the labial face (Fig. 11.1E). The mesial cutting edge of the crown is convex. The distal edge is shorter, sub-vertical with a more or less developed notch that produces a small, convex distal blade. Both edges of the crown are crenate (round-toothed), with denticles decreasing in size toward both the base and apex. The distal blade is also crenate. The teeth usually present constrictions at the base of the crown on both mesial and distal margins. The crown–root boundary is marked by a wide V-shaped band (collar) on the lingual face, whereas on the labial face there is a bulge (cingulum) that overhangs the root. Several nutritive foramina may occur under the labial bulge. The root is basally compressed and higher on the lingual face, with a shallow basal notch in labial/lingual view, which separates two round-ended lobes. One or two nutritive foramina are present on the lingual protuberance. The specimen MCNA 5659 (Fig. 11.1A), which corresponds to a lateral tooth, has a crown lacking a clear distal blade. The distal edge

Figure 11.1 *Squalicorax* ex gr. *kaupi* (Agassiz, 1843). A, lateral tooth in labial view, MCNA 5659; B, lateral tooth in labial view, MCNA 5658; C, lateral tooth in lingual view, MCNA 6493; D, lateral tooth in labial view, MCNA 5452; E, lateral tooth in labial view, MCNA 14665; F, lateral tooth from a posterior position in lingual view, OIGM-GM11; G, lateral tooth from a posterior position in labial view, MCNA 15160; H–J, anterolateral tooth in lingual (H), labial (I), and distal (J) views, MCNA 10500; K–M, anterolateral tooth in lingual (K), labial (L), and distal (M) views, MCNA 10498; N–P, lateral tooth in lingual (N), labial (O), and mesial (P) views, MCNA 10496; Q–R, anterolateral tooth in lingual (Q) and labial (R) views, MCNA 14666. A–G from lithofacies-2, H–R from lithofacies-1. ▶



of the crown is concave and also crenate from apex to base. The crenate, convex mesial cutting edge is worn but still retains thick denticles on the basal one-third. The crown apex is also damaged by functional use. The crown–root boundary is marked by a bulge, under which several foramina are vaguely observed. The root is broad and low with a wide basal notch between the root lobes. Both ends of the lobes are rounded, but the distal one is more square-edged.

Remarks. When Agassiz erected the species *S. kaupi* in 1843 (as *Corax kaupii* in the original description) he used a series of syntypes from two widely separate Campanian areas, namely the localities Aachen and Haldem in the western part of Germany and a single site in Delaware (USA)¹. These specimens have the distal edge and distal blade of the crown separated by either a slight or a noticeable notch (elsewhere also referred to as indentation), which was a diagnostic feature used to differentiate them from those of the species *S. pristodontus* Agassiz (1843). The species *S. pristodontus* has larger-sized teeth (in comparison to those of *S. kaupi*) with a triangular-shaped crown that lacks the distal blade (or heel) in addition to a characteristic high root², being found in the middle-upper Maastrichtian of Europe, Africa, Asia, and America (see Cappetta, 2012). The anacoracid species *S. lindstromi* (Davis, 1890) and *S. pristodontus-plicatus* (Priem, 1898), occurring in the Campanian of Europe, have similarly shaped teeth. A diagnostic feature in *S. lindstromi* is the mesial edge of the crown, which is noticeably convex and overhangs the root. Moreover, the posterior margin is straight and extends at the base, forming a right angle, or an angle greater than 90°, with the distal and often convex heel. An important characteristic of *S. pristodontus-plicatus* is the presence of strong labial folds on the base of the crown (this feature is barely noticeable in *S. lindstromi*). On the basis of morphological dental characteristics, Davis (1890) noticed that representatives of *S. lindstromi* seemed to occupy an intermediate position between *S. pristodontus* and *S. falcatus*³. However, as he ignored in his discussion the Agassiz's (1843) species *S. kaupi*, it is hard to know his viewpoint with respect to the senior species *S. kaupi*, and in fact, Cappetta (2006) synonymised *S. lindstromi* and *S. pristodontus-plicatus* with *Squalicorax kaupi*. Determining whether they are valid species or merely morphological variations within *S. kaupi*, and hence being considered junior synonyms, is something to be approached anytime in the future after a revision of the related *Squalicorax* species (Siverson et al., 2007).

The Glikman's (1980: 123) phylogenetic relationships of the anacoracids, relying on their morphological dental modifications, have been used to provide a biostratigraphical zonation of the Upper Cretaceous strata in the Russian Platform and the West Siberian Basin. Glikman (1980) and Zhelezko (1988), using *Squalicorax* teeth from the southern Urals region (Mugodzhzar Mountains, northwestern Kazakhstan) and nearby regions

¹ Probably from the fine to medium silty glauconitic Mount Laurel Formation at Delaware (USA), which is very fossiliferous in invertebrates as well as in fish remains (see Lauginiger and Hartstein, 1983).

² See Chapters 13 to 15 for an examination of the Maastrichtian *Squalicorax pristodontus*.

³ The lineage *S. falcatus*–*S. kaupi*–*S. pristodontus* in the Upper Cretaceous was later confirmed by Cappetta (1987).

in Russia, subdivided the Campanian into three successive biozones (from older to younger): *S. kaupi*, *S. lindstromi*, and *S. plicatus* (= *S. pristodontus-plicatus*). Amon et al. (1997), for their part, subdivided the Campanian into three biozones (from older to younger), namely *S. lindstromi*, *S. plicatus*, and *S. ex gr. pristodontus*, considering *S. kaupi* an upper Santonian species. But both schemes need to be cautiously used until the group of *S. kaupi*, to which belong the Gometxa specimens, is revised on the basis of clear taxonomic criteria.

Teeth of the group *S. kaupi* have been reported in many worldwide Campanian and Maastrichtian deposits. The species is known in North America from Alberta, Canada (Beavan, 1995; Beavan and Russell, 1999), Montana (Case, 1978, 1979), Big Horn Basin in Wyoming (Case, 1987), the Atlantic and Gulf coastal plain (Cappetta and Case, 1975b; Lauginiger and Hartstein, 1983; Case and Schwimmer, 1988), and Texas (Welton and Farish, 1993; Schubert et al., 2016, and references therein). In Europe, it occurs in the B-CB in northern Spain (Corral et al., 2004, 2011), the Kristianstad Basin, southern Sweden (Siverson, 1992; Einarsson et al., 2010), the Liege-Limburg Basin at Aachen in Germany (Albers and Weiler, 1964), the Mons Basin in Belgium (Herman, 1973, 1977), the Anglo-Paris Basin (France and the UK) (Leriche, 1902; Guinot et al., 2013, and references therein), Charentes in West France (Vullo, 2005), Tercis-les-Bains in the southwest of France (Cappetta and Odin, 2001), the North German Basin in Hannover, Germany (Schneider and Ladwig, 2013), the Münsterland Cretaceous Basin (Müller, 1989, 2014; Thies and Müller, 1993), and the Urals in Russia and their continuation in northwestern Kazakhstan (i.e. Mugodzhar Hills) (Glikman, 1980; Zhelezko, 1988; Amon et al., 1997). Other localities reported to contain the species are in Israel, in the phosphate-rich chalk of the Menuha Formation (Lewy and Cappetta, 1989), Jordan (Zalmout and Mustafa, 2001), and the Angolan exclave of Cabinda (Antunes and Cappetta, 2002).

Family CRETOXYRHINIDAE Glikman, 1958

Genus *CRETOXYRHINA* Glikman, 1958

Type species. *Oxyrhina mantelli* Agassiz, 1843; from the Chalk Group (Turonian–Coniacian) of Lewes in Sussex (England, UK).

Cretoxyrhina mantelli (Agassiz, 1843)

Fig. 11.2

For the synonymy see Siverson (1992), add Siverson and Lindgren (2005).

Material. One tooth from lithofacies-2, MCNA 10491.

Locality. Gometxa in Vitoria-Gasteiz municipality, Álava (Basque Country, Spain).

Age. Lower upper Campanian (*G. aegyptiaca* zone).

Description. A detailed description of the dentition of *C. mantelli* is given in Eastman

(1895) and Shimada (1997c). The specimen MCNA 10491 corresponds to a lateral tooth of moderate size, with a triangular, distally inclined crown that gradually widens to its base (crown with height similar to width). The labial face of the crown is nearly flat and bears subtle vertical wrinkles in the mid-basal region of the cusp. The lingual face, which is gently convex, is smooth. The cutting edge is continuous and extends to the basis of the crown's edges. Both marginal sides have a wide notch in the enameloid-root boundary. The root is wider than the coronal portion and shows a wide central basal notch in labial/lingual view, separating two divergent branches with round, labiolingually compressed ends.

Remarks. *Cretoxyrhina mantelli* is a cosmopolitan species, whose first appearance is in the upper Albian, while its last known occurrence is in the Campanian (Siverson and Lindgren, 2005). The presence of this species in post-Santonian deposits was confirmed in the following areas: the upper Santonian to lower Campanian Mooreville Chalk in Alabama, USA (Shimada and Hooks, 2004), the Kristianstad Basin in southern Sweden, where it ranges from the uppermost lower Campanian (*Belemnellocamax mammillatus* zone) to lowermost upper Campanian (*Belemnellocamax balsvikensis* zone) according to Siverson (1992), the Liege-Limburg Basin in the Aachen area, Germany (Albers and Weiler, 1964), the Campanian of the Anglo-Paris Basin in the departments of Aisne, Somme, and Marne, northern France (Leriche, 1902), the Mugodzhar Hills (southern Urals) in northwestern Kazakhstan (Glikman, 1980), the Mount Laurel Formation in New Jersey (Cappetta and Case, 1975b), the lower Campanian Smoky Hill Chalk Member of the Niobrara Chalk in Logan County, western Kansas, USA (Siverson and Lindgren, 2005), and the upper Campanian Bearpaw Formation at Dorothy in southern Alberta, Canada (Cook et al., 2017). The presence of *C. mantelli* in Gometxa site confirms the known lowermost upper Campanian disappearance of the species and extends its palaeogeographical distribution southward to the northern margin of the Tethys.



Figure 11.2 *Cretoxyrhina mantelli* (Agassiz, 1843) from lithofacies-2, upper (?) lateral tooth in lingual (A), labial (B), mesial (C), and basal (D), MCNA 10491.

Family MITSUKURINIDAE Jordan, 1898

Genus *ANOMOTODON* Arambourg, 1952

Type species. *Anomotodon plicatus* Arambourg, 1952; from the Maastrichtian of Ouled Abdoun, Morocco.

Anomotodon hermani Siverson, 1992

Figs. 11.3A–L

For the synonymy see Guinot et al. (2013).

Material. Eleven teeth from lithofacies-1, MCNA 3685, MCNA 10507, MCNA 10508, OIGM-GM7, and seven other catalogued specimens.

Locality. Gometxa in Vitoria-Gasteiz municipality, Álava (Basque Country, Spain).

Age. Lower upper Campanian (*G. aegyptiaca* zone).

Description. A recent description of the dentition of this mitsukurinid shark is provided by Guinot et al. (2013) on the basis of a great number of teeth found in the Anglo-Paris Basin (France and the UK). The teeth of this species are medium to large sized. Anterior teeth are tall and erect with a narrowly triangular cusp, sigmoid in profile view, which extends basally along the root branches without forming a real heel (Fig. 11.3C). The continuous cutting edge runs along the anterior and posterior sides, from apex to base. The labial face is slightly convex and smooth with a short vertical bulge flanked by depressions on the medio-basal part of the cusp (Fig. 11.3B). The lingual face is convex and ornamented with sinuous vertical folds (approximately 15 to 17) that extend upwards about two-thirds the length of the cusp (Fig. 11.3A). A distinct lingual furrow (neck) separates the crown and root. The root has two long, convex lobes with round ends. They diverge at an angle of about 80°. There is a marked lingual protuberance with a net nutritive groove. A second specimen (Figs. 11.3D–F) is more asymmetrical, having the main cusp slightly inclined distally, which would indicate that is from an anterolateral position. Another specimen (Figs. 11.3G–I), referred to as an upper lateral tooth, has a wider crown that is compressed labiolingually. The long, triangular cusp is distally inclined. The mesial and distal cutting edges, which are almost straight and convex respectively, reach the lateral root extremities to form lateral heels. The labial face of the cusp is flat and smooth, while the slightly convex lingual face bears approximately 12 faint vertical folds on its basal half. The crown is separated from the root by a furrow on the lingual side. The root is low, sub-rectangular with two divergent branches with slightly rounded marginal edges. The lingual protuberance has a very marked nutritive groove, which contains a large circular foramen. The basal notch is shallow and broad, forming an obtuse angle in lingual/labial view.

Remarks. Contrary to other mitsukurinid sharks, including the extant goblin shark, the genus *Anomotodon* has lateral teeth devoid of lateral cusplets, which indicate that these sharks may have differentiated from a common ancestral form with a *Scapanorhynchus*-type dentition (Cappetta, 2012).

The species *Anomotodon hermani* is currently known in Western Europe. Apart from Havré, province of Hainaut in SW Belgium (the type locality in the Mons Basin) (Herman, 1977), this species has been reported in the Kristianstad Basin, southern Sweden (Siverson, 1992), the Anglo-Paris Basin, France and the UK (Guinot et al., 2013), and the North German Basin, northern Germany (Schneider and Ladwig, 2013). *Anomotodon hermani* ranges from middle Santonian through the Campanian (Guinot et al., 2013). In the Anglo-Paris Basin the youngest occurrence of this species is reported from the lower part of the lower Campanian (in the echinoid *Offaster pilula* zone) (Guinot et al., 2013). According to Herman (1977), in Belgium *A. hermani* ranges from the lower to lowermost upper Campanian (spanning the belemnite *Goniotenthis granulataquadrata* to *Belemnitella mucronata* zones) of the Trivières Chalk Formation, and is less frequently found in the base of the Obourg Chalk Formation (in the *B. mucronata* zone). The presence of *A. hermani* in the Gomecha Member extends southward to North Iberia the previously known geographical distribution of the species and constitutes together with the specimens cited by Herman (1977) its youngest record.

Genus *SCAPANORHYNCHUS* Woodward, 1889

Type species. Rhinognathus lewisii Davis, 1887; Santonian of Sahel Alma, Lebanon.

Scapanorhynchus cf. *texanus* (Roemer, 1849)

Figs. 11.3M–Q

For the synonymy see Cappetta and Case (1975b), add Cappetta and Case (1999).

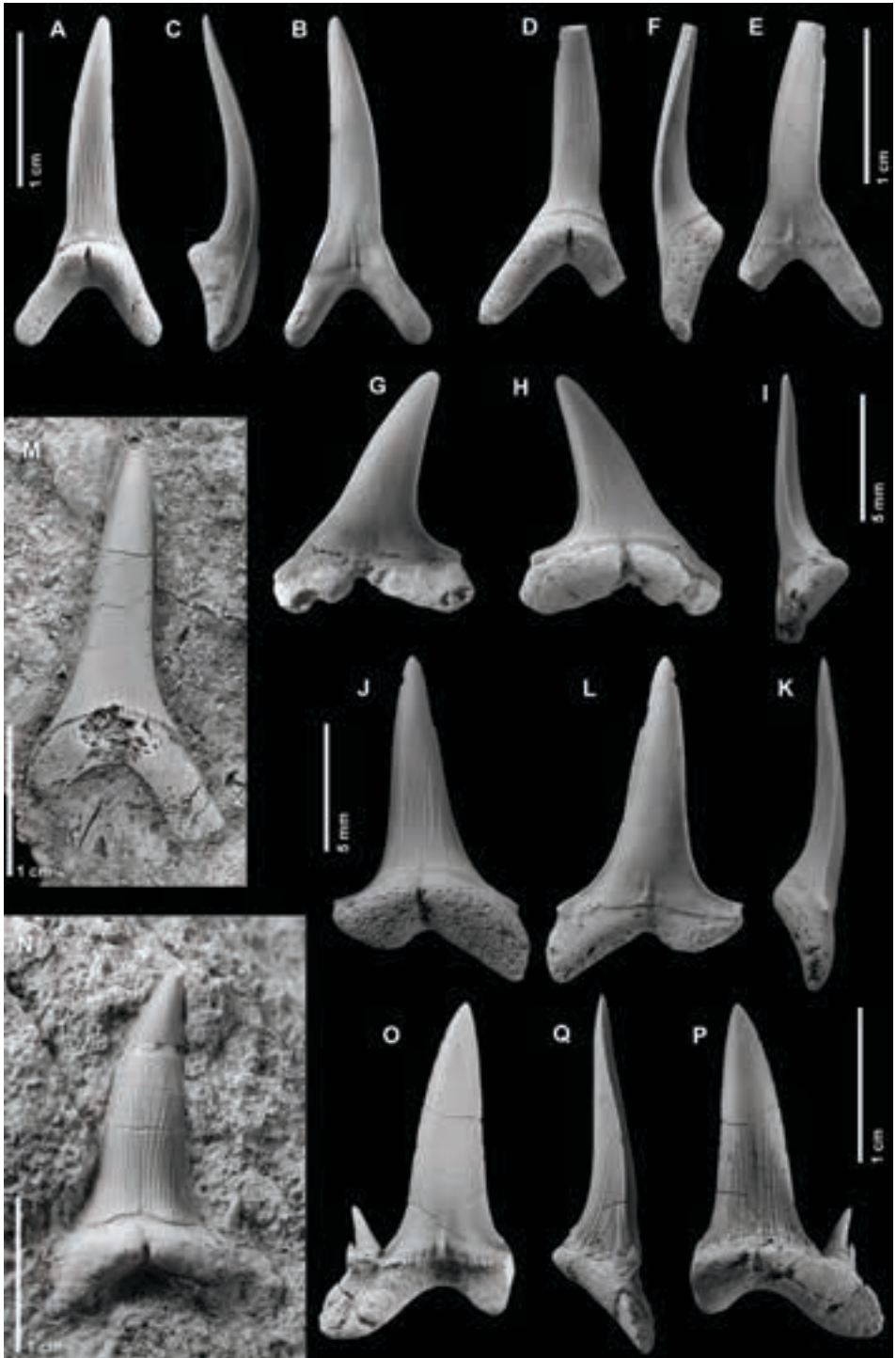
Material. Three teeth from lithofacies-2, MCNA 2591, MCNA 5453, and MCNA 8527.

Locality. Gometxa in Vitoria-Gasteiz municipality, Álava (Basque Country, Spain).

Age. Lower upper Campanian (*G. aegyptiaca* zone).

Description. Species characterised by its medium-sized teeth. The upper anterior tooth (MCNA 2591) has a tall, erect, narrowly triangular crown with continuous cutting edges from apex to base (Fig. 11.3M). The crown does not have lateral cusplets, and the main cusp broadens basally but without developing proper lateral heels (the cutting edge extends basally along the lobes of the root). The lingual face of the crown is convex with numerous short basal folds (over 50) in addition to six faint folds that extend upwards two-thirds the length of the cusp. The crown–root boundary does

Figure 11.3 A–L, *Anomotodon hermani* Siverson, 1992, from lithofacies-1: A–C, anterior tooth in lingual (A), labial (B), and profile (C) views, MCNA 3685; D–F, anterior tooth in lingual (D), labial (E), and profile (F) views, OIGM-GM7; G–I, upper lateral tooth in labial (G), lingual (H), and distal (I) views, MCNA 10508; J–L, lower lateral tooth in lingual (J), mesial (K), and labial (L) views, MCNA 10507. M–Q, *Scapanorhynchus* cf. *texanus* (Roemer, 1849) from lithofacies-2: M, upper anterior tooth in lingual view, MCNA 2591; N, lateral tooth in lingual view, MCNA 5453; O–Q, lateral tooth in labial (O), lingual (P), and lateral (Q) views, MCNA 8527. ▶



not present a clear neck. Despite not being well preserved, the root is bilobate with a barely noticeable lingual protuberance. The best-preserved distal lobe is long, narrow, and distally flattened with a squared end.

Two teeth with labiolingually flattened cusps, which are more broadly triangular than that in the previous specimen, are referred to as lateral teeth (Figs. 11.3N, O–Q). The main cusp, which bends toward the rear, is flanked by paired sharp lateral cusplets with short vertical striations, only on the lingual face. The inner pair is larger and divergent, while the smaller outer pair is inclined toward the main cusp. The labial face of the crown is flattened and smooth, although many short folds develop at the crown–root boundary, and a shallow depression is centrally located at the base of the main cusp (Fig. 11.3O). The lingual face is convex, folded with approximately 15 to 17 vertical parallel striations extending three-quarters the length of the cusp. Distally, they slightly deviate towards the edges of the crown with the presence of short additional striations (Fig. 11.3N). The cutting edges terminate at the base of the cusp. A vague longitudinal groove (neck) on the lingual face marks the crown–root boundary. In profile, the main cusp of specimen MCNA 5453 shows a slight sigmoid curvature, being the apex slightly curved labially (Fig. 11.3Q). Root is short and bilobate. A well-developed protuberance and an elongated nutritive groove are distinguished on the lingual face of both tooth specimens. The lobes are well separated by a broad, round basal notch (Fig. 11.3P).

Remarks. *Scapanorhynchus texanus* was first described by Roemer (1849) – and figured in a posterior paper (Roemer, 1852) – on the basis of specimens from the latest Cretaceous of New Braunfels, Texas, USA (most likely from the Campanian Pecan Gap Chalk of the Taylor Marl Group, but also possible from the Maastrichtian Navarro Group). *Scapanorhynchus texanus* and *S. raphiodon* are two closely related species. When discussed the taxonomic status of the genus *Scapanorhynchus*, Bourdon et al. (2011) stated that under the current trend in North America, teeth of the genus *Scapanorhynchus* are assigned either to the species *S. raphiodon* or *S. texanus*, preferably using *S. raphiodon* for the Santonian finds. Thus, *S. texanus* chronologically replaces *S. raphiodon* with the latter occurring in Santonian strata or earlier rocks (Case et al., 2001b). Moreover, the European specimens are generally assigned to *S. raphiodon* and the North American material to *S. texanus* (Case and Cappetta, 1997). *Scapanorhynchus raphiodon* (Agassiz, 1843) is the species of the genus most widely cited in the literature, despite the taxon being erected on poorly-preserved material from the Upper Cretaceous – probably Turonian, Woodward (1911) – of Lewes, East Sussex, UK (Cappetta, 1987; Siverson, 1992). The species *S. raphiodon* is known from a number of localities in Belgium, France, UK, Ukraine, Uzbekistan, North America, ranging from upper Cenomanian to Santonian (Herman, 1977; Hamm and Shimada, 2002). Some specimens from Santonian to lower Campanian age deposits of Bas-Congo in the Democratic Republic of the Congo and the Angolan exclave of Cabinda have been assigned to *Scapanorhynchus raphiodon* (Dartevelle and Casier, 1943; Taverne, 1970). The species *S. texanus* is mainly known from Campanian and Maastrichtian deposits in

North America (Cappetta and Case, 1999), but it has also been reported in southern Trans-Urals (Kachar quarry), in the Mangyshlak region of Kazakhstan (Zhelezko, 1988, 1990). A similar form assigned to *Scapanorhynchus* cf. *texanus* has been reported from the Coniacian?–Santonian of Nigeria by Vullo and Courville (2014).

Known occurrences of *Scapanorhynchus* in the Campanian include those in Belgium (Herman, 1977), Sweden (Siverson, 1992), Hampshire in the UK (Underwood and Ward, 2008), Kazakhstan (Zhelezko, 1988, 1990), Morocco (Cappetta, 2012), Egypt (Priem, 1914), Angola (Antunes and Cappetta, 2002), an array of fossil sites throughout northern America including the Big Horn Basin in Wyoming (Case, 1987), Texas (Cappetta and Case, 1999; Roemer, 1849; Schubert et al., 2016; Welton and Farish, 1993), Alabama (Cappetta and Case, 1975b), the Blufftown Formation in Western Georgia (Case and Schwimmer, 1988), the Merchantville and Marshalltown formations in Delaware (Lauginiger and Hartstein, 1983), the Mount Laurel Formation in New Jersey (Cappetta and Case, 1975b), and the Herbert Sound Member of the Santa Marta Formation in James Ross Island, Antarctic Peninsula (Kriwet et al., 2006). Moreover, three isolated dental cusps from the lower Campanian of the Faucouzy site (Aisne, France) were referred as the teeth of *Scapanorhynchus* aff. *raphiodon* by Guinot et al. (2013) on the basis of both size and characteristic lingual folding. Some anterior teeth of *Scapanorhynchus perssoni* Siverson, 1992, recovered from the Campanian Kristianstad Basin in Sweden, significantly differ from those found in Gometxa by having tall, moderately thick crowns in the anterior teeth, which are also flanked by a sharp accessory cusplets. Moreover, the lingual face of the crown is more densely ornamented with finer vertical folds in *S. perssoni*. The teeth of the Maastrichtian species *S. rapax* (Quaas, 1902) from Africa (Arambourg, 1952) and the Middle East (Bardet et al., 2000) are much larger, having numerous striations on the labial face of the crown and a strongly developed root. Moreover, the cutting edge does not extend to the base of the crown in *S. rapax* (Cappetta and Case, 1975b). The species *Scapanorhynchus minimus* – erected by Landemaine (1991) – has more gracile crowns with lateral cusplets in both anterior and lateral teeth. Thus, the Gometxa specimens, although smaller, closely resemble those of *S. texanus* in having short lower labial folds (Bourdon et al., 2011). However, the only anterior tooth preserved (Fig. 11.3M) differs from the American species by showing thinner lingual striations in the crown and a less robust appearance. Despite not being well preserved, the neck also lacks of vertical folds. All in all, the scapanorhynchid teeth from Gometxa could be assigned to *Scapanorhynchus* cf. *texanus* due to the dearth of material so far found.

Family ODONTASPIDIDAE Müller and Henle, 1839

Genus *CARCHARIAS* Rafinesque, 1810

Type species. *Carcharias taurus* Rafinesque, 1810; Recent, Sicily, Italy.

For the discussions concerning the taxonomical status of this genus see Ward (1988).

Carcharias aasenensis Siverson, 1992

Fig. 11.4

1992 *Carcharias aasenensis* Siverson, p. 536, Pl. 3, Figs. 1–6.

2014 *Carcharias aasenensis* Siverson, 1992; Ladwig, p. 2, Pl. 2, Figs. a–d.

Material. Two teeth from lithofacies-1, MCNA 10501 and MCNA 15517.

Locality. Gometxa in Vitoria-Gasteiz municipality, Álava (Basque Country, Spain).

Age. Lower upper Campanian (*G. aegyptiaca* zone).

Description. Teeth of small to medium size. The anterior tooth (Figs. 11.4A–D) contains a tall, erect, triangular cusp that is flanked on each side by a triangular, little divergent cusplet. The cutting edge reaches the base of the cusp and continues into the cusplets. The lingual face is markedly convex and smooth, but bears short and faint plications at the base of the enameloid that continue into the collar (or neck). The labial face is slightly convex and smooth, with two well-developed shoulders that overhang the root to form an inverted V-shape, at the vertex of which there is faint running vertically fold. Below this point, a clear foramen opens in the root (Fig. 11.4B). The root is bilobed with a marked lingual protuberance and two elongated branches that are separated by a deep nutritive groove. The root presents a tight basal concavity in labial/lingual view (angle between branches ca. 75°). Another upper lateral tooth (Figs. 11.4E–G) has a smooth-faced triangular cusp with a continuous cutting edge, inclined distally but almost straight in profile. The lingual face of the cusp is moderately convex and bears short plications located at the central basal portion of the cusp. The labial face has a mesial triangular fossa located basally. The only preserved lateral cusplet is more mesiodistally expanded, when compared to those cusplets in the anterior tooth, and shows the development of an additional, short marginal cusplet lingually folded (Fig. 11.4G). A collar, which is pierced by several foramina, is developed lingually at the crown–root boundary. A central foramen occurs on the labial side at the crown–root boundary (Fig. 11.4F). The bilobed root is low and bears a weak lingual protuberance with a short nutritive groove. The distal lobe is partially lost by abrasion.

Remarks. The teeth of this species are very similar in appearance to those of the broadly coeval *Carcharias latus*¹ (Davis, 1890) from the Kristianstad Basin in southern Sweden and *Carcharias samhammeri*² (Cappetta and Case, 1975b) from the New Jersey

¹ The species *Carcharias latus* has been known from temperate regions of northwest Europe. In addition to the type locality described by Davis (1890), Siverson (1992) reported it from a limited number of localities in the province of Scania (Kristianstad Basin, Sweden). *Carcharias latus* also occurs in the upper Campanian (CIV) of Le Pilou and Le Caillaud, Charente-Maritime, France (Vullo, 2005) and the lower Campanian (*O. pilula* zone) of Villers-devant-le-Thours in France (Guinot et al., 2013).

² The North American species *Carcharias samhammeri* was described by Cappetta and Case (1975b) from the Mount Laurel Formation of New Jersey, and additionally from the Mount Laurel and Marshalltown formations in Delaware by Lauginiger and Hartstein (1983). The Marshalltown and Mount Laurel formations in the New Jersey and Delaware (USA) are respectively considered upper Campanian and uppermost Campanian on the basis of ammonites and calcareous nannoplankton (see Kennedy and Cobban, 1994; Sugarman et al., 1995).



Figure 11.4 *Carcharias aasenensis* Siverson, 1992, from lithofacies-1. A–D, anterolateral tooth in lingual (A), labial (B), profile (C), and basal (D), MCNA 10501; E–G, lateral tooth in lingual (E), labial (F), and mesial (G) views, MCNA 15517.

Coastal Plain, USA. However, *C. aasenensis* differs from *C. latus*, among other features according to Siverson (1992), in possessing a more massive root, relatively larger lateral cusplets, lingually flattened cusps in lateral teeth, and in lacking basal folds on the labial side of the crown. *C. aasenensis* differs from *C. samhammeri* in being considerably smaller (*C. samhammeri* becomes as much as one and a half times larger) and in having a more developed shoulder and a crown overhanging the root. *Carcharias aasenensis* differs in its larger size from *Carcharias adneti* Vullo, 2005 (which is another odontaspimid of relatively younger age recorded in the Vitoria Pass site; see Chapter 12), and in having a thicker root and lacking clear lingual folds on the cusp.

In addition to the type locality in Åsen (Scania, Sweden), *C. aasenensis* has also been reported by Ladwig (2014) at the upper Campanian locality of Krons Moor in the North German Basin (Schleswig-Holstein, Germany). The upper Campanian Gometxa locality in northern Spain represents the southernmost occurrence of this species, and considerably extends its known distribution.

Family OTODONTIDAE Glikman, 1964

Genus *CRETOLAMNA* Glikman, 1958

Type species. *Otodus appendiculatus* Agassiz, 1843; Turonian of Lewes, East Sussex (England).

The genus *Cretolamna* has been given a wide geographical and stratigraphical range from Albian to Ypresian (Cappetta, 2012). A large number of records have been given to the species *C. appendiculata*, but many of such forms may correspond to different species (Cappetta, 2012). More recently, Siversson et al. (2015) have also noted that many of these *C. appendiculata*-type teeth have been misclassified, and consequently they have assigned them to either different or new species based on the current analysis of their dental characters, mostly those diagnostic ones present in the root.

An explanation over the controversial spelling of the genus, either *Cretolamna* or *Cretalamna*, is given in Cappetta (2012: 234) and Siversson et al. (2015). Here, I will follow Cappetta's opinion in retaining the traditional spelling.

Cretolamna borealis (Priem, 1897)

Figs. 11.5–6

For the synonymy see Siversson et al. (2015).

Material. Twenty one teeth, OIGM-GM5, OIGM-GM6, OIGM-GM12, MCNA 5456, MCNA 8521, MCNA 10503, MCNA 10504, MCNA 10505, and ten other catalogued specimens from lithofacies-1; OIGM-GM8, MCNA 14667, and another catalogued specimen from lithofacies-2.

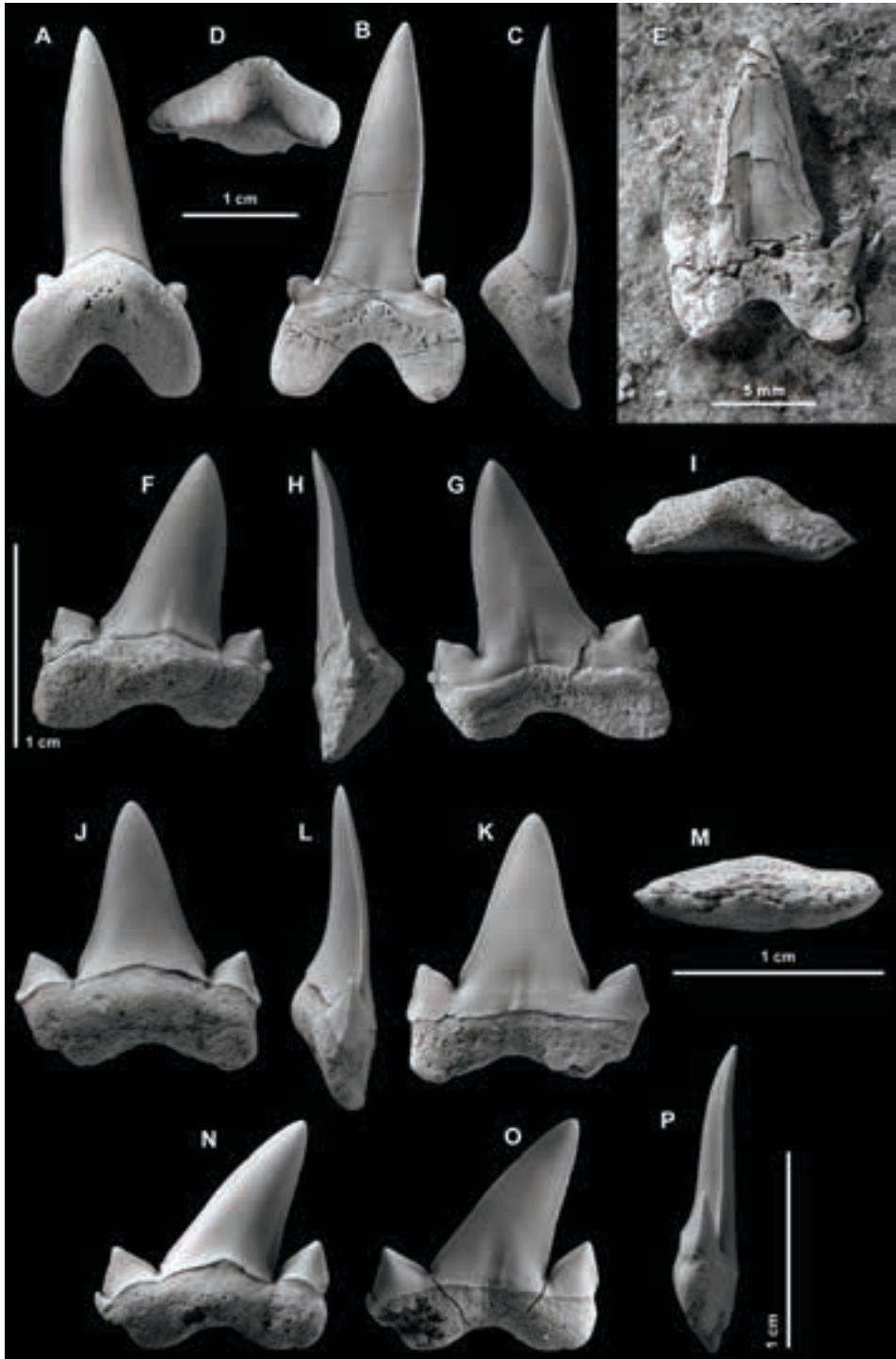
Locality. Gometxa in Vitoria-Gasteiz municipality, Álava (Basque Country, Spain).

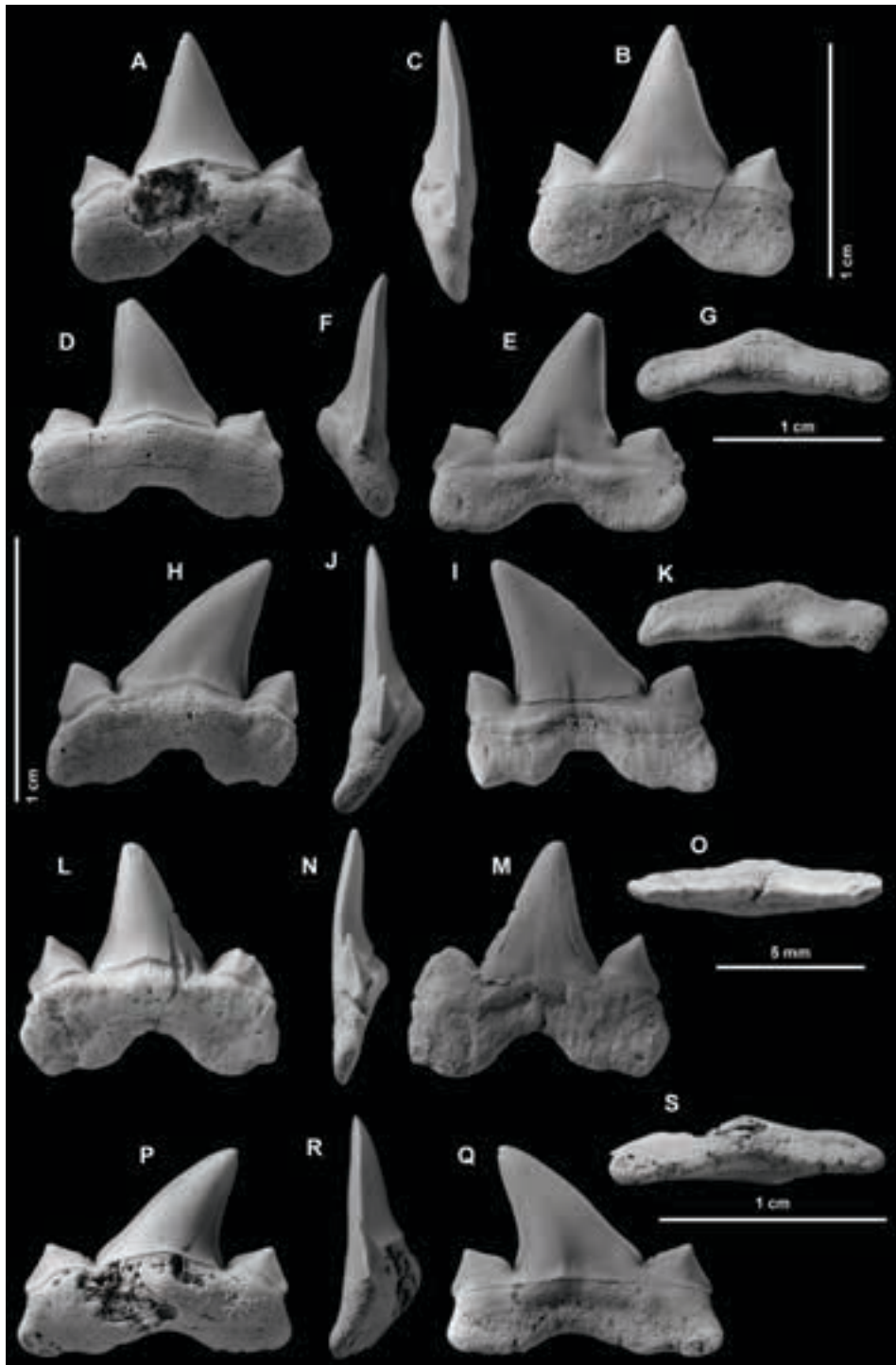
Age. Lower upper Campanian (*G. aegyptiaca* zone).

Description. A detailed description of the species is provided by Siversson et al. (2015), which is summarised below. The teeth are of medium to large size. The crown is distinguished by having a triangular, labiolingually flattened cusp flanked by a small, divergent cusplet on each side. Both labial and lingual faces of the crown are generally smooth, except in posterolateral teeth, where vertical folds can occur on the labial face. The cutting edge is continuous. The root is short. However, variations to this general morphology may occur depending on the tooth position in the jaws.

An anterior tooth (Figs. 11.5A–D) is slender – taller than wide – measuring 32 mm in height. The relatively high median cusp, which presents a recurved apex in labial/

Figure 11.5 *Cretolamna borealis* (Priem, 1897). A–D, upper anterior tooth in lingual (A), labial (B), mesial (C), and basal (D) views, OIGM-GM5; E, anterior tooth in labial view, MCNA 14667; F–I, upper anterior (?) tooth in lingual (F), labial (G), mesial (H), and basal (I) views, MCNA 10503; J–M, posterolateral tooth in lingual (J), labial (K), mesial (L), and basal (M) views, MCNA 10504; N–P, posterolateral tooth in lingual (N), labial (O), and distal (P) views, MCNA 8521. A–C, F–P from lithofacies-1, E from lithofacies-2. ►





lingual view and a sigmoid curvature in profile (Fig. 11.5C), is flanked by a single pair of short, divergent broad-tipped cusplets. The labial and lingual faces of the median cusp are slightly flattened and convex, respectively. The cutting edge does not run continuously from the main cusp to the cusplets. The base of the crown on the labial side is marked by a curvy boundary line, giving rise to faint shoulders (Fig. 11.5B). The root is bilobed, short, and slightly asymmetrical in labial/lingual view. The lobes are labiolingually compressed and round-ended. A well-developed lingual protuberance is pierced by several foramina. On the labial side, a line of foramina runs parallel to the crown–root boundary. The basal edge in labial/lingual view forms a deep U-shape. In basal view, the root shows a triangular outline (Fig. 11.5D).

The specimen MCNA 10503 (Figs. 11.5F–I) comes from an anterior to anterolateral tooth file. The main cusp of the crown is broad, shorter, and more labiolingually compressed (probably because it belongs to the upper row) than that of anterior teeth, and also presents a recurved apical part in labial/lingual view. Both triangular cusplets are divergent and tipped and are, in addition, split into secondary smaller cusplets. This characteristic is also observed in other lateral teeth of the series (tooth row).

The lateral (i.e. anterolateral to posterolateral) teeth of this species are comparable, varying only the morphology according to their row position, as well as whether they are from the upper or lower jaw. Having said that, the main cusp in upper lateral teeth is broad, labiolingually compressed, and distally inclined (in contrast to lower lateral teeth, whose cusp is more upright). The labial face is more flattened than the lingual one. There are two triangular, wider than high, lateral cusplets, one on each side of the main cusp. In labial/lingual view, the inside cutting edge of the cusplets is convex, whereas the outer edge is concave. The crown–root boundary is highlighted by a clear neck on the lingual face of the crown (Fig. 11.6D), whereas that boundary is almost straight on the labial face (Fig. 11.6E). The labial face of the crown may present short vertical ridges in its basal part (Fig. 11.6I). The root is short, labiolingually compressed, and slightly asymmetrical in labial/lingual view. The lingual protuberance is not particularly robust; this results in a rectangular shaped outline in basal view (Fig. 11.6K). The lobes of the root are separated by a round to acute median notch in labial/lingual view. The end of the mesial lobe is generally more pointed than that of the distal lobe.

◀ **Figure 11.6** *Cretolamna borealis* (Priem, 1897). A–C, posterolateral tooth in lingual (A), labial (B), and mesial (C) views, MCNA 10505; D–G, posterolateral tooth in lingual (D), labial (E), mesial (F), and basal (G) views, OIGM-GM6; H–K, posterolateral tooth in lingual (H), labial (I), mesial (J), and basal (K) views, OIGM-GM12; L–O, posterolateral tooth in lingual (L), labial (M), distal (N), and basal (O) views, OIGM-GM8; P–S, posterolateral tooth in lingual (P), labial (Q), mesial (R), and basal (S) views, MCNA 5456. A–K, P–S from lithofacies-1; L–O from lithofacies-2.

In general, posterolateral teeth are wider than tall, having a short root, whose lobes are separated by a shallow, median notch in lingual/labial view (Figs. 11.6P, Q).

Remarks. In 1897, Priem described a shark tooth coming from the Campanian (*Belemnitella mucronata* zone) at Köping in the province of Scania (Kristianstad Basin, Sweden). Although this fossil element exhibited notable similarities in overall morphology to the species *Cretolamna appendiculata* (Agassiz, 1843), Priem (1897: 41) thought that this individual tooth represented a new species on the basis of marked basal folds on the labial face of the crown, which he named *Lamna borealis*. However, this particular feature (vertical folds in the basal third of the cusp) is not present in many of the specimens from Sweden, according to Siversson et al. (2015), as there is not either among the Gometxa material (this is only observable in lateroposterior teeth).

Compared with *C. sarcoportheta*, another otodontid species known from the Campanian of the Vitoria Sub-basin, several differences in dentition are observed between them. *Cretolamna borealis* can be distinguished by having (after Siversson et al., 2015): (i) more elongated cusps in anterior teeth, some of them with recurved apices in labial/lingual view, and elongated root lobes, labiolingually compressed; (ii) lateroposterior teeth with a smaller lingual protuberance in the root (giving a rectangular root in basal view); (iii) upper lateral teeth with a main cusp more distally inclined in labial/lingual view, but straight in profile view, and large lateral cusplets having convex inner and concave outer cutting edges; (iv) lateroposterior teeth commonly with vertical folds in the basal part of the labial face of the cusp; and (v) teeth with more symmetrical roots.

According to Siversson et al. (2015), the species *C. borealis* is known to range from Santonian through Campanian. It has been reported from the Tamayama Formation (probably lower Santonian) in Fukushima Prefecture, Honshu, Japan (Shimada et al., 2010), occurring with *Cretolamna hattini* Siversson et al., 2015. Younger records of *C. borealis* include the uppermost lower Campanian (Kristianstad Basin) in the province of Scania, Sweden (Priem, 1897; Siverson, 1992; Siversson et al., 2015), the lower upper Campanian (Obourg Chalk Formation, Mons Basin) in the province of Hainaut, Belgium (Herman, 1977), the Campanian of northern France in the Anglo-Paris Basin (Leriche, 1902), the lower upper Campanian in Charente-Maritime, France (Vullo, 2005), the Campanian in the Saratov province, Lower Volga region, Russia (Glikman, 1980; Averianov and Popov, 1995), the Campanian in the Kyzylkum desert of southern Kazakhstan (Glikman, 1980), and the uppermost Campanian (Mount Laurel Formation) in Delaware, USA (Lauginiger and Hartstein, 1983). The specimens figured by Schneider and Ladwig (2013) as *C. appendiculata* from Hannover in the North German Basin (Germany) should be referred to *C. borealis*, instead.

In addition to the new occurrence at Gometxa site, this species is well represented in the studied section at Vitoria Pass site, where is commonly found in the upper Campanian Eguleta Member (see Chapter 12).

Cretolamna sarcoportheta Siversson, Lindgren, Newbrey, Cederström, and Cook, 2015
Fig. 11.7

For the synonymy see Siversson et al. (2015).

Material. Five teeth from lithofacies-1, MCNA 15518, MCNA 5455, and three other catalogued specimens.

Locality. Gometxa in Vitoria-Gasteiz municipality, Álava (Basque Country, Spain).

Age. Lower upper Campanian (*G. aegyptiaca* zone).

Description. For the description of this species see by Siversson et al. (2015). Teeth of medium size (measuring up to 18 mm in height), which would correspond to the first and second upper anterior positions according to the reconstructed tooth set given by Siversson et al. (2015: Fig. 19). The crown is formed by a moderately tall, triangular cusp that is greatly labiolingually compressed, and two small triangular acute-tipped cusplets, one to each side of the cusp. The cusplets are separated from the main cusp by blunt notches. In profile view, the main cusp presents a sigmoid curvature (Figs. 11.7C, G). The base of the crown is marked on the labial side by the presence of a faint, curvy

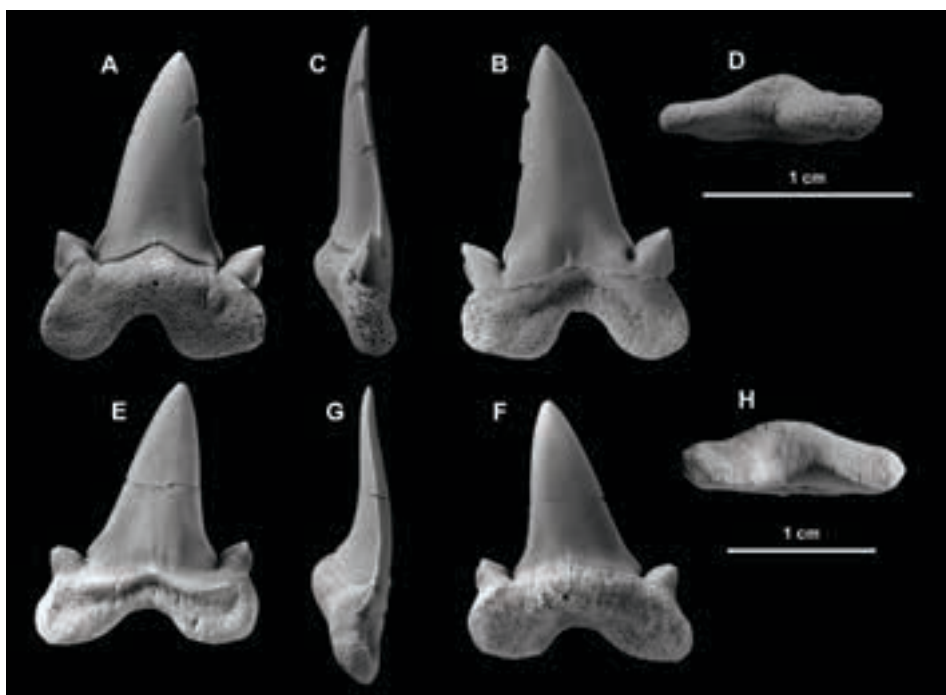


Figure 11.7 *Cretolamna sarcoportheta* Siversson et al., 2015. A–D, upper anterior tooth in lingual (A), labial (B), distal (C), and basal (D) views, MCNA 15518; E–H, upper anterior tooth in labial (E), lingual (F), mesial (G), and basal (H) views, MCNA 5455. All from lithofacies-1.

bulge that overhang the root in the middle part (Fig. 11.7E). The root is asymmetrical in labial/lingual view, being the distal lobe narrower than the round-squared, mesial lobe. The moderate lingual protuberance in the root exhibits a median foramen. The basal edge of the root forms an U-shaped notch in the middle, in labial/lingual view.

Remarks. The teeth of this *Cretolamna* species from Gometxa conform to the description of those of *C. sarcoportheta* given by Siversson et al. (2015). This species is characterised by having a triangular main cusp, either straight or slightly inclined, which is broader in lateral teeth more anteriorly situated. The root is generally asymmetrical in basal view (subtriangular in anterior teeth), with a distal lobe narrower than the mesial one. A comparison with the species *C. borealis* has been stated above. Contrary to the Gometxa site, where this taxon is poorly represented, the teeth of *C. sarcoportheta* are common in the upper Campanian strata of the Eguileta Member (Montes de Vitoria Formation) at Vitoria Pass site. Further remarks will be considered when dealing with the examination of this species from the latter site (see Chapter 12).

LAMNIFORMES incert. fam.

Genus *PARANOMOTODON* Herman in Cappetta and Case, 1975b

Type species. *Oxyrhina angustidens* Reuss, 1845; Upper Cretaceous, Turonian, southern foot of Boren hills, near Bílina, northwest Bohemia, Czech Republic.

Paranomotodon cf. *angustidens* (Reuss, 1845)

Fig. 11.8

For the synonymy see Vullo (2005), add Leriche (1902).

1902 *Oxyrhina angustidens* (Reuss, 1845); Leriche, p. 117, Pl. 3, Figs. 59–65.

Material. Five teeth, MCNA 10493, MCNA 15598, MCNA 15599, MCNA 15604 from lithofacies-1; MCNA 10492 from lithofacies-2.

Locality. Gometxa in Vitoria-Gasteiz municipality, Álava (Basque Country, Spain).

Age. Lower upper Campanian (*G. aegyptiaca* zone).

Description. The teeth are of small to medium size. In anterior teeth (Figs. 11.8A–E), the crown is formed by a long, triangular cusp, slightly sigmoid in profile view, with two (mesial and distal) enameloid expansions forming small heels, which are recurved inwardly. Both the labial and lingual faces are weakly convex and smooth. A longitudinal fold in the midline, flanked by parallel grooves on each side, is present at the base

Figure 11.8 *Paranomotodon* cf. *angustidens* (Reuss, 1845). A–C, upper anterior tooth in lingual (A), labial (B), and mesial (C) views, MCNA 10492; D–F, lower anterior tooth in lingual (D), labial (E), and profile (F) views, MCNA 15599; G–I, lower (?) anterolateral tooth in lingual (G), labial (H), and distal (I) views, MCNA 15604; J–L, lateral tooth in lingual (J), labial (K), and distal (L) views, MCNA 10493; M–N, lateral tooth in lingual (M) and labial (N) views, MCNA 15598. A–C from lithofacies-2, D–N from lithofacies-1.



of the cusp on the labial face (Figs. 11.8B, E). An anterolateral tooth from lithofacies-2 shows axial fractures in the crown, caused by compaction, and a root surface slightly abraded (Fig. 11.8B). The specimen MCNA 15599 presents on the labial side of the cusp numerous small plications at the edge of the enameloid (Fig. 11.8E). Moreover, its root is low, having a well preserved faint neck on the lingual side, below the enameloid-covered crown, and a moderate lingual protuberance that is divided by a median thin nutritive groove. A wide notch separates the lobes (angle between lobes ca. 100°); the completely preserved one appears to have a round end. The basal edge of the root is wide concave in labial/lingual view. Lateral teeth (Figs. 11.8J–N) have a smooth, labiolingually compressed main cusp, which is distally inclined and meets the distal heel at nearly a right angle. The labial face of the crown has a clear medio-basal depression (delta-shaped fossa). The root is more labiolingually compressed, and also carries a well-marked nutritive groove.

Remarks. This species was placed within Alopiidae for a long time, but the tooth similarities shared with extant members of this family may be well due to convergence (Cappetta, 2012). *Paranomotodon angustidens* is a frequently reported selachian species in the European rock formations, ranging from the Cenomanian through Santonian (see Cappetta, 2012 for a summary of its occurrences). Moreover, there are other tooth specimens closely related to the type species known from Campanian and Maastrichtian localities in New Jersey and Texas, USA (Cappetta and Case, 1975b; Welton and Farish, 1993), the Kristianstad Basin, southern Sweden (Siverson, 1992), the North German Basin near Hannover in northern Germany (Schneider and Ladwig, 2013), the Anglo-Paris Basin at the Aisne department in northern France (Leriche, 1902), the Aquitaine Basin in Charentes, West France (Vullo, 2005), and Gometxa in northern Spain (this work), which may belong to an undescribed species of *Paranomotodon* on the basis of a more robust appearance, and because they have broader cusps and root branches less developed than those of *P. angustidens* (Cappetta and Case, 1975b; Guinot et al., 2013).

Order ORECTOLOBIFORMES Applegate, 1972

Family HEMISCYLLIIDAE Gill, 1862

Genus *HEMISCYLLIUM* Müller and Henle, in Smith, 1837

Type species. *Squalus ocellatus* Bonnaterre, 1788; Recent, Western South Pacific Ocean.

Hemiscyllium hermani Müller, 1989

Figs. 11.9A–K

1982 *Hemiscyllium* sp.; Herman, p. 141, pl. 2, fig. 4.

1989 *Chiloscyllium greeni* (Cappetta, 1973); Müller, p. 37, pl. 8, figs. 2a–d.

1989 *Hemiscyllium* ? sp.; Müller, p. 37, pl. 9, figs. 1a–d.

?2007 *Hemiscyllium* sp.; Kriwet et al., p. 1050, pl. 1, figs. 1–5.

Material. Ten teeth from lithofacies-1, MCNA 15615, MCNA 15616, MCNA 15623, and seven other catalogued specimens.

Locality. Gometxa in Vitoria-Gasteiz municipality, Álava (Basque Country, Spain).

Age. Lower upper Campanian (*G. aegyptiaca* zone).

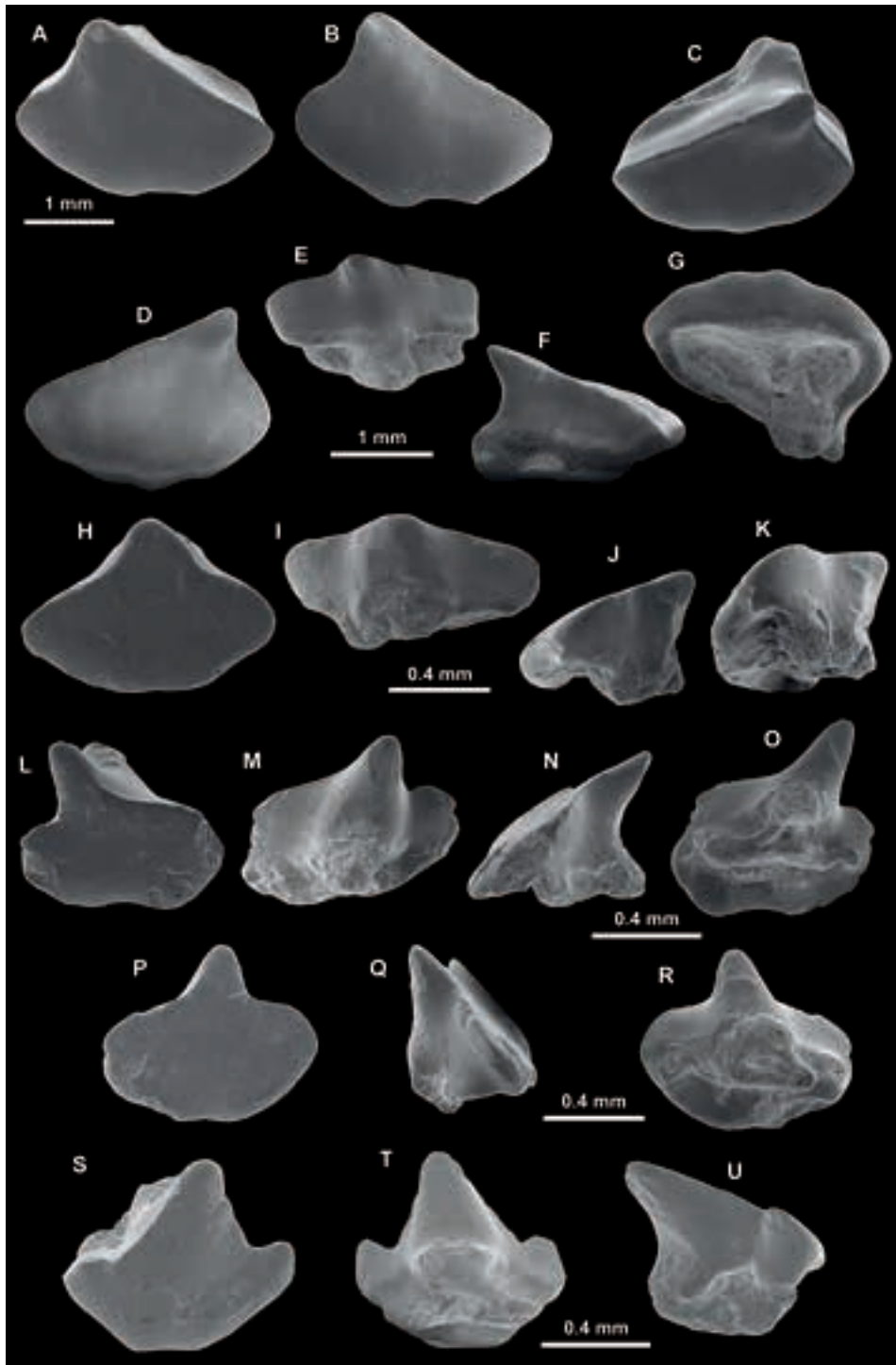
Description. Although this species has small teeth, usually less than 1 mm wide, according to Müller (1989), two samples of our material double this value (MCNA 15615 and MCNA 15616). These teeth have a cuspidate, smooth crown, mesiodistally expanded, which inclines towards the commissure in laterals when viewed labially. The crown is approximately triangular in profile view (Fig. 11.9F). An anterolateral tooth has a cusp more symmetrical in labial view (Fig. 11.9H). The labial face of the crown is almost flat, having the shape of a circular sector. The base has a regularly convex profile, except in its medial part where is roughly concave (i.e. bifid basal contour). The lingual face is strongly convex, with a tapered median protuberance (uvula). A continuous, sharp crest separates the labial and lingual crown faces. The crown strongly overhangs the root labially, forming a visor (Fig. 11.9F). The crown–root boundary forms a rounded bulge on the lingual side (Fig. 11.9E), except in the protuberance area because of abrasion during bedload transport. Due to the state of preservation of the material, details of the root are only observed in specimen MCNA 15616 (Figs. 11.9E, F–G). Thus, the root is much narrower than the crown, and is lingually projected. The lingual face of the root possesses a median protuberance with a round foramen in its centre. This protuberance is flanked on each side by a lateral concavity. The root lobes diverge labially to form a V-shape in basal view (Fig. 11.9G). The basal face was presumably flat.

Remarks. The species was first described by Müller (1989) from the basal Billerbecker Greensand of the upper Campanian Baumberge Formation in the Münster Basin (NW Germany), and it likely also occurs in the Campanian of the Kristianstad Basin, southern Sweden (Sørensen et al., 2013). In addition, an incomplete tooth from the Maastrichtian of Hemmoor (northern Germany), and formerly classified as an unassigned species of *Hemiscyllium* by Herman (1982), was examined by Müller (1989), who included it in the synonymy of the species. Additional occurrences are reported in the chalky Sigerslev Member of the upper Maastrichtian Tor Formation and the Fiskeler and *Cerithium* Limestone members of the lowermost Danian Rødvig Formation, both in eastern Zealand, Denmark, according to Adolphssen and Ward (2014, 2015).

The teeth of *H. hermani* are easily differentiated from those of *Chiloscyllium greeni* (Cappetta, 1973) in lacking lateral cusplets, and in having a main cusp with the labial face flat to slightly convex and a less squared-edged median protuberance. An unassigned anterolateral tooth of *Hemiscyllium*, figured by Kriwet et al. (2007) from the upper Campanian of the Trepmp Basin (eastern Pyrenees, Lleida, Spain), probably corresponds to *H. hermani*. This species is also differentiated from *Chiloscyllium frequens* Guinot et al., 2013 (see below) by the lack in the teeth of a pair of reduced lateral cusplets flanking the main cusp.

Genus *CHILOSCYLLIUM* Müller and Henle, 1837

Type species. *Scyllium plagiosum* Bennett, 1830; Recent, Sumatra, Indo-West Pacific.



Chiloscyllium cf. *gaemersi* Müller, 1989

Figs. 11.9L–R

Material. Seventeen teeth, MCNA 15622, MCNA 15624, and fifteen other catalogued specimens from lithofacies-1.

Locality. Gometxa in Vitoria-Gasteiz municipality, Álava (Basque Country, Spain).

Age. Lower upper Campanian (*G. aegyptiaca* zone).

Description. Teeth of small size, usually less than 1 mm wide. These anterolateral teeth are characterised by having an asymmetrical wide crown, whose cusp is inclined towards the commissure (Figs. 11.9L, P). The cusp is short. The labial face of the crown, which is almost flat except in the cusp, extends basally to form a visor that overhangs the root (Fig. 11.9N). The basal edge of this face is round or slightly bilobed in labial view. The lingual face is strongly convex in the median part and almost flat towards the margins. Both crown faces are smooth. The cutting edge is continuous and extends to the asymmetrical heels, being the distal one smaller. The specimen MCNA 15624 has the distal heel separated from the cusp by a faint notch (Fig. 11.9M). The root in both figured specimens is poorly preserved and incomplete. Despite that, it is observed that roots are bilobate and projected lingually. Their lingual face has a median protuberance that is flanked by two lateral depressions. In basal view, the lobes diverge labially (are V-shaped), and in the middle a relatively large baso-medial foramen is observed (Fig. 11.9O).

Remarks. Despite the difficulty of interpreting a drawing, I do not see great differences between the Gometxa teeth and those figured by Müller (1989) as *Chiloscyllium gaemersi*, first discovered from the upper Campanian basal Billerbecker Greensand in the Münster Basin (NW Germany). The species *Chiloscyllium gaemersi* has also been reported to occur in the Kristianstad Basin, southern Sweden (Sørensen et al., 2013).

The teeth of *C. gaemersi* differ from those of *Hemiscyllium hermani* by being smaller, by having curved cutting edges, which give the crown a characteristic cusp flanked with incipient lateral heels, and by having a flat labial face of the crown. *Adnetoscyllium angloparisensis* Guinot et al., 2013 is a very close related hemiscylliid species described from the Anglo-Paris Basin (France and the UK), ranging from upper Santonian to lower upper Campanian. However, the teeth of the latter species differ from those of *C. gaemersi* in having a crown with a more acute cusp apex, fang-like in appearance, convex

- ◀ **Figure 11.9** A–K, *Hemiscyllium hermani* Müller, 1989, A–B, lateral tooth in occlusal (A) and labial (B) views, MCNA 15615; C–G, lateral tooth in occlusal (C), and labial (D), lingual (E), profile (F), and basal (G) views, MCNA 15616; H–K, anterolateral tooth in labial (H), lingual (I), profile (J), and oblique basal (K) views, MCNA 15623. L–R, *Chiloscyllium* cf. *gaemersi* Müller, 1989, L–O, anterolateral tooth in occlusal–labial (L), lingual (M), profile (N), and basal (O) views, MCNA 15624; P–R, anterolateral tooth in labial (P), profile (Q), and basal (R) views, MCNA 15622. S–U, *Chiloscyllium* cf. *vulloi* Guinot et al., 2013, anterolateral tooth in labial (S), basal (T), and profile (U) views, MCNA 15626; apron digitally restored in basal view. All from lithofacies-1.

cutting edges running to the margins forming inclined heels, and a weak ridge running parallel to the outer edge of the labial apron, and by bearing a thin, continuous bulge in the basal edge of the lingual face (Guinot et al., 2013).

Chiloscyllium cf. *vulloi* Guinot, Underwood, Cappetta, and Ward, 2013
Figs. 11.9S–U

?1988 *Ginglymostoma globidens* Cappetta and Case, 1975b; Case and Schwimmer, p. 294, figs. 4.13–16.

?2010 *Chiloscyllium* sp.; Hübner and Müller, p. 447, figs. 5a–d.

Material. Two teeth from lithofacies-1, MCNA 15626 and another catalogued specimen.

Locality. Gometxa in Vitoria-Gasteiz municipality, Álava (Basque Country, Spain).

Age. Lower upper Campanian (*G. aegyptiaca* zone).

Description. This anterolateral tooth is small (less than 1 mm in width). The crown is smooth and formed by a triangular main cusp flanked by a pair of low, outward-diverging lateral cusplets (Fig. 11.9S). The main cusp is inclined distally. The labial face of the crown is relatively flat, and overhangs the root by a truncate, slightly bifid apron. Lingually, the main cusp is convex, and widens basally to connect with a lingual protuberance. The cutting edge is continuous and extends to the margins of the crown. The root is badly eroded, but what remains of it suggests that it was formed by a pair of V-shaped lobes, laterally expanded (Fig. 11.9T).

Remarks. The fossil tooth MCNA 15626 from Gometxa belongs to a group of hemiscylliid species mainly recognised by having crowns with a main cusp triangular and one pair of well-formed lateral cusplets. Among these taxa are *Chiloscyllium vulloi* Guinot et al., 2013, *Chiloscyllium* cf. *vulloi sensu* Guinot et al. (2013), and *Chiloscyllium frequens* Guinot et al., 2013. Additional diagnostic features in *Chiloscyllium vulloi*, which is known from the middle Turonian Justine-Herbigny site (Ardennes, France), are a strongly concave median area on the lingual face of the crown, a well-formed triangular lingual protuberance, a bifid apron, a heart-shaped root with a bulging lingual protuberance perforated by a broad central foramen, and finally concave root marginolingual edges pierced by foramina. Some specimens described by Guinot et al. (2013: Figs. 9E'–L') from the Coniacian glauconitic sandstone of Minnis North in Antrim, Northern Ireland (UK), appears to be closely related to *C. vulloi*, being referred to as *Chiloscyllium* cf. *vulloi*. A larger overall size, a crown with a convex labial face, in profile view, and lateral cusplets more developed are differences that distinguish *C.* cf. *vulloi* from *C. vulloi*, according to these authors. *Chiloscyllium* cf. *vulloi* may be also present in the Cenomanian of the Münster Basin (near Halle, NW Germany), according to Guinot et al. (2013). *Chiloscyllium frequens* is a recently erected species ranging from upper Santonian to lower upper Campanian in the Anglo-Paris Basin (France and the UK), which is separated from the above species by its teeth generally larger in size (Guinot et al., 2013). Moreover, *C. frequens* have teeth with an elongate main cusp

flanked by one to two pairs of short, lateral cusplets (often underdeveloped or absent in anterior teeth), and a strongly overhanging apron with a basal edge generally convex.

The Gometxa teeth resemble most closely with those of *Chiloscyllium* cf. *vulloi* by its characteristic crown outline in labial view. Moreover, it is easily differentiated from those of the cooccurring species *Chiloscyllium gaemersi* in having well-formed lateral cusplets, and a trapezoidal basal outline of its labial face, which is defined by its straight marginal edges. A more precise description of this taxon in Gometxa is not possible based on the poor condition of the found teeth.

Order CARCHARHINIFORMES Compagno, 1973

Family SCYLORHINIDAE Gill, 1862

Genus *PROHAPLOBLEPHARUS* Underwood and Ward, 2008

Type species. *Scyliorhinus riegrafi* Müller, 1989; (lower) upper Campanian, Baumberge-Schichten, Münster Basin (west Münsterland, Westphalia in NW Germany).

Prohaploblepharus riegrafi (Müller, 1989)

Fig. 11.10

Material. Eighteen teeth from lithofacies-1, MCNA 15619, MCNA 15620, MCNA 15621, and fifteen other catalogued specimens.

Locality. Gometxa in Vitoria-Gasteiz municipality, Álava (Basque Country, Spain).

Age. Lower upper Campanian (*G. aegyptiaca* zone).

Description. The teeth of this species are small (barely exceeding 1 mm in height). The crown has a slender cusp, flanked by two pairs of lateral, divergent cusplets, being the outer ones much reduced than the inner ones. The main cusp, which leans toward the commissure in more lateral files, has a slightly convex labial face, displaying well-marked longitudinal ridges that run apically to reach about half the length of the cusp (Figs. 11.10C, G, K). The lingual face of the cusp is basally rounded, convex, and ornamented with thin ridges. The cutting edge is continuous and extends toward the cusplets. The crown–root boundary is curved medially on the labial side, overhangs the root, and also displays a series of regularly spaced ridges and troughs (Fig. 11.10C). All the teeth have their roots considerably abraded, lacking the distal part of the lobes. However, it can be appreciated that in this species the root is low with a flat basal face. The root also has a pronounced lingual protuberance with a large medial foramen, or incomplete nutritive groove. In the figured specimens the mesiolingual foramen has been further exaggerated by erosion and is not to be mistaken with a true nutritional groove.

Remarks. *Prohaploblepharus riegrafi* was previously recorded in the Upper Cretaceous of northwest Europe. The species was first described by Müller (1989) from the basal Billerbecker Greensand of the lower upper Campanian Baumberge Formation in the Münster Basin (NW Germany) (see also, Müller, 2014; Thies and Müller, 1993). These beds are regarded to represent the *Bostrychoceras polyplocum* zone, according to Kaplan

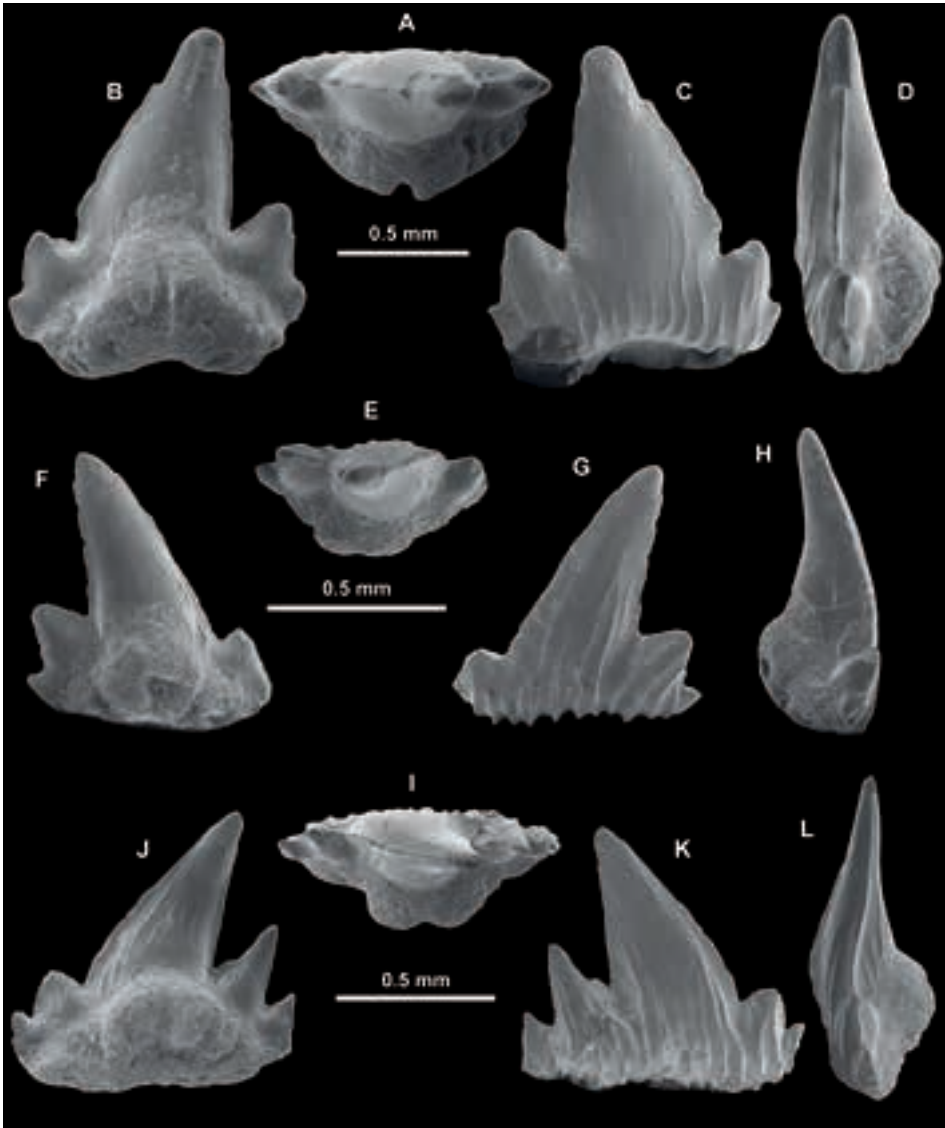


Figure 11.10 *Probaploblepharus riegrafi* (Müller, 1989). A–D, anterolateral tooth in apical (A), lingual (B), labial (C), and profile (D), views, MCNA 15619; E–H, anterolateral tooth in apical (E), lingual (F), labial (G), and profile (H), views, MCNA 15621; I–L, lateral tooth in apical (I), lingual (J), labial (K), and profile (L), views, MCNA 15620. All from lithofacies-1.

et al. (2005). Additional records outside the type area are described in the Upper Cretaceous of the British Islands (UK) by Underwood and Ward (2008), who also extended the stratigraphical range of the species from Coniacian to lower Campanian. Thus, according to these authors, the older occurrence of the species is within a phosphatic

bed of the Hibernian Greensand Formation (Coniacian, *Micraster cortestudinarium* zone) in Antrim County, Northern Ireland, while a calcarenite of early Campanian age (Culver Chalk Formation) that crops out in Downend (Hampshire) and a phosphatic horizon (lower Campanian, *Offaster pilula* zone) in Winterbourne (Berkshire) are the youngest occurrences in the UK.

Order SYNECHODONTIFORMES Duffin and Ward, 1993

Family PALAEOSPINACIDAE Regan, 1906

Genus *SYNECHODUS* Woodward, 1888

Type species. *Hybodus dubrisiensis* Mackie, 1863; from the Lower Chalk (Cenomanian) of Dover (Kent, UK).

Synechodus aff. *filipi* Siverson, Cook, Cederström, and Ryan, 2016

Figs. 11.11A–H

1989 *Synechodus perssoni* Siverson, 1989; *nomen invalidum*, p. 11, pl. 1, figs. 1–3, pl. 2, figs. 1–2.

1989 *Synechodus lerichei* Herman, 1977; Siverson, p. 13, pl. 1, figs. 4–5, pl. 2, figs. 3–4.

1995 *Scyliorhinus reyndersi* Halter, 1995; Halter (partim), p. 84, pl. 7, figs. 1–2, pl. 8, fig. 2, pl. 9, fig. 1.

Material. Two teeth from lithofacies-1, MCNA 15613 and MCNA 15614.

Locality. Gometxa in Vitoria-Gasteiz municipality, Álava (Basque Country, Spain).

Age. Lower upper Campanian (*G. aegyptiaca* zone).

Description. These two anterolateral teeth are rather small (1.5–2 mm in width). They have a low central cusp, wider at its base, which leans commissurally. Two pairs of lateral cusplets, the outer ones smaller, flank the cusp. The lingual face of the cusp is more convex than the labial one, at least in the specimen MCNA 15613 (Figs. 11.11A–D). The cutting edge seems to be continuous. The crown bears on both faces well-marked vertical ridges that radiate from apex toward the base (Fig. 11.11C). This ornamentation also extends toward the lateral cusplets. Additional folds on the base of the labial face produce a cell-like pattern (Fig. 11.11B). The crown overhangs the root labially with a rounded edge, while a vague neck connects the crown with the root lingually. The root is low and projected lingually, having a flat base perforated by irregular foramina. The lingual root-face bears several foramina in addition to a rounded, square-edged medial protuberance that is pierced by a teardrop-shaped foramen (Fig. 11.11E). The basal outline of the root forms a wide arch in labial/lingual view (Figs. 11.11A, E).

Remarks. The species *Synechodus filipi* has been recently described by Siverson et al. (2016) from Åsen (Kristianstad Basin, Sweden), and likely includes one *Synechodus* specimen reported by Herman (1977) from the Obourg Chalk Formation in Belgium, according to Siverson et al. (2016). According to these authors, the taxon includes the teeth described by Siverson (1989) as *Synechodus lerichei* Herman, 1977 and

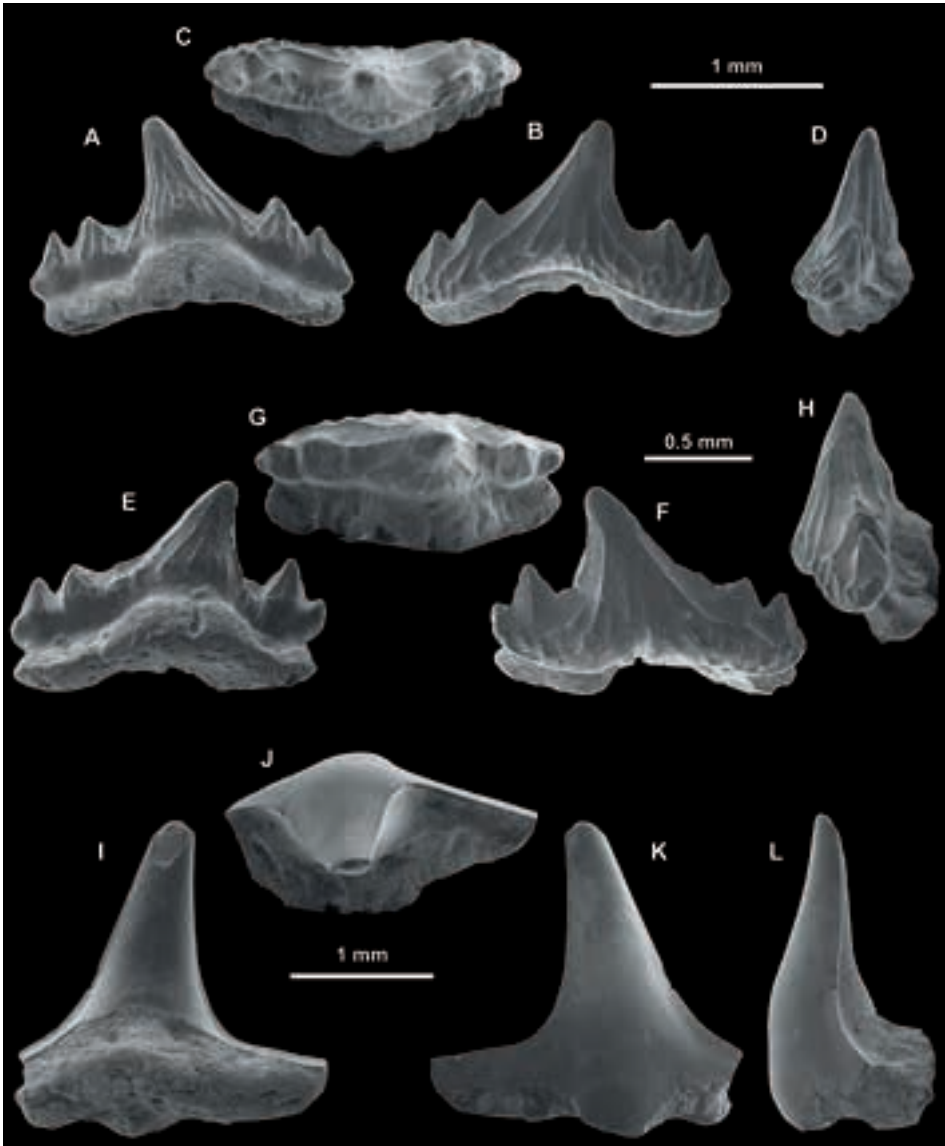


Figure 11.11 A–H, *Synechodus* aff. *filipi* Siverson et al., 2016, A–D, anterolateral tooth in lingual (A), labial (B), apical (C), and profile (D) views, MCNA 15613; E–H, anterolateral tooth in lingual (E), labial (F), apical (G), and profile (H) views, MCNA 15614. I–L, *Squatina bassei* Leriche, 1929, anterolateral tooth in lingual (I), apical (J), labial (K), and profile (L) views, MCNA 15612. All from lithofacies-1.

Synechodus perssoni Siverson, 1989, the latter being a *nomen invalidum* because it was not effectively published in accordance to the ICZN rules. *Synechodus filipi* is known to occur from upper lower Campanian to lower upper Campanian (*Belemnellocamax*

mammillatus to *Belemnellocomax balsvikensis* informal zones), as stated in Siverson (1989) and Siverson et al. (2016). Among the primary types used in the description of species *Scyliorhinus reyndersi* Halter, 1995, there are some teeth that are closely related to *Synechodus* aff. *filipi*. This material was collected at Halembaye in the Belgian Limburg, where quarries produce fine-grained chalk of the Zeven Wegen Member (Gulpen Formation, lower upper Campanian), as reported by Halter (1995).

Synechodus turneri Case, 1987, *S. lerichei* Herman, 1977, and *Synechodus faxensis* (Davis, 1890) are three further species within the genus *Synechodus* with teeth that closely resemble those of *S. filipi*, according to Siverson et al. (2016). So far, the species *S. turneri* is restricted to the Western Interior of North America, being present in the upper Campanian Mesaverde Formation of Wyoming, USA (Case, 1987) and the Campanian Foremost Formation in southeast Alberta, Canada (Peng et al., 2001). The species *S. lerichei* Herman, 1977 was described using material from several Belgians formations, namely Lonzée Member [?Coniacian–Santonian to ?basal Campanian, according to Robaszynski et al. (2001)], Obourg Chalk and Spiennes formations [lower upper Campanian to upper Campanian, as stated in Robaszynski et al. (2001)], Cibly Phosphatic Chalk Formation [lower Maastrichtian, according to Robaszynski et al. (2001)], and the Maastrichtian Maastricht Formation in the Dutch Limburg. The taxon *Synechodus lerichei* was found previously by Priem (1897) in the lower upper Campanian (*Belemnitella mucronata* zone) of Meudon (Hauts-de-Seine, France), but he failed to give a species name for the material. Recently, Guinot et al. (2013) have also reported its presence in the Anglo-Paris Basin, and, more specifically, in Boxford, Berkshire, UK (lower Santonian; *Micraster coranguinum* zone) and the French sites of Hallencourt in Somme (lower Campanian; *Offaster pilula* zone) and Mont-Août in Marne (lower upper Campanian; *Belemnitella mucronata* zone). Teeth of *S. lerichei* are also known from the basal Billerbecker Greensand of the Campanian Baumberge Formation in the Münster Basin (NW Germany) (Müller, 1989). These beds are regarded as representing the upper Campanian (*Bostrychoceras polyplacum* zone), according to Kaplan et al. (2005).

The species *Synechodus faxensis* was first described from specimens collected in a Danian calcarenite at the type locality of Faxe in Zealand, Denmark. This species was revised by Adolfssen and Ward (2014, 2015) on the basis of additional material collected from calcarenite deposits occurring at Kulstirenden (Stevns Klint) and two quarries – Stevns Kridtbrud and Faxe – in the Zealand Region of Denmark, with a stratigraphical range from Maastrichtian to middle Danian (Tor and Rødvig formations, respectively), according to Adolfssen et al. (2017). Leriche (1929) noticed that the teeth of *S. faxensis* closely resembled other *Synechodus* specimens from the lower Maastrichtian Cibly Phosphatic Chalk Formation in the Hainaut province (Belgium) and from the Maastrichtian Maastricht Formation in the Dutch Limburg, but neither fossil collection, nor repository details, nor figurations were given.

When J. Herman defined the species *S. lerichei* in 1977, he included different aged specimens with distinctive morphological appearance (called here morphotypes).

Guinot et al. (2013) has noticed that the slender morphotype of this species is also found in some Campanian sites of northern France.

Although the teeth of *Synechodus* from Gometxa are small, they differ from those of the Campanian-aged slender morphotype of *S. lerichei* in having irregular vertical ridges in the crown, a less number of lateral cusplets (only two pairs), and a more pronounced lingual protuberance of the root. They also differ in lacking the characteristic short, parallel folds in the labiobasal edge of the root (i.e. pseudopolyaulacorhize arrangement). The teeth of *S. turneri* are also slender, but they differ from those of Gometxa in having the main cusp lingually inclined, more pairs of lateral cusplets, an arched root, in basal view, with many large labial foramina, and a pseudopolyaulacorhize arrangement of the root. Moreover, these teeth lack the reticulate ornamentation at the base of the labial side of the crown.

The teeth of *S. filipi* generally have a crown with acute cusplets. The enameloid ornamentation in this species is characterised by weak vertical ridges, commonly restricted to the cusplets and the basal half of the main cusp. Thus, the main differences of the Gometxa material with *S. filipi* are in the crown ornamentation, stronger in the former, and in having less and blunter cusplets. By its general morphology, the teeth from Gometxa are closely related with those classified as *Synechodus* aff. *filipi* by Siversson et al. (2016: Figs. 10C–D), which show stronger enameloid ornamentation and blunter cusplets. The teeth of this taxon are easily distinguished from those of *Synechodus faxensis* by having a smaller size and a coarse irregular ornamentation of the crown, and by lacking the pseudopolyaulacorhize arrangement of the root.

Superorder SQUALOMORPHII Compagno, 1973

Order SQUATINIFORMES Buen, 1926

Family SQUATINIDAE Bonaparte, 1838

Genus *SQUATINA* Duméril, 1806

Subgenus *CRETASCYLLIUM* Müller and Diedrich, 1991

Type species. *Squatina cranei* Woodward, 1888; upper middle to lower upper Cenomanian, Grey Chalk subgroup, from Clayton (Sussex, UK).

The subgenus *Cretascyllum* was proposed by Guinot et al. (2012b) to define those squatinid sharks with clear heterodont dentition, including in this rank the species *Squatina cranei* Woodward, 1888 and *Squatina hassei* Leriche, 1929. The name of the subgenus comes after the junior synonym of the species *Cretascyllum expansum* Müller and Diedrich (1991). The teeth of this subgenus are easily distinguished from those of the extant species *Squatina* (*Squatina*) *squatina* (Linnaeus, 1758), as stated by Guinot et al. (2012b), by the following: (i) their strong heterodonty; (ii) anterior teeth higher than wide with a crown roughly triangular in outline; (iii) anterolateral and lateral teeth wider than high, and labiolingually compressed; (iv) heels weakly developed or

absent in anterior teeth, but well-developed in anterolateral and lateral ones; (v) anterior teeth with a labiolingually compressed, heart-shaped root that have a large lingual protuberance with a wide central foramen and two lingual foramina on each side; and (vi) lateral teeth having a well-developed root with slightly oblique branches pierced by numerous marginolingual foramina.

Squatina (Cretascyllium) hassei Leriche, 1929

Figs. 11.11I–L

For the synonymy see Guinot et al. (2012b).

Material. Two teeth from lithofacies-1, MCNA 15612 and another catalogued specimen.

Locality. Gometxa in Vitoria-Gasteiz municipality, Álava (Basque Country, Spain).

Age. Lower upper Campanian (*G. aegyptiaca* zone).

Description. The MCNA 15612 specimen is a broken and incomplete anterolateral tooth of small-to-medium size. It possesses a high, slightly inclined cusp that broadens basally and narrows apically. The apex is chipped. The continuous cutting edge of the main cusp extends laterally, creating a pair of low lateral heels, although the proximal one is practically missing (broken off recently). The main cusp is sigmoid in profile view (Fig. 11.11L). The labial face is markedly less convex than the lingual one, being both faces smooth. A well-developed rounded apron is present on the labial face, basally. The relatively poor preservation of the root does not prevent from observing that it is low, and extends horizontally. Moreover, a pair of pits, which are flanking the lingual root protuberance near the crown–root boundary, may be the remnants of two foramina.

Remarks. Despite the relatively poor preservation of the figured tooth, both the shape of the cusp and that what remains of the root indicate that this specimen belongs to *Squatina (C.) hassei* Leriche, 1929. The teeth *S. hassei* are very similar in their general appearance to those of *S. cranei*, especially the anterior ones, but anterolateral and lateral teeth clearly differ from the latter, among other features, in possessing horizontal to subhorizontal root branches, lower heels, and a parallel-sided labial apron often projected over the root base, as stated in Guinot et al. (2012b).

The species *Squatina (C.) hassei* was described by Leriche, 1929 from a Maastrichtian carbonate-dominated succession of the Maastricht Formation at Maastricht, Dutch Limburg (Netherlands), and subsequently reported by Geyn (1937). Its presence has been also noticed in other localities of Belgium by Herman (1977), who reported it in the upper Maastrichtian white chalks of the Liege-Limburg Region (near the stratotype area) and in the Jauche Member (= Tuffeau d'Orp-le-Grand), cropping out at Orp-Jauche, Brabant (East Belgium). Another documented occurrence of this taxon is in the Maastrichtian of Morocco (Noubhani and Cappetta, 1997).

Squatina (C.) hassei has been found in the Campanian of the North German Basin near Hannover in North Germany (Schneider and Ladwig, 2013) and the Liege-Limburg Basin at Aachen in westernmost Germany (Albers and Weiler, 1964). Herman

(1973, 1977) also found the species in the Campanian of the Mons Basin (Obourg Chalk and Trivières Chalk formations), province of Hainaut (SW Belgium). Vullo (2005) described *Squatina* cf. *hassei* from the upper Campanian (CIV and CV) of Le Pilou and Le Caillaud (Charente-Maritime, France), which has been referred to *S. (C.) hassei* by Guinot et al. (2012b). The latter authors have also reported this species generally distributed across several fossil sites in the Anglo-Paris Basin, spanning the lower Santonian (e.g. Berkshire, UK) through lower upper Campanian (e.g. Hampshire in the UK; Ardennes, Aisne, and Marne in France). Other possible occurrences are in the lower Campanian of the Münster Basin in west Münsterland, Westphalia (NW Germany), where an incomplete tooth has similarities with *S. (C.) hassei*, according to Hübner and Müller (2010).

The marine phosphate-rich deposits deposited during the Campanian in Israel are also reported to contain *S. hassei* (Lewy and Cappetta, 1989). Moreover, the Campanian Foremost Formation in southeastern Alberta (Canada) and, possibly, the Campanian turbiditic deposits of the Gamma Member (Santa Marta Formation) in the James Ross Island (Antarctica) are points where the species has been found (Peng et al., 2001; Richter and Ward, 1990; respectively).

Some tooth specimens described by Lauginiger and Hartstein (1983) from the Marshalltown and Mount Laurel formations (aged upper to uppermost Campanian, respectively) in Delaware, USA, and by Cappetta and Case (1975b) from the Mount Laurel Formation (aged uppermost Campanian) in the New Jersey Coastal Plain, eastern North America, USA, have also been referred to *S. hassei*. But according to Guinot et al. (2012b), they are likely to belong to different species within the Orectolobiformes.

Superorder BATOMORPHII Cappetta, 1980a

Order RAJIFORMES Berg, 1940

Family PARAPALAEOBATIDAE Cappetta, 1992

Genus *PARAPALAEOBATES* Weiler in Stromer and Weiler, 1930

Type species. Strophodus pygmaeus Quaas, 1902; lower Maastrichtian of Gasr, Dachel Oasis, Libyan Desert, Egypt.

Parapalaeobates pygmaeus (Quaas, 1902)

Fig. 11.12

1902 *Strophodus pygmaeus*; Quaas, p. 312, Pl. XXVII, Figs. 16–18.

1920 *Cestracion pygmaeus* (Zittel in Quaas, 1902); Gemmellaro, p. 158, Pl. 1, Figs. 1–7.

1930 *Parapalaeobates pygmaeus* (Quaas); Stromer and Weiler, p. 17, Pl. II, Figs. 14–18; Pl. IV, Fig. 7.

1943 *Parapalaeobates* cf. *pygmaeus* (Quaas); Darteville and Casier, p. 180, Pl. XI, Figs. 26, 28.

1991 *Parapalaeobates pygmaeus* (Quaas); Landemaine, p. 11, Pl. 2, Figs. 1–5.

2001 *Parapalaeobates* sp.; Zalmout and Mustafa, p. 400, Pl. 6, Figs. 5–8.

2002 *Parapalaeobates pygmaeus* (Quaas); Mustafa et al., p. 434, Figs. 6.5–6.

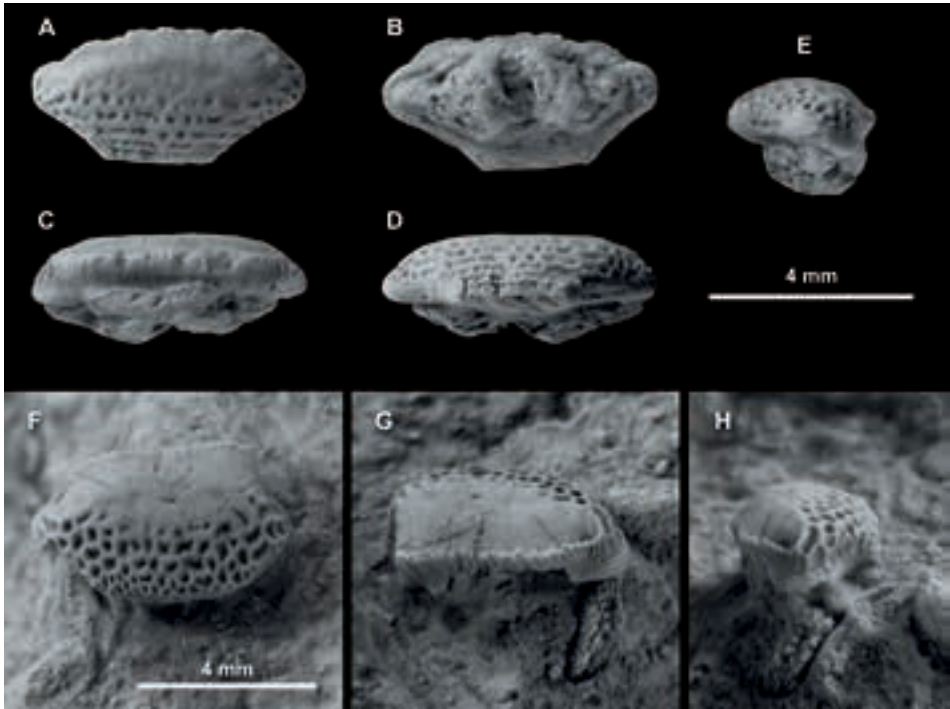


Figure 11.12 *Parapalaebates pygmaeus* (Quaas, 1902) from lithofacies-2, A–E, lateroposterior tooth in occlusal (A), basal (B), lingual (C), labial (D), and profile (E) views, MCNA 10499; F–H, lateral tooth in occlusal (F), lingual (G), and profile (H) views, OIGM-GM13.

Material. Four teeth, OIGM-GM13 from lithofacies-2; MCNA 10499 and two other fragmentary specimens from lithofacies-1.

Locality. Gometxa in Vitoria-Gasteiz municipality, Álava (Basque Country, Spain).

Age. Lower upper Campanian (*G. aegyptiaca* zone).

Description. The specimens reach a maximum mesodistal width of 5.75 mm. These teeth have a convex crown, displaying a roughly hexagonal face in occlusal view. This face is strongly ornamented in the anterior (labial) half with an alveolar decoration formed by several small polygonal pits (Figs. 11.12A, F). A well-developed labial apron overhangs the root (Fig. 11.12D). The vestige of a broad central uvula is visible on the lingual face of the crown in the specimen MCNA 10499 (Fig. 11.12C). Two large foramina open on the lingual root face, one on each side of the uvula (Fig. 11.12C). The holaulacorhize root has two broad lobes separated by a deep furrow (Fig. 11.12B). The specimen OIGM-GM13 is a lateral tooth that displays parallel vertical folding at the base of the crown on the lingual face (Fig. 11.12G).

Remarks. The genus *Parapalaebates* is a member of Rajiformes with specialised, crushing-grinding dentition (Cappetta, 1992). Arambourg (1952: 2014) described

the species *Parapalaeobates atlanticus* Arambourg, 1952 from the Maastrichtian of Morocco on the basis of teeth that showed a regularly convex crown with a honeycomb ornamented occlusal (oral) face lacking a transverse crest. According to Cappetta (2012), the species may be a junior synonym of *Parapalaeobates pygmaeus*. In fact, the transverse crest may appear only on some specimens, and Quaas (1902) himself took this feature into account when described the species.

The Upper Cretaceous genus *Parapalaeobates* is mainly restricted to northern and central Africa, Middle East, Central Asia, and Madagascar, being most often found in Campanian to Maastrichtian rocks (Cappetta, 2012). Averianov and Nessov (1995: Table 1) listed the presence of *Parapalaeobates* cf. *glickmani* Nessov, Mertiniene and Udovichenko in Nessov and Udovichenko, 1986 at the base of the Darbasa Formation (lower?–lower upper Campanian) in southern Kazakhstan. *Parapalaeobates atlanticus* is reported from upper Santonian to Maastrichtian age deposits of the Angolan exclave of Cabinda and the Bas-Congo in the Democratic Republic of the Congo (Dartevelle and Casier, 1959; Taverne, 1970), and from the Maastrichtian of Morocco (Arambourg, 1952; Noubhani and Cappetta, 1997). Cappetta (2012) also reported unassigned material to the genus *Parapalaeobates* from the Campanian of Morocco. In western Europe, the only record of *Parapalaeobates pygmaeus* was until now in the Santonian of Dordogne, France (Landemaine, 1991). These upper Campanian specimens from Gometxa increase the known geographical distribution of the species.

Suborder RHINOBATOIDEI Fowler, 1941
Family RHINOBATIDAE Müller and Henle, 1838
Genus RHINOBATOS Link, 1790

Type species. *Raja rhinobatos* Linnaeus, 1758; Recent, Genoa and Venice, Italy.

Rhinobatos casieri Herman, in Cappetta and Case, 1975b
Figs. 11.13A–I

Material. Two teeth from lithofacies-1, MCNA 15607 and MCNA 15608.

Locality. Gometxa in Vitoria-Gasteiz municipality, Álava (Basque Country, Spain).

Age. Lower upper Campanian (*G. aegyptiaca* zone).

Description. The specimens are small, about 1 mm in mesiodistal width. The oral face of the crown is keeled and weakly cuspidate. A transverse occlusal crest is split into labial and lingual segments to produce a triangle-shaped margino-occlusal face on each side of the crown (Fig. 11.13A). The labial outline of the crown is gently curved. Marginal edges of the crown are parallel with no or very weak marginal constrictions. The median uvula is rather long and round-ended, having lateral edges subparallel (Figs. 11.13A, F). The lateral (i.e. marginal) uvulae are wider, much shorter, and also round ended. A prominent notch separates the medial uvula from the lateral uvulae. The crown is triangle-shaped in profile view (Fig. 11.13B). The root–crown edge is

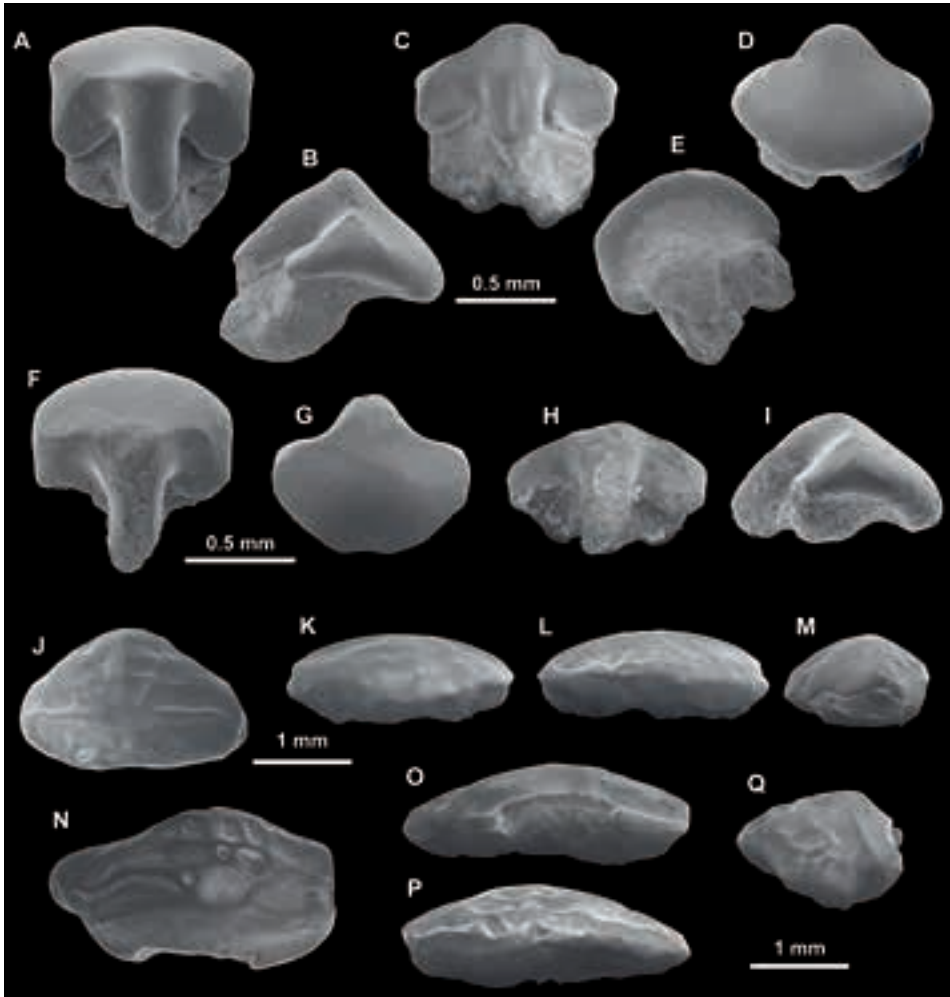


Figure 11.13 A–I, *Rhinobatos casieri* Herman, in Cappetta and Case, 1975, A–E, lateroanterior tooth in occlusal (A), profile (B), lingual (C), labial (D), and oblique basal (E) views, MCNA 15607; F–I, lateroanterior tooth in occlusal (F), labial (G), lingual (H), and profile (I) views, MCNA 15608. J–Q, *Ptychotrygon* sp., J–M, anterior tooth in occlusal (J), lingual (K), labial (L), and profile (M) views, MCNA 15617; N–Q, lateral tooth in occlusal (N), lingual (O), labial (P), and profile (Q) views, MCNA 15618. All from lithofacies-1.

rounded and labially overhangs the root to form a broad visor. The root, which is projected lingually when viewed on profile, is bilobed, being the branches separated by a deep nutritive groove. There is, at least, a pair of large foramina on the lingual face of the root, one on each marginolingual side.

Remarks. Although small, the specimens from Gometxa are morphologically similar to the teeth of *R. casieri* figured elsewhere. Herman first described *R. casieri* in

1973 using specimens from Loncée in Namur, Belgium (Santonian, Glauconie de Loncée Formation), Hainaut, Belgium (lowermost upper Campanian, Obourg Chalk Formation), and Aachen, Germany (lower Campanian, Vaals Formation), but it was not until later, in 1975, that the species became scientifically available (Cappetta and Case, 1975b). Previously, Albers and Weiler (1964) seemed to have found this taxon in the Campanian of Aachen in the Liege-Limburg Basin (Germany) without giving the teeth a species name, according to Cappetta and Case (1975b). The specimen *R. echavei* described by Vullo (2005) from western France (Le Pilou and Meschers sites; upper Campanian) should probably be referred to as *R. casieri* on the basis of their occlusal morphological characters, especially the presence of a transverse crest, depressed marginal regions, and the shape of the notches that separate the medial uvula from the lateral ones. The lack of a clear cusped crown may be due to wearing. Several specimens of the same species have been recently reported by Guinot et al. (2012a) from the lower Campanian (*Offaster pilula* zone) of northern France (Faucouzy and Hallencourt in the Aisne and Somme departments, respectively) and by Underwood and Ward (2008) in lower Campanian calcarenite rocks from Downend, in Hampshire (UK). The species is also present in the Campanian of the Kristianstad Basin in southern Sweden, according to Sørensen et al. (2013). *Rhinobatos seruensis* Guinot et al., 2012a is another rhinobatid from the Anglo-Paris Basin, but its teeth can be easily differentiated from those of *R. casieri* in having a short occlusal crest that reaches the marginolingual areas in addition to a wider medial uvula. Some *Rhinobatos* specimens from the upper lower Campanian of the Kristianstad Basin in Sweden have been referred to as well to the species *R. casieri* (Sørensen et al., 2013).

Rhinobatos casieri is also known from the Campanian of the Western Interior Seaway of North America, from Canada to Texas. This species is a relevant element of the elasmobranch assemblage found in the Milk River area, southeastern Alberta, Canada (Peng et al., 2001). These elasmobranchs, which are associated with mollusc invertebrates, lie within a silty sandstone and interbeds of finely laminated mudstone of the Foremost Formation. This lithostratigraphical unit was deposited during the upper Campanian in shallow marine settings within a regressive phase of the Judith River Group (McNeil et al., 1995). Case (1987) has also reported the presence of *R. casieri* within the upper Campanian Teapot Sandstone Member of the Mesaverde Formation in north Wyoming, USA. The Teapot Sandstone Member represents a deltaic environment and includes both marine and nonmarine lithologies which were deposited in delta plain, delta front, and prodelta settings (Anna, 2009).

The teeth of *Rhinobatos* sp., described by Schubert et al. (2016) from the Aguja Formation (upper Campanian) in West Texas, resemble those attributed to *R. casieri*, according to the authors. Some specimens from Texas referred to as *R. casieri* by Welton and Farish (1993) belong, in fact, to the Maastrichtian species *R. uvulatus* Case and Cappetta, 1997 on the basis of their low crown and the poor development of the marginal uvulae with respect to the medial one, according to the authors who erected

the latter species from coeval strata of the Kemp Clay Formation in Texas, USA. In the Atlantic and Gulf Coastal Plains, the species *R. casieri* was reported by Cappetta and Case (1975b) as occurring in the Campanian of New Jersey (USA). Moreover, *R. casieri* is present in the Campanian of South Carolina, USA, according to Cicimurri (2007), where the Donoho Creek Formation has yielded a diverse selachian assemblage representing different species that inhabited the subaqueous part of a delta.

Suborder SCLERORHYNCHOIDEI Cappetta, 1980a
Family PTYCHOTRYGONIDAE Kriwet, Nunn and Klug, 2009
Genus PTYCHOTRYGON Jaekel, 1894

Type species. *Ptychodus triangularis* Reuss, 1845; Upper Cretaceous, Turonian, Kosstitz and southern foot of Boren hills, near Bílina, northwest Bohemia, Czech Republic.

Ptychotrygon sp.
Figs. 11.13J–Q

Material. Two teeth from lithofacies-1, MCNA 15617 and MCNA 15618.

Locality. Gometxa in Vitoria-Gasteiz municipality, Álava (Basque Country, Spain).

Age. Lower upper Campanian (*G. aegyptiaca* zone).

Description. Teeth of small size. An anterior tooth (Figs. 11.13J–M) has a crown that is mesiodistally elongated and roughly triangular in occlusal view (Fig. 11.13J). Three vague mesiodistally oriented crests – obscured by abrasion – extend across the labial crown face, being the main crest the longest and mid-located. Additional small ridges, transversal to the crests, give an irregular vermiculated pattern in the labial region. The crown is dome-shaped on profile view (Fig. 11.13M). A lateral tooth (Figs. 11.13N–Q) has an oval-shaped crown. It is mesiodistally wider than labiolingually, and shows margino-lingual and margino-labial constrictions on the only preserved margin. Transverse crest are fairly raised. The crown ornamentation consists of irregular, vermiculate rugae on the labial region of the crown, below the main transverse crest. The highly abraded state of these teeth prevents from making any comments on the anatomical characteristics of the root.

Remarks. *Ptychotrygon* is a genus with a temporal range from upper Albian through Maastrichtian (Cappetta, 2012). The oldest known *Ptychotrygon* batoid is *Ptychotrygon geyeri* Kriwet, 1999a, collected in the upper Albian (uppermost part of the Utrillas Formation) of the Iberian Range in the east of Spain. Further prospecting fieldwork by Kriwet et al. (2009) in the Aliaga Sub-basin, Teruel (eastern Spain) produced the discovery of a younger elasmobranch deposit in the lower Cenomanian (Mosqueruela Formation) including isolated teeth of *Ptychotrygon geyeri*, *P. pustulata*, *P. striata*, and one unassigned species (*Ptychotrygon* sp.). The species *P. geyeri* is also known to occur in the upper Albian of Asturias (North Spain), and *Ptychotrygon slaughteri* Cappetta

and Case, 1975a is present in relatively younger deposits of the same area (lower Cenomanian: La Manjora Formation), as stated in Bernárdez (2002). *Ptychotrygon triangularis* (Reuss, 1845) has been described by Herman (1977) from the Cenomanian of Portugal and the Turonian of the Czech Republic and Nord Department in France. An unassigned species of the genus *Ptychotrygon* occurs in the Santonian of Vendée, Western France, according to Cappetta (1981).

Several species, some of which endemic to one particular locality, have been described in different areas of North America, including the Western Interior Basin, Western Texas, Arkansas, Alabama, and the Gulf Coastal Plain. *P. slaughteri* Cappetta and Case, 1975a is the oldest known North American representative of the genus, occurring in the Cenomanian Woodbine Formation of Texas (see also Cappetta and Case, 1999). *Ptychotrygon triangularis*, cooccurring with *Ptychotrygon ledouxi*, is also known from the Turonian Carlile Shale of South Dakota (Cappetta, 1973). *Ptychotrygon triangularis* is also found in the Turonian Atarque Sandstone Member of the Tres Hermanos Formation in New Mexico, a unit formed by near-shore calcareous sandstone with shale interbeds (Wolberg, 1985).

Ptychotrygon eutawensis Case et al., 2001b was first discovered in the Eutaw Formation (lower to middle Santonian) of Georgia, USA, and it has been additionally recorded by Bourdon et al. (2011) in the Santonian of New Mexico, USA. The teeth of this species possess generally a triangular outline in occlusal view; however, the presence of vermiculate rugae on the lingual region of the crown is not reported in *P. eutawensis*.

Among the species assigned to *Ptychotrygon*, the following are known to occur in Campanian strata, according to Case and Cappetta (1997) and Cappetta and Case (1999): *P. agujaensis* McNulty and Slaughter, 1972; *P. blainensis* Case, 1978; *P. boothi* Case, 1987; *P. cuspidata* Cappetta and Case, 1975b; *P. ellae* Case, 1987; *P. greybullensis* Case, 1987; and *P. vermiculata* Cappetta, 1975b. The teeth of *P. blainensis*, which are found in the Judith River Formation in Montana (USA), are easily differentiated from those of Gometxa by having a high cuspidate crown with a basilo-labial bulge, two transverse crests, and distinctive striated enameloid ornamentation on the labial face. *P. boothi*, *P. ellae*, and *P. greybullensis* are reported to occur in the upper Campanian Mesaverde Formation of Wyoming (USA), but the teeth of all these three species are easily differentiated from those of Gometxa by lacking the particular vermiculated pattern on the crown.

Many well preserved teeth of *Ptychotrygon* have been described from several uppermost Cretaceous localities across Texas in USA (see McNulty and Slaughter, 1972; Welton and Farish, 1993; Case and Cappetta, 1997). Recently, Schubert et al. (2016) have described several forms from a fossil-rich Campanian site in the Aguja Formation of West Texas. There, the cooccurring species are: *P. agujaensis*, *Ptychotrygon* aff. *P. cuspidata*, *Ptychotrygon triangularis*, and one unassigned species within the genus *Ptychotrygon*. The species *P. agujaensis* is identified – after the original diagnosis – by having teeth with a low and rounded crown, with an apparent main keel and several

closely spaced, low and rounded, transverse corrugations on the labial face. The Campanian teeth of *P. triangularis* are distinguished in having triangular crowns with three coarse, relatively distant transverse ridges on the labial face and smaller corrugations on the lower labial area. Due to their high cusp morphology, the teeth of neither the unassigned *Ptychotrygon* species nor the taxon that is systematically close to *P. cuspidata* can be related to those of Gometxa in the Vitoria Sub-basin.

P. vermiculata is a distinctive species that occurs with *P. cuspidata* in Campanian rocks of the Atlantic and Gulf Coastal Plains (USA). Cappetta and Case (1975b) fully described teeth of this species in the Mount Laurel Formation (aged uppermost Campanian) of the New Jersey Coastal Plain, eastern North America. According to Cicimurri (2007), *P. vermiculata* is present in the Campanian Donoho Creek Formation of South Carolina. Moreover, Lauginiger and Hartstein (1983) found *P. vermiculata* in the Marshalltown Formations (aged upper Campanian) of Delaware.

The youngest representatives of *Ptychotrygon* are known from the Maastrichtian of South Dakota (Becker et al., 2004), Arkansas (Becker et al., 2006), and Texas (Case and Cappetta, 1997) in North America (USA), where several teeth of *P. vermiculata* and *Ptychotrygon* cf. *P. vermiculata* have been reported. Moreover, *P. vermiculata* cooccurs in Texas with *Ptychotrygon winni* Case and Cappetta, 1997, whose teeth are distinct in having sharp cuspidate crowns, strongly triangular in occlusal view, with a well-marked keel and undulating transverse ridges in their labial face.

Contrarily to the many North American and European occurrences, the African record of the genus is scarce, and *Ptychotrygon henkeli* Werner, 1989 from the upper Cenomanian (Gebel Dist Member of the Bahariya Formation) of Egypt is the only species so far found.

Clearly, the overall shape of the crown in the Gometxa material allows an assignment to the genus *Ptychotrygon*, and therefore, these specimens are the youngest occurrence of the genus in Western Europe. Although the teeth from Gometxa differ from all the above species in having coarser vermiculate ornamentation, the specimen MCNA 15617 (Figs. 11.13J, M) can be compared to that of *P. triangularis* described by Schubert et al. (2016: Fig. 7.15). However, the scarcity and poor preservation of the material prevents a confident assignment to such species, and thus, until new material becomes available, the Gometxa specimens are referred to *Ptychotrygon* sp. indet.

Chapter 12
NEOSELACHIANS FROM THE VITORIA PASS SITE (EGUILETA MEMBER,
UPPER CAMPANIAN)

12.1 Introduction

The previous chapter reviewed the elasmobranch description of the lowermost upper Campanian. Here I will consider various anatomical and taxonomic issues relating to a younger assemblage of lamniform and carcharhiniform sharks found at Vitoria Pass site and referred to the Eguileta Member (EM) of the Montes de Vitoria Formation (in the B-CB). These strata have also yielded an ammonite fauna readily assignable to the upper Campanian (see Chapter 6). Selachians are the most common marine vertebrates in this geologic unit. The faunal remains include some lamniform semipelagic elements, also reported from the relatively older Gomecha Member (GM). But, contrary to the latter site, selachian taxa of deeper open-water regions are lacking in the EM. An ecological change in the marine environment is a major reason for this, as sedimentology and cooccurring fossil macroinvertebrates have revealed. The fossiliferous horizons of the EM indicate lower species richness comparing to the younger assemblages of the GM, but this is because bulk sampling has not yet been made. The fossils here examined are housed in the Arabako Natur Zientzien Museoa/Museo de Ciencias Naturales de Álava (MCNA) and the Luberri-Oiartzungo Ikasgune Geologiko Museoa (OIGM).

12.2 Systematic palaeontology

- Class CHONDRICHTHYES Huxley, 1880
- Subclass ELASMOBRANCHII Bonaparte, 1838
- Cohort EUSELACHII Hay, 1902
- Subcohort NEOSELACHII Compagno, 1977
- Superorder GALEOMORPHII Compagno, 1973
- Order LAMNIFORMES Berg, 1958
- Family ANACORACIDAE Casier, 1947
- Genus *SQUALICORAX* Whitley, 1939

Type species. *Corax pristodontus* Agassiz, 1843; Maastrichtian of Maastricht, Netherlands.

Squalicorax ex gr. *kaupi* (Agassiz, 1843)

Figs. 12.1–2

For the synonymy see Siverson (1992), Antunes and Cappetta (2002), and Vullo (2005).

Material. Fifty teeth, including OIGM-GM3, MCNA 3622, MCNA 3675, MCNA 3677, MCNA 5217, MCNA 10551, MCNA 10553, MCNA 10554, MCNA 10555, MCNA 10556, MCNA 10557, MCNA 10562, MCNA 13936, and MCNA 13946.

Locality. Vitoria Pass: Castillo-Gardelegi in the municipality of Vitoria-Gasteiz, Álava (Basque Country, Spain).

Age. Upper Campanian (*G. gansseri* zone, *Rugoglobigerina rotundata* subzone).

Description. The general morphology of these anacoracid teeth has been well described in the previous chapter, so I will not reiterate on it here, except to make the point that large morphotypes may exhibit some folds in the mid-basal region of the labial (Figs. 12.1B, H) and lingual (Fig. 12.1A) faces of the crown. Moreover, the crown is straight, or curved to a small degree, in profile view. The general contour of the mesial edge of the crown is gibbous, regularly convex, but occasionally it is modified in some specimens by having a notch in the midway (Fig. 12.1A), or a slightly recurved apex in others (Figs. 12.1J, K).

Remarks. The classification of this material is still unsatisfactory, and is tentatively assigned to the *S. kaupi* group, pending the needed revision of the *Squalicorax* species (see Siverson et al., 2007). Despite their varied morphology, the teeth commonly attributed to the species *Squalicorax kaupi* (Agassiz, 1843) are characterised by having a crown with a relatively straight distal cutting edge and a more or less developed distal heel separated from the main cusp by a deep notch. On the basis of these features, many specimens from the Vitoria Pass section may easily be assigned to *Squalicorax* ex gr. *kaupi*. However, some other specimens from the same beds lack the distal heel, and hence the posterior cutting edge runs continuously from apex to base, forming a concave outline in labial/lingual view. Despite of that, the latter tooth-design is easily distinguishable from that found in *S. pristodontus* (see Cappetta, 2012).

It is noticeable the presence of large-sized teeth of *Squalicorax* in the EM (Figs. 12.1A–I). However, the current state of knowledge does not allow an easy assignment of these specimens, as they may either correspond to fully grown adults or to a different species, the latter of which is regarded plausible by Einarsson et al. (2010) when they validated the species *S. lindstromi* erected by Davis (1890). The teeth of the latter differ from those of the Maastrichtian species *S. pristodontus* in having proportionally higher roots and crenations (serrations) more evenly distributed along the cutting edges of the crown. Teeth of *Squalicorax* ex gr. *kaupi* not only are frequently collected in exposures of the Eguileta Member, but they commonly occur in the Gomecha Member of the Vitoria Formation (see Ch. 11). The species *S. kaupi* has been found in many Campanian and Maastrichtian deposits worldwide as mentioned in the previous chapter (see also Table 17.2 in Ch. 17), but as anticipated, the taxon may include several species yet to be established.

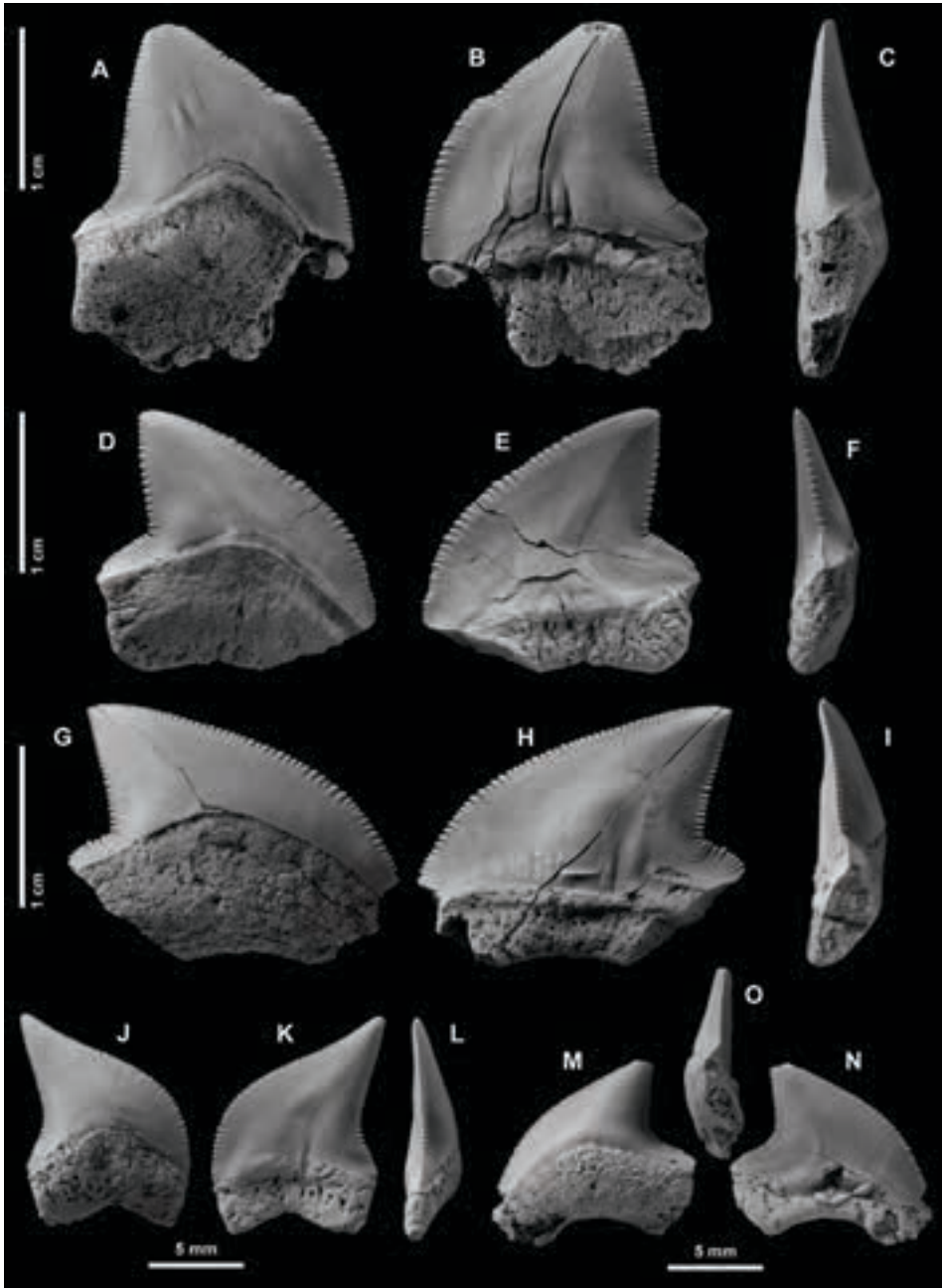
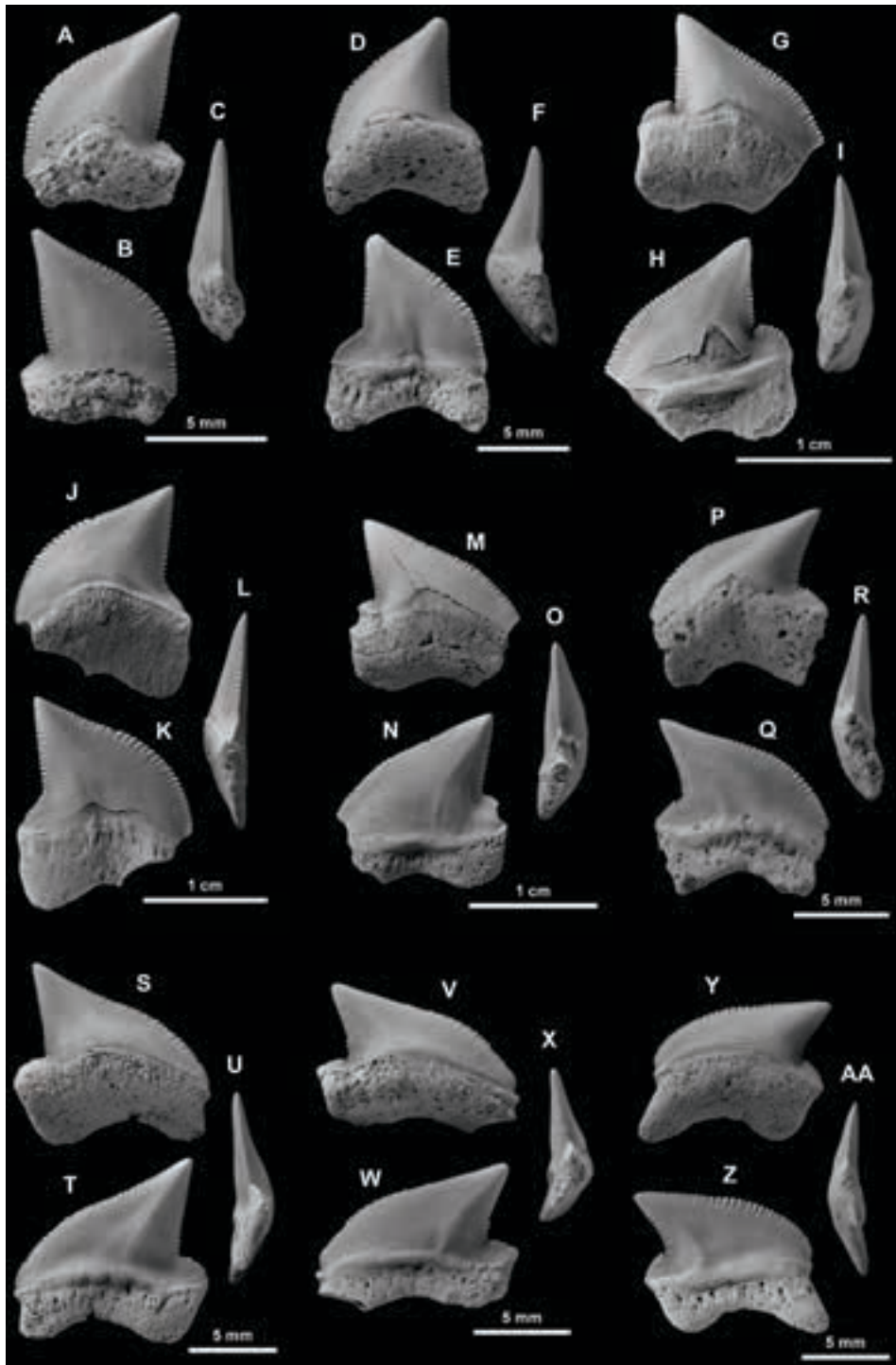


Figure 12.1 *Squalicorax* ex gr. *kaupi* (Agassiz, 1843). A–C, anterolateral tooth in lingual (A), labial (B), and distal (C) views, MCNA 5217; D–F, lateral tooth in lingual (D), labial (E), and distal (F) views, MCNA 3675; G–I, lateral tooth in lingual (G), labial (H), and mesial (I) views, MCNA 10557; J–L, anterolateral tooth in lingual (J), labial (K), and (L) views, MCNA 10553; M–O, lateral tooth in lingual (M), labial (N), and (O) views, MCNA 13946.



Family ODONTASPIDIDAE Müller and Henle, 1839
Genus *CARCHARIAS* Rafinesque, 1810

Type species. *Carcharias taurus* Rafinesque, 1810; Recent, Sicily, Italy.

For the discussions concerning the taxonomical status of this genus see Ward (1988).

Carcharias adneti Vullo, 2005
Fig. 12.3

2001 *Carcharias* sp.; Cappetta and Odin, p. 650, Pl. 1, Fig. 5.

2005 *Carcharias adneti*; Vullo, p. 618, Figs. 4D–L.

2013 *Carcharias adneti*; Guinot et al., p. 58, Figs. 20E–Z.

Material. Seven teeth, including MCNA 5655, MCNA 5665, MCNA 10542, and MCNA 14241.

Locality. Vitoria Pass: Castillo-Gardelegi in the municipality of Vitoria-Gasteiz, Álava (Basque Country, Spain).

Age. Upper Campanian (*G. gansseri* zone, *Rugoglobigerina rotundata* subzone).

Description. The species can be diagnosed, as stated in Vullo (2005), by the following characteristic features: (i) small-sized teeth, upper lateral teeth are broader than anterior ones and have a labiolingually compressed crown; (ii) cutting edges of teeth smooth, main cusp flanked by one pair of lateral cusplets; (iii) labial face of the main cusp smooth, while lingual face with faint and irregular vertical folds not reaching the apex; (iv) root lobes narrow and arched; and (v) basal outline vary depending on the tooth types. Anterior teeth have a relatively narrow, nearly symmetrical, main cusp in labial/lingual view (Figs. 12.3A, E) flanked by two pointed, awl-shaped lateral cusplets. In profile the main cusp is sigmoidal (tip recurved labially) (Figs. 12.3C, G). The labial face is flat and smooth, while the lingual face is convex and ornamented with many faint folds in the lower mid part. Enameloid shoulders, which may have short vertical ridges, extend onto the root lobes (Fig. 12.3C). The crown–root boundary is well-marked by a neck on the lingual side, while on the labial side there is an arched bulge that overhangs the root (Figs. 12.3B, L). The root is bilobate with long, round-ended lobes. The lingual protuberance of the root is pronounced and bears a long nutritive groove. The basal outline of the root forms a pointed arch in labial/lingual view (Figs. 12.3B, L).

- ◀ **Figure 12.2** *Squalicorax* ex gr. *kaupi* (Agassiz, 1843). A–C, anterolateral tooth in lingual (A), labial (B), and distal (C) views, MCNA 13936; D–F, anterolateral tooth in lingual (D), labial (E), and distal (F) views, MCNA 3622; G–I, lateral tooth in lingual (G), labial (H), and distal (I) views, MCNA 3677; J–L, lateral tooth in lingual (J), labial (K), and distal (L) views, MCNA 10556; M–O, lateral tooth in lingual (M), labial (N), and distal (O) views, OIGM-GM3 (Gorka Martin coll.); P–R, lateral tooth in lingual (P), labial (Q), and distal (R) views, MCNA 10555; S–U, lateral tooth in lingual (S), labial (T), and distal (U) views, MCNA 10554; V–X, posterolateral tooth in lingual (V), labial (W), and distal (X) views, MCNA 10562; Y–AA, posterolateral tooth in lingual (Y), labial (Z), and distal (AA) views, MCNA 10551.



Figure 12.3 *Carcharias adneti* Vullo, 2005. A–D, anterior tooth in lingual (A), labial (B), profile (C), and basal (D) views, MCNA 5665; E–H, anterior tooth in lingual (E), labial (F), profile (G), and basal (H) views, MCNA 5655; I–J, lateral tooth in lingual (I) and labial (J) views, MCNA 14241; K–N, anterior tooth in lingual (K), labial (L), profile (M), and basal (N) views, MCNA 10542.

One upper lateral specimen, MCNA 14241 (Figs. 12.3I–J), has a triangular cusp, wide at its base and inclined distally, which is flanked on each side by moderately long, triangular cusplets well separated from the cusp by notches. The distal cusplet is par-

tially preserved. Both mesial and distal cutting edges are continuous, regularly curved, and run from the apex to the base of the crown. Small chipping along the cutting edges is present. The labial face is flat and smooth. The lingual face is slightly convex and bears many faint folds running vertically in the lower half. A neck is developed lingually at the crown–root boundary. On the labial side, the enamelled crown is separated from the root by a well-marked bulge. The root is short and bilobed with a lingual protuberance cut by a nutritive groove. The root lobes are labiolingually compressed. The basal outline of the root in labial/lingual view forms a wide, inverted V-shape.

Remarks. This taxon is included among those species of the genus *Carcharias* with ornamented cusps. However, surface folding is only present on the lingual face of the cusp, a diagnostic feature shared with only three other species, as stated in Vullo (2005): *C. hardingi* (Cappetta and Case, 1975b), *C. holmdelensis* (Cappetta and Case, 1975b), and *C. tenuis* (Davis, 1890). Overall tooth size, shape of the cusplets, and type of ornamentation are features that separate *C. adneti* from those species, according to Vullo (2005). Moreover, the lack of short, vertical basal folding on the labial face of the crown easily differentiates these odontaspidid teeth found at Vitoria Pass site from the species *Carcharias latus* (Davis, 1890).

The species *C. adneti* was described by Vullo (2005) from the upper Campanian (CIV) at Le Pilou cliffs, near Barzan (Charente-Maritime, France), with an additional discovery at Le Caillaud, near Tercis in the Landes department (Aquitaine region in southwest France). According to Guinot et al. (2013), one unassigned species of *Carcharias* found by Cappetta and Odin (2001) at Tercis-les-Bains in southwestern France (Aquitaine Basin) should be referred to *C. adneti*. Moreover, *C. adneti* is a common element in the Campanian selachian assemblages of the Anglo-Paris Basin (France and the UK), having been found in southeast England (Berkshire, Hampshire, Isle of Wight, and West Sussex) and northern France (departments of Ardennes, Aisne, and Marne), as stated in Guinot et al. (2013). These authors have also extended its stratigraphical range from Santonian to lowermost upper Campanian. The presence of this species in the upper Campanian rocks of northern Spain provides a southward extension of the geographical range.

Family OTODONTIDAE Glikman, 1964

Genus *CRETOLAMNA* Glikman, 1958

Type species. *Otodus appendiculatus* Agassiz, 1843; Turonian of Lewes, East Sussex (England).

Diagnostic characters of the *Cretolamna* species are discussed by Siversson et al. (2015). See comments in Chapter 11 regarding some aspects of the genus.

Cretolamna borealis (Priem, 1897)

Fig. 12.4

For the synonymy see Siversson et al. (2015).

Material. Thirty-two teeth, including MCNA 1666, MCNA 3663, MCNA 3669, MCNA 3674, MCNA 5461, and MCNA 10522.

Locality. Vitoria Pass: Castillo-Gardelegi in the municipality of Vitoria-Gasteiz, Álava (Basque Country, Spain).

Age. Upper Campanian (*G. gansseri* zone, *Rugoglobigerina rotundata* subzone).

Description. Teeth of medium to large size, measuring up to 20 mm high. Crown with smooth enameloid surfaces, and root symmetrical in basal view. The relatively symmetrical specimen MCNA 10522 has been identified as an upper anterior tooth (Figs. 12.4A–D). Its crown has an erect, triangular central cusp with a broad base. Its labial face is nearly flat, while the lingual one is convex. In profile view, the main cusp shows a faint sigmoid curvature. There is a single pair of short and robust cusplets. The lingual crown–root boundary is marked by a neck. The crown overhangs the root on the labial face by means of a faint bulge. The robust root is quite symmetrical, despite the mesial lobe appearing to be more developed than the distal one. Both lobes have round ends. Several dispersed foramina are present in the mid part of the labial face, below the labial bulge. A swollen lingual protuberance exhibits two medial foramina. The base of the root has a regular curved outline in lingual/labial view.

A lower anterior tooth (MCNA 3674; Figs. 12.4E–H) has a crown formed by a high, triangular and broadly based median cusp that is flanked by a single pair of relatively long, divergent cusplets. These are well separated from the cusp by notches. The cutting edges are continuous and quite straight in lingual/labial view. The labial face of the main cusp is flat to slightly convex with a small median fossa, basally located, whereas the lingual face is convex. Both crown faces are smooth. A well-marked, arched neck is developed at the lingual crown–root boundary. On the labial side, the crown is separated from the root by a curved edge that overhangs the root. This is quite symmetrical, and has two relatively short, flattened lobes; having a round end the distal one, and being tapered the mesial one. The lingual protuberance is not pronounced. The basal outline of the root depicts a wide, inverted U-shape, in either lingual or labial view.

Upper lateral teeth have a triangular cusp that is shorter than that of those teeth situated in anterior positions, and moreover, is distally inclined in labial/lingual view. In profile view, the central cusp is straight. Two large and divergent cusplets, one on each side, are tightly bounded to the central cusp. Specimen MCNA 3663 (Figs. 12.4I–L) shows typical crown cusplets in teeth from this position, having convex inner cutting edges, but concave outer edges when observed in labial/lingual view (Figs. 12.4I, J). A faint bulge, which is more marked on the mid part, highlights the labial crown–root boundary in the labial side. The root is slightly asymmetrical with two short, labiolingually compressed lobes and a faint lingual protuberance (better seen in basal view). The median notch of the basal edge of the root is either wide or narrow in teeth of this position.

Lower lateral teeth have a central cusp that is more slender than that of teeth from the upper row, and they are sigmoid (recurved apex) in profile view (Figs. 12.4S, W). The acute-tipped cusplets are slightly separated from the central cusp (Fig. 12.4V). As

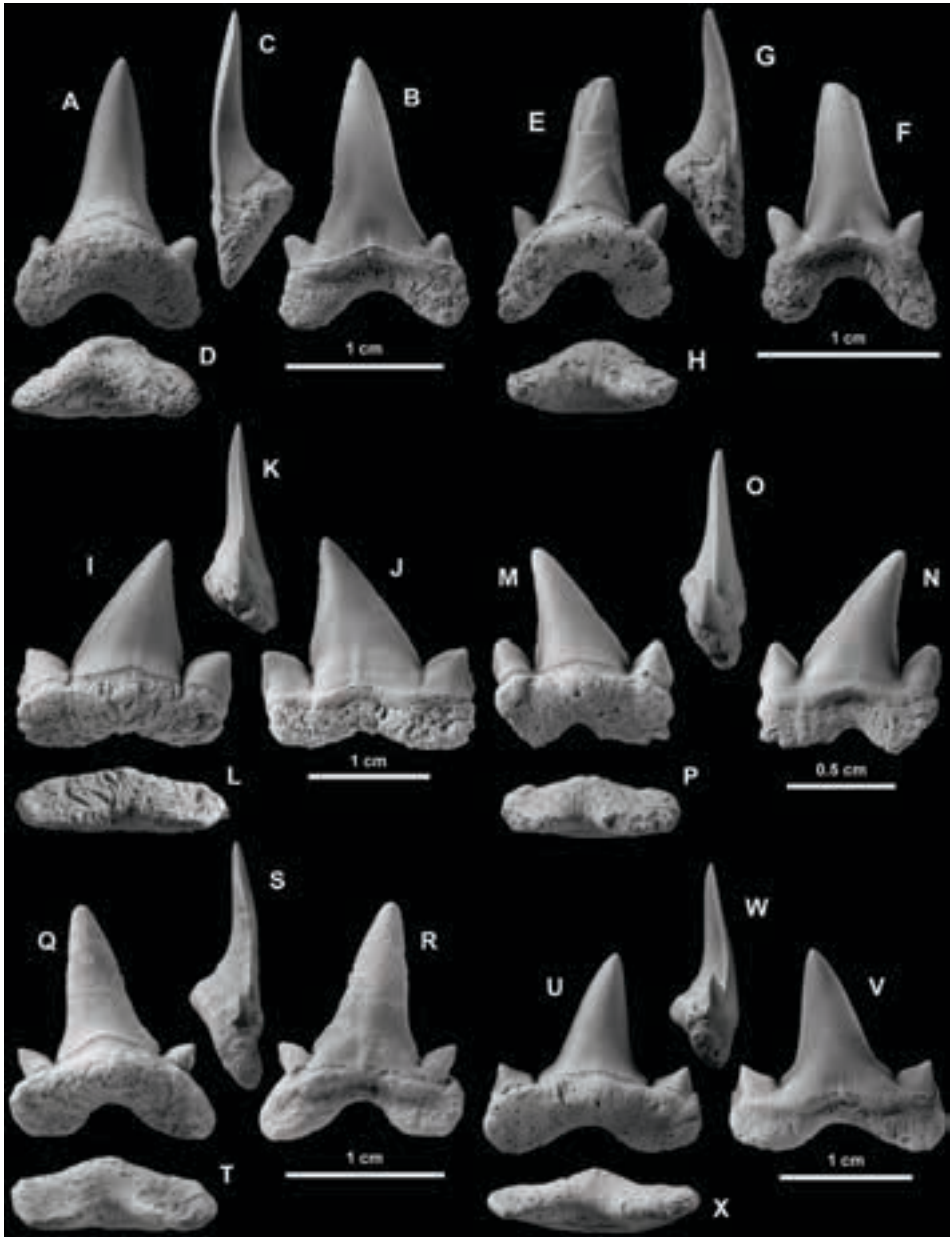


Figure 12.4 *Cretolamna borealis* (Priem, 1897). A–D, upper anterior tooth in lingual (A), labial (B), profile (C), and basal (D) views, MCNA 10522; E–H, lower anterior tooth in lingual (E), labial (F), profile (G), and basal (H) views, MCNA 3674; I–L, upper posterolateral tooth in lingual (I), labial (J), profile (K), and basal (L) views, MCNA 3663; M–P, upper posterolateral tooth in lingual (M), labial (N), profile (O), and basal (P) views, MCNA 3669; Q–T, lower anterolateral tooth in lingual (Q), labial (R), profile (S), and basal (T) views, MCNA 5461; U–X, lower posterolateral tooth in lingual (U), labial (V), profile (W), and basal (X) views, MCNA 1666.

in upper lateral teeth, a curvy crown–root boundary is observed on the labial face of the crown. The root is slightly asymmetrical with two short, labiolingually compressed lobes, being the mesial lobe thinner and longer. The basal edge of the root is characterised by being either semi-circular or semi-oval in the middle.

Remarks. The species *Cretolamna borealis* is also well represented in the Gomecha Member. Some general comments on aspects regarding the geographical and stratigraphical ranges of this species, and comparison with other closely related species, have been stated in Chapter 11 (in the species remarks) and will not be repeated here.

Cretolamna sarcoportheta Siversson, Lindgren, Newbrey, Cederström, and Cook, 2015
Figs. 12.5–6

For the synonymy see Siversson et al. (2015).

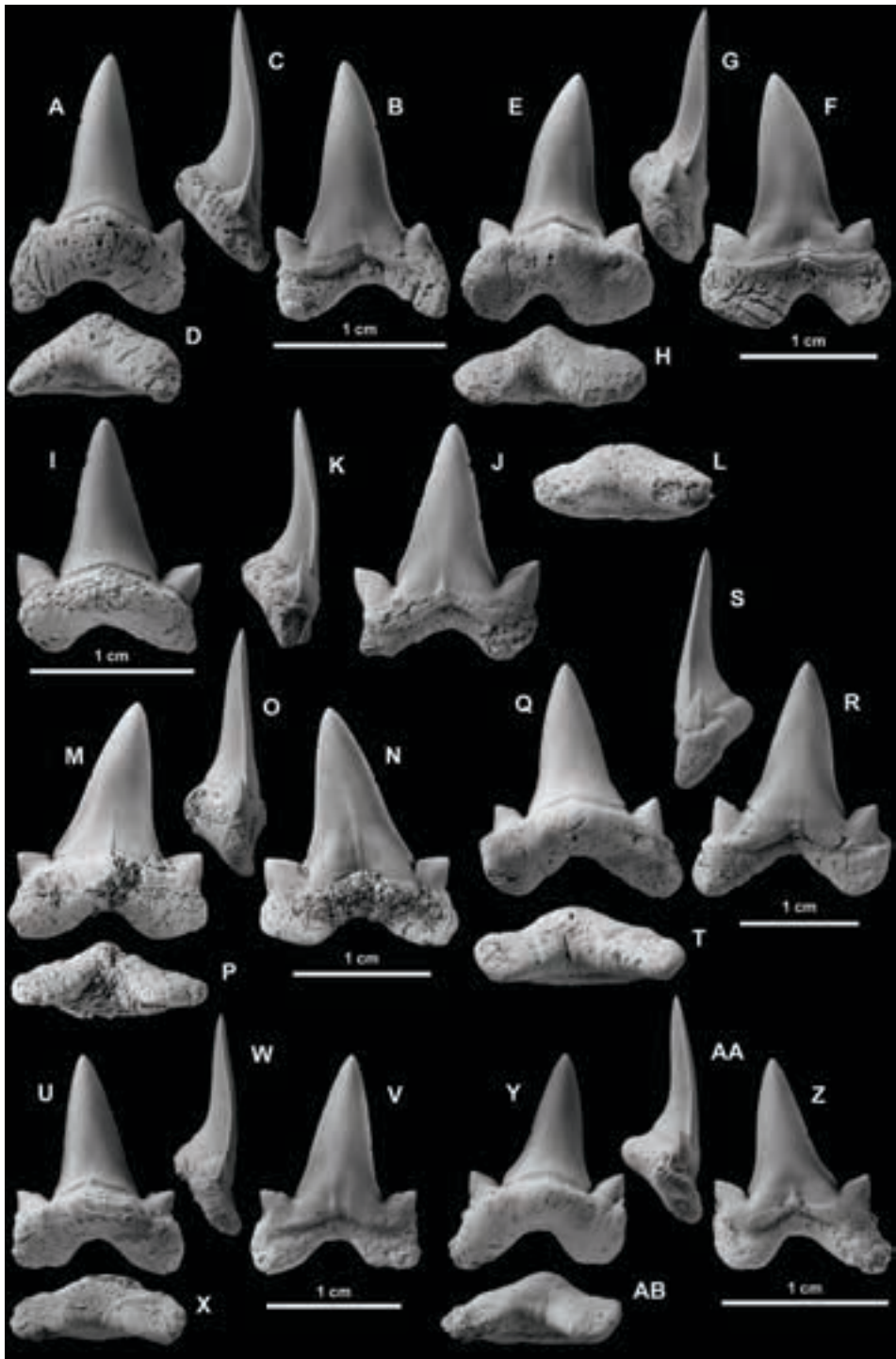
Material. Thirty-three teeth, including OIGM-GM2, OIGM-GM1, MCNA 3666, MCNA 5662, MCNA 5663, MCNA 8516, MCNA 8519, MCNA 10511, MCNA 10512, MCNA 10513, MCNA 10514, MCNA 10519, MCNA 10520, MCNA 10521, and MCNA 10532.

Locality. Vitoria Pass: Castillo-Gardelegi in the municipality of Vitoria-Gasteiz, Álava (Basque Country, Spain).

Age. Upper Campanian (*G. gansseri* zone, *Rugoglobigerina rotundata* subzone).

Description. Moderate-sized teeth (measuring up to 19 mm high). The crown is formed by a triangular central cusp, thickened labiolingually, which is flanked by two acute and generally broad cusplets, one to each side. The enameloid surfaces are unornamented. The cutting edge is continuous. The specimen MCNA 10521 (Figs. 12.5A–D) corresponds to a lower anterior, or a first anterolateral tooth, by comparison to the artificial tooth set given by Siversson et al. (2015). This tooth is characterised by a slender central cusp with a sigmoid curvature in profile view. The mesial cutting edge is slightly sigmoid in labial/lingual view, while the distal edge is straight. The triangular cusplets are moderately long, divergent, and acute-tipped. A noticeable, arched collar (neck) marks lingually the boundary between the crown and the root. On the labial side, the crown–root boundary is highlighted by a wavy bulge (or cingulum) with a V-shaped

Figure 12.5 *Cretolamna sarcoportheta* Siversson et al., 2015. A–D, lower anterior or anterolateral tooth in lingual (A), labial (B), profile (C), and basal (D) views, MCNA 10521; E–H, upper anterior tooth in lingual (E), labial (F), profile (G), and basal (H) views, OIGM-GM2; I–L, lower anterior tooth in lingual (I), labial (J), profile (K), and basal (L) views, MCNA 10511; M–P, upper anterolateral tooth in lingual (M), labial (N), profile (O), and basal (P) views, MCNA 8519; Q–T, lower anterolateral tooth in lingual (Q), labial (R), profile (S), and basal (T) views, MCNA 10514; U–X, lower anterolateral tooth in lingual (U), labial (V), profile (W), and basal (X) views, MCNA 3666; Y–AB, lower anterolateral tooth in lingual (Y), labial (Z), profile (AA), and basal (AB) views, MCNA 10512. ►

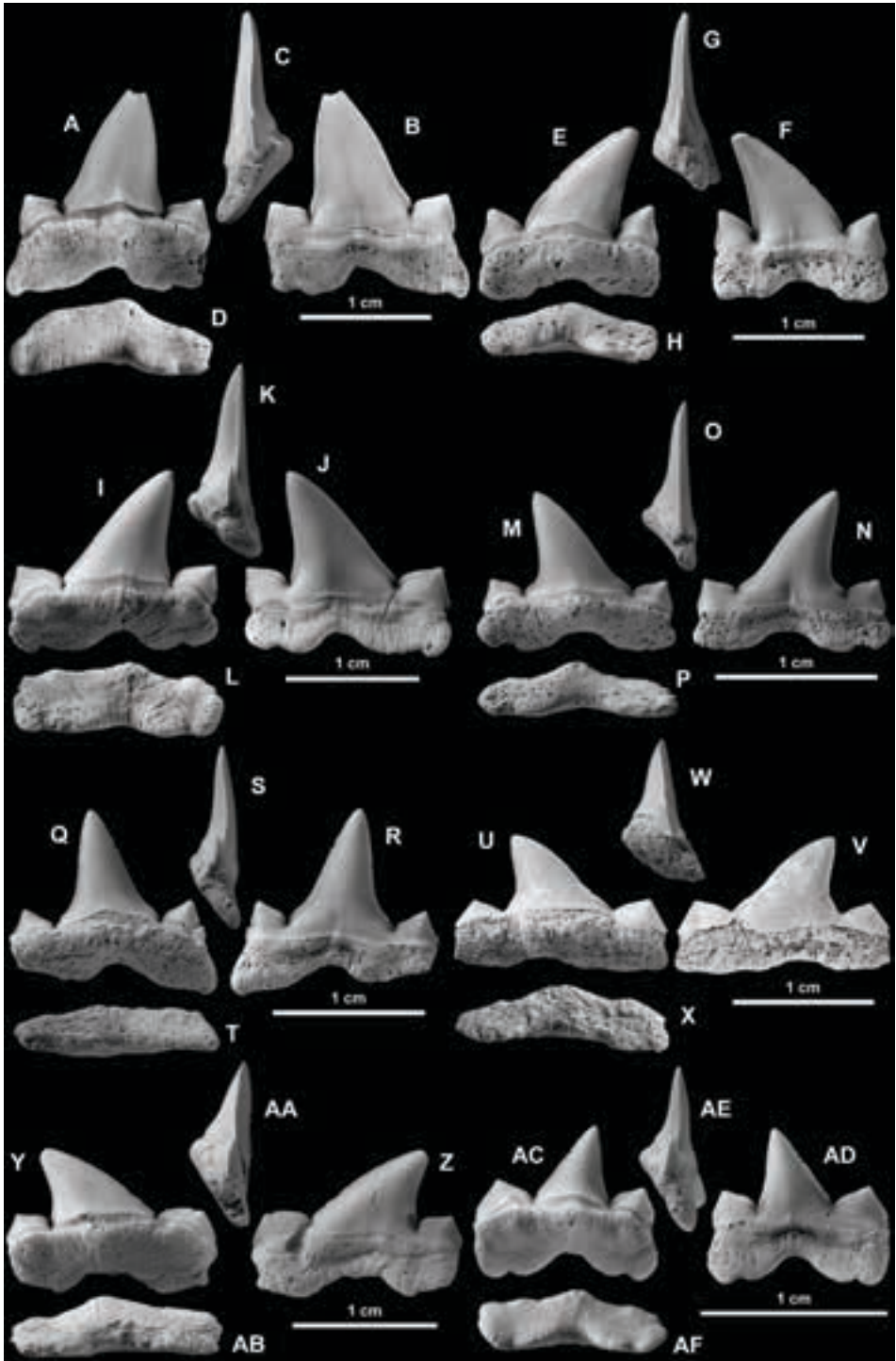


notch in the middle. The root is massive and asymmetrical, subtriangular in basal view, with a distal lobe that is considerably broader and tapered than the mesial one. The lingual protuberance shows a median foramen. Several dispersed foramina occur on the median part of the root, below the labial bulge. The basal edge of the root in lingual/labial view has a wide, semi-oval notch that is offset from the apicobasal axis.

The tooth OIGM-GM2 (Figs. 12.5E–H) corresponds to a second upper anterior position. The cusp is triangular, being lightly compressed labiolingually, and with the apex slightly recurved to the mesial position. The cusplets are triangular, acute, and divergent. The labial face of the main cusp is flat with a middle basal fossa, while the lingual face is slightly convex and flattened in the median part. On the labial face, there is a wavy cingulum at the base of the crown, which extends from the mesial to the distal margins of the tooth. The lingual neck forms an obtuse angle. The root is markedly asymmetrical in basal view, with two unequal lobes. The mesial lobe is broad and has a straight to slightly convex basal edge. The distal lobe is less developed and rounded-ended. Both lobes are labiolingually compressed, distally. The root has a well-marked lingual protuberance, under which a median foramen opens. The basal edge of the root has a semi-circular notch, distally displaced, in lingual/labial view.

Lateral teeth from the upper rows (i.e. anterolaterals to posterolaterals) show a clear monognathic heterodont condition with broad cusps that vary in height, and are somewhat inclined to the distal position. The main cusp is broadly triangular and labiolingually compressed, with a lingual face more convex than the labial one, which is almost flat. In profile view, the cutting edge of the main cusp is straight to slightly concave in those teeth anteriorly situated. There is one pair of relatively broad and divergent triangular cusplets, one to each side. The labial root–crown junction forms a neck along the lingual enameloid boundary, while it is usually wavy and somewhat bulging on the labial side. The root in first anterolateral teeth is asymmetrical in lingual/labial view, being the distal lobe sub-quadrangular, while the mesial lobe is pointed, as indicated by Siverson et al. (2015). Teeth more laterally positioned show more symmetrical roots, the latter condition is also observed in basal view. The lingual protuberance is not particularly pronounced, being perforated by a median foramen that is generally displaced with respect to its peak height. The basal edge of the root exhibits a generally wide

Figure 12.6 *Cretolamna sarcoporheta* Siverson et al., 2015. A–D, upper anterolateral tooth in lingual (A), labial (B), profile (C), and basal (D) views, MCNA 5662; E–H, upper posterolateral tooth in lingual (E), labial (F), profile (G), and basal (H) views, MCNA 10520; I–L, upper posterolateral tooth in lingual (I), labial (J), profile (K), and basal (L) views, MCNA 10519; M–P, upper posterolateral tooth in lingual (M), labial (N), profile (O), and basal (P) views, MCNA 10532; Q–T, lower posterolateral tooth in lingual (Q), labial (R), profile (S), and basal (T) views, MCNA 10513; U–X, upper posterolateral tooth in lingual (U), labial (V), profile (W), and basal (X) views, MCNA 5663; Y–AB, upper posterior tooth in lingual (Y), labial (Z), profile (AA), and basal (AB) views, MCNA 8516; AC–AF, lower posterior tooth in lingual (AC), labial (AD), profile (AE), and basal (AF) views, OIGM-GM1. ▶



median notch in labial/lingual view. A pair of very small notches below the mesial and distal lobes may be additionally found in the root of more distally situated teeth (Fig. 12.6J). The upper posterolateral teeth, which are most posteriorly situated in the jaws, are smaller and mesiodistally elongated (Figs. 12.6U, Y). They have a main cusp distally inclined, which is approximately straight in profile view (Figs. 12.6W, AA). Their roots are similar to those of most anteriorly positioned teeth.

Lower lateral teeth have a triangular cusp that varies from broad and labiolingually compressed (in more anteriorly situated teeth) to slender, widening at the base (i.e. narrower in the distal two-thirds of the cusp). In the latter morphotype, the apicobasal axis is almost vertical. The labial face of the main cusp is weakly convex to flat, with a median basal fossa and a short vertical fold in the middle (Figs. 12.5V, Z). The most posterolateral teeth are smaller and have the main cusps more distally inclined than those previously regarded. Moreover, their cusps are straight to labially incurved in profile view (Fig. 12.6AE). The crown also includes one pair of relatively broad and divergent, triangular cusplets, one on each side of the main cusp (Fig. 12.6AD), contrary to those teeth anteriorly positioned in jaws, which have sharper and slender cusplets (Figs. 12.5V, Z). In labial/lingual view, the root is more symmetrical in those teeth posteriorly placed (Fig. 12.6AC), while is noticeably asymmetrical in teeth from anteriormost files (Figs. 12.5U, Y). The root lobes are short, being the distal lobe rounded to quadrangular and the mesial lobe elongated and bluntly pointed. The labial face of the root has a curved, depressed region in the middle part, below the fossa formed on the base of the cusp. The lingual protuberance is rather developed in those teeth anteriorly situated in the dental file (Fig. 12.5AB), while is not particularly strong in the teeth posteriorly placed, as seen in basal views (Fig. 12.6AF). The basal outline of the root in these teeth is marked by a wide U-shaped notch in the central part. Moreover, the basal end of the root lobes are basally notched in more posteriorly situated teeth (Fig. 12.6AC).

Remarks. The most common selachian teeth collected by surface picking in the Eguileta Formation are those of *Cretolamna sarcoportheta*. The differences between this species and *Cretolamna borealis* have been covered above in Chapter 11 (in the remarks on *C. borealis*). According to Siversson et al. (2015), *Cretolamna sarcoportheta* is most similar to *C. appendiculata* in having teeth with a labiolingually thick cusp, upper lateroposterior teeth, anteriorly situated in jaws, with a markedly asymmetrical root (and triangular in basal view), upper anterior teeth with a strongly compressed distal lobe of the root, lower anterior teeth with a prominent lingual protuberance of the root, and lateroposterior teeth also with a pronounced lingual protuberance in profile view, but differs in having tooth cusps somewhat broader, upper lateroposterior teeth with labial faces less concave, and roots with more swelling lingual protuberance.

The species *C. sarcoportheta* has been previously reported from the lower upper Campanian of the Obourg Chalk Formation in the province of Hainaut, Belgium [described as *C. appendiculata* var. *pachyrhiza* by Herman (1977)], the uppermost lower Campanian (*Belemnellocamax mammillatus* zone: informal equivalent to the *Belemni-*

tella mucronata/*Gonioteuthis quadrata gracilis* belemnite zone) of Scania in the Kristianstad Basin, Sweden (Siverson, 1992; Siverson et al., 2015), and the phosphatic limestones occurring at Beauval in the Somme department, France (Siverson et al., 2015). It is most likely that the species is present in other classic Campanian areas, and therefore a research review of *C. appendiculata*-type teeth is needed, following the diagnostic characters given by Siverson et al. (2015) for a correct species placement.

Family PSEUDOCORACIDAE Cappetta, 2012

Genus *PSEUDOCORAX* Priem, 1897

Type species. *Corax affinis* Münster in Agassiz, 1843; Maastrichtian of Maastricht, Netherlands.

Pseudocorax ranges from the Turonian to Maastrichtian, with specimens being found in Europe, North America, northern Africa, and Middle East (Cappetta, 2012).

Pseudocorax laevis (Leriche, 1906)

Figs. 12.7A–D

For the synonymy see Herman (1977) and Guinot et al. (2013).

Material. Two teeth, MCNA 10561 and OIGM-GM16.

Locality. Vitoria Pass: Castillo-Gardelegi in the municipality of Vitoria-Gasteiz, Álava (Basque Country, Spain).

Age. Upper Campanian (*G. gansseri* zone, *Rugoglobigerina rotundata* subzone).

Description. Teeth of small size. The tooth crown is strongly compressed labiolingually, having a triangular, and relatively elongated, distally inclined cusp with a sharp apex. The labial face of the crown is flat to convex, whereas the lingual face is convex. Both enameloid faces are smooth, apart from two faint longitudinal grooves that are present in the middle part, near the labial root–crown boundary (Fig. 12.7A). The mesial edge of the crown is gently curved over most of its extension, but basally produces a weakly differentiated mesial heel (Fig. 12.7B). The distal edge is gently sigmoid, or almost straight, with a V-shaped basal notch that produces a wide convex distal blade. The continuous cutting edge extends to the heels. A faint neck separates crown from root on the lingual side, whereas the crown–root boundary is gently concave or wavy on the labial side. The asymmetrical, bilobed root (the distal lobe is slightly more developed than the mesial one) is wider than tall, and is provided with a mesially arranged nutritive groove pierced by a rather large foramen.

Remarks. The species *Pseudocorax laevis* was first described by Leriche in 1906 from the Campanian of an unspecified location in northern France. The morphological characters of the specimens collected in the Vitoria Pass site coincide with those given for the lateral teeth of the species. There are some large species of *Paratriakis* with which one specimen of the Vitoria Pass could be compared (Figs. 12.7C–D). *Paratriakis* has

been cited in southwest France by Cappetta and Odin (2001) and northern France by Guinot et al. (2013). However, our specimen differs from those of *Paratriakis* in its larger size, and, despite having lost most of the mesial part of the root, in having the remnant of a mesial blade-shaped heel (notice the mesiobasal notch of the cutting edge), and thus the specimen represents a very lateral tooth of *Pseudocorax laevis*. The upper Campanian to Maastrichtian *Pseudocorax affinis* (Münster in Agassiz, 1843) is a morphologically related species, but it differs from *P. laevis* in having finely crenate cutting edges (Leriche, 1906; Guinot et al., 2013). *Pseudocorax laevis* is represented in the Santonian–Campanian of Belgium (Herman, 1977), the mid-Santonian–upper Campanian of the Anglo-Paris Basin in France and the UK (Herman, 1977; Guinot et al., 2013), the lower upper Campanian in Charente-Maritime, centralwestern France (Vullo, 2005), and the Campanian of west Hannover in Westphalia, Germany (Schneider and Ladwig, 2013). This new record of *P. laevis* in the Vitoria Sub-basin is the southernmost known occurrence in Europe to date. Although *P. laevis* seems to be better distributed in western Europe (Guinot et al., 2013), it also occurs in the Mooreville Chalk Formation (lower Santonian to lower Campanian) of Alabama, on the North America Gulf Coastal Plain, as stated in Applegate (1970) and Herman (1977).

Family PSEUDOSCAPANORHYNCHIDAE Herman, 1979
Genus *PROTOLAMNA* Cappetta, 1980b

Type species. *Protolamna sokolovi* Cappetta, 1980b; upper Aptian of La Tuilière, Vaucluse, SE France.

Protolamna borodini (Cappetta and Case, 1975b)
Figs. 12.7E–K

For the synonymy see Cappetta and Case (1975b), Siverson (1992), and Vullo (2005).

Material. Three teeth, MCNA 3623, MCNA 10548, and OIGM-GM15.

Locality. Vitoria Pass: Castillo-Gardelegi in the municipality of Vitoria-Gasteiz, Álava (Basque Country, Spain).

Age. Upper Campanian (*G. gansseri* zone, *Rugoglobigerina rotundata* subzone).

Figure 12.7 A–D, *Pseudocorax laevis* (Leriche, 1906), A–B, lateral tooth in labial (A) and lingual (B) views, Gorka Martin coll., OIGM-GM16; C–D, posterolateral tooth in lingual (C) and labial (D) views, MCNA 10561. E–K, *Protolamna borodini* (Cappetta and Case, 1975), E–F, anterolateral tooth in lingual (E) and labial (F) views, OIGM-GM15; G–H, anterolateral tooth in lingual (G) and labial (H) views, MCNA 3623; I–K, anterior tooth in lingual (I), labial (J), and profile (K) views, MCNA 10548. L–U, *Serratolamna khderii* (Zalmout and Mustafa, 2001), L–N, upper anterior tooth in lingual (L), labial (M), and distal (N) views, MCNA 10544; O–P, lower lateral tooth in lingual (O) and labial (P) views, MCNA 5657; Q–R, upper lateral tooth in lingual (Q) and labial (R) views, MCNA 5656; S–U, upper lateral tooth in lingual (S), labial (T), and mesial (U) views, MCNA 13947. ►



Description. Teeth of small size (reaching a maximum length of 8 to 9 mm). A typical anterior tooth (Figs. 12.7I–K) has a slender, symmetrical cusp, which is slightly inclined lingually. The cusp, which is faintly sigmoid in profile view, is flanked by a pointed denticle (the opposite one presumably became lost with the corresponding root lobe) that is ornamented with vertical ridges on both lingual and labial sides. The cutting edge is continuous, extending to the cusplets. The labial face of the cusp is gently convex and has strong and discontinuous, subparallel vertical ridges that extend onto the apex (Fig. 12.7J). The lingual face exhibits faint vertical ridges, which are limited to the margins of the cusp and do not reach the apex (Figs. 12.7I, K). The basal boundary of the crown is U-shaped on the labial side, and overhangs the root. The collar is well formed on the lingual side. The root is high and has a very strong lingual protuberance, pierced by a median foramen. The only root lobe preserved in the specimen MCNA 10548 is compressed mesiodistally and has a round end. It can be predicted that root lobes in the tooth were slightly splayed or subparallel. Anterolateral teeth (Figs. 12.7E–F, G–H) have a narrow cusp that slightly broadens basally. The cusp is flanked by a pair of acute, not too divergent lateral cusplets, which are labially and lingually ornamented with faint vertical ridges. The main cusp is slightly inclined towards the commissure. The labial face of the crown is almost flat and ornamented with short flexuous vertical ridges, which are limited to the entire basal part in the cusp, but run onto the apex in the cusplets. This face overhangs what remains of the root. The lingual face is strongly convex basally, and smooth. The cutting edge is continuous along the main cusp and does not reach the base of the cusp. The boundary between the crown and the root is marked on the lingual face by a well-defined dental band (collar) with parallel borders. That boundary on the labial face is a curved line. Unfortunately, the root is not fully preserved, but at least the presence of a strong lingual protuberance, which is pierced by a median foramen, can be observed (Fig. 12.7G).

Remarks. Most of the currently recognised species in the genus *Protolamna* occur throughout the Lower Cretaceous and lowermost Upper Cretaceous strata (see Cappetta, 2012). *Protolamna borodini* is easily differentiated from the species *P. carteri* Cappetta and Case, 1999 and *P. roanokeensis* Cappetta and Case, 1999 from the upper Cenomanian and Albian, respectively, of Texas (USA) in having smooth surfaces on the lingual side of the main cusp (i.e. not ornamented with ridges). The slender species *Protolamna acuta* Müller and Diedrich, 1991 from the Cenomanian of the Lower Saxony Basin (near Bielefeld, Westphalia, NW Germany) differs from *P. borodini* in having pointed cusplets, a narrow nutritive groove (at least in anterior and anterolateral teeth), and weaker labial ornamentation on the crown. The species *Protolamna sarstedtensis* Schmitz, Thies, and Kriwet, 2010 from the lower Barremian marls of the Hannover region (west Germany) is similar to *P. borodini* in having vertical ridges on the labial side of the crown, being only restricted to its basal part, but it differs in having the main cusp slender with non-diverging, thin cusplets. The species *Protolamna sokolovi* Cappetta, 1980b from the upper Aptian of southern France also differs from *P. borodini* in having

lingual ornamentation on the cusp of anterior teeth, cusplets strongly separated from the main cusp, and in lacking a regularly curved enameloid boundary of the crown on the labial face (i.e. a wide, inverted U-shaped edge overhanging the root).

The species *P. borodini* is restricted to the Campanian–Maastrichtian interval. *P. borodini* is a characteristic species of the Upper Cretaceous of North America, with specimens being described for the first time in the upper Campanian Mount Laurel Formation of New Jersey (Cappetta and Case, 1975b) and also present in the Marshalltown Formations of Delaware, which is also upper Campanian (Lauginiger and Hartstein, 1983). This species also occurs in Campanian rocks of the Kristianstad Basin in southern Sweden (Siverson, 1992), the upper Campanian (CIV) at Le Pilou, Le Caillaud and Meschers (Charente-Maritime) in southwest France (Vullo, 2005), the Campanian phosphate beds of the Mishash Formation in south Israel (Vullo, 2005), and the Maastrichtian phosphate series of Ouled Abdoun in Morocco (Vullo, 2005; Cappetta, 2012). *P. borodini* is extremely rare in the Vitoria Sub-basin with the current state of knowledge.

Family SERRATOLAMNIDAE Landemaine, 1991

Genus *SERRATOLAMNA* Landemaine, 1991

Type species. *Otodus serratus* Agassiz, 1843; from the Maastrichtian of the Montagne de Saint-Pierre, Maastricht, Netherlands.

Serratolamna khderii (Zalmout and Mustafa, 2001)

Figs. 12.7L–U

For the synonymy see Vullo (2005), add:

1902 *Lamna serrata* (Agassiz, 1843); Leriche, p. 113, Pl. 3, Figs. 39–46.

Material. Five teeth, MCNA 5656, MCNA 5657, MCNA 10544, MCNA 13947, and another catalogued tooth.

Locality. Vitoria Pass: Castillo-Gardelegi in the municipality of Vitoria-Gasteiz, Álava (Basque Country, Spain).

Age. Upper Campanian (*G. gansseri* zone, *Rugoglobigerina rotundata* subzone).

Description. The teeth of this species are medium-sized. An anterior tooth (MCNA 10544; Figs. 12.7L–N) has a crown with a straight and flattened main cusp, the base of which is broad. The apex of the cusp is slightly incurved linguallly when seen in profile. The cutting edge is continuous. There is a short and pointed cusplet on each side of the main cusp, being the distal one larger. The lingual face of the cusp is gently convex, whereas the labial one is almost flat and has a median basal fossa. Although the enameloid is apparently smooth on both sides of the cusp, very faint vertical ridges are appreciated on the lingual side (Fig. 12.7L). A collar is present on the lingual crown–root boundary. The root lobes are mesiodistally spread, with a distinct bulge and a well marked nutritive groove (Fig. 12.7L). Moreover, the lobes are unequal, being the anteri-

or one longer and thinner. The basal outline of the root forms a wide pointed arch (Fig. 12.7M). Lateral teeth have a triangular main cusp, and also labiolingually compressed, but inclined distally (Figs. 12.7Q, S). The main cusp is almost straight in profile, with the apex labially incurved (Fig. 12.7U). The lingual face of the crown is smooth in these teeth and slightly convex. The labial face appears nearly flat, having a triangular fossa, located basally, which has a faint, vertical fold in the middle (Figs. 12.7P, R). The cutting edge is continuous, extending to the cusplets that flank both sides of the main cusp. The mesial cusplet is triangular in shape and has straight marginal edges, except for the exterior basal part where the edge have produced an additional, minute cusplet (Figs. 12.7O, S). The distal part of the crown have multiple, triangular cusplets (up to three), being the nearest to the main cusp the longest, wider and most inclined distally (Figs. 12.7O, Q, S). The basal margin of the crown is wavy on the labial face because of the enameloid shoulders, which have short, vertical scratch-like grooves in the marginal part below the cusplets (Figs. 12.7P, R). The labiobasal edge of the crown, just below the main cusp, slightly overhangs the root and forms a wide, inverted U-shaped line that runs parallel to the basal notch of the root (Figs. 12.7P, T). The root is short, labiolingually compressed with two round-ended, asymmetric lobes. A well-developed nutritive groove is formed in the central part of the lingual protuberance. The basal notch of the root forms a wide inverted U-shape in labial/lingual view.

Remarks. Cappetta (2012) has indicated that the species *Serratolamna khderii* follows an odontospidid tooth design with lingual ornamentation in anterior files. The species *S. khderii* was established by Zalmout and Mustafa (2001) on tooth specimens from the lower Maastrichtian strata of Jordan. It has since extended its distribution to include Benguérir (lower Maastrichtian, Ganntour Basin) in Morocco (Cappetta et al., 2014b). Other Maastrichtian records of this species include the small teeth assigned to odontospidids from the upper Campanian–lower Maastrichtian of Angola (reported by Antunes and Cappetta, 2002) and some specimens from the lower Maastrichtian of Syria (reported by Bardet et al., 2000), as stated in Vullo (2005). This species seems to be also present in the lower Campanian (*Goniotheutis quadrata* zone) of the Anglo-Paris Basin (departments of Aisne and Somme), according to illustrations provided by Leriche (1902), and possibly at the Aachen area (Germany) in the Liege-Limburg Basin (Albers and Weiler, 1964). Vullo (2005) have extended the stratigraphical and geographical ranges of this species assigned to the genus *Serratolamna* to include the upper Campanian (CVIII bed) specimens of Meschers (Charente-Maritime) in France. The discovery of *S. khderii* in the Vitoria Pass section (Vitoria Sub-basin) constitutes so far the southernmost European occurrence of this taxon in Campanian rocks.

Order CARCHARHINIFORMES Compagno, 1973

Family TRIAKIDAE Gray, 1851

Genus *GALEORHINUS* Blainville, 1816

Type species. *Squalus galeus* Linnaeus, 1758; Recent, European seas.

Galeorhinus girardoti Herman, 1977

Fig. 12.8

For the synonymy see Vullo (2005).

Material. One tooth, MCNA 10547.

Locality. Vitoria Pass: Castillo-Gardelegi in the municipality of Vitoria-Gasteiz, Álava (Basque Country, Spain).

Age. Upper Campanian (*G. gansseri* zone, *Rugoglobigerina rotundata* subzone).

Description. This lateral tooth is relatively small, barely reaching 2 mm. The crown is formed by a triangular main cusp, which is distally inclined and labiolingually compressed, and at least two cusplets decreasing in size distally (Fig. 12.8A). Both mesial and distal cutting edges of the cusp are straight and continuous. The mesial edge is chipped by use (Fig. 12.8B). The enameloid is smooth on both sides of the crown. The basilolabial bulge of the crown is wide arched and smooth. There is a thin collar separating the crown and the root on the lingual side. The root, being broad and flattened, is partly preserved and this raises the question as to whether or not it had nutritive groove. Several holes throughout the lingual side of root may correspond to foramina.

Remarks. The species *G. girardoti* was originally described by Herman (1977) from the Campanian–Maastrichtian of Belgium. According to Herman (1977) and Case and Cappetta (1997), the teeth of the Campanian forms seem to have more basal folds on

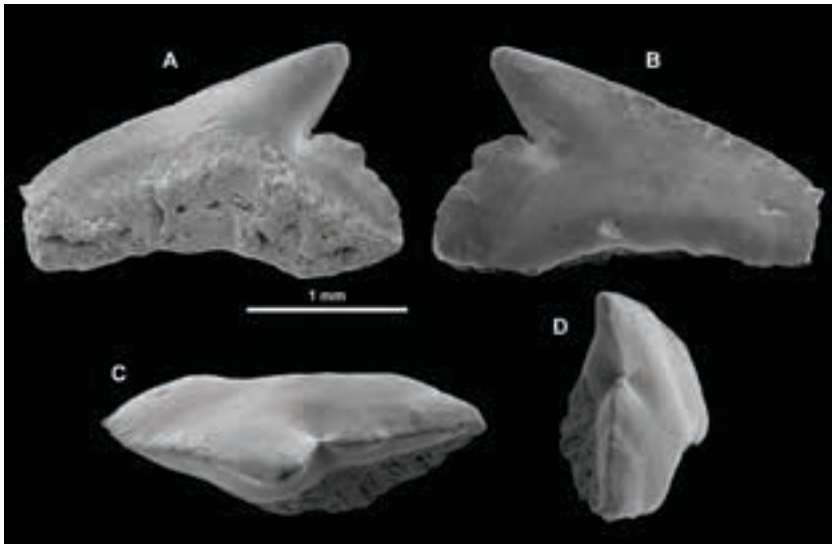


Figure 12.8 *Galeorhinus girardoti* Herman, 1977, lateral tooth in lingual (A), labial (B), apical (C), and distal (D) views, MCNA 10547.

the labial face of the crown than those of the Maastrichtian, which are unornamented. Our specimen from the Vitoria Pass and those of the same species reported in France by Vullo (2005) are unornamented forms, despite of coming in both cases from Campanian rocks. The species *G. girardoti* differs from ?*Galeorhinus unilateralis* described by Averianov (1997) from the upper Santonian–Campanian Russian Platform Sea (Kikino locality in Penza province, Russia) in having a lingual collar, less developed and relatively shorter lateral cusplets, and a less arched basiolabial bulge.

The stratigraphical range of the genus *Galeorhinus* is from Cenomanian to Recent (see Cappetta, 2012). Those specimens assigned to *Galeorhinus girardoti* are found in its type locality in Hainaut, Belgium (base of the Obourg Chalk Formation in the Mons Basin; lower upper Campanian, *Belemnitella mucronata* zone¹) and in Aachen, western part of Germany (Vaalser Grünsand, lower Campanian), according to Herman (1977). Although rare, *G. girardoti* is also found in the Osterwicker Schisten of the central area of the Cretaceous Münster Basin (west Münsterland, Westphalia in NW Germany), as stated in Muller (1989, 2014). Moreover, the localities Le Pilou and Le Caillaud in the Charente-Maritime (southwest France), where lower upper Campanian CIV and CV beds are reported to include *G. girardoti* according to Vullo (2005), should be also added to the northwestern European sites.

Moreover, the following three unassigned species to the genus *Galeorhinus* have been described from the Campanian. *Galeorhinus* sp. was reported by Schneider and Ladwig (2013) at the base of the upper Campanian (*Patagiosites stobaei*/*Galeola basiplana* zone² in the zonal scheme for the northern Germany) in the North German Basin in Hannover, Germany, and also by Siverson (1993) in rocks of latest early Campanian age of the Kristianstad Basin (Scania, Sweden). Finally, Lewy and Cappetta (1989) have also included *Galeorhinus* sp. in the marine phosphatic chalk occurring at the top of the Menuha Formation of Israel, which corresponds to the lowermost Campanian.

¹ Named after the belemnite *Belemnitella mucronata* (von Schlotheim, 1813)

² Named after the ammonites *Patagiosites stobaei* (Nilsson, 1827), and the echinoid *Galeola basiplana* Ernst, 1971.

Chapter 13
 NEOSELACHIANS FROM THE QUINTANILLA LA OJADA SITE
 (VALDENOCEDA FORMATION, MAASTRICHTIAN)

13.1 Introduction

In this chapter I describe the occurrence of two selachian assemblages that were discovered at Quintanilla la Ojada site in the northern flank of the Vienda Mountains (northern Burgos) by geologists of the Universidad del País Vasco/Euskal Herriko Unibertsitatea (UPV/EHU) during the doctorate field research undertaken by Ana Berreteaga (Berreteaga, 2008). This material mainly consists of isolated teeth, with a particular taphonomic and geochemical history, which extends our knowledge about the chondrichthyan taxa in the Basque-Cantabrian Region. Selachian teeth are the conspicuous elements of this assemblage but osteichthyan (bony fish), but mosasaurid fossils also occur (Berreteaga, 2008; Berreteaga et al., 2010, 2011). All material is housed in the collections of the MCNA (Vitoria-Gasteiz, Spain).

13.2 Systematic palaeontology

Class CHONDRICHTHYES Huxley, 1880
 Subclass ELASMOBRANCHII Bonaparte, 1838
 Cohort EUSELACHII Hay, 1902
 Subcohort NEOSELACHII Compagno, 1977
 Superorder GALEOMORPHII Compagno, 1973
 Order LAMNIFORMES Berg, 1958
 Family ANACORACIDAE Casier, 1947
 Genus *SQUALICORAX* Whitley, 1939

Type species. *Corax pristodontus* Agassiz, 1843; Maastrichtian of Maastricht, Netherlands.

See Chapter 15 about some comments on the genus.

Squalicorax kaupi (Agassiz, 1843)

Figs. 13.1A–H

Material. Twelve teeth including MCNA 14690 from QLO-1, and MCNA 14682, MCNA 14683 and MCNA 14684 from QLO-2.

Horizon and locality. Valdenoceda Formation, lower upper Maastrichtian, Quintanilla la Ojada (Burgos, Spain).

Description. A detailed description of the species is given in Cappetta and Case (1975b: 8). These teeth are slightly smaller than the average size of the teeth of this species (the larger tooth is 11 mm wide). The crown is triangular and seems to have had an acute apex. The mesial cutting edge of the crown is convex, sometimes gibbous (i.e. in anterior teeth), while the distal edge is usually shorter and straight. The distal heel is low and straight (Figs. 13.1G–H). Serrations on both cutting edges are fine to medium and regularly distributed. When finely preserved, the root is flattened and shows a broad, shallow basal notch characteristic of the species. Small irregular foramina are present on the labial face of the root (Fig. 13.1A).

Discussion. This is a relatively abundant taxon at Quintanilla la Ojada. Apart from having a well differentiated distal heel, the teeth of *S. kaupi* differ from those of *S. pristodontus* in the angle between distal and heel cutting edges of the cusp, which may even be up to 90° in the former taxon (Figs. 13.1G–H).

The stratigraphical range of *Squalicorax kaupi* is Coniacian to Maastrichtian (Cappetta, 2012) and its known occurrences in other locations across the world during the Maastrichtian are listed in Table 20.3 (in Chapter 20). The species is also known in the Maastrichtian of the southcentral Basque-Cantabrian Region, identified at Albaina by teeth belonging to juvenile individuals (Cappetta and Corral, 1999). Close-resembling teeth of this species are relatively abundant in the Campanian (Bardet et al., 1993; see also Chapters 11 and 12 in this thesis).

Squalicorax pristodontus (Agassiz, 1843)

Figs. 13.1I–Q

Material. Eleven teeth including MCNA 14853 and MCNA 14680 from QLO-1, and MCNA 14679 and MCNA 14811 from QLO-2.

Horizon and locality. Valdenoceda Formation, lower upper Maastrichtian, Quintanilla la Ojada (Burgos, Spain).

Description. A detailed description of the species is given in Cappetta and Case (1975b: 8). Teeth of *Squalicorax pristodontus* are relatively large. The crown is broad and triangular with a convex mesial edge especially in its lower end. The distal cutting edge is straight or slightly concave. Cutting edges bear strong serrations that are evenly distributed. The root is labiolingually flattened with a row of small irregular foramina on the labial face (Figs. 13.1P–Q) and a medially placed basal notch (Figs. 13.1K, M). The

teeth are slightly curved in lateral view (Fig. 13.1L), being the lingual face concave and the labial one convex.

Discussion. The teeth of *Squalicorax pristodontus* morphologically resemble those of *Squalicorax kaupi*, although the former are larger and the serrations tend to be more asymmetrical. The distal edge of the crown is almost straight or slightly concave, no developing a distal heel. Teeth of this taxon are rare in Quintanilla la Ojada, representing approximately 6% of all teeth collected from the site. Cappetta et al. (2014b: 229) have observed a drop in the number of teeth collected along the Maastrichtian series in Morocco. This suggests that the taxon abundance dropped at the end of the Maastrichtian, which is in line with its extinction before the K–Pg event (Adolfsson and Ward, 2014).

Squalicorax pristodontus was apparently globally widespread in tropical and warm-temperate seas in the Late Cretaceous. The known occurrences of this species during the Maastrichtian in other locations across the world are listed in Table 20.3 in Chapter 20.

Squalicorax sp.

Figs. 13.1R–U

Material. Four teeth (MCNA 14693, MCNA 14857) from QLO-2.

Horizon and locality. Valdenoceda Formation, lower upper Maastrichtian, Quintanilla la Ojada (Burgos, Spain).

Description. Medium-sized teeth having a broad triangular crown with serrated cutting edges. The mesial edge of the crown is convex bearing stronger compound serrations (i.e. with small serrations superimposed to the large ones) in the medial part (Figs. 13.1T–U). The distal cutting edge is shorter and equally convex, and is separated from a gibbous heel by a deep notch. Small indentations are noticeable at the base of the crown in both medial and distal cutting edges. The boundary between the enameloid and the root forms a slightly curved line in both labial and lingual faces. The root is high, rather thick with nearly straight lateral edges, except for a small notch in the mesial edge (Fig. 13.1U) and a marked basal notch. Several small and irregular foramina open on the labial face below the enameloid/root boundary (Fig. 13.1R).

Discussion. The teeth of this taxon may resemble those of *S. kaupi* by their general dental morphology, but the compound serrations on the cutting edges of the crown and the shape of the heel differentiates from them. Moreover, the teeth from Quintanilla la Ojada are also thicker than those of *S. kaupi*. The teeth of Quintanilla la Ojada show a certain similarity in size and morphology, including compound serrations, to some specimens from the Upper Cretaceous of Angola and the DR Congo figured by Dartevelle and Casier (1943, 1959) and assigned to *S. yangaensis*. Other *Squalicorax* species having compound serrations occur in the lower Maastrichtian of the Ouled Abdoun and Gantour basins, Morocco (Arambourg, 1952; Cappetta et al., 2014b) and in Syria (Bardet et al., 2000). Recently, Cappetta et al. (2014a) have erected the species *Squalicorax benguirensis* for the latter specimens, but only lateral teeth ex-

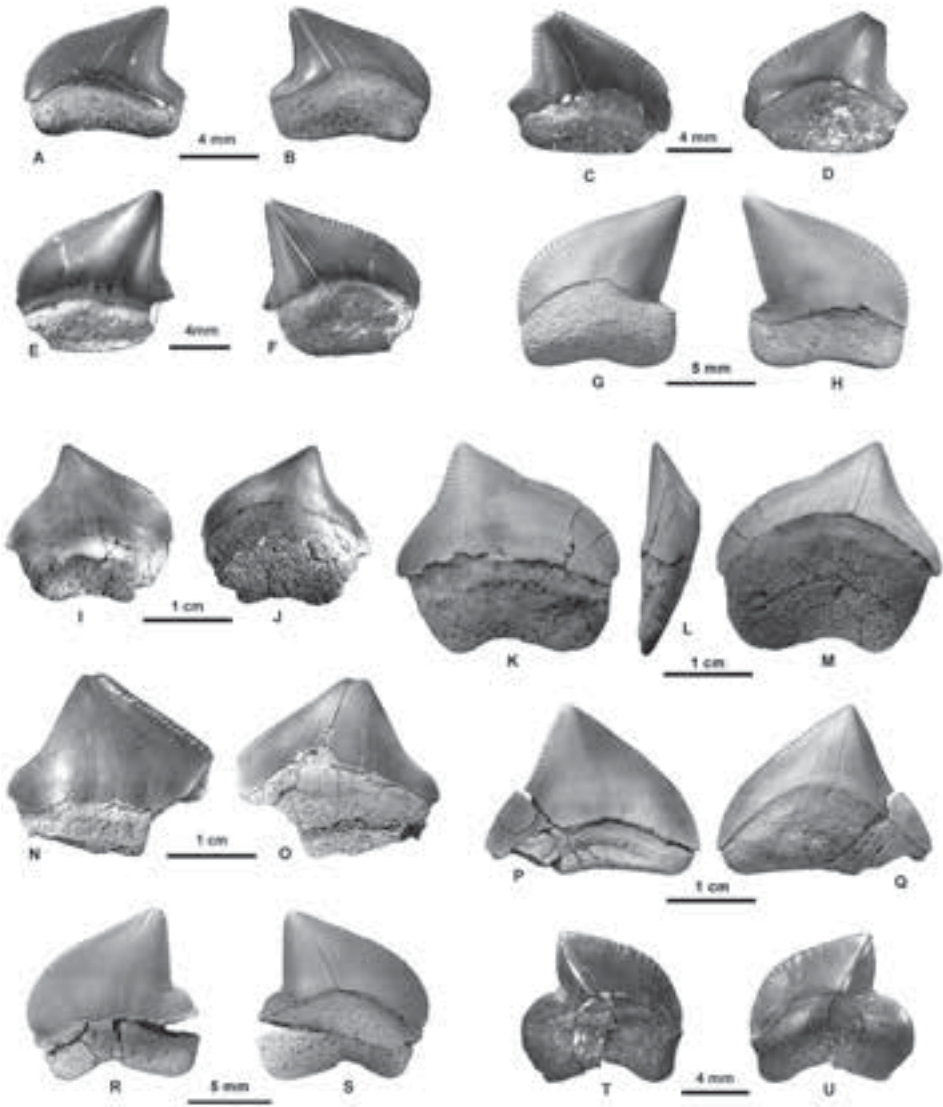


Figure 13.1 A–H, *Squalicorax kaupi* (Agassiz, 1843), A–B, lateral tooth in labial (A) and lingual (B) views, MCNA 14682; C–D, lateral tooth in labial (C) and lingual (D) views, MCNA 14683; E–F, lateral tooth in labial (E) and lingual (F) views, MCNA 14684; G–H, lateral tooth in lingual (G) and labial (H) views, MCNA 14690. I–Q, *Squalicorax pristodontus* (Agassiz, 1843), I–J, lateral tooth in labial (I) and lingual (J) views, MCNA 14679; K–M, lateral tooth in labial (K), mesial (L) and lingual (M) views, MCNA 14811; N–O, lateral tooth in labial (N) and lingual (N) views, MCNA 14680; P–Q, lateral tooth in labial (P) and lingual (Q) views, MCNA 14853. R–U, *Squalicorax* sp., R–S, anterolateral tooth in labial (R) and lingual (S) views, MCNA 14857; T–U, anterolateral tooth in labial (T) and lingual (U) views, MCNA 14693. Teeth G–H, N–O, and P–Q were recovered from the discontinuous lag deposit QLO-1 and the rest from the bone assemblage QLO-2.

hibit a clear heel within this species, and most notoriously, they have secondary serrations evenly superimposed on the overall sinuate cutting edge. However, none of these species above mentioned seems to correspond to our specimens whose cutting edges also bear double serrations. For the moment this taxon is left in open nomenclature because of the scarcity of specimens.

Family OTODONTIDAE Glikman, 1964

Genus *CRETOLAMNA* Glikman, 1958

Type species. *Otodus appendiculatus* Agassiz, 1843; Turonian of Lewes, East Sussex (England).

Cretolamna sp. aff. *Cretolamna appendiculata* (Agassiz, 1843)

Figs. 13.2A–B

Material. One tooth (MCNA 14802) and other incomplete tooth attributable to this species, both from QLO-2.

Horizon and locality. Valdenoceda Formation, lower upper Maastrichtian, Quintanilla la Ojada (Burgos, Spain).

Description. This is a small, very lateral tooth with a low triangular main cusp flanked by two broad lateral cusplets, one on each side. Cutting edges are smooth. Both lingual and labial faces are flattened and smooth. The root is nearly rectangular with a shallow basal notch.

Discussion. Despite not being finely preserved, this small tooth of a lamniform shark is provisionally considered to be a commissural tooth, and the scarcity of the material prevents us to go further in the species assignment. The species *Cretolamna appendiculata* has been given a wide geographical distribution and stratigraphical range from Albian to Priabonian (Cappetta, 2012). However, Siversson et al. (2015) have pointed out that the taxon *C. appendiculata*, as usually identified, constituted in reality a number of different species occurring within the Late Cretaceous (from the Cenomanian to the Campanian). Maastrichtian morphotypes of *Cretolamna* with low height/width ratio were first described as *C. appendiculata* var. *lata* by Herman (1977) and later elevated to species rank [*Cretolamna lata* (Herman, 1977)] by Herman and Van Waes (2012), having a relatively low and wide crown with very wide lateral cusplets. However, a revision of such Maastrichtian forms taking into consideration their root characters is still pending. This taxon, along with other Maastrichtian forms of having a low height/width ratio, are listed in Table 20.3 (in Chapter 20).

Family SERRATOLAMNIDAE Landemaine, 1991

Genus *SERRATOLAMNA* Landemaine, 1991

Type species. *Otodus serratus* Agassiz, 1843; Maastrichtian of the Montagne de Saint-Pierre, Maastricht, Netherlands.

Serratolamna serrata (Agassiz, 1843)
Figs. 13.2C–N

Material. Twenty-three teeth from QLO-2, including MCNA 14694, MCNA 14695, MCNA 14696, MCNA 4697, MCNA 14858, and MCNA 14832.

Horizon and locality. Valdenoceda Formation, lower upper Maastrichtian, Quintanilla la Ojada (Burgos, Spain).

Description. See Arambourg (1952: 98) and Cappetta and Corral (1999: 347) for a detailed description of the species. Teeth of this species are labiolingually flattened and have a smooth triangular crown with continuous cutting edge. The main cusp is high and can be either symmetrical or slanted towards the commissure, depending on whether they belong to teeth from the anterior (Figs. 13.2E–F) or lateral files (Figs. 13.2I–J). The cusp is flanked on both sides by two pairs of small diverging cusplets. An additional third cusplet develops in the commissural side of the crown on some lateral teeth (Figs. 13.2G–H), and therefore the distal heel is longer than the mesial one. Faint folds occur where the labial face of the main cusp merges with the root, giving a sinuous enameloid boundary. On the lingual face, the boundary between the enamelled cusp and the root face is not straight but irregular, developing a medial chevron. In lateral view the cusp is slightly concave labially. In posterior teeth the main cusp is short in relation to the root height and slant commissurally (Figs. 13.2M–N). The root is rectangular and flattened labiolingually. It has two asymmetric root lobes that are divided by a well-defined axial groove, where a foramen occurs. The root may be as high as the crown in posterior teeth (Figs. 13.2M–N).

Discussion. This species seems to be restricted worldwide during the Maastrichtian (Underwood and Mitchell, 2000). Its presence in the Campanian of Alabama (Shimada and Brereton, 2007) needs to be confirmed, as they may well represent a closely related taxon (K. Shimada pers. com., 2010). The species *Serratolamna serrata* is a common and abundant element in the fossil assemblages of the Basque-Cantabrian Region (both in Albaina and Quintanilla la Ojada). Table 20.3 in Chapter 20 lists the known world occurrences of this species.

Family ODONTASPIDIDAE Müller and Henle, 1839
Genus *CARCHARIAS* Rafinesque, 1810

Type species. *Carcharias taurus* Rafinesque, 1810; Recent, Sicily, Italy.

Carcharias heathi Case and Cappetta, 1997
Figs. 13.3A–L

Material. Fifteen teeth, including MCNA 14815 from QLO-1, and MCNA 14711, MCNA 14712, MCNA 14713, and MCNA 14714 from QLO-2.

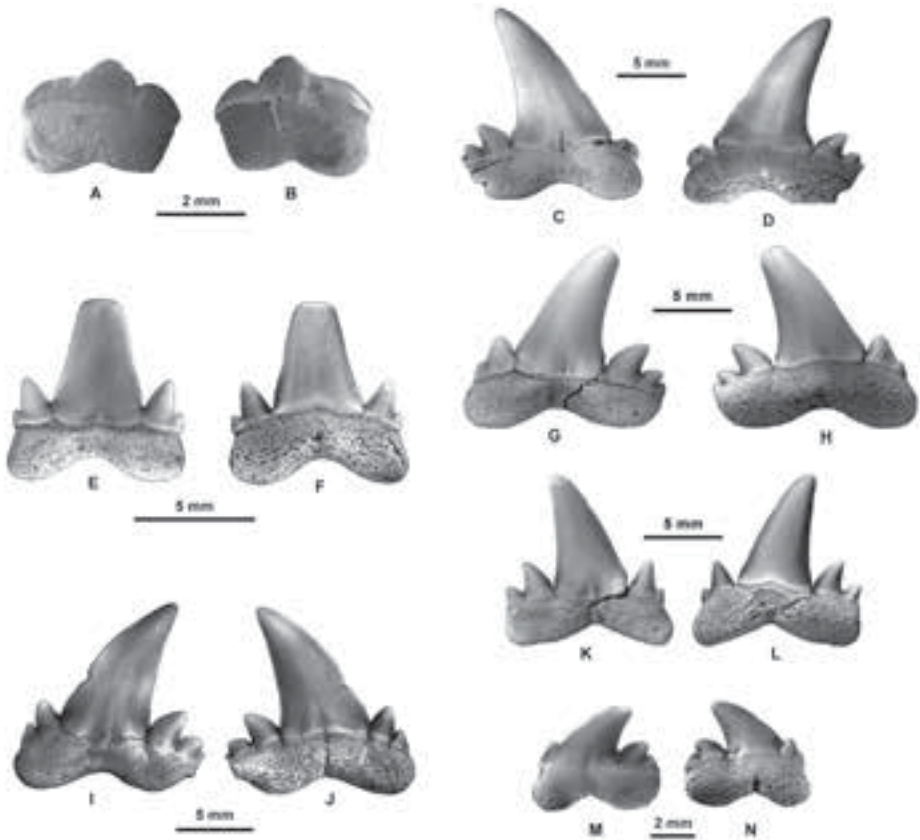


Figure 13.2 A–B, *Cretolamna* sp. aff. *Cretolamna appendiculata* (Agassiz, 1843), anterior tooth in labial (A) and lingual (B) views, MCNA 14802. C–N, *Serratolamna serrata* (Agassiz, 1843), C–D, upper anterior tooth in labial (C) and lingual (D) views, MCNA 14694; E–F, upper anterior tooth in labial (E) and lingual (F) views, MCNA 14695; G–H, upper lateral tooth in labial (G) and lingual (H) views, MCNA 14858; I–J, upper lateral tooth in labial (I) and lingual (J) views, MCNA 14697; K–L, lower? lateral tooth in labial (K) and lingual (L) views, MCNA 14832; M–N, posterior tooth in labial (M) and lingual (N) views, MCNA 14696. All the teeth from bone assemblage QLO-2.

Horizon and locality. Valdenoceda Formation, lower upper Maastrichtian, Quintanilla la Ojada (Burgos, Spain).

Description. A detailed description of the species is given in Case and Cappetta (1997: 140) and Cappetta and Corral (1999: 347). Teeth are medium-sized (up to 20 mm high) with a triangular crown, not very high, that broadens at its base. The labial face is slightly convex whereas the lingual one is moderately convex and both show smooth enamelled surfaces. Two lateral cusplets flank the main cusp. They are triangular and divergent, shorter in lateral teeth, where exhibit an expanded process but without developing a secondary cusplet (Figs. 13.3G–H). Additionally, lateral cusplets show a di-

vergent recurved apex in anterior teeth (Figs. 13.3B, E). The inner cutting edge reaches the base of the cusp and is regularly concave. The main cusp of anterior teeth shows a slight sigmoidal curve in lateral view (Fig. 13.3B) and the cutting edges do not reach the base of the crown. The labial boundary of the enameloid slightly overhangs the root and in some specimens it develops a visible chevron pattern (Figs. 13.3A, D). The root bears a shallow groove on a weak lingual protuberance. The lobes are divergent, with a high basal deep notch in anterior teeth (Fig. 13.3A), much wider in lateral ones (Figs. 13.3D, G, I). Both lobes have round ends.

Discussion. The main differences with respect to the type series lie in the presence of a weak lingual protuberance and the shape of the groove at the centre of the root, much shallower in the Quintanilla la Ojada teeth, but this is probably due to a slight abrasion of the root. In addition, the chevron mark located at the base of the cusp on the labial face is hardly seen on lateral teeth. Apart from the Spanish material and specimens from the type locality in Texas (USA), other occurrences of this typical Maastrichtian species are shown in Chapter 20 (Table 20.3).

Carcharias sp.
Figure 13.3M–P

Material. Three teeth from QLO-2 including MCNA 14715 and MCNA 14850.

Horizon and locality. Valdenoceda Formation, lower upper Maastrichtian, Quintanilla la Ojada (Burgos, Spain).

Description. One tooth, which is mesiodistally compressed, has a curved cusp without lateral cusplets (Figs. 13.3M–N). The labial face of the crown of this small specimen is almost flat, whereas the lingual one is convex; both of them are devoid of ornamentation. The irregular root is high and narrow, with a strong lingual protuberance and two asymmetrical and few divergent lobes. Another small tooth (Figs. 13.3O–P) has smooth lingual and labial faces of the crown. The main cusp, which is short and slants distally, is flanked by a pair of broad and divergent lateral cusplets. A lingual collar is developed. The root is nearly as large as the crown, and have two well-differentiated lobes with round ends separated by a V-shaped interlobe area. The lingual protuberance is cut by a deep root groove.

Discussion. These two teeth are much modified; the first is a parasymphyseal tooth (Figs. 13.3M–N), and the second is regarded as an intermediate tooth (Figs. 13.3O–P). It is difficult to give an accurate taxonomic assignment for these tooth elements, and thus both specimens according to size, asymmetry, and overall aspect comparing with the extant *Carcharias taurus* (Rafinesque, 1810) are cautiously assigned to the genus *Carcharias*, but they could also belong to the only well-identified species of *Carcharias* (i.e. *C. heathi*) collected in the locality.

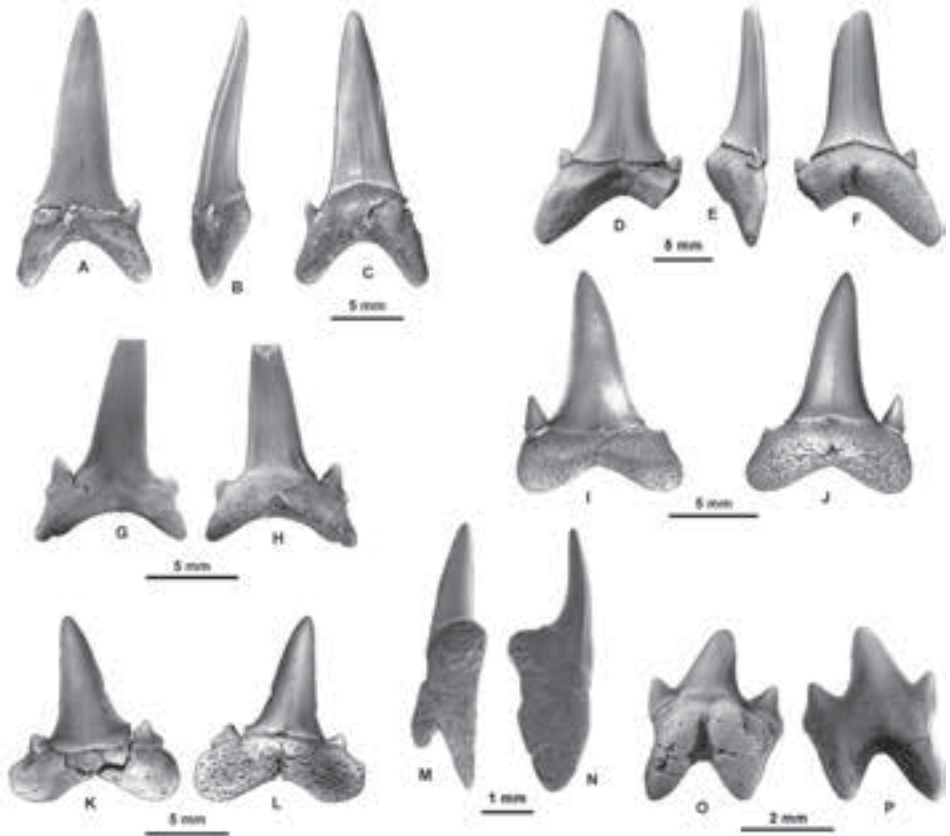


Figure 13.3 A–L, *Carcharias beathi* Case and Cappetta, 1997, A–C, anterior tooth in labial (A), lateral (B) and lingual (C) views, MCNA 14714; D–F, anterolateral tooth in labial (D), lateral (E) and lingual (F) views, MCNA 14815; G–H, lower lateral tooth in labial (G) and lingual (H) views, MCNA 14713; I–J, upper lateral tooth in labial (I) and lingual (J) views, MCNA 14711; K–L, upper lateral tooth in labial (K) and lingual (L) views, MCNA 14712. M–P, *Carcharias* sp., M–N, parasymphyseal tooth in oblique lingual (M) and lateral (N) views, MCNA 14715; O–P, intermediate tooth in lingual (O) and labial (P) views, MCNA 14850. Tooth D–F recovered from the discontinuous lag deposit QLO-1 and the rest from the bone assemblage QLO-2.

Order ORECTOLOBIFORMES Applegate, 1972

Family GINGLYMOSTOMATIDAE Gill, 1862

Genus *PLICATOSCYLLIUM* Case and Cappetta, 1997

Type species. *Plicatoscyllium derameei* Case and Cappetta, 1997; upper Maastrichtian of Texas.

This genus *Plicatoscyllium* was erected for those Upper Cretaceous representatives of the family Ginglymostomatidae showing teeth with a more or less strongly folded labial face. The teeth of all species within this extinct genus have a hemiaulacorhize root

with a massive medial lingual protuberance. The crown is triangular with a main cusp and three to four pairs of large lateral cusplets. The labial face of the crown has a typical ornamentation consisting of three to more than twenty-two strong sinuous enameloid folds (Herman and Van Waes, 2014).

All the representatives of the genus *Plicatoscyllium* were inhabitants of shallow waters in tropical to subtropical regions (Cappetta, 2012).

Plicatoscyllium lehneri (Leriche, 1938)

Figs. 13.4A–G

Material. Three incomplete teeth from QLO-2 (MCNA 14722, MCNA 14723, and MCNA 14848).

Horizon and locality. Valdenoceda Formation, lower upper Maastrichtian, Quintanilla la Ojada (Burgos, Spain).

Description. The teeth are symmetrical and of medium size. Four lateral cusplets flank the broad conical cusp, the inner ones being larger. The labial face of the crown shows a marked ornamentation consisting in irregular folds or wrinkles confined to a triangular area (Fig. 13.4E). The inner cusplets are also ornamented with labial folds. The basal end of the labial face develops a short and wide apron with a central notch. The labial face of the crown slopes down at approximately 45° angle, in profile view. The root, which is hemiaulacorhizous, has a roughly triangular V-shape, viewed basally, encircled by the crown outline, and with a large elongated foramen situated in the centre. On each lateral side of the lingual face a marginal foramen is observed. The lingual root protuberance, although not completely preserved, is strong and bears a central foramen (Fig. 13.4B).

Discussion. A typical ornamentation with a triangular design develops at the base of the labial surface of the crown. This peculiar pattern characterises the teeth of this species (Noubhani and Cappetta, 1997; Cappetta and Corral, 1999). *Plicatoscyllium lehneri* was mistakenly regarded as a synonym of *Plicatoscyllium minutum* (Forir, 1887) by Herman (1977), and after him by Noubhani and Cappetta (1997) and Cappetta and Corral (1999). The review of Maastrichtian material of *P. minutum* from the Maastrichtian of Kanne, NE Belgium by H. Cappetta allowed to confirm the morphological differences between the teeth of both species (Corral et al., 2015b). Thus, the labial ornamentation of the crown is much simpler in *P. minutum* than in *P. lehneri*, particularly because of the absence of a triangular zone in anterior teeth and the less numerous folds in lateral teeth (see Herman, 1977). The separation of *P. minutum* and *P. lehneri* (see Figs. 13.5–6) was formalised by Cappetta (2006). Table 20.3 in Chapter 20 lists the regions where this Maastrichtian species has been found, in some cases described under the name *Ginglymostoma rugosum* (Dartevelle and Casier, 1943) or assigned to the closely related species *P. minutum* in others (Noubhani and Cappetta, 1997; Cappetta and Corral, 1999).

Order CARCHARHINIFORMES Compagno, 1973

Family TRIAKIDAE Gray, 1851
Genus *PALAEOGALEUS* Gurr, 1962

Type species. *Scyllium vincenti* Daimeries, 1888; Selandian (middle Palaeocene) of Belgium.

Palaeogaleus faujasi (Geyn, 1937)
Figs. 13.4H–I

Material. Three teeth from QLO-2, including MCNA 14724.

Horizon and locality. Valdenoceda Formation, lower upper Maastrichtian, Quintanilla la Ojada (Burgos, Spain).

Description. See Geyn (1937: 42) and Herman (1977: 261) for a detailed description of the species. The best preserved specimen is an abraded lateral tooth that lacks most of the distal heel. The cusp is high, subconical and biconvex in cross section. The enameloid is smooth in both lingual and labial faces. The mesial cutting edge is slightly concave, whereas the distal one is shorter and approximately subvertical. The main cusp is flanked by two short cusplets mesially, but only by one cusplet on the distal part of the crown due to abrasion of the heel. Short basilolabial folds are located in the marginal zone of the mesial heel. The rounded labial base of the crown is reminiscent of a transversal bulge. Despite that only part of the root has been preserved, a lingual protuberance and the remnants of a broad and deep nutritive groove that would separate both lobes are still recognised. In addition, a large marginolingual foramen has also been preserved.

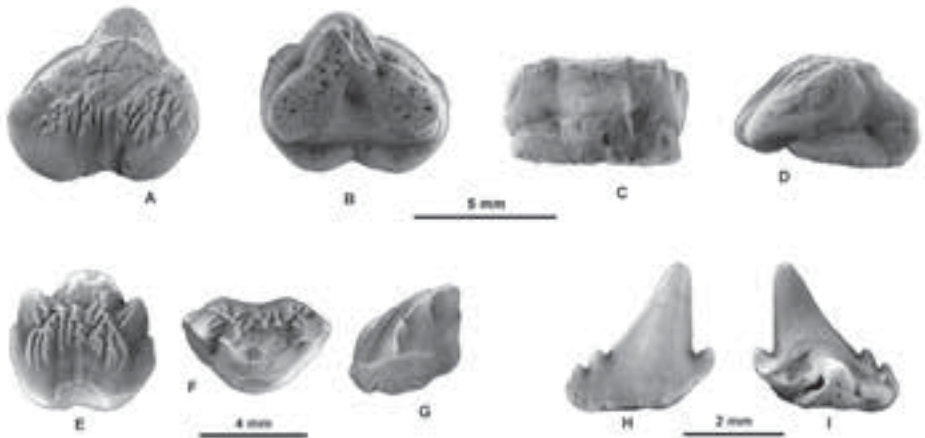


Figure 13.4 A–G, *Plicatoscyllium lehneri* (Leriche, 1938), A–D, anterolateral tooth in labial (A), basal (B), lingual (C) and profile (D) views, MCNA 14848; E–G, anterolateral tooth in labial (E), apical (F) and profile (G) views, MCNA 14722. H–I, *Palaeogaleus faujasi* (Geyn, 1937), lateral tooth in labial (H) and lingual (I) views, MCNA 14724. All the teeth from the bone assemblage QLO-2.



Figure 13.5 Original figuration of *Plicatoscyllium lehneri* (Leriche, 1939). 1–6, lateral teeth with a gradually more distal position.

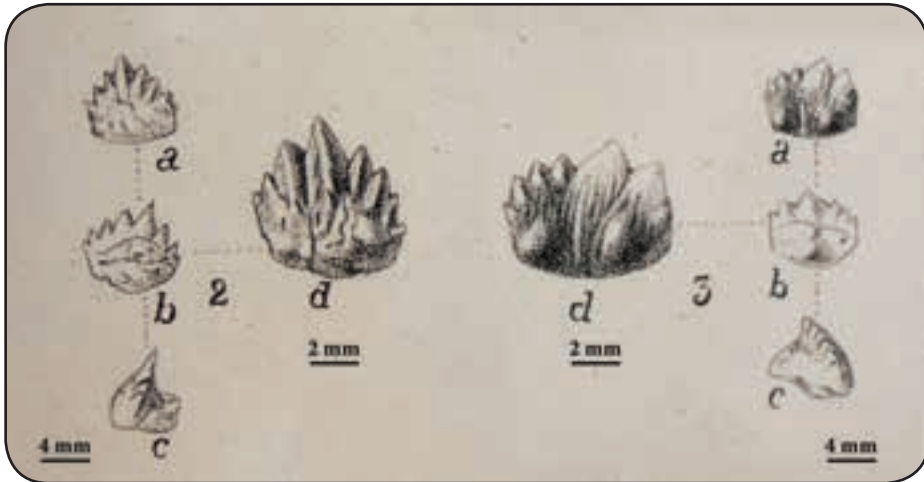


Figure 13.6 Original figuration of *Plicatoscyllium minutum* (Forir, 1887). 2, anterolateral tooth; 3, lateral tooth.

Discussion. The teeth of *Palaeogaleus faujasi* are the largest and more robust among the species assigned to the genus (Cappetta and Corral, 1999). This Maastrichtian species seems to be restricted mainly to the northeastern Atlantic Region (see Table 20.3 in Chapter 20). Generally regarded as a Maastrichtian species, the stratigraphical range of *P. faujasi* was extended down by Vullo (2005) to the upper Campanian on the basis of a single tooth found in Charente (France). Subtle folds on the lingual face of mesial and the distal cusplets, and the existence of short but strong folds along the basiolabial bulge, which give it a jagged appearance, are features that make the Campanian specimen slightly distinct from the Maastrichtian forms of *P. faujasi*.

Superorder BATOMORPHII Cappetta, 1980a
 Order RAJIFORMES Berg, 1940
 Suborder RHINOBAIDOIDEI Fowler, 1941
 Family RHINOBATIDAE Müller and Henle, 1838
 Genus *RHINOBATOS* Link, 1790

Type species. *Raja rhinobatos* Linnaeus, 1758; Recent, Genoa and Venice, Italy.

Rhinobatos echavei Cappetta and Corral, 1999
 Figs. 13.7A–M

Material. Three teeth from QLO-2 (MCNA 14728, MCNA 14730, and MCNA 14731).
Horizon and locality. Valdenoceda Formation, lower upper Maastrichtian, Quintanilla la Ojada (Burgos, Spain).

Description. See Cappetta and Corral (1999: 354) for a complete description of the species. Teeth rather thick with a crown mesiodistally elongated in occlusal view. There is a well marked transverse keel that is concave labially and mesiodistally meets the margins at an angle greater than 90°. Distinct constrictions occur behind both marginal angles (Figs. 13.7A, E, I). The labial margin of the crown is regularly convex, whereas the lingual margin is cut out by a relatively broad, protruding medial uvula and two short marginal uvulae (Fig. 13.7I). Each uvula is broad, rounded and circumscribed by a short crest behind the constriction. The labial face of the crown, which is round-to-diamond shaped (Figs. 13.7D, H, M), extends labially to form a medially broad visor. In profile view the sloping labial face is steep upwards but rounded at the visor level (Fig. 13.7K). The lingual face is bulged up but flattened above the uvula. It can be seen in the best preserved specimen (Figs. 13.7I–M) that the root is slightly narrower than the crown, and the labial face of the former is oblique and downwards projected. Moreover, the root branches into two lobes separated by a deep groove inside which a large foramen opens. The marginolingual faces of the root are also provided with large circular foramens (Fig. 13.7I). The lingual notch of the root is broad and rounded.

Discussion. The specimens from Quintanilla la Ojada broadly match the original description of *R. echavei* from Albaina. However, they slightly differ from the types because of the rounded and poorly salient process on the middle part of the labial visor of the crown, which is less developed. Vullo (2005) reported this species from western France, extending thus its distribution and its stratigraphical range to the lower-upper Campanian, where would occur with the closely related species *R. casieri* Herman in Cappetta and Case (1975b). See remarks in Chapter 11.

Rhinobatos ibericus Cappetta and Corral, 1999
 Figs. 13.7N–R

Material. One tooth from QLO-2 (MCNA 14729).

Horizon and locality. Valdenoceda Formation, lower upper Maastrichtian, Quintanilla la Ojada (Burgos, Spain).

Description. See Cappetta and Corral (1999: 356) for a complete description of the species. Practically, the crown is the only preserved part of this small tooth. The crown is slightly longer than wide and has a labial margin regularly convex. Behind the rounded marginal angles no constrictions occur. In occlusal view, a transverse cuspidate keel forms a slight open concavity, being cuspidate in the medial part. The labial face of the crown distinctly shows a round-to-diamond shape. The lingual face bears a long median uvula that is narrow long and has a lanceolate end (Fig. 13.7N). It is accompanied by two labially-pointing marginal uvulae that are sort and rounded. A strong median process occurs under the visor (Fig. 13.7N).

Discussion. The cuspidate keel of the crown suggests that this tooth corresponds to a male individual. Teeth of *R. uvulatus* figured by Case and Cappetta (1997) are quite similar to *R. ibericus* but the former differentiates by having a less rounded labial outline of the crown, a short median protuberance under the visor, and a long and less acute median uvula. Despite lacking the root we see enough characters in the crown as to assign this tooth to *R. ibericus*, a taxon previously known from the type locality of Albaina (Cappetta and Corral, 1999).

RHINOBATOIDEI incert. fam.

Genus *VASCOBATUS* Cappetta and Corral, 1999

Type species. *Vascobatis albaitensis* Cappetta and Corral, 1999; from the Maastrichtian of Albaina (Treviño County, Burgos, Spain).

Vascobatis albaitensis Cappetta and Corral, 1999

Figs. 13.8

Material. Fourteen teeth from QLO-2, including MCNA 14727, MCNA 14733, MCNA 14734, MCNA 14735, and MCNA 14736.

Horizon and locality. Valdenoceda Formation, lower upper Maastrichtian, Quintanilla la Ojada (Burgos, Spain).

Description. See Cappetta and Corral (1999: 361) for a complete description of the species. Teeth with a smooth cuspidate crown with a diamond-shaped labial face forming a tilted plane. This face becomes convex above the lingual margin, and overhangs the root in the form of a projecting visor (Figs. 13.8C, K). The wide lingual face is concave in profile. Two straight transverse keels run across the crown when viewed occlusally (Figs. 13.8E, M). The upper outline of the labial face forms an angle of 90° or higher with respect to the two well defined keels, being the lower basal side either convex or truncated (Figs. 13.8H, Q). The lingual margin is much more convex and constrictions on the outline differentiate a short rounded median uvula (Fig. 13.8I). The root

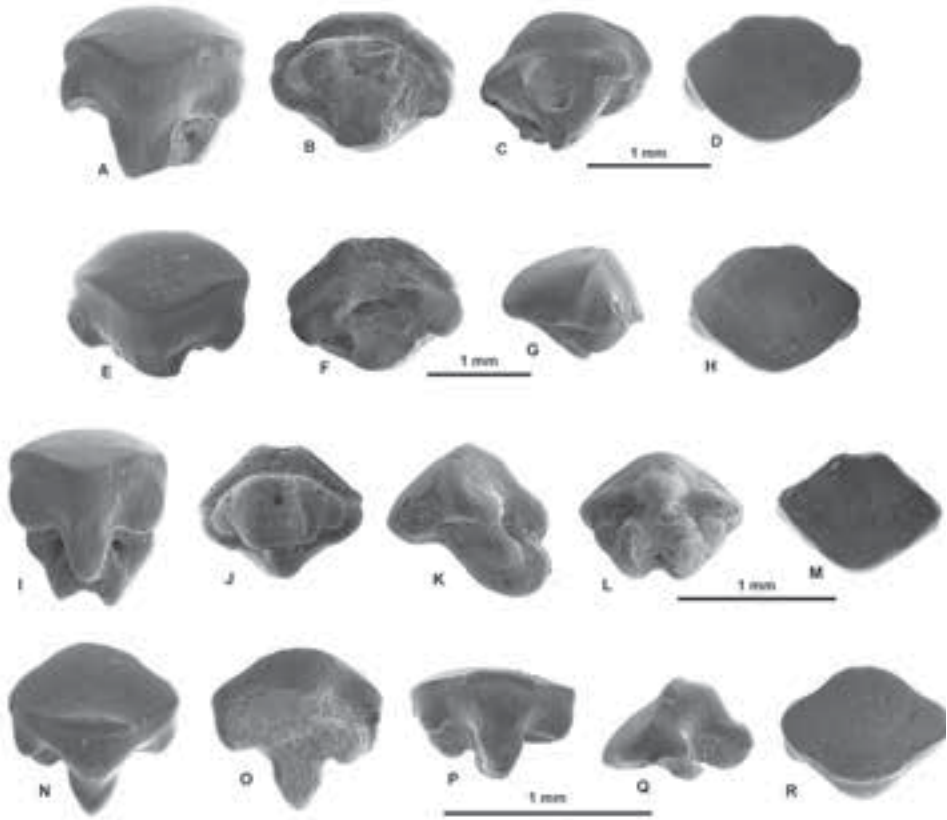


Figure 13.7 A–M, *Rhinobatos echavei* Cappetta and Corral, 1999, A–D, lateral tooth in occlusal (A), basal (B), lateral (C) and labial (D) views, MCNA 14728; E–H, anterolateral tooth in occlusal (E), basal (F), lateral (G) and labial (H) views, MCNA 14731; I–M, anterolateral tooth in occlusal (I), basal (J), lateral (K), lingual (L), labial (M) and views, MCNA 14730. N–R, *Rhinobatos ibericus* Cappetta and Corral, 1999, lateroanterior tooth in oblique occlusal (N), basal (O), lingual (P), lateral (Q) and labial (R) views, MCNA 14729. All the teeth from the bone assemblage QLO-2.

is short, narrower than the crown and lacks the medial groove. When unabraded, the root is heart-shaped in basal view, and has a concave labial area where opens a large circular foramen (Figs. 13.8J, O). A lingual foramen, which opens just below the limit of the enameloid, also occurs and is flanked by two small foramina located on the marginolingual faces of the root (Figs. 13.8L, P).

Discussion. The specimens clearly fit the diagnosis of the species given by Cappetta and Corral (1999). Some specimens (Figs. 13.8E–H, M–P) have more cuspidate crowns, probably corresponding to male individuals. The lower side of the visor is generally unornamented, although three irregular pits are observed in a lateral tooth (Fig. 13.8N). The basal face of the root in the Quintanilla la Ojada specimens is also slightly convex, as in the type specimens. However, we cannot ascertain here if this character was enhanced by

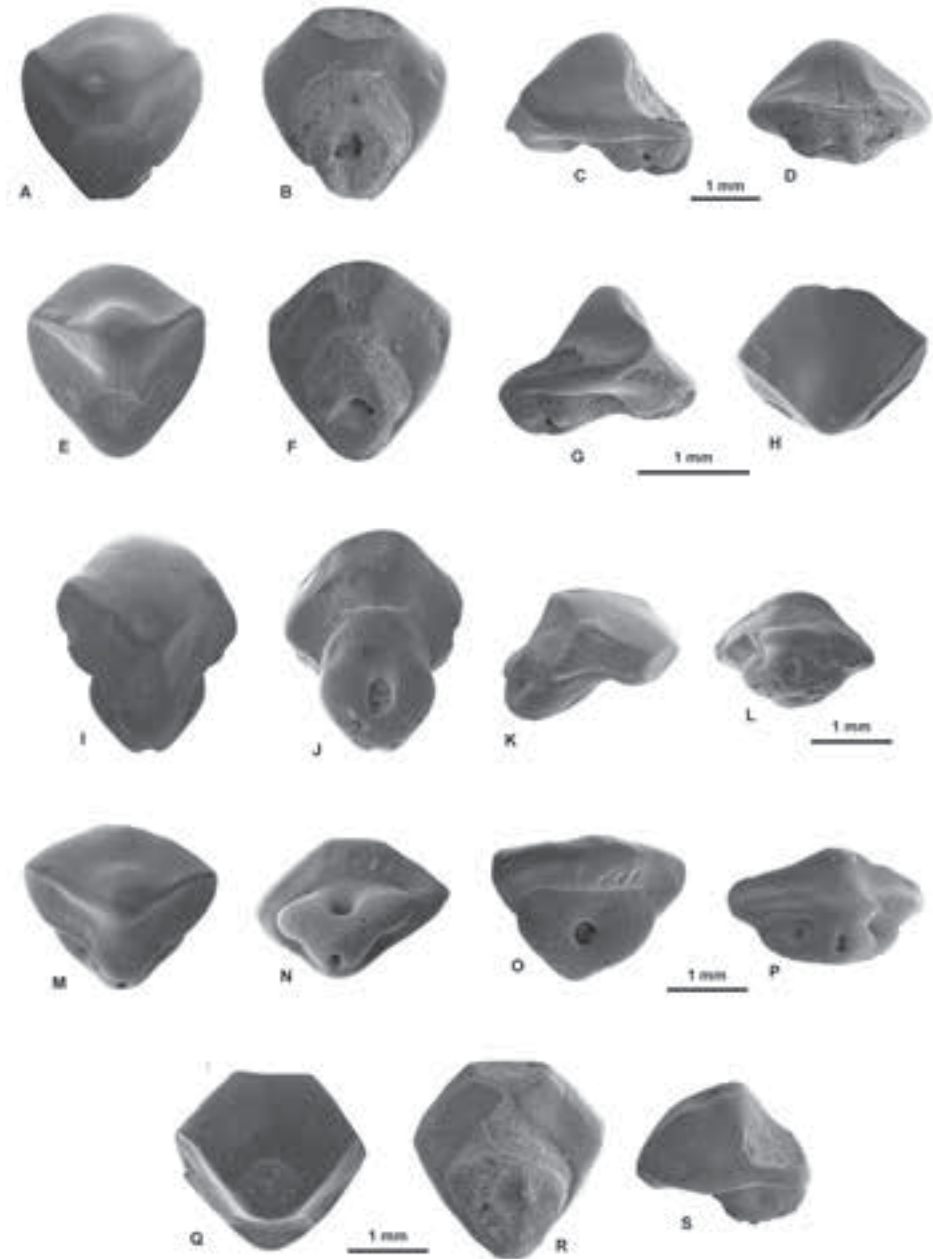


Figure 13.8 *Vascobatis albaitensis* Cappetta and Corral, 1999, A–D, lateroanterior tooth in occlusal (R), basal (S), lateral (T) and lingual (U) views, MCNA 14727; E–H, lateroanterior tooth in occlusal (E), basal (F), lateral (G) and labial (H) views, MCNA 14734; I–L, anterior tooth in occlusal (I), basal (J), lateral (K) and lingual (L) views, MCNA 14733; M–P, lateral tooth in occlusal (M), basal (N), oblique basal (O) and lingual (P) views, MCNA 14736; Q–S, lateroanterior tooth in occlusal (Q), basal (R) and lateral (S) views, MCNA 14735. All the teeth from the bone assemblage QLO-2.

abrasion. Outside the north Iberian Peninsula, the species occurs in the Maastrichtian of Belgium (Cappetta, 2012; Herman and Van Waeas, 2014) (see Table 20.3 in Chapter 20).

Suborder SCLERORHYNCHOIDEI Cappetta, 1980a

Family SCLERORHYNCHIDAE Cappetta, 1974

Genus *GANOPRISTIS* Arambourg, 1935

Type species. *Ganopristis leptodon* Arambourg, 1935; from the Maastrichtian of the Ouled Abdoun Basin, Morocco.

Ganopristis leptodon Arambourg, 1935

Figs. 13.9A–I

Material. Four incomplete rostral teeth including MCNA 14748 and MCNA 14749, and two incomplete oral teeth (MCNA 14745, MCNA 14746), all from QLO-2.

Horizon and locality. Valdenoceda Formation, lower upper Maastrichtian, Quintanilla la Ojada (Burgos, Spain).

Description. See Cappetta and Corral (1999) for a description of the species. Rostral teeth are long and dorsoventrally compressed with a smooth pointed and slightly sigmoidal cap. In specimen MCNA 14749, the anterior cutting edge runs straight towards the base of the cusp but the posterior one is convex and does not reach the basal bulge (Figs. 13.9H–I). Its peduncle is short and exhibits a rounded abraded shape. The specimen MCNA 14748 lacks most of the cusp (Fig. 13.9G), but despite this, most of the peduncle has been preserved showing the widening of its base, which is typical of the species. The latter rostral tooth also retains the characteristic bulge that overhangs the peduncle, the base of which is depressed in the centre but raised on either side. The anterior face is convex but a scar on the posterior face replaces the two missing small bifurcate lobes. Oral teeth are small, wider than long, with a cuspidate crown, the labial contour of which is regularly convex forming a subtle apron. The labial face of the crown is inclined and can be either smooth (Figs. 13.9A–B) or bear some thin folds converging toward the apex (Figs. 13.9E–F). The subvertical lingual face is reduced and has a small uvula that projects downward. In basal view, two flat root lobes are roughly subtriangular, being separated by a deep groove in which a foramen opens.

Discussion. This is a typical Maastrichtian species with an antiequatorial distribution that has been reported from Limburg and Brabant in Netherlands and Belgium (Albers and Weiler, 1964; Herman, 1977) and from the phosphate deposits of Morocco (Arambourg, 1935, 1952), where oral teeth are frequent in the upper beds of the Maastrichtian (Cappetta et al., 2014b). It is also present in the Maastrichtian of Albaina (Cappetta and Corral, 1999).

Order MYLIOBATIFORMES Compagno, 1973

Superfamily DASYATOIDEA Whitley, 1940

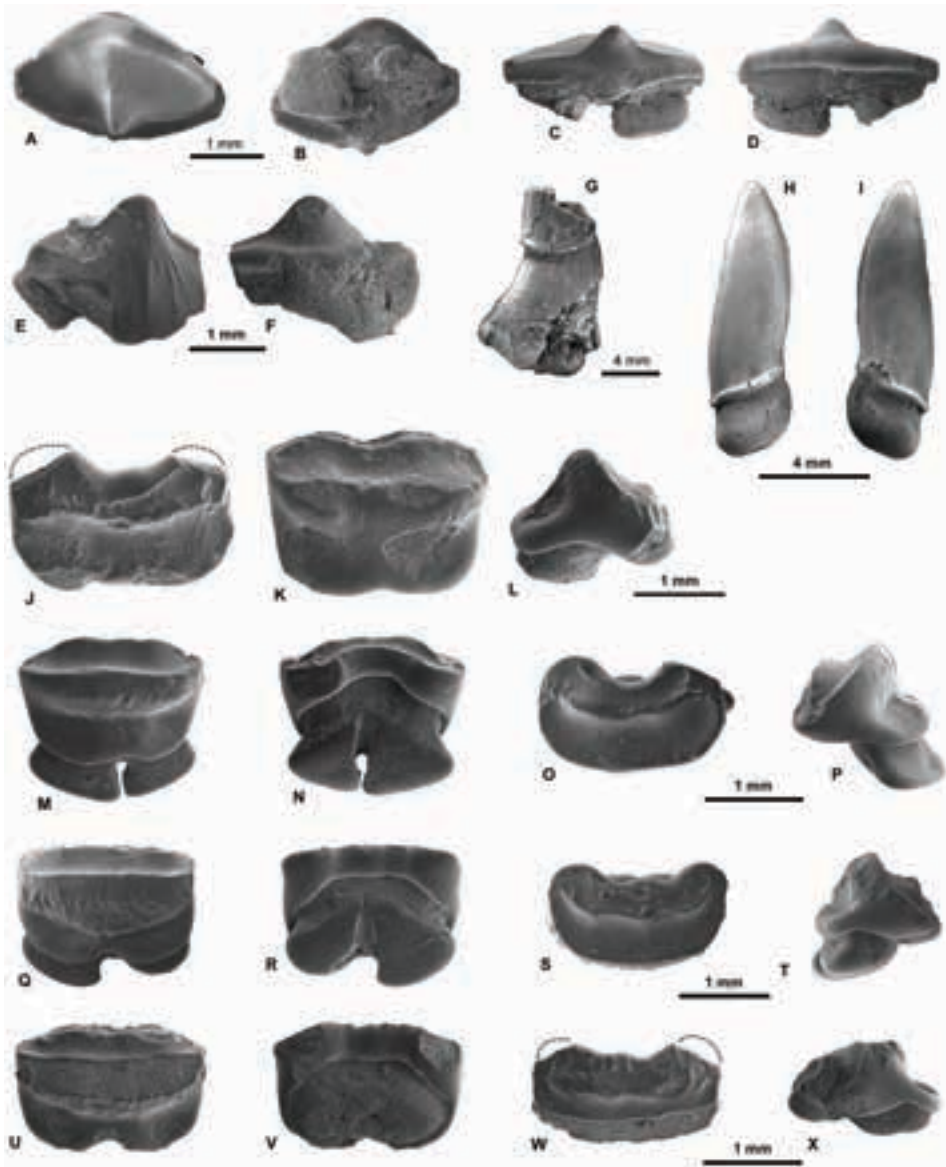


Figure 13.9 A–I, *Ganopristis leptodon* Arambourg, 1935, A–D, oral tooth in occlusal (A), basal (B), oblique lingual (C) and labial (D) views, MCNA 14745; E–F, oral tooth in labial (E) and lingual (F) views, MCNA 14746; G, fragment of rostral tooth in dorsal or ventral view, MCNA 14748; H–I, rostral tooth in dorsal and ventral views, MCNA 14749. J–X, *Coupatezia fallax* (Arambourg, 1935), J–L, lateral tooth in labial (J), occlusal (K) and lateral (L) views, MCNA 14754; M–P, lateral tooth in occlusal (M), oblique basal (N), labial (O) and lateral (P) views, MCNA 14751; Q–T, lateral tooth in occlusal (Q), basal (R), labial (S) and lateral (T) views, MCNA 14753; U–X, lateral tooth in occlusal (U), basal (V), labial (W) and lateral (X) views, MCNA 14752. Dashed lines indicate missing parts. All the teeth from the bone assemblage QLO-2.

DASYATOIDEA incert. fam.

Genus *COUPATEZIA* Cappetta, 1982

Type species. *Coupatezia woutersi* Cappetta, 1982; from the middle Eocene of Belgium.

Coupatezia fallax (Arambourg, 1952)

Figs. 13.9J–X

Material. Six teeth from QLO-2 (MCNA 14751, MCNA 14752, NCNA 14753, MCNA 14754 and two unregistered teeth).

Horizon and locality. Valdenoceda Formation, lower upper Maastrichtian, Quintanilla la Ojada (Burgos, Spain).

Description. See Arambourg (1952:178) and Noubhani and Cappetta (1997: 112) for a detailed description of the species. All teeth are small and mesiodistally elongated (typically from 1.8 mm up to 2.8 mm). The crown is low, bears a straight transverse cutting crest (Figs. 13.9M, Q, U), and has well defined marginal angles. All labial faces are reniform with different grades of vermiculation (Figs. 13.9J, O, S, W). A transverse ridge, that runs parallel to the cutting crest, divides the face into a smooth upper part and a vermiculated lower part. The lingual face is concave, with a thin vermiculated ornamentation and two marginal fossetae. In profile (Figs. 13.9L, P, T, X), the lingual face is shorter and steeper than the labial face. The labial visor is regularly concave, and the enameloid/root boundary occurring below has a trapezoidal outline (Figs. 13.9N, R, V). A medially depressed bulge overhangs the root lingually. The root is low, nearly as large as the crown, and lingually displaced in relation to the median plane of the tooth. It has a pair of lobes separated by a rather large and deep horseshoe-shaped groove (Fig. 13.9M). The bases of both lobes are triangular and practically flat (Figs. 13.9N, R).

Discussion. According to the general morphology, all the specimens collected from Quintanilla la Ojada belong to female individuals and resemble the typical forms found in Morocco (H. Cappetta, pers. observ.). Individuals of this species also occurs in Albaina (Cappetta and Corral, 1999), where they display only minor differences from their Moroccan counterparts, such as a less marked transverse crest and a thinner ornamentation on the labial face. Additional occurrences are listed in Chapter 20 (Table 20.3). The species *Coupatezia fallax* is only known from Maastrichtian deposits and seems to be confined to the upper Maastrichtian according to Cappetta et al. (2014b).

Superfamily MYLIOBATOIDEA Compagno, 1973

Family RHOMBODONTIDAE Cappetta, 1987

Genus *RHOMBODUS* Dames, 1881

Type species. *Rhombodus binkhorsti* Dames, 1881; from the Maastrichtian of Maastricht, Netherlands.

Rhombodus binkhorsti Dames, 1881

Fig. 13.10

Material. Sixty-one teeth from QLO-2, including MCNA 14757, MCNA 14758, MCNA 14759, MCNA 14800, and MCNA 14834.

Horizon and locality. Valdenoceda Formation, lower upper Maastrichtian, Quintanilla la Ojada (Burgos, Spain).

Description. See Noubhani and Cappetta (1994: 11) and Cappetta and Corral (1999: 366) for a description of the species. Medium-sized teeth easily identified by a diamond shape outline in occlusal view (Figs. 13.10A, G, N). The crown is high, when is unworn, and has four subvertical marginal faces that join the occlusal face through sharp edges. Marginal faces are covered with dense vertical wrinkles. The occlusal face is slightly convex, and quite often is worn out. Only minor patches of the original enamel ornamentation remain preserved. A transversal bulge, which is medially salient, arises along the base of the lingual face (Fig. 13.10B, E, K), but a half-round groove is on the labial one. Above this lingual bulge a deep transverse groove occurs, cutting the very salient and straight mesiolingual crest. The labial visor is salient (Figs. 13.10P, L). The root is narrower than the crown, from which is separated by a smooth depressed ring pierced by small foramina (Figs. 13.10E, H). In basal view, each root lobe forms a triangle with rounded corners, and each of the lobes are separated from the other by a deep median groove that follows the shorter diagonal of the rhombic outline of the teeth.

Discussion. These teeth, which belong to the characteristic grinding dentition type (sensu Cappetta, 1987), are easily distinguished from other Upper Cretaceous genera by both their size and rhombic crown. The specimens MCNA 14757, MCNA 14758, and MCNA 14834 exhibit an asymmetrical crown, wider than longer, when seen in occlusal view, and thus they are interpreted as corresponding to lateral teeth (Figs. 13.10D–F, G–H, N–Q). The species *Rhombodus binkhorsti* is considered a good marker for the Maastrichtian stage (Cappetta, 1987). The species is practically cosmopolitan in distribution, with the exception of the Asia-Pacific Region (see Table 20.3 in Chapter 20).

Rhombodus sp.

Fig. 13.11

Material. Fourteen teeth from QLO-2, including MCNA 14767, MCNA 14771, MCNA 14777, MCNA 14781, and MCNA 14801.

Horizon and locality. Valdenoceda Formation, lower upper Maastrichtian, Quintanilla la Ojada (Burgos, Spain).

Description. All the teeth are small. Anterolateral teeth are identified by their diamond shape outline in occlusal view (Figs. 13.11A, E). The crown of the teeth is as high as the root. The occlusal face is flat, but abrasion may lead to a round profile in some specimens (Figs. 13.11C, F). Marginolingual faces have a transversal bulge at the base.

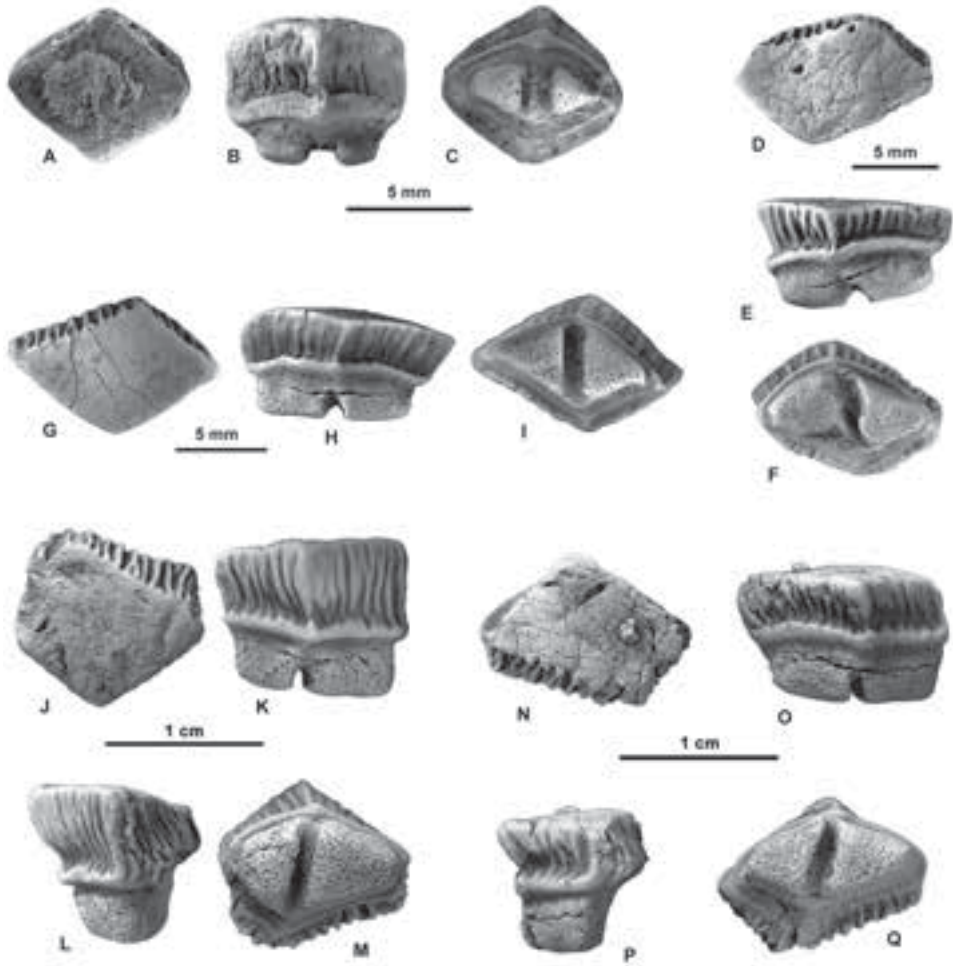


Figure 13.10 *Rhombodus binkhorsti* Dames, 1881. A–C, anterior tooth in occlusal (A), lingual (B) and basal (C) views, MCNA 14800; D–F, lateral tooth in occlusal (D), lingual (E) and basal (F) views, MCNA 14757; G–I, lateral tooth in occlusal (G), lingual (H) and basal (I) views, MCNA 14758; J–M, anterolateral tooth in occlusal (J), lingual (K), lateral (L) and basal (M) views, MCNA 14759; N–Q, lateral tooth in occlusal (N), lingual (O), lateral (P) and basal (Q) views, MCNA 14834. All the teeth from the bone assemblage QLO-2.

Above it, a groove occurs in where the remnants of vertical wrinkles are still visible. The root, which is narrower than the crown, has two short lobes, triangular in basal view. They are separated by a deep median groove. Lateral teeth (Figs. 13.11I–T), on the contrary, are longer than wide in occlusal view and not so symmetric. A low crown, which is not excessively worn by usage, bears alveolate ornamentation on the occlusal face (Figs. 13.11M, Q). The presence of extra marginal facets can create a hexagonal outline of the

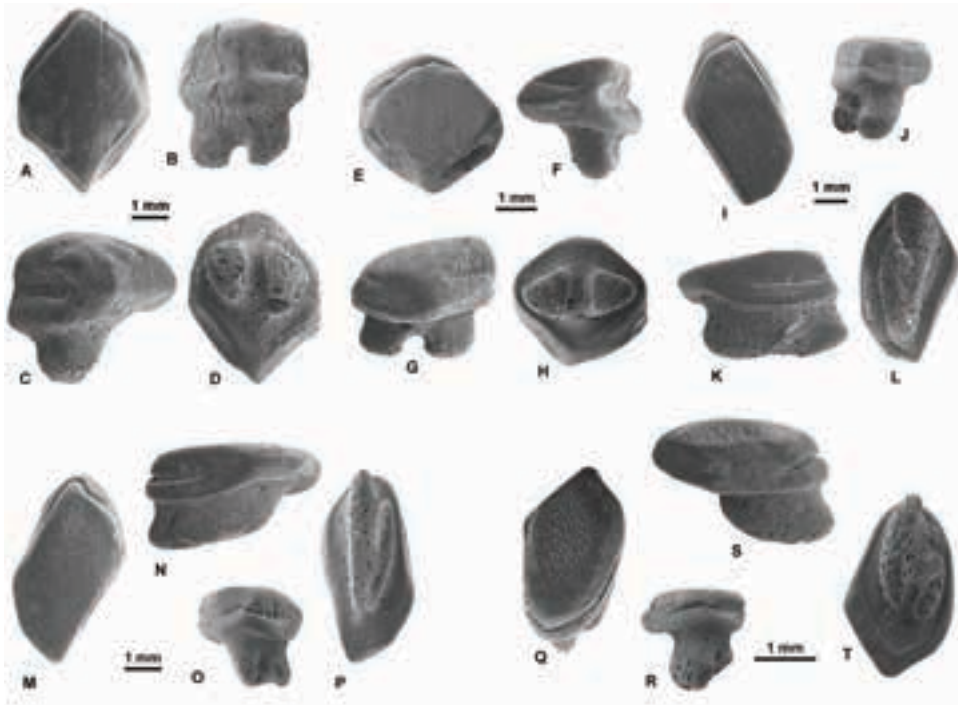


Figure 13.11 *Rhombodus* sp. A–D, anterolateral tooth in occlusal (A), lingual (B), lateral (C) and basal (D) views, MCNA 14777; E–H, lateral tooth in occlusal (E), lateral (F), labial (G) and basal (H) views, MCNA 14771; I–L, lateral tooth in occlusal (I), lingual (J), lateral (K) and basal (L) views, MCNA 14767; M–P, lateral tooth in occlusal (M), lateral (N), lingual (O) and basal (P) views, MCNA 14781; Q–T, lateral tooth in occlusal (Q), lingual (R) and lateral (S) and basal (T), views, MCNA 14801. All the teeth from the bone assemblage QLO-2.

crown. The root is lingually axis-displaced and this feature results in a long labial visor. Root lobes are labiolingually elongated and are also divided by a groove.

Discussion. The teeth of this taxon are uncommon. Three species of the genus *Rhombodus* are known to occur in the Iberian Peninsula: *Rhombodus andriesi* and *Rhombodus binkhorsti* from the upper Maastrichtian of Albaina (Cappetta and Corral, 1999), and *Rhombodus ibericus* Kriwet et al., 2007 from the upper lower Maastrichtian beds exposed at Fontllonga 6 in the Tremp area (southern Pyrenees, Spain) (Kriwet et al., 2007). The Quintanilla la Ojada teeth most closely resemble those of *Rhombodus ibericus*, mainly by size and the rhombic outline of the crown, whose marginolabial faces are ornamented but the marginolingual ones are smooth. Lateral teeth of both taxa are subpentagonal or hexagonal in outline, in occlusal view, by the development of one or two marginal extra facets. Lateralmost teeth in both taxa also share an asymmetrical outline in occlusal view (i.e. longer than wide), with two lobes of different height. However, the major differences between them lie in the shape and type of ornamenta-



Figure 13.12 Rajiformes indet. Dermal denticle in occlusal (A) and lateral (B) views from the bone assemblage QLO-2, MCNA 14803.

tion of the occlusal face of the crown, which is convex and decorated with coarser irregular shaped hollows in *R. ibericus*. On the contrary, the occlusal face of the crown of *Rhombodus* sp. is slightly concave, being ornamented with crescent pits. Lateral teeth from the two species are also separated from each other by differences in the transverse depression above the lingual bulge, which in *Rhombodus* sp. is deeper and narrower. Moreover, the lingual bulge is less overhanging in *Rhombodus* sp. than in *R. ibericus*.

Rajiformes indet.

Fig. 13.12

Material. One specimen (MCNA 14803) from QLO-2.

Horizon and locality. Valdenoceda Formation, lower upper Maastrichtian, Quintanilla la Ojada (Burgos, Spain).

Description. The only specimen is an isolated dermal denticle, or thorn, with conical profile in lateral view. The enamelled cusp has two sharpened edges, and forms a flat sloped surface that is round-pointed in the highest part (apex) but fringed in the lower end. The basal face is flat and rounded in contour with irregular folds on the neck.

Discussion. Thorns are specialised denticles that are common to all Rajiformes (Cappetta, 1987). Morphologically the specimen resembles the denticles described by Cappetta (1980a) in an articulated skeleton of *Rhinobatos latus* from the Santonian of Lebanon. However, this single unrelated type of denticle prevents us from giving more accurate assignation to any Rhinobatoidei.

Chapter 14
 NEOSELACHIANS FROM THE ALBAINA SITE (TORME FORMATION,
 UPPER MAASTRICHTIAN)

14.1 Introduction

In this chapter I deal with the systematics of the selachian material discovered in the late 1980s by a research team made up of scientists from Argentine, French and Spanish universities during a series of palaeontological excavations led by geologists of the Universidad del País Vasco/Euskal Herriko Unibertsitatea (UPV/EHU) in the then recently discovered fossil site of Laño quarry (Treviño County, Burgos) (see Astibia et al., 1990). Initially, some French members first noticed only a few shark and ray teeth scattered on the surface of fallen rocks at the toe of the quarry face, but the identified taxa (*Cretolamna appendiculata*, *Cretolamna* sp., *Ganopristis leptodon* and *Rhombodus binkhorsti*) allowed a preliminary dating of the underlying part of the series in which the terrestrial tetrapod remains were located. Since then, further explorations have been carried out and the number of chondrichthyan specimens has grown to become a significant collection. Over 1200 isolated teeth and other skeletal hard parts, including placoid scales, dermal thorns, fragments of caudal stings, and a few vertebrae have been collected. These fossils are curated and stored at the Arabako Natur Zientzien Museoa/Museo de Ciencias Naturales de Álava (MCNA). Additional remains in the private collection of J.I. Sáez Laría (Vitoria-Gasteiz) were considered for study.

14.2 Systematic palaeontology

Class CHONDRICHTHYES Huxley, 1880
 Subclass ELASMOBRANCHII Bonaparte, 1838
 Cohort EUSELACHII Hay, 1902
 Subcohort NEOSELACHII Compagno, 1977
 Superorder GALEOMORPHII Compagno, 1973

Order LAMNIFORMES Berg, 1958

Family ANACORACIDAE Casier, 1947

A list of nominal species within Anacoracidae is provided by Cappetta et al. (2014a).

Genus *SQUALICORAX* Whitley, 1939

Type species. *Corax pristodontus* Agassiz, 1843; Maastrichtian of Maastricht, Netherlands.

Some comments about the status of the genus have been given in Chapter 15.

Squalicorax kaupi (Agassiz, 1843)

Fig. 14.1

For the synonymy see Siverson (1992).

Material. MCNA 8236, MCNA 8237, MCNA 15248, MCNA 15401, MCNA 15402, and over one hundred and fifty catalogued teeth in the MCNA.

Locality. Albaina in the municipality of Treviño County (Burgos, northern Spain).

Age. Upper Maastrichtian (*Menuites fresvillensis* zone).

Description. See Cappetta and Case (1975b). The teeth are medium-sized, smaller than those of *S. pristodontus*. The mesial cutting edge is usually convex, sometimes gibbous and shows a well marked concavity. A noticeable notch occurs at the junction between the distal cutting edge of the cusp and the distal heel. The serrations of the cutting edges are strong. The root is strongly labiolingually flattened, with oblique marginal border in labial view. The basal notch of the root is wide and not very deep.

Discussion. Many found teeth of this species are about one-half the size of *Squalicorax pristodontus*. Cappetta and Corral (1999) reported that the teeth of this species in the Albaina locality have a very small size compared to teeth of other localities in Europe or North America and that they probably correspond to juvenile fishes. Since then the author of this thesis has collected additional specimens belonging to adult and juvenile individuals. This species is quite abundant in the upper Campanian of New Jersey (Cappetta and Case, 1975b), and occurs up to upper Maastrichtian in Texas (Case and Cappetta, 1997). The species is scarce in the Maastrichtian of Morocco (see Table 20.3 in Chapter 20).

Squalicorax pristodontus (Agassiz, 1843)

Fig. 14.2

For the synonymy see Cappetta and Case (1975b) and Herman (1977).

Material. Five teeth, including MCNA 8297, MCNA 9042.1, and JISL-271 (J.I. Sáez Laría private collection).

Locality. Albaina in the municipality of Treviño County (Burgos, northern Spain).

Age. Upper Maastrichtian (*Menuites fresvillensis* zone).

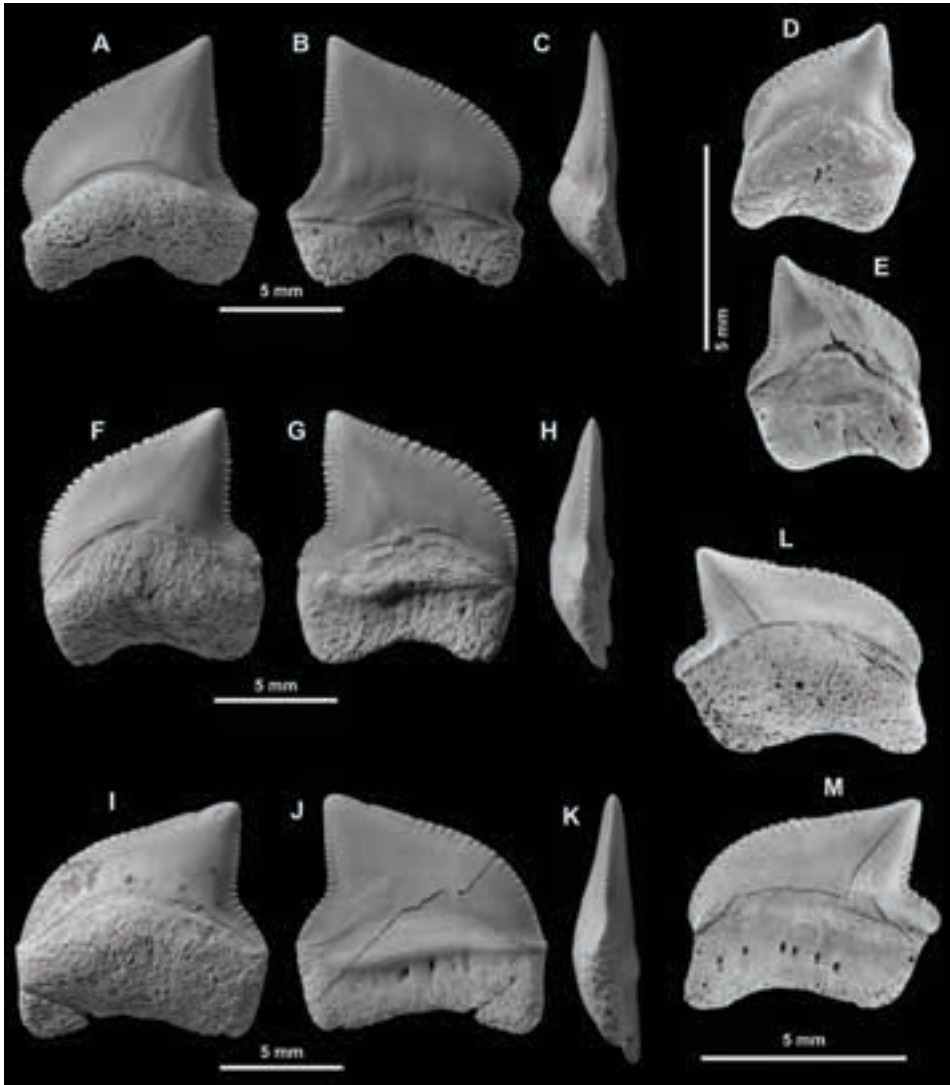


Figure 14.1 *Squalicorax kaupi* (Agassiz, 1843). A–C, anterolateral tooth in lingual (A), labial (B), and mesial (C) views, MCNA 15401; D–E, anterior tooth in lingual (D) and labial (E) views, MCNA 8236; F–H, anterolateral tooth in lingual (F), labial (G), and mesial (H) views, MCNA 15402; I–K, lateral tooth in lingual (I), labial (J), and mesial (K) views, MCNA 15248; L–M, lateral tooth in lingual (L) and labial (M) views, MCNA 8237. Photographs D–E, L–M from Cappetta and Corral (1999).

Description. See Cappetta and Case (1975b). The general morphology of the teeth in this species is roughly similar in the various tooth files of the jaws, being differentiated by its relative height that decreases towards the commissure (Arambourg, 1952). Cutting edges are strongly serrated (e.g. serrate to crenate) with larger serrations located

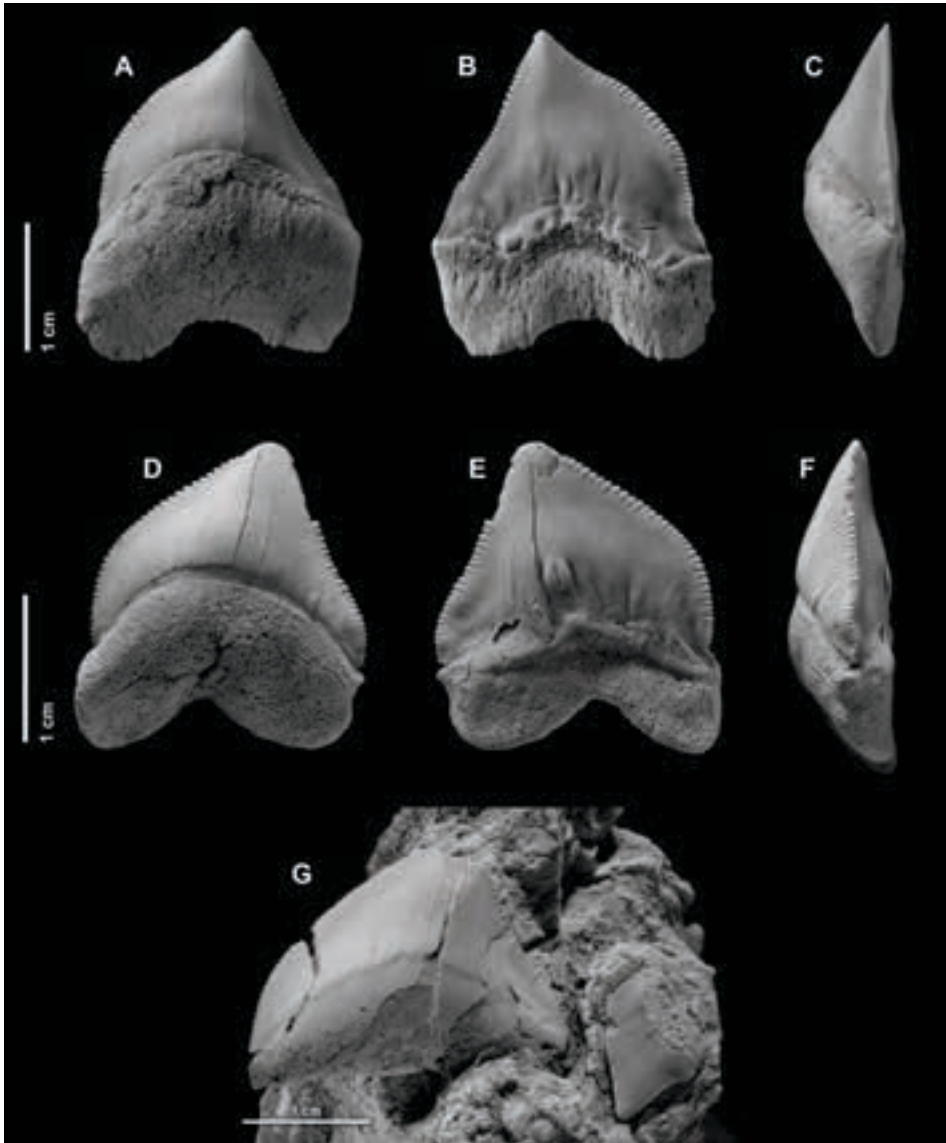


Figure 14.2 *Squalicorax pristodontus* (Agassiz, 1843). A–C, anterior tooth in lingual (A), labial (B), and mesial (C) views, JISL-271 (J.I. Sáez Laría private collection); D–F, anterolateral tooth in lingual (D), labial (E), and mesial (F) views, MCNA 8297; G, lateral tooth in lingual view (left specimen), MCNA 9042.1.

mid-way along the crown margin. The crown is erect in anterior files. It has a gibbous mesial cutting edge in its median region and a practically straight abrupt distal one. The labial face of the crown is decorated with vertical irregular folds (Fig. 14.2B). The crown-root boundary is marked by a collar and a bulge in the lingual and labial faces,

respectively. The root is high and labiolingually flattened with a well marked basal median notch. A line of lingual foramina occurs in the upper part of the root. Lateral teeth are mesiodistal expanded and the crown is distally inclined (Fig. 14.2G).

Discussion. It is a rare tooth in the Albaina locality when compared to the nearby Quintanilla la Ojada site, where relatively more specimens occur given the size of the current sample in the latter. The few teeth collected in Albaina are quite identical by size and morphology with typical teeth of the species (see also discussion in Chapters 13 and 15). Teeth of the species have been found in other Maastrichtian locations across the world (see Table 20.3 in Chapter 20).

Family OTODONTIDAE Glikman, 1964

Genus *CRETOLAMNA* Glikman, 1958

Type species. *Otodus appendiculatus* Agassiz, 1843; Turonian of Lewes, East Sussex (England, UK).

Cretolamna appendiculata (Agassiz, 1843)

Fig. 14.3

For the synonymy see Herman (1977) and Siverson (1996).

Material. MCNA 8294, MCNA 8295, MCNA 8296, MCNA 14995, and about twenty-five additional, catalogued teeth in the MCNA.

Locality. Albaina in the municipality of Treviño County (Burgos, northern Spain).

Age. Upper Maastrichtian (*Menuites fresvillensis* zone).

Description. The teeth are small-sized, with rather broad cusps. The denticles are low and widen mesiodistally, particularly in lateral files, with a proximal cutting edge longer than the external one; on some very lateral teeth, small and short folds appear on the lingual face of the denticles (Fig. 14.3M). The root is not very high in lingual view and the basal notch is wide and shallow.

Discussion. Many teeth of this species are particularly small in the Albaina locality. The stratigraphical range of *Cretolamna appendiculata* is noteworthy because it ranges from Albian in Texas (Cappetta and Case, 1999) to Ypresian in Europe, southwestern Morocco and North America (Cappetta, 2012). This suggests that different species are lumped under this name (Cappetta and Corral, 1999; Siverson et al., 2015). Several sub-species ranging from the Cenomanian to the Paleocene were differentiated by Herman (1977), namely *C. appendiculata appendiculata*, *C. appendiculata lata* and *C. appendiculata pachyrhiza*. A revision of the Maastrichtian forms with low height/width ratio individuals is still pending, but they may well belong to *Cretolamna lata* (Herman, 1977), which has been recently elevated to species rank by Herman and Van Waes (2012) (see also discussion in Chapter 13). This species also has a large geographical range, including Europe, Africa, Asia, and North America (see Table 20.3 in Chapter 20).

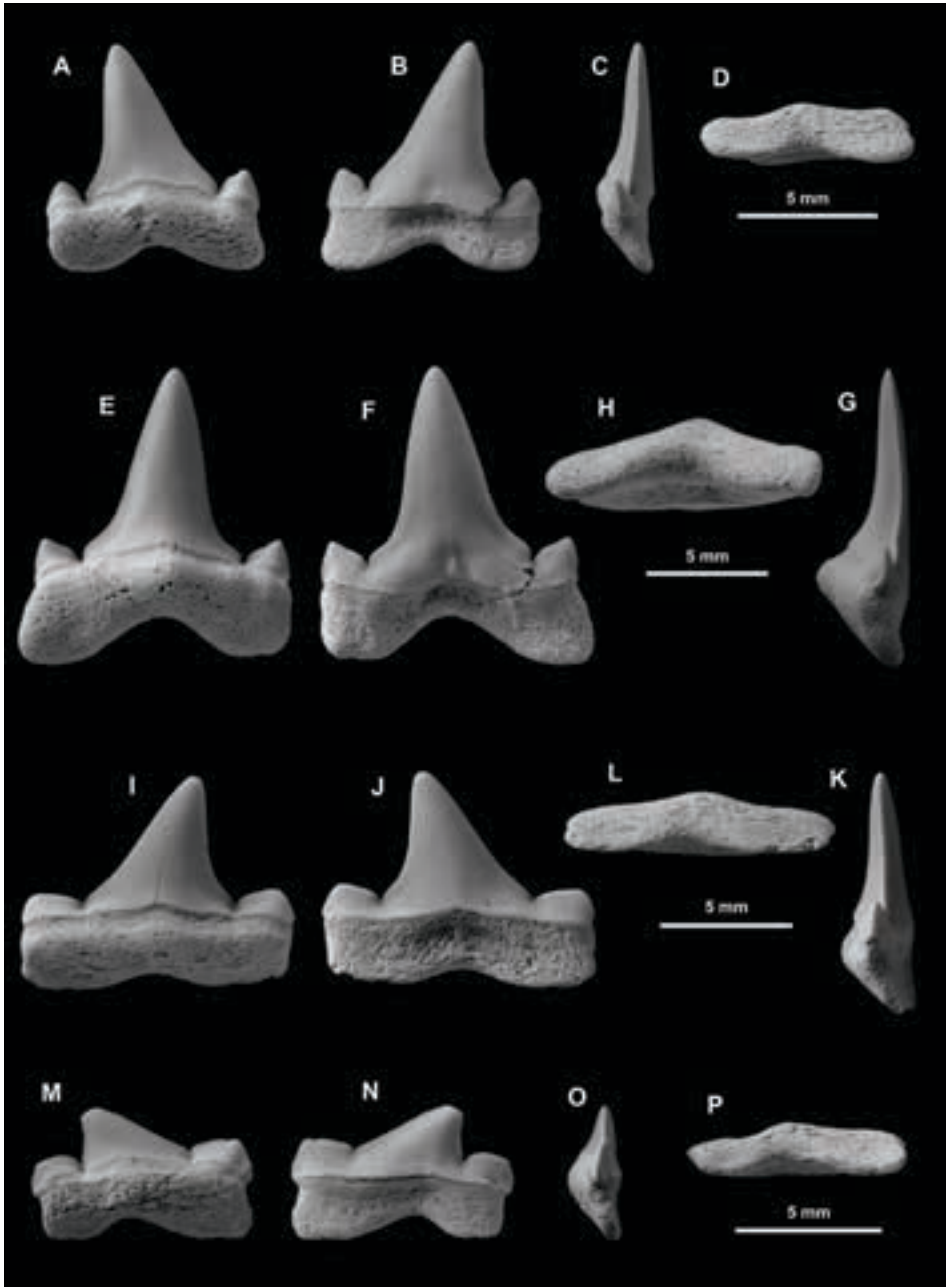


Figure 14.3 *Cretolamna appendiculata* (Agassiz, 1843). A–D, anterior tooth in lingual (A), labial (B), mesial (C), and basal (D) views, MCNA 8294; E–H, lower anterior tooth in lingual (E), labial (F), distal (G), and basal (H) views, MCNA 14995; I–L, lateral tooth in lingual (I), labial (J), distal (K), and basal (L) views, MCNA 8295; M–P, very lateral tooth in lingual (M), labial (N), mesial (O), and basal (P) views, MCNA 8296.

Genus *SERRATOLAMNA* Landemaine, 1991

Type species. *Otodus serratus* Agassiz, 1843; Maastrichtian of the Montagne de Saint-Pierre, Maastricht, Netherlands.

When Landemaine erected the genus *Serratolamna*, he included several species belonging in reality to other genera like *Carcharias* and *Cretolamna* (Case and Cappetta, 1997). For the discussion concerning the genus *Serratolamna* and its content, the reader is invited to see the Case and Cappetta's article dealing with the Maastrichtian faunas of Texas (1997).

Serratolamna serrata (Agassiz, 1843)

Fig. 14.4

For the synonymy see Cappetta and Case (1975b), Herman (1977), and Case and Cappetta (1997).

Material. MCNA 8238, MCNA 8239, MCNA 8240, and two hundred and sixty catalogued teeth in the MCNA.

Locality. Albaina in the municipality of Treviño County (Burgos, northern Spain).

Age. Upper Maastrichtian (*Menuites fresvillensis* zone).

Description. An anterior tooth (Figs. 14.4A–C) shows a triangular, straight and rather flat crown; it possesses a pair of lateral cusplets, the main one of which is wide and separated from the cutting edges of the cusp by a deep notch. The enameloid boundary shows an angular median sinuosity at the base of the labial face. The root lobes are transversely spread, with a flat basal face and a well marked groove. On a lateral tooth (Figs. 14.4G–H) the crown is tilted and widened; the distal heel is longer than the mesial one. A posterior tooth shows a very bedded and reduced crown; the distal heel bears two denticles; the mesial one is limited to a small denticle extending the mesial cutting edge of the cusp. The root in posterior teeth is stout and as high as the crown.

Discussion. This species is a typical element present in the selachian fauna during the Maastrichtian, being described worldwide. Its occurrences are listed in Table 20.3 (Chapter 20).

Family ODONTASPIDIDAE Müller and Henle, 1839

Genus *CARCHARIAS* Rafinesque, 1810

Type species. *Carcharias taurus* Rafinesque, 1810; Recent, Sicily, Italy.

For the discussions concerning the taxonomical status of this genus see Ward (1988).

Carcharias heathi Case and Cappetta, 1997

Figs. 14.5A–F

1997 *Carcharias heathi* Case and Cappetta, p. 140, Pl. 7, Figs. 7–9.

2015b *Carcharias heathi* Case and Cappetta; Corral et al., p. 649, Figs. 7A–L.

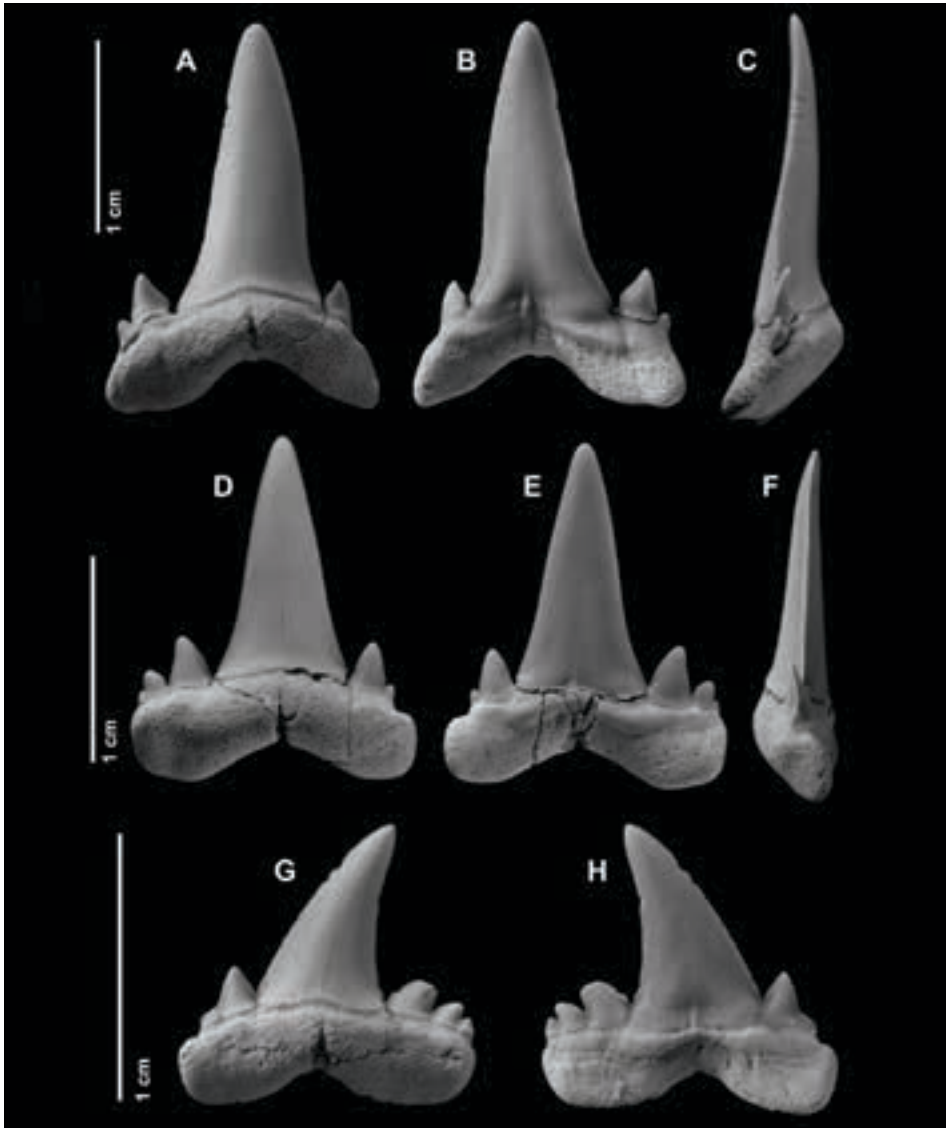


Figure 14.4 *Serratolamna serrata* (Agassiz, 1843). A–C, anterior tooth in lingual (A), labial (B), and distal (C) views, MCNA 8238; D–F, lower lateral tooth in lingual (D), labial (E), and distal (F) views, MCNA 8239; G–H, upper lateral tooth in lingual (G), and labial (H) views, MCNA 8240.

Material. MCNA 8241, MCNA 8242, and other one hundred and six catalogued teeth in the MCNA.

Locality. Albaina in the municipality of Treviño County (Burgos, northern Spain).

Age. Upper Maastrichtian (*Menuites fresvillensis* zone).

Description. For a description of this species see Case and Cappetta (1997). The teeth of this species have a triangular crown narrowing gradually towards the apex, with a slightly sigmoidal profile. In anterior teeth the cutting edges do not reach the base of the crown. The lateral cusplets are not high. The root lobes are well diverging even in anterior files. The lingual face of the crown is always smooth.

Discussion. This taxon, erected from material of the upper Maastrichtian of Texas, also occurs in the Maastrichtian of Morocco (Arambourg, 1952), where it was sometimes mistaken for the Danian species *Carcharias tingitana* (Arambourg, 1952). In *Carcharias tingitana*, the lateral cusplets are smaller but sharper than in *Carcharias heathi*, the cusp is more rounded on its lingual face, and the cutting edges of the crown are shorter. The specimens from Albaina are identical with those from Texas. It is possible that *Carcharias heathi* also occurs in northern Europe where may have been mistaken with other odontaspidid species. See other occurrences in Table 20.3 (Chapter 20).

Carcharias aff. *gracilis* (Davis, 1890)

Figs. 14.5G–H

2015 *Carcharias* aff. *gracilis* (Davis); Adolfssen and Ward, p. 327, Fig 6A–C.

Material. MCNA 8243, and other three catalogued teeth in the MCNA.

Locality. Albaina in the municipality of Treviño County (Burgos, northern Spain).

Age. Upper Maastrichtian (*Menuites fresvillensis* zone).

Description. This lower lateral tooth is small and symmetrical; a lateral cusplet is broken. The remaining cusplet is relatively high, compared with the cusp, wide, triangular and separated from the cutting edge of the cusp by a deep and narrow notch stopping far from the labial limit of the enameloid. The cusp is erect and rather flat; it widens at its base and the outline of both cutting edges is concave in labial (or lingual) view. The basal bulge of the labial face of the cusp bears numerous very short and vertical folds, the strongest being situated below the cusplets level. The root lobes are very separated, with a basal edge regularly concave. The labial face of the root is not very high; the lingual face of the root is well developed and oblique (Fig. 14.5H), and the basal face rather rounded. The lingual groove is deep.

Discussion. The type-specimens of *Carcharias gracilis* (Davis, 1890: 386, Pl. 38, Figs. 18–20) are three broken anterior teeth whose morphological features are difficult to establish on the basis of a so poorly preserved material. Siverson (1995) considers the specimen figured by Davis (1989, Pl. 38, Fig. 20) as representing a tooth of *Odontaspis speyeri* Darteville and Casier, 1943, which is characterised by having coarse labial folds and often a second pair of cusplets. The types of *Carcharias gracilis* come from Danian deposits, so, the assignment of these teeth of Albaina to the species must be considered with reservations. However, the material from Albaina corresponds perfectly with *Carcharias gracilis* (Davis, 1890) from the Maastrichtian of Belgium and Netherlands (Cappetta and Corral, 1999), and represent the only occurrence outside northwest

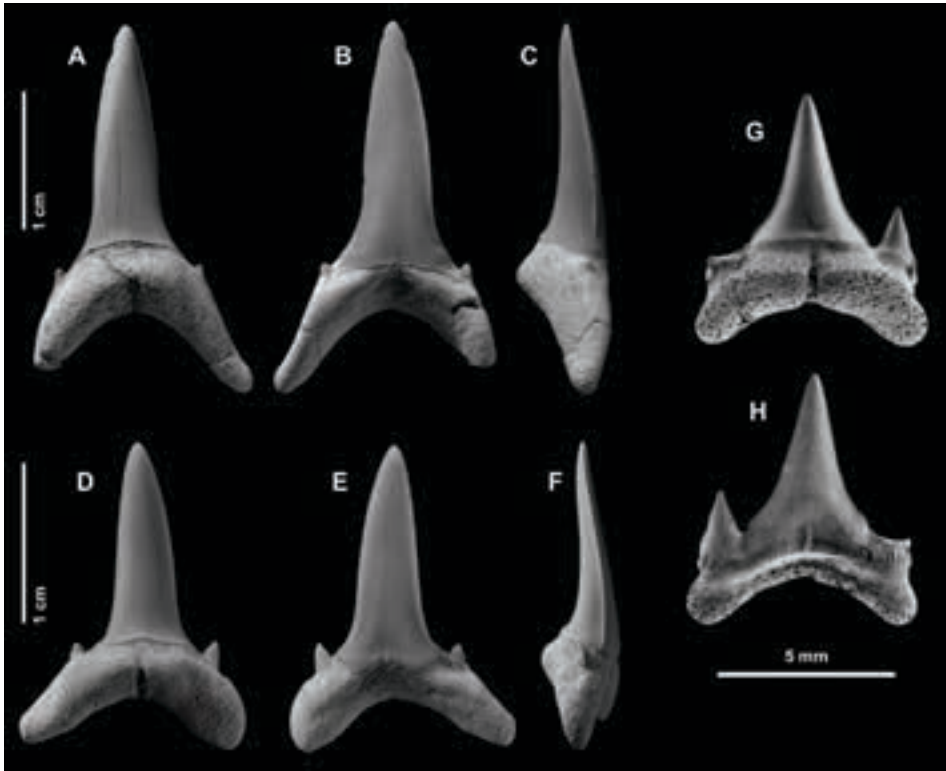


Figure 14.5 A–F, *Carcharias beathi* Case and Cappetta, 1997, A–C, anterior tooth in lingual (A), labial (B), and profile (C) views, MCNA 8241; D–F, lateral tooth in lingual (D), labial (E), and profile (F) views, MCNA 8242. G–H, *Carcharias* aff. *gracilis* (Davis, 1890), lower lateral tooth in lingual (G), and labial (H) views, MCNA 8243. Photographs G–H from Cappetta and Corral (1999).

continental Europe, where *C. gracilis* was defined (see Table 20.3 in Chapter 20). Some of the specimens figured by Geyn (1937) may also belong to this taxon.

Genus *ODONTASPIS* Agassiz, 1838

Type species. *Squalus ferox* Risso, 1810; Recent, Mediterranean coastline, southern France.

Odontaspis bronni (Agassiz, 1843)

Fig. 14.6

1843 *Lamna* (*Odontaspis*) *bronni* Agassiz, Vol. 3, p. 297, Pl. 37a, Figs. 8–9.

1929 *Odontaspis bronni* (Agassiz, 1843); Leriche, p. 240–241.

1937 *Odontaspis* (*Odontaspis*) *bronni* (Agassiz, 1843); Geyn, p. 31, p. 33, Figs. 117–123.

1977 *Palaeohypotodus bronni* (Agassiz, 1843); Herman, p. 230, Pl. 10, Fig. 2.

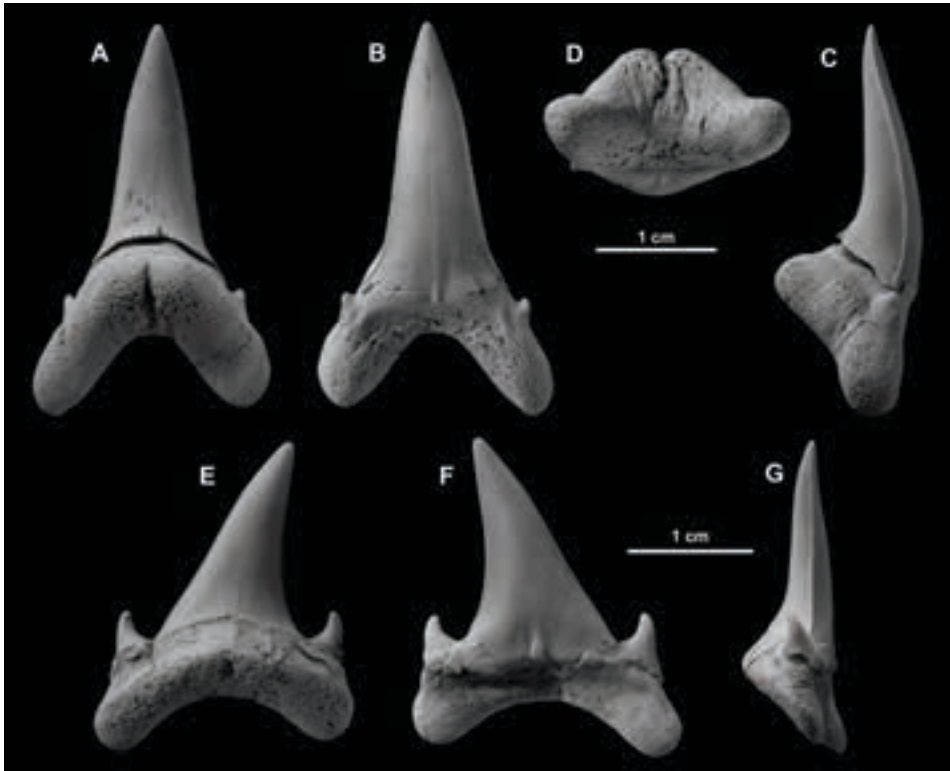


Figure 14.6 *Odontaspis bronni* (Agassiz, 1843), A–D, anterior tooth in lingual (A), labial (B), profile (C) view, and basal (D) views, JISL-273; E–G, lateral tooth in lingual (E), labial (F), and profile (G) views, JISL-2075.

Material. Two teeth; JISL-273 and JISL-2075 (J.I. Sáez Laría private collection).

Locality. Albaina in the municipality of Treviño County (Burgos, northern Spain).

Age. Upper Maastrichtian (*Menuites fresvillensis* zone).

Description. The anterior tooth is large-sized (3 cm high) and stout (Figs. 14.6A–C). The cusp is erect, rather wide at its base, and slightly tilted lingually. The cutting edges are continuous and slightly sigmoidal in profile view. The labial face of the cusp is transversely convex, mainly at the base, and overhangs the root by a not very salient bulge. The lingual face is strongly convex transversely with a completely smooth enameloid surface. The lateral cusplets are small, not very sharp and slightly divergent; they are separated from the cusp cutting edges. The root is massive, with rather short and thick lobes that are well separated and rounded at their ends. The lingual protuberance is well developed, with a deep groove. A lateral tooth (Figs. 14.6E–G) is slender, broader (particularly at the base) and labiolingually compressed. The main cusp, which is distally

inclined, is flanked on each side by a well-developed cusplet, the apexes of which are both pointing to the cusp and curved lingually. The cutting edges of the crown are continuous, straight in profile view, and do not reach the base of the main cusp. The root has a moderate lingual protuberance and two round-ended, well-splayed root lobes.

Discussion. The anterior tooth from Albaina is quite identical to one of the teeth figured by Geyn (1937: 33, Fig. 121) from the Maastrichtian of the Dutch Limburg. The teeth studied by Herman (1977) from the Maastrichtian of Belgium and Netherlands show usually two pairs of lateral cusplets, which is not the case on the Albaina specimens. The large specimens from Albaina are smaller than the biggest ones collected in northern Europe. Some large specimens from the Maastrichtian of Belgium are quite identical to the anterior tooth from Albaina (H. Cappetta, pers. observ.). Until now, this species was only known in northwestern Europe and its discovery in Albaina extends its range southwards. Albaina is the only occurrence outside the area where the species was defined.

Order ORECTOLOBIFORMES Applegate, 1972
Family GINGLYMOSTOMATIDAE Gill, 1862
Genus *PLICATOSCYLLIUM* Case and Cappetta, 1997

Type species. *Plicatoscyllium derameei* Case and Cappetta, 1997; upper Maastrichtian of Texas.

This genus was erected by Case and Cappetta (1977) for the Upper Cretaceous Ginglymostomatidae showing teeth with a more or less strongly folded labial face. The teeth of all species within this extinct genus have a hemiaulacorhize root with a massive medial lingual protuberance. The crown is triangular with a main cusp and three to four pairs of large lateral cusplets. The labial face of the crown has a typical ornamentation consisting of three to more than twenty-two strong sinuous enameloid folds (Herman and Van Waes, 2014). All the representatives of the genus *Plicatoscyllium* were inhabitants of shallow waters in tropical to subtropical regions (Cappetta, 2012).

Plicatoscyllium lehneri (Leriche, 1938)
Figs. 14.7A–L

- 1938 *Ginglymostoma lehneri* Leriche, p. 22, Pl. 4, Figs. 1–6.
- 1943 *Ginglymostoma rugosum* Darteville and Casier, p. 106, Pl. 3, Fig. 9.
- 1952 *Ginglymostoma lehneri* Leriche; Arambourg, p. 131, Pl. 21, Figs. 12–29, Fig. 24 in the text.
- 1952 *Ginglymostoma rugosum* Darteville and Casier; Arambourg, p. 130, Pl. 21, Figs. 9–11.
- 1958 *Ginglymostoma lehneri* Leriche; Casier, p. 54, Pl. 3, Fig. 1.
- 1959 *Ginglymostoma lehneri* Leriche; Signeux, p. 224, Pl. 7, Figs. 18–20.
- 1959 *Ginglymostoma rugosum* Darteville and Casier; Signeux, p. 235, Pl. 9, Figs. 3–4.
- 1997 *Plicatoscyllium minutum* (Forir, 1887); Noubhani and Cappetta, Pl. 15, Figs. 1–8.
- 2015b *Plicatoscyllium lehneri* (Leriche); Corral et al., p. 650, Figs. 8A–G.

Material. JISL- 272 (J.I. Sáez Laría private collection), MCNA 8244, MCNA 8245, MCNA 8246, MCNA 8247, MCNA 8248, MCNA 8249, and other sixteen catalogued teeth in the MCNA.

Locality. Albaina in the municipality of Treviño County (Burgos, northern Spain).

Age. Upper Maastrichtian (*Menuites fresvillensis* zone).

Description. For the description see Arambourg (1952) and Noubhani and Cappetta (1997). The teeth of this species are characterised by particularly strong labial folds delimiting a triangular area on the labial face of the crown. One latero-anterior tooth (Figs. 14.7C–F) shows the typical morphology and ornamentation. The apron is usually concave medially in labial view and the lingual protuberance is wide and prominent. In profile view (Fig. 14.7E), the labial face of the crown is very oblique, making an angle of about 45° with the basal face of the root. Very lateral teeth (Fig. 14.7L) are rather mesiodistally compressed. In lateral files, the folds are less strong and not delineate a triangular area. In very lateral teeth, the main cusp and lateral cusplets are very reduced, the outline of the apron is regularly convex in labial view and the folds are much less numerous and less prominent.

Discussion. The teeth of the ginglymostomatids *Plicatoscyllium minutum* and *Plicatoscyllium lehneri* are similar to such an extent that the latter species has been considered a junior synonym (Herman 1977; Arambourg, 1952; Noubhani and Cappetta 1997; Cappetta and Corral, 1999). The species *Plicatoscyllium minutum* (Forir, 1887) is based on isolated teeth that have been collected over the years in the Maastricht Formation (upper Maastrichtian) of the Dutch Limburg province (Netherlands), and the Limburg and Liege provinces (Belgium) (Herman and Van Waes, 2014). The labial ornamentation of the crown is much simpler in *Plicatoscyllium minutum* than in *Plicatoscyllium lehneri*, particularly because the absence of a triangular zone in anterior teeth and the occurrence of less numerous folds in lateral teeth (see Herman, 1977).

The species *Plicatoscyllium lehneri* (Leriche, 1938) was erected on the basis of isolated teeth discovered in the Vista Bella Formation (Maastrichtian) of Trinidad Island (Trinidad and Tobago), and presents a main distribution in the Tethyan realm. It also occurs in the Maastrichtian of DR Congo (as *Ginglymostoma rugosum*; Darteville and Casier, 1943) and the Maastrichtian phosphate deposits of Morocco (Noubhani and Cappetta, 1997: as *Plicatoscyllium minutum*; Cappetta et al., 2014b). See other occurrences in Table 20.3 (Chapter 20).

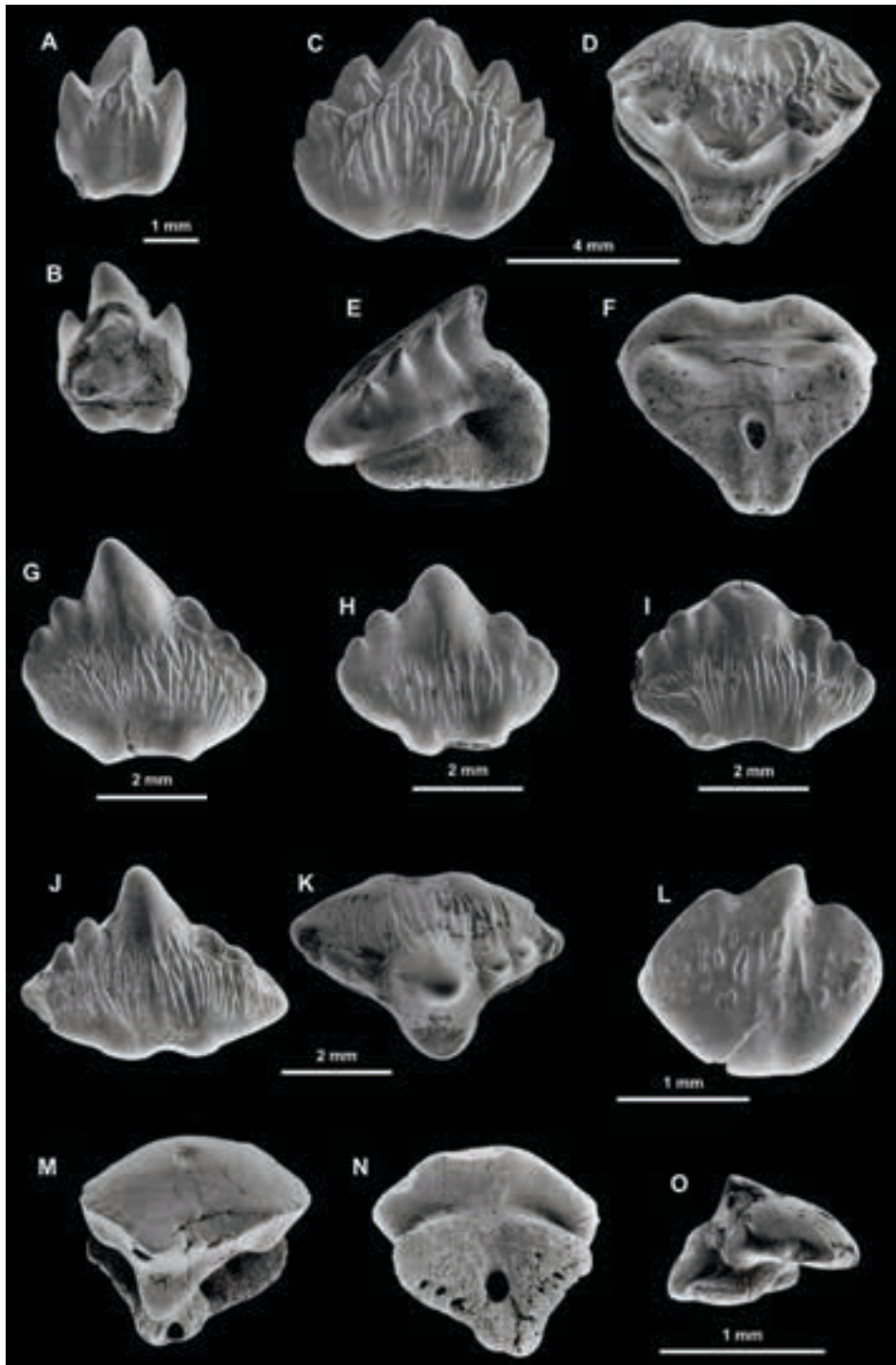
Family HEMISCYLLIIDAE Gill, 1862

Genus *CHILOSCYLLIUM* Müller and Henle, 1837

Type species. *Scyllium plagiosum* Bennett, 1830; Recent, Sumatra, Indo-West Pacific.

Chiloscyllium sp.

Figs. 14.7M–O



Material. MCNA 8250, and other seventeen catalogued teeth in the MCNA.

Locality. Albaina in the municipality of Treviño County (Burgos, northern Spain).

Age. Upper Maastrichtian (*Menuites fresvillensis* zone).

Description. A lateral tooth shows a not very high crown and a very short cusp; its root is strongly flattened with a large central foramen; in occlusal view, the lingual margin of the crown shows sorts of very short lateral uvulae.

Discussion. By its morphology, this tooth reminds those of the genus *Vascobatis* (see below). Yet, its root is much more flattened, with the central foramen opening basally and not on the labial face of the root as in *Vascobatis*. Moreover, the apron is not horizontal but oblique in profile view, the root is much more developed transversely and the enameloid lingual protuberance is narrower. So this tooth can be assigned to the Orectolobiformes and more precisely to the genus *Chiloscyllium*. In the genus *Hemiscyllium*, the labial face of the crown is flatter, with often a bifid apron and a basal median process issuing from the lower part of the apron and directed lingually.

Order CARCHARHINIFORMES Compagno, 1973

Family TRIAKIDAE Gray, 1851

Genus *PALAEOGALEUS* Gurr, 1962

Type species. *Scyllium vincenti* Daimeries, 1888; from the Selandian (middle Palaeocene) of Belgium.

Palaeogaleus faujasi (Geyn, 1937)

Fig. 14.8

Material. MCNA 8251, MCNA 8252, MCNA 8253, MCNA 8254, MCNA 8255, MCNA 8256, MCNA 8257, MCNA 8258, and other thirty-five catalogued teeth in the MCNA.

Locality. Albaina in the municipality of Treviño County (Burgos, northern Spain).

Age. Upper Maastrichtian (*Menuites fresvillensis* zone).

Description. For a detailed description of this species see Herman (1977). The teeth of this species are robust with a high and thick cusp; lateral cusplets are widely united to the base of the cusp and are not very high nor sharp. The labial face of the crown is usually smooth; when folds are present, they are short, not very salient and located under the heels.

-
- ◀ **Figure 14.7** A–L, *Plicatoscyllium lebneri* (Leriche, 1938), A–B, anterior tooth in labial (A) and lingual (B) views, MCNA 8244; C–F, lateroanterior tooth in labial (C), occlusal (D), profile (E) and basal (F) views, JISL-272 (J.I. Sáez Laría private coll.); G, lateral tooth in labial view, MCNA 8245; H, lateral tooth in labial view, MCNA 8246; I, lateral tooth in labial view, MCNA 8247; J–K, lateral tooth in labial (J) and occlusal (K) views, MCNA 8248; L, very lateral tooth in labial view, MCNA 8249. M–O, *Chiloscyllium* sp., lateral tooth in occlusal (M), basal (N) and profile (O) views, MCNA 8250. Photographs from Cappetta and Corral (1999).

Discussion. *Palaeogaleus* first occurs in the Campanian (Herman, 1977) and continues on into the end of the lower Ypresian (Noubhani and Cappetta, 1997). Very few species of *Palaeogaleus* have been described in Cretaceous deposits, as follows:

- *Palaeogaleus dahmanii* Noubhani and Cappetta, 1997; Maastrichtian from the Ouled Abdoun Basin, Morocco.
- *Palaeogaleus faujasi* (Geyn, 1937); Maastrichtian from Geulem and Kunrade, Dutch Limburg, Netherlands.
- *Palaeogaleus havreensis* Herman, 1977; Campanian (Craie d'Obourg) from Obourg, province of Hainaut, Belgium.
- *Palaeogaleus navarroensis* Case and Cappetta, 1997; late Maastrichtian (Navarroan, Kemp Clay Fm) from South Sulphur River, near Commerce, Hunt County, Texas, USA.

Palaeogaleus faujasi is the largest amongst the *Palaeogaleus* species. It differs from the other species by its much thicker and much less folded teeth; moreover, the lateral cusplets are less developed and the bulge at the base of the labial face of the crown is thicker and more salient than in the other species. Outside the area where the species was defined, the western Pyrenees is the only region where teeth of this species have been reported (see Table 20.3 in Chapter 20).

Superorder BATOMORPHII Cappetta, 1980a
 Order RAJIFORMES Berg, 1940
 Suborder RHINOBATOIDEI Fowler, 1941
 Family RHINOBATIDAE Müller and Henle, 1838
 Genus *RHINOBATOS* Linck, 1790

Type species. *Raja rhinobatos* Linnaeus, 1758; Recent, Genoa and Venice, Italy.

The rhinobatids are well represented in the Cretaceous deposits by many species. Usually, only teeth are known, but at some localities, complete or partial skeletons with dentitions are present (Schweizer, 1964; Cappetta, 1980a). It must be underlined that many of the fossil species assigned to the extant genus *Rhinobatos* possess dental morphological features that do not fit with the extant species, which shows on the whole a rather homogeneous dental design. A revision of the fossil species and a comparison with the extant taxa is needed with the aim of making clear their systematics and relationships. Such a revision will probably lead to the definition of new fossil genera.

Rhinobatos echavei Cappetta and Corral, 1999
 Fig. 14.9

Material. MCNA 8269, MCNA 8270, MCNA 8271, MCNA 8272, MCNA 8273, MCNA 8274, and twelve additional, catalogued teeth in the MCNA.

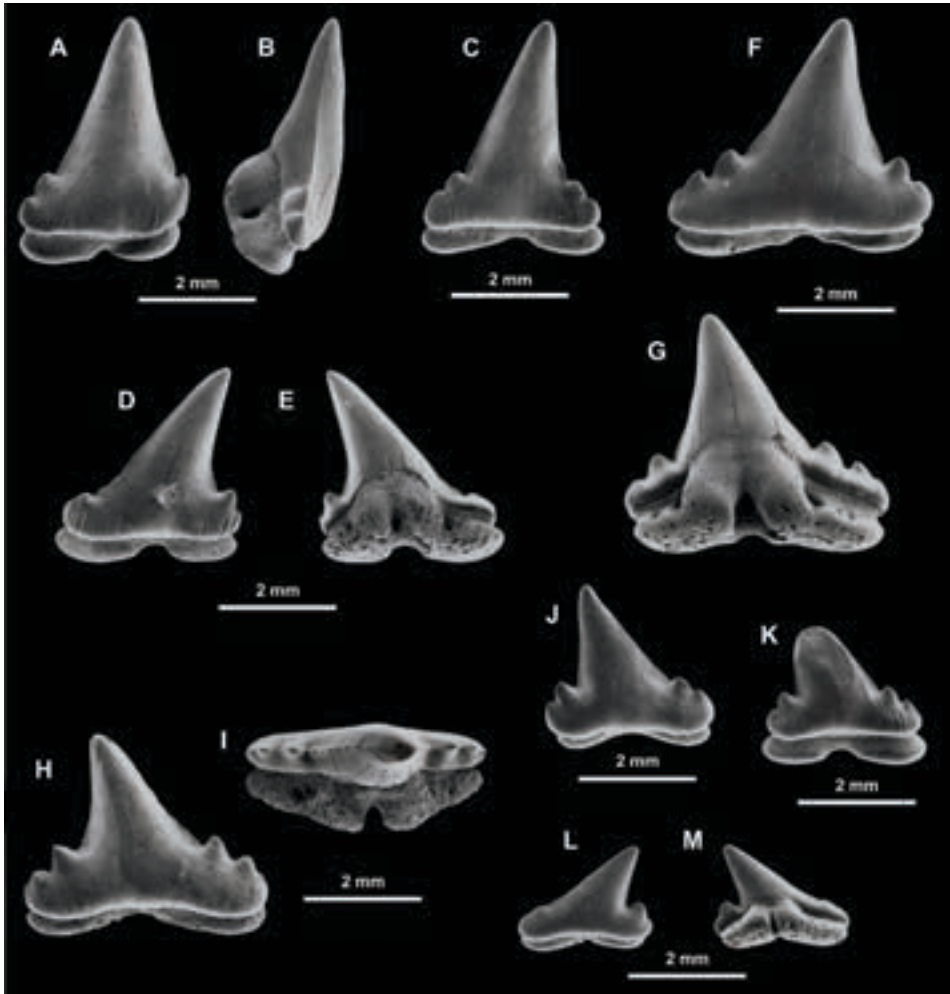


Figure 14.8 *Palaeogaleus faujasi* (Geyn, 1937). A–B, anterior tooth in labial (A) and profile (B) views, MCNA 8251; C, anterior tooth in labial view, MCNA 8252; D–E, lateroanterior tooth in labial (D) and lingual (E) views, MCNA 8253; F–G, lateral tooth in labial (F) and lingual (G) views, MCNA 8254; H–I, lateral tooth in labial (H) and occlusal (I) views, MCNA 8255; J, lateral tooth in labial view, MCNA 8256; K, lateral tooth in labial view, MCNA 8257; L–M, very lateral tooth in labial (L) and lingual (M) views, MCNA 8258. Photographs from Cappetta and Corral (1999).

Locus typicus. Albaina in the municipality of Treviño County (Burgos, northern Spain).
Age. Upper Maastrichtian (*Menuites fresvillensis* zone).

Derivatio nominis. Species named in honour of Mr Juan Echave, the permit holder of the Albaina-Laño quarry.

Holotype. MCNA 8272, Figs. 14.9G–I.

Mensurations. As follows:

	8269	8270	8271	8272	8273	8274	no. 7
L	1.52	1.66	1.62	1.70	1.49	2.60	1.56
W	1.60	1.52	1.65	1.93	1.72	2.60	1.44

L: maximum length; W: maximum width; in mm.

Diagnosis. Rhinobatid species with rather thick teeth, usually broader than long, with a clear constriction behind marginal angles. Transverse cutting crest, and labially concave in occlusal view. Median uvula rather long, most often very wide and with a rounded extremity; marginal uvulae broad and rounded, often bearing a short crest just behind the constriction. Root high and as broad as the crown.

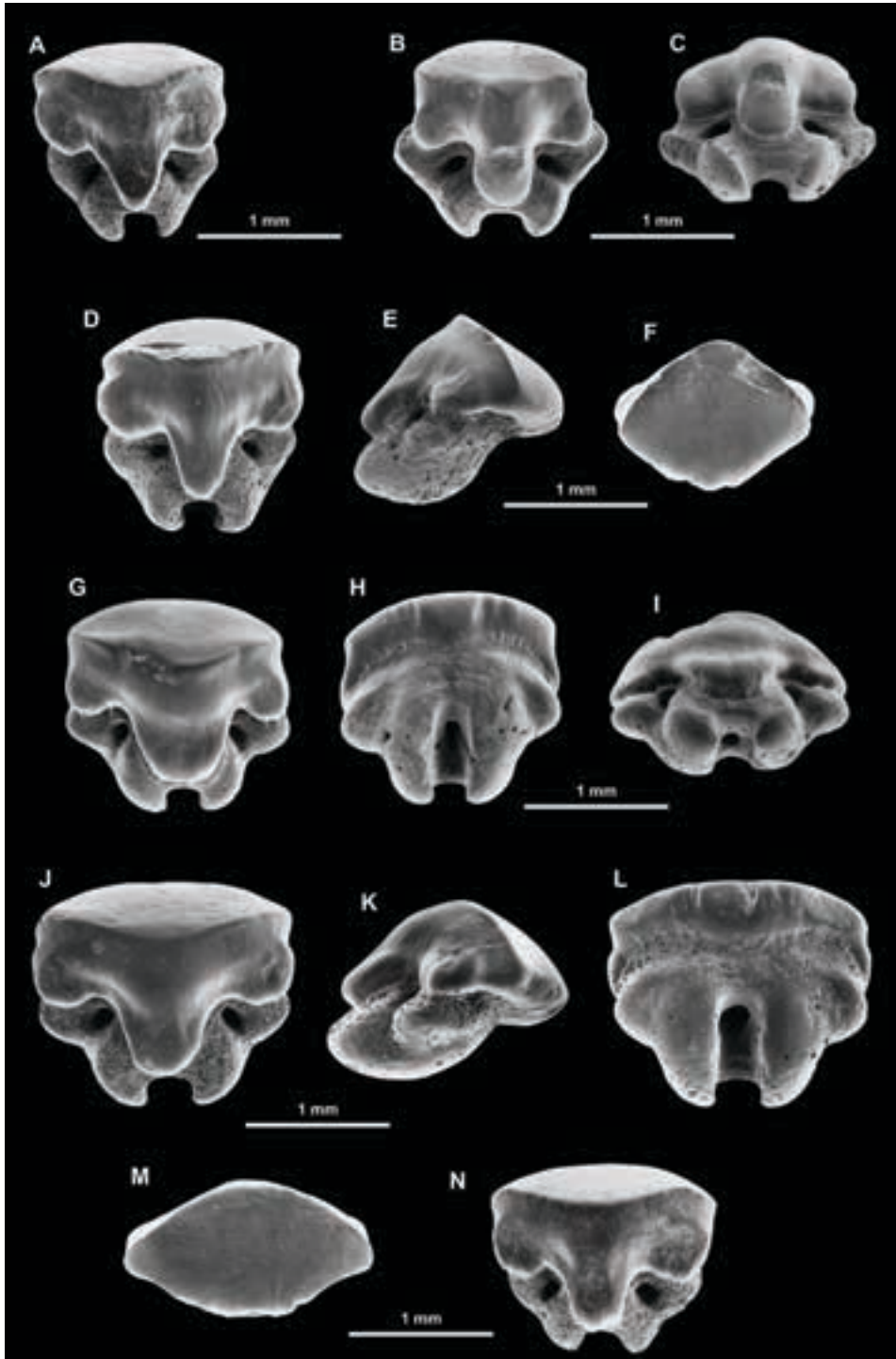
Description. The type specimen is a lateral tooth, broader than long. The crown is rather high, lacking a cusp, with a well marked transverse crest, labially concave in occlusal view and joining rounded marginal angles that make just more than 90°; a well distinct constriction occurs behind the marginal angles. The labial margin of the crown is regularly convex; the lower edge of the visor is hardly concave, broader medially where a large, rounded and poorly salient labial process differentiates; some short, irregular and smooth folds occur on either side of the process.

The lingual margin is cut out by a salient, broad and rounded median uvula and by two short but well distinct marginal uvulae. In profile view, the labial face is abrupt in its upper part and clearly convex at the visor level; the lingual face is bulged in its upper part and flattened above the uvula (Fig. 14.9I).

The root is as broad as the crown, and rather thick. In profile view (Fig. 14.9K), its labial face is rather long and very oblique, joining the lobes that are convex. The lobes are separated by a wide and deep groove where a large foramen opens in a rather labial position. The basal face of the lobes is transversely and labiolingually convex. The marginolingual faces of the root bear, each one, a large circular foramen. The lingual notch of the root, corresponding to the extremity of the groove, is broad, deep and rounded. In anterior files, the teeth are less mesiodistally spread (Fig. 14.9A). The uvula is sometimes broader (Fig. 14.9J), or on the contrary narrower and more slender than on the type specimen (Fig. 14.9D).

In some teeth, short crests can be observed on the upper part of the marginal uvulae, just behind the marginal constrictions (Figs. 14.9A–B, D). In others, the transverse crest is sometimes more salient (Fig. 14.9E).

Figure 14.9 *Rhinobatos echavei* Cappetta and Corral, 1999. A, lateroanterior tooth in occlusal view, MCNA 8269; B–C, lateroanterior tooth in occlusal (B) and lingual (C) views, MCNA 8270; D–F, lateroanterior tooth in occlusal (D), profile (E), and labial (F) views, MCNA 8271; G–I, lateral tooth in occlusal (G), basal (H), and lingual (I) views, holotype MCNA 8272; J–M, lateral tooth in occlusal (J), profile (K), basal (L), and labial (M) views, MCNA 8273; N, lateral tooth in occlusal view, MCNA 8274. Photographs from Cappetta and Corral (1999). ▶



Discussion. This species can be distinguished from *Rhinobatos ibericus* Cappetta and Corral, 1999 by its broader teeth showing a clear constriction behind the marginal angles in occlusal view. Moreover, in *R. echavei* the root is higher, thicker and often is as large as the crown. There is no labial median process on the lower part of the visor. It can be separated from *R. uvulatus* Case and Cappetta, 1997, from the Maastrichtian of Texas, by its much stronger median uvula and by its broader root. The species also occurs at Quintanilla la Ojada site (see Chapter 13).

Rhinobatos ibericus Cappetta and Corral, 1999

Fig. 14.10

Material. MCNA 8275, MCNA 8276, MCNA 8277, MCNA 8278, MCNA 8279, MCNA 8280, and other ten additional, catalogued teeth in the MCNA.

Locus typicus. Albaina in the municipality of Treviño County (Burgos, northern Spain).

Age. Upper Maastrichtian (*Menuites fresvillensis* zone).

Derivatio nominis. From the Latin adjective *ibericus* meaning from Iberia, being the latter as the Greeks called the southwesternmost territory of mainland Europe.

Holotype. MCNA 8279, Figs. 14.10K–N.

Mensurations. As follows:

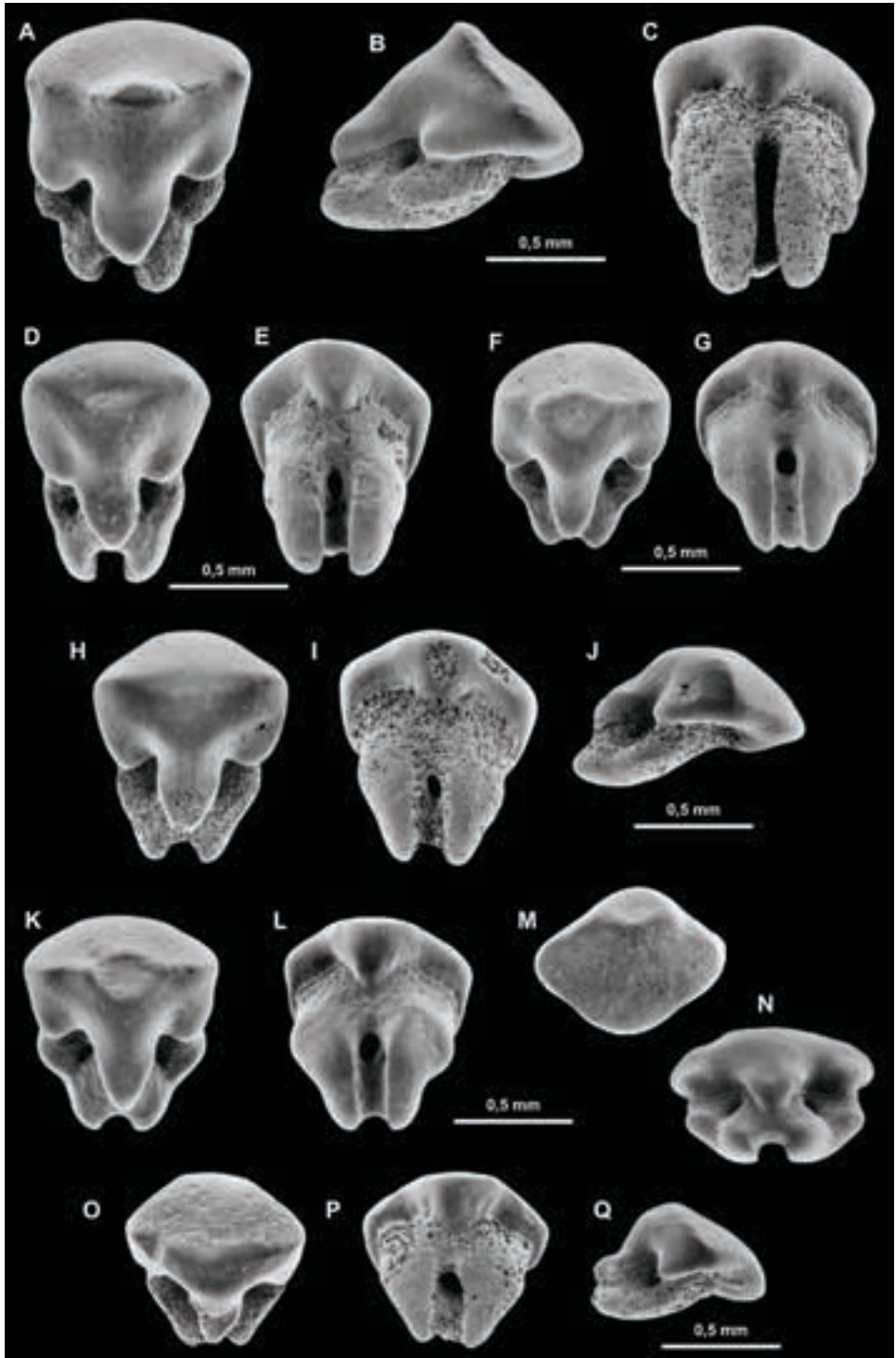
	8275	8276	8277	8278	8279	8280
L	1.18	1.03	0.90	1.04	0.95	0.75
W	1.02	0.90	0.85	0.92	0.88	0.85

L: maximum length; W: maximum width; in mm.

Diagnosis. Rhinobatid ray with teeth longer than wide and not very thick. In occlusal view, the transverse crest is practically straight and not sharp; no constriction behind the marginal angles. The median uvula is long with a rounded to acute extremity; marginal uvulae are not wide nor salient and close to the median one. There is a strong median process on the lower part of the labial visor. Root not very thick, narrower than the crown, with a long and oblique labial face in profile view.

Description. The type-specimen is a latero-anterior tooth (Fig. 14.10K–N). It is longer than wide and the root is narrower than the crown in occlusal view. The labial margin of the crown is regularly convex, the marginal angles are rounded and there is no constriction behind them. The transverse crest is not very sharp and transversely straight in

Figure 14.10 *Rhinobatos ibericus* Cappetta and Corral, 1999. A–C, anterior tooth in occlusal (A), profile (B) and basal (C) views, MCNA 8275; D–E, anterior tooth in occlusal (D) and basal (E) views, MCNA 8276; F–G, anterior tooth in occlusal (F) and basal (G) views, MCNA 8277; H–J, lateroanterior tooth in occlusal (H) view, basal (I), and profile (J) views, MCNA 8278; K–N, lateroanterior tooth in occlusal (K), basal (L), labial (M), and lingual (N) views, holotype MCNA 8279; O–Q, lateral tooth in occlusal (O), basal (P), and profile (Q) views, MCNA 8280. Photographs from Cappetta and Corral (1999). ▶



occlusal view. The median uvula is long, narrowing lingually; the marginal uvulae are short, rounded and separated from the median one by a shallow notch. The lower part of the labial visor shows a strong median process. In profile view, the labial face of the crown is oblique and slightly convex. The root is not very thick and narrower than the crown. In profile view, the labial face of the root is very oblique, and the basal face of the lobes is slightly convex. The lobes are labiolingually elongated and separated by a deep and rather broad groove with a foramen opening in its labial region (Fig. 14.10L). There is a pair of large marginolingual foramina.

A larger tooth corresponding probably to a male specimen shows a cuspidate crown with a transverse crest limited to the top of the apex of the tooth (Fig. 14.10A); the median uvula is not very long and wide, but the root remains not thick (Fig. 14.10B). In some teeth, the marginal uvulae are very short (Fig. 14.10D). A lateral tooth shows a very deep and concave lingual profile (Fig. 14.10Q).

Discussion. The teeth of this species are easy to separate from those of *R. echavei* Cappetta and Corral, 1999. On the whole, they are much smaller, narrower, and more labiolingually elongated. The broadest part of the crown in *R. ibericus* is situated at the level of the marginal angles, and usually there is not a constriction between these angles and the marginal uvulae. The marginal uvulae are much less developed. The root is less high, much narrower than the crown, in occlusal view, with lobes more elongated labiolingually. Moreover, in basal view, a clear median process (much more salient than in *R. echavei*) differentiates at the lower part of the labial visor; there are no folds on each side of this process.

Many fossil species are actually assigned to the genus *Rhinobatos*; these species are founded on isolated teeth or on skeletons. If the latter ones are more numerous, it must be pointed out that many species remain undescribed in the Cretaceous and Paleogene deposits of North Africa and Middle East (Cappetta, 1991; Noubhani and Cappetta, 1997).

Nominal species based on isolated teeth:

- *Rhinobatos casieri* Herman in Cappetta and Case, 1975b; Santonian; Lonzée, Namur province, Belgium.
- *Rhinobatos craddocki* Case and Cappetta, 1997; upper Maastrichtian (Navarroan, Kemp Clay Fm); South Sulphur River, near Commerce, Hunt County, Texas, USA.
- '*Rhinobatos*' *gonzalo* Bernárdez, 2002; upper Cenomanian, Cab-1, Asturias, northwestern Spain.
- *Rhinobatos halteri* Biddle and Landemaine, 1988; upper Barremian; La Soulaire, bone-bed 2, Unienville, Aube, France.
- *Rhinobatos incertus* Cappetta, 1973; Turonian (Carlile Shale Fm.); 13 km of Hot Springs, Fall River County, South Dakota, USA.
- *Rhinobatos incidens* (Kriwet, 1999b); lower Barremian, Alcaine, Province of Teruel, Spain.

- *Rhinobatos kiestensi* Cappetta and Case, 1999; Turonian–Coniacian boundary (contact Eagle Ford Shale–Austin Chalk), Kiest Bd., Dallas, Texas, USA.
- *Rhinobatos ladoniaensis*, Cappetta and Case, 1999; lower Campanian (Taylor Marl Fm.), North Sulphur River, Ladonia, Fannin County, Texas, USA.
- *Rhinobatos lobatus*, Cappetta and Case, 1999; Turonian–Coniacian boundary (contact Eagle Ford Shale–Austin Chalk), Kiest Bd., Dallas Co., Texas, USA.
- *Rhinobatos mariannae* Bor, 1983; upper Maastrichtian; Canal Albert near Cast-er, Liege province, Belgium and NEKAMI quarry (Groeve 't Rooth), near Margraten (Limburg, Netherlands).
- *Rhinobatos picteti* Cappetta, 1975a; Gargasian (upper Aptian); Les Barbiers, near la Tuilière, Vaucluse, southern France.
- *Rhinobatos seruensis* Guinot et al., 2012a; latest Santonian (*Marsupites testudinarius* zone), Séru, Aisne, France.
- '*Rhinobatos*' *sotoi* Bernárdez, 2002; lower Turonian (*Whiteinella archaeocretacea* zone), Aro-25, Asturias, northwestern Spain.
- *Rhinobatos uvulatus* Case and Cappetta, 1997; upper Maastrichtian (Navarroan, Kemp Clay Fm.); South Sulphur River, near Commerce, Hunt Co., Texas, USA.

Species based on skeletons:

- *Rhinobatos grandis* (Davis, 1887); Cenomanian; Hakel, Lebanon.
- *Rhinobatos hakelensis* Cappetta, 1980a; Cenomanian; Hakel, Lebanon.
- *Rhinobatos intermedius* (Davis, 1887); upper Santonian; Sahel Alma, Lebanon.
- *Rhinobatos latus* (Davis, 1887); upper Santonian; Sahel Alma, Lebanon.
- *Rhinobatos maronita* (Pictet and Humbert, 1866); Cenomanian; Hakel, Lebanon.
- *Rhinobatos obtusatus* Costa, 1865; Aptian–Albian; Pietraraja, Naples area, Italy.
- *Rhinobatos tenuirostris* (Davis, 1887); upper Santonian; Sahel Alma, Lebanon.
- *Rhinobatos tessellatus* (Marck, 1894); Campanian; Westphalia, southern Germany.
- *Rhinobatos whitfieldi* (Hay, 1903); Cenomanian; Hadjula, Lebanon.

Some species like *Rhinobatos craddocki*, *R. intermedius*, *R. latus*, *R. maronita*, *R. hakelensis*, *R. picteti* and *R. whitfieldi* have teeth with poorly developed or even absent marginal uvulae, a feature that allows to separate them easily from the species described above; the teeth of *R. whitfieldi*, furthermore, show a strongly indented labial visor. The teeth of *R. mariannae* possess few salient marginal uvulae, in addition to a crown with marginolingual faces bearing smooth folds.

The teeth of *Rhinobatos halteri* are lacking marginal uvulae; their labial outline shows a rounded and very prominent median protuberance; their lingual profile is clearly concave at the beginning of the median uvula. *Rhinobatos incertus* is characterised by teeth strongly cuspidate and lacking a cutting transverse crest, with hardly salient but transversely developed marginal uvulae. The teeth of *Rhinobatos grandis* have a particularly broad median uvula with a rounded extremity. *Rhinobatos* sp. from the Turonian of South Dakota (Cappetta, 1973) has also teeth with broad median uvula

but usually spreading out at their extremity. *Rhinobatos casieri* and *R. uvulatus* show teeth with usually well developed marginal uvulae, as the other pre-Maastrichtian species from Texas (Cappetta and Case, 1999); their general morphology allows to distinguish them easily. *Rhinobatos obtusatus* and *R. tessellatus* are represented by skeletons but unfortunately, their dentitions are unknown. The species *Rhinobatos ibericus* is also present at the site of Quintanilla la Ojada (see Chapter 13).

RHINOBATOIDEI incert. fam.

Genus *ATAKTOBATIS* Cappetta and Corral, 1999

Type species. *Ataktobatis variabilis* Cappetta and Corral, 1999; from the Maastrichtian of Albaina (Treviño County, Burgos, Spain).

Derivatio nominis. Combination of the Greek *ataktos* (i.e. irregular), in allusion to the lingual margin of the crown, and of suffix *batis* (i.e. ray in Greek).

Diagnosis. Rhinobatoidei with teeth of small size, not very high, with a lingual limit of the crown irregular with a short median uvula and more or less differentiated and dissymmetric lateral uvulae; a constriction occurs behind the marginal angles and the transverse cutting edge is convex labially in occlusal view. Root elongated lingually and very oblique with lobes separated by a deep groove.

Ataktobatis variabilis Cappetta and Corral, 1999

Fig. 14.11

Material. Four teeth, MCNA 8265, MCNA 8266, MCNA 8267, and MCNA 8268.

Locus typicus. Albaina in the municipality of Treviño County (Burgos, northern Spain).

Age. Upper Maastrichtian (*Menuites fresvillensis* zone).

Holotype. MCNA 8267, Figs. 14.11G–H.

Derivatio nominis. From the Latin *variabilis* (i.e. variable).

Mensurations. As follows:

	8265	8266	8267	8268
L	1.57	1.57	1.55	1.61
W	1.16	1.54	1.61	1.53

L: maximum length; W: maximum width; in mm.

Diagnosis. The same as for the genus.

Description. The holotype is a latero-anterior tooth practically as long as broad. In occlusal view, the labial outline of the crown is regularly convex; the marginal angles are rounded, in a labial position; behind them, the lateral margins are concave, due to a well marked constriction. Lingually, these margins join the marginal uvulae that are not symmetrical; one is broader and more irregular than the other one. They are well separated from the median uvula by narrow and short notches.

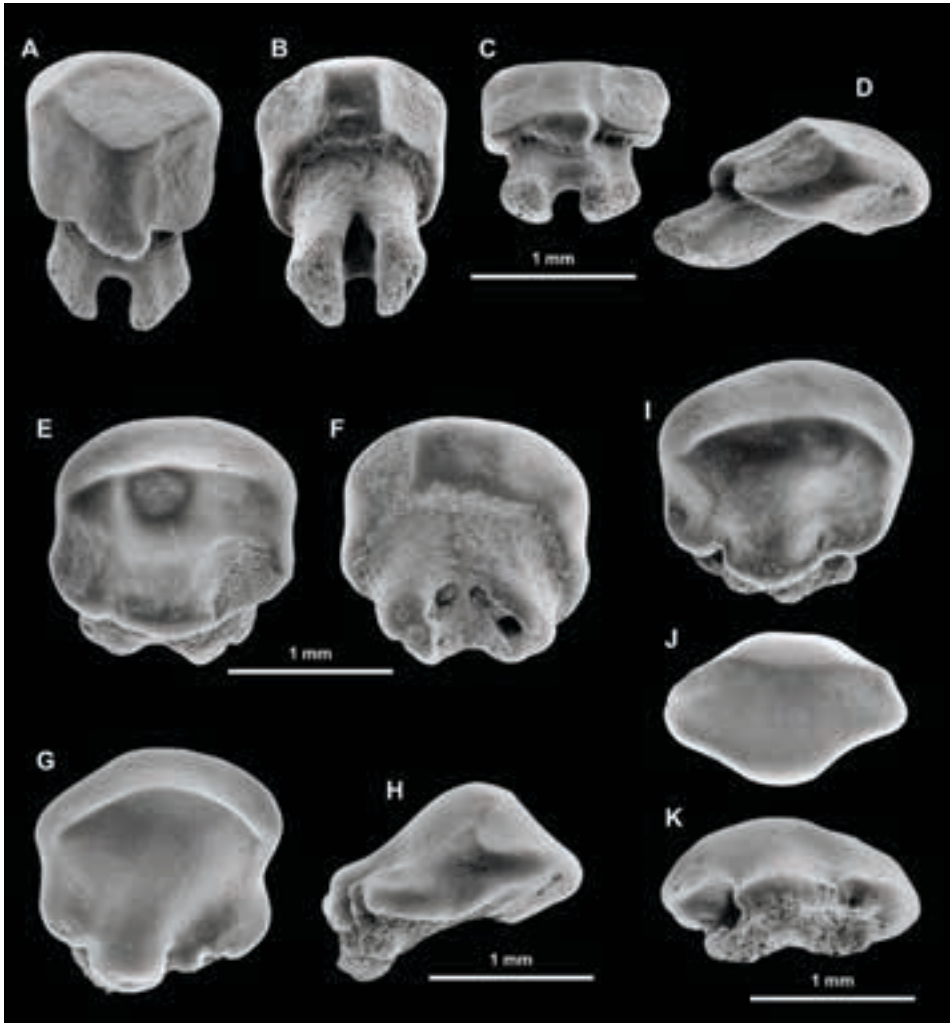


Figure 14.11 *Ataktobatis variabilis* Cappetta and Corral, 1999. A–D, anterior tooth in occlusal (A), basal (B), lingual (C), and profile (D) views, MCNA 8265; E–F, lateral tooth in occlusal (E) and basal (F) views, MCNA 8266; G–H, lateroanterior tooth in occlusal (G) and profile (H) views, holotype MCNA 8267; I–K, lateral tooth in occlusal (I), labial (J), and lingual (K) views, MCNA 8268. Photographs from Cappetta and Corral (1999).

The crown is not very thick, with a labial face much more reduced and more abrupt than the lingual one. The lower part of the visor is well developed, wide and very oblique in profile view (Fig. 14.11H). In basal view, the median part of the visor is angular and the lateral parts show wear surfaces corresponding to tooth-to-tooth friction areas. The root is not very well preserved on the type specimen (Fig. 14.11G–H); it is narrower than the crown, with a very oblique labial part in profile view.

Morphological variations are not observed to be important. One tooth shows a cuspidate crown and probably corresponds to a male specimen (Fig. 14.11E). The marginal constrictions are less deep and the lingual outline of the crown is more regular in occlusal view; the median uvula is wide and short, hardly separated from the lateral uvulae that are not well differentiated. The lingual face of the crown shows wear surfaces above the lateral uvulae (Fig. 14.11E). The root is damaged but exhibits a broad groove with two foramina; due to the wear of lobes, a foramen opens in the middle of one of the lobes. On another tooth, the marginal constriction of the crown is lacking on one side (Fig. 14.11I). An anterior tooth is attributed to the same species (Figs. 14.11A–D). This tooth is complete, longer than broad. It shows hardly differentiated marginal constrictions and not protruding marginal uvulae. The top of the crown is strongly truncated by functional wear. The root is well preserved, not thick, strongly developed lingually and narrow. The lobes are separated by a deep groove; their basal faces are small and slightly convex. Except the fact that it is narrower and labiolingually elongated, the other features correspond well to those of the latero-anterior teeth.

Discussion. By their general morphology, these teeth can be referred to Rhinobatoidei; yet, in the extant members of this suborder, no individuals exhibit similar dental features, namely a very irregular lingual limit of the crown. Fossil teeth with such morphology have not yet been described but they also occur in the Maastrichtian of Morocco and Egypt (H. Cappetta collection, Université de Montpellier, France).

Genus *VASCOBATIS* Cappetta and Corral, 1999

Type species. *Vascobatis albaitensis* Cappetta and Corral, 1999; from the Maastrichtian of Albaina (Treviño County, Burgos, Spain).

Derivatio nominis. From the demonym of *vasco* (i.e. Basque in Spanish) and the suffix *batis* (i.e. ray in Greek).

Diagnosis. Rhinobatoidei having rhombic-shaped teeth, in occlusal view, with a high and cuspidate crown; cutting edges salient. Strong median uvula, sometimes bifid. Labial visor strongly overhanging with a wide and flat lower part, horizontal in profile view. Root much narrower than the crown, few developed lingually, oblique and concave labially. A large foramen opening on the upper part of the lingual protuberance; a broad and circular central foramen on the basal face of the root and a pair of large marginolingual foramina.

Vascobatis albaitensis Cappetta and Corral, 1999

Fig. 14.12

Material. MCNA 8281, MCNA 8282, MCNA 8283, MCNA 8284, MCNA 8285, MCNA 8286, MCNA 8287, and two additional, catalogued teeth in the MCNA.

Locus typicus. Albaina in the municipality of Treviño County (Burgos, northern Spain).

Age. Upper Maastrichtian (*Menuites fresvillensis* zone).

Holotype. MCNA 8281, Figs. 14.12A–D.

Derivatio nominis. From Albaita, the Latin name of the current Albaina locality.

Mensurations. As follows:

	8281	8282	8283	8284	8285	8286	8287
L	2.78	2.50	2.57	2.80	2.30	2.60	1.40
W	2.79	2.27	2.42	2.50	2.50	2.60	1.50

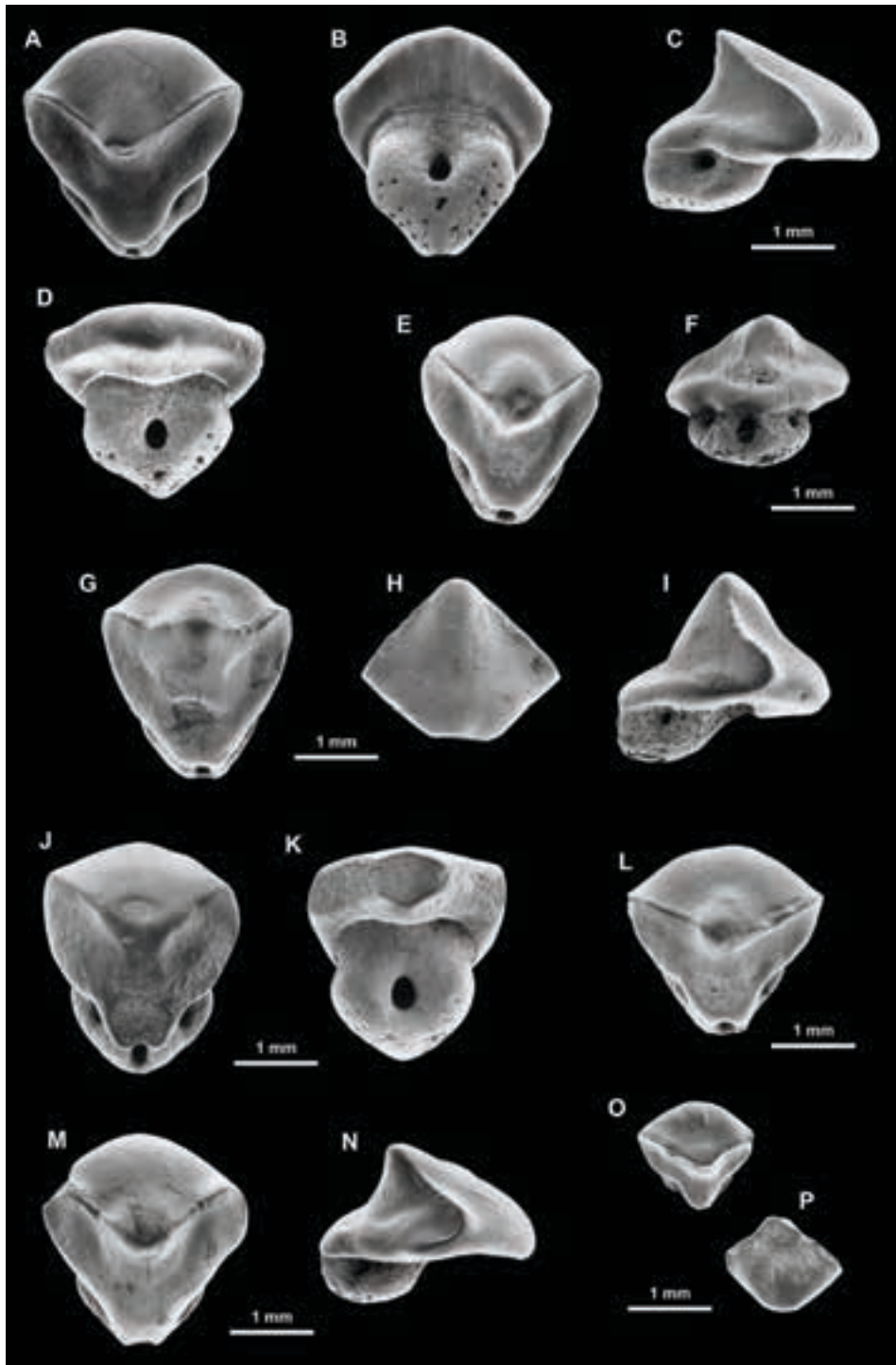
L: maximum length; W: maximum width; in mm.

Diagnosis. Same as for the genus.

Description. The type specimen (Figs. 14.12A–D) is a tooth longer than broad that occupied a latero-anterior position in the jaw. The crown is not very high but well cuspidate. The transverse crest is well differentiated and salient; the marginal angles are just above 90° and in a rather labial position. In occlusal view, the labial margin of the crown is regularly convex; the lingual margin is much more convex with a rounded and not very high median uvula that is separated from the general outline by a rather well marked constriction. The two segments of the crest, which join to make the cusp, are practically straight and form an open V-shape (Fig. 14.12A). In profile view (Fig. 14.12C), the labial face is very oblique and straight except above the labial margin where it becomes convex. The lingual face is very concave. The visor is very salient, strongly overhanging the root, with a lower part very broad (Fig. 14.12D) and horizontal in profile view (Fig. 14.12C). In labial view, the lower limit of the crown is very convex, almost angular in its median part. The root is short, narrower than the crown, relatively slender mesiodistally, and lacks a groove; it is not developed lingually. In basal view its outline is heart-shaped with a concave labial area where a large and circular central foramen opens (Fig. 14.12B); the lingual foramen is also large and opens just below the limit of the enameloid. A pair of large foramina occurs on the marginolingual faces of the root. Its basal face is slightly convex.

Dental morphological variations are not very important, but some particular features can be noted. In occlusal view, the cusp can be in a more labial (Fig. 14.12G) or more lingual (Fig. 14.12O) position. On some teeth, the uvula outline is not regularly convex but more or less notched medially (Figs. 14.12G, J). Some teeth show a constriction at the beginning of the uvula (Fig. 14.12J) and, in some cases, the outline of the labial face is truncated at its base (Fig. 14.12H). Very lateral teeth bear sometimes small folds on the labial face of the crown (Fig. 14.12P).

Discussion. By the general morphology of its teeth, the genus *Vascobatis* can be assigned to Rhinobatoidei; by its crown morphology, it could be attributed to the Rajoidei but the occurrence of large marginolingual foramina is not in favour with this hypothesis. The resemblance with the Orectolobiformes, particularly with the genera *Hemiscyllium* and *Chiloscyllium*, is superficial, as the teeth of this group have their roots much more transversely developed in comparison with the crown. *Vascobatis albaitensis* also occurs at Quintanilla la Ojada site (see Chapter 13).



Suborder SCLERORHYNCHOIDEI Cappetta, 1980a
 Family SCLERORHYNCHIDAE Cappetta, 1974
 Genus *DALPIAZIA* Checchia-Rispoli, 1933

Type species. *Dalpiazia stromeri* Checchia-Rispoli, 1933; from the Maastrichtian of Tripolitania, Libya.

Dalpiazia stromeri Checchia-Rispoli, 1933
 Figs. 14.13A–E

- 1902 *Problematicum*, Quaas, p. 320, Pl. 28, Fig. 15.
 1933 *Dalpiazia stromeri* Checchia-Rispoli, p. 7, Pl. 1.
 1935 *Onchosaurus maroccanus* Arambourg, p. 421, Pl. 19, Fig. 8.
 1940 *Onchosaurus maroccanus* Arambourg; Arambourg, p. 143, Pl. 3, Figs. 2–5.
 1943 *Onchosaurus manzadinensis* Darteville and Casier, p. 166, Pl. 14, Figs. 1–8, Text-fig. 55.
 1952 *Onchosaurus (Ischirbiza) maroccanus* Arambourg; Arambourg, p. 191, Pl. 19, Figs. 34–43.
 1987 *Dalpiazia stromeri* Checchia-Rispoli; Cappetta, p. 147, p. 148, Fig. 125.

Material. Two rostral tooth; an almost complete specimen, MCNA 8259, and a portion of the peduncle of another specimen.

Locality. Albaina in the municipality of Treviño County (Burgos, northern Spain).

Age. Upper Maastrichtian (*Menuites fresvillensis* zone).

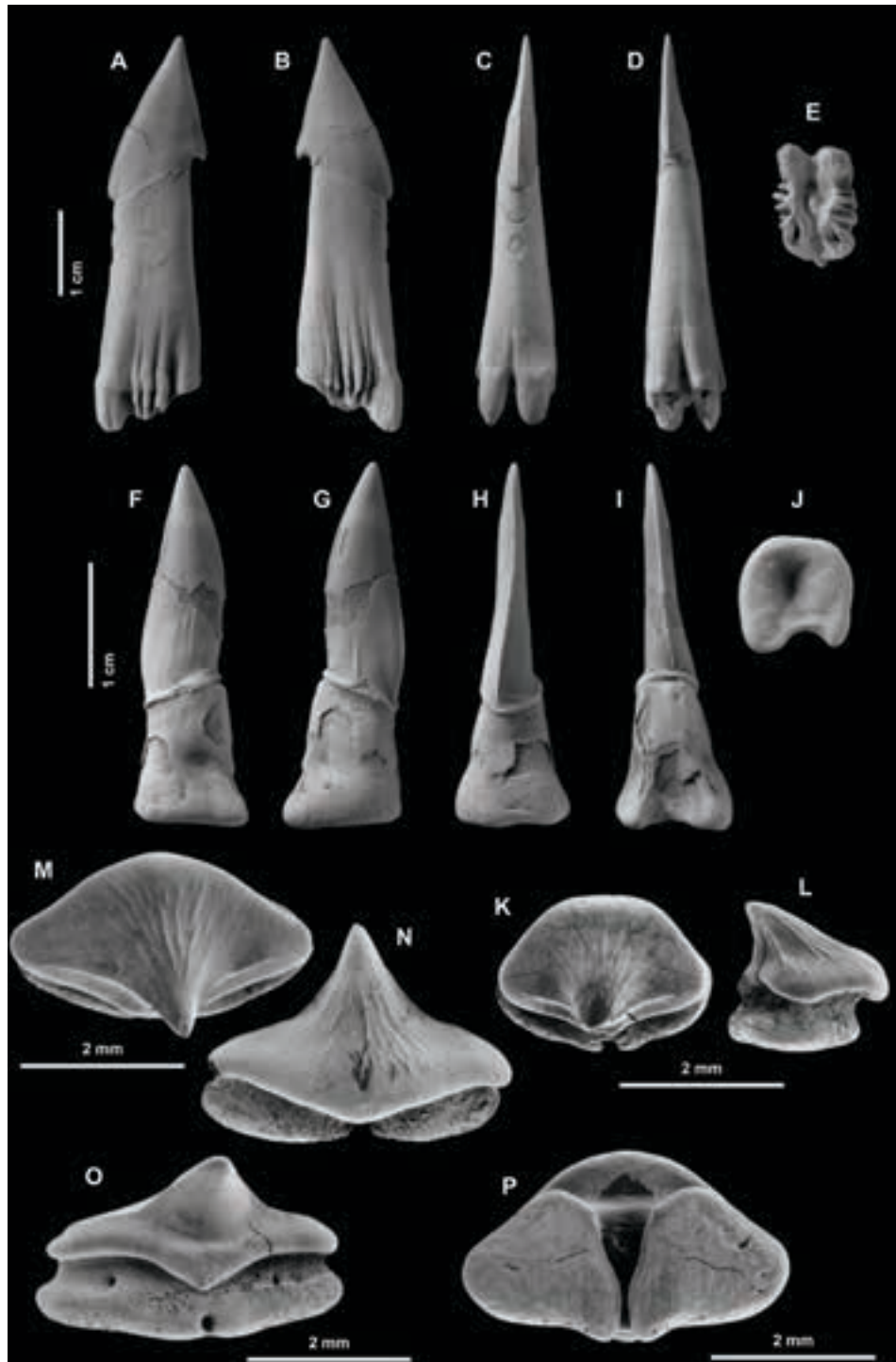
Description. For a full description of this species, see Arambourg (1952) and Cappetta (1972). For a description of oral teeth, see Cappetta (1991). The rostral tooth shows a triangular cusp with an oblique boundary and a clear posterior barb. The peduncle is much longer than the cusp with strong basal grooves on the upper and lower faces.

Discussion. For a detailed discussion concerning the taxonomic status of this sclerorhynchid genus, see Cappetta (1972). This species is recorded for the first time in Europe; until now, it was only pointed out in Africa (see Table 20.3 in Chapter 20).

Genus *GANOPRISTIS* Arambourg, 1935

Type species. *Ganopristis leptodon* Arambourg, 1935; from the Maastrichtian of Ouled Abdoun, Morocco.

-
- ◀ **Figures 14.12** *Vascobatis albaitensis* Cappetta and Corral, 1999. A–D, lateroanterior tooth in occlusal (A), basal (B), profile (C) and oblique basal (D) views, holotype MCNA 8281; E–F, anterior tooth in occlusal (E) and lingual (F) views, MCNA 8282; G–I, anterior tooth in occlusal (G), labial (H), and profile (I) views, MCNA 8283; J–K, lateroanterior tooth in occlusal (J) and oblique basal (K) views, MCNA 8284; L, lateroanterior tooth in occlusal view, MCNA 8285; M–N, anterior tooth in occlusal (M) and profile (N) views, MCNA 8286; O–P, lateral tooth in occlusal (O) and labial (P) views, MCNA 8287. Photographs from Cappetta and Corral (1999).



Ganopristis leptodon Arambourg, 1935

Figs. 14.13F–P

- 1935 *Ganopristis leptodon* Arambourg, p. 421, Pl. 19, Fig. 11.
 1940 *Ganopristis leptodon* Arambourg; Arambourg, p. 133, Fig. 8 and p. 141, Pl. 4, Figs. 2–3.
 1952 *Sclerorhynchus leptodon* Arambourg; Arambourg, p. 189, Pl. 29, Figs. 21–33.
 1964 *Sclerorhynchus leptodon* Arambourg; Casier, p. 5, p. 9, Fig. 1 and Pl. 1, Figs. 1–11.
 ?1964 *Sclerorhynchus batavicus* Albers and Weiler, p. 15, p. 17, Fig. 51.
 1987 *Ganopristis leptodon* Arambourg; Cappetta, p. 148, p. 149, Figs. 126 A–H.
 2015b *Ganopristis leptodon* Arambourg; Corral et al., p. 654, Figs. 11A–I.

Material. MCNA 8260, MCNA 8261, MCNA 8262, MCNA 8263, MCNA 8264, and about thirty additional oral teeth in the MCNA.

Locality. Albaina in the municipality of Treviño County (Burgos, northern Spain).

Age. Upper Maastrichtian (*Menuites fresvillensis* zone).

Description. The rostral tooth is quite typical of the genus, with a dorsoventrally flattened cusp longer than the peduncle (see Cappetta, 1987 for a full description). The oral teeth are well cuspidate. The radiating folds covering the labial face in oral teeth are not always very marked and some teeth can be almost smooth. The root is wide, high, with important lobes, whose basal face is broad and flat.

Discussion. The genus *Ganopristis* is known as early as late Santonian in Israel (Lewy and Cappetta, 1989). Rostral teeth have been described in the Maastrichtian of Netherlands (Albers and Weiler, 1964) as *Sclerorhynchus batavicus*; by their morphology, the figured tooth can be assigned to the genus *Ganopristis*, and could even correspond to *Ganopristis leptodon*. Other rostral tooth figured by these authors from the Maastrichtian of Germany (*Sclerorhynchus germaniae*) can be attributed to the genus *Ischyrbiza* rather than to the *Sclerorhynchus* or *Ganopristis* genera, on the basis of their morphological features. In fact, they could correspond to the species described by Casier (1964) as *Ischyrbiza* cf. *avonicola* from the Santonian of Loncée (Belgium); this author also described oral and rostral teeth of *Ganopristis leptodon* from the Maastrichtian of Netherlands.

In Morocco, oral teeth of *Ganopristis leptodon* are frequent in the upper part of the Maastrichtian; the ornamentation of the labial face of the crown is very variable, from practically smooth to strongly folded and with many intermediate forms; rostral teeth are much scarcer than oral ones. See other occurrences of the species in Table 20.3 in Chapter 20.

- ◀ **Figure 14.13** A–E, *Dalpiazia stromeri* Checchia-Rispoli, 1933, rostral tooth in upper/lower (A–B), anterior (C), posterior (D), and basal (E) views, MCNA 8259. F–P, *Ganopristis leptodon* Arambourg, 1935, F–J, rostral tooth in upper/lower (F–G), anterior (H), posterior (I), and basal (J) views, MCNA 8260; K–L, oral tooth in occlusal (K) and profile (L) views, MCNA 8261; M–N, oral lateral tooth in occlusal (M) and labial (N) views, MCNA 8262; O, oral lateral tooth in lingual view, MCNA 8263; P, oral lateral tooth in basal view, MCNA 8264. Photographs M–P from Cappetta and Corral (1999).

Order MYLIOBATIFORMES Compagno, 1973
Superfamily DASYATOIDEA Whitley, 1940
DASYATOIDEA incert. fam.
Genus *COUPATEZIA* Cappetta, 1982

Type species. *Coupatezia woutersi* Cappetta, 1982; from the middle Eocene of Belgium.

Coupatezia fallax (Arambourg, 1952)
Fig. 14.14

- 1952 *Raja fallax* Arambourg, p. 178, Pl. 28, Figs. 54–59 and Fig. 40 in the text.
1977 *Dasyatis fallax* (Arambourg); Herman, p. 277, Pl. 13, Fig. 4.
1987 *Coupatezia fallax* (Arambourg); Cappetta, p. 168 (name only).
1997 *Coupatezia fallax* (Arambourg); Noubhani and Cappetta, Pl. 60, Figs. 1–6.
2015b *Coupatezia fallax* (Arambourg); Corral et al., p. 655, Figs. 11J–X.

Material. MCNA 8288, MCNA 8289, MCNA 8290, and twenty-one additional, catalogued teeth in the MCNA.

Locality. Albaina in the municipality of Treviño County (Burgos, northern Spain).

Age. Upper Maastrichtian (*Menuites fresvillensis* zone).

Description. See Arambourg (1952) and Noubhani and Cappetta (1997). The teeth of this species reach a rather large size (up to 3 mm in total width).

Discussion. Compared to the specimens from Morocco, some differences can be noted; no tooth from the Spanish locality shows such a high and salient transverse crest as that observed in the Moroccan specimens; no one bears a so strong granular ornamentation on the labial face of the crown; yet, this feature mainly occurs on lateral teeth, and we have few teeth corresponding to this position among the material from Albaina. Outside Morocco, where it was first described, this species was only known in the Maastrichtian of Belgium (Herman, 1977); it also occurs in the Maastrichtian of southern France (Gheerbrant et al., 1997) (see Table 20.3 in Chapter 20).

Superfamily MYLIOBATOIDEA Compagno, 1973
Family RHOMBODONTIDAE Cappetta, 1987
Genus *RHOMBODUS* Dames, 1881

Type species. *Rhombodus binkhorsti* Dames, 1881; from the Maastrichtian of Maastricht, Netherlands.

Rhombodus andriesi Noubhani and Cappetta, 1994
Figs. 14.15A–E

- 1994 *Rhombodus andriesi* Noubhani and Cappetta, p. 8, Pl. 1, Figs. 1–8.

Material. MCNA 8291, and another additional tooth in the MCNA.

Locality. Albaina in the municipality of Treviño County (Burgos, northern Spain).

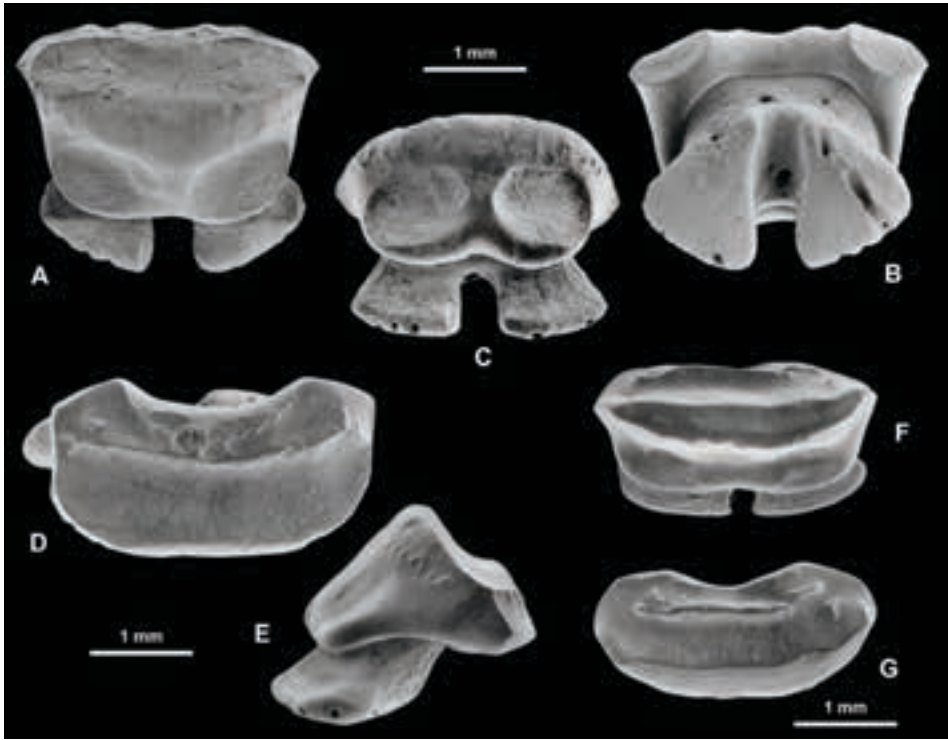


Figure 14.14 *Coupatetia fallax* Arambourg, 1952. A–C, lateroanterior tooth in occlusal (A), basal (B), and lingual (C) views, MCNA 8288; D–E, lateral tooth in labial (D) and profile (E) views, MCNA 8289; F–G, lateral tooth in occlusal (F) and labial (G) views, MCNA 8290. Photographs from Cappetta and Corral (1999).

Age. Upper Maastrichtian (*Menuites fresvillensis* zone).

Description. For the description of this species see Noubhani and Cappetta (1994). This species is mainly characterised by the deep transverse depression located above the lingual basal bulge of the crown.

Discussion. The teeth of this species are morphologically close to those of *Rhombodus binkhorsti*. In *Rhombodus andriesi* the occlusal face of the crown is narrower than its base, in occlusal view (Fig. 14.15A); but the main difference is the occurrence of a deep transversal groove at the base of the marginolingual faces of the crown, just above the lingual bulge; the root is also relatively less high.

In Morocco, this species is not widespread and seems to be located in some layers of the half part of the upper Maastrichtian. It was only known in the type-locality of Ould-er-Rami (Ganntour Basin), but in 1996, it has been also collected in the localities of Foug Tizi and Sidi el Maati where it is rather frequent (Cappetta's personal observation in Cappetta and Corral, 1999). The discovery of this species in the Basque-Cantabrian Region (northern Spain) represents the northernmost occurrence known to date (see Table 20.3 in Chapter 20).

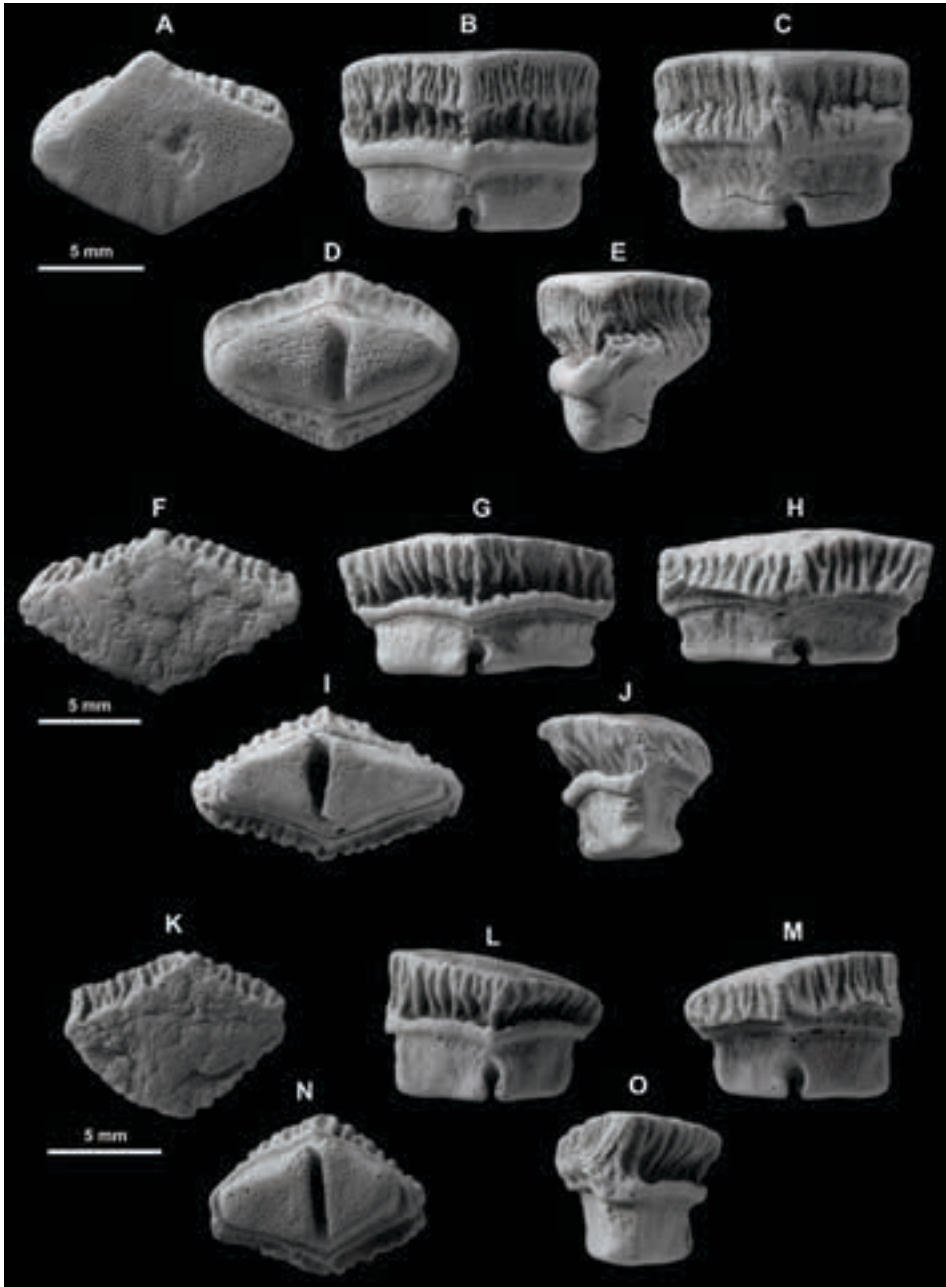


Figure 14.15 *Rhombodus andriesi* Noubhani and Cappetta, 1994, A–E, lateroanterior tooth in occlusal (A), lingual (B), labial (C), basal (D), and profile (E) views, MCNA 8291. F–O, *Rhombodus binkhorsti* Dames 1881, F–J, lateral tooth in occlusal (F), lingual (G), labial (H), basal (I), and profile (J) views, MCNA 8293; K–O, very lateral tooth in occlusal (K), lingual (L), labial (M), basal (N), and profile (O) views, MCNA 8292.

Rhombodus binkhorsti Dames, 1881

Figs. 14.15F–O

For the synonymy see Noubhani and Cappetta (1994); add:

- 1988 *Rhombodus binkhorsti* Dames; McLellan, p. 6–7.
- 1993 *Rhombodus binkhorsti* Dames; Welton and Farish, p. 155, Figs. 1–6.
- 1994 *Rhombodus binkhorsti* Dames; Noubhani and Cappetta, p. 11, Pl. 2, Figs. 1–5.
- 1997 *Rhombodus binkhorsti* Dames; Case and Cappetta, Pl. 15, Figs. 4–5.
- 2015b *Rhombodus binkhorsti* Dames; Corral et al., p. 655, Figs. 12A–F.

Material. MCNA 8292, MCNA 8293, and over three hundred and ten additional, catalogued teeth in the MCNA.

Locality. Albaina in the municipality of Treviño County (Burgos, northern Spain).

Age. Upper Maastrichtian (*Menuites fresvillensis* zone).

Description. See Arambourg (1952) and Chapter 13 of this thesis.

Discussion. As far as known, this species occurs only in Maastrichtian deposits. The species is frequently collected in Maastrichtian deposits worldwide (see Chapter 13 and Table 20.3 in Chapter 20).

Chapter 15
NEOSELACHIANS FROM THE ENTZIA SITES (PUERTO DE OLAZAGUTÍA
FORMATION, UPPER MAASTRICHTIAN)

15.1 Introduction

The present chapter gives the systematic descriptions of selachians collected from two localities on the northern slopes of the Entzia Mountain Range (eastern Álava) and further develops the Corral's (1996) paper. Previously, selachian teeth fragments were found nearby by Ruiz de Gaona (1943) at the type section of the Puerto de Olazagutía Formation (POF) in Navarre. The taxonomic diversity of the Entzia selachians is comparatively much lower than that in other Maastrichtian sites of the Basque-Cantabrian Region, which could be related to the collecting techniques (i.e. surface hand picking), but also to the depositional environment of the POF in the Basque-Cantabrian Basin. Future bulk sampling and intensive wet sieving of the fossil beds could provide coeval additional taxa.

The phosphatic composition of the fossil teeth makes them low durable to weathering. As a consequence, they often occur broken and fragmented, which over time give rise to open fractures and eventually broken tooth crowns (rootless teeth). If not collected soon after being freed from the rock, the specimens are at risk of being swept down over the steeply outcrops by water runoff and destroyed, as it has recently been found out at the Entzia-I fossil site. The material is deposited in the collections of the MCNA (Vitoria-Gasteiz, Spain).

15.2 Systematic palaeontology

Class CHONDRICHTHYES Huxley, 1880
Subclass ELASMOBRANCHII Bonaparte, 1838
Cohort EUSELACHII Hay, 1902
Subcohort NEOSELACHII Compagno, 1977

Superorder GALEOMORPHII Compagno, 1973
 Order LAMNIFORMES Berg 1958
 Family ANACORACIDAE Casier 1947
 Genus *SQUALICORAX* Whitley 1939

Type species. *Corax pristodontus* Agassiz, 1843; Maastrichtian of Maastricht, Netherlands.

Whitley (1939) created *Squalicorax* to replace the genus *Corax* of Agassiz (1843) because the later had been used by Ledru (1810: 204) to describe a raven (corvid). European palaeontologists did not understand the generic reallocation proposed by Whitley, or it was unknown to them, and accepted instead the junior synonym *Anacorax* White and Moy-Thomas, 1940 (see discussion in Herman, 1977). In these circumstances, it is not surprising that Ruiz de Gaona (1943) used the Agassiz's initial generic allocation, given the imprecise taxonomic status of the taxon at the time. Even after the publication of the Ruiz de Gaona (1943) paper, the selachian genus *Corax* was still in use by renowned palaeontologists, including Arambourg (1952: 111) who justified its use on the basis that 'birds and sharks were easily distinguishable'¹.

Squalicorax kaupi (Agassiz, 1843)

Fig. 15.1

Material. Two teeth; MCNA 1080 and MCNA 10591.

Locality. Entzia-I: Vicuña in San Millán/Donemiliaga municipality, Álava (Basque Country, Spain).

Age. Upper Maastrichtian (*Menuites fresvillensis* zone).

Description. See Cappetta and Case (1975b: 8) for the description of the species.

Discussion. This species is easily distinguishable from the coeval *Squalicorax pristodon-*

¹ According to Whitley (1939), Ledru (1810) is credited as being the first to use the genus *Corax* for a corvid, but in fact, Daudin (1800) had already listed several corvids, such as "*Corax varius*" from Mexico, "*Corax borealis*" from Faroe Islands, "*Corax candidus*" from Northern Europe and "*Corax crucirostris*" from Puerto Rico. All these species are now considered either nomina dubia or junior synonyms of other *Corvus* spp. Furthermore, the genus *Corax* has also been used to describe the species of ground beetle (Carabidae): *Corax ghiliani* Putzeys, 1846, from Andalusia (Spain). Later taxonomic revisions relegated *Corax* to subgenus status, becoming then *Steropus* (*Corax*) *ghiliani* (Putzeys, 1846). When Ortuño (1990) revised the *Steropus* and *Corax* genera (Carabidae), he validates the genus *Corax*; therefore that endemic Iberian ground beetle is now *Corax* (*Corax*) *ghiliani* Putzeys, 1846. All this raised a question whether *Squalicorax* Whitley, 1939 should be considered as a junior synonym and therefore rejected (Arambourg, 1952). The reasons given by Whitley (1939) appear to be less relevant even more so when the corvids *Corax* are nowadays considered either nomina dubia or junior synonyms of other *Corvus* spp. Entomologists have not followed the Whitley's proposal and have not rejected the generic name *Corax* Putzeys, 1846 for a kind of ground beetle. In sum, the opinion of Arambourg (1952: 111) on the validity of *Corax* Agassiz, 1843, as it has priority to *Corax* Putzeys, 1846, have not succeed, and *Squalicorax* Whitley, 1939 is nowadays widely used.

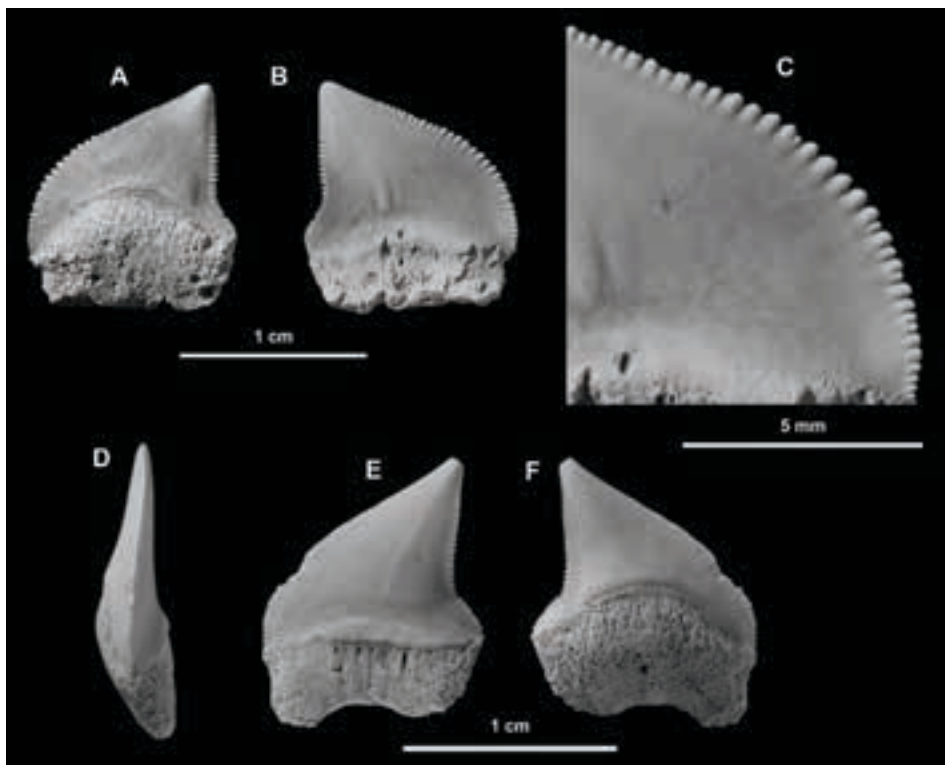


Figure 15.1 *Squalicorax kaupi* (Agassiz, 1843). A–C, anterolateral tooth from Entzia-I (San Millán, Álava) in lingual (A) and labial (B) views, (C) detail of serrations in labial view along mesial edge, MCNA 1080; D–F, lower anterolateral tooth from Entzia-I (San Millán, Álava) in mesial profile (D), labial (E), and lingual (F) views, MCNA 10591.

tus by the presence of a distinct notch on the distal edge of the crown. Moreover, the teeth are small- to medium-sized, typically less than 1.5 cm in width. For further information on the species distribution during the Maastrichtian the reader is referred to Chapters 13, 14, and Table 20.3 in Chapter 20.

Squalicorax pristodontus (Agassiz, 1843)

Fig. 15.2

Material. Four teeth; MCNA 1364, MCNA 3616, MCNA 5451, and MCNA 9665.

Localities. Entzia-I: Vicuña in San Millán/Donemiliaga municipality, Álava; Entzia-II: Andoin in Asparrena municipality, Álava. Basque Country, Spain.

Age. Upper Maastrichtian (*Menuites fresvillensis* zone).

Description. The specimens collected in the Entzia Mountain Range (Álava) show the dental characters of the species indicated by Cappetta and Case (1975b: 8). The teeth

are large and labiolingually compressed with labial and lingual faces slightly concave and convex, respectively. The crown is triangular in form, with the apex leaning towards the commissure. Both cutting edges of the crown are crenate, being convex the mesial cutting edge and slightly concave and shorter the distal one.

One of the specimens (Figs. 15.2A–D) corresponds to a lateral tooth, possibly from the lower jaw. It is slightly wider than high, measuring 29 mm wide and a minimum of 26 mm height. The apical end of the crown is slightly acute. At the base of the labial face of the crown two well-marked folds run towards the top, giving a lobulate surface. On the contrary, the lingual face is smooth and convex, but has faint folds at the base, more marked at the crown/root boundary. The mesial cutting edge developed 60 crenations, while 45 ones are in the distal cutting edge. Crenations are tapered and slightly asymmetrical, pointing downwards to the base of the tooth (Fig. 15.2D). In the midway of the edge, crenations became thicker and some of them are doubly crenate. A labial bulge overhangs the root. The root in the species is higher on the lingual face and becomes thinner towards the basal end (Figs. 15.2C, E, I). Below the bulge there are many irregular foramina. In contrast, only two clear foramina, which are centrally located, occur on the lingual face of the root. Although both basal lobes are missing, a notched basal edge can be inferred. The MCNA 5451 specimen (Fig. 15.2F–G) is a tooth from a more anterior position in the jaw. The crown is more triangular; its labial face is flat and has no folds on it. The lingual face of the crown is convex. The mesial cutting edge of the crown has 45 crenations, while 34 ones ornate the distal cutting edge. Nothing else can be said of a poorly preserved root, as most of its basal end is missing. The teeth of this species usually exhibit a faint curvature when seen in lateral view (Figs. 15.2E, I).

Discussion. This is the most common species in the Maastrichtian of Entzia (Álava). Despite difficulties in delimiting their interspecific boundaries, the morphologically distinct species *Squalicorax falcatus*, *S. kaupi* and *S. pristodontus* are regarded as forming a continuous evolutionary lineage through the Upper Cretaceous (Cappetta, 1987). It appears that *S. pristodontus* was similar in shape to *S. kaupi* although the former species was bigger and had larger-sized teeth. Moreover, the lacking of a notch basally placed in the distal cutting edge of the crown is a distinctive feature that differentiates *S. pristodontus* from *S. kaupi*. Such characteristic feature prevents the formation of a distinctive distal heel, giving a variable concavity in the distal cutting edge according to the tooth position in the dental series. The mesial cutting edge of *S. pristodontus* teeth is arched, but not gibbous; moreover, crenations in both cutting edges are more numerous and more irregular than in *S. kaupi* teeth.

The species *Squalicorax pristodontus* has a very wide distribution range (see Chapter 20 in this thesis). It has been reported from the upper Campanian to the Maastrichtian (see Arambourg, 1952 and Herman, 1977 for a detailed account), but the taxon is much more abundant in the middle–upper Maastrichtian according to Case (1987). Older reports in the upper Campanian of northern European basins (in Belgium, France, and Netherlands) may well correspond to a closely related species *Squalicorax*

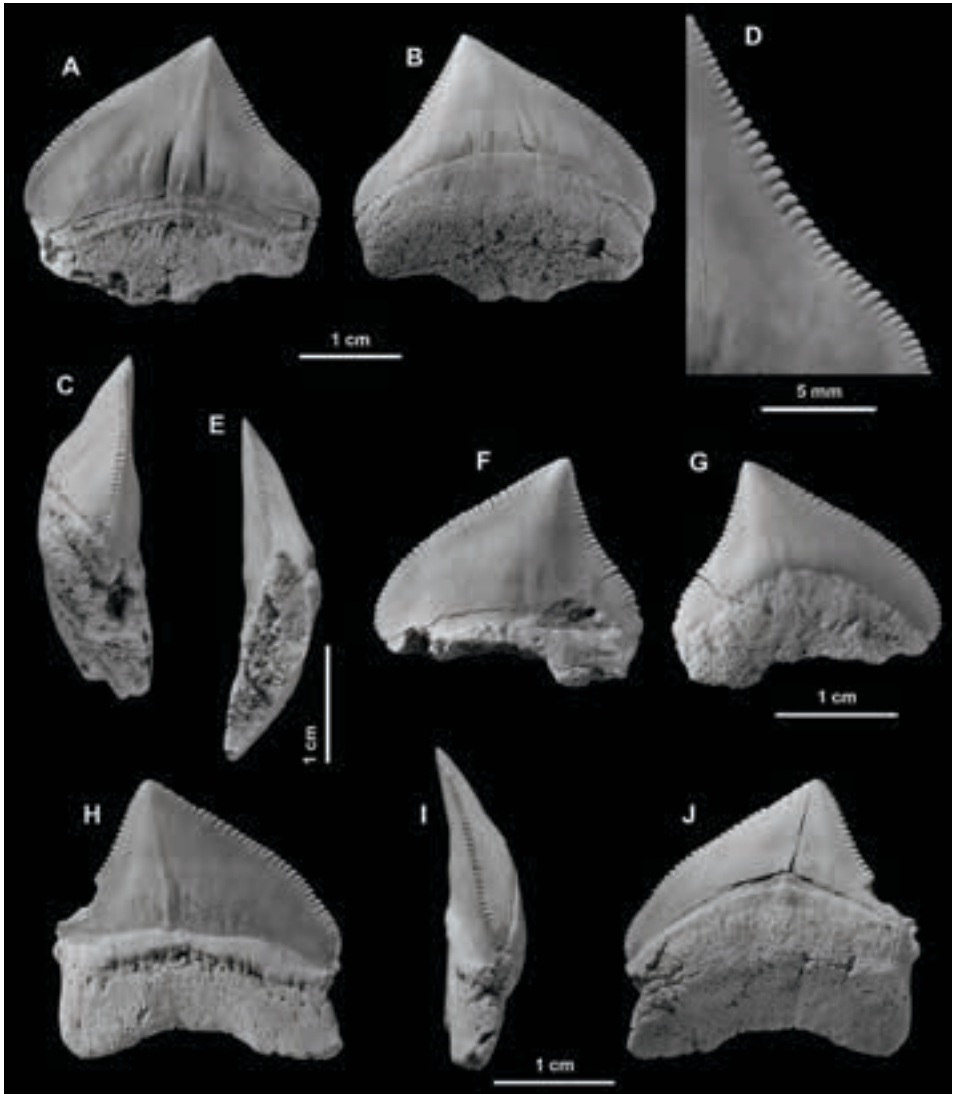


Figure 15.2 *Squalicorax pristodontus* (Agassiz, 1843). A–D, lateral tooth (? lower) from Entzia-I (San Millán, Álava) in labial (A), lingual (B), and mesial profile (C) views, (D), detail of serrations along the distal edge in labial view, MCNA 1364; E, distal view of an incomplete lateral tooth from Entzia-I (San Millán, Álava), MCNA 3616; F–G, anterolateral tooth from Entzia-II (Asparrena, Álava) in labial (F) and lingual (G) views, MCNA 5451; H–I, anterolateral tooth from Entzia-I (San Millán, Álava) in labial (H), mesial profile (I) and lingual (J) views, MCNA 9665.

lindstromi (Davis, 1890), if the validity of this species is finally approved. Therefore, its presence in pre-Maastrichtian deposits must be cautiously considered until a major revision of the genus is accomplished.

Family ODONTASPIDIDAE Müller and Henle, 1839
Genus *CARCHARIAS* Rafinesque, 1810

Type species. *Carcharias taurus* Rafinesque, 1810; Recent, Sicily, Italy.

For the discussions concerning the taxonomical status of this genus see Ward (1988).

Carcharias beathi Case and Cappetta, 1997
Fig. 15.3

1997 *Carcharias beathi* Case and Cappetta, p. 140, Pl. 7, Figs. 7–9.

1999 *Carcharias beathi* Case and Cappetta; Cappetta and Corral, p. 347, Pl. 1, Figs. 7–8.

2015b *Carcharias beathi* Case and Cappetta; Corral et al., p. 649, Figs. 7A–L.

Material. Three incomplete teeth; MCNA 8530, MCNA 10593, and MCNA 10594.

Locality. Entzia-I: Vicuña in San Millán/Donemiliaga municipality, Álava (Basque Country, Spain).

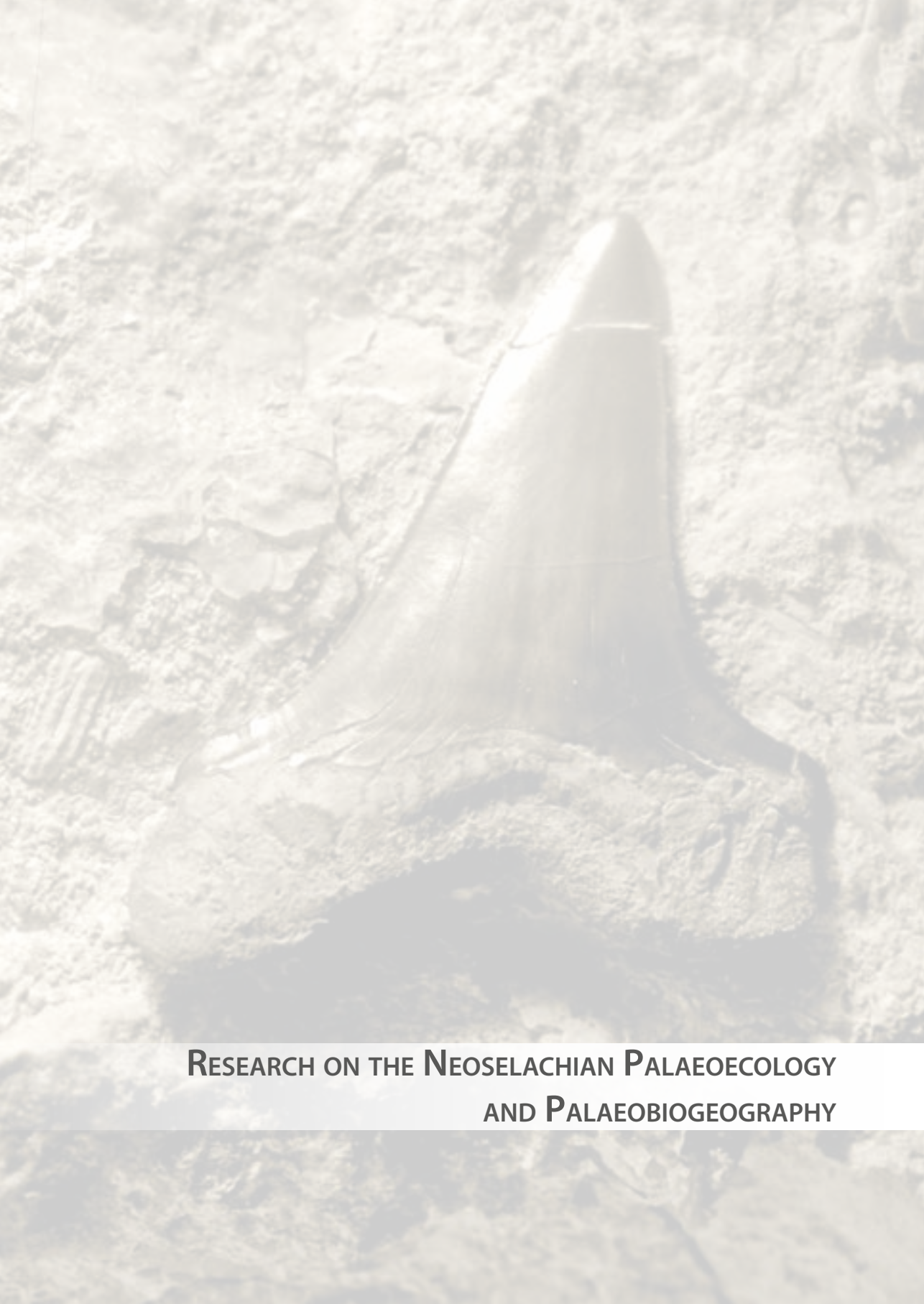


Figure 15.3 *Carcharias beathi* Case and Cappetta, 1997. A–C, anterior tooth from Entzia-I (San Millán, Álava) in labial (A), lingual (B) and profile (C) views, MCNA 10594; D–E, intermediate tooth from Entzia-I (San Millán, Álava) in labial (D) and lingual (E) views, MCNA 10593; F–G, lateral tooth from Entzia-I (San Millán, Álava) in labial (F) and lingual (G) views, MCNA 8530.

Age. Upper Maastrichtian (*Menuites fresvillensis* zone).

Description. For a full description of this species, see Case and Cappetta (1997). Teeth are slightly sigmoid in lateral view. The crown bears a triangular smooth cusp, which is narrower and vertical in anterior teeth but leans distally in lateral ones and is flanked by one pair of short lateral cusplets. A nutritive groove separates the lobes of a wide bilobate root. The line that limits the enameloid crown and the root forms a characteristic wide V-shape.

Discussion. This taxon is rare at the Entzia sites, and only fragmentary teeth are usually found. Morocco in Africa, according to Case and Cappetta (1997), the type locality in Northern America (Texas, USA), and the Basque-Cantabrian Region (central-northern Spain) are the reported occurrences of this upper Maastrichtian species, but it seems possible for *Carcharias heathi* also to occur in northern Europe, perhaps mistaken with closely related species (see also Chapters 13, 14, and Table 20.3 in Chapter 20).

A close-up photograph of a fossilized shark tooth. The tooth is dark, almost black, and has a triangular shape with a sharp point. It is embedded in a light-colored, textured rock matrix. The background is a soft, out-of-focus light green color.

**RESEARCH ON THE NEOSELACHIAN PALAEOECOLOGY
AND PALAEOBIOGEOGRAPHY**

During the Maastrichtian, after the peak Cretaceous Greenhouse warmth...



BANNER: STOP GLOBAL COOLING!

AMMONITE #1. Ice sheets found in Gondwana!!

AMMONITE #2. We should fight

AMMONITE #1. Let's face the truth, we have no future!

Chapter 16
STRATIGRAPHICAL AND PALAEOBIOGEOGRAPHICAL DISTRIBUTION
OF THE SAWFISH *ONCHOSAURUS* (NEOSELACHII, SCLERORHYNCHIDAE)

16.1 Introduction

The discovery of vertebrate remains in the Coniacian marine deposits of the Basque-Cantabrian Region is very unusual. One such discovery is the sawfish *Onchosaurus* specimen from Barrio Panizares (Burgos, Spain), which also constitutes the first record of this species in the Iberian Peninsula. On the basis of the known occurrences of *Onchosaurus* in the Upper Cretaceous a tentative pattern of palaeobiogeographical distribution of the genus is provided.

16.2 Distribution of *Onchosaurus*

As previously mentioned in Chapter 10, fossil remains of *Onchosaurus* are worldwide known, except for Australia and Antarctica, from the Turonian through upper Campanian. However, only a few and often fragmentary skeletal remains are so far described (Fig. 16.1, Table 16.1). In spite of this scarcity, both chronostratigraphical and geographical ranges permit to address tentative palaeobiogeographical distributions of this genus during the Upper Cretaceous (Fig. 16.2).

Stratigraphical distribution

The oldest occurrence of *Onchosaurus radicalis* is from the Turonian of Ecuador (Dunkle, 1951). Coniacian records of this species are reported in New Mexico, USA (Spielmann and Lucas, 2006) and in the Iberian Peninsula (Corral et al., 2012). The youngest occurrence of *O. radicalis* is from the upper Campanian of Meudon, France (type locality; Gervais, 1852). Priem (1908) and later Arambourg (1940) reported additional material of *O. radicalis* from the Senonian of Chemillé-sur-Indre (Indre-et-Loire Department, western France). Post-Turonian stages around this area are not

Table 16.1 Global distribution of *Onchosaurus* across the Late Cretaceous. Fossil localities listed from younger to older; numbers are the same than those of Figure 16.1.

No.	Locality	Age	Status	Reference
<i>Onchosaurus radicalis</i> Gervais, 1852				
1	Napo (Ecuador)	Turonian	Figured	Dunkle, 1951
2	Bernalillo County, New Mexico (USA)	Coniacian	Cited	Spielmann and Lucas, 2006
3	Barrio Panizares, Burgos (Spain)	upper Coniacian	Figured	Corral et al., 2012
4	Chemillé-sur-Indre, Indre-et-Loire (France)	'Senonian'	Figured	Priem, 1908; Arambourg, 1940
5	Meudon (France)	upper Campanian	Figured	Gervais, 1852
<i>Onchosaurus pharao</i> (Dames, 1887)				
6	Magdalena (Colombia)	Turonian	Figured	Páramo Fonseca, 1997
7	Damergou (Niger)	Turonian	Figured	Arambourg and Joleaud, 1943
8	S. Anna d'Alfaedo, Verona (Italy)	middle–upper Turonian	Figured	Amalfitano et al., 2016
9	Iembe, Kwanza Basin (Angola)	upper Turonian	Figured	Antunes and Cappetta, 2002
10	Otuzco, Department of Cajamarca (Peru)	Coniacian	Figures	Kriwet and Klug, 2012
11	Iwaki, Fukushima Prefecture (Japan)	lower Santonian	Figured	Uyeno and Hasegawa, 1986
12	Cairo West of Gizah; Sinai (Egypt)	Santonian	Figured	Dames, 1887a; Kriwet and Klug, 2012
13	Ain el Hâss, Baharya Basin (Egypt)	upper "Senonian"	Figured	Stromer, 1917
14	Jabal Abtar, Palmyrides (Syria)	Santonian	Cited	Al Maleh and Bardet, 2003
15	Bulu-Zambi (DR Congo)	Santonian	Figured	Darteville and Casier, 1943
16	Sergipe State (Brazil)	Santonian	Cited	Cappetta, 1987
17	Quars Helqum (Iraq)	Campanian	Figured	Kriwet and Klug, 2012
18	Aldama, Chihuahua (Mexico)	Campanian	Figured	Delgado-Escobar et al., 2015
19	Presidio County, Texas (USA)	middle Campanian	Figured	Lehman, 1989

individually mapped in recent geological maps, but Alcaydé (1990) assigns a Coniacian–late Campanian age for the decalcified white marlstone with chert and siliceous sponges that crops out near Chemillé-sur-Indre, France.

Onchosaurus pharao is first known from the Turonian of South America (Colombia: Páramo Fonseca, 1997; Peru: Kriwet and Klug, 2012), northern and western Africa (Niger: Arambourg and Joleaud, 1943; Angola: Antunes and Cappetta, 2002), and Europe (Amalfitano et al., 2016). Santonian occurrences are restricted to Africa (Egypt: Dames, 1887a; Democratic Republic of Congo: Darteville and Casier, 1943), Middle East (Syria: Al Maleh and Bardet, 2003), South America (Brazil: Cappetta, 1987), and possibly Japan (Uyeno and Hasegawa, 1986). The material from the middle Campanian of Texas (USA) represents the youngest occurrence of the species (Lehman, 1989).

Palaeobiogeographical distribution

Whereas *Onchosaurus radicalis* was apparently confined to northern South America during the Turonian, the coeval species *O. pharao* disseminated rapidly across the margins of two main Gondwanan landmasses, namely northern South America and western Africa (localities 6, 7, 9), and southern European areas (locality 8) (see Fig. 16.1, Table 16.1). Therefore, a Gondwanan origin in the South Temperate Realm is likely for the ge-

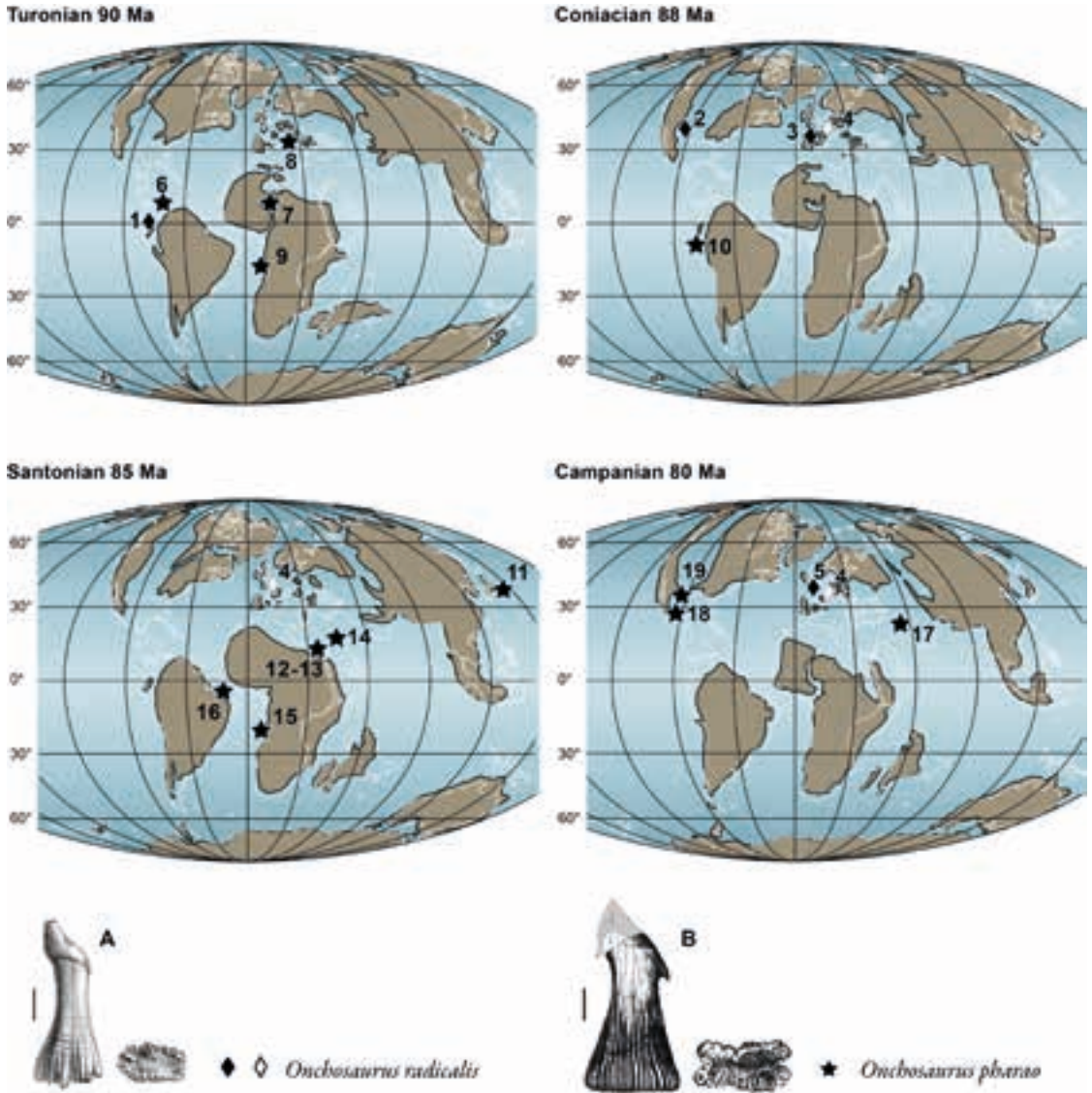


Figure 16.1 Main occurrences of the species of *Onchosaurus*. Palaeocoastlines after Smith et al., 1984. Key: diamond (◆) and lozenge (◇), *Onchosaurus radicalis* Gervais, 1852; star (★), *Onchosaurus pharao* (Dames, 1887a). A, *O. radicalis* Gervais, 1852, original figuration of the holotype; B, *O. pharao* (Dames, 1887a), original figuration of the syntype, scale bar 1 cm. Localities discussed: 1, Ecuador; 2, New Mexico, USA; 3, Spain; 4, Chemillé-sur-Indre, France; 5, Meudon, France; 6, Colombia; 7, Niger; 8, Italy; 9, Angola; 10, Peru; 11, Japan; 12, Cairo-Sinai, Egypt; 13, Baharya, Egypt; 14, Syria; 15, DR Congo; 16, Brazil; 17, Iraq; 18, Mexico; 19, Texas, USA. Note: the tooth from Chemillé-sur-Indre, France (locality 4) has been plotted as a white lozenge in all post Turonian palaeogeographical maps since its precise stratigraphical position is unknown. See Table 16.1 for full references.

nus *Onchosaurus*. The Turonian records the largest eustatic rise of the whole Cretaceous (Haq et al., 1987; Van Sickle et al., 2004), thus favouring the formation of large epicontinental marine basins and a high primary food production (Briggs, 1995). This transgression probably facilitated a worldwide dispersion of these marine fishes (Fig. 16.2), as occurred at the same time for marine squamates (Bardet et al., 2008). While a dispersal scenario can be established for *O. radicalis* from its putative South American centre of origin, a dispersal scenario of *O. pharao* from the putative Nigerien centre of origin (locality 7) implies a very rapid dispersal towards both the north (across the Tethys Ocean into Italy; locality 8) and the south (western Africa, and across the South Atlantic into South America (localities 9 and 6, respectively), according to the supposed sea surface currents at the time (see Fig. 16.2). During the Coniacian, *Onchosaurus radicalis* is known to occur in the northern temperate platform margins of Europe and North

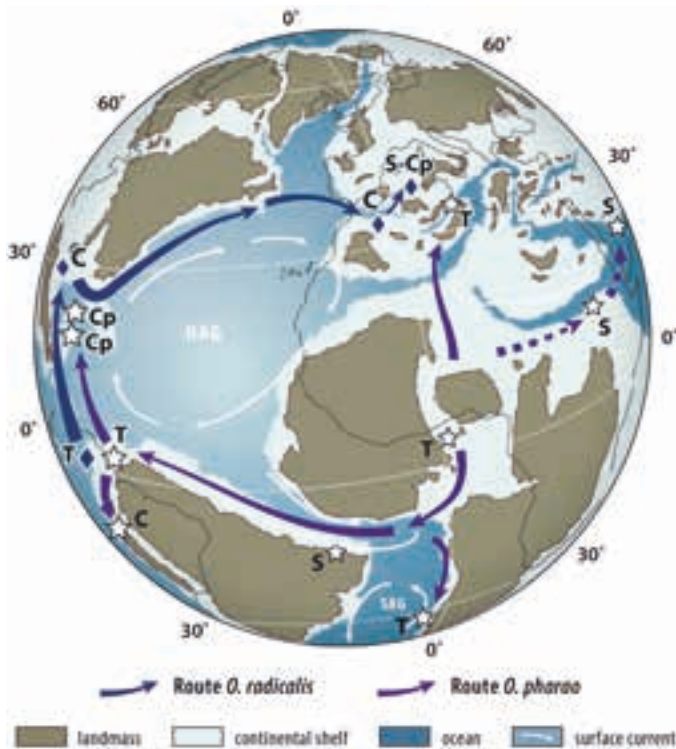


Figure 16.2 Palaeogeographical globe for the Turonian (90 my), showing hypotheses about dispersal routes of *Onchosaurus radicalis* (◆) in dark blue, and *Onchosaurus pharao* (☆) in purple. The Globe was built from a Blakey's palaeogeographical map of the Turonian (Global Palaeogeography, cpgeosystems.com/090Marect.jpg) modified with Google Earth. Present-day coastlines outlined in grey. Supposed surface ocean currents in the North Atlantic palaeo-ocean and Equatorial Gulf are represented in grey white arrows. Symbols and capital letters indicate the occurrence of the species at any geological stage: T, Turonian; C, Coniacian; S, Santonian; CP, Campanian. NAG: North Atlantic Gyre; SAG: South Atlantic Gyre.

America (localities 2, 3 and 5, Fig. 16.1, Table 16.1), suggesting that the species already crossed the equatorial barrier formed by the tropical waters of the Tethys Sea. The Coniacian record of *Onchosaurus pharao* is until now restricted to a single occurrence in South America (locality 10; Kriwet and Klug, 2012). Subsequent dispersal during the Coniacian–Santonian time interval probably occurred to the southern Atlantic (localities 15, 16), and possibly Japan (locality 11). The presence of *O. pharao* in the southern margin of the Mediterranean Tethys (localities 12, 13, and 14) at that time is thought to have been derived from an older, African dwelling stock. But it was not until the Campanian that this species reached the northern temperate regions, as the Lehman's (1989) specimens from Texas corroborate it (locality 19).

Both species of *Onchosaurus* have persisted in Laurasia at least up to the Campanian time, in North America (localities, 18 and 19), Europe (locality 5), and Middle East (locality 17). The decline of *Onchosaurus* after the Campanian could be explained by steady lowering of the sea level after the Campanian (Haq et al., 1987) and the consequent lost of propitious dwelling environments. In post Campanian times, the ecological role played by *Onchosaurus* in shore environments was mainly replaced by other Sclerorhynchidae genera, such as *Ischyrbiza* Leidy, 1856 in the Western Interior Sea of North America and *Ganopristis* Arambourg, 1935 and *Dalpiazia* Checchia-Rispoli, 1933 in Africa and Europe, as the fossil record indicates.

Chapter 17

PALAEOECOLOGY AND PALAEOBIOGEOGRAPHY OF THE CAMPANIAN SELACHIANS IN THE GOMETXA AND VITORIA PASS BEDS

17.1 Introduction

Gometxa and Vitoria Pass sites are two productive localities in the province of Álava (Vitoria Sub-basin of the Basque-Cantabrian Basin) that have been studied for their palaeontological value. Surface collecting and bulk sampling from these sections have yielded a good number of teeth and other non-dental remains. The most diverse unit for selachian fossils is the Gomecha Member (GM) in the former site. This selachian collection is represented by 122 teeth, and at least 17 taxa within six orders and 13 families occur, being split into two ecological assemblages (from lithofacies 1 and 2, respectively). The selachian assemblage of the Vitoria Pass beds, which is also much less diverse than the previously indicated, is represented by 133 teeth. At least eight taxa within two orders and seven families represent this assemblage. The Campanian selachians recognised in this thesis work (Table 17.1) comprise 22 taxa, of which at least 15 are new for the Campanian record of the Iberian Peninsula.

The relative age of the deposits from which the selachian material comes has been established on the basis of planktonic foraminifers and associated ammonite fauna, as seen in Chapters 5 and 6. Isolated teeth of fossil selachians and other invertebrate taxa are relatively abundant in the GM of the Vitoria Formation. The dominant lithologies are a glauconite-rich calcarenite (lithofacies-2) and – underlying this interval – a marly unit with intercalated parallel-laminated calcarenite seams (lithofacies-1) from which the most diverse vertebrate assemblage comes. The dating of this underlying marl unit is supported by the occurrence of the scaphitid ammonites *Scaphites* (*S.*) *gibbus*, which is reported to occur from the uppermost lower Campanian to the lowermost upper Campanian (Machalski et al., 2004). The same unit is restricted to the lower upper Campanian planktonic foraminiferal zone of *G. aegyptiaca* (*G. aegyptiaca* subzone) on the basis of a preliminary microfossil study (J.A. Arz, pers. comm.).

In comparison with the slightly younger fauna of the GM, the selachian remains in the Vitoria Pass beds occur in prodelta deposits of the Eguileta Member (EM), within

the ammonite *Hoplitoplacenticeras marroti* zone of the upper Campanian (Santamaría Zabala, 1996; and own observations). However, its foraminiferal association is characteristic of the *Gansserina gansseri* zone, *Rugoglobigerina rotundata* subzone (J.A. Arz, pers. comm.). Thus, there is an eight-million-year discrepancy between ammonite and planktonic foraminiferal dating, which requires to be further investigated. The stratigraphical relationships of the mid Upper Cretaceous rock units of the Vitoria Sub-basin have been graphically given in Fig. 6.10 (in Chapter 6).

Finally, this chapter is also aiming to analyse the palaeobiogeographical spectrum of the Campanian selachian genera, and to discuss the results, by means of using a taxonomic data set of 18 operational geographical units (OGU) reported to contain selachians of this age (the published and unpublished sources are all shown in Table 17.3 given below). However, this study is at best incomplete, since the taxonomic composition of selachian assemblages needs to overcome some sort of biases in the collection and identification of the samples, and a major drawback is the notable number of geographical sites reported in the Northern Hemisphere compared to those in the Southern Hemisphere.

17.2 Species diversity and faunal affinities

Fossil selachians in the Álava Campanian, as determined in this study, are represented by 17 families with 22 described taxa (Tables 17.1, 17.2).

The Gometxa site

Despite the fact that only a relatively small quantity of marly matrix of the GM has been screen washed for selachian microteeth, this locality has produced the most diverse Campanian selachian fauna known from the Basque-Cantabrian Region. Lamniformes, Carcharhiniformes, Orectolobiformes, Squatiniformes, Synechodontiformes, and Rajiformes are the orders that occur at Gometxa site. But, we should note that this selachian diversity is in accordance with a generalised taxonomic drop in the oceans during the Campanian times, as reported by Guinot (2013b) and discussed below.

Teeth of Lamniformes and Orectolobiformes are mostly found, with values of 51.6% and 23.8% respectively (Fig. 17. 1). Particularly, Lamniformes is the most diverse order in the sharks with six families recognised (i.e. Anacoracidae, Cretoxyrhinidae, Lamniformes incert. fam., Mitsukurinidae, Odontaspidae, and Otodontidae) representing eight species. Orectolobiformes are constituted only by the single family Hemiscylliidae with three species (*Chiloscyllium* cf. *gaemersi*, *Chiloscyllium* cf. *vulloi*, and *Hemiscyllium hermani*) accounting for 23.8% of the total sample. Carcharhiniforms are represented by the family Scyliorhinidae with the single species *Prohaploblepharus riegrafi* (14.7% of the total sample). Squatiniform and synechodontiform sharks are a minor component of the GM palaeobiodiversity with a single family each (Squatinidae and Palaeospinacidae, respectively). As far as Rajiformes is concerned,

Table 17.1 Occurrence list of elasmobranch taxa in the studied sampling sites with a subjective estimation of their abundance. Percentage values are based on a sample of 122 teeth for Gometxa and 133 teeth for Vitoria Pass (no., number of teeth). Relative abundance ranges (RA): A, abundant (>30% teeth in total assemblage); C, common (10%–30% teeth in total assemblage); UC, uncommon (5%–10% teeth in total assemblage); R, rare (4%–5% teeth in total assemblage); ER, extremely rare (1%–4% teeth in total assemblage).

Order	Taxa	Gometxa			Vitoria Pass		
		RA	no.	%	RA	no.	%
Orectolobiformes	<i>Chiloscyllium</i> cf. <i>gaemersi</i> Müller, 1989	C	17	13.93	—	—	—
	<i>Chiloscyllium</i> cf. <i>vulloi</i> Guinot et al., 2013	ER	2	1.64	—	—	—
	<i>Hemiscyllium hermani</i> Müller, 1989	UC	10	8.20	—	—	—
Lamniformes	<i>Anomotodon hermani</i> Siverson, 1992	UC	11	9.02	—	—	—
	<i>Carcharias aasenensis</i> Siverson, 1992	ER	2	1.64	—	—	—
	<i>Carcharias adneti</i> Vullo, 2005	—	—	—	UC	7	5.26
	<i>Cretolamna borealis</i> (Priem, 1897)	C	21	17.21	C	32	24.06
	<i>Cretolamna sarcoportheta</i> Siverson et al., 2015	R	5	4.10	C	33	24.81
	<i>Cretoxyrhina mantelli</i> (Agassiz, 1843)	ER	1	0.82	—	—	—
	<i>Paranomotodon</i> cf. <i>angustidens</i> (Reuss, 1845)	R	5	4.10	—	—	—
	<i>Protolamna borodini</i> (Cappetta and Case, 1975b)	—	—	—	ER	3	2.26
	<i>Pseudorax laevis</i> (Leriche, 1906)	—	—	—	ER	2	1.50
	<i>Scapanorhynchus</i> cf. <i>texanus</i> (Roemer, 1849)	ER	3	2.46	—	—	—
	<i>Serratolamna kbderii</i> (Zalmout and Mustafa, 2001)	—	—	—	ER	5	3.76
	<i>Squalicorax</i> ex gr. <i>kaupi</i> (Agassiz, 1843)	C	15	12.30	A	50	37.59
	Carcharhiniformes	<i>Galeorhinus girardoti</i> Herman, 1977	—	—	—	ER	1
<i>Prohaploblepharus riegrafi</i> (Müller, 1989)		C	18	14.75	—	—	—
Synechodontiformes	<i>Synechodus</i> aff. <i>filipi</i> Siverson et al., 2016	ER	2	1.64	—	—	—
Squatiformes	<i>Squatina</i> (<i>Cretascyllium</i>) <i>hassei</i> Leriche, 1929	ER	2	1.64	—	—	—
Rajiformes	<i>Parapalaeobates pygmaeus</i> (Quaas, 1902)	ER	4	3.28	—	—	—
	<i>Ptychotrygon</i> sp.	ER	2	1.64	—	—	—
	<i>Rhinobatos casieri</i> Herman, in Cappetta and Case, 1975b	ER	2	1.64	—	—	—

three families (Parapalaeobatidae, Ptychotrygonidae, and Rhinobatidae) occur representing the following three taxa (6.6% of the total sample): *Parapalaeobates pygmaeus*, *Ptychotrygon* sp., and *Rhinobatos casieri*.

More precisely, the GM has yielded two assemblages of selachians, as follows: (1) a large assemblage from the lithofacies-1 consisting of *Anomotodon hermani*, *Carcharias aasenensis*, *Chiloscyllium* cf. *gaemersi*, *Chiloscyllium* cf. *vulloi*, *Cretolamna borealis*, *Cretolamna sarcoportheta*, *Hemiscyllium hermani*, *Paranomotodon* cf. *angustidens*, *Parapalaeobates pygmaeus*, *Prohaploblepharus riegrafi*, *Ptychotrygon* sp., *Rhinobatos casieri*, *Squalicorax* ex gr. *kaupi*, *Squatina* (*Cretascyllium*) *hassei*, and *Synechodus* aff. *filipi*; and (2) a slightly younger, much poorer assemblage from the lithofacies-2 consisting of *Cretolamna borealis*, *Cretoxyrhina mantelli*, *Paranomotodon* cf. *angustidens*, *Parapalaeobates pygmaeus*, *Scapanorhynchus* cf. *texanus*, and *Squalicorax* ex gr. *kaupi*.

Non-dental remains, including vertebral centra, dermal denticles, and coprolites are also found at this site, although in less numbers than the teeth. They remain to be described in future works.

The Vitoria Pass site

The Eguileta Member (EM) at the Vitoria Pass site has yielded a selachian assemblage of lower diversity than that of the Gometxa site, being Lamniformes and Carcharhiniformes the two only orders represented. However, there is undoubtedly some degree of biased fossil material due to the collecting techniques (only surface prospecting). In terms of abundance, lamniform sharks is the almost exclusive component of the Vitoria Pass fauna, having found the following taxa: *Carcharias adneti*, *Cretolamna borealis*, *Cretolamna sarcoportheta*, *Protolamna borodini*, *Pseudocorax laevis*, *Serratolamna khderii*, and *Squalicorax* ex gr. *kaupi*. The otodontids *Cretolamna borealis* and *C. sarcoportheta* (referred to as *C. appendiculata* in older accounts) and the anacoracid *Squalicorax* ex gr. *kaupi* are by far the most abundant found in the EM (accounting for 24.1%, 24.8%, and 37.6%, respectively of the total sample), but their abundance can represent a sampling bias in favour of large tooth specimens. Carcharhiniform sharks are only represented by the sole family Triakidae with the single species *Galeorhinus girardoti*.

17.3 Palaeoecology and biogeographical faunal patterns

Neoselachii (sharks, rays and their relatives) are very conservative in retaining many body morphological features along the geological time, so knowledge of the extant analogues may well give a representative picture of the fossil ancestors (Musick et al., 2004). With the exception of some oceanic filter-feeders forms (i.e. planktivorous predators), neoselachians are adapted for an active, carnivorous lifestyle. However, the majority of them are not apex predators but instead they collectively function as mesopredators, occupying a lower trophic level and feeding upon small fishes and marine invertebrates (Klimley, 2013). Second, but also related, is that fossil selachians can be used to acquire bathymetric estimations on the basis of the known depth range of their extant analogues.

Neoselachians were an essential part of the marine ecosystem occurring in the Vitoria Sub-basin during the Campanian. Scant attention has been given to their ecological relationships or to the habitat diversity that occupied (Corral et al., 2011). Here are presented some preliminary ecological observations (general ecology and habitat preferences) of these fossil neoselachians.

The pie chart of Fig. 17.1 shows graphically the aggregated tooth percentage of the selachians found in the Gometxa Member. In modern seas, the order Lamniformes is over-balanced toward highly-mobile, oceanic and semipelagic species inhabiting the epipelagic zone in oceanic and sublittoral waters (Compagno, 2008). The highest proportion of shark teeth at Gometxa corresponds to lamniforms, which are represented by the important pelagic families Anacoracidae, Cretoxyrinidae, Mitsukurinidae, Od-

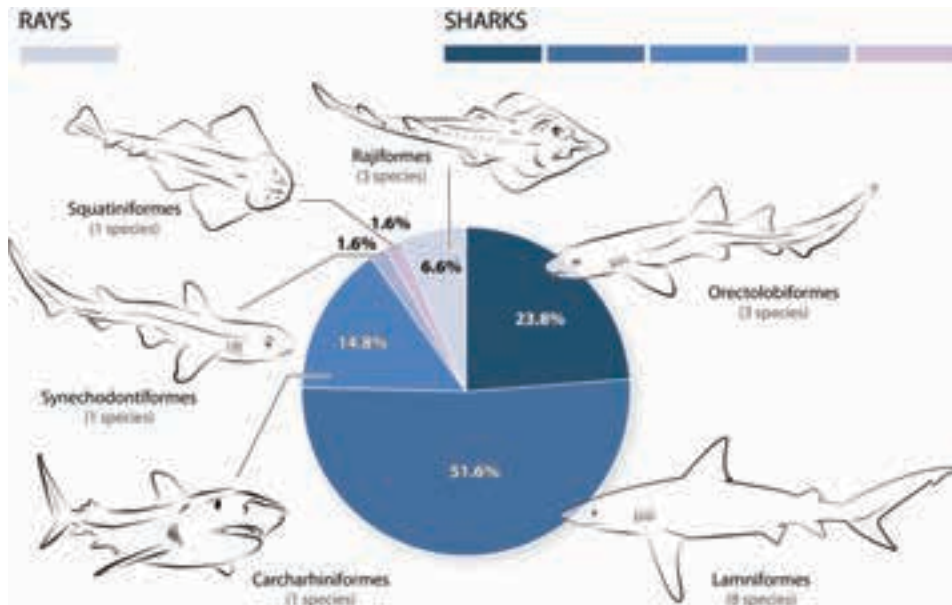


Figure 17.1 Relative abundance of Elasmobranchii teeth from the Gometxa Member at Gometxa site (Álava, northern Spain) from data shown in Table 17.1. Silhouettes depict a member of the group (not to scale).

ontaspidae, and Otodontidae (one of the species found is not assigned to any family). Their ecology and other key characteristics are summarised here.

Squalicorax is an extinct genus of sharks belonging to the also extinct family Anacoracidae (Albian–Maastrichtian), whose blade-like teeth show a clear morphological convergence with modern carcharhinids and sphyrnids (Cappetta, 2012). Its cutting type dentition is interpreted as evidence that many large species from the Upper Cretaceous were active, generalist predators, or more likely opportunistic scavengers, well adapted to kill and dismember large prey (see Schwimmer et al., 1997).

Only a few Campanian shark species from the Vitoria Sub-basin are considered apex predators, and *Cretoxyrhina* is among them. This is an extinct genus of large toothed sharks with a tearing-to-cutting type dentition, belonging to the Cretaceous family Cretoxyrhinidae. Although a rare element of the fish assemblage at Gometxa (0.82% of the total sample), the shark *Cretoxyrhina mantelli* was at the highest trophic position in the food web, according to both its dentition and inferred relatively large body size. The common anacoracid *Squalicorax* ex gr. *kaupi* and the otodontids *Cretolamna* spp. were also important apex predators in the epipelagic zone, being present in great numbers according to the proportional abundance of teeth recovered.

A relatively small number of teeth have been identified as belonging to *Paranomotodon* cf. *angustidens*, which is considered a macrooceanic shark of small-to-moderate

Table 17.2 List of neoselachians identified from the Campanian of the Basque-Cantabrian Region (northern Spain) and their presence in approximately coeval deposits of other world regions.

	Europe						
	Kristianstad Basin (Sweden)	North German Basin (N Germany)	Münsterland Cretaceous Basin (N Germany)	Liege-Limburg Basin (BE, DE, NL)	Mons Basin (Belgium)	Anglo-Paris Basin (France, UK)	Aquitaine Basin (W France)
Sharks							
<i>Anomotodon hermani</i> Siverson, 1992	43, 48	39			25, 26	24	
<i>Carcharias aasenensis</i> Siverson, 1992	43, 48	28					
<i>Carcharias adneti</i> Vullo, 2005						24	11, 51
<i>Chiloscyllium cf. gaemersi</i> Müller, 1989	48		33, 34, 49				
<i>Chiloscyllium cf. vulloi</i> Guinot et al., 2013						24	
<i>Cretolamna borealis</i> (Priem, 1897)	36, 43, 46	?39			25, 26	30	51
<i>Cretolamna sarcophorheta</i> Siverson et al., 2015	43, 46				25, 26	46	
<i>Cretoxyrhina mantelli</i> (Agassiz, 1843)	43, 48			2		30	
<i>Galeorhinus girardoti</i> Herman, 1977			33, 34, 49	25, 26	25, 26		51
<i>Hemiscyllium hermani</i> Müller, 1989	48		33, 34				
<i>Paranomotodon cf. angustidens</i> (Reuss, 1845)	43	39				30	51
<i>Prohaploblepharus riegrafi</i> (Müller, 1989)			33, 34, 49, 50			50	
<i>Protolamna borodini</i> (Cappetta and Case, 1975b)	43						51
<i>Pseudocorax laevis</i> (Leriche, 1906)		39			25, 26	24, 25, 26, 31	51
<i>Scapanorhynchus cf. texanus</i> (Roemer, 1849)						?24	
<i>Serratolamna khderii</i> (Zalmout and Mustafa, 2001)				?2		30	51
<i>Squalicorax ex gr. kaupi</i> (Agassiz, 1843)	20, 43, 48	39	33, 34, 49	1, 2, 49	25, 26	24, 30	11, 51
<i>Squatina (Cretascyllium) hassei</i> Leriche, 1929		39	27	2, 49	25, 26	23	51
<i>Synechodus aff. filipi</i> Siverson et al., 2016	42, 47				25, 26		
Rays							
<i>Parapalaebates pygmaeus</i> (Quaas, 1902)							
<i>Ptychotrygon</i> sp.							
<i>Rhinobatos casieri</i> Herman, in Cappetta and Case 1975b	48			2, 25, 26	25, 26	22, 50	51

Data taken from the following sources: (●) this research thesis; 1, Agassiz, 1843; 2, Albers and Weiler, 1964; 3, Amon et al., 1997; 4, Antunes and Cappetta, 2002; 5, Applegate, 1970; 6, Averianov and Popov, 1995; 7, Beavan, 1995; 8, Beavan and Russell, 1999; 9, Cappetta and Case, 1975b; 10, Cappetta and Case, 1999; 11, Cappetta and Odin, 2001; 12, Case, 1978; 13, Case, 1979; 14, Case, 1987; 15, Case and Schwimmer, 1988; 16, Cicimurri, 2007; 17, Cook et al., 2017; 18, Corral et al., 2004; 19, Corral et al., 2011; 20, Einarsson et al., 2010; 21, Glikman, 1980; 22, Guinot et al., 2012a; 23, Guinot et al., 2012b; 24, Guinot et al., 2013; 25, Herman, 1973; 26, Herman, 1977; 27, Hübner and Müller, 2010; 28, Ladwig, 2014; 29, Lauginiger and Hartstein, 1983; 30, Leriche, 1902; 31, Leriche, 1906; 32, Lewy and Cappetta, 1989; 33, Müller, 1989; 34, Müller, 2014; 35, Peng et al., 2001; 36, Priem, 1897; 37, Richter and Ward, 1990; 38, Roemer, 1849; 39, Schneider and Ladwig, 2013; 40, Schubert et al., 2016; 41, Shimada and Hooks, 2004; 42, Siverson, 1989; 43, Siverson, 1992; 44, Siverson, 1993; 45, Siverson and Lindgren, 2005; 46, Siverson et al., 2015; 47, Siverson et al., 2016; 48, Sorensen et al., 2013; 49, Thies and Müller, 1993; 50, Underwood and Ward, 2008; 51, Vullo, 2005; 52, Welton and Farish, 1993; 53, Williamson and Lucas, 1992; 54, Zalmout and Mustafa, 2001; 55, Zhelezko, 1988. The numbers in ruby colour indicate type localities. Country codes: BE, Belgium; DE, Germany; KZ, Kazakhstan; NL, Netherlands; RU, Russia; UK, United Kingdom.

Vitoria Sub-basin, B-CB (N Spain)	Eurasia		North America							Middle East		Africa	Antarctica
	Urals, Mughalzhar (RU, KZ)	Alberta (Canada)	Montana (USA)	Wyoming (USA)	New Mexico (USA)	New Jersey, Delaware, (USA)	Alabama, Georgia (USA)	Kansas, Texas (USA)	Israel	Jordan	Cabinda (Angola)	Ross Island	
•, 19													
•													
•, 19													
•													
•													
•, 18	6, 21							9, 29					
•													
•, 18, 19	21	17					9	41	45				
•													
•							9		52				
•													
•, 19							9, 29			51			
•, 19								5, 25, 26					
•	55			14			9, 29	9, 15	10, 38, 40, 52		4		
•							9						
•, 18, 19	3, 21, 55	7, 8	12, 13	14	53	1, 9, 29	15	40, 52	32	54	4		
•		35					9		32			37	
•													
•													
•		35		14			9	16	40				

size with an uncertain family status, according to Cappetta (2012), but with teeth morphologically similar to those of Alopiidae. The extant sharks of the latter family are oceanic but occasionally visit littoral waters, as stated in Compagno (2008).

Although very rare, the odontaspimid *Carcharias aasenensis* is also represented. The extant odontaspimid *Carcharias taurus* is regarded as a coastal shark, having a wide-ranging distribution alongshore in temperate to tropical waters at depths of generally less than 200 m (Compagno, 1984a). This swimming efficient, but slow moving, shark is a voracious feeder on bony fishes, small selachians, cephalopods and crustaceans according to the latter author.

While many selachians from Gometxa are mainly inhabitants of coastal waters (from the shore to a depth of 200 m), some others are completely adapted to live within an extensive depth range (see also Chapter 19). Thus, among these are two mitsukurinid lamniforms, *Anomotodon* and *Scapanorhynchus*, which infrequently occur in the Gomecha Member (9% and 2.5% respectively). According to Compagno (1984a), the extant members of Mitsukurinidae are completely adapted to live in outer continental shelves and slopes down to depths of at least 550 m, being mostly considered slope-dwellers as well as semipelagic (Compagno, 2008).

Many other important selachians, all of which are primarily bottom-dwellers (e.g. demersal sharks and batoids), are assumed to have occurred over shelf and upper slope habitats. Among these are the species *Hemiscyllium hermani* and the two taxa referred to *Chiloscyllium*, belonging to the family Hemiscylliidae. The extant members of this family are small, mostly less than 1 m in length, possessing a cylindrical-shaped body (Compagno, 1984a). Their clutching-type dentition is specifically designed to either clutch soft-bodied animals or crush hard-shelled invertebrate preys. Modern hemiscylliids are bottom-dwelling sharks, predominantly found on the continental shelf (from inshore waters up to 100 m depth) and are reported to live in warm, tropical waters, from the Indian Ocean to the Indo-West Pacific, as stated in Compagno (1984a).

Prohaploblepharus riegrafi is the sole recognised species at Gometxa site belonging to Scyliorhinidae. This is a large family of sharks with numerous extant species, each having its own characteristic geographical range from cold temperate to tropical waters and diverse depth distributions. Modern scyliorhinids are generally small (most of them less than 0.8 m in length) bottom-dwelling sharks, moving either on hard sediments or muddy soft bottoms from the upper continental shelf to depths greater than 2,000 m, as reported by Compagno (1984b). The general tooth design is characterised by a sharp main cusp with extra cusplets on each side (clutching-type dentition; Cappetta, 2012). Small bony fishes, crustaceans, and cephalopods are as well in the diet of scyliorhinid sharks.

Palaeospinacidae is an extinct family of synechodontiform sharks with elongated body and a clutching-type dentition (Cappetta, 2012), being represented by *Synechodus* aff. *filipi* at Gometxa. It has been suggested a dominantly benthic or nektobenthic lifestyle in off-shore environments for *Synechodus* sharks, which could have consumed both soft-bodied and shelled marine invertebrates (Underwood et al., 1999).

Extant members of the monogenetic family Squatinidae are adapted to life near or on the sea bed (i.e. bottom-dwelling sharks). They possess cuspidate, clutching-type teeth. All squatinids remain buried on sandy or muddy sea bottoms during day, waiting to ambush small fishes or a wide range of benthic invertebrates found living on the sea bottom, but become active swimmers at night (Compagno, 1984a; Klimley, 2013). *Squatina* sharks are predominantly shelf inhabitants, with several species occurring on the middle slope to a depth of at least 1,300 m, also being quite widespread in cool temperate to tropical waters of all oceans (Compagno, 1984a).

Rajiforms (Batoidea) are also described but they occur in lower numbers. Only the taxa *Parapalaebates pygmaeus*, *Ptychotrygon* sp., and *Rhinobatos casieri* are represented in the two Gometxa assemblages (from lithofacies 1 and 2). The former species has grinding-type teeth (i.e. durophagous dentition), being able to feed largely on hard-shelled preys such as echinoderms, molluscs, and crustaceans, in agreement with Cappetta (2012). *Ptychotrygon* sp. and *Rhinobatos casieri* are also regarded bottom-dwellers but with a crushing-type dentition that allowed them to consume small fishes, crustaceans and cephalopods (Cappetta, 2012). Modern representatives of Rhinobatidae are strong-swimming, bottom-dwellers with a circumglobal distribution in subtropical and temperate regions (Compagno and Last, 1999; Cappetta, 2012). They may be found on either sandy or muddy bottoms, usually in shallow coastal areas of the continental shelf, but some species occur on the uppermost continental slope (i.e. from depths of a few metres down to over 200–300 m), according to the same authors.

The illustrative food-web of the Fig. 17.2 depicts the trophic interactions among the recognised fossil assemblages in the pelagic ecosystem that existed at this time in Gometxa. The proposed model is composed of the following five trophic positions: primary producers (phytoplankton), zooplankton, lower trophic level (micronektonic and macronektonic elements: bony fish species and cephalopods), mesopredators (medium- and small-sized selachians, among which the species *Anomotodon hermani*, *Scapanorhynchus* cf. *texanus*, *Carcharias aasenensis*, and *Paranomotodon* cf. *angustidens*), and the above mentioned apex predators in the highest trophic level.

Previous sedimentological and micropalaeontological studies have given an estimated depth range of 80 to 400 m, with a general eastward deepening of the depositional basin (Ramírez del Pozo, 1971), or in a depth of water below 100–150 m (Engeser, 1985). The above selachians provide extra information, as well, for interpreting the palaeoenvironmental conditions in the Vitoria Sub-basin during the deposition of the Gomecha Member. A mixed assemblage of pelagic (oceanic and semipelagic) and bottom-dwelling selachians that lived close to the continental shelf and upper slope have been found – especially in the oldest assemblage from lithofacies-1. The oceanic fauna is dominated by the sharks *Cretolamna*, *Cretoxyrhina*, and *Paranomotodon*, while the semipelagic (or neritic) *Carcharias* is considered a shallow inshore inhabitant that occasionally entered oceanic waters. Among the bottom dwellers are included small sharks such as the hemiscylliids (e.g. *Chiloscyllium* and *Hemiscyllium*), scyliorhinids (e.g. *Prohaploblepharus*), and palaeospinacids (e.g. *Synechodus*), but also a few batoids living close to or on the continental shelf- and perhaps upper slope (e.g. *Parapalaebates*, *Ptychotrygon*, and *Rhinobatos*). Moreover, other important cooccurring shark taxa belong to sharks considered to be deep-water inhabitants, although with an extensive depth range (e.g. the mitsukurinids *Anomotodon* and *Scapanorhynchus*, and *Squatina*). However, the presence of the latter taxa does not imply deep-water mesopelagic or bathyal habitats for the Gometxa site, and when comparing its faunal elements with those of the Münsterland Cretaceous Basin (NW Germany), genuine deep-water squalomorph and hexanchid sharks are lacking.

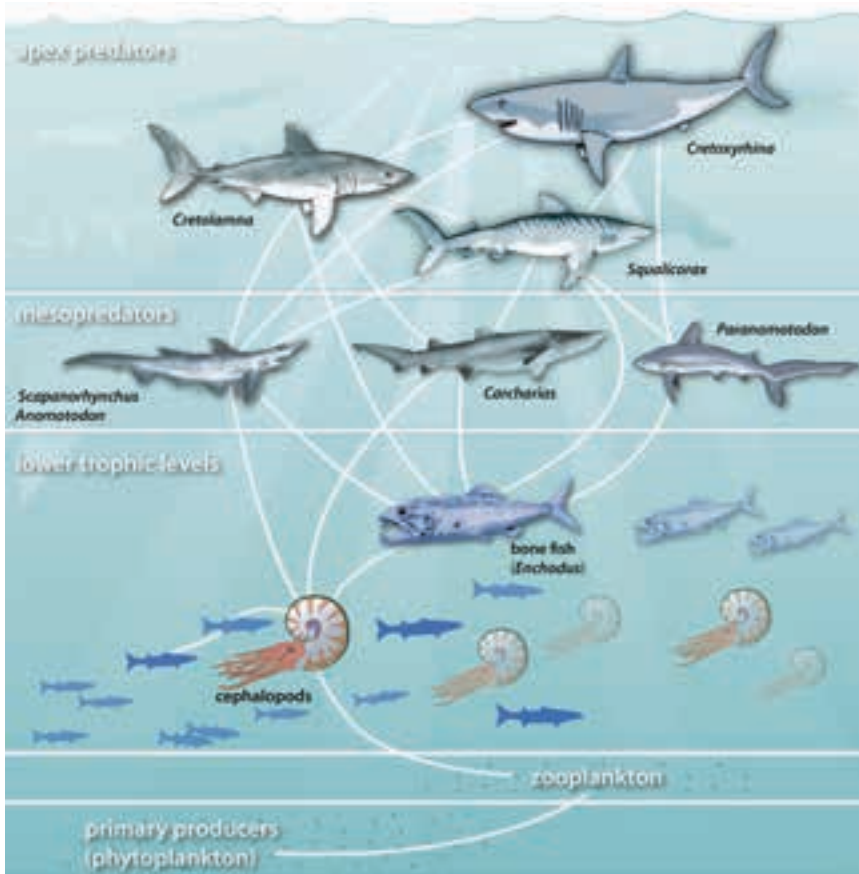


Figure 17.2 A general representation of the pelagic food web with the five trophic levels of the Gometxa ecosystem during the earliest late Campanian. White lines show assumed interactions among the components (fish drawings modified from several sources; not to scale).

The younger selachian assemblage recovered at Vitoria Pass from the upper Campanian Eguileta Member, which represents a subaqueous, lower energy delta slope according to Engeser (1985), is marked by a lower diversity with only a few species belonging to the lamniform and carcharhiniform orders (see Table 17.1)¹. This rock unit also contains a rich and diverse assemblage of marine invertebrates (see Chapter 6), and from its micropalaeontological analysis a well-oxygenated water column to depths greater than 50 m is deduced at the time of sedimentation (San Martín, 1986).

The medium- to large lamniform sharks *Squalicorax* ex gr. *kaupi*, *Cretalamna borealis*, and *C. sarcoportheta* (representing an aggregated 86.5% of the total lamniform

¹This assemblage is remarkably biased toward large specimens due to the collecting techniques.

teeth) occupied the highest trophic level within the pelagic ecosystem, but despite extensive prospecting, *Cretoxyrhina mantelli* is unknown at this fossil site, indicating that either the marine habitat was unfavourable for this pelagic shark or the species was in very short individuals at a time that coincides with its global extinction (see remarks in Chapter 11). It was also found that mosasaurids, which were also specialised hunters of the marine vertebrate fauna, represented in the Eguileta Member were top predators in these marine ecosystem at the expense of large sharks of the genus *Cretolamna* (Bardet et al., 1993, 1997, 2006; Corral et al., 2004). But mosasaurids also had in the largest sharks their natural predators, as bite marks on a mosasaurid vertebra from Jauregi (Eguileta Member) were purportedly inflicted by a shark (Corral et al., 2004). The next two chapters further expand on this.

The Vitoria Pass faunal assemblage also includes the uncommon odontaspidid *Carcharias adneti*. At present, many of inshore waters are abundant in the extant species *Carcharias taurus*. This raises the question whether the higher proportion of odontaspidid teeth present in the Vitoria Pass assemblage, comparing to that of Gometxa site (see Table 17.1), reinforces the idea of a shallower depositional environment for the Eguileta Member, as first proved by sedimentological data. Further collecting work is needed to clarify it.

The triakid *Galeorhinus girardoti* is the sole carcharhiniform shark recognised in the Vitoria Pass assemblage. The extant analogue *Galeorhinus galeus* Linnaeus, 1758 is a strong-swimming, coastal-pelagic shark that also ventures offshore, being abundant in cold to warm temperate waters of the continental shelf and upper continental slope (Compagno, 1984b). This shark species often occurs close to the sea bottom (benthopelagic habits) from a few metres to depths of over 400 m, as also reported in Compagno (1984b). Galeorhinids possess cutting-clutching teeth, suitable for primarily feeding on bottom-dwelling cephalopods, crustaceans, and fishes (Cappetta, 2012).

From a biogeographical perspective, the Campanian selachians from the Vitoria Sub-basin include cosmopolitan taxa [e.g. *Cretolamna sarcoportheta* (also referred to as *C. appendiculata* in earlier times), *Rhinobatos casieri*, *Scapanorhynchus* cf. *texanus*, *Squalicorax* ex gr. *kaupi*, and *Squatina hassei*], also occurring in coeval deposits of Western Europe and other parts of the world (see Table 17.2). Considering the whole taxa list of Gometxa and Vitoria Pass sites as an aggregate assemblage (i.e. intended to represent a relatively extended period of time from a reduced geographical area), the artificial set may show a different biogeographical history to that of North Temperate regions, but not clearly Tethyan and it can be in part comparable to that of Aquitaine from southwestern France reported by Vullo (2005).

Particularly, the oldest fossil assemblage from lithofacies-1 at Gometxa has provided some species that are considered inhabitants of relatively deep-water habitats, or in other words, mesopelagic and bottom-dweller selachians. In addition to common coastal and epipelagic selachians, some few scyliorhinids (i.e. *Probaploblepharus*), orectolobiforms (i.e. *Chiloscyllium*), palaeospinacids (i.e. *Synechodus*), and mitsukurinids (i.e. *Amonoto-*

don) also occur in the following areas of the epicontinental sea of the warm-temperate North European province: the Kristianstad Basin (Siversson et al., 2015, 2016; Sørensen et al., 2013), the Anglo-Paris Basin (Guinot et al., 2012a; 2012b), and the Münsterland Cretaceous Basin within the same biogeographical province (Müller, 1989, 2014; Thies and Müller, 1993; Hübner and Müller, 2010). However, in the latter basin it cooccurs both deep- and shallow-water selachians, which is the result of a typical taphonomic assemblage originated within turbiditic deposits (Hübner and Müller, 2010).

The sharks *Squatina hassei*, *Scapanorhynchus* cf. *texanus*, and *Squalicorax* ex gr. *kaupi* present a possible antiequatorial distribution. Although this is difficult to fully asseverate in the last two examples, because there seems to be several different species included in the cosmopolitan species *Squalicorax kaupi*, as noted earlier (see Chapters 11 and 12).

A clear modification in the faunal composition between the lower upper Campanian (Gometxa site) and upper Campanian selachian associations (Vitoria Pass site) has been observed, but this cannot be solely attributed to the progressive cooling conditions reported in Western Europe during the Campanian stage (Guinot, 2013b). Rather, local palaeogeography accounted for this faunal adjustment, since a regional regressive event affected the south central part of the Basque-Cantabrian Basin by the end of the Campanian, as reported by many geologists (Engeser, 1985; Floquet, 2004; Wiedmann et al., 1983). Thus, the ecological impact caused by changes in the marine environment with challenging shallower regressive conditions and the loss of a suitable habitat, is a major cause related to the decline of some selachian groups and their eventual disappearance in the Vitoria Sub-basin near the end of the upper Campanian.

17.4 Global patterns in the biogeographical distribution of neoselachians during the Campanian time

Common multivariate ordinations and parsimony analysis

This research study involves using several statistical techniques to analyse similarity (or dissimilarity) in taxa composition among several geographical regions. Simple ordination methods used are as follows: principal coordinate analysis (PCoA), non-metric multidimensional scaling (NMDS), clustering, and parsimony analysis of endemism (PAE). Early applications of these techniques in other fossil groups include those by Hanger (1996), Seeling et al. (2004), and Fryrda and Blodgett (2008).

A data matrix has been generated from the literature and personal observation for the presence (and absence) of 86 selachian genera representing 42 families and 10 orders known to occur in 18 geographical areas named operative geographical units (or OGUs) after Seeling et al. (2004), most of them strikingly distributed across the Northern Hemisphere. The 18 distributional regions compared herein are: (A) the Kristianstad Basin (Sweden); (B) the North German Basin (N Germany); (C) the Münster-

land Cretaceous Basin (northwest Germany); (D) the Liege-Limburg Basin (Belgium, Germany, and the Netherlands); (E) the Mons Basin (Belgium); (F) the Anglo-Paris Basin (France and the UK); (G) the Aquitaine Basin (W France); and (H) the Vitoria Sub-basin of the B-CB (northern Spain) in Western Europe; (I) the Urals (Russia and Kazakhstan) in easternmost Europe; (J) the Dinosaur Park and Bearpaw formations of Alberta (Canada); (K) the Judith River Formation of Montana; (L) the Mesaverde Formation in the Big Horn Basin of Wyoming; (M) the Picture Cliff Formation of New Mexico; (N) the Marshalltown and Mount Laurel formations in the Atlantic Coastal Plain of New Jersey and Delaware; (O) the Bluffton and Donoho Creek formations in the Gulf Coastal Plain of southwestern Georgia and South Carolina; and (P) the Aguja Formation of West Texas in the USA; (Q) the Menuha and Mishash formations (Israel and Jordan) in the Middle East; and finally (R) the distributional unit of Cabinda (Angola's exclave province) in western Africa (see Table 17.3).

For two-OGU comparison, the more similar they are, the closer they will be presented in tables and graphs (see Table 17.4). However, this has to be carefully evaluated because the sedimentological context in the deposit formation (e.g. depositional environment and oceanic currents) may have played a characteristic role in the final composition of the fossil assemblage. PCoA analysis of the studied data set, using the Jaccard's similarity index (JI), has resulted in the plot of the Fig. 17.3. Except for the Africa site (locality R), the coordinates of the PCoA show positive eigenvalues (i.e. 12.797 to 7.28E-16), so the results can be considered valid (see Hammer and Harper, 2006). The data representation by this method depicts a group of points with a reasonably logical geographical distribution. A NMDS ordination was also undertaken using the JI (Fig. 17.4 is the two-dimensional scattergram of the data matrix constructed from Table 17.3). This ordination analysis is very similar to PCoA, and therefore the resulting scatter graph is comparable in shape. However, the distances between the data points in NMDS space are distorted, contrary to what happens in PCoA, and the axes only form an arbitrary system of coordinates. Despite obtaining a stress value of 0.1755, as depicted in the Shepard plot (Fig. 17.5), the scattergram is considered relatively acceptable – for figures above 0.1, some information has been lost in the reduction of dimensionality, as indicated in Hammer and Harper (2006). Generally, this map-like graph allows to visualise the distribution of the 18 OGU in an rather intuitive way. Other informative biogeographical diagrams about faunal relationships can be obtained by cluster analysis. The similarity among the 18 OGU units of the data set is readily interpretable with this method. Both Jaccard and Dice indices and the average linked (UPGMA) algorithm have been used in information retrieval, having found that the outcome has not differed significantly after choosing any of the two similarity indices. The results are presented in the form of dendrograms (Fig. 17.6) where coupled geographical units with shorter branches are more closely related. Finally, on the basis of the distribution matrix of the genera, a parsimony analysis of endemicity (PAE) was performed to further test any faunal relationships among the

Table 17.3 Data matrix of 86 selachian genera collected from relevant deposits formed during the Campanian. Conversion to a presence/absence table is needed for its application to biogeography (bullets represent the 1 values and voids the 0 values). Letters denote the considered operational geographical units (OGU).

Order	Family	Genera	Operational geographical units (OGU)																	
			A	B	C	D	E	F	G	H	I	J	K	L	M	N	O	P	Q	R
Lam	Hemiscylliidae	<i>Acantboscyllium</i>						•	•											
Lam	Cretoxyrhinidae	<i>Acrolamna</i>																		•
Raj	Hypsobatidae	<i>Angolabatis</i>																		•
Raj	Sclerorhynchidae	<i>Ankistrohynchus</i>						•						•			•			
Lam	Mitsukurinidae	<i>Anomotodon</i>	•	•	•			•	•		•									
Lam	Cretoxyrhinidae	<i>Archaeolamna</i>	•					•	•				•	•	•	•	•	•	•	
Car	Triakidae	<i>Archaeotriakis</i>												•	•	•				
Raj	Sclerorhynchidae	<i>Borodinoprists</i>																		•
Myl	Myliobatidae	<i>Brachyrhizodus</i>																	•	•
Ore	Ginglymostomatidae	<i>Cantioscyllium</i>													•	?			•	•
Lam	Odontaspidae	<i>Carcharias</i>	•	•				•	•	•	•			•	•	•	•	•	•	•
Ore	Orectolobidae	<i>Cederstroemia</i>	•					•	•					•						
Sql	Squalidae	<i>Centrophoroides</i>			•	•		•	•						•					
Sql	Somniosidae	<i>Centrosymnus</i>			•	•														
Ore	Hemiscylliidae	<i>Chiloscyllium</i>	•		•			•		•			•	•	•		•	•	•	•
Hex	Chlamydoselachidae	<i>Chlamydoselachus</i>																		•
Ore	Orectolobidae ?	<i>Columbusia</i>													•		•			?
Car	Scyliorhinidae	<i>Crassescyliorhinus</i>	•		•			•	•	•										
Raj	Platyrrhinidae	<i>Cretaplatyrhinoidis</i>								•										
Sql	Somniosidae	<i>Cretascymnus</i>			•	•														•
Lam	Otodontidae	<i>Cretolamna</i>	•	•	•	•	•	•	•	•	•	•					•	•	•	•
Ore	Orectolobidae	<i>Cretoectolobus</i>	•											•	•	•				
Lam	Cretoxyrhinidae	<i>Cretoxyrhina</i>	•			•		•		•	•	•					•			
Ech	Echinorhinidae	<i>Echinorhinus</i>																		•
Sql	Etmopteridae	<i>Eoetmopterus</i>			•	•														
Lam	Cretoxyrhinidae	<i>Eotriatolamia</i>						•	•			•								
Lam	Anacoracidae	<i>Galeocorax</i>																		•
Car	Triakidae	<i>Galeorhinus</i>	•	•	•			•	•	•	•								•	•
Raj	Sclerorhynchidae	<i>Ganoprists</i>																		•
Ore	Hemiscylliidae	<i>Hemiscyllium</i>	•	•	•					•										
Het	Heterodontidae	<i>Heterodontus</i>	•	•	•	•	•	•	•	•		•					•	•	•	
Hex	Hexanchidae	<i>Hexanchus</i>			•	•		•	•			•							•	•
Hyb	Hybodontidae	<i>Hybodus</i>	•			•						•	•	•	•	•	•	•	•	
Myl	Myliobatidae	<i>Igdabatis</i>																		?
Raj	Sclerorhynchidae	<i>Ischyrbiza</i>					•							•	•	•	•	•	•	•
Lam	Odontaspidae	? <i>Jaekelotodus</i>								•										
Car	Leptochariidae	<i>Leptocharias</i>								•										
Hyb	Lonchidiidae	<i>Lissodus</i>																•	•	•
Hyb	Lonchidiidae	<i>Lonchidion</i>						•	•						•	•				•
Hyb	Hybodontidae	<i>Meristodon</i>										•		•	•					•
Hyb	Hybodontidae	<i>Meristodonoides</i>											•				•			
Raj	Sclerorhynchidae	<i>Microprists</i>									•									
Raj	Rhinobatoidei incert. fam	<i>Myledaphus</i>											•	•	•	•				

Table 17.3 (continued, footnote)

Data set from the following sources: **A**, Kristianstad Basin, Sweden (Siverson, 1989; Siverson, 1992; Siverson, 1993; Siverson et al., 2015, 2016; Sørensen et al., 2013); **B**, North German Basin, N Germany (Ladwig, 2014; Schneider and Ladwig, 2013; Thies and Müller, 1993); **C**, Münsterland Cretaceous Basin, northwest Germany (Hübner and Müller, 2010; Müller, 1989, 2014; Thies and Müller, 1993); **D**, Liege-Limburg Basin, Belgium, Germany, and the Netherlands (Albers and Weiler, 1964; Herman, 1977); **E**, Mons Basin, Belgium (Herman, 1977); **F**, Anglo-Paris Basin, France and the UK (Gervais, 1852; Guinot et al., 2012a, 2012b, 2013; Herman, 1977; Leriche, 1902; Leriche, 1906; Priem, 1897; Underwood and Ward, 2008); **G**, Aquitaine Basin, W France (Cappetta and Odin, 2001; Vullo, 2005); **H**, Vitoria Sub-basin, B-CB, northern Spain (this research); **I**, The Urals, Russia and Kazakhstan (Averianov and Nessov, 1995; Glikman, 1980; Zhelezko, 1988, 1990); **J**, Alberta, Canada (Beavan, 1995; Beavan and Russell, 1999; Cook et al., 2017; Peng et al., 2001); **K**, Judith River Formation, Montana, USA (Case, 1978, 1979); **L**, Big Horn Basin, Wyoming, USA (Case, 1987; Schubert et al., 2016); **M**, Mesa Portales, New Mexico, USA (Schubert et al., 2016; Williamson and Lucas, 1992); **N**, Atlantic Coastal Plain, New Jersey and Delaware, USA (Callahan et al., 2014; Cappetta and Case, 1975b; Case and Cappetta, 2004; Lauginiger and Hartstein, 1983); **O**, Gulf Coastal Plain, southwestern Georgia and South Carolina, USA (Case and Schwimmer, 1988; Cicimurri, 2007); **P**, Texas, USA (Cappetta and Case 1975a, 1999; Schubert et al., 2016; Welton and Farish, 1993); **Q**, Middle East, Israel and Jordan (Lewy and Cappetta, 1989; Zalmout and Mustafa, 2001); **R**, West Africa, Angola (Antunes and Cappetta, 2002; Cappetta, 2012).

revised fossiliferous units considered in this research. These calculations generated by the PAST v1.91 software resulted in a strict consensus tree based on 162 equally parsimonious trees discovered by heuristic search (mode TBR or tree bisection and reconnection) and under the Fitch criterion (Fig. 17.7).

Discussion of the results

The barriers that shape the geographical distribution of marine fishes in modern seas result from the sea-continent distribution, in addition to several major environmental limiting factors, such as salinity, ocean currents, oxygen concentration, degree of turbidity and significantly seawater temperature. But also the dispersal ability (or vagility) of the elasmobranchs, which is clearly different in pelagic oceanic species compared with small nectobenthic taxa¹, and the rifting apart of the continents, which may create either barriers or new marine connections, are accounting aspects that have affected their biogeographical boundaries. Benthic sharks have a distribution range five times smaller than pelagic sharks (Musick et al., 2004). This characteristic has been noticed in the Jurassic seas by Kriwet and Klug (2008), where the squatinids, orectolobiforms,

¹ Dispersal in elasmobranchs requires active swimming because of their reproductive habits (i.e. oviparism and anchoring large, horny capsules to the sea bottom after deposition); fertilised eggs are not broadcasted to the water column as many marine bony fishes do (Musick et al., 2004).

Table 17.4 Similarity among 18 operational geographical units (OGU) calculated from the genera raw-data matrix in Table 17.3 using the Jaccard's index (lower triangle) and Dice's index (upper grey triangle). The value reduces as a pair of units gets less similar.

OGUs	A	B	C	D	E	F	G	H	I	J	K	L	M	N	O	P	Q	R	
A	1	0.533	0.600	0.514	0.667	0.636	0.634	0.711	0.444	0.489	0.429	0.392	0.286	0.593	0.542	0.464	0.410	0.167	
B	0.364	1	0.711	0.333	0.609	0.492	0.611	0.513	0.350	0.158	0.111	0.267	0.200	0.333	0.333	0.449	0.471	0.276	
C	0.429	0.552	1	0.389	0.654	0.567	0.488	0.500	0.304	0.311	0.190	0.314	0.114	0.302	0.340	0.500	0.450	0.278	
D	0.346	0.200	0.241	1	0.389	0.320	0.320	0.500	0.533	0.483	0.308	0.400	0.421	0.541	0.500	0.359	0.333	0.300	
E	0.500	0.438	0.486	0.241	1	0.746	0.571	0.444	0.435	0.311	0.286	0.431	0.286	0.407	0.417	0.464	0.400	0.167	
F	0.467	0.326	0.396	0.190	0.595	1	0.491	0.500	0.393	0.333	0.281	0.364	0.240	0.406	0.349	0.507	0.400	0.118	
G	0.464	0.440	0.323	0.190	0.400	0.326	1	0.514	0.286	0.171	0.125	0.244	0.231	0.455	0.474	0.522	0.414	0.154	
H	0.552	0.345	0.333	0.333	0.286	0.333	0.346	1	0.421	0.421	0.286	0.364	0.286	0.596	0.488	0.449	0.516	0.207	
I	0.286	0.212	0.179	0.364	0.278	0.245	0.167	0.267	1	0.410	0.389	0.400	0.345	0.468	0.390	0.360	0.294	0.200	
J	0.324	0.086	0.184	0.318	0.184	0.200	0.094	0.267	0.258	1	0.800	0.682	0.643	0.553	0.439	0.327	0.188	0.138	
K	0.273	0.059	0.105	0.182	0.167	0.163	0.067	0.167	0.241	0.667	1	0.683	0.640	0.409	0.368	0.261	0.138	0.077	
L	0.244	0.154	0.186	0.250	0.275	0.222	0.139	0.222	0.250	0.517	0.519	1	0.606	0.566	0.511	0.519	0.263	0.114	
M	0.167	0.111	0.061	0.267	0.167	0.136	0.130	0.167	0.208	0.474	0.471	0.435	1	0.378	0.452	0.308	0.087	0.100	
N	0.421	0.200	0.178	0.370	0.256	0.255	0.294	0.424	0.306	0.382	0.257	0.395	0.333	1	0.760	0.596	0.350	0.158	
O	GULFCOAST.PL.	0.371	0.200	0.205	0.333	0.263	0.212	0.310	0.323	0.242	0.281	0.226	0.343	0.292	0.613	1	0.615	0.353	0.188
P	TEXAS	0.302	0.289	0.333	0.219	0.302	0.340	0.353	0.289	0.220	0.195	0.150	0.350	0.182	0.425	0.444	1	0.512	0.200
Q	MIDD-EAST	0.258	0.308	0.290	0.200	0.250	0.250	0.261	0.348	0.172	0.103	0.074	0.152	0.045	0.212	0.214	0.344	1	0.250
R	ANGOLA	0.091	0.160	0.161	0.176	0.091	0.063	0.083	0.115	0.111	0.074	0.040	0.061	0.053	0.086	0.103	0.111	0.143	1

The analysed regions are: A) Kristianstad Basin, Sweden; B) North German Basin, N Germany; C) Münsterland Cretaceous Basin, northwest Germany; D) Liege-Limburg Basin, Belgium, Germany, and the Netherlands; E) Mons Basin, Belgium; F) Anglo-Paris Basin, France and the UK; G) Aquitaine Basin, W France; H) Vitoria Sub-basin, B-CB, northern Spain; I) The Urals, Russia and Kazakhstan; J) Alberta, Canada; K) Judith River Formation, Montana, USA; L) Big Horn Basin, Wyoming, USA; M) Mesa Portales, New Mexico, USA; N) Atlantic Coastal Plain, New Jersey and Delaware, USA; O) Gulf Coastal Plain, southwestern Georgia and South Carolina, USA; P) Texas, USA; Q) Middle East, Israel and Jordan; and R) West Africa, Angola.

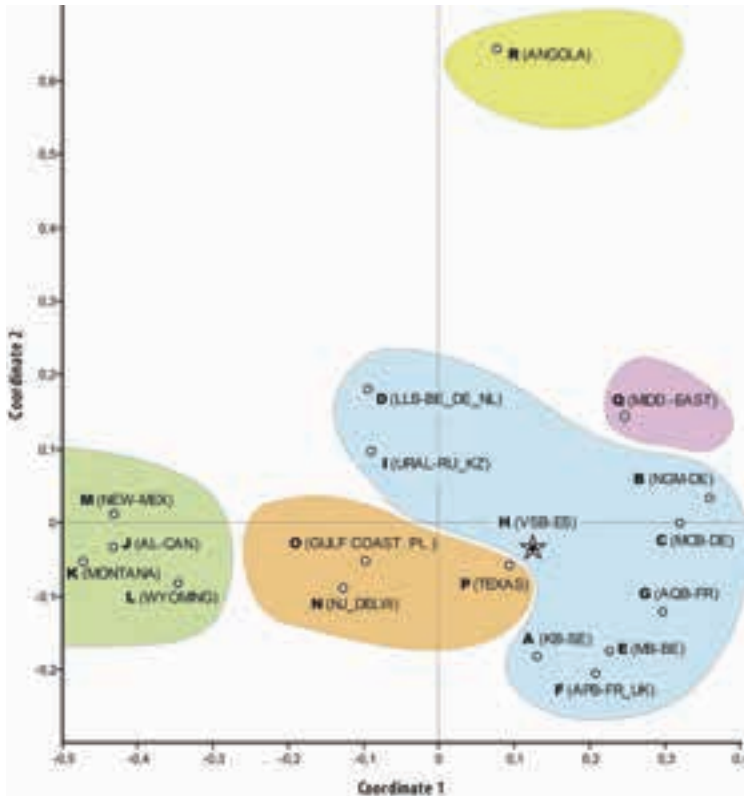


Figure 17.3 Ordination diagram (PCoA) applied to 18 operational geographical units (OGU), using the Jaccard coefficient of similarity. The site of this study is marked with a star. Supposed distribution of the selachian palaeobioprovinces is represented by different colours. Geographical abbreviations are defined in Table 17.4.

and batoids generally show lower levels of geographical distribution and have the highest levels of endemism, and on the contrary, the degree of endemism is low in sharks that are able to move alongshore and migrate long distances across oceans, as in Lamniform representatives. Moreover, it has been adequately observed a strong relationship between total shark length and range of distribution in extant individuals. Thus, small species, less than 1 m long, have very small ranges, while species over 3 m often have circumglobal distributions; and ranges are, on average, smaller in coastal sharks than in those occurring primarily in bathyal or oceanic habitats (Musick et al., 2004).

The key to explain the distribution of a geographically detached group of taxa, according to a dispersal or vicariance model, is to assess the age of the geographical barriers and then see if they are older, or not, than the allopatric taxa (Musick et al., 2004). Many genera reported in the Campanian are assigned to species that appeared earlier in the Jurassic and Lower Cretaceous (see Cappetta, 2012), therefore a vicariance scenario

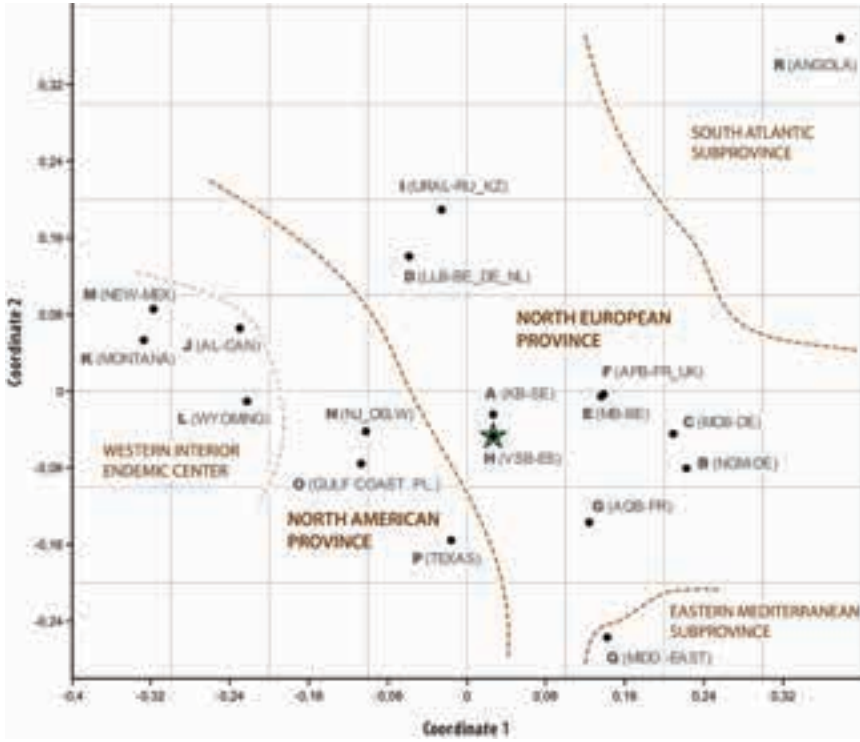


Figure 17.4 Non-metric multidimensional scaling (NMDS) graph applied to 18 operational geographical units (OGU), using the Jaccard coefficient of similarity. Tentative distribution of the paleobioprovinces is marked. The site of this study is marked with an star. Geographical abbreviations are defined in Table 17.4.

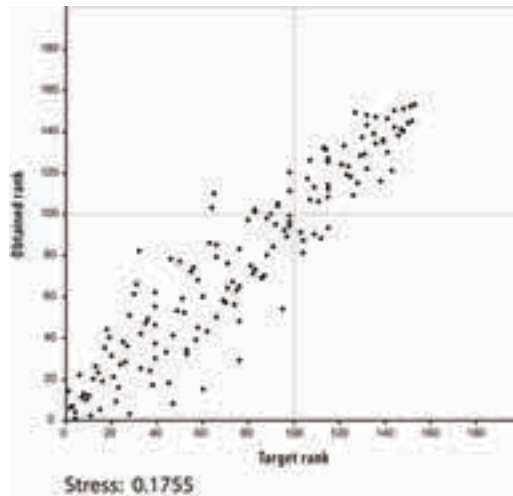


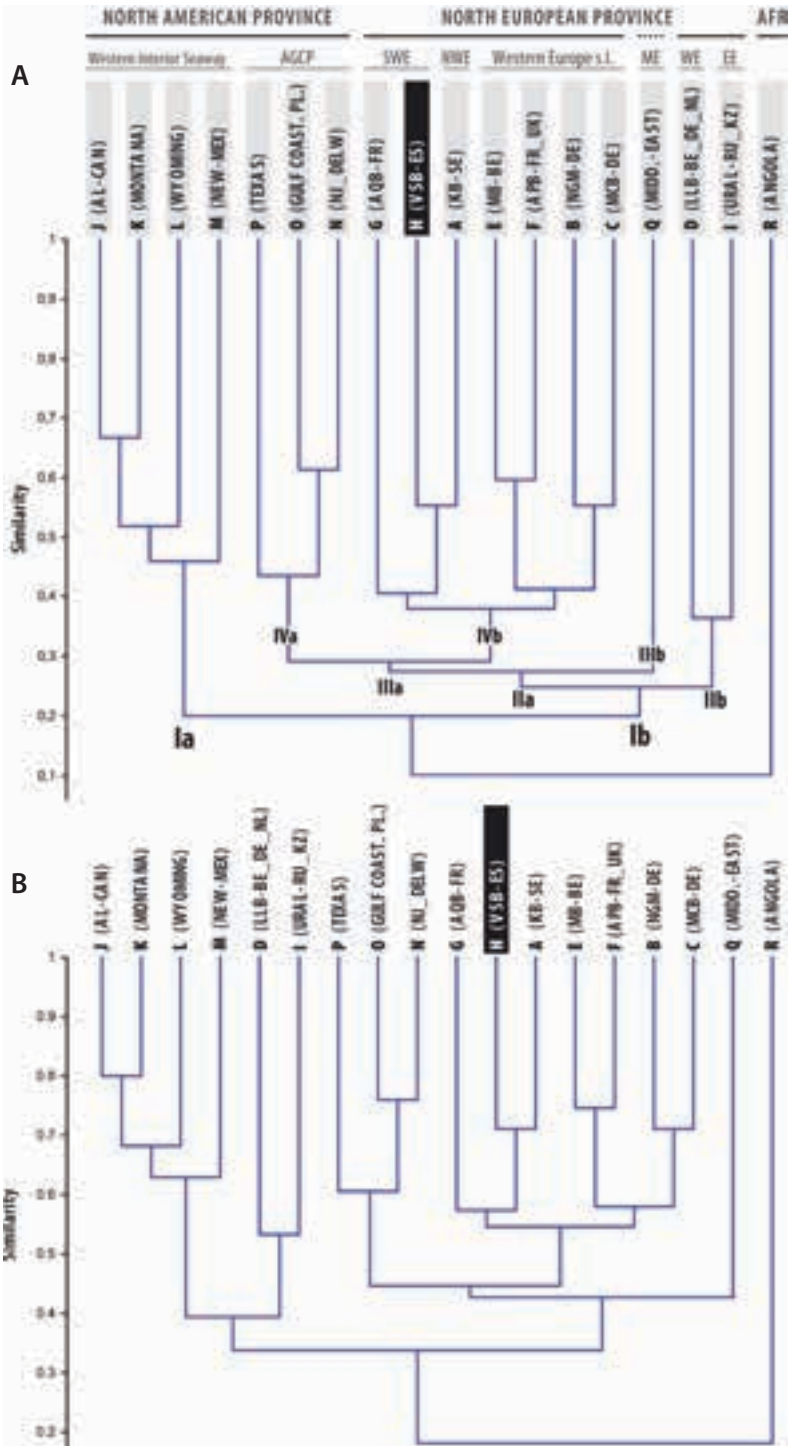
Figure 17.5 Shepard plot from the NMDS analysis of Fig. 17.4.

favoured by the continental separation of shelf margins would better explain the distribution of two separated clusters of a genus in benthic and benthopelagic selachians that are characterised by a low dispersal rate. Contrarily, a wide geographical distribution of large bodied, pelagic elasmobranchs that are able to overcome geographical and ecological barriers is better explained by dispersal.

Form both PCoA and NMDS diagrams (Figs. 17.3–4), it is clearly observed that the selachian distribution in the North American Province seems to be associated with particular geographical (latitudinal) and possibly ecological conditions. A shallow inner sea, named Western Interior Seaway (WIS), occupied the continent during the late Campanian from places in Alberta, in the North, to western Texas at the southern end. This biogeographical unit – between two landmasses and isolated from the main Atlantic and Oceanic oceans – developed across Alberta, Montana, Wyoming, and New Mexico, and corresponds to the endemic centre of the Western Interior of North America referred by Kauffman (1973). In order to explain the selachian diversity of the Texas area, which is more closely related to those areas in the Gulf and Atlantic Coastal Plain, ecological variables (i.e. zone of warm southern water currents) can be regarded. Moreover, it is likely that ocean surface currents would have enabled several North Atlantic genera to colonize the southern end of the WIS. Within the European Province, the geographical zones are more or less evenly distributed, with a significantly closer relation between paired regions with similar faunal composition, such as the Anglo-Paris Basin (France and the UK conjoined) and the Mons Basins in Belgium, and the North German and Münsterland Cretaceous basins, both in northern Germany. The Kristianstad Basin in Sweden and the Aquitaine Basin in western France also show a latitudinal gradient of north temperate and warm temperate water seas, respectively. The proximity of the Liege-Limburg Basin (Belgium, Germany, and the Netherlands) in Western Europe to the Urals unit (Russia and Kazakhstan) in Eastern Europe is a mayor inconsistency that may be attributed to the lack of a recent systematic review of the fossil sharks occurring in the involved areas. In contrast, similarity indices reveal very low faunal affinity with the rests of the groups of the poorly known Campanian deposits of Africa (Angola). Faunal data in the Middle-East zone (Israel and Jordan), located in between Eastern Europe and Africa, are in a proper position in the Indo-Mediterranean region.

The cluster analysis has produced dendrograms almost similar for Jaccard and Dice indices (Fig. 17.6). Despite of differences in the splitting (branching) values, which have no significance respecting to the palaeobiogeographical affinities, the only signifi-

Figure 17.6 Cluster analysis of the 18 OGU's studied. A, dendrogram constructed with the paired group algorithm and Jaccard's index; B, analysis of the same data using Dice's index (note that similarity is deflated compared to JI). Some root branches has been reoriented to visualise the geographical data. AFR, Africa; AGCP, Atlantic and Gulf Coastal Plain; EE, Eastern Europe; ME, Middle East; NWE, north-western Europe; SWE, southwestern Europe, WE, Western Europe (s.l.). Abbreviations of the OGU's are defined in Table 17.4. ►



cant divergences exist with regard to the position of units D and I of the OGU (refer to Table 17.4 for unit identification). Thus, I will further comment on the Jaccard index dendrogram (Fig. 17.6A), as these results are most consistent with those obtained with the previous PCoA and NMDS analysis. Two major groups (cut at 0.2 on the similarity axis), each with valid subgroups are evident in the cluster analysis (Fig. 17.6A). The main group Ia is formed by geographical units J, K, L, and M, which correspond in broad terms to the WIS. The second, and more complex main group Ib, is in turn split into subgroups IIa, which comprises most of the geographical units across North America, Western Europe, and Middle-East, and IIb consisting of Eastern Europe (unit I) and the outlier Liege-Limburg grouping (unit D). Clustering of IIa then proceeds with subgroups IIIa and IIIb, producing two distinctive geographical groupings. Thus, whereas the grouping of IIIa comprises geographical units that still belong to the North Temperate Realm, the IIIb subgroup corresponds to the phosphate-rich units of the Middle East, within the Tethyan Realm. Then a new splitting within the IIIa cluster occurs at point 2.9 on the y-axis. The grouping of IVa corresponds to those units located in the North American Province (Atlantic and Gulf Coastal Plain, and the southern end of the WIS), whereas the grouping of IVb represents the European units. The results of the cluster dendrogram also indicate that there are notable links between the paired geographical units O–N, E–F, B–C, and A–H.

The analysis of similarity based on the Jaccard (JI) and Dice (DI) indices (Table 17.4) reveals that the selachian fauna of the Vitoria Sub-basin shows closest faunal affinity with that of the Kristianstad Basin in Sweden (JI = 0.552, DI = 0.711) and slightly lower affinity with other faunas in the Atlantic Coastal Plain of North America (New Jersey and Delaware, USA) (JI = 0.424, DI = 0.596). Similarity analyses also demonstrate a very low faunal affinity with Angola (JI = 0.115, DI = 0.207), New Mexico (JI = 0.167, DI = 0.286), and Montana assemblages (JI = 0.167, DI = 0.286).

The calculation for PAE using the distribution data of 60 selachian taxa was done for the geographical zones after data cleansing (i.e. automorphic- and plesiomorphic-like data removed)¹. The corresponding parsimonious tree is depicted in Fig. 17.7 (L = 162, CI = 0.37; RI = 0.57)². The advantages of using this method to study patterns of endemism are explained in Cecca (2002) and Seeling et al. (2004; and references therein).

Some African taxa represented in the PAE cladogram are so characteristic that can be used to separate this South Atlantic area (R) from all other OGU units, forming thus the sister group to the other geographical units. However, some genera included there (e.g. *Cretolamna*, *Scapanorhynchus*, and *Squalicorax*) are known to occur also in distant geographical locations of North America, Europe, and the southern margin of the Tethys. This could be explained as an antiequatorial distribution of the genera (i.e.

¹ A PAE cladogram contains several geographical lineages that represent zones with biotic interchange or divergence (Cecca, 2002).

² L, tree length; CI, consistence index; RI, retention index.

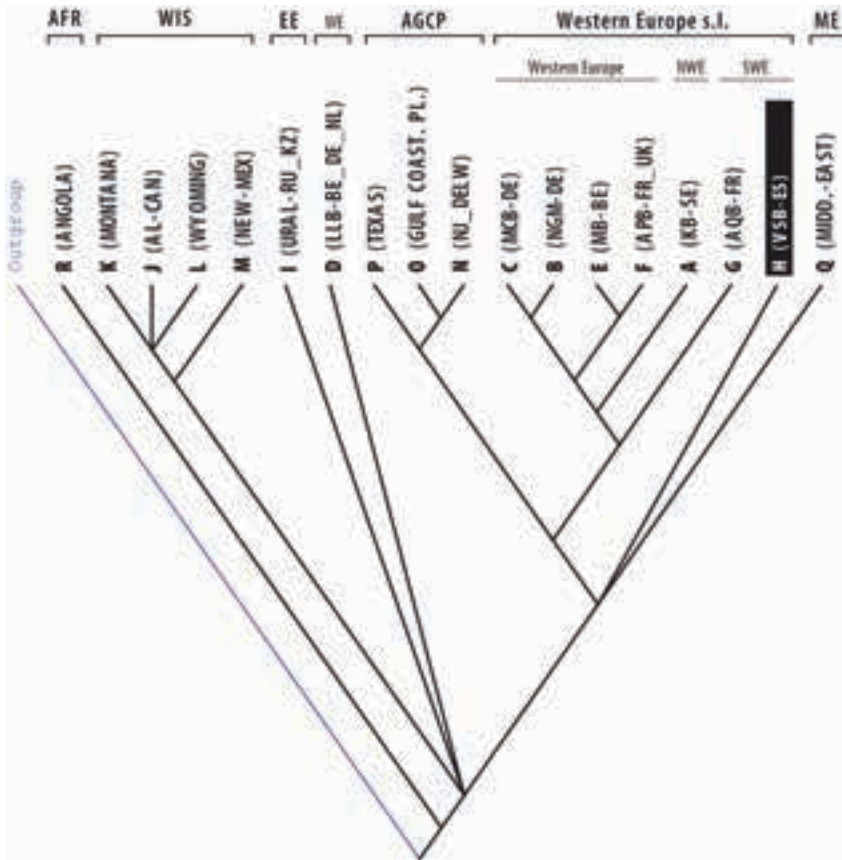


Figure 17.7 Strict consensus tree based on the two most parsimonious trees calculated in a heuristic search TBR (tree bisection and reconnection) and Fitch criterion. This tree is based on analysis of the genera/distribution matrix of the Campanian selachians. AFR, Africa; AGCP, Atlantic and Gulf Coastal Plain; EE, Eastern Europe; ME, Middle East; NWE, northwestern Europe; SWE, southwestern Europe; WIS, Western Interior Seaway. OGU abbreviations are defined in Table 17.4.

being present on both sides of the equatorial thermal division), which is a current phenomenon in bony fishes and sharks, as stated in Nelson (2006). The PAE results, as also proved by cluster analysis, shows a large endemic area in the northernmost and central zones of North America (WIS). This is depicted by a small subtree (clade) formed by a three-way fork (sister-groups to each other), namely Alberta (J), Montana (K), and Wyoming (L), and the New Mexico (M) region as the sister group. The isolation of the marine biota in these northern and middle parts of North America – allegedly with low water circulation – resulted in an adequate area for taxonomic differentiation (area of endemism), as stated in Kauffman (1973). These areas are separated from the two other North American OGUs, namely the Atlantic and Gulf Coastal Plain (AGCP)

with New Jersey and Delaware (N) and southwestern Georgia and southern Carolina (O), and the western Texas (P), which seemed to be well influenced by major surface currents in the proto-Atlantic Ocean at the Campanian time.

The geographical areas Urals (I) and Liege-Limburg Basin (D) are basally rooted in the consensus tree to the WIS area of North America (J to M). This introduces an uncertainty in the expected distribution of the fossil faunae that may be related with missing taxa in the data set or the presence of genera with wide geographical distributions inhabiting similar shelfal environments (e.g. *Cretolamna*, *Cretoxyrhina*, *Heterodontus*, *Hybodus*, *Scapanorhynchus*, *Squalicorax*, *Squatina*, and *Synechodus*). Therefore an updated revision of the faunal list of these two European OGU is required to solve the question.

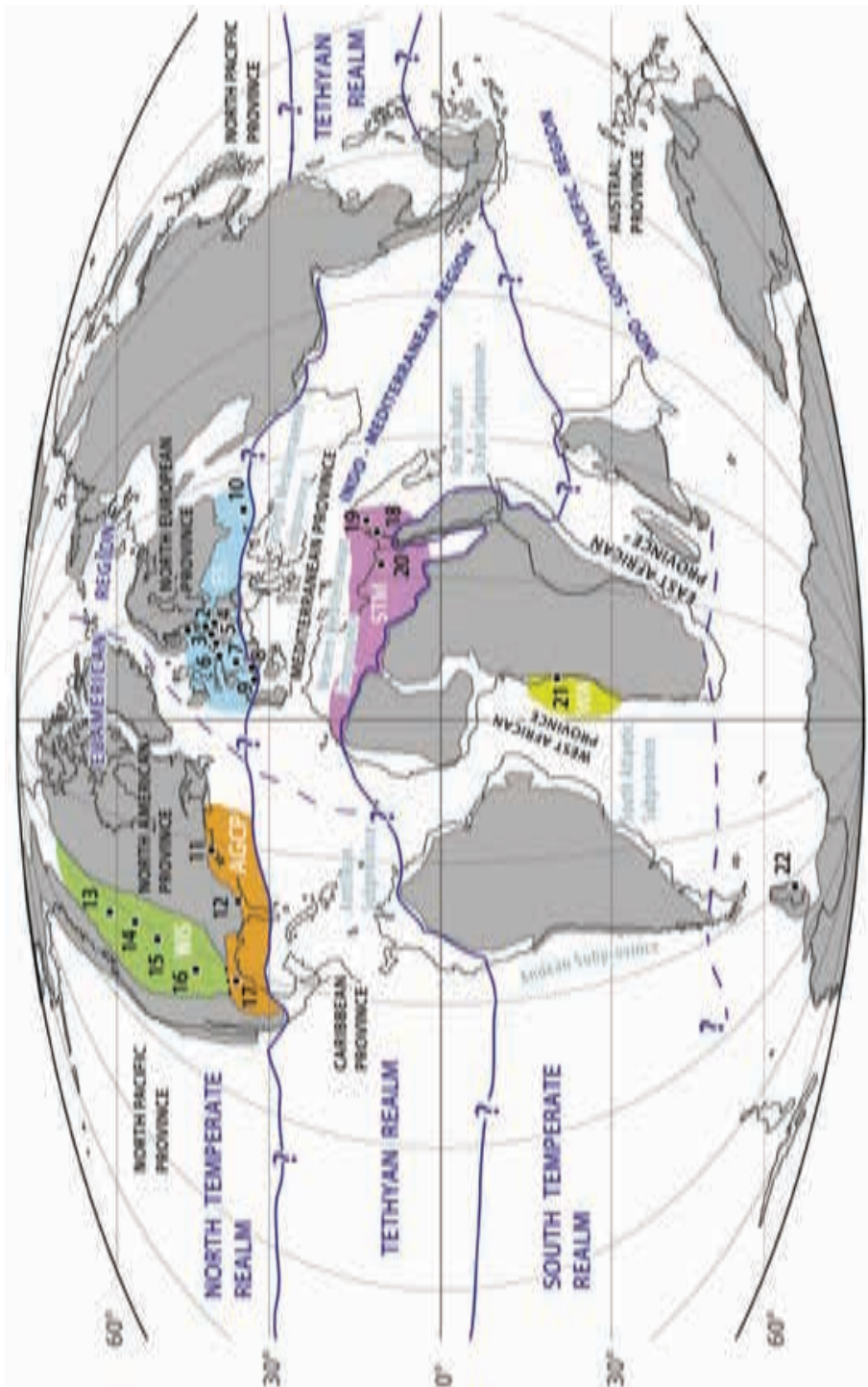
The remaining of the geographical units is included in large cladogram that contains an unresolved trichotomy formed by a large clade containing the AGCP (N to P) and almost all Western Europe geographical areas placed along both margins of the North Atlantic Ocean (A to C, E–F, and G), and two sister groups basally rooted one on each margin of the Tethyan Sea, namely the Vitoria Sub-basin of the B-CB in southwestern Europe (H) and the Israel/Jordan area in the Middle East (Q).

The North Atlantic clade (N to P) along the eastern North American coast successfully represents the relationships between areas of the Atlantic and Gulf Coastal Plain (AGCP). Thus, the geographical units New Jersey and Delaware (N) and the conjoined southwestern Georgia and South Carolina (O) here occur with Texas (P) as the sistergroup, despite being the latter geographically circumscribed to the southern end of the WIS. Species dispersal in this part of North America could be easily achieved in favour of major oceanic currents within a passive margin, and the clear faunal ties of the Texas unit (P) with the N and O groupings of eastern North America, would represent a westward extension of the Atlantic and Gulf Coastal Plain (AGCP) faunae.

All geographical areas in the European Atlantic margin are contained in a predominantly Western Europe clade, with the exception of the Vitoria Sub-basin area (H). The Aquitaine Basin unit (G) is shown to be less inclusive single branch within the major Western European (s.l.) clade, which embraces all of the western geographical units (A, C–B, E–F), except the Liege-Limburg Basin (D). The next less inclusive clade is formed by the basal Kristianstad Basin (A), which is called here northwestern Europe, and two clades resolved in 'more derived' positions in evolutionary terms, namely the North German Basin and Münsterland Cretaceous Basin (C+B), and the Mons Basin and the Anglo-Paris Basin (E+F). Not surprisingly, these pairs of localities show a high degree of similarity with respect to each other, as discussed before.

After all the above observations, the following five palaeobiogeographical units (PBU) sensu Seeling et al. (2004) have been recognised on the basis of using multivariate ordination techniques and parsimony analysis. They are shown on a palaeogeographical reconstruction of the Earth during the Campanian, where the major biogeographical units of Kauffman (1973) are also given (Fig. 17.8). They are as follows:

- i. *Western Interior Seaway (WIS)*. This unit includes the OGU's Alberta (J), Montana (K), Wyoming (L), and New Mexico (M). It is characterised by a mixture of cosmopolitan and endemic genera, and represents a separate warm temperate unit. However, latitudinal differences are observed in the faunal data set, which may indicate that distribution along the WIS was influenced by environmental parameters. It is worth to note the lack of genus *Cretolamna*, the ecological role of the latter perhaps was played here by *Archaeolamna*.
- ii. *Atlantic and Gulf Coastal Plain (AGCP)*. This unit is defined to include the eastern area of North America with the OGU's of New Jersey-Delaware (N), the conjoined southwestern Georgia and South Carolina (O), and the adjacent area of Texas (P). As in the cluster dendrograms, the latter deposit is included here, despite of being situated at the southernmost sector of the WIS units. A very different regime of ocean currents in the area seems to have been a major factor in the distribution of faunal assemblages in this northern warm-temperate unit. The diversity of selachians is high in the AGCP unit, especially in the Texas area with 32 genera. Pelagic or oceanic sharks from open waters are relatively diverse with six to nine families of Lamniformes present. This PBU is also recognised on the basis of the following endemic genera of batomorphs: *Borodinopristis*, *Brachyrhizodus*, and *Pseudohypolophus*.
- iii. *European seas (ES)*. This large area is defined here to include all OGU's from the eastern margin of the Russian and Kazakhstani platform, here named the Urals (I), to the Western European margin of Eurasia (A to H). Within the Western European clade, the highest-diversity of neoselachians is recorded from the Anglo-Paris Basin (F) with at least 41 genera. The data set suggests strong links between this latter area and the closely related Mons Basin (F), which resulted in a dichotomy, with the presence of the endemic *Acanthoscyllium*, *Cretaplatyrhinoidis*, *Leptocharias*, *Palaeoscyllium*, *Palaeotriakis*, *Parasquatina*, *Pseudoscylliorhinus*, *Sigmoscyllium*, and *Squatirhina*. The faunal differences between the grouping of the North German and Münsterland basins (B and C, respectively) and the Mons and Anglo-Paris basins (E and F, respectively) are considered to be the result of ecological changes, favoured by the weight of the Squaliformes taxa present in the German areas (e.g. *Centrophoroides*, *Centroscymnus*, *Cretascymnus*, *Eoetmopterus*, *Paraphorosoides*, *Proetmopterus*, and *Squalus*). In temperate and tropical regions, modern representatives of the family Squalidae are distributed throughout the water column in epipelagic, mesopelagic, and probably bathypelagic environments, living primarily along the outer shelf and upper continental slope to depths of more than 3,000 m, having a higher diversity in deeper waters (Compagno, 1984a). Basinal conditions during the Campanian in the Anglo-Paris Basin are mostly pelagic, with coccolith and foraminiferal chalk deposited in the epicontinental sea that covered the region (Guinot et al., 2013). These sedimentary facies are significantly



different when compared to the sandy calcarenites and calcirudites deposited in the relatively small-sized Kristianstad Basin (A) at the northeastern margin of the epicontinental Chalk Sea (see Surlyk and Sørensen, 2010; Sørensen et al., 2013). Here, higher-latitude vertebrate and invertebrate biota inhabited shallow coastal shelf environments (i.e. rocky shore), and the endemic shark *Polyacrodus* represent a difference with respect to the aforementioned basins. The Aquitaine Basin (G) is certainly separated from the other reported areas because of its particular shallow-water taxa with Tethyan affinity, according to Guinot (2013a). The biota, although less diverse with respect to that of the previously mentioned areas, includes many pelagic and benthopelagic sharks with suggested links to the AGCP unit (e.g. *Carcharias*, *Cretolamna*, *Galeorhinus*, *Heterodontus*, *Palaeogaleus*, *Paranomotodon*, *Pararhincodon*, *Plicatoscyllium*, *Protolamna*, *Pseudocorax*, *Scyliorhinus*, *Serratolamna*, *Squalicorax*, and *Squatina*). Finally, the southernmost adjacent area in this PBU is the Vitoria Sub-basin (H) in the B-CB. The fact that this area emanates from a trichotomy could be the result of biased sampling, or possibly, that the conjoined assemblage of the Basque-Cantabrian Region presents more affinity with the fossil Tethyan fauna. This should be solved in a future work. Many of the taxa of the European unit are also shared at generic level with the AGCP unit. According to the above, the biogeographical proximity during the Campanian of areas

-
- ◀ **Figure 17.8** The Earth during the Campanian times with the main areas exhibiting selachian faunae. Notice that most of the sites are distributed in the Northern Hemisphere. Palaeobiogeographical units (PBU) explained in text. Localities: 1, Kristianstad Basin, southern Sweden (Siverson, 1989, 1992, 1993; Siverson et al., 2015, 2016; Sørensen et al., 2013); 2, North German Basin, Westphalia, Germany (Ladwig, 2014; Schneider and Ladwig, 2013; Thies and Müller, 1993); 3, Münsterland Cretaceous Basin, northwest Germany (Hübner and Müller, 2010; Müller, 1989, 2014; Thies and Müller, 1993); 4, Liege-Limburg Basin, Belgium, Germany, and the Netherlands (Albers and Weiler, 1964; Herman, 1977); 5, Mons Basin, Belgium (Herman, 1977); 6–6', Anglo-Paris Basin, France and the UK (Gervais, 1852; Guinot et al., 2012a, 2012b, 2013; Herman, 1977; Leriche, 1902; Leriche, 1906; Priem, 1897; Underwood and Ward, 2008); 7, northern Aquitaine Basin, Charente, W France (Vullo, 2005); 8, southern Aquitaine Basin, Tercis-les-Bains, SW France (Cappetta and Odin, 2001); 9, Vitoria Sub-basin, Basque-Cantabrian Region, northern Spain (this research); 10, Urals, Russia and northwestern Kazakhstan (Averianov and Nessov, 1995; Glikman, 1980; Zhelezko, 1988, 1990); 11, New Jersey and Delaware, USA (Callahan et al., 2014; Cappetta and Case, 1975b; Cappetta and Case, 1999; Lauginiger and Hartstein, 1983); 12, Alabama and southwestern Georgia, USA (Case and Schwimmer, 1988; Cicimurri, 2007); 13, Alberta, Canada (Beavan, 1995; Beavan and Russell, 1999; Cook et al., 2017; Peng et al., 2001); 14, Judith River Formation, Montana (Case, 1978, 1979); 15, Big Horn Basin, Wyoming, USA (Case, 1987; Schubert et al., 2016); 16, New Mexico, USA (Schubert et al., 2016; Williamson and Lucas, 1992); 17, Texas (Cappetta and Case 1975a, 1999; Schubert et al., 2016; Welton and Farish, 1993); 18, Israel (Lewy and Cappetta, 1989); 19, Jordan (Zalmout and Mustafa, 2001); 20, Egypt (Cappetta, 2012); 21, Angola (Antunes and Cappetta, 2002); 22, Ross Island, Antarctica (Richter and Ward, 1990; Kriwet et al., 2006). Palaeogeographical map based on Smith et al. (1994) and biogeographical units after Kaufmann (1973).



Figure 17.9 Biogeographical distribution of the main selachian areas in Western Europe and Middle East at the late Campanian (~ 75 Ma). Localities: 1, Kristianstad Basin (Sweden); 2, North German Basin (Westphalia, Germany); 3, Münsterland Cretaceous Basin (northwest Germany); 4, Liege-Limburg Basin (Belgium, Germany, and the Netherlands); 5, Mons Basin (Belgium); 6–6', Anglo-Paris Basin (France and the UK); 7, northern Aquitaine Basin (Charente, W France); 8, southern Aquitaine Basin (Tercis-les-Bains, SW France); 9, Vitoria Sub-basin, Basque-Cantabrian Region (Spain); 10, Urals (Russia and northwestern Kazakhstan); 18, Israel; 19, Jordan. Palaeogeographical reconstruction redrawn from R. Blakey (https://deeptimemaps.com/wp-content/uploads/2016/05/75_Cret_EurMap.png); surface palaeocurrents modified from Pucéat et al. (2005). NAG: North Atlantic gyre.

embracing Western Europe and the AGCP in North America demands the assumption of sea-ways between both sides of the Atlantic Ocean, promoted by the moving-eastward, off-shore surface circulation of the North Atlantic gyre (Fig. 17.9). This hypothesis would be also supported by analogy with the modern system of currents.

- iv. *South-Tethyan margin (STM)*. This unit is a clearly, low-latitude region known from a number of phosphate-bearing deposits in Israel and Jordan (Middle East, Q). Additionally, some other fossil sites recognised by Capetta (2012) on the southern margin of the Tethys Ocean (Morocco and

Egypt) can be included. This area appears to be an open marine biogeographical unit, influenced by ecological factors, with a rich representation of lamniform sharks (including six families) and, at least, two endemic selachian forms (i.e. *Nanocorax* and *Ganopristis*).

- v. *Western Africa (WA)*. This area appears to be recognisable in the South Atlantic continental passive margin of Africa on the basis of the only known site of Angola (R). This arid subtropical region records a unique composition formed by a mixture of wide-range lamniform sharks (i.e. *Cretolamna*, *Scapanorhynchus*, and *Squalicorax*) and characteristic endemic forms, among the latter are certain rajiforms (i.e. *Angolabatis*), echinorhiniforms (i.e. *Echinorhinus*) and hexanchiforms (i.e. *Chlamydoselachus*, *Notidanodon*, and *Sphenodus*). It is noteworthy the presence here of the squalid genus *Squalus*, where cold water upwelling near the coast occurred at the time.

In addition to these PBU units, there was a southern warm temperate unit in the Antarctic Peninsula during the Campanian, recognised with ostracods by Seeling et al. (2004). Although this high-latitude unit is still poorly surveyed for selachians, it is represented by the genera *Chlamydoselachus*, *Notidanodon*, *Sphenodus*, and *Squatina* (Richter and Ward, 1990).

In sum and following the Kauffman's (1973) scheme, the highest biogeographical units during the Campanian include the warm North Temperate Realm (units A to P), the warm South Temperate Realm (units R and Antarctica) and the Tethyan Realm (unit Q and other North African localities the southern margin of the Tethys, not studied here). The North European province extended from Northern Ireland in the west to the Urals (southern Russia and Kazakhstan). The Western Europe and Urals subprovinces are well-defined at the Campanian. The selachian faunae of the Vitoria Subbasin are regarded as belonging to the Western Europe Subprovince. However, further researches are needed to solve the observed trichotomy in the PAE dendrogram (Fig. 17.7) and confirm its putative Tethyan affinity. The North American province includes two well differentiated areas (or subprovinces), the WIS with a high level of endemism and the AGCP. The faunal record of the Antarctica Peninsula is interesting as provides a preliminary estimate of the Cretaceous conditions in the high southern palaeolatitudes.

According to data given in Table 17.3, only the anacoracid shark *Squalicorax* is considered a truly pandemic (cosmopolitan) element. However, there are other genera with a wide geographical distributions across the Northern Hemisphere, among which the most notorious elements are *Archaeolamna*, *Cretolamna*, *Cretoxyrhina*, *Rhinobatos*, *Scapanorhynchus*, *Squalicorax*, *Squatina*, and *Synechodus*.

Chapter 18

BITE MARKS ATTRIBUTED TO A SHARK ON A MOSASAURID VERTEBRA (VITORIA SUB-BASIN, CAMPANIAN)

18.1 Introduction

The available documentation on the dietary habits and food consumption of extant sharks is relatively abundant (see Schwimmer et al., 1997, and references therein; see also Klimley, 2013). However, cases of bioerosion structures caused by neoselachian sharks were more rare in the palaeontological literature at the time of the writing of the article from which this chapter derives (see Corral et al., 2004), even though it was reported by Schwimmer et al. (1997), Shimada (1997a), Bardet et al. (1998), and Everhart (1999). In addition to those cases, Neumann (2000) also described predatory (or scavenging) marks on marginal ossicles of Cretaceous goniasterid asteroids, which, in his opinion, were perpetrated by a shark of the genus *Squalicorax*. But, as it will be discussed later, common predator-prey relationships in the Mesozoic fossil record include shark-marine tetrapod interactions, among the latter are plesiosaurs (Williston and Moodie, 1917; Welles, 1943; Shimada et al., 2010; Einarsson et al., 2010), ichthyosaurs (Zammit and Kear, 2011), mosasaurs (Welton and Farish, 1993, Everhart, 2004, 2008; Schwimmer et al., 1997, Bardet et al., 1998; Rothschild et al., 2005), and marine turtles (Lingham-Soliar, 1991). Moreover, sharks themselves may become prey to other larger sharks (Shimada, 1997a).

This research is based on a caudal vertebra of a mosasaurid (a marine varanoid lizard) discovered in the upper Campanian marine deposits in the southern Basque-Cantabrian Basin (B-CB), north central part of the Iberian Peninsula. The fossil was discovered shattered into distinct fragments by the fossil enthusiast Javier Sáenz when prospecting a new fossiliferous exposure created during the construction of an irrigation reservoir and details of its preparation have been included in Chapter 2 (Section 2.10).

The bone surface of the vertebra shows several marks that are considered an indirect evidence of predation or scavenging by a shark. Some other fossil remains of marine reptiles, in particular teeth and vertebrae of mosasaurs, have been described

from the Upper Cretaceous of Álava and proximate regions (Bardet et al., 1993, 1997, 1999, 2006, 2013). Apart from an invertebrate-rich assemblage, the fossil deposit at this site has yielded a few isolated teeth of bony fish and selachians, the latter being present in large number.

18.2 Location and geological setting

The site is located about 1.5 km southwest the hamlet of Jauregi, which is approximately 18 km southeast of the city of Vitoria-Gasteiz in the province of Álava (Fig. 18.1). The Jauregi site lies in the Vitoria Sub-basin, central part of the Navarre-Cantabrian Ramp of the B-CB, where uppermost Cretaceous rocks (Campanian to Maastrichtian) record three short term transgressive–regressive depositional cycles deposited in a shallow ramp-like setting with marine and continental environments (see Chapter 1).

This section records the sedimentary history of a shallow carbonate ramp during the upper Campanian. Good exposures of marl strata (upper beds of the Vitoria Formation) and alternating prodelta silty marl containing mica and calcareous marlstone (Eguileta Member within the Montes de Vitoria Formation) (Fig. 18.2) are found

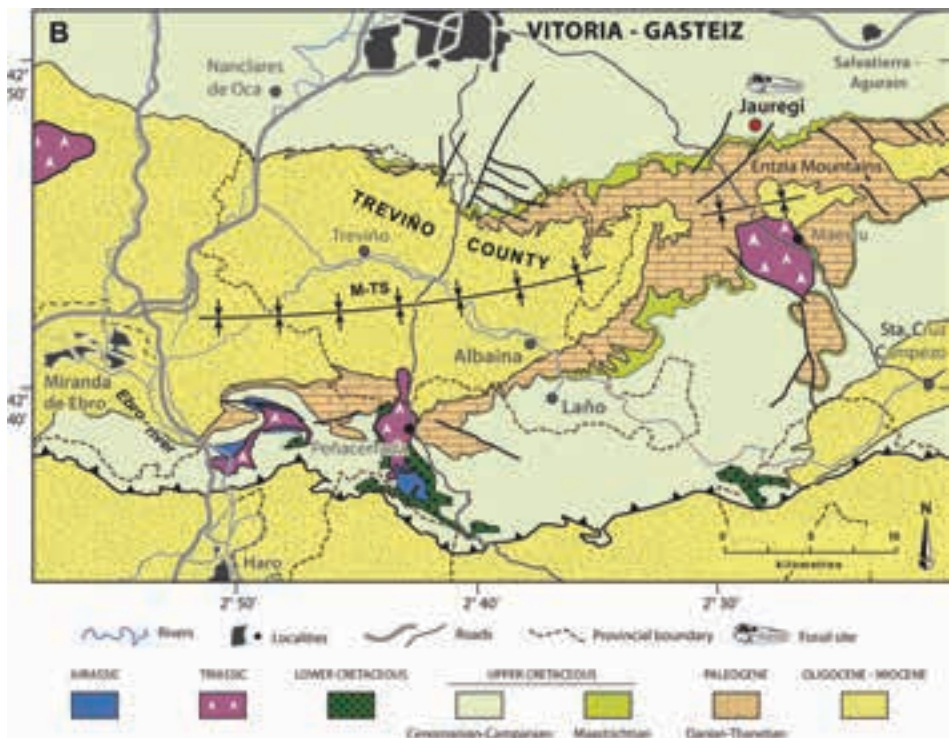


Figure 18.1 Geographical setting and simplified geological map of the studied area (Vitoria Sub-basin in the B-CB, Basque-Cantabrian Region) (modified from Corral et al., 2015a, Fig 1). The site of the discovery is marked with a red dot. Redrawn from Corral et al. (2004).



Figure 18.2 A, Rotalde reservoir near Jauregi (view to the west), note the prominent indurated marlstones dipping southward; B, the Eguileta Member at Jauregi is dominated by marls with few argillaceous marlstone interbeds as seen along the eastern side of the reservoir.

along the northern slopes of the Iturrieta-Entzia Mountains (northern limb of the Miranda-Treviño Syncline). The Eguileta Member has produced interesting assemblages of ammonites and inoceramids that have been studied by López (1993a, 1996), Santamaría Zabala (1996), and Küchler (2000a). Santamaría Zabala (1996) noted the presence of the zonal ammonite species *Nostoceras* (*B.*) *polyplocum* (Roemer, 1841). A subsequent review of the faunal assemblages of the site by Küchler (2000a) also confirmed the presence of *Nostoceras* (*Euskadicerias*) *unituberculatum* (Błaszczewicz, 1980) and the subspecies *Nostoceras* (*Euskadicerias*) *euskadiense* II sensu Küchler, 2000a. The

presence of both ammonite taxa in the upper beds, which are equivalent to the zone of *Trachyscaphites pulcherrimus* Roemer, 1841, argues for a very late Campanian age for the Eguileta Member at the Jauregi section (Küchler, 2000a).

18.3 Description of the specimen

Order SQUAMATA Opper, 1811
Family MOSASAURIDAE Gervais, 1853
Subfamily MOSASAURINAE Williston, 1897

Mososaurinae gen. et sp. indet.
Figs. 18.3, and 2.22 in Chapter 2

Material. MCNA 5359, a caudal vertebra.

Locality. Jauregi¹, Iruraz-Gauna municipality (Álava province, Basque County, Spain).

Age and stratigraphical horizon. Upper Campanian (*B. polyplacum* zone); Eguileta Member (Montes de Vitoria Formation).

Description. The centrum have the normal procoelous morphology (i.e. concave on the anterior articular surface and convex on the posterior one), as is typical of mososaurid vertebrae (Fig. 18.3B). The neural arch is fused to the centrum, so that it could belong to an adult or subadult individual. The presence of hemal arches (chevrons) and the lack of transverse processes indicate that it is a distal caudal vertebra (Russell, 1967). The subtriangular shape of the articular surfaces and the size of the centrum (45 mm long, 40 mm wide, and 65 mm high) suggest that it is one of the first distal caudal vertebrae. This vertebra has been preliminarily attributed to a Mososaurinae indet. because the chevrons are fused to the centrum (Bardet et al., 1997). In the Campanian of Europe several species of mososaurines (*sensu* Bell, 1997) are known: *Carinodens fraasi* (Dollo, 1913), *Globidens dakotaensis* Russell, 1975, *Leiodon anceps* Owen, 1840–1845, *Mososaurus compressidens* Gaudry, 1892, *Prognathodon* cf. *sectorius* (Cope, 1871), *Prognathodon giganteus* Dollo, 1904, and *Tylosaurus* sp. (Bardet and Pereda Suberbiola, 1996; Bardet et al., 2006, 2012). Unfortunately, distal caudal vertebrae are not preserved in any of the known specimens, so it is not possible to give a more accurate systematic determination for the Jauregi vertebra. With reference to the mososaurid skeletal reconstructions (Russell, 1967) and the size of the vertebra, the mososaurid from Jauregi is thought to have reached 3 to 5 m in length.

Bioerosion structures. The left lateral side of the vertebral centrum is marked by at least six deep tooth impressions arranged into two parallel marks that run to the longitudinal axis of the vertebra (Figs. 18.3A, 18.4A); the dimensions of each mark are listed

¹ The current official name is Jauregi, but it is also found written Jáuregi in previous geological works.

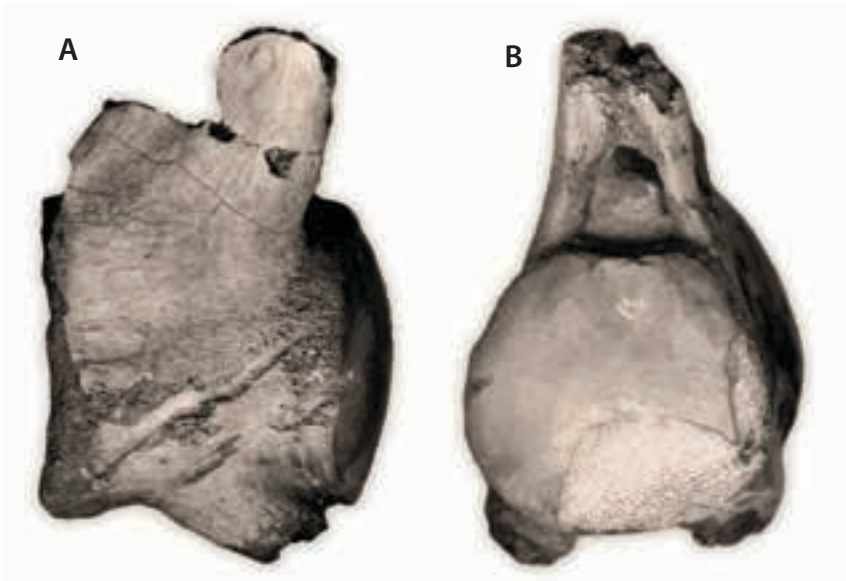


Figure 18.3 MCNA 5359. Mosasaurinae indet., Eguileta Member (upper Campanian), Jauregi. A, specimen condition after being mechanically prepared. The marl filling in the area of the marks is clearly seen. B, caudal vertebra in caudal view.

in Table 18.1. The upper series forms a nearly continuous puncture (43 mm long and approximately 2 mm depth), though it is possible to distinguish four successive cuttings aligned in pairs (Nos. 1 to 4, Fig. 18.4B). Numbers 3 and 4 (Fig. 18.4B), near the anterior articular face of the centrum, are offset aligned to the cutting line. The lower series has two clear cuts perfectly aligned and are well preserved (Nos. 5 and 6, Fig. 18.4B). One cut of the lower series has slightly damaged the convex articular face of the vertebral centrum, while the other one, more ventrally located, is at the base of the left hemal arch (which is fused to the centrum). A precise observation of the cuts, especially those of the lower series, shows that they have forked endpoints (see Fig. 18.4A).

Interpretation. At first, the morphology of the structures observed in the vertebra closely resembles the characteristic feeding punctures produced by a selachian with cutting-type dentition, or a tendency towards such model. In modern seas, the main predatory sharks belong to the Galeomorphii, with representatives of the orders Lamniformes, Carcharhiniformes, Orectolobiformes, and Heterodontiformes (Compagno, 1988).

The Jauregi site has yielded a few isolated teeth of Lamniformes, but in nearby coeval outcrops, shark teeth are common. Among those identified are the anacoracid *Squalicorax* ex gr. *kaupi* (Agassiz, 1843) (Figs. 18.5A–B) and the otodontid *Cretolamna borealis* (Priem, 1897) (Figs. 18.5D–E), all of which are in addition the most common taxa in the site and the ones with larger teeth. The teeth of *S.* ex gr. *kaupi* are medium-sized (up to 17–20 mm wide), labiolingually flattened with a wide triangu-

Table 18.1. Mark measurements referred to shark bite punctures sketched in Figure 18.4B (in mm).

Mark no.	1	2	3	4	5	6
length	14	14	14	6	15	14
width	2.5	3	3	2	2	3
depth	3	4.5	3	2	1.5	1.5



Figure 18.4 A, close-up of the marks on the vertebral centrum (after full chemical preparation). B, interpretation of the shark bites on the mosasaurid vertebra, MCNA 5359. Both the direction of the tooth row and the trend of the bite paths are indicated. Black holes: relative bites towards the left; white holes: relative bites towards the right (from Corral et al., 2004).

lar crown and crenate cutting edges that give them a serrate appearance. The teeth of *Squalicorax* represent a good example of cutting-type dentition (Cappetta, 1987). On the other hand, the teeth of *Cretolamna* are characterised by a crown with a flattened main cusp, triangular in shape and wide at the base (up to 15–17 mm), flanked by a pair of wide, small-sized and well-developed lateral cusplets. Monognathic heterodonty within this species is clearly evident (Cappetta, 1986); that is, the main cusp is sharp and straight in anterior teeth while it widens in the upper lateral teeth. According to Cappetta (1987), sharks of the genus *Cretolamna* have tearing-type teeth, although its lateral teeth show a tendency to a cutting-type dentition, working as a shearing blade. The teeth of both *Cretolamna* and *Squalicorax* taxa have pointed, laterally compressed cusps with lenticular cross section, being thicker in the former genus.

When interpreting the marks in the mosasaurid vertebra it seems important to understand how the dental differences in sharks (i.e. heterodonty, tooth shape and size, and interdental spacing) and the functional mechanics of their feeding apparatus affect. Several cutting tests were made on plasticine using loose teeth of *Cretolamna* and *Squalicorax* in order to establish the morphological differences of the caused indentations (Figs. 18.5C, F). Obviously, plasticine and bone tissue are materials with different mechanical response to the dynamics of the bite, but this simple test helps us to see

clear differences between the marks left by the teeth of these two genera. Deméré and Cerutti (1982) used paraffin for the same purpose. A prime conclusion drawn from the test is that the crenate cutting edges of the teeth of *Squalicorax* make distinctive parallel grooves when the cutting direction is perpendicular or oblique to the mesial plane of the tooth. But when the cutting path is parallel to the mesial plane of the tooth, both species produce very similar marks (i.e. elongated incisions with pointed ends), although *Squalicorax* teeth produce sharper cutting marks with less force.

According to Schwimmer et al. (1997), bite marks on bones attributed to *Squalicorax* are characterised by parallel striae produced by the crenate edges of the tooth crown. Striae produced by teeth with crenate or serrate cutting edges would be the combined result of both the lateral head movements during biting and the shape of the dental arcade (i.e. arch-shaped arrangement of the teeth in the jaws), which favour rotation and slide movements of the teeth (Cigala-Fulgosi, 1990). On the contrary, neat cuts or punctures without serrated marks produced by the same sharks are the result of 'investigative bites', where there are not repeated lateral head movements. This is the result of a predatory strategy known as 'bite, spit and wait' (Tricas and McCosker, 1984), for which the shark inflicts mortal wounds on vulnerable parts of the prey that cause immobilization, haemorrhagic shock and a reduced fighting capacity (Klimley et al., 1996).

If a member of the genus *Squalicorax* was the perpetrator of the bites in the Jauregi vertebra, such deep marks without serrated edges would either reflect a predatory behaviour (i.e. investigative bites) or indicate manipulation bites to dismember larger preys (scavenging in this case), after the feeding behaviour for chondrichthyans established by Motta et al. (1997). Similar marks in skeletal remains of a dolphin from the Pliocene, allegedly caused by a *Carcharodon carcharias* (Linnaeus, 1758), have been interpreted by Cigala-Fulgosi (1990, Fig 2b) as the result of a cutting process in which the teeth run along their mesial plane.

The presence on the vertebra of two sets of bite marks (upper and lower one, as shown in Fig. 18.4A) would represent two successive bites by assuming that *Squalicorax* sharks had a single functional dental series (as observed in extant sharks with analogue dental morphology). Individuals of *Cretolamna* would have, on the contrary, more than one functional tooth set, so if this species had caused the marks, these could have been originated after a single bite during a predatory attack or opportunistic scavenging of a carcass. On the other hand, the morphology of the marks also allows to infer the direction of movement during cutting. As the greatest bite force occurs when biting, the impact point on the bone should match the main cusp of the selachian tooth. When the tooth runs along the cutting path makes asymmetrical marks, being blunt at the proximal end and very sharp at the opposite one, mainly due to the lowering of the bite force before releasing the prey. A feasible explanation of the forked ends of the punctures observed in the Jauregi vertebra (Fig. 18.4) is that each individual mark was made in fact by two superimposed cuttings, each one running in an opposite direction, being thus the result of a forward and reverse movement of the teeth after a back-and-forth

shaking motion of the head. This behaviour is typical of sharks, and are used to tear and sever body pieces of their prey. Closely resembling bite marks to those observed in the mosasaurid vertebra from Jauregi were described by Budinoff (1991) on a human humerus, dated 789–1033 BC, belonging to a pre-Columbian inhabitant of Puerto Rico. Such injuries have recently been interpreted by Keegan (2003) —after discussion with ichthyologists— as the result of a shark attack. Some of these marks have also sharp forked ends resulting from two opposite cutting directions.

Finally, the fact that some cuttings reach the cancellous bone suggests a violent shark bite on the Jauregi mosasaurid. Furthermore, it should be noted that the punctures only affect one side of the centrum, making it difficult to discern which tooth series of the shark jaw (either from the palatoquadrate or the Meckel's cartilage) hit the vertebra.

18.4 Discussion

Examples of predation in the fossil record have regularly increased over the years. Bambach (in Kowalewski, 2002: 3–4) defined predators as organisms that “hunt or trap, subdue, and kill individual animals that have some capacity for either protection or escape”. However, when assessing individual palaeontological cases it is not easy to verify that such biological interactions are predator-prey relationships, scavenging or parasitism (Kowalewski, 2002). In the opinion of this author, there is a continuous spectrum from lethal predation to scavenging, including in the middle partial predation without causing the death of the prey. Thus, unless there are clear evidences that differentiate such behaviour, Kowalewski (2002) expresses a preference for using predator in the broader sense, which would mean either predator or scavenger. The same reasoning terms are applied to prey or carrion.

Bioerosion structures (boring marks, tooth and biting traces, scars, or fractures), coprolites and intestinal casts with identifiable remains of the prey, or preserved exceptional events like a fish buried while eating another fish, are direct indicators of predation, whereas some taphonomic models in which skeletal accumulations are not explained by sedimentological processes, individuals with defensive skeletal structures or with body structures designed for hunting or grinding animals with hard skeleton come into the category of indirect evidence (Kowalewski, 2002). Despite the fact that the predatory evidence is mostly destroyed, “literally eaten” during the early stages of its formation in the fossil record (Brett, 1990), predation traces are common in organisms with biomineralised skeletons —from protists to land vertebrates, including humans. This is because the bioerosion traces left on the prey skeletons are so well preserved as the skeletons themselves (Kowalewski, 2002). However, literature regarding to the predatory behaviour of marine vertebrates are less habitual due to the scarcity of specimens in the fossil record with this type of evidence.

The apparition of scars, bone tissue with evidence of necrotic areas around cuts or bone regeneration in clearly bioeroded areas indicates that the prey survived the at-

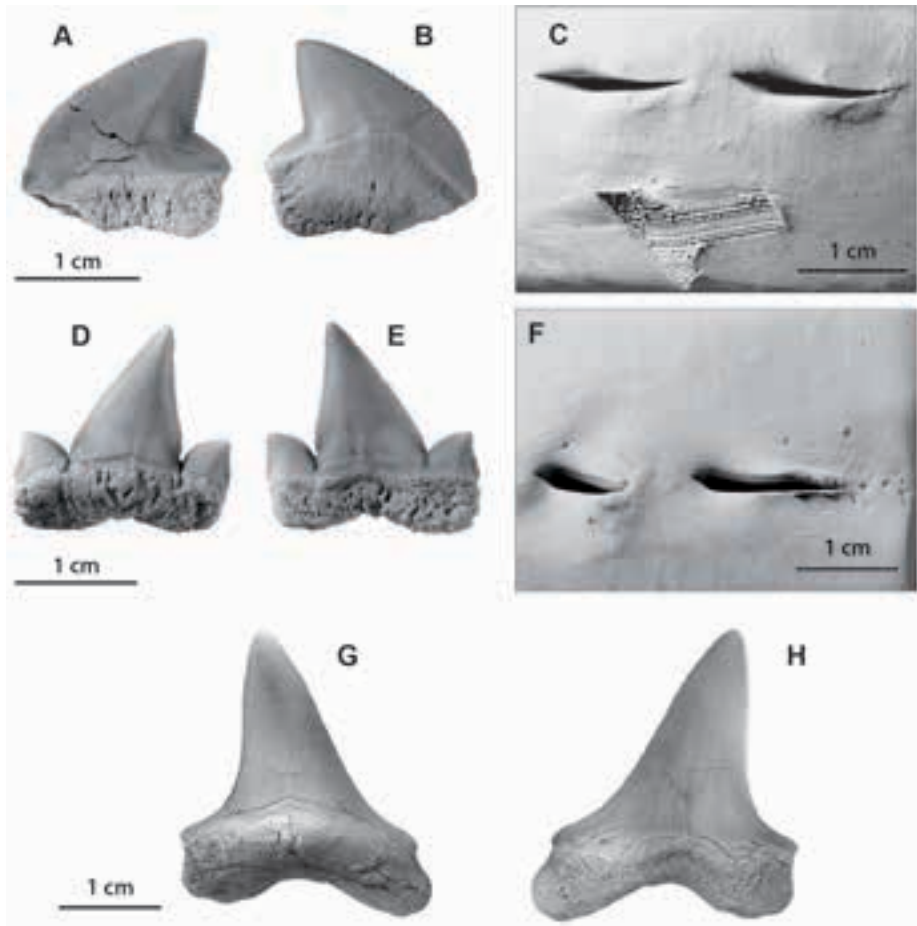


Figure 18.5 A–B, *Squalicorax ex gr. kaupi* (Agassiz, 1843) from Gardelegi (Álava), Eguileta Member (upper Campanian), lateral tooth in labial and lingual views, MCNA 3675; C, indentation marks made in plasticine with a tooth of *S. ex gr. kaupi*: cutting punctures along its mesiodistal plane (above), dragging the tooth perpendicularly to its mesiodistal plane (below); D–E, *Cretolamna borealis* (Priem, 1897) from Gardelegi (Álava), Eguileta Member (upper Campanian), upper lateral tooth in lingual and labial views, MCNA 3663; F, indentation marks made in plasticine with a tooth of *C. borealis*: cutting punctures along its mesiodistal plane; G–H, *Cretoxyrbina mantelli* (Agassiz, 1843) from Gometxa (Álava), Gomecha Member (lower upper Campanian), lateral tooth in lingual and labial views, MCNA 10491. Modified from Corral et al. (2004).

rack (Martin and Rothschild, 1989; Everhart et al., 1995; Schwimmer et al., 1997). But when bioerosion structures do not show any evidence of healed bite marks, as in the case of the mosasaurid vertebra from Jauregi, it may indicate that the prey succumbed to the attack or, more likely, that the mosasaurid was already dead at the time of attack. The scavenging activity can be inferred from a direct evidence (e.g. a lost tooth of a

predator piercing a decaying bone) or indirectly (e.g. different types of tooth marks on prey bones or that the teeth of predators and prey remains appear together in the same bone bed) (Schwimmer et al., 1997).

Einarsson et al. (2010) have reported parallel sets of cuts on plesiosaurian bones, which are consistent with feeding traces produced by the lamniform shark *Squalicorax lindstromi* (Davis, 1890)¹. Bardet et al. (1998) also described a caudal vertebra of the mosasaurid *Plioplatecarpus marshi* Dollo, 1882 from the Gulpen Formation (upper Maastrichtian) of Liege (Belgium), which has fine and elongated marks in its neural spine. The authors interpret such structures as bite marks caused by a small scavenger with cutting-type teeth, suggesting the squalid shark *Centrophoroides appendiculatus* (Agassiz, 1843). Dortangs et al. (2002) also found direct and indirect evidence of selachian scavenging when studying the remains of *Prognathodon saturator* Dortangs et al., 2002, a Maastrichtian mosasaurid discovered in the region of Maastricht, Netherlands. The existence of marks in some parts of the skeleton and a highly relative concentration of *Plicatoscyllium* and *Squalicorax* teeth associated to the remains of the mosasaurid indicate that the carcass was partially devoured before burial by those selachians (Dortangs et al., 2002). To these authors, the possible gathering of shark teeth inside the mosasaurid stomach before being released on the sea bottom after the mosasaurid death (and hence the shark is the prey), is discarded because the teeth do not display evidence of digestion (i.e. dissolution caused by acid in the stomach of the predator).

The cutting-type dentition of *Squalicorax* may be compared to that of the extant tiger shark *Galeocerdo cuvier* (Peron and Lesueur, in Lesueur, 1822). Despite that this apparent similarity is a case of convergence, it is suggested that the feeding habits of *Galeocerdo* should not be very different from those of *Squalicorax* (Schwimmer et al., 1997; Shimada, 1997a). Modern tiger sharks have different feeding strategies, including active predation on fish, turtles, invertebrates, etc., and opportunistic scavenging (Compagno, 2001). Based on fossil evidence from the Gulf Coastal Plain and the Western Interior Sea in North America, Schwimmer et al. (1997) suggested that scavenging in vertebrate carcasses could be one of the primary feeding strategies of *Squalicorax*. On the other hand, *Cretolamna* sharks have a tearing type dentition, particularly well adapted for piscivory (Springer, 1961) but disadvantageous for dismembering large prey (Schwimmer et al., 1997). However, it is most likely that large individuals of this genus, with rows of wide teeth in the palatoquadrate (upper jaw), were able to cut large pieces of flesh and dismember large vertebrates, in much the same way as modern ecomorphs do. Among these are the porbeagle sharks [*Lamna nasus* (Bonnaterre, 1788)], with teeth very similar to those of *Cretolamna*, or large mako sharks (*Isurus oxyrinchus* Rafinesque, 1810) measuring about three meters in length, whose upper teeth are more triangular and flattened in larger individuals of the species (Compagno, 2001).

¹ This species has been considered a questionable junior synonym of *Squalicorax kaupi* (Agassiz, 1843) by Cappetta (2006).

Both *Squalicorax* ex gr. *kaupi* and *Cretolamna borealis* were moderately medium-sized sharks by comparing their teeth to those of *Squalicorax kaupi* and *Cretolamna appendiculata* respectively and whose total length usually did not exceed 3 m (Schwimmer et al., 1997). Strategically, it is quite likely that these sharks individually did not attack prey larger than or equal to their own size (as would be the case with the Jauregi mosasaurid). The evolutionary success of *Squalicorax*, a shark with a wide temporal and spatial distribution during the Cretaceous, has been interpreted as related to their opportunistic feeding habits (Schwimmer et al., 1997; Shimada, 1997a).

On the other hand, the large lamniform shark *Cretoxyrhina mantelli* (Agassiz, 1843)¹ could be an active predator, ecologically comparable to the extant members of the genus *Isurus* (H. Cappetta, pers. comm.). Actinopterygians, plesiosaurs, mosasaurids, marine turtles, and other sharks were the most important components of its diet, so it is conceivable that this top level predator occupied the apex of the marine food web in Late Cretaceous times (Martin and Rothschild, 1989; Siverson, 1992; Schwimmer et al., 1997). Individuals of the species *Cretoxyrhina mantelli* were probably distributed globally during most of the Upper Cretaceous. The species, ubiquitous throughout the Santonian, has extended its stratigraphical range to the Campanian. In North America, the species ranges in age from Turonian to lowermost Campanian (nannoplankton zone 18) (D.R. Schwimmer, pers. comm.). In Europe, this taxon has also been collected from upper lower Campanian to lower upper Campanian strata in the Kristianstad Basin of Scania, Sweden (Siverson, 1992), as well as in the early late Campanian calcarenites of the Gomecha Member (Vitoria Formation in the Vitoria Sub-basin, B-CB, northern Spain) (Figs. 18.5G–H). However, this shark species has been ruled out as the attacker of the Jauregi mosasaurid because the last individuals of the species seem not to have lasted until the uppermost Campanian.

A further argument against the involvement of this taxon can be obtained by measuring the dent spacing (i.e. between crown apex distances) along a tooth row, which obviously will depend on the size of the teeth and especially on the root width. By analysing the tooth of *Cretoxyrhina mantelli* housed in the MCNA collections (Figs. 18.5G–H) and artificial tooth sets figured in the palaeontological literature (see Siverson, 1992; Shimada, 1997c; Welton and Farish, 1993), the minimum dent spacing is about 25–30 mm. But when measuring the distance between two homologous points in the marks left on the mosasaurid vertebra from Jauregi values of 15 to 16 mm are obtained. These figures are consistent with the expected values in selachian taxa with smaller teeth, such as *Squalicorax* ex gr. *kaupi* and *Cretolamna borealis*.

¹ Typically 4.5–5 m in length, although occasionally there were specimens that reached 6 m, according to Shimada (1993, 1997b).

Chapter 19
MARINE VERTEBRATE PREDATORS (ACTINOPTERYGII,
CHONDRICHTHYES, AND MOSASAURIDAE) IN THE CAMPANIAN OF
THE BASQUE-CANTABRIAN BASIN

19.1 Introduction

The Campanian carbonate series of silty marlstone and clay limestone reflect the influence of inner ramp and mid- to outer ramp sedimentation in extensive areas of the passive continental margin of the Iberian Peninsula, corresponding to the Navarre-Cantabrian Ramp domain (or 'Álava Block') of the Basque-Cantabrian Basin (B-CB), as outlined in Chapter 1.

Carbonate outer ramp deposition during the lower upper Campanian led to the formation of the Gomecha Member of the Vitoria Formation in the Vitoria Sub-basin of the B-CB (see Chapter 5). This unit, which is accessible on the northern slopes of the Vitoria Mountains (Álava province), is especially rich in teeth of diverse selachians (see Chapter 11). Sedimentation from upper Campanian to lower Maastrichtian first occurred in open oceanic conditions evolving later into a shallow-marine, neritic environment with the deposition of the Montes de Vitoria Formation, whose Eguileta Member is characterised by silty clayey marls with authigenic glauconite. This unit is particularly fossiliferous, containing abundant marine invertebrate and vertebrate species (Bardet et al., 1993). Pelagic biota from the shallow neritic environments of the Eguileta Member includes cephalopods (carnivorous predators) (see Chapter 6) and many remains of predatory (carnivorous) vertebrates, including isolated teeth of diverse bony fishes, selachians, and mosasaurids, with the latter (although rare) being represented by a vertebra of Mosasaurinae and most commonly by isolated teeth (Bardet et al., 1993, 1997, 2006; Corral et al., 2004; see also Chapters 12 and 18).

In an attempt to analyse the shark diversity, some of the identified selachian taxa are typified within given ecomorphotypes (or body adaptations and dental characteristics that give clues about the trophic structure of these fishes in their habitat), following Compagno's (1990) work.

19.2 Marine vertebrate groups

Actinopterygii (Bony Fish)

The salmoniform fish genus *Enchodus* sp. (Figs. 19.1A–B) is the most common taxon. Their jaws are provided with fang-shaped teeth which indicate that they mainly fed on cephalopods and small bony fish.

Selachians (*Chondrichthyes: Euselachii: Neoselachii*)

The selachians, with a polyphiodont dentition, is the most frequent and diverse group of vertebrates found in the localities of the study area (see Chapters 11 and 12). A total of twenty-two taxa of Neoselachii have been identified, including many that had not previously been reported for the Campanian of the Iberian Peninsula (some of them are included in Table 19.1 and Fig. 19.1).

Mosasaurids (*Squamata: Mosasauridae*)

Three species are, at least, recorded in the Campanian deposits of Álava (Table 19.1): *Mosasaurus lemonnieri* Dollo, 1889 (Figs. 19.1V–W), *Tylosaurus* sp., and *Prognathodon* sp. (Bardet et al., 1993, 1997, 2006). Moreover, an isolated caudal vertebra assigned to an indeterminate mosasaurine with shark-inflicted teeth punctures (Fig. 19.1X) completes the list to date; this is one of the few known examples of such type of bioerosion in the European fossil record (Corral et al., 2004; see Chapter 18).

Mosasaurids were megapredators (some species over 8 meters in length) whose niche was at the top of the food web. Their cutting-type teeth reflect dietary adapta-

Figure 19.1 Marine vertebrates from the upper Campanian rocks of the Vitoria Sub-basin, Álava province. A–B, *Enchodus* sp., caniniform tooth in labial (A) and lateral (B) views, MCNA 14240; C–D, *Carcharias adneti* Vullo, 2005, anterolateral tooth in labial (C) and lingual (D) views, MCNA 14241; E–F, *Squalicorax* ex gr. *kaupi*, anterolateral tooth in lingual (E) and labial (F) views, MCNA 10500; G–H, *Cretolamna sarcoportheta* Siverson et al., 2015, upper anterior tooth in labial (G) and lingual (H) views, MCNA 8519; I–J, *Scapanorhynchus* cf. *texasus*, anterolateral tooth in labial (I) and lingual (J) views, MCNA 10508; K–L, *Anomotodon hermani* Siverson, 1992, anterior tooth in lingual (K) and labial (L) views, MCNA 3685; M, *Galeorhinus girardoti* Herman, 1977, lateral tooth in lingual view, MCNA 10547; N–O, *Protolamna borodini* (Cappetta and Case, 1975b), anterior tooth in lingual (N) and labial (O) views, MCNA 10548; P–Q, *Squatina bassei* Leriche, 1929, anterolateral tooth in lingual (P) and labial (Q) views, MCNA 15612; R–S, *Parapalaeobates pygmaeus* (Quaas, 1902), lateroposterior tooth in occlusal (R) and basal (S) views, MCNA 10499; T–U, *Rhinobatos casieri* Herman, in Cappetta and Case, 1975b, lateroanterior tooth in occlusal (T) and profile (U) views, MCNA 15607; V–W, *Mosasaurus lemonnieri* Dollo, 1889, tooth in labial (V) and lingual (W) views, MCNA 5360; X, Mosasaurinae indet., caudal vertebra in lateral view, MCNA 5359. A–B, C–D, G–H, M, and N–O from the upper Campanian (Eguileta Member) of the Vitoria Pass, Gardelegi, Álava; E–F, I–J, K–L, P–Q, R–S, and T–U from the lowermost upper Campanian (Gomecha Member) of Gometxa, Álava; V–W, from the lower Campanian of Bóveda, Álava; X, from the upper Campanian (Eguileta Member) of Jauregi, Álava. Modified from Corral et al. (2011). ▶

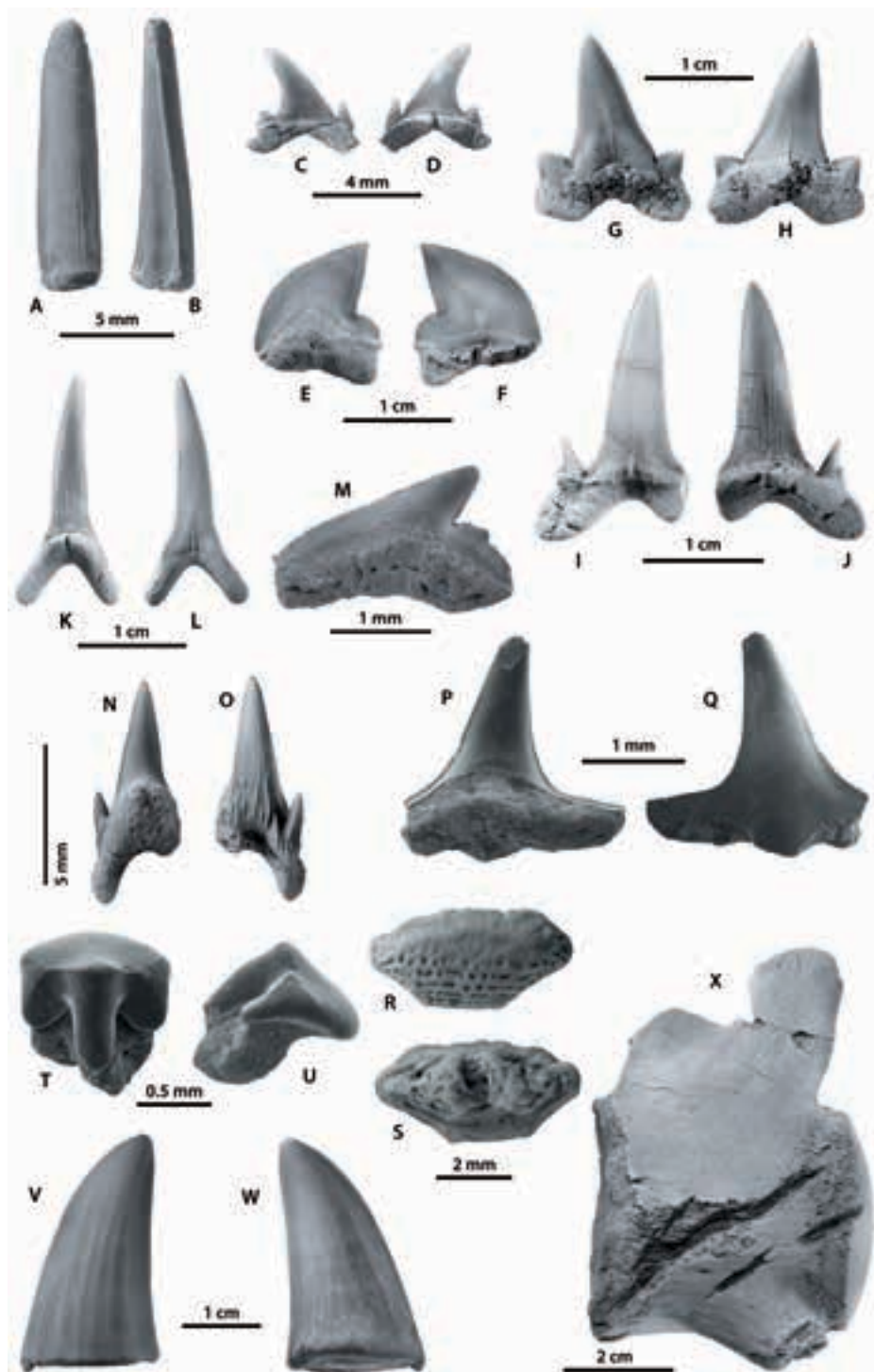


Table 19.1 Selected selachian and mosasaurid predators known to have occurred during the Campanian in the southern domains of the B-CB (modified from Corral et al., 2011).

Taxa	Dentition type ¹	Ecomorphotype ²
Selachians		
<i>Carcharias aasenensis</i>	tearing	Littoral mesotrophic
<i>Carcharias adneti</i>	tearing	Littoral mesotrophic
<i>Serratolamna kbderii</i>	tearing	Littoral mesotrophic
<i>Galeorhinus girardoti</i>	cutting-clutching	Littoral mesotrophic
<i>Squalicorax</i> ex gr. <i>kaupi</i>	cutting	Littoral eurytrophic
<i>Pseudocorax laevis</i>	cutting	Littoral eurytrophic
<i>Cretoxyrhina mantelli</i>	tearing-to-cutting	Tachypelagic
<i>Cretolamna borealis</i>	tearing-to-cutting	Tachypelagic
<i>Cretolamna sarcophorheta</i>	tearing-to-cutting	Tachypelagic
<i>Paranomotodon</i> cf. <i>angustidens</i>	tearing	Macroceanic
<i>Protolamna borodini</i>	tearing	Macroceanic
<i>Anomotodon hermani</i>	tearing	Rhynchobathic
<i>Scapanorhynchus</i> cf. <i>texasus</i>	tearing	Rhynchobathic
<i>Squatina bassei</i>	clutching	Squatino-benthic
<i>Parapalaebates pygmaeus</i>	grinding	Durophagous
<i>Ptychotrygon</i> sp.	crushing	Rhinobenthic
<i>Rhinobatos casieri</i>	crushing	Rhinobenthic
Mosasaurids		
<i>Mosasaurus lemnierii</i>	cutting	
<i>Tylosaurus</i> sp.	cutting	
<i>Prognathodon</i> sp.	cutting	

¹ dentition type in selachians after Cappetta (1986) and in mosasaurids after Massare (1987), Bardet et al. (2015).

² after Compagno (1990).

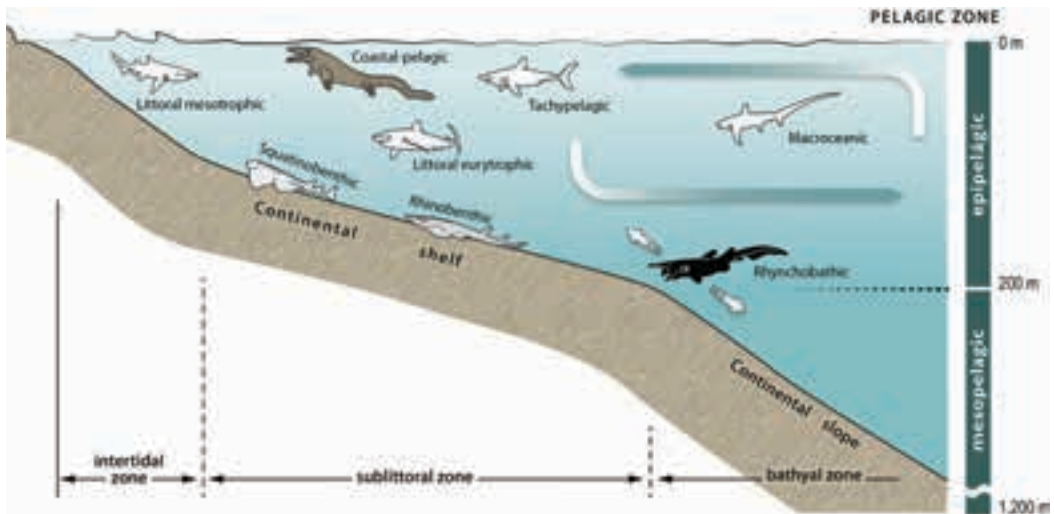


Figure 19.2 Simplified palaeoenvironmental distribution of major selachian ecomorphotypes (silhouettes in white and black; not to scale) and mosasaurs (silhouette in brown colour) across the shelf-basin transect of northern Iberian margin (B-CB) based on Campanian specimens found in Álava. Modified from Corral et al. (2011).

tions of the dentition (Massare, 1987; Bardet et al., 2015). *Mosasaurus* and *Prognathodon*, whose fossils have often been found associated, are cosmopolitan genera in the Campanian and Maastrichtian. The Tylosaurinae have a more restricted distribution, being known only in palaeolatitudes either above 30°N or below 30°S. This discovery in the B-CB (latitude 35°N) represents the southernmost registration in Northern Hemisphere (Bardet et al., 2006). The species *Mosasaurus lemonnieri* has also been identified in the Maastrichtian of Belgium (Dollo, 1889), DR Congo (Lingham-Soliar, 1994), and Syria (Bardet et al., 2000).

19.3 Selachian ecomorphotypes

Neoselachians are a very morphologically and functionally conservative fish group. They are highly specialised predators which compete for food with other groups of marine vertebrates (Compagno, 1990). Despite its heterodontic dentition, postpalaeozoic selachians exhibit only a few general dental types (Cappetta, 1986). Compagno (1990) has also noted the strong relationship between diet and habitat in neoselachians, establishing different ecomorphotypes or taxa groups that share similar shape, habitat and behaviour, regardless of their phylogeny or evolutionary relation.

The morphotypes proposed for the selachian palaeobiodiversity in the Campanian of Álava are based on the Compagno's (1990) observations, and some of the taxa found can be grouped into seven ecomorphotypes with clutching, crushing, cutting, cutting-clutching, grinding, tearing, and tearing-to-cutting dental types (Table 19.1, Fig. 19.2).

Modern littoral eurytrophic¹ shark species are opportunistic predators, or even scavengers, able to attack preys larger than themselves, with cutting-type teeth (in some species the cutting edge of the teeth is crenate). The cosmopolitan taxon *Squalicorax* ex gr. *kaupi* (Fig. 19.1E–F) and the Euamerican *Pseudocorax laevis* are two species that are represented in the fossil record of Álava. These sharks with documented habits of scavenging (Schwimmer et al., 1997) would be in a lower trophic position than those of the tachypelagic group (see below).

Modern littoral mesotrophic selachians are slow swimming demersal generalist predators. The fossil taxa *Carcharias aasenensis*, *Carcharias adneti* (Fig. 19.1C–D) and *Serratolamna khderii*, which are less common in Álava during the Campanian, have pointed teeth with main cusps flanked by lateral cusplets (tearing-type teeth). Although the shark *Galeorhinus girardoti* (Fig. 19.1M) is placed in this category, it may have occasionally ventured into deeper areas of the shelf to broaden its food range (cutting-clutching dentition).

Extant tachypelagic² sharks are rapid, active swimmers with fusiform bodies and a mean body temperature above sea temperature. These super-predators of nearshore and

¹ From the Greek *eury*, wide and *trophikos*, pertaining to food.

² From the Greek *takhos*, speed and *pelages*, sea.

ocean habitats make long-distance seasonal migrations and prey on bony fish and other elasmobranchs. While the Upper Cretaceous otodontid sharks *Cretolamna borealis* or *Cretolamna sarcophorheta* (Fig. 19.1G–H) are successful species within this category, being represented in many worldwide locations (principally the former one) and commonly found in Álava, the apex predator *Cretoxyrhina mantelli* (about 6 m long) is rare and would be in recession in the upper Campanian, with the last individuals being limited to western Europe.

Modern macrooceanic shark species are active swimmers with a wide geographical distribution. These sharks of stylised body live in oceanic waters, although they may enter into the nearshore and the mesopelagic zones. They feed on shoaling fish and cephalopods. The species *Protolamna borodini* (Fig. 19.1N–O) and *Paranomotodon* cf. *angustidens* would represent this ecomorphotype in the Vitoria Sub-basin (B-CB).

Extant rhynchobathic¹ selachians are demersal and poor swimmers as their body shape reflects. They inhabit mid-waters (shelf edge or upper slope), and make daily vertical migrations in search of food. Their main diet is fish and soft-bodied cephalopods. The species *Anomotodon hermani* (Fig. 19.1K–L) and *Scapanorhynchus* cf. *texanus* (Fig. 19.1I–J), with a tearing-type dentition, are good representatives of this ecomorphotype. In the Vitoria Sub-basin the teeth of the latter taxa are found associated with those sharks characteristic of epibathyal areas.

The extant squatinid angel shark, which represents the squatinobenthic ecomorphotype, shows a flattened, ray-like body and a terminal mouth with cuspidate, clutching-type teeth. This bottom-dwelling shark remains hidden in the sea bottom to ambush small fishes and consume a variety of benthic invertebrates. *Squatina hassei* (Fig. 19.1P–Q) belongs to this morphotype.

Two morphotypes are typically observed among the bottom-dweller rajiforms. The extant guitarfish is a good example to represent the rhinobenthic² ecomorphotype. Such batoids, which have an elongated and flattened body, tend to swim slowly along the sea bottom. Thus, they are bottom feeders with dentitions adapted to consume small fishes and crush hard-shelled invertebrate preys. *Rhinobatos casieri* (Fig. 19.1T–U) and possibly *Ptychotrygon* sp. are included here.

Finally, the durophagous³ batoid type is represented by the Upper Cretaceous *Parapalaebates pygmaeus* (Fig. 19.1R–S), which is characterised by having jaws with tooth pavements, suitable for grinding and breaking hard-shelled prey (i.e. molluscs and other invertebrates).

¹ From the Greek *rhynchos*, snout and *báth(os)*, depth.

² From the Greek *rhino-*, nose and *bénthos*, depth of the sea, bottom.

³ From the Latin *durus*, hard and the Greek *phagein*, to eat.

Chapter 20

SELACHIAN PALAEOECOLOGY, STRATIGRAPHICAL DISTRIBUTION,
AND PALAEOBIOGEOGRAPHY OF THE MAASTRICHTIAN ASSEMBLAGES
(QUINTANILLA LA OJADA, ALBAINA, AND ENTZIA)

20.1 Introduction

The main marine stratigraphical units in the study area with significant Maastrichtian selachian content are (in decreasing age order): the upper part of the Valdenoceda Formation (VNF) at Quintanilla la Ojada (Burgos), the Torme Formation (TF) at Albaina (Treviño County, Burgos), and finally the Puerto de Olazagutía Formation at Vicuña and Andoin (Entzia/Urbasa Mountains, Álava) (see Fig. 7.7 in Chapter 7). Among them, the richest and most diverse fossil deposits derive from the shallow environments of the TF in the southern part of the Basque-Cantabrian Region (Albaina site in Treviño County, Burgos). In contrast, a limited set of selachian specimens from the Entzia/Mountains represents the youngest and less diverse assemblage of marine vertebrates recorded in the Upper Cretaceous of the region. These selachian faunas have also been important in order to better understand the different aspects about the geologic history of the Maastrichtian shelfal systems and the palaeoecological history of their marine biota.

On the whole, these assemblages from the Basque-Cantabrian Region (western Pyrenees) represent the most diverse and rich Maastrichtian neoselachian fauna so far discovered in Southern Europe. Additional records are the small assemblage collected by Gheerbrant et al. (1997) in the Haute-Garonne (southern France) and the tooth assemblages from restricted environments of the Catalonian Pyrenees, northeastern Spain (Soler-Gijón and López-Martínez, 1998; Kriwet et al., 2007), whose palaeoecological and environmental characteristics clearly differ from those that existed in the western Pyrenees at that time. Other Maastrichtian elasmobranch faunas in the Northern European basins (Belgium, Netherlands, and Germany) are more diversified, but many taxa remain to be described and many others need a revision (Cappetta and Corral, 1999).

20.2 Palaeoecology

Sharks and rays, in addition to many actinopterygian fishes (Berreteaga et al., 2011) and mosasaurs (Berreteaga, 2008) were able to take advantage of the shallow-marine environments developed in the Castilian Ramp (southern part of the B-CB) during the Maastrichtian. Identified teeth from Quintanilla la Ojada (Burgos) represent at least 17 taxa of small nekto-benthic rays and larger coastal pelagic sharks. The taxa and relative abundance are summarised in Table 20.1. Differences in degree of preservation and ecologic mixing suggest that the assemblage originated by biostratinomic processes, and the extent of reworking or the diagenetic changes can be ascertained by both REE patterns and total composition of rare earth elements (Berreteaga, 2008). Concerning the differential REE uptake into biogenic apatite, the enameloid always shows lower total trace-element content than the dentine and therefore REE pattern curves are often different (i.e. intra-fossil variation). Thus, the study on REE from the youngest and richest assemblage QLO-2 has concluded that the effects of taphonomic mixing are minor or non-existent, as samples from similar type of tissue practically show the same pattern. However, as other taphonomic signatures indicate, re-sedimentation is a process to be regarded. Furthermore, REE changes during late diagenesis seem to be minimal as indicated by Berreteaga (2008).

The material from Quintanilla la Ojada shows a diversified association of rays (including Rhinobatidae, Rhinobatoidei, Sclerorhynchidae, Dasyatoidea, and Rhombodontidae), bottom-dwelling sharks (including Ginglymostomatidae and Triakidae) and nektonic sharks (including Anacoracidae, Odontaspidae, Otodontidae, and Serrolamniidae) based on data from the assemblage QLO-2 (Fig. 20.1).

According to Compagno (1984b), many modern triakids (Carcharhiniformes) are opportunistic carnivores that inhabit muddy bottoms in water depths from intertidal to outermost shelf, and modern ginglymostomatids (Orectolobiformes) are inshore bottom sharks that occur in shallow littoral areas and reefal lagoons (although some species may also occur along the shelf up to several tens of metres deep). As seen in Fig. 20.1, both orders Carcharhiniformes and Orectolobiformes are underrepresented in the fossil record of Quintanilla la Ojada, which makes problematic a palaeoecological explanation. On the other hand, the Lamniformes is the most diversified order with seven species (44% of the total of the assemblage) distributed among four families. Modern sharks of this order are regarded as hunting carnivores (and opportunistic scavengers) feeding on bony fish, occurring within inshore waters from the intertidal zone to the outer shelf. According to the number of species recorded from this fossil site, batoid taxa represent almost half of the assemblage. In terms of abundance, the Quintanilla la Ojada assemblage is dominated by teeth of the myliobatoid *Rhombodus binkhorsti* (no. of specimens = 61), which may reflect more individuals of this species being present, considered to be better-adapted to shallow-water environments, but it could also result from a bias related to the overall shape of teeth and tooth number in the jaws of this species. Both factors have made them abundant and very durable

Table 20.1 Relative abundance of selachian species at Quintanilla la Ojada site. Percentage values are based on a sample of 180 teeth. Relative abundance ranges: A, abundant (>30% teeth in total assemblage); C, common (10%–30% teeth in total assemblage); UC, uncommon (5%–10% teeth in total assemblage); R, rare (4%–5% teeth in total assemblage); ER, extremely rare (1%–4% teeth in total assemblage).

Order	Species	Relative abundance	no	%
Orectolobiformes	<i>Plicatoscyllium leheri</i> (Leriche, 1938)	extremely rare	3	1.67
Lamniformes	<i>Carcharias beathi</i> Case and Cappetta, 1997	uncommon	15	8.33
	<i>Carcharias</i> sp.	extremely rare	3	1.67
	<i>Cretolamna</i> sp. aff. <i>C. appendiculata</i> (Agassiz, 1843)	extremely rare	1	0.56
	<i>Serratolamna serrata</i> (Agassiz, 1843)	common	23	12.78
	<i>Squalicorax kaupi</i> (Agassiz, 1843)	uncommon	12	6.67
	<i>Squalicorax pristodontus</i> (Agassiz, 1843)	uncommon	11	6.11
	<i>Squalicorax</i> sp.	extremely rare	4	2.22
Carcharhiniformes	<i>Palaeogaleus faujasi</i> (Geyn, 1937)	extremely rare	3	1.67
Rajiformes	<i>Ganopristis leptodon</i> Arambourg, 1935	extremely rare	6	3.33
	<i>Rhinobatos echavei</i> Cappetta and Corral, 1999	extremely rare	3	1.67
	<i>Rhinobatos ibericus</i> Cappetta and Corral, 1999	extremely rare	1	0.56
	<i>Vascobatis albatensis</i> Cappetta and Corral, 1999	uncommon	14	7.78
Myliobatiformes	<i>Coupagezia fallax</i> (Arambourg, 1952)	extremely rare	6	3.33
	<i>Rhombodus binkhorsti</i> Dames, 1881	abundant	61	33.89
	<i>Rhombodus</i> sp.	uncommon	14	7.78

Note: species abundance is a subjective measure and only reflects own views.

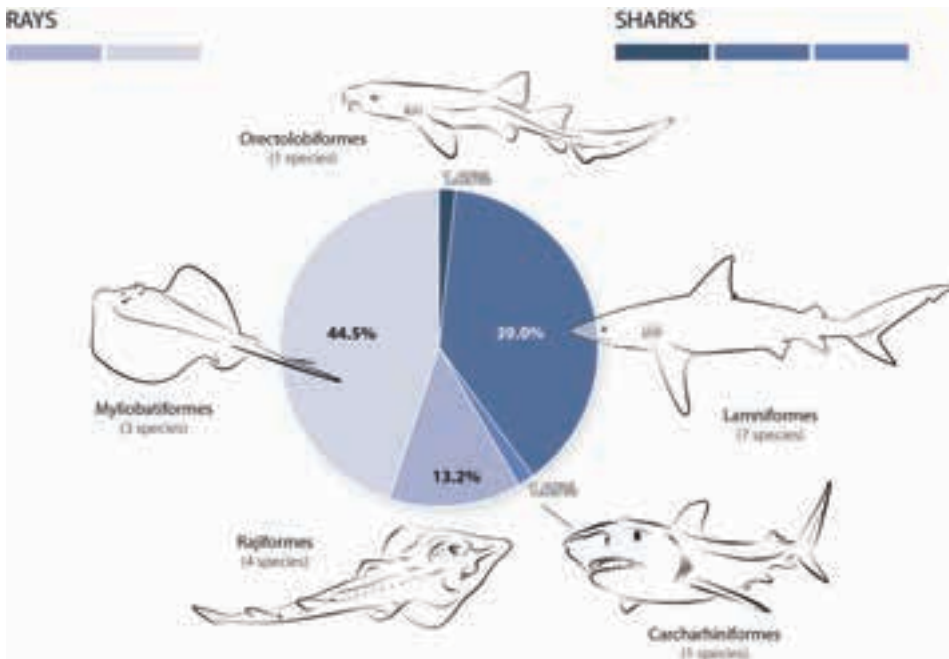


Figure 20.1 Relative abundances of Elasmobranchii teeth from Quintanilla la Ojada site (Burgos, Spain). Silhouettes depict a member of the group (not to scale).

elements before burial and therefore more likely to survive as fossils. Both Rajiformes (sclerorhynchids, rhinobatids and the closest relatives) and Myliobatiformes (rhombodontids and dasyatoids) are regarded as benthic carnivores that feed on small preys within or close to the sea bottom.

Examination of the elasmobranch assemblage (19 species) from Albaina site has allowed to distinguish as well a mixture of faunae from different ecological habitats (i.e. active swimming forms and bottom dwelling species), enclosed in five systematic orders (Fig. 20.2). These species and their relative abundance are indicated in Table 20.2.

Considering the depositional framework, the fauna of Albaina represents typical marine conditions, yet the selachian assemblage includes many small-sized teeth (for instance in the species *Cretolamna appendiculata* and *Squalicorax kaupi*) that would correspond to juvenile individuals of these two species, indicating probably nearshore environmental conditions (Cappetta and Corral, 1999). But it is important to note that the presence of numerous small-size teeth of a particular species does not necessarily indicate a large concentration of juvenile schooling fish. Since juvenile sharks produce and shed many teeth to keep pace with the growth of the jaws, which is faster in young stages as indicated by Kemp (1999: 59), and thus many small-sized teeth are incorporated into the fossil record. The relative abundance of guitarfishes (Suborder Rhinobatoidei), which nowadays prefer tropical and sub-tropical waters, in addition to their scarcity in coeval North European basins indicates that sea temperature in the area of Albaina was probably warmer than those in the Belgian and German basins. It is noteworthy that three off-shore sharks (*Carcharias beathi*, *Serratolamna serrata* and *Squalicorax kaupi*) and a bottom-dweller batoid (*Rhombodus binkhorsti*) are the most frequently found at Albaina site (accounted for the 78% of the selachian remains), but as these teeth are easily noticeable to the naked eye it may only mean a bias in the collecting of the specimens.

The pie chart of Fig. 20.2 graphically depicts the percentage of elasmobranch orders within the Albaina assemblage. These results are close to those observed in the Maastrichtian of Morocco where Rajiformes and Myliobatiformes represent 45%, and Orectolobiformes, Carcharhiniformes, Lamniformes represent 47%. The remaining Moroccan elements are represented by Heterodontiformes, Squatiniformes, Squaliformes, Hexanchiformes, and Pristiophoriformes (Noubhani and Cappetta, 1997), all of them lacking at Albaina. In terms of ecological meaning, this rate is normal for a neritic fauna (an artistic depiction of the Maastrichtian sea in the Albaina locality is represented in Fig. 20.3).

The offshore marine environment in the Entzia Mountains during the upper Maastrichtian was dominated by the individuals of the large anacoracid *Squalicorax pristodontus*. It can be assumed that individuals of that extinct species would be at the top of the food chain by inference from the extant tiger shark, *Galeocerdo cuvier* (Peron and Lesueur, in Lesueur, 1822) with an analogous dentition. Thus, *S. pristodontus* must have been a good swimmer and well adapted to the rich life in a marine habitat. A great variety of marine invertebrates, such as cephalopods, bivalves and crustaceans, and bony

Table 20.2 Relative abundance of selachian species at Albaina site. Percentage values are based on a sample of 1,078 teeth (modified from Cappetta and Corral, 1999). Relative abundance ranges as in Table 20.1.

Order	Species	Relative abundance	no	%
Orectolobiformes	<i>Plicatoscyllium lehneri</i> (Leriche, 1938)	extremely rare	23	2.13
	<i>Chiloscyllium</i> sp.	extremely rare	18	1.67
Lamniformes	<i>Carcharias aff. gracilis</i> (Davis, 1890)	extremely rare	4	0.37
	<i>Carcharias heathi</i> Case and Cappetta, 1997	common	108	10.02
	<i>Cretolamna appendiculata</i> (Agassiz, 1843)	extremely rare	29	2.69
	<i>Odontaspis bronni</i> (Agassiz, 1843)	extremely rare	2	0.19
	<i>Serratolamna serrata</i> (Agassiz, 1843)	common	263	24.40
	<i>Squalicorax kaupi</i> (Agassiz, 1843)	common	157	14.56
	<i>Squalicorax pristodontus</i> (Agassiz, 1843)	extremely rare	5	0.46
Carcharhiniformes	<i>Palaeogaleus faujasi</i> (Geyn, 1937)	extremely rare	43	3.99
Rajiformes	<i>Ataktobatis variabilis</i> Cappetta and Corral, 1999	extremely rare	4	0.37
	<i>Dalpiazia stromeri</i> Checchia-Rispoli, 1933	extremely rare	2	0.19
	<i>Rhinobatos echavei</i> Cappetta and Corral, 1999	extremely rare	18	1.67
	<i>Rhinobatos ibericus</i> Cappetta and Corral, 1999	extremely rare	16	1.48
	<i>Vascobatis albatensis</i> Cappetta and Corral, 1999	extremely rare	9	0.83
	<i>Ganopristis leptodon</i> Arambourg, 1935	extremely rare	35	3.25
Myliobatiformes	<i>Couatezia fallax</i> (Arambourg, 1952)	extremely rare	24	2.23
	<i>Rhombodus andriesi</i> Noubhani and Cappetta, 1994	extremely rare	2	0.19
	<i>Rhombodus binckhorsti</i> Dames, 1881	common	316	29.31

Note: species abundance is a subjective measure and only reflects own views.

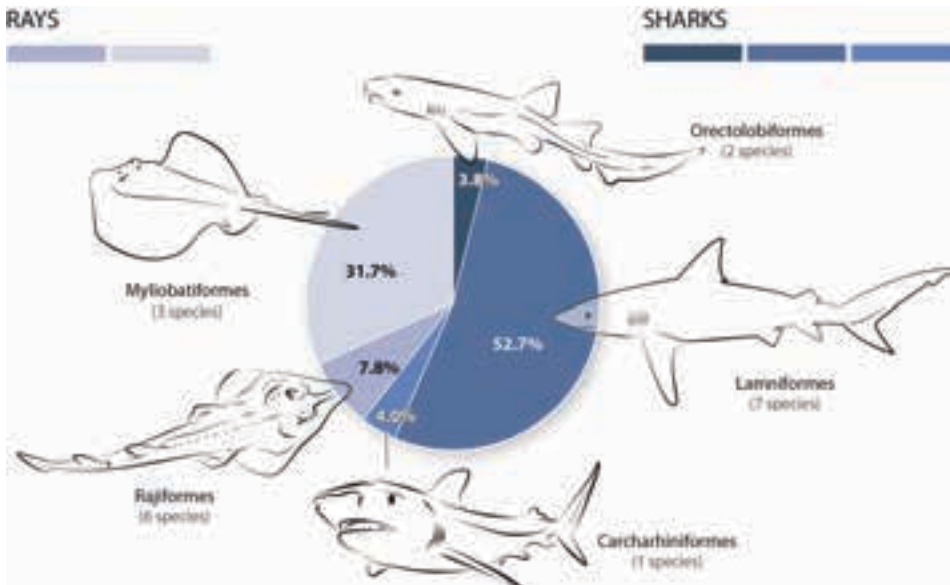


Figure 20.2 Relative abundance of Elasmobranchii teeth from Albaina site (Treviño County, Burgos, Spain). Silhouettes depict a member of the group (not to scale).

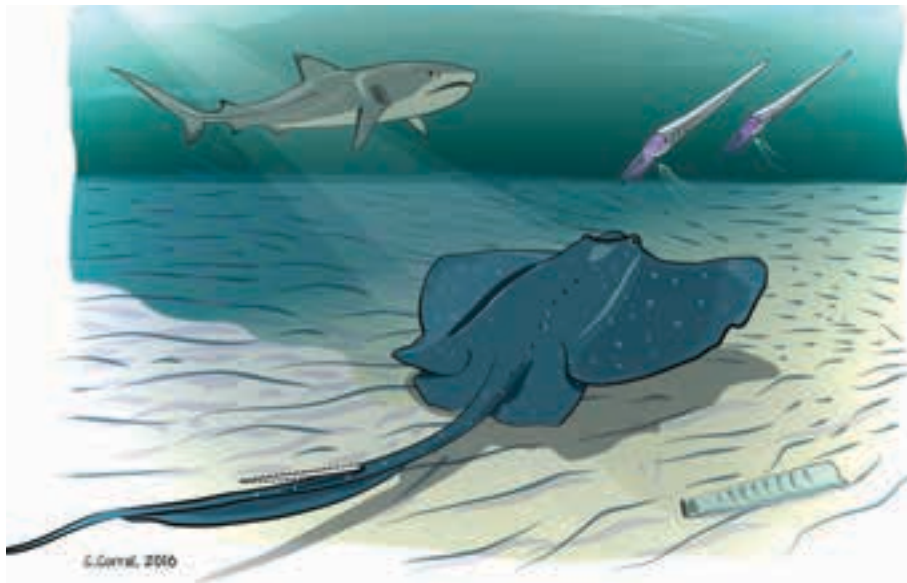


Figure 20.3 Artist's impression of sea life at Albaina (Treviño County, Burgos) during the Maastrichtian depicting a myliobatiform ray (bottom), a lamniform shark (top left), and two baculitid ammonites (top right). Drawing by the author.

fishes, sharks and other marine reptiles, among vertebrates, accounted for the bulk of its diet. A scavenging habit is also inferred from its specialised dentition (Schwimmer et al., 1997). The elevated tooth ratio of *Squalicorax* to other lamniforms (*Cretolamna* and *Serratolamna*) has been considered as an indicative of open and deeper marine environments (see Antunes and Cappetta, 2002; Cappetta et al., 2014b).

20.3 Species diversity, faunal affinities, and palaeobiogeographical implications

The taxonomic composition found in a determined fossil site is primarily the result of the palaeoenvironmental conditions, palaeobathymetry, water temperature and bottom substrate of the ancient sea (Cappetta et al., 2014b). All these factors help to depict a better understanding of ancient ecosystems.

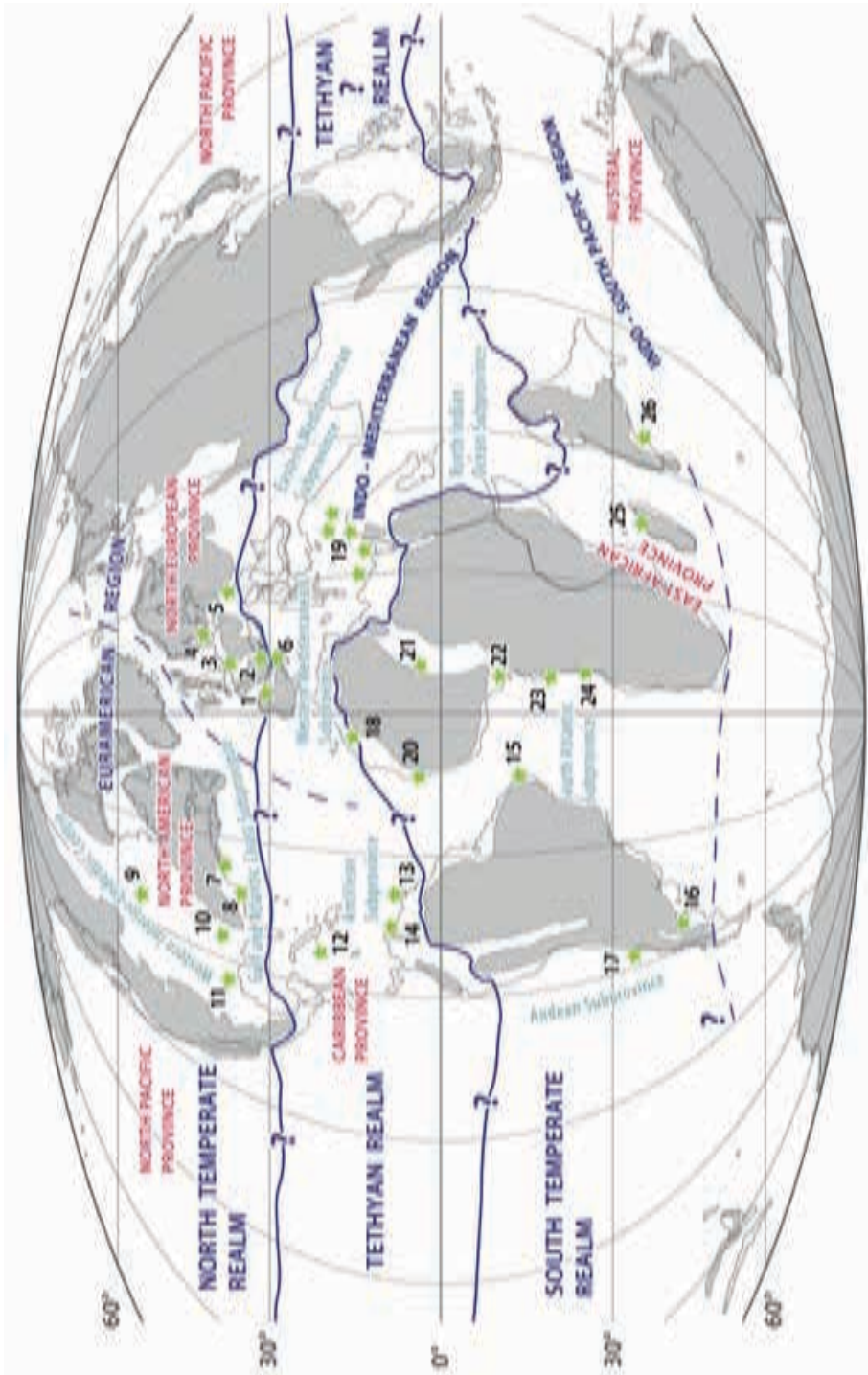
The Maastrichtian selachian diversity found in the Basque-Cantabrian Region and in the major fossil localities (Fig. 20.4) is shown in Table 20.3. It is easily observed that the selachian faunae of Quintanilla la Ojada and Albaina are compositionally very similar to one another, despite that the former site has been found less rich in terms of number of specimens. Minor faunal differences observed (regardless of the collection bias, that is, with a smaller sample size in Quintanilla la Ojada) may be due to either ecological or biostratigraphic causes. As sedimentological data suggests, the Quintanilla la Ojada material accumulated in typical shoreface-proximal ramp environments, as

explained earlier, whereas Albaina fossils appear to have been deposited in relatively open-marine environments (Cappetta and Corral, 1999).

Selachian records from the Maastrichtian in southwestern Europe are circumscribed to the French and Spanish slopes of the Pyrenees. Tercis-les-Bains (Aquitaine Region, France) has yielded a faunule characterised by *Pseudocorax affinis* and *Paratriakis* sp. (Cappetta and Odin, 2001), whereas fossil material from the Marnes d'Auzas Formation in Peyrecave (Haute-Garonne, France) includes at least four taxa: *Palaeogaleus* sp., *Paratrygonorrhina amblysoda*, *Rhombodus binkhorsti*, and *Coupatezia* sp. (Gheerbrant et al., 1997). Particular mention is to be made of the selachian associations found in the Tremp area (located on the eastern Spanish Pyrenees), which are dominated by small myliobatid rays. As pointed out in the Kriwet et al. (2007) paper, Fontllonga-6 fossil site is quite a productive early Maastrichtian deposit (within Chron C31r). Unfortunately, such coastal deposit is devoid of shark remains and only the small myliobatoid rays *Rhinobatos ibericus* and *Igdabatis indicus* occur (Soler-Gijón and López-Martínez, 1998; Kriwet et al., 2007).

In contrast to the open marine settings that characterise the Basque-Cantabrian Region during the upper Maastrichtian, the Tremp sequences were deposited in coastal lagoons (Kriwet et al., 2007), and hence they show a restricted diversity of elasmobranch species. Authors working in that region (Soler-Gijón and López-Martínez, 1998; Kriwet et al., 2007) have suggested a Late Cretaceous shallow trans-Tethyan connection between Eurasia and India on the basis of the occurrence of the myliobatoid ray *Igdabatis indicus*. The most likely scenario is that *Igdabatis indicus* originated in southern Europe – as the Campanian of Tremp has yielded the oldest known occurrence (Kriwet et al., 2007) – and then dispersed during the Maastrichtian across the Tethys Ocean to the northern margins of Africa, farther south to Niger (Cappetta, 1972) and eastwards to the Indian continent (Prasad and Cappetta, 1993). Paradoxically, the shallow marine environments formed along the Pyrenean Region during the Maastrichtian became a sort of environmental/geographical barrier with a low interconnection between eastern and western sea regions, which prevented a westward dispersal of *I. indicus*.

From a palaeoecological perspective, the selachian fauna from Quintanilla la Ojada is dominated by large pelagic lamniforms such as *Squalicorax kaupi*, *Squalicorax pristodontus*, *Serratolamna serrata*, *Carcharias heathi*, in addition to the myliobatiform *Rhombodus binkhorsti*, but the endemic nektobenthic rays *Vascobatis albaitensis*, *Rhinobatos echavei*, and *Rhinobatos ibericus* are a significant part of the selachian assemblages. Other elasmobranch species include orectolobiform (*Plicatoscyllium lehneri*) and carcharhiniform (*Palaeogaleus faujasi*) sharks, sclerorhynchid sawfishes (*Ganopristis leptodon*), and the demersal dasyatid ray (*Coupatezia fallax*). This association of taxa indicates a shallow-marine neritic environment with natural connection to open sea. Other important aspect is that the faunal interchange across the North Atlantic (between the North European and North American provinces) and between the North European



and western Tethyan basins was possible during the Late Cretaceous, as indicated by the cooccurrence of the species *Squalicorax kaupi*, *S. pristodontus*, *Serratolamna serrata*, and *Plicatoscyllium lehneri* on both sides of the Atlantic Ocean (Darteville and Casier, 1943; Welton and Farish, 1993; Noubhani and Cappetta, 1997).

The coastal pelagic sharks *Squalicorax kaupi*, *S. pristodontus*, *Carcharias beathi*, *Cretolamna* sp. aff. *C. appendiculata*, and *Serratolamna serrata* were active swimmers that could easily migrate moving alongshore and offshore favoured by surface ocean currents, according to their distribution in the Gulf and Atlantic Coast subprovince of North America and the North European Province. Such transoceanic migrations in the North Temperate Zone may be related to a clockwise-rotating North Atlantic gyre (in the proto-North Atlantic), which allowed these species to inhabit Europe and North America regions. Other less efficient swimmers, such as the orectolobiform *Plicatoscyllium lehneri*, present a peri-Atlantic distribution and, therefore, the species is regarded as a demersal shallow-water swimmer with populations in the North Temperate, Tropical and South Temperate regions of the Palaeo-Atlantic (see Table 20.3). On the basis of the present distribution of the orectolobiform sharks, which are mostly found in shelfal waters, the idea of dispersal by ocean currents is less probable; thus a vicariance process through the upper Cretaceous could better explain their past distribution. Other demersal species such as the triakid *Palaeogaleus faujasi* did not migrate large distances and was it restricted to the North European Province (Cappetta and Corral, 1999).

Therefore, the selachian faunae from the Basque-Cantabrian Region (mainly Quintanilla la Ojada and Albaina associations) appear to have well-supported affinities with other European faunae (northern France, Belgium, and Netherlands) and with the Moroccan one to a lesser extent (see Cappetta and Corral, 1999). But contrarily to that of Albaina, where *Rhombodus andriesi* and *Dalpiazia stromeri* occur, the Quintanilla la Ojada assemblages do not contain any exclusive Gondwanan element and, in fact, they are a mixture of cosmopolitan and endemic taxa (including two small rhinobatoidei rays among the latter: *Rhinobatos ibericus* and *Vascobatis albaitensis*). Also worth noting is that the demersal myliobatid *Rhombodus binkhorsti* shows a markedly circumtropical

- ◀ **Figure 20.4** The Earth during the Maastrichtian times with the main selachian sites indicated. Fossil localities: 1, Basque-Cantabrian Region, Spain (17, 25, 26); 2, Southern France (34); 3, Netherlands and Franco-Belgian basins (2, 3, 11, 14, 28, 33, 36, 37, 39); 4, Denmark (1); 5, Bulgaria (38); 6, North Catalonia, Spain (Kriwet et al., 2007; Soler-Gijón and López-Martínez, 1998); 7, New Jersey (15, 22, 31); 8, North Carolina (23); 9, Western Interior, South Dakota (8); 10, Arkansas (9); 11, Texas (16, 21, 49); 12, Jamaica (46); 13, Trinidad (40); 14, Venezuela (20); 15, Brazil (44); 16, Argentina (10); 17, Chile (14, 50); 18, Morocco (5, 6, 10, 19, 42, 43); 19, Libya, Egypt, Jordan, Syria, Israel (7, 13, 18, 24, 32, 41, 45, 48, 51); 20, Senegal (14, 27); 21, Niger (47); 22, Nigeria (12); 23, DR Congo (29, 30); 24, Angola (4, 29); 25, Madagascar (35); 26, India (Prasad and Cappetta, 1993). Palaeogeographical map based on Smith et al. (1994) and biogeographical units after Kaufmann (1973). Note: numbers in parentheses refer to publications given in the caption of Table 20.3.

Table 20.3 List of neoselachians identified from the Maastrichtian of the Basque-Cantabrian Region (northern Spain) and their presence in coeval world deposits.

	Europe					North
	Quintanilla la Ojada (Spain)	Albaina (Spain)	Southern France	Netherlands, Franco-Belgian basins	Denmark, Bulgaria	Western Interior (South Dakota, Texas)
Sharks						
<i>Squalicorax pristodontus</i> (Agassiz, 1843)	26	17, 25		2, 33, 36, 39	1, 38	49
<i>Squalicorax kaupi</i> (Agassiz, 1843)	26	17		33		16, 21, 49
<i>Squalicorax</i> sp.	26					
<i>Cretolamna</i> sp. aff. <i>Cretolamna appendiculata</i> (Agassiz, 1843)	26	17		33, 36, 37		49
<i>Serratolamna serrata</i> (Agassiz, 1843)	26	17		2, 33, 36		8, 21, 49
<i>Carcharias heathi</i> Case and Cappetta, 1997	26	17				21
<i>Carcharias</i> aff. <i>gracilis</i> (Davis, 1890)		17		33		
<i>Carcharias</i> sp.	26					
<i>Odontaspis bronni</i> (Agassiz, 1843)		17		2, 33		
<i>Plicatoscyllium lehneri</i> (Leriche, 1938)	26	17				49
<i>Palaeogaleus fajasi</i> (Geyn, 1937)	26	17		33, 36		
<i>Chiloscyllium</i> sp.		17				
Rays						
<i>Rhinobatos echavei</i> Cappetta and Corral, 1999	26	17				
<i>Rhinobatos ibericus</i> Cappetta and Corral, 1999	26	17				
<i>Ataktobatis variabilis</i> Cappetta and Corral, 1999		17				
<i>Vascobatis albaitensis</i> Cappetta and Corral, 1999	26	17		14, 37		
<i>Ganopristis leptodon</i> Arambourg, 1935	26	17		3, 36		
<i>Dalpiazia stromeri</i> Checchia-Rispoli, 1933		17				
<i>Coupatanzia fallax</i> (Arambourg, 1952)	26	17	34	11, 36		
<i>Rhombodus</i> sp.	26					
<i>Rhombodus andriesi</i> Noubhani and Cappetta, 1994		17				
<i>Rhombodus binkborsti</i> Dames, 1881	26	17	34	3, 28, 33		21, 49

Data taken from the following sources: 1, Adolfssen and Ward (2014); 2, Agassiz (1843); 3, Albers and Weiler (1964); 4, Antunes and Cappetta (2002); 5, Arambourg (1935); 6, Arambourg (1952); 7, Bardet et al. (2000); 8, Becker et al. (2004); 9, Becker et al. (2006); 10, Bogan and Agnolin (2010); 11, Bruggen et al. (1993); 12, Cappetta (1972); 13, Cappetta (1991); 14, Cappetta (2012); 15, Cappetta and Case (1975b); 16, Cappetta and Case (1999); 17, Cappetta and Corral (1999); 18, Cappetta et al. (2000); 19, Cappetta et al. (2014b); 20, Carrillo et al. (2008); 21, Case and Cappetta (1997); 22, Case et al. (2001a); 23, Case et al. (2017); 24, Checchia-Rispoli (1993); 25, Corral (1996); 26, Corral et al. (2015b); 27, Cuny et al. (2012); 28, Dames (1881); 29, Darteville and Casier (1943); 30, Darteville and Casier (1959); 31, Gallagher (2002); 32, Gemmellaro (1920); 33, Geyn (1937); 34, Gheerbrant et al. (1997); 35, Gottfried et al. (2001); 36, Herman (1977); 37, Herman and Van Waes (2014); 38, Jagt et al. (2006); 39, Leriche (1929); 40, Leriche (1938); 41, Lewy and Cappetta (1989); 42, Noubhani and Cappetta (1994); 43, Noubhani and Cappetta (1997); 44, Rebouças and Santos (1956); 45, Signeux (1959); 46, Underwood and Mitchell (2000); 47, Vullo and Courville (2014); 48, Stromer and Weiler (1930); 49, Welton and Farish (1993); 50, Wetzel (1930); 51, Zalmout and Mustafa (2001). Type localities are marked in ruby colour; modified from Corral et al. (2015b).

bodus andriesi). Three of the species occurring both in Albaina and the North European Province are absent in Africa (i.e. *Odontaspis bronni*, *Carcharias* aff. *gracilis*, and *Palaeogaleus faujasi*). Seven of the species are common to the three areas (i.e. *Squalicorax kaupi*, *Squalicorax pristodontus*, *Cretolamna* sp. aff. *C. appendiculata*, *Serratolamna serrata*, *Ganopristis leptodon*, *Coupatanzia fallax*, and *Rhombodus binkhorsti*). Some remarkable features at Albaina site are the presence of *Dalpiazia stromeri*, *Rhombodus andriesi*, and *Carcharias heathi* – previously unknown to Europe but present in the rich phosphate deposits of Morocco – and that *Palaeogaleus faujasi* and *Odontaspis bronni* – usually regarded North European species – also inhabited the marine shelf of the North Iberian margin (Cappetta and Corral, 1999). It must be noted that the four species limited to the Albaina locality belong to the order Rajiformes and are represented by teeth of small to very small sizes.

Faunal differences between two given fossil sites can be quantified by the Simpson's (1969) coefficient [$SC: 100 C/N1$], where C is the taxa number common to the faunas to be compared with each other and N1 the total number of taxa of the smallest fauna. In this regard, the comparison between Albaina and Morocco faunas, on a side, and Albaina and Northern Europe faunas, on the other side, gives similar results. The Simpson coefficient is the same in both cases ($SC = 55.5$).

The biogeographical characterization of the assemblages from North Iberia is summarised by Cappetta and Corral (1999) and Corral et al. (2015b) as being a combination of cosmopolitan elements, such as the lamniform sharks *Squalicorax* spp., *Cretolamna* spp., *Serratolamna serrata*, the orectolobiform *Plicatoscyllium lehneri*, and the myliobatiform ray *Rhombodus binkhorsti* (by far the most common species at the sites), some south-Tethyan species (i.e. *Dalpiazia stromeri* and *Rhombodus andriesi*), and some species restricted to the North European Region and northern margin of the Tethys (i.e. *Rhinobatos echavei*, *Rhinobatos ibericus*, and *Vascobatis albaitensis*) (see Table 20.3).



CONCLUSIONS



... beyond a light bulb moment!

Chapter 21 CONCLUSIONS

The main aim of this thesis is to describe and evaluate the remains of fossil neoselachians collected in Upper Cretaceous rocks from the southern part of the Basque-Cantabrian Basin (B-CB) over a period of more than 30 years. There, several outcrops have been shown to be a particularly important source for marine fossil vertebrates, among which the neoselachians (subclass Elasmobranchii) are the most common and diverse. Moreover, this thesis is a contribution to decipher the geological history of southern parts of the Basque-Cantabrian Region during the Upper Cretaceous. However, the research does not, or at least should not, end here. There are still many invertebrate and vertebrate fossil specimens from this region in crowded museum cabinets – collected by fossil enthusiasts and renowned geologists – which are deserving of future attention.

21.1 General conclusions

- Historical records of fossil sharks from this region are scarce in the geological literature. Those that occurred date back to the end of the 19th century and the first half of the 20th century (by the work of Adán de Yarza in 1885 and Ruiz de Gaona in 1943), and are limited to a mention of the presence of few lamniform specimens whose whereabouts are unknown today.
- This work represents a major advance in the knowledge of the Upper Cretaceous selachians (Galeomorphii, Squalomorphii, and Batomorphii) known to occur in the Basque-Cantabrian Region – mainly for the Campanian and Maastrichtian stages.
- The shallow carbonate-ramp successions of the B-CB – within the northern Iberian continental margin – have shown a high diversity of selachian fishes through the upper half of the Upper Cretaceous. The list includes over 43 taxa, representing 7 orders and 20 families, ranging from highly mobile pelagic species to demersal species (i.e. found living and feeding near the sea bottom). The selachian remains compose a significant fraction of the marine vertebrates finds, especially in the Campanian glauconite-rich beds and the Maastrichtian marine phosphate-rich deposits and marl–limestone alternations.

- While the real picture of the elasmobranchs that inhabited the more shallow neritic parts of the B-CB through the uppermost Cretaceous is relatively good, the faunal composition of them in earlier geological ages is far from being knowable. It is a fact that pre-Campanian selachians are unknown or rarely found in the Basque-Cantabrian Region. This is, for instance, the case for the Santonian thick marine sequences cropping out in the central part of the B-CB, which have yielded only occasional selachian finds and, unfortunately, none of them is yet housed in public institutions for consultation and study. In this context, those Santonian exposures are in need of future research.

21.2 Conclusions on the Coniacian stratigraphy and associated faunal remains

- The Coniacian open-marine, neritic carbonate series of the Nidáguila Formation at Barrio Panizares site (Castilian Platform, B-CB) has yielded, so far, a single rostral spine of the sawfish *Onchosaurus radicalis*, which represents the first record of this species in the Iberian Peninsula.

- The specimen occurs with many derived shell debris, having been interpreted to represent a storm bed deposit. This helped reinforce the idea that it was transported from an adjacent shallower area, as the extant analogous sclerorhynchids are well suited to living in shallow-water habitats. However, a semipelagic lifestyle for the Cretaceous sawfish is not completely ruled out.

- From its stratigraphic position (i.e. above the first occurrence of *Protexanites bourgeoisianus* and below the first occurrence of *Hemitissotia turzoi*), the age of the *Onchosaurus* bed is estimated to be late Coniacian.

- *Onchosaurus* is an extinct Cretaceous sawfish ranging from the Turonian through upper Campanian, and whose fossil remains are worldwide known except for Australia and Antarctica. However, fossil specimens are scarce, being assigned either to *Onchosaurus radicalis* Gervais, 1852 or *Onchosaurus pharao* (Dames, 1887).

- A Gondwanan origin is inferred for *Onchosaurus* in accordance with the 19 worldwide known occurrences. But soon after, the genus spread northwards favoured by newly-formed continental margins during the maximum sea level rise attained in the Turonian. It is assumed that this pelagic sawfish was able to cross oceans, aided by surface currents.

21.3 Conclusions on the Campanian stratigraphy and associated faunal remains

- Two distinctive lithostratigraphical units in the Vitoria Sub-basin (southern part of the B-CB) are known to produce fossil neoselachian remains, namely the Gomecha Member (GM) of the Vitoria Formation and the Eguileta Member (EM) of the younger Montes de Vitoria Formation.

- The GM records two successive sedimentary episodes: (1) a basal subunit – lithofacies-1 – of alternating bluish-grey marls and marly limestones, from which most of the fossil remains has been obtained, and (2) a glauconite-rich, packstone calcarenite/

calcirudite subunit – lithofacies-2 –, which is the most prominent rock of the unit. The GM was deposited on a mid-to-outer ramp to fore slope, with a depth range of 80 to 400 m (Ramírez del Pozo, 1971) or below 100–150 m (Engeser, 1985).

- The GM has yielded two selachian assemblages. The first of these – from lithofacies-1 – is a mixture of pelagic, shelf and slope-dwelling selachians. It consists of the following taxa: *Anomotodon hermani*, *Carcharias aasenensis*, *Chiloscyllium* cf. *gaemersi*, *Chiloscyllium* cf. *vulloi*, *Cretolamna borealis*, *Cretolamna sarcophortheta*, *Hemiscyllium hermani*, *Paranomotodon* cf. *angustidens*, *Parapalaeobates pygmaeus*, *Probaploblepharus riegrafi*, *Ptychotrygon* sp., *Rhinobatos casieri*, *Squalicorax* ex gr. *kaupi*, *Squatina* (*Cretoscyllium*) *hassei*, and *Synechodus* aff. *filipi*. A slightly younger assemblage – from lithofacies-2 –, poorer in specimen number and less diverse, consists of the following taxa: *Cretolamna borealis*, *Cretoxyrhina mantelli*, *Paranomotodon* cf. *angustidens*, *Parapalaeobates pygmaeus*, *Scapanorhynchus* cf. *texanus*, and *Squalicorax* ex gr. *kaupi*.

- The order Lamniformes shows the highest species richness with eight species (accounting over 50% of the global tooth sample). Extant members of the Lamniformes mainly inhabit pelagic waters, including both oceanic and semipelagic environments. The oceanic selachian fauna of the GM is dominated by the genera *Cretolamna*, *Cretoxyrhina*, and *Paranomotodon*, while the semipelagic *Carcharias* genus – with coastal nektobenthic habits – is considered a shallow inshore inhabitant that occasionally entered oceanic waters. Two mitsukurinid genera, *Anomotodon* and *Scapanorhynchus*, have also been found (although are uncommon to extremely rare, respectively). The species of these genera could be considered as mesopelagic, based on the ecology of the only extant member of this family (i.e. the goblin shark *Mitsukurina owstoni* Jordan, 1898), which has adapted to live within an extensive depth range, farther from the shore on the continental shelf break and upper slope. About more than half of the selachian species found are bottom-dwelling forms (i.e. demersal species) living on the continental ramp (or shelf) and upper slope. These belong to small hemiscylliids (e.g. *Chiloscyllium* and *Hemiscyllium*), scyliorhinids (e.g. *Probaploblepharus*), palaeospinacids (e.g. *Synechodus*), and batoids (e.g. *Parapalaeobates*, *Ptychotrygon*, and *Rhinobatos*).

- The GM also contains a relatively diverse assemblage of invertebrate fossils, which occurs with the selachian teeth, consisting of sponges, oysters, ammonites, microbrachiopods, stalked crinoids, echinoids, calcareous worm tubes, and decapod remains. All of them indicative of well oxygenated environments.

- The fossil productive lithofacies-1 of the GM is regarded as late Campanian in age (~73.5 Ma) based on the recognition of the *Globotruncana aegyptiaca* subzone (*G. aegyptiaca* zone) (J. Arz, pers. comm.). Additionally, other diagnostic fossils such as ammonites have also been used.

- The EM is dominantly represented by bluish-grey fossiliferous glauconitic marls of commonly homogenous appearance that grade upward into a bioclastic mudstone (i.e. a turbiditic subunit containing glauconite and abundant siderite grains). This unit records a prodelta depositional environment in the shallow sea that throughout the Campanian

occupied most of the southern part of the Vitoria Sub-basin (Engeser, 1985).

- The selachians found in these deposits of the EM at Vitoria Pass site are assigned to the following taxa: *Carcharias adneti*, *Cretolamna borealis*, *Cretolamna sarcoportheta*, *Protolamna borodini*, *Pseudocorax laevis*, *Serratolamna khderii*, and *Squalicorax* ex gr. *kaupi*. It is acceptable that all lamniform species inhabited this semipelagic environment on the continental ramp, with the odontaspimid *C. adneti* and the serratolamnid *S. khderii* occupying coastal benthic areas. The teeth of *C. borealis*, *C. sarcoportheta*, and *S.* ex gr. *kaupi* are numerically predominant in these deposits, but this feature surely represents a sampling bias toward large and more easily found species.

- The selachian community found in the EM inhabited well-oxygenated waters based on the rich diversity of cooccurring invertebrates, but dysoxic–anoxic conditions may have existed below the sediment–water interface (at periods of low sedimentation rate) during the deposition of the unit, as evidenced by the presence of diagenetic phosphate concretions and pyritised internal moulds of molluscs.

- Rock samples from the Vitoria Pass site (EM) are assignable to the *Rugoglobigerina rotundata* subzone (*Gansserina gansseri* zone), and therefore are upper Campanian (~ 72 Ma) (J. Arz, pers. comm.).

- The overall selachian fauna of the two conjoined Gometxa and Vitoria Pass sites in the Vitoria Sub-basin shows its closest faunal affinities to that of the Kristianstad Basin in Sweden (Jaccard and Dice similarity coefficients are 0.552 and 0.711, respectively), and is slightly less similar to other faunae in the Atlantic Coastal Plain of North America (New Jersey and Delaware, USA) (Jaccard and Dice similarity coefficients are 0.424 and 0.596, respectively), as assessed using the current data. This faunal similarity with the geographically distant Swedish area – observed in non-metric multidimensional scaling (NMDS) and clustering analyses – is strikingly notorious, but this finding may have been biased as a result of analysing two ecologically unequal faunae. On the other hand, the faunal affinities with the Atlantic and Gulf Coastal Plain (AGCP) unit may be due to the high number of pelagic lamniform sharks present in the sample, which in general would have had a high dispersal potential favoured by surface currents in the North Atlantic gyre. It is very likely that the differences with other western European regions will be less noticeable as our knowledge of the Vitoria Sub-basin faunal composition is increased. The application of the parsimony analysis of endemism (PAE) for identifying biogeographical areas has given a more parsimonious view of the relationships of the selachian areas during the Campanian. Both the Vitoria Sub-basin and Tethyan Middle East are rooted at a basal node with almost all western European areas and the AGCP region, however. This pattern of distribution of selachian genera introduces an uncertainty, and again is something to be solved at some point in the future.

- Five palaeobiogeographical units (PBU) – sensu Seeling et al. (2004) – have been recognised on the basis of multivariate ordination techniques and by parsimony analysis applied to a matrix of Campanian selachian genera. The units are named as follow: (i) Western Interior Seaway (WIS) and (ii) Atlantic and Gulf Coastal Plain

(AGCP), both in the North American province, (iii) European seas (ES) in the North European province, (iv) South-Tethyan margin (STM) in the Mediterranean province, and finally (v) Western Africa (WA) in the West African province. The obtained ordination patterns also show that the water temperature gradient, ocean circulation patterns, and biogeographical barriers are considered main factors controlling the distribution of selachians in the PBUs.

- Despite the cooling climatic evolution during the latest Cretaceous (Guinot, 2013b), the Campanian elasmobranchs of the Vitoria Sub-basin are still typical of warm temperate waters.

- Campanian deposits with selachian assemblages occur in limited areas of the Basque-Cantabrian Region, and with the current state of knowledge the central part of the Álava province is its main source. Moreover, many of the selachian taxa from the Gomecha and Eguileta members of the Vitoria Sub-basin (B-CB) are reported to occur for the first time in the Campanian of the Iberian Peninsula.

- The Gomecha and Eguileta members constitute a singular resource for the study of the marine ecosystems occurring in southern Europe during the Campanian. These lithostratigraphical units not only have yielded interesting selachian assemblages – as seen –, but also vertebrate remains of mosasaurids and a faunule of marine bony fishes (actinopterygians) not yet fully studied.

21.4 Conclusions on the cut marks on a mosasaurid vertebra from the Campanian of the Vitoria Sub-basin

- Marks observed on a mosasaurid caudal vertebra discovered at Jauregi site, in eastern Álava (Eguileta Member of the Montes de Vitoria Formation; upper Campanian) was likely the result of opportunistic scavenging by a lamniform shark on a mosasaurid carcass. However, active predation on the mosasaurid cannot be completely discarded.

- Cooccurring shark teeth are scarce but the numerous isolated teeth of *Squalicorax* ex gr. *kaupi* and *Cretolamna borealis* collected in nearby coeval deposits supports the idea that such encounter could be possible.

- Some asymmetric, overlapping cut marks on the bone surface are interpreted as a result of the predator's tooth during food manipulation (i.e. piercing and cutting flesh along the mesial plane of the tooth when feeding on prey).

- The shape of the bite marks alludes to a shark with a cutting-type dentition, or with a tendency towards this model, as the producer. A member of the genus *Squalicorax* – with tooth crowns having a wide cross-section and marginal serrations – is the main shark candidate, rather than *Cretolamna*, even though serration grooves were not made on the bone surface of the vertebra.

- The species *Cretoxyrhina mantelli* is ruled out as the biter on the basis of its teeth size and the interspace length between the punctures. Moreover, Jauregi site is biostratigraphically placed well above the taxon's last appearance datum, according to Siverson (1992).

- The elongated, sharp-edged shape of the punctures precludes an attribution to other potential predators, such as plesiosaurs, crocodiles, or mosasaurids, because the teeth of these would have produced round to oval, relatively more spaced marks (see references in Chapter 18).
- The bioerosion structures on the Jauregi mosasaurid vertebra represent an indirect evidence of shark–mosasaur trophic interaction during the Campanian, and allow us both to hypothesize about the feeding behaviour of fossil sharks and to highlight the ecological role of sharks in the Cretaceous marine food webs.

21.5 Conclusions on the marine vertebrate predators (Actinopterygii, Chondrichthyes, and Mosasauridae) in the Campanian of the Basque-Cantabrian Basin (B-CB)

- During the Campanian, selachians were most abundantly represented in the Vitoria Sub-basin (B-CB, northern of the Iberian Peninsula), both in terms of diversity, with twenty-two taxa, and abundance. But they were not the only carnivorous marine vertebrates in the region, as at least three mosasaurid taxa and a single actinopterygian (enchodontid) were also present.

- Among selachians, some lamniform species are considered to be apex predators (i.e. *Cretoxyrhina mantelli*, *Cretolamna borealis*, and *Cretolamna sarcoportheta*) or purportedly opportunistic (i.e. *Squalicorax* ex gr. *kaupi*). Moreover, an enchodontid fish has been identified, – occupying a lower trophic level, possibly preying on ammonites and small invertebrates – but this group of fishes is still underrepresented.

- Although most selachian species in the Vitoria Sub-basin are restricted to the marine epipelagic and neritic environments, some mitsukurinid sharks were deep-water species (e.g. *Anomotodon* and *Scapanorhynchus*), venturing down to the upper slope zone. The cooccurrence of the mitsukurinid sharks with a rhynchobathic habitus, which are characteristic ecomorphotypes of the mesopelagic zone, with selachians linked to the oceanic epipelagic zone (e.g. tachypelagic and macrooceanic types), is related to diel vertical migrations of the former, a particularity that has been observed in extant shark populations (Heithaus, 2004).

- Batoid fishes in the Vitoria Sub-basin were not statistically significant, but they represented a noteworthy role in the sea bottom. These include the clearly durophagous *Parapalaebates pygmaeus* and two small predators with a crushing-type dentition, namely *Rhinobatos casieri* and *Ptychotrygon* sp.

21.6 Conclusions on the Maastrichtian stratigraphy and associated faunal remains

- The following Maastrichtian formations in the B-CB have yielded shark and ray remains: the Valdenoceda Formation (VNF), the Torme Formation (TF), and the Puerto de Olazagutía Formation (POF).

- The VNF (Castilian Ramp, southern part of the B-CB) is composed of small,

shallowing upward sequences of alternating dolostone and dolomitised bioturbated marlstone rocks that were originally deposited as carbonate sand and lime mud on a proximal platform (inner to mid ramp) close to a lagoon connected with the open sea, as suggested by lithological, sedimentological, and palaeontological observations. The presence of miliolid foraminifers and small gastropods may be indicative of a shallow-marine, restricted environment, but a more accurate reconstruction of the depositional environment would be confirmed by a further analysis of the benthic foraminifers.

- The fossil vertebrates found in the VNF at Quintanilla la Ojada (assemblages QLO-1 and QLO-2) consist of a relatively diverse fauna of selachians – with at least 17 taxa –, many actinopterygian fish remains, and a few mosasaurid teeth.

- Each fossil assemblage differs significantly from the other in the faunal abundance, preservation, and colour. Thus, the reddish brown teeth from QLO-1 (associated to the transgressive lag) exhibit a high degree of abrasion and breakage, while those tooth elements from QLO-2 (associated to the dolomitised marlstone) are dark grey and occur either pristinely preserved or with an abraded-polished appearance. Observed differences in the degree of preservation and ecologic mixing suggest that the richest assemblage QLO-2 originated by biostratinomic processes (i.e. deposition and abrasion in a varying degree). The extent of abrasion, reworking, and diagenetic changes are ascertained by the patterns of variation and total composition of rare earth elements (REE). Concerning the differential REE uptake into biogenic apatite, enameloid always has lower total trace-element content than dentine, just as it was assumed, and therefore their corresponding REE pattern curves are different (i.e. intra-fossil variation). The effects of taphonomic mixing are minor or non-existent, as samples with similar bone tissue type show practically the same patterns. However, element re-sedimentation is a process to be regarded, as taphonomic signatures indicate.

- In terms of selachian diversity, the taxa represented in the VNF are similar to those occurring at Albaina site – located about 60 kilometres eastwards in a straight line –, although fossil specimens are much less abundant in the VNF.

- An early to early late Maastrichtian age was indicated for the VNF, according to the biozonation based on rudist bivalves (Floquet, 1991). However, the cooccurrence of the selachian species *Carcharias heathi*, *Coupatezia fallax*, *Plicatoscyllium lehneri*, and *Rhombodus binkhorsti* in assemblage QLO-2 would give a younger age for, at least, the upper part of the VNF (comparing with the results obtained in Moroccan exposures by Cappetta et al., 2014b). Further investigation is needed in order to clarify the causes of this inconsistency.

- The fossiliferous deposits of the TF at Albaina (Navarre-Cantabrian domain of the B-CB) have produced the richest and most diverse record of Maastrichtian elasmobranchs in the Iberian Peninsula and, along with the previously described from Quintanilla la Ojada, are practically unique to southern Europe.

- The faunal list includes 10 taxa of galeomorph sharks and 9 batomorphs (mainly skates, rays, and guitarfishes). The lamniform species *Serratolamna serrata*, *Squalicorax*

kaupi, and *Carcharias heathi* are the most common sharks, while the Myliobatoidea *Rhombodus binkhorsti* is the most common batomorph in the formation.

- The composition of this original assemblage is conditioned by the palaeogeographical location of the northern Iberia margin in Maastrichtian times between the northern European and northern African seas. Therefore, it is not surprisingly formed by a mixture of wide range (or cosmopolitan) elements mixed with south-Tethyan and boreal warm-temperate species, in addition to some local taxa, the latter of which are four rajiform species of small to very small size (i.e. *Rhinobatos echavei*, *Rhinobatos ibericus*, *Ataktobatis variabilis*, and *Vascobatis albaitensis*, designed new when were first described by Cappetta and Corral in 1999). Eight of the species are common to the three geographical areas: *Squalicorax kaupi*, *Squalicorax pristodontus*, *Cretolamna appendiculata*, *Serratolamna serrata*, *Plicatoscyllium lehneri*, *Ganopristis leptodon*, *Coupatezia fallax*, and *Rhombodus binkhorsti*. Three of the species that occur in both Albaina and Northwestern Europe are lacking in Africa: *Odontaspis bronni*, *Carcharias* aff. *gracilis*, and *Palaeogaleus faujasi*). Moreover, it has been shown that two of the species, for a long time considered as northern European, reached northern Iberia: *Palaeogaleus faujasi* and *Odontaspis bronni*. Finally, five of the species cooccurring in both Morocco and northern Iberia did not reached North European latitudes: *Carcharias heathi*, *Rhombodus andrieusi*, *Plicatoscyllium lehneri*, *Dalpiazia stromeri*, and *Ganopristis leptodon*.

- The Simpson's (1969) coefficient (SC) was used to identify the faunal similarities between the pairs of comparison Albaina/Morocco and Albaina/Northern Europe, obtaining in both cases the identical numeric value = 55.5.

- The aggregate tooth number of elasmobranchs belonging to the orders Orectolobiformes, Carcharhiniformes, and Lamniformes at Albaina represents 60.5% of the total assemblage, whereas the teeth assigned to Rajiformes plus Myliobatiformes make up 39.5% of the total sample. Such figures are 47% and 45% respectively in the Maastrichtian of Morocco (Cappetta and Corral, 1999).

- The elasmobranch association from Albaina is composed of a mixture of faunal components from two different ecological habitats (i.e. active swimming forms and bottom dwelling species), living under normal shallow marine conditions. It is noteworthy that the most common shark species are epipelagic neritic forms: *Carcharias heathi*, *Serratolamna serrata*, and *Squalicorax kaupi*. The former two are considered to be ichthyophagous/teuthyophagous in terms of feeding habits, while the latter is a generalist-opportunistic predator. The other more frequently faunal component is the bottom-dweller batoid *Rhombodus binkhorsti*, which is equipped with a durophagous dentition suitable for feeding on crustaceans, echinoids, and molluscs. The relative abundance in Albaina of fossil elements belonging to the suborders Rhinobatoidei and Sclerorhynchoidei, whose living members mainly inhabit warm-temperate to subtropical waters, contrasts with their scarce representation in other Northwestern European deposits (e.g. in the Belgian, Dutch, and German basins), thus indicating, presumably, that water temperature was warmer in Albaina settings. The assemblage also includes

small-sized teeth of the species *Cretolamna appendiculata* and *Squalicorax kaupi*. They are assigned to juvenile shark individuals, which in modern environments are most frequently found in shallow-water nursery areas, thus suggesting nearshore marine conditions for Albaina (Cappetta and Corral, 1999).

- Biostratigraphically, the TF at Albaina is upper Maastrichtian (*Menuites fresvillensis* zone). This formation is informally divided into lower, middle, and upper subunits. The bioclastic nankin-type limestone of the middle subunit (i.e. lithofacies LF-II) includes the taxa *Squalicorax pristodontus*, *Odontaspis bronni*, *Serratolamna serrata*, *Plicatoscyllium lehneri*, *Palaeogaleus faujasi*, *Dalpiazia stromeri*, *Ganopristis leptodon*, *Coupatetzia fallax*, *Rhombodus binkhorsti*, and *Rhombodus andriesi*, which are considered typical Maastrichtian. The presence of the species *Rhombodus andriesi* is in favour of a late – but not latest – Maastrichtian age, according to Cappetta and Corral (1999). Moreover, this subunit includes a mollusc faunule with baculitid ammonite material considered to be late Maastrichtian.

- The shark tooth collection from the upper part of the POF (Entzia-I and Entzia-II sites) is the poorest of the three Maastrichtian selachian accumulations in terms of species diversity and abundance. These shark faunule is typified by the anacoracids *Squalicorax kaupi* and *Squalicorax pristodontus* and the odontaspidid *Carcharias heathi*, which are thought to inhabit warm temperate, inshore epipelagic seas (littoral zone). Based on the known findings, *Squalicorax pristodontus* was the largest marine predator occurring in this area.

- A late Maastrichtian age for the deposits of the POF is well supported by the ammonites *Baculites anceps*, *Hoploscaphites constrictus*, *Menuites fresvillensis*, and *Pseudophyllites indra*.



REFERENCES



REFERENCES

A

- Adán de Yarza, R., 1885. Descripción Física y Geológica de la Provincia de Álava. Memorias de la Comisión del Mapa Geológico de España. Imprenta y fundición de Manuel Tello, Madrid, 176 pp.
- Adkins, W.S., 1929. Some Upper Cretaceous Taylor ammonites from Texas. *University of Texas Bulletin* 2901, 203–211.
- Adolfssen, J.S., Milàn, J., Friedman, M., 2017. Review of the Danian vertebrate fauna of southern Scandinavia. *Bulletin of the Geological Society of Denmark* 65, 1–23.
- Adolfssen, J.S., Ward D.J., 2014. Crossing the boundary: an elasmobranch fauna from Stevns Klint, Denmark. *Palaeontology* 57(3), 591–629.
- Adolfssen, J.S., Ward, D.J., 2015. Neoselachians from the Danian (early Paleocene) of Denmark. *Acta Palaeontologica Polonica* 60(2), 313–338.
- Agassiz, L., 1833–1843. Recherches sur les poissons fossiles, Volume 3. Imprimerie de Petit-pierre, Neuchâtel et Soleure, 390 + 32 pp.
- Al Maleh, A.K., Bardet, N., 2003. Découverte de niveaux phosphatés associés à des restes de vertébrés dans les dépôts carbonatés du Coniacien–Santonien du Jabal Abtar: épisode précoce de la phosphatogenèse sénonienne des Palmyrides (Syrie centrale). *Comptes Rendus Géosciences* 335, 391–400.
- Albers, H., Weiler, W., 1964. Eine fischfauna aus der oberen Kreide von Aachen und neuer funde von Fischresten aus dem Maestricht des angrenzenden belgisch-holländischen Raumes. *Neues Jahrbuch für Geologie und Paläontologie - Abhandlungen* 120(1), 1–33.
- Alcaydé, G., 1990. Carte géologique de la France à 1/50000, Châtillon-sur-Indre (516). Bureau de recherches géologiques et minières, Orléans. Notice explicative par Alcaydé, G. (1990), 37 pp.
- Alonso, J., 1986. El Cretácico Superior de la Sierra de Entzia. I-Estratigrafía. *Estudios del Instituto Alavés de la Naturaleza* 1, 9–33.
- Alonso, J., 1987. El Cretácico Superior de la Sierra de Entzia. II-Bioestratigrafía y Taxonomía. *Estudios del Instituto Alavés de la Naturaleza* 2, 29–90.
- Alonso-Zarza, A.M., Armenteros, I. et al., 2002. Tertiary, in: Gibbons, W., Moreno, T. (Eds), *The Geology of Spain*. The Geological Society, London, pp. 293–334.

- Amalfitano, J., Giusberti, L., Dalla Vecchia, F.M., Kriwet, J., 2016. First skeletal remains of the giant sawfish *Onchosaurus* (Neoselachii, Sclerorhynchiformes) from the Upper Cretaceous of northeastern Italy. *Cretaceous Research* 69 (2017), 124–135.
- Amaral, W.W., 1994. Microscopic preparation, in: Leiggi, P., May, P. (Eds), *Vertebrate Paleontological Techniques*, Volume 1. Cambridge University Press, Cambridge, pp. 129–140.
- Amiot, M., 1982. El Cretácico Superior de la Región Navarro-Cántabra, in: *El Cretácico de España*. Universidad Complutense, Madrid, pp. 88–111.
- Amiot, M., 1983a. L'évolution transgressive au cours du Coniacien-Santonien inférieur dans les parties occidentale et médiane du domaine, in: Institut des Sciences de la Terre (Ed.), *Vue sur le Crétacé basco-cantabrique et nord-ibérique. Une marge et son arrière-pays, ses environnements sédimentaires*. Mémoires Géologiques de l'Université de Dijon 9, pp. 131–132.
- Amiot, M., 1983b. La Mégaséquence régressive du Sénonien. Effacement Graduel du Domaine Navarro-Cantabre, in: Institut des Sciences de la Terre (Ed.), *Vue sur le Crétacé basco-cantabrique et nord-ibérique. Une marge et son arrière-pays, ses environnements sédimentaires*. Mémoires Géologiques de l'Université de Dijon 9, pp. 134–136.
- Amiot, M., Floquet, M., Mathey, B., 1983. Relation entre les trois domaines de sédimentation du Crétacé supérieur, in: Institut des Sciences de la Terre (Ed.), *Vue sur le Crétacé basco-cantabrique et nord-ibérique. Une marge et son arrière-pays, ses environnements sédimentaires*. Mémoires Géologiques de l'Université de Dijon 9, pp. 169–180.
- Amon, E.O., Blueford, J.R., De Wever, P., Zhelezko, V.I., 1997. An essay on regional geology and stratigraphy of the Upper Cretaceous deposits of southern Urals territories. *Geodiversitas* 19(2), 293–317.
- Anna, L.O., 2009. Geologic assessment of undiscovered oil and gas in the Powder River Basin Province: U.S. Geological Survey Digital Data Series DDS-69-U, 93 pp.
- Antunes, M.T., Cappetta H., 2002. Sélaciens du Crétacé (Albien-Maastrichtien) d'Angola. *Palaontographica A* 264 (5–6), 85–146.
- Applegate, S.P., 1965. Tooth terminology and variation in sharks with special reference to the sand shark, *Carcharias taurus* Rafinesque. *Contributions in Science*, Los Angeles County Museum 86, 18 pp.
- Applegate, S.P., 1970. The vertebrate fauna of the Selma formation of Alabama, Part VIII, The Fishes. *Fieldiana: Geology Memoirs* 3(8), 385–433.
- Applegate, S.P., 1972. A revision of the higher taxa of orectolobids. *Publication of the Marine Biological Association of India* 14, 743–751.
- Applegate, S.P., Espinosa-Arrubarrena, L., 1996. The fossil history of *Carcharodon* and its possible ancestor, *Cretolamna*: a study in tooth identification, in: Klimley, A.P., Ainley, D. (Eds), *Great White Sharks. The biology of *Carcharodon carcharias**. Academic Press, San Diego, pp. 19–36.
- Arambourg, C., 1935. Note préliminaire sur les vertébrés fossiles des phosphates du Maroc. *Bulletin de la Société Géologique de France* 5, 413–440.
- Arambourg, C., 1940. Le groupe des Ganopristinés. *Bulletin de la Société Géologique de France* 10(5), 127–147.
- Arambourg, C., 1952. Les vertébrés fossiles des gisements de phosphates (Maroc-Algérie-Tunisie). *Notes et Mémoires du Service Géologique du Maroc* 92, 1–372.
- Arambourg, C., Joleaud, L., 1943. Vertébrés fossiles du Bassin du Niger. *Bulletin de la Direction des Mines de l'Afrique Occidentale Française* 7, 27–84.

- Arz, J.A., Molina, E., 2002. Bioestratigrafía y Cronoestratigrafía con foraminíferos planctónicos del Campaniense superior y Maastrichtiense de latitudes templadas y subtropicales (España, Francia y Tunicia). *Neues Jahrbuch für Geologie und Paläontologie - Abhandlungen* 224(2), 161–195.
- Astibia, H., García-Garmilla, F., Orue-Etxebarria, X., Rodríguez-Lázaro, J., Buscalioni, A.D., Sanz, J.L., Jiménez-Fuentes, E., 1987. The Cretaceous-Tertiary boundary in a sector of the south limb of the Miranda-Treiviño synclinal: the first appearance of Chelonia and Archosauria in the Basque Country. *Cretaceous Research* 8, 15–27.
- Astibia, H., Buffétau, E., Buscalioni, A.D., Cappetta, H., Corral, C., Estes, R., García-Garmilla, F., Jaeger, J.J., Jiménez-Fuentes, E., Le Loeuff, J., Mazin, J.M., Orue-Etxebarria, X., Pereda-Suberbiola, J., Powell, J.E., Rage, J.-C., Rodríguez-Lázaro, J., Sanz, J.L., Tong, H., 1990. The fossil vertebrates from Albaina, Condado de Treiviño, Northern Spain (Basque Country, Spain); new evidence on the composition and affinities of the Late Cretaceous continental faunas of Europe. *Terra Nova* 2, 460–466.
- Astibia, H., del Valle de Lersundi, J., Murelaga, X., Serra-Kiel, J. (Coords), 1996. Homenaje a Máximo Ruiz de Gaona, naturalista y paleontólogo (1902–1971). Príncipe de Viana. Suplemento de Ciencias 14/15, 206 pp.
- Astibia, H., Corral, J.C., Murelaga, X., Orue-Etxebarria, X., Pereda-Suberbiola, X. (Coords), 1999a. Geology and Palaeontology of the Upper Cretaceous vertebrate-bearing beds of the Laño quarry (Basque-Cantabrian Region, Iberian Peninsula). *Estudios del Museo de Ciencias Naturales de Álava* 14(Número especial 1), 1–380.
- Astibia, H., Corral, J.C., Murelaga, X., Orue-Etxebarria, X., Pereda Suberbiola, X., 1999b. Introduction. Laño discovery. Palaeontological and geocultural setting. *Estudios del Museo de Ciencias Naturales de Álava* 14(Número especial 1), 7–12.
- Atabekian, A.A., Akopian, V.T., 1969. Late Cretaceous ammonites of the Armenian SSR (Pachydiscidae). *Izvestiya Akademii Nauk Armyankoi SSR Nauki o Zemle* 6, 3–20 [in Russian; not seen].
- Averianov, A.O., 1997. Additions to the selachian fauna of the Russian Cretaceous. 2. A new species of *Paracorax* Cappetta, 1977 (Chondrichthyes: Anacoracidae). *Zoosystematica Rossica* 6(1/2) 1996, 315–316.
- Averianov, A., Nesson, L., 1995. A new Cretaceous mammal from the Campanian of Kazakhstan. *Neues Jahrbuch für Geologie und Paläontologie - Monatshefte* 1995 H2, 65–74.
- Averianov, A., Popov, E., 1995. A new species of chimaeroid fish from the Upper Cretaceous of the Saratov Region, Russia. *Palaeontology* 38(3), 659–664.
- Azkarate, A., 1988. Arqueología cristiana de la antigüedad tardía en Álava, Guipúzcoa y Vizcaya. Diputación Foral de Álava, Servicio de Publicaciones, 586 pp.
- Azkarate, A., Solaun, J.L., 2008. Excavaciones arqueológicas en el exterior de los conjuntos rupestres de Las Gobas (Laño, Burgos), *Archivo Español de Arqueología* 81, 133–149.

B

- Baceta, J.I., 1996. El Maastrichtiense superior, Paleoceno e Ilerdiense basal de la Región Vasco-Cantábrica: secuencias deposicionales, facies y evolución paleogeográfica. Doctoral Thesis, Universidad del País Vasco/EHU, Leioa, 372 pp.
- Baceta, J.I., Pujalte, V., Orue-Etxebarria, X., 1999. The vertebrate fossil-bearing sites of the Laño quarry (Basque Cantabrian Region): stratigraphical and palaeogeographical context. *Estudios del Museo de Ciencias Naturales de Álava* 14(Número especial 1), 13–28.

- Balaram, V., 1996. Recent trends in the instrumental analysis of rare earth elements in geological and industrial materials. *Trends in Analytical Chemistry* 15, 475–482.
- Banerjee, S., Udita, B., Kanchan, P., Mena, S.S., 2016. Compositional variability of glauconites within the Upper Cretaceous Karai Shale Formation, Cauvery Basin, India: Implications for evaluation of stratigraphic condensation. *Sedimentary Geology* 331, 12–29.
- Banner, F., Blow, W., 1960. Some primary types of species belonging to the superfamily Globigerinaceae. *Contributions from the Cushman Foundation for Foraminiferal Research* 11(1), 1–41.
- Bardet, N., Pereda Suberbiola, X., 1996. Las faunas de reptiles marinos del Cretácico final de Europa (margen norte del Tétis mediterráneo). *Revista Española de Paleontología* 11, 91–99.
- Bardet, N., Corral, J.C., Pereda, J., 1993. Primeros restos de reptiles marinos en el Cretácico superior de la Cuenca Vasco-Cantábrica. *Estudios del Museo de Ciencias Naturales de Álava* 8, 27–35.
- Bardet, N., Corral, J.C., Pereda Suberbiola, X., 1997. Les mosasaures (Squamata) du Crétacé supérieur du Bassin Basco-Cantabrique. *Geobios - Mémoire spécial* 20, 19–26.
- Bardet, N., Jagt, J.W.M., Kuypers, M.M.M., Dortangs, R.W., 1998. Shark tooth marks on a vertebra of the mosasaur *Plioplatecarpus marsbi* from the Late Maastrichtian of Belgium. *Natuurhistorisch Genootschap in Limburg* 41, 52–55.
- Bardet, N., Corral, J.C., Pereda Suberbiola, X., 1999. Marine reptiles from the uppermost Cretaceous of the Laño quarry (Iberian Peninsula). *Estudios del Museo de Ciencias Naturales de Álava* 14(Número especial 1), 373–380.
- Bardet, N., Cappetta, H., Pereda Suberbiola, X., Mouty, M., Al Maleh, A.K., Ahmad, A.M., Khata, O., Gannoum, N., 2000. The marine vertebrate faunas from the Late Cretaceous phosphates of Syria. *Geological Magazine* 137(3), 269–290.
- Bardet, N., Pereda Suberbiola, X., Corral, J.C., 2006. A tylosaurine Mosasauridae (Squamata) from the Late Cretaceous of the Basque-Cantabrian Region. *Estudios Geológicos* 62(1), 213–218.
- Bardet, N., Houssaye, A., Rage, J.-C., Pereda-Suberbiola, X., 2008. The Cenomanian-Turonian (late Cretaceous) radiation of marine squamates (Reptilia): the role of the Mediterranean Tethys. *Bulletin de la Société Géologique de France* 179, 605–622.
- Bardet, N., Pereda Suberbiola, X., Corral, J.-C., Baceta, J.I., Torres, J.A., Botantz, B., Martin, G., 2012. A skull fragment of the mosasaurid *Prognathodon* cf. *sectorius* from the Late Cretaceous of Navarre (Basque-Cantabrian Region). *Bulletin de la Société Géologique de France* 183(2), 117–121.
- Bardet, N., Martin, G., Corral, J.C., Pereda Suberbiola, X., Astibia, H., 2013. New mosasaurid teeth (Reptilia: Squamata) from the Maastrichtian of Albaina (Laño Quarry, Condado de Treviño). *Spanish Journal of Palaeontology* 28(1), 69–78.
- Bardet, N., Houssaye, A., Vincent, P., Pereda Suberbiola, X., Amaghaz, M., Jourani, E., Meslouh, S., 2015. Mosasaurids (Squamata) from the Maastrichtian Phosphates of Morocco: biodiversity and palaeoecology based on tooth morphoguilds. *Gondwana Research* 27(3), 1068–1078.
- Barnolas, A., Pujalte, V., 2004. Cordillera Cantábrica: Rasgos distintivos y división, in: Vera, J.A. (Ed.), *Geología de España*. SGE-IGME, Madrid, pp. 237–241.
- Barroso Barcenilla, F., 2004. Acanthoceratidae y zonación de ammonites del Cenomaniense superior y del Turoniense inferior en el área de Puente de Eja, Cuenca Vasco-Cantábrica, España. *Coloquios de Paleontología* 54, 83–114.

- Barroso-Barcenilla, F., Goy, A., 2007. Revision and new data of the ammonite family Pseudotisotiidae in the Iberian Trough, Spain. *Geobios* 40, 455–487.
- Basse, E., 1947. Les peuplements Malagaches de *Barroisicerias*. (Revision du genre *Barroisicerias* De Gross.) *Paléontologie de Madagascar* 26. *Annales Paleontology* 22: 97–190 (1–82).
- Bataller, J.R., 1960. Los vertebrados del Cretácico español. *Notas y Comunicaciones del Instituto Geológico y Minero de España* 60, 141–164.
- Beavan, N.R., 1995. A marine fossil assemblage from the Foremost Formation (Cretaceous, Campanian), southern Alberta, and an evaluation of North American Cretaceous elasmobranch biostratigraphy. M.Sc. Thesis, University of Calgary, 162 pp.
- Beavan, N.R., Russell, A.P., 1999. An elasmobranch assemblage from the terrestrial-marine transitional Lethbridge Coal zone (Dinosaur Park Formation; upper Campanian), Alberta, Canada. *Journal of Paleontology* 73, 494–503.
- Becker, M.A., Chamberlain, J.A. Jr., Terry, D.O. Jr., 2004. Chondrichthyans from the Fairpoint Member of the Fox Hills Formation (Maastrichtian), Meade County, South Dakota. *Journal of Vertebrate Paleontology* 24(4), 780–793.
- Becker, M.A., Chamberlain, J.A. Jr., Wolf, G.E., 2006. Chondrichthyans from the Arkadelphia formation (Upper Cretaceous: Upper Maastrichtian) of Hot Spring County, Arkansas. *Journal of Paleontology* 80(4), 700–716.
- Bell, G.L. Jr., 1997. A phylogenetic revision of North American and Adriatic Mosasauoidea, in: Callaway, J.M., Nicholls E.L. (Eds), *Ancient Marine Reptiles*. Academic Press, San Diego, pp. 293–332.
- Bennett, E.T., 1830. Class Pisces, in: Raffles, S., *Memoir of the life and public services of Sir Thomas Stamford Raffles, F.R.S. &c. John Murray, London*, pp. 686–694.
- Benton, M., 2004. *Vertebrate Paleontology*, 3rd edition. Blackwell, Oxford UK, 455 pp.
- Benton, M., 2015. *Vertebrate Palaeontology*, 4th edition. Wiley-Blackwell, Oxford UK, 480 pp.
- Berg, L.S., 1940. Classification of fishes, both recent and fossil. *Transactions of the Institute of Zoology, Academy of Sciences of the URSS* 5, 85–517 [in Russian].
- Berg, L.S., 1958. *System der Rezenten und Fossilen Fischartigen und Fische*. Deutscher Verlag der Wissenschaft, Berlin, 310 pp.
- Bernárdez, E., 2002. Los dientes de seláceos del Cretácico de la depresión central asturiana. Doctoral Thesis, University of Oviedo, Oviedo, 1–476.
- Berreteaga, A., 2008. Estudio estratigráfico, sedimentológico y paleontológico de los yacimientos con fósiles de vertebrados del Cretácico final de la Región Vasco-Cantábrica. Doctoral Thesis, Universidad del País Vasco/EHU, Leioa, 410 pp.
- Berreteaga, A., Badiola, A., Astibia, H., Pereda-Suberbiola, X., Elorza, J., Etxebarria, N., Álvarez, A., 2004. Estudio geoquímica de fósiles de vertebrados de varias localidades del Cretácico Superior y Paleógeno de los Pirineos occidentales. *Geogaceta* 36, 167–170.
- Berreteaga, A., Pereda Suberbiola, X., Floquet, M., Olivares, M., Etxebarria, N., Iriarte, E., Badiola, A., Elorza, J., Astibia, H., 2008a. Datos sedimentológicos y tafonómicos de enclaves finicretácicos con fósiles de vertebrados de la Formación Sobrepeña (Burgos, Región Vasco-Cantábrica). *Geo-Temas* 10, 1277–1280.
- Berreteaga, A., Pereda Suberbiola, X., Floquet, M., Iriarte, E., Astibia, H., 2008b. Geological setting of the Late Cretaceous (Campanian-Maastrichtian) vertebrate fossil-bearing sites from the southern Basque-Cantabrian Region (Iberian Peninsula). 33rd International Geological Congress (Oslo), Abstracts, HPP1363P.

- Berreteaga, A., Pereda Suberbiola, X., Corral, J.C., Poyato-Ariza, F.J., Floquet, M., Iriarte, E., Bardet, B., López-Horge, M., Badiola, A., Astibia, H., 2010. A new marine vertebrate fauna from the latest Cretaceous of Quintanilla la Ojada (Burgos, Basque-Cantabrian Region). STRATI 2010, 4th French Congress on Stratigraphy, UPMC, Paris, 34–35.
- Berreteaga, A., Poyato-Ariza, F.J., Pereda Suberbiola, X., 2011. A new actinopterygian fauna from the latest Cretaceous of Quintanilla la Ojada (Burgos, Spain). *Geodiversitas* 33(2), 285–301.
- Biddle, J.-P., Landemaine, O., 1988. Contribution à l'étude des sélaciens du Crétacé du Bassin de Paris. Découverte de quelques nouvelles espèces associées à une faune de type wealdien dans le Barrémien supérieur (Crétacé inférieur) des environs de Troyes (Aube). *Musée de Saint-Dizier, Saint-Dizier, Cahiers* 2, 1–22.
- Bieda, F., 1933. Sur les Spongiaires siliceux du Senonien des environs de Cracovie. *Rocznik Polskiego Towarzystwa Geologicznego* 9, 1–41.
- Bitner, M.A., Pisera, A., 1979. Brachiopods from the Upper Cretaceous chalk of Mielnik (Eastern Poland). *Acta Geologica Polonica* 29(1), 67–88.
- Blainville, H.M.D. de, 1816. Prodrome d'une distribution systématique du règne animal. *Bulletin des Sciences par la Société Philomathique de Paris* 8, 113–124.
- Błaszkiwicz, A., 1980. Campanian and Maastrichtian ammonites of the Middle Vistula River valley, Poland: a stratigraphic-paleontological study. *Prace Instytutu Geologicznego* 92, 1–63.
- Bogan, S., Agnolin, F.L., 2010. Primera ictiofauna marina del Cretácico Superior (Formación Jaguel, Maastrichtiano) de la provincia de Río Negro, Argentina. *Papéis Avulsos de Zoologia* 50(12), 175–188.
- Böhm, J., 1907. Über *Inoceramus Cripsi* Mant. *Zeitschrift der Deutschen geologischen Gesellschaft* 59 (Monatsberichte der Deutschen geologischen Gesellschaft 4), 113–114.
- Bolli, H., 1951. The Genus *Globotruncana* in Trinidad, B.W.I.: Notes on Occurrence, Nomenclature and Relationships between Species. *Journal of Paleontology* 25(2), 187–199.
- Bonaparte, C.L., 1838. *Selachorum Tabula analytica*. *Nuovi Annali della Scienze Naturali, Bologna* 2, 195–214.
- Bonnaterre, J.P., 1788. *Tableau encyclopédique et méthodique des trois règnes de la nature. Ichthyologie*. Panckoucke, Paris, 215 pp.
- Bor, T.J., 1983. A new species of *Rhinobatos* (Elasmobranchii, Batomorphii) from the upper Maastrichtian of the Netherlands and Belgium. *Geologie en Mijnbouw* 62, 297–300.
- Botella, H., Donoghue, P.C.J., Martínez-Pérez, C., 2009. Enameloid microstructure in the oldest known chondrichthyan teeth. *Acta Zoologica* 90 (Suppl. 1), 103–108.
- Bourdon, J., Wright, K., Lucas, S.G., Spielmann, J.A., Pence, R., 2011. Selachians from the Upper Cretaceous (Santonian) Hosta Tongue of the Point Lookout Sandstone, Central New Mexico. *New Mexico Museum of Natural History and Science Bulletin* 52, 1–52.
- Braillon, J., 1973. Utilisation de techniques chimiques et physiques dans le dégagement et le triage des fossiles de vertébrés. *Bulletin du Muséum National d'Histoire Naturelle 3e série* 176, 141–166.
- Breder, C.M., 1952. On the utility of the saw of the sawfish. *Copeia* 1952, 90–91.
- Brett, C.E., 1990. Predation. Marine, in: Briggs, D.E.G., Crowther, P.R. (Eds), *Palaeobiology: A Synthesis*. Blackwell Scientific Publications, Oxford, pp. 368–372.
- Bridge, J., Demicco, R., 2008. *Earth Surface Processes, Landforms and Sediment Deposits*. Cambridge University Press, Cambridge, UK, 815 pp.
- Briggs, J.C., 1995. *Global Biogeography. Developments in Paleontology and Stratigraphy*. Elsevier, New York, 452 pp.

- Brönnimann, P., 1952. Globigerinidae from the Upper Cretaceous (Cenomanian–Maestrichtian) of Trinidad, B.W.I. *Bulletin of American Paleontology* 34(140), 1–70.
- Bruggen, W. van der, Quack-Potteboom, E.Z.M., Odé, H., 1993. Einige opmerkingen over de Horizont van Lichtenberg in de groeve ENCI en de aangetroffen kraakbeenvissenfauna. *Grondboor en Hamer* 6, 162–166.
- Brunton, C.H., Besterman, T.P., Cooper, J.A., 1985. Guidelines for the curation of geological materials. Geological Society of London, Miscellaneous Paper 17, 1–182.
- Buckley, L.G., McCrea, R.T., 2009. The sodium hypochlorite solution for the Removal of lichen from vertebrate track surfaces. *Ichnos* 16, 230–234.
- Budinoff, L., 1991. An osteological analysis of the human burials recovered from Maisabel: An Early Ceramic Site on the North Coast of Puerto Rico, in: Robinson, L.S. (Ed.), *Proceedings of the 12th Congress of the International Association for Caribbean Archaeology*. A.I.A.C. Martinique, pp. 117–134.
- Buen, F. de, 1926. Catálogo ictiológico del Mediterráneo español y de Marruecos recopilando lo publicado sobre peces de las costas mediterráneas y próximas del Atlántico (Mar de España). Resultados de las Campañas realizadas por acuerdos internacionales, 2. Instituto Español de Oceanografía, Madrid, 222 pp.
- Burst, J.F., 1958. Glauconite pellets; their mineral nature and applications to stratigraphic interpretations. *Bulletin of American Association of Petroleum Geologists* 42, 310–327.

C

- Calderón, S., 1875. Guía del Geólogo y Mineralogista Expedicionario en España. Reseña geológica de la provincia de Álava. *Estudios Geológicos de España*. Primera parte. Imprenta Gregorio Juste, Madrid, 31 pp.
- Callahan, W.R., Mehling, C.M., Denton, R.K. Jr., Parris, D.C., 2014. Vertebrate paleontology and stratigraphy of the Late Cretaceous Holmdel Park Site, Monmouth County, New Jersey. *Dakoterra* 6, 163–169.
- Calzada, S., Pocovi, A., 1980. Braquiópodos senonienses de la sierra del Mont-Roig (Prepirineo de Lérida). *Boletín de la Real Sociedad Española de Historia Natural (Secc. Geología)* 78, 5–19.
- Cappetta, H., 1972. Les poissons crétacés et tertiaires du bassin des Iullemeden (République du Niger). *Palaeovertebrata* 5(5), 179–251.
- Cappetta, H., 1973. Selachians of the Carlile Shale (Turonian) of South Dakota. *Journal of Paleontology* 47(3), 504–514.
- Cappetta, H., 1974. Sclerorhynchidae nov. fam., Pristidae et Pristiophoridae: un exemple de parallélisme chez les sélaciens. *Comptes Rendus de l'Académie des Sciences, Paris* 278, 225–228.
- Cappetta, H., 1975a. Sélaciens et Holocéphale du Gargasien de la région de Gargas (Vaucluse). *Géologie méditerranéenne* 2(3), 115–134.
- Cappetta, H., 1975b. *Ptychotrygon vermiculata* nov. sp., sélacien nouveau de Campanien du New Jersey (U.S.A.). *Comptes Rendus Sommaires de la Société Géologique de France* fasc. 5, 164–166.
- Cappetta, H., 1980a. Les sélaciens du Crétacé Supérieur du Liban. II: Batoïdes. *Palaeontographica A* 168(5–6), 149–229.
- Cappetta, H., 1980b. Modification du statut générique de quelques espèces de sélaciens crétacés et tertiaires. *Palaeovertebrata* 10(1), 29–42.
- Cappetta, H., 1981. Sur la découverte des genres *Ischyrrhiza* et *Ptychotrygon* (Selachii,

- Batomorphii) dans le Crétacé supérieur de Vendée (France). *Geobios* 14(6), 807–812.
- Cappetta, H., 1982. Revision de *Cestracion duponti* Winkler, 1874 (Selachii, Batomorphii) du Bruxellien de Woluwe-Saint-Lambert (Eocene moyen de Belgique). *Mededelingen van de Werkgroep voor Tertiaire en Kwartaire Geologie* 19, 113–125.
- Cappetta, H., 1986. Types dentaires adaptatifs chez les sélaciens actuels et postpaléozoïques. *Palaeovertebrata* 16, 57–76.
- Cappetta, H., 1987. Chondrichthyes II. Mesozoic and Cenozoic Elasmobranchii, in: Schultze, H.-P. (Ed.), *Handbook of Paleichthyology* vol. 3B. Gustav Fischer Verlag, Stuttgart, 193 pp.
- Cappetta, H., 1991. Découverte de nouvelles faunes de sélaciens (Neoselachii) dans les phosphates maastrichtiens de la Mer Rouge, Égypte. *Münchner Geowissenschaftliche Abhandlungen A* 19, 17–56.
- Cappetta, H., 1992. Nouveaux Rhinobatoidei (Neoselachii, Rajiformes) à denture spécialisée du Maastrichtien du Maroc. Remarques sur l'évolution dentaire des Rajiformes et des Myliobatiformes. *Neues Jahrbuch für Geologie und Paläontologie – Abhandlungen* 187(1), 31–52.
- Cappetta, H., 2006. Elasmobranchii Post-Triadici, (Index specierum et generum), in: Riegraf, W. (Ed.), *Fossilium Catalogus, I: Animalia*, 142. Backhuys Publishers, Leiden, 472 pp.
- Cappetta, H., 2012. Chondrichthyes (Mesozoic and Cenozoic Elasmobranchii: teeth), in: Schultze, H.-P. (Ed.), *Handbook of Paleichthyology* 3E. Verlag F. Pfeil, Stuttgart, 512 pp.
- Cappetta, H., Case, G.R., 1975a. Sélaciens nouveaux du Crétacé du Texas. *Geobios* 8(4), 303–307.
- Cappetta, H., Case, G.R., 1975b. Contribution à l'étude des sélaciens du groupe Monmouth (Campanien-Maastrichtien) du New Jersey. *Palaeontographica A* 151(1–3), 1–46.
- Cappetta, H., Case, G.R., 1999. Additions aux faunes de sélaciens du Crétacé du Texas (Albien supérieur-Campanien). *Palaeo Ichthyologica* 9, 5–111.
- Cappetta, H., Corral, J.C., 1999. Upper Maastrichtian selachians from the Condado de Treviño (Basque-Cantabrian Region, Iberian Peninsula). *Estudios del Museo de Ciencias Naturales de Álava* 14(Número especial 1), 339–372.
- Cappetta, H., Odin, G.S., 2001. Les sélaciens du Campanien-Maastrichtien de Tercis les Bains (SO France), in: Odin G.S. (Ed.), *The Campanian - Maastrichtian Boundary: characterisation and correlation from Tercis (Landes, SW France) to Europe and other continents. Developments in Palaeontology and Stratigraphy* 19, Elsevier Science Publishers, Amsterdam, pp. 645–651.
- Cappetta, H., Pfeil, F., Schmidt-Kittler, N., 2000. New biostratigraphical data on the marine Upper Cretaceous and Palaeogene of Jordan. *Newsletters on Stratigraphy* 38(1), 81–95.
- Cappetta, H., Adnet, S., Akkrim, D., Amalik, M., 2014a. New *Squalicorax* species (Neoselachii: Lamniformes) from the Lower Maastrichtian of Ganntour phosphate deposit, Morocco. *Palaeovertebrata* 38(2), 13 pp., (online publication).
- Cappetta, H., Bardet, N., Pereda Suberbiola, X., Adnet, S., Akkrim, D., Amalik, M., Benabdallah, A., 2014b. Marine vertebrate faunas from the Maastrichtian phosphates of Benguerir (Ganntour Basin, Morocco): Biostratigraphy, palaeobiogeography and palaeoecology. *Palaeogeography, Palaeoclimatology, Palaeoecology* 409, 217–238.
- Caron, M., 1985. Cretaceous planktic foraminifera, in: Bolli, H.M., Saunders, J.B., Perch-Nielsen, K. (Eds), *Plankton stratigraphy Volume 1*. Cambridge University Press, Cambridge, pp. 17–86.
- Carreras Suárez, F, Ramírez del Pozo, J., 1978. Memoria explicativa de la hoja nº 139 (Eulate) del

- Mapa Geológico de España, segunda serie. E 1:50 000. IGME, Madrid, 36 pp.
- Carrillo, J.D.B., Ayala, R., Chávez, E.O.A., González, G.B., 2008. Registro de (Elasmobranchii: Serratolamnidae) en el Cretácico Superior (maastrichtiense) de los andes venezolanos. *Geominas* 36(47), 160–163.
- Carroll, R.L., 1988. *Vertebrate paleontology and evolution*. Freeman and Company, New York, 698 pp.
- Carsey, D.O., 1926. Foraminifera of the Cretaceous of Central Texas. *University of Texas Bulletin* 2612, 56 pp.
- Case, G.R., 1978. A new selachian fauna from the Judith River Formation (Campanian) of Montana. *Palaeontographica A* 160, 176–205.
- Case, G.R., 1979. Additional records from the Judith River Formation (Campanian) of Montana. *Geobios* 12(2), 223–233.
- Case, G.R., 1987. A new Selachian Fauna from the Late Campanian of Wyoming (Teapot Sandstone Member, Mesaverde Formation, Big Horn Basin). *Palaeontographica A* 197, 1–37.
- Case, G.R., Cappetta, H., 1997. A new selachian fauna from the late Maastrichtian of Texas (Upper Cretaceous/Navarroan; Kemp Formation). *Münchner Geowissenschaftliche Abhandlungen A* 34, 131–189.
- Case, G.R., Cappetta, H., 2004. Additions to the elasmobranch fauna from the Late Cretaceous of New Jersey (lower Navesink Formation, early Maastrichtian). *Palaeo-vertebrata*, 33(1–4), 1–16.
- Case, G.R., Schwimmer, D.R., 1988. Late Cretaceous fish from the Blufftown Formation (Campanian) in Western Georgia. *Journal of Paleontology* 62(2), 290–301.
- Case, G.R., Borodin, P.D., Leggett, J.J., 2001a. Fossil selachians from the New Egypt Formation (Upper Cretaceous, Late Maastrichtian) of Arneytown, Monmouth County, New Jersey. *Palaeontographica A* 261(4–6), 113–124.
- Case, G.R., Schwimmer, D.R., Borodin, P.D. and Leggett, J.J., 2001b. A new selachian fauna from the Eutaw Formation (Upper Cretaceous/Early to Middle Santonian) of Chatahoochee County, Georgia. *Palaeontographica A* 261, 83–102.
- Case, G.R., Cook, T.D., Sadorf, E.M., Shannon, K.R., 2017. A late Maastrichtian selachian assemblage from the Peedee Formation of North Carolina, USA. *Vertebrate Anatomy Morphology Palaeontology* 3, 63–80.
- Casier, E., 1947. Constitution et évolution de la racine dentaire des Euselachii. II. Étude comparative des types. *Bulletin du Musée Royal d'Histoire Naturelle de Belgique* 23, 1–32.
- Casier, E., 1958. Contribution à l'étude des poissons fossiles des Antilles. *Mémoires Suisses de Paléontologie* 74, 1–95.
- Casier, E., 1964. Contributions à l'étude des poissons fossiles de la Belgique. XIII. – Présence de Ganopristinés dans la Glaucionie de Loncée et le Tuffeau de Maestricht. *Institut Royal des Sciences naturelles de Belgique, Bulletin* 40(11), 1–25.
- Cavigelli, J.P., 2009. Micropreparation... one sand grain at a time, in: Brown, M.A., Kane, J.F., Parker, W.G. (Eds), *Methods in fossil preparation: Proceedings of the First Annual Fossil Preparation and Collections Symposium, Petrified Forest national Park*, pp. 41–52.
- Cecca, F., 2002. *Palaeobiogeography of marine fossil invertebrates - concepts and methods*. Taylor & Francis, London, 273 pp.
- Chaney, D.S., 1989. Hand-Held, Mechanical Preparation Tools, in: Feldmann, R.M., Chap-

- man, R.E., Hannibal, J.T. (Eds), Paleotechniques. Paleontological Society Special Publication 4, 186–203.
- Checchia-Rispoli, G., 1933. Di un nuovo genere di ‘Pristidae’ del Cretaceo superiore della Tripolitania. Memorie della Reale Accademia italiana, Classe Scienze Fisiche Matematiche e Naturale 4, 1–6.
- Cicimurri, D.J., 2007. A late Campanian (Cretaceous) selachian assemblage from a classic locality in Florence County, South Carolina. *Southeastern Geology* 45(2), 59–72.
- Cifelli, R.L., Madsen, S.K., Larson, E.M., 1996. Screenwashing and associated techniques for the recovery of microvertebrate fossils, in: Cifelli, R.L. (Ed.), Techniques for recovery and preparation of microvertebrate fossils. Oklahoma Geological Survey Special Publication 96(4), 1–24.
- Cigala-Fulgosi, F., 1990. Predation (or possible scavenging) by a great white shark on an extinct species of bottlenosed dolphin in the Italian Pliocene. *Tertiary Research* 12, 17–36.
- Ciry, R., 1939. Étude géologique d’une partie des provinces de Burgos, Palencia, León et Santander. Thèse à la Faculté de Sciences de l’Université de Paris. Douladoure imprimeurs, Toulouse, 519 pp.
- Clarke, J., Etches, S., 1991. Predation among Jurassic marine reptiles. *Proceedings of the Dorset Natural History Archaeological Society* 113, 202–205.
- Cobban, W.A., Kennedy, W.J., 1992. Campanian *Trachyscaphites spiniger* ammonite fauna in north-east Texas. *Palaeontology* 35(1), 63–93.
- Collignon, M., 1932. Fossiles du Crétacé supérieur du Menabe. *Annales de Paléontologie* 21, 35–87.
- Collignon, M., 1948. Ammonites néocrétacées du Menabe (Madagascar), I - Les Texanitidae. *Annales géologiques du Service des mines, Madagascar* 13, 49–108.
- Collignon, M., 1955. Ammonites néocrétacées du Menabe (Madagascar), II - Les Pachydiscidae. *Annales géologiques du Service des mines, Madagascar* 21, 1–98.
- Compagno, L.J.V., 1973. Interrelationships of living elasmobranchs, in: Greenwood P.H., Miles R.S., Patterson, C. (Eds), Interrelationships of fishes. *Zoological Journal of the Linnean Society* 53 (Supplement), 15–16.
- Compagno, L.J.V., 1977. Phyletic relationships of living sharks and rays. *American Zoologist* 17, 303–322.
- Compagno, L.J.V., 1984a. FAO Species Catalogue. Vol 4 Sharks of the world, an annotated and illustrated catalogue of shark species known to date. Part 1 – Hexanchiformes to Lamniformes. *FAO Fisheries Synopsis* 125 4(1), 1–249.
- Compagno, L.J.V., 1984b. FAO Species Catalogue. Vol 4 Sharks of the world, an annotated and illustrated catalogue of shark species known to date. Part 2 – Carcharhiniformes. *FAO Fisheries Synopsis* 125 4(2), 251–633.
- Compagno, L.J.V., 1988. *Sharks of the order Carcharhiniformes*. Princeton University Press, Princeton, N.J., 486 pp.
- Compagno, L.J.V., 1990. Alternative life-history styles of cartilaginous fishes in time and space. *Environmental Biology of Fishes* 28, 33–75.
- Compagno, L.J.V., 1999a. Systematics and body form, in: Hamlett, W.C. (Ed.), *Sharks, Skates, and Rays: The Biology of Elasmobranch Fishes*. Johns Hopkins University Press, Baltimore, pp. 1–42.
- Compagno, L.J.V., 1999b. Endoskeleton, in: Hamlett, W.C. (Ed.), *Sharks, Skates, and Rays: The Biology of Elasmobranch Fishes*. Johns Hopkins University Press, Baltimore, pp. 69–92.
- Compagno, L.J.V., 2001. *Sharks of the world. An annotated and illustrated catalogue*

- of shark species known to date. Volume 2. Bullhead, mackerel and carpet sharks (Heterodontiformes, Lamniformes and Orectolobiformes). FAO Species Catalogue for Fishery Purposes 1(2), 1–269.
- Compagno, L.J.V., 2008. Pelagic Elasmobranch Diversity, in: Camhi, M.D., Pikitch, E.K., Babcock, E.A. (Eds), *Sharks of the Open Ocean: Biology, Fisheries and Conservation*. Blackwell Science, Oxford, pp. 14–23.
- Compagno, L.J.V., Last, P.R., 1999. Rhinobatidae, Guitarfishes, in: Carpenter, K.E., Niem, V.H. (Eds), *The living marine resources of the Western Central Pacific. Volume 3, Batoid fishes, chimaeras and bony fishes part 1 (Elopidae to Linophrynidae)*. FAO species identification guide for fishery purposes, Rome, pp. 1423–430.
- Converse, H.H., 1989. *Handbook of Paleo-Preparation Techniques*. Florida Paleontological Society Inc., Gainesville, Florida, 109 pp.
- Cook, T.D., Brown, E., Ralrick, P.E., Konishi, T., 2017. A late Campanian Euselachian Assemblage from the Bearpaw Formation of Alberta, Canada: Some Notable Range Extensions. *Canadian Journal of Earth Sciences* 54(9), 973–980.
- Cope, E.D., 1871. Supplement to the ‘Synopsis of the extinct Batrachia and Reptilia of North America’. *Proceedings of the American Philosophical Society* 12, 41–52.
- Coquand, H., 1859. Synopsis des animaux et des végétaux fossiles observés dans la formation crétacée du sud-ouest de la France. *Bulletin de la Société Géologique de France* (2ème serie) 16, 945–1023.
- Corral, J.C., 1996. *Squalicorax pristodontus* (Agassiz 1843), selacio citado por M. Ruiz de Gaona en la Sierra de Urbasa (Navarra). Descripción de nuevo material en Álava. *Príncipe de Viana. Suplemento de Ciencias* 14/15, 125–136.
- Corral, J.C., 2012. Técnicas aplicadas en la preparación de un cráneo cuaternario de *Panthera pardus* (Linneo, 1758) de Ataura (cueva Allekoaitze, Guipúzcoa). *Boletín Geológico y Minero* 123(2), 127–138.
- Corral, J.C., Pereda Suberbiola, X., Bardet, N., 2004. Marcas de ataque atribuidas a un selacio en una vértebra de mosasaurio del Cretácico Superior de Álava (Región Vasco-Cantábrica). *Revista Española de Paleontología* 19(1), 23–32.
- Corral, J.C., Bardet, N., Pereda Suberbiola, X., Arz, J.A., 2011. Depredadores marinos (osteíctios, selacios y mosasaurios) en el Campaniense de la Cuenca Vasco-Cantábrica. *Paleontología i evolució, Memoria especial* 5, 83–87.
- Corral, J.C., Bardet, N., Pereda-Suberbiola, X., Cappetta, H., 2012. First occurrence of the sawfish *Onchosaurus* from the Late Cretaceous of Spain. *Journal of Vertebrate Paleontology* 32(1), 212–218.
- Corral, J.C., Pueyo, E.L., Berreteaga, A., Rodríguez-Pintó, A., Sánchez, E., Pereda-Suberbiola, X., 2015a. Magnetostratigraphy and lithostratigraphy of the Laño vertebrate-site: Implications in the uppermost Cretaceous chronostratigraphy of the Basque-Cantabrian Region. *Cretaceous Research* 57 (2016), 473–489.
- Corral, J.C., Berreteaga, A., Cappetta, H., 2015b. Upper Maastrichtian shallow marine environments and neoselachian assemblages in North Iberian palaeomargin (Castilian Ramp, Spain). *Cretaceous Research* 57 (2016), 639–661.
- Costa, O.G., 1865. Studi sopra i terreni ad ittioliti delle provincie napolitane diretti a stabilire l’eta’ geologica de’ medesimi. Parte Seconda. *Atti della Reale Accademia delle Scienze Fisiche e Matematiche* 2(16), 1–33.

- Cotteau, G., Gauthier, V., 1895. Échinides fossiles, in: de Morgan, J., Mission scientifique en Perse, 1889–1891, Vol. 3(1) Paléontologie. Leroux, Paris, 142 pp.
- Cuny, G., Benton, M., 1999. Early radiation of the neoselachian sharks in western Europe. *Geobios* 32(2), 193–204.
- Cuny, G., Martin, J.E., Sarr, R., 2012. A neoselachian shark fauna from the Late Cretaceous of Senegal. *Cretaceous Research* 34, 107–115.
- Cunningham, S.C., 2000. Tooth Study of a Recent Sand Tiger Shark *Carcharias taurus* (Rafinesque, 1810). http://www.elasmo.com/cunningham/sc_ctaurus.html (accessed 18 September 2015).
- Cushman, J.A., 1926. Some foraminifera from the Mendez shale of eastern Mexico. Contributions from the Cushman Laboratory for Foraminiferal Research, 2(1), 16–26.
- Cushman, J.A., 1938. Cretaceous species of *Guembelina* and related genera. Contributions from the Cushman Laboratory for Foraminiferal Research 14(1), 1–28.

D

- Daimeries, A., 1888. Notes ichthyologiques, I–III. Annales de la Société royale malacologique de Belgique, Bulletin des Séances 23, 42–43, 45–48, 101–104.
- Dalbiez, F., 1955. The genus *Globotruncana* in Tunisia. *Micropaleontology* 1(2), 161–171.
- Dames, W., 1881. Ueber zähne von *Rhombodus* aus der obersenenen Tuffkreide von Maastricht. Sitzungsberichte der Gesellschaft naturforschender Freunde 1, 1–3.
- Dames, W., 1887a. Ueber *Titanichthys pharao* nov. gen., nov. sp., aus der Kreideformation Aegyptens. Sitzungsberichte der Gesellschaft naturforschender Freunde 5, 69–72.
- Dames, W., 1887b. Bemerkung zu seiner früheren Mitteilung über *Titanichthys*. Sitzungsberichte der Gesellschaft naturforschender Freunde 1887, 137.
- d'Archiac, E.J.A., 1859. Note sur le genre *Otostoma*. Bulletin de la Société Géologique de France (2ème série), 16, 871–879.
- Dartevelle, E., Casier, E., 1943. Les poissons fossiles du Bas-Congo et des régions voisines, (première partie). Annales du Musée du Congo Belge Série A 3(2, 1), 1–200.
- Dartevelle, E., Casier, E., 1959. Les poissons fossiles du Bas-Congo et des régions voisines, (troisième partie). Annales du Musée du Congo Belge Série A 3(2, 3), 257–568.
- Daudin, F.M., 1800. Traité élémentaire et complet d'ornithologie, ou histoire naturelle des oiseaux. Imprimerie de Bertrandet, Paris, 473 pp.
- Davidson, A., Brown, G.W., 2012. Paraloid™ B-72: practical tips for the vertebrate fossil preparator. *Collection Forum* 26(1–2), 99–119.
- Davis, J.W., 1887. The fossil fishes of the chalk of Mount Lebanon, in Syria. The Scientific Transactions of the Royal Dublin Society 3(2), 457–636.
- Davis, J.W., 1890. On the fossil fish of the Cretaceous formations of Scandinavia. The Scientific Transactions of the Royal Dublin Society 4(2), 363–434.
- Dean, M.N., Summers, A.P. (2006). Mineralized cartilage in the skeleton of chondrichthyan fishes. *Zoology* 109 (2006), 164–168.
- DeKay, J.E., 1828. Report on several fossil multilocular shells from the State of Delaware: with observations of a second specimen of the new fossil genus *Eurypterus*. *Annals of the Lyceum of Natural History of New York* 2, 273–279.
- Delgado-El Escobar, A.A., Rodríguez de la Rosa, R.A., Saenz-Quiñones, A.I., Gutiérrez-Martín-

- ez, J.A., 2015. The first record of *Onchosaurus* (†Sclerorhynchidae) from the Late Cretaceous of northern Mexico. *Boletín de la Sociedad Geológica Mexicana* 67(1), 113–117.
- Deméré, T. A., Cerutti, R. A., 1982. A Pliocene shark attack on a cethotheriid whale. *Journal of Paleontology* 56, 1480–1482.
- Desmarest, A.G., 1822. Histoire naturelle des crustacés fossiles, sous les rapports zoologiques et géologiques. Les crustacés proprement dites. Chez F.-G. Levrault, Paris, 154 pp.
- Desmoulins, C., 1837. Études sur les Échinides, 3e mémoire. Actes de la Société Linnéenne de Bordeaux 9, 45–364.
- Dollo, L., 1882. Note sur l'ostéologie des Mosasauridae. *Bulletin du Musée d'Histoire Naturelle de Belgique* 1, 55–80.
- Dollo, L., 1889. Première note sur les mosasauriens de Mesvin. *Bulletin de la Société belge de Géologie, de Paléontologie et d'Hydrogéologie, Mémoires* 3(5), 271–304.
- Dollo, L., 1904. Les mosasauriens de la Belgique. *Bulletin de la Société belge de Géologie, de Paléontologie et d'Hydrogéologie, Mémoires* 18(3), 207–216.
- Dollo, L., 1913. *Globidens fraasi*, mosasaurien mylodonte nouveau du Maestrichtien (Crétacé supérieur) du Limbourg, et l'éthologie de la nutrition chez les mosasauriens. *Archives de Biologie* 28, 609–626.
- d'Orbigny, A., 1839. Foraminifères, in: de la Sagra, R. (Ed.), *Histoire physique, politique et naturelle de l'île de Cuba*, vol. 2. A. Bertrand, Paris, 244 pp.
- d'Orbigny, A., 1840a. Paléontologie française. Terrains crétacés. 1, Céphalopodes. Chez l'Auteur, Paris, 662 pp.
- d'Orbigny, A., 1840b. Mémoire sur les foraminifères de la craie blanche du bassin de Paris. *Mémoires de la Société Géologique de France (1ère série)* 4(1), 1–51.
- d'Orbigny, A., 1845. Paléontologie française. Terrains crétacés. 3, Lamellibranchia. Arthus Bertrand, Paris, 807 pp.
- d'Orbigny, A., 1850. *Prodrome de Paléontologie stratigraphique universelle des animaux mollusques et rayonnés*, vol. 2. Masson, Paris, 427 pp.
- Dortangs, R.W., Schulp, A.S., Mulder, E.W.A., Jagt, J.W.M., Peeters, H.H.G., de Graaf, D.Th., 2002. A large new mosasaur from the Upper Cretaceous of The Netherlands. *Netherlands Journal of Geosciences / Geologie en Mijnbouw* 81, 1–8.
- Duffin, C.J., Ward, D.J., 1993. The Early Jurassic palaeospinacid sharks of Lyme Regis, southern England, in: Herman, J., van Waes, H. (Eds), *Elasmobranches et Stratigraphie*. Belgian Geological Survey, Professional Papers 1993/6, 264, 53–101.
- Dujardin, F., 1837. Mémoire sur les couches du sol en Touraine et description des coquilles de la craie et des faluns. *Mémoires de la Société Géologique de France (1ère série)* 2(9), 211–311.
- Duméril, A.M.C., 1806. *Zoologie analytique, ou méthode naturelle de classification des animaux, rendue plus facile à l'aide de tableaux synoptiques*. Allais, Paris, 344 pp.
- Dunkle, D.H., 1951. New Western Hemisphere occurrences of fossil selachians. *Journal of the Washington Academy of Science* 41, 344–347.

E

- Eastman, C.R., 1895. Beiträge zur Kenntniss der Gattung *Oxyrhina*, mit besonderer Berücksichtigung von *Oxyrhina Mantelli* Agassiz. *Palaeontographica - Beiträge zur Naturgeschichte der Vorzeit* 41, 149–191.

- Eastman, C.R., 1904. On the dentition of *Rhynchodus* and other fossil Fishes. *The American Naturalist* 38(448), 295–299.
- Ehrenberg, C.G., 1840. Über die Bildung der Kreidefelsen und des Kreidemergels durch unsichtbare Organismen. *Abhandlungen der Königlichen Akademie der Wissenschaften zu Berlin* (for 1838), 59–147.
- Einarsson, E., Lindgren, J., Kear, B.P., Siverson, M., 2010. Mosasaur bite marks on a plesiosaur propodial from the Campanian (Late Cretaceous) of southern Sweden. *GFF* (Transactions of the Geological Society in Stockholm) 132(2), 123–128.
- Einsele, G., 1992. *Sedimentary Basins, Evolution, Facies, and Sediment Budget*. Springer-Verlag, Berlin, 628 pp.
- El-Naggar, Z.R., 1966. Stratigraphy and planktonic foraminifera of the Upper Cretaceous–lower Tertiary succession in the Esna-Idfu region, Nile Valley, Egypt, U.A.R. *Bulletin of the British Museum (Natural History) Supplement* 2, 291 pp.
- Elorza, J., Orue-Etxebarria, X., 1985. An example of silicification in *Gryphaea* sp. shells from Laño (south of Vitoria, Spain), in: 6th European Regional Meeting of the International Association of Sedimentologists, Lleida'85, Abstracts, pp. 556–559.
- Elorza, J., Astibia, H., Murelaga, X., Pereda Suberbiola, X., 1999. Francolite as a diagenetic mineral in dinosaur and other Upper Cretaceous reptile bones (Laño, Iberian Peninsula): microstructural, petrological and geochemical features. *Cretaceous Research* 20(2), 169–187.
- Enault, S., Guinot, G., Koot, M.B., Cuny, G., 2015. Chondrichthyan tooth enameloid: past, present, and future. *Zoological Journal of the Linnean Society* 174, 549–570.
- Enax, J., Prymak, O., Raabe, D., Epple, M., 2012. Structure, composition, and mechanical properties of shark teeth. *Journal of Structural Biology* 178, 290–299.
- Enax, J., Janus, A.M., Raabe, D., Epple, M., Fabritius, H.-O., 2014. Ultrastructural organization and micromechanical properties of shark tooth enameloid. *Acta Biomaterialia* 10, 3959–3968.
- Engeser, T., 1985. *Sedimentologische, fazielle und tektonogenetische Untersuchungen in der Oberkreide des Basko-Kantabrischen Beckens (Nordspanien)*. Doctoral thesis, University of Tübingen, Tübingen, 232 pp.
- Ernst, G. 1971. Biometrische Untersuchungen über die Ontogenie und Phylogenie der *Offaster/Galeola*-Stammesreihe (Echin.) aus der nordwesteuropäischen Oberkreide. *Neues Jahrbuch für Geologie und Paläontologie - Abhandlungen* 139(2), 169–225 [not seen].
- Ernst, H., 1984. Ontogenie, Phylogenie und Autökologie des inarticulaten Brachiopoden *Isocrania* in der Schreibkreidefazies NW-Deutschlands (Coniac bis Maastricht). *Geologisches Jahrbuch A* 77, 3–105.
- Everhart, M.J., 2004. Late Cretaceous interaction between predators and prey. Evidence of feeding by two species of shark on a mosasaur. *PalArch, vertebrate palaeontology series* 1(1), 1–7.
- Everhart, M.J., 2008. A bitten skull of *Tylosaurus kansasensis* (Squamata: Mosasauridae) and a review of mosasaur-on-mosasaur pathology in the fossil record. *Kansas Academy of Science, Transactions* 111(3-4), 251–262.
- Everhart, M.J., 1999. Evidence of feeding on mosasaurs by the late Cretaceous lamniform shark, *Cretoxyrhina mantelli*. *Journal of Vertebrate Paleontology* 17(Supplement to 3), 43A–44A.
- Everhart, M.J., Everhart, P.A., Shimada, K., 1995. A new specimen of shark bitten mosasaur vertebrae from the Smoky Hill Clark (Upper Cretaceous) in western Kansas. *Abstracts of Papers 127th Annual Meeting of the Kansas Academy of Science* 14, 19.

F

- Feldmann, R.M., 1989. Whitening fossils for photographic purposes, in: Feldman, R.M., Chapman, R.E., Hannibal, J.T. (Eds), *Paleotechniques*. The Paleontological Society, Special Publication 4, 342–346.
- Fernández López, S., 1998. Tafonomía and fosilización (capítulo III), in: Meléndez, B. (Ed.), *Tratado de Paleontología*, tomo I, 3ª ed. Consejo Superior de Investigaciones Científicas, Madrid, pp. 51–107.
- Feuillée, P., P. Rat, 1971. Structures et Paléogéographie paléocantabriques, in: *Histoire structural du golfe de Gascogne*, Éditions Technip, Paris, v. 22, pp. V1.1–V1.48.
- Floquet, M., 1983. La plate-forme nord-castillane et les faciès proximaux, in: Institut des Sciences de la Terre (Ed.), *Vue sur le Crétacé basco-cantabrique et nord-ibérique. Une marge et son arrière-pays, ses environnements sédimentaires*. Mémoires Géologiques de l'Université de Dijon 9, pp. 141–168.
- Floquet, M., 1991. La plate-forme nord-castillane au Crétacé supérieur (Espagne). Arrière-pays ibérique de la marge passive Basco-Cantabrique. Sédimentation et vie. Mémoires Géologiques de l'Université de Dijon 14, 925 pp.
- Floquet, M., 1998. Outcrop cycle stratigraphy of shallow ramp deposits, the Late Cretaceous series on the Castilian Ramp (Northern Spain), in: Graciansky, P.C. de, Hardenbol, J., Jacquín, T., Vail, P.R. (Eds), *Mesozoic and Cenozoic Sequence Stratigraphy of European Basins*. SEPM Society for Sedimentary Geology, special publication 60, 343–361.
- Floquet, M., 2004. El Cretácico Superior de la Cuenca Vasco-Cantábrica y áreas adyacentes, in: Vera, J.A. (Ed.), *Geología de España*. Sociedad Geológica de España and Instituto Geológico y Minero de España, Madrid, pp. 299–306.
- Floquet, M., Alonso, A., Meléndez, A., 1982. Cameros-Castilla. El Cretácico Superior, in: García, A. (Ed.), *El Cretácico de España*. Editorial Complutense, Madrid, pp. 387–456.
- Forbes, E., 1846. Report on the fossil invertebrata from southern India, collected by Mr. Kaye and Mr. Cunliffe. *Transactions of the Geological Society of London*, 2nd series 7(3), 97–174.
- Forir, H., 1887. Contributions à l'étude du système crétacé de la Belgique. Sur quelques poissons et crustacés nouveaux ou peu connus. *Annales de la Société Géologique de Belgique* 14, 25–56.
- Fowler, H.W., 1941. The fishes of the groups Elasmobranchii, Holocephali, Isospondyli and Ostariophysi obtained by the U. S. Bureau of Fisheries steamer 'Albatross' in 1907 to 1910, chiefly in the Philippine Islands and adjacent seas. *Bulletin of the United States National Museum* 100, 1–879.
- Fryrdá, J., Blodgett, R.B., 2008. Paleobiogeographic affinities of Emsian (late Early Devonian) gastropods from Farewell terrane (west-central Alaska), in: Blodgett, R.B., Stanley, G.D. Jr. (Eds), *The terrane puzzle: new perspectives on paleontology and stratigraphy from the North American Cordillera*. Geological Society of America Special Paper 442, 107–120.

G

- Gallagher, W.B., 2002. Faunal changes across the Cretaceous-Tertiary (K-T) boundary in the Atlantic coastal plain of New Jersey: Restructuring the marine community after the K-T mass-extinction event, in: Koeberl, C., MacLeod, K.G. (Eds), *Catastrophic Events and*

- Mass Extinctions: Impacts and Beyond. Geological Society of America Special Paper 356, 291–301.
- Gallémí, J., López, G., Martínez, R., Pons, J.M., 2007. Macrofauna of the Villamartín Section: Coniacian/Santonian boundary, North Castilian Platform, Burgos, Spain. *Cretaceous Research* 28, 93–107.
- Gandolfi, R., 1955. The genus *Globotruncana* in northeastern Colombia. *Bulletin of American Paleontology* 36(155), 1–118.
- García-Mondéjar, J., 1990. The Aptian-Albian carbonate episode of the Basque-Cantabrian Basin (northern Spain): general characteristics, controls and evolution, in: Tucker, M.E., Wilson, J.L., Crevello, P.D., Sang, J.F., Read, J.F. (Eds), *Carbonate Platforms: Facies, Sequences and Evolution*. International Association of Sedimentology, Special Publication 9, 257–290.
- Garman, S., 1913. The Plagiostomia - Sharks, skates, and rays. *Memoirs of the Museum of Comparative Zoölogy at Harvard College* 36(1–2), 1–515.
- Gaudry, A., 1892. Les Pythonomorphes de France. *Mémoire de la Société Géologique de France* 10, 1–13.
- Gemmellaro, M., 1920. Ittiodontoliti Maëstrichtiani di Egitto. *Atti della Reale Accademia di scienze, lettere e belle arte di Palermo*, 3° Série 11, 151–204.
- Gervais, M.P., 1852. *Zoologie et paléontologie françaises (animaux vertébrés) ou nouvelles recherches sur les animaux vivants et fossiles de la France*. Arthus Bertrand Libraire - Éditeur, Paris, 271 pp.
- Gervais, P., 1953. Observations relatives aux reptiles fossiles de France. *Comptes Rendus hebdomadaires des Séances de l'Académie des Sciences* 36, 374–377, 470–474.
- GESSAL, 1990. Documentos sobre la geología del subsuelo de España, Año 1990. IGME, Madrid (unpublished).
- Geyn, W. van de, 1937. Les élasmobranches du Crétacé marin du Limbourg Hollandais. *Naturhistorisch Maandblad* 26, 16–21, 28–33, 42–53, 56–60, 66–69.
- Gheerbrant, E., Abrial, C., Cappetta, H., 1997. Nouveaux sites à microvertébrés du Crétacé supérieur des Petites Pyrénées (Haute-Garonne et Ariège, France). *Geobios Mémoire spécial* 20, 257–269.
- Gill, T., 1862. Analytical analysis of the order Squali and revision and nomenclature of Henera. *Annals of the Society of Natural History of New York* 7, 367–408.
- Gischler, E., Gräfe, K.-U., Wiedmann, J., 1994. The Upper Cretaceous *Lacazina* Limestone in the Basco-Cantabrian and Iberian Basins of Northern Spain: Cold-water Grain Associations in Warm-water Environments. *Facies* 30, 209–246.
- Glikman, L.S., 1958. Rates of evolution in lamnoid sharks. *Akademii Nauk SSSR* 123, 568–571 [in Russian].
- Glikman, L.S., 1964. Paleogene sharks and their stratigraphic significance. Nauka Press, Moscow-Leningrad, 229 pp. [in Russian].
- Glikman, L.S., 1980. Evolution of Cretaceous and Cenozoic lamnoid sharks. Nauka Press, Moscow, 247 pp. [in Russian].
- Goldfuss, G.A., 1826–1933. *Petrefacta Germaniæ tam ea, quae in Museo Universitatis Regiae Borussicae Fridericiae Wilhelmae Rhenanae servantur quam alia quaecunque in Museis Hoeninghusiano Muensteriano aliisque*, I. Arnz & Comp., Düsseldorf, 252 pp.
- Goldfuss, A., 1834–1940. *Petrefacta Germaniae ...*, II. Arnz & Comp., Düsseldorf, 312 pp.
- Gómez Alday, J.J., 1999. Stratigraphic and depositional environments of the Upper Cretaceous

- of the Laño quarry. Evidence of diapiric activity. *Estudios del Museo de Ciencias Naturales de Álava* 14(Número especial 1), 29–35.
- Gómez Alday, J.J., García-Garmilla, F., Elorza, J., 1994. Evidencias de actividad diapírica sobre las unidades deposicionales del Maastrichtiense en la zona de Albaina (C. de Treviño) (Sur de Vitoria, cuenca Vasco-Cantábrica). *Geogaceta* 16, 90–93.
- Gómez-Alday, J.J., García-Garmilla, F., Elorza, J., 2002. Origin of quartz geodes from Laño and Tubilla del Agua sections (middle-upper Campanian, Basque-Cantabrian Basin, northern Spain): isotopic differences during diagenetic processes. *Geological Journal* 37, 117–134.
- Gottfried, M.D., Rabarison, J.A., Randriamiarimanana, L.L., 2001. Late Cretaceous elasmobranchs from the Mahajanga Basin of Madagascar. *Cretaceous Research* 22, 491–496.
- Gräfe, K.-U., 1994. Sequence stratigraphy in the Cretaceous and Paleogene (Aptian to Eocene) of the Basco-Cantabrian Basin (N. Spain). *Tübinger geowissenschaftliche Arbeiten (A)* 18, 418 pp.
- Gräfe, K.-U., 2005. Late Cretaceous benthic foraminifers from the Basque-Cantabrian Basin, Northern Spain. *Journal of Iberian Geology* 31, 277–298.
- Gräfe, K.-U., Floquet, M., Rosales, I., 2002. Late Cretaceous of the Basque-Cantabrian Basin, in: Gibbons, W., Moreno, T. (Eds), *The Geology of Spain*. The Geological Society, London, pp. 281–284.
- Grambast, L., 1971. Remarques phylogénétiques et biocronologiques sur les *Septorella* du Crétacé terminal de Provence et les charophytes associés. *Paléobiologie Continentale* 2(2), 1–38.
- Grambast, L., Gutiérrez, G., 1977. Espèces nouvelles de charophytes du Crétacé supérieur terminal de la province de Cuenca (Espagne). *Paléobiologie Continentale* 8(2), 1–34.
- Gray, J.E., 1851. List of the specimens of Fish in the Collection of the British Museum. Pt. I. British Museum of Natural History, London, 106 pp.
- Green, O.R., 2001. *A Manual of Practical Laboratory and Field Techniques in Palaeobiology*. Kluwer Academic Publishers, Dordrecht, 538 pp.
- Griepenkerl, O., 1889. Die Versteinerungen der senonen Kreide von Königslutter im Herzogthum Braunschweig. *Paläontologische Abhandlungen* 4(5), 305–419.
- Grossouvre, A. de, 1894. Recherches sur la Craie supérieure, 2ème Partie Paléontologie, Les ammonites de la Craie supérieure. Mémoires pour servir à l'explication de la Carte géologique de la France. Imprimerie Nationale Paris, 264 pp. (dated 1893 in title page).
- Guinot, G., 2011. Selachians from the Late Cretaceous of the Anglo-Paris Basin: systematics, diversity, palaeoecology. Doctoral Thesis, Université Montpellier 2 Sciences et Techniques, Montpellier, 503 pp.
- Guinot, G., 2013a. Late Cretaceous elasmobranch palaeoecology in NW Europe. *Palaeogeography, Palaeoclimatology, Palaeoecology* 388, 23–41.
- Guinot, G., 2013b. Regional to global patterns in Late Cretaceous selachian (Chondrichthyes, Euselachii) diversity. *Journal of Vertebrate Paleontology* 33(3), 521–531.
- Guinot, G., Cappetta, H., Underwood, C.J., Ward, D.J., 2012a. Batoids (Elasmobranchii: Batomorphii) from the British and French Late Cretaceous. *Journal of Systematic Palaeontology* 10(3), 445–474.
- Guinot, G., Underwood, C.J., Cappetta, H., Ward, D.J., 2012b. Squatiniformes (Chondrichthyes, Neoselachii) from the Late Cretaceous of southern England and northern France with redescription of the holotype of *Squatina cranei* Woodward, 1888. *Palaeontology* 55(3), 529–551.
- Guinot, G., Underwood, C.J., Cappetta, H., Ward, D.J., 2013. Sharks (Elasmobranchii:

- Euselachii) from the Late Cretaceous of France and the UK. *Journal of Systematic Palaeontology* 11(6), 589–671.
- Guitart, D., 1966. Nuevo nombre para una especie de tiburón del género *Isurus* (Elasmobranchii: Isuridae) de aguas cubanas. *Poeyana (Ser. A)* 15, 1–9.
- Gunnerus, J.E., 1765. Brugden (*Squalus maximus*), Beskrvenen ved J. E. Gunnerus. *Det Trondhiemske Selskabs Skerifter* 3, 33–49 [not seen].
- Gurr, P.R., 1962. A new fish fauna from the Woolwich Bottom Bed (Sparnacian) of Herne Bay, Kent. *Proceedings of the Geologists' Association* 73(4), 419–447.

H

- Hall, B.K., 2005. Bones and cartilage. *Developmental and Evolutionary Skeletal Biology*. Elsevier, London, 760 pp.
- Hall, J., Meek, F.B., 1855. Descriptions of new species of fossils, from the Cretaceous formations of Nebraska, with observations upon *Baculites ovatus* and *B. compressus*, and the progressive development of the septa in *Baculites*, *Ammonites* and *Scaphites*. *Memoirs of the American Academy of Arts and Sciences* 5, 379–411
- Halstead, B.W., 1971. Venomous fishes, in Bürcherl, W., Buckley, E.E., (Eds), *Venomous animals and their venoms*. Vol. 2 *Venomous vertebrates*. Academic Press, New York, 587–626.
- Halter, M.C., 1995. Additions to the Fish Fauna of N.W. Europe. 3. Three new species of the genus *Scyliorhinus* from the Late Cretaceous (Campanian and Maastrichtian) of the Limburg area (Belgium and The Netherlands) with a reassignment of four additional fossil species to the genus *Scyliorhinus* sensu stricto, in: Herman, J., van Waes, H. (Eds), *Elasmobranches et Stratigraphie*. Belgian Geological Survey, Professional Papers 1995/3, 278, 65–109.
- Hamm, S.A., Shimada, K., 2002. Associated Tooth Set of the Late Cretaceous Lamniform Shark, *Scapanorhynchus raphiodon* (Mitsukurinidae), from the Niobrara Chalk of Western Kansas. *Transactions of the Kansas Academy of Science*, 105(1–2), 18–26.
- Hammer, Ø., Harper, D.A.T., 2006. *Paleontological Data Analysis*. Blackwell, Malden, 351 pp.
- Hammer, Ø., Harper, D.A.T., Ryan, P.D., 2001. PAST: Paleontological Statistics Software Package for Education and Data Analysis. *Palaeontologia Electronica* 4(1), 9pp.
- Hancock, J.M., 1991. Ammonite scales for the Cretaceous System. *Cretaceous Research* 12, 259–291.
- Hanger, R.A., 1996. Permian Brachiopod paleobiogeography of South America, in Copper, P., Jisuo, J. (Eds), *Brachiopods*. A.A. Balkema, Rotterdam, 107–119.
- Haq, B.U., 1991. Sequence stratigraphy, sea-level change, and significance for the deep sea, in: MacDonald, D.I.M. (Ed.), *Sedimentation, Tectonic and Eustasy: Sea-Level Changes at Active Margins*. International Association of Sedimentologists Special Publication 12, 3–39.
- Haq, B.U., Hardenbol, J., Vail, P.R., 1987. Chronology of fluctuating sea levels since the Triassic (250 million years ago to present). *Science* 235, 1156–1167.
- Hardenbol, J., Thierry, J., Farley, M.B., Jacquin, T., Graciansky, P.-C. de, Vail, P.R., 1998. Appendix to: Mesozoic and Cenozoic sequence chronostratigraphic framework of European basins. Chart 5, Cretaceous Biochronostratigraphy, in: Graciansky, P.-C. de, Hardenbol, J., Thierry, J., Vail, P.R., (Eds), *Mesozoic and Cenozoic Sequence Stratigraphy of European Basin*. SEPM (Society for Sedimentary Geology), Special Publication 60, 763–781.
- Hay, O.P., 1902. Bibliography and Catalogue of Fossil Vertebrata of North America. *Bulletin of the United States Geological Survey* 179, 1–868.

- Hay, O.P., 1903. On a collection of upper Cretaceous fishes from Mount Lebanon, Syria, with descriptions of four new genera and nineteen new species. *Bulletin of the American Museum of Natural History* 19(10), 395–452.
- Hébert, E., 1875a. Description de deux espèces d'*Hemipneustes* de la Craie supérieure des Pyrénées. *Bulletin de la Société Géologique de France* (3ème série) 3, 592–595.
- Hébert, E., 1875b. Classification du terrain crétacé supérieur. *Bulletin de la Société Géologique de France* (3ème série) 3, 595–599.
- Heithaus, M.R., 2004. Predator–Prey Interactions, in: Carrier, J.C., Musick, J.A., Heithaus, M.R. (Eds), *Biology of sharks and their relatives*. CRC Press, Boca Raton, pp. 488–521.
- Hellawell, J., Nicholas, C.J., 2012. Acid treatment effects on the stable isotopic signatures of fossils. *Palaeontology* 55(1), 1–10.
- Herman, J., 1973. Les sélaciens des terrains néocrétacés & paléocènes de Belgique & des contrées limitrophes Éléments d'un biostratigraphie intercontinentale. Unpublished Doctoral Thesis. Université libre de Bruxelles, Faculté des sciences, Bruxelles, 598 pp.
- Herman, J., 1977. Les sélaciens des terrains néocrétacés et paléocènes de Belgique et des contrées limitrophes. Éléments d'une biostratigraphie intercontinentale. Mémoires pour servir à l'explication des Cartes géologiques et minières de la Belgique 15 (for 1975), 1–401.
- Herman, J., 1979. Réflexions sur la systématique des Galeoidei et sur les affinités du genre *Cetorhinus* à l'occasion de la découverte d'éléments de la denture d'un exemplaire fossile dans les sables du Kattendijk à Kallo (Pliocène inférieur, Belgique). *Annales de la Société Géologique de Belgique* 102, 357–377.
- Herman, J., 1982. Die Selachier-Zähne aus der Maastricht-Stufe von Hemmoor, Niederelbe (NW-Deutschland). *Geologisches Jahrbuch, Reihe A*, 61, 129–159.
- Herman, J., Van Waes, H., 2012. Observations concernant l'Évolution et la Systématique de quelques Euselachii, Neoselachii et Batoidei (Pisces - Elasmobranchii), actuels et fossiles. *Géominpal Belgica* 2, 89 pp.
- Herman J., Van Waes, H., 2014. Observations concerning the Evolution and the Parasytematics of all the living and fossil Chlamydoselachiformes, Squatiniformes, Orectolobiformes, and Pristiophoriformes, based on both biological and odontological data. Suggestion of a possible origin of the Order Pristiophoriformes, of the Order Ganopristiformes and a global Synthesis of the previous Systematics proposals. *Géominpal Belgica* 6, 1–364.
- Hewitt, T.A., Westermann, G.E.G., 1989. Mosasaur tooth on the ammonite *Placenticerus* from the Upper Cretaceous of Alberta, Canada. *Canadian Journal of Earth Sciences* 27, 469–472.
- Hodson, M.E., Valsami-Jones, E., Cotter-Howells, J.D., Dubbin, W.E., Kemp, A.J., Thornton, I., Warren, A., 2001. Effect of bone meal (calcium phosphate) amendments on metal release from contaminated soils – a leaching column study. *Environmental Pollution* 112(2), 233–243.
- Holthuis, L.B., 1991. An annotated and illustrated catalogue of species of interest to fisheries known to date. *FAO Fisheries Synopsis* 125, v. 13. Food and Agriculture Organization, Rome, 292 pp.
- Hubbell, G., 1996. Using tooth structure to determine the evolution history of the white sharks, in: Klimley, A.P., Ainley, D. (Eds), *Great White Sharks - The biology of *Carcharodon carcharias**. Academic Press, San Diego, pp. 9–18.
- Hubert, J.F., Panish, P.T., Prostack, K.S., Chure, D.J., 1996. Chemistry, microstructure, petrology, and diagenetic model of Jurassic dinosaur bones, Dinosaur National Monument, Utah. *Journal of Sedimentary Research* 66, 531–547.

Hübner, T., Müller, A., 2010. Selachian teeth from Campanian sediments (Upper Cretaceous) of the Münsterland Cretaceous Basin (NW-Germany). *Paläontologische Zeitschrift* 84(4), 437–455.

Hurcewicz, H., 1966. Siliceous sponges from the Upper Cretaceous of Poland; Part I, Tetraxonia. *Acta Palaeontologica Polonica* 11, 15–129.

Huxley, T.H., 1880. On the application of the laws of evolution to the arrangement of the Vertebrata, and more particularly of the Mammalia. *Proceedings of the Scientific Meetings of the Zoological Society of London* 1880, 649–662.

I

Institut des Sciences de la Terre, 1983. Le domaine navarro-cantabre et les faciès de plate-forme distale, in: *Vue sur le Crétacé basco-cantabrique et nordibérique. Une marge et son arrière-pays, ses environnements sédimentaires. Mémoires Géologiques de l'Université de Dijon* 9, pp. 117–140.

J

Jaekel, O., 1894. Die eocänen Selachier vom Monte Bolca. Ein Beitrag zur Morphogenie der Wirbelthiere. Julius Springer, Berlin, 176 pp.

Jagt, J.-W.M., Motchurova-Dekova, N., Ivanov, P., Cappetta, H., Schulp, A.-S., 2006. Latest Cretaceous mosasaurs and lamniform sharks from Labirinta cave, Vratsa district (northwest Bulgaria): a preliminary note. *Annales Géologiques de la Péninsule Balkanique* 67, 51–63.

Jeppsson, L., Anehus, R., 1995. A buffered formic acid technique for conodont extraction. *Journal of Paleontology* 69(4), 790–794.

Jeppsson, L., Fredholm, D., Mattiasson, B., 1985. Acetic Acid and Phosphatic Fossils: A Warning. *Journal of Paleontology* 59(4), 952–956.

Jeppsson, L., Anehus, R., Fredholm, D., 1999. The optimal acetate buffered acetic acid technique for extracting phosphatic fossils. *Journal of Paleontology* 73(5), 964–972.

Jordan, D.S., 1898. Description of a species of fish (*Mitsukurina owstoni*) from Japan, the type of a distinct family of Lamnoid sharks. *Proceedings of the California Academy of Sciences (Series 3, Zoology)* 1(6), 199–204.

K

Kalfayan, L., 2008. *Production Enhancement with Acid Stimulation*. 2nd edition. PennWell Corporation, Tulsa, Oklahoma, 270 pp.

Kaplan, U., Kennedy, W.J., Hiss, M., 2005. Stratigraphie und Ammonitenfaunen des Campan im nordwestlichen und zentralen Münsterland. *Geologie und Paläontologie in Westfalen* 64, 1–171.

Karrenberg, M., 1935. Ammoniten aus der Nordspanischen Oberkreide. *Palaeontographica A* 82, 125–161.

Kauffman, E.G., 1973. Cretaceous Bivalvia, in: Hallam, A. (Ed.), *Atlas of Palaeobiogeography*. Elsevier, Amsterdam, pp. 353–383.

Kauffman, E.G., 1990. Mosasaur predation on ammonites during the Cretaceous – an evolu-

- tionary history, in: Boucot, A.J. (Ed.), *Evolutionary Palaeobiology of Behaviour and Coevolution*. Elsevier, Amsterdam, pp. 184–189.
- Kauffman, E.G., Kesling, R.V., 1960. An Upper Cretaceous ammonite bitten by a mosasaur. *University of Michigan Museum Paleontological Contribution* 15, 193–248.
- Keegan, W.F., 2003. The first documented shark attack in the Americas, cal AD 789–1033. *Caribbean Archaeology*. www.flmnh.ufl.edu/anthro/caribarch/sharks.htm. Accessed 20/08/2003.
- Keene, S., 1987. Some adhesives and consolidants used in conservation. *Geological Curator* 4(7) (for 1986), 421–425.
- Kemp, N.E., 1999. Integumentary system and teeth, in: Hamlett, W.C. (Ed.), *Sharks, Skates, and Rays: The Biology of Elasmobranch Fishes*. Johns Hopkins University Press, Baltimore, pp. 43–68.
- Kennedy, W.J., 1984. Systematic palaeontology and stratigraphic distribution of the ammonite faunas of the French Coniacian. *Special Papers in Palaeontology* 31, The Palaeontological Association, London, 160 pp.
- Kennedy, W.J., 1986. The ammonite fauna of the type Maastrichtian with a revision of *Ammonites colligatus* Binkhorst, 1861. *Bulletin de l'Institut Royal des Sciences Naturelles de Belgique, Sciences de la Terre* 56, 151–267.
- Kennedy, W.J., Cobban, W.A., 1994. Upper Campanian (Upper Cretaceous) ammonites from the Marshalltown Formation-Mount Laurel boundary beds in Delaware. *Journal of Paleontology* 68(6), 1285–1305.
- Kennedy, W.J., Cobban, W.A., 1999. Campanian (Late Cretaceous) ammonites from the Bergstrom Formation in Central Texas. *Acta Geologica Polonica* 49(1), 67–80.
- Kennedy, W.J., Cobban, W.A., 2001. Campanian (Late Cretaceous) Ammonites from the upper part of the Anacacho Limestone in South Central Texas. *Acta Geologica Polonica* 51(1), 15–30.
- Kennedy, W.J., Henderson, R.A., 1992a. Non-heteromorph ammonites from the Upper Maastrichtian of Pondicherry, south India. *Palaeontology* 35(2), 381–442.
- Kennedy, W.J., Henderson, R.A., 1992b. Heteromorph ammonites from the upper Maastrichtian of Pondicherry, south India. *Palaeontology* 35(3), 693–731.
- Kennedy, W.J., Jagt, J.W.M., 1995. Lower Campanian heteromorph ammonites from the Valls Formation around Aachen, Germany, and adjacent parts of Belgium and The Netherlands. *Neues Jahrbuch für Geologie und Paläontologie - Abhandlungen* 197(3), 275–294.
- Kennedy, W.J., Bilotte, M., Lepicard, B., Segura, F., 1986. Upper Campanian and Maastrichtian ammonites from the Petites-Pyrénées, southern France. *Eclogae Geologicae Helvetiae* 79(3), 1001–1037.
- Kidwell, S.M., 1991. The stratigraphy of shell concentrations, in: Allison P.A., Briggs D.E.G. (Eds), *Taphonomy, Releasing the Data Locked in the Fossil Record*. Plenum Press, New York, pp. 211–290.
- Kidwell, S.M., 1998. Time-averaging in the marine fossil record: overview of strategies and uncertainties. *Geobios* 30(7), 977–995.
- Kind, H.D., 1967. Diapire und Alttertiär im südöstlichen Baskenland (Nordspanien). *Beihefte zum Geologischen Jahrbuch* 66, 127–174.
- Klimley, P.A., 2013. *The Biology of Sharks and Rays*. University of Chicago Press, Chicago, Illinois, 512 pp.

- Klimley, P.A., Pyle, P., Anderson, S.D., 1996. The behavior of white sharks and their pinniped prey during predatory attacks, in: Klimley, A.P., Ainley, D.G. (Eds), *Great White Sharks. The biology of *Carcharodon carcharias**. Academic Press, San Diego, pp. 175–191.
- Klinger, H.C., Kennedy, W.J., 1993. Cretaceous faunas from Zululand and Natal, South Africa. The heteromorph ammonite genus *Eubaculites* Spath, 1926. *Annals of the South African Museum* 102(6), 185–264.
- Koeppenkastrop, D., De Carlo, E.H., 1992. Sorption of rare-earth elements from seawater onto synthetic mineral particles – an experimental approach. *Chemical Geology* 95, 251–263.
- Kohn, M.J., Schoeninger, M.J., Barker, W.W., 1999. Altered states: Effects of diagenesis on fossil tooth chemistry. *Geochimica et Cosmochimica Acta* 63(18), 2737–2747.
- Koob, S., 1986. The Use of Paraloid B72 as an adhesive: its application for archaeological ceramics. *Studies in Conservation* 31, 7–13.
- Kossmat, F., 1897. Untersuchungen über die Südindische Kreideformation, part III. Beiträge zur Paläontologie und Geologie Österreich-Ungarns und des Orients 11, 89–152.
- Kowalewski, M., 2002. The fossil record of predation: an overview of analytical methods, in: Kowalewski, M., Kelley, P.H. (Eds), *The fossil record of predation. The Paleontological Society Papers* 8, 3–42.
- Kriwet, J., 1999a. *Ptychotrygon geyeri* n. sp. (Chondrichthyes, Rajiformes) from the Utrillas Formation (upper Albian) of the central Iberian Ranges (East-Spain). *Profil* 16, 337–346.
- Kriwet, J., 1999b. Neoselachier (Pisces, Elasmobranchii) aus der Unterkreide (unteres Barremium) von Galve und Alcaine (Spanien, Provinz Teruel). *Palaeo Ichthyologica* 9, 113–142.
- Kriwet, J., 2004. The systematic position of the Cretaceous sclerorhynchid sawfishes (Elasmobranchii, Pristiorajea), in: Arratia, G., Tintori, A. (Eds), *Mesozoic fishes 3 – Systematics, palaeoenvironments and biodiversity*. Verlag Dr. Fritz Pfeil, München, Germany, pp. 57–73.
- Kriwet, J., Klug, S., 2008. Diversity and biogeography patterns of Late Jurassic neoselachians (Chondrichthyes, Elasmobranchii). *Journal of the Geological Society London* 295, 55–69.
- Kriwet, J., Klug, S., 2012. Presence of the extinct sawfish, *Onchosaurus* (Neoselachii, Sclerorhynchiformes) in the Late Cretaceous of Peru with a review of the genus. *Journal of South American Earth Sciences* 39, 52–58.
- Kriwet, J., Lirio, J.M., Nuñez, H.J., Puceat, E., Lécuyer, C., 2006. Late Cretaceous Antarctic fish diversity, in: Francis J.E., Pirrie D., Crame J.A. (Eds), *Cretaceous–Tertiary high-latitude palaeoenvironments, James Ross Basin, Antarctica*. Geological Society, London, Special Publications 258, 83–100.
- Kriwet, J., Soler-Gijón, R., López-Martínez, N., 2007. Neoselachians from the upper Campanian and lower Maastrichtian (Upper Cretaceous) of the southern Pyrenees, northern Spain. *Palaeontology* 50(5), 1051–1071.
- Kriwet, J., Nunn, E.V., Klug, S., 2009. Neoselachians (Chondrichthyes, Elasmobranchii) from the Lower and lower Upper Cretaceous of north-eastern Spain. *Zoological Journal of the Linnean Society* 155(2), 316–347.
- Küchler, T., 2000a. *Nostoceras (Euskadiceras) euskadiense*, a new ammonite subgenus and species from the higher Upper Campanian (Upper Cretaceous) of northern Spain. *Berliner Geowissenschaftliche Abhandlungen, Reihe E* 34, 291–307.
- Küchler, T., 2000b. *Scaphites hippocrepis* (Dekay) IV, a new chronological subspecies from the Lower – Upper Campanian (Upper Cretaceous) boundary interval of northern Spain. *Acta Geologica Polonica* 50(1), 161–167.

- Küchler, T., 2000c. Upper Cretaceous of the Barranca (Navarra, northern Spain); integrated litho-, bio- and event stratigraphy. Part II: Campanian and Maastrichtian. *Acta Geologica Polonica* 50(4), 441–499.
- Küchler, T., Kutz, A., Wägreich, M., 2001. The Campanian-Maastrichtian boundary in northern Spain (Navarra Province): the Imiscoz and Erro sections, in: Odin, G.S. (Ed.), *The Campanian-Maastrichtian stage boundary: characterisation at Tercis les Bains (France): correlation with Europe and other continents*. IUGS Special Publication (monograph) Series, 36, *Developments in Palaeontology and Stratigraphy Series*, vol. 19, Elsevier, Amsterdam, pp. 723–744.
- L**
- Ladwig, J., 2014. Zähne der Hai-Gattung *Carcharias* aus dem oberen Campanium der Schreibkreidegrube „Saturn“ in Kronsmoor (Schleswig-Holstein). *Arbeitskreis Paläontologie Hannover* 42, 1–11.
- Lalicker, C.G., 1948. A new genus of Foraminifera from the Upper Cretaceous. *Journal of Paleontology* 22(5), 624.
- Lamarck, J.B., 1801. *Système des Animaux sans vertèbres*. L'Auteur, Darteville, Paris, 432 pp.
- Lamarck, J.B., 1806. *Mémoires sur les fossiles des environs de Paris, comprenant la détermination des espèces qui appartiennent aux animaux marins sans vertèbres, et dont la plupart sont figurés dans la collection des vélins du Muséum*. *Annales du Muséum d'Histoire naturelle (Paris)*, 8: 156–166.
- Lamarck, J.B., 1816. *Histoire naturelle des animaux sans vertèbres*. Vol. 2, Verdière Libraire, Paris, 568 pp.
- Lamarck, J.B., 1819. *Histoire naturelle des animaux sans vertèbres*, v. 6(1). Chez l'Auteur, Paris, 232 pp.
- Landemaine, O., 1991. Sélaciens nouveaux du Crétacé supérieur du Sud-Ouest de la France. Quelques apports à la systématique des éla-smobranches. *Société Amicale des Géologues Amateurs* 1, 1–45.
- Latasa, J.H., 1996. M. Ruiz de Gaona. Reseña humana de un escolapio. *Príncipe de Viana. Suplemento de Ciencias* 14/15, 13–19.
- Lauginiger, E.M., Hartstein, E.F., 1983. A guide to fossil sharks, skates, and rays from the Chesapeake and Delaware Canal Area, Delaware. *Delaware Geological Survey, OFR 21*, 63 pp.
- Laurent, Y., Cavin, L., Bilotte, M., 1999. Découverte d'un gisement à vertébrés dans le Maastrichtien supérieur des Petites-Pyrénées. *Comptes Rendus de l'Académie des sciences de Paris, Sciences de la terre et des planètes* 328, 781–787.
- Lawley, R., 1876. *Nuovi studi sopra ai pesci ed altri vertebrati fossili delle Colline toscane*. Tipografia dell'Arte della Stampa, Firenze, 122 pp.
- Lawley, R., 1881. *Studi comparativi sui pesci fossili coi viventi dei generi *Carcharodon*, *Oxyrhina* e *Galeocerdo**. Tipografia T. Nistri e C., Pisa, 151 pp.
- Lebrun, P., 2001. Requins, raies et autres chondrichthyes fossiles. Tome I: Diversité, anatomie, classification et phylogénèse des requins et autres chondrichthyes. *Minéraux & fossiles, hors-série* 12, 112 pp.
- Lécuyer, C., Bogey, C., Garcia, J.-P., Grandjean, P., Barrat, J., Floquet, M., Bardet, N., Pereda-Suberbiola, X., 2003. Stable isotope composition and rare earth element content of vertebrate remains from the Late Cretaceous of northern Spain (Laño): did the environ-

- mental record survive? Palaeogeography, Palaeoclimatology, Palaeoecology 193, 457–471.
- Ledru, A.P., 1810. Voyage aux îles de Ténériffe, la Trinité, Saint-Thomas, Sainte-Croix et Porto-Rico. Arthus Bertrand, Paris, vol. 2, 324 pp.
- Lehman, T.M., 1989. Giant Cretaceous sawfish (*Onchosaurus*) from Texas. Journal of Paleontology 63, 533–535.
- Leidy, J., 1856. Notice of remains of extinct vertebrate animals of New-Jersey, collected by Prof. Cook of the State Geological Survey under the direction of Dr. W. Kitchell. Proceedings of the Academy of Natural Sciences of Philadelphia 8, 220–221.
- Leriche, M., 1902. Révision de la faune ichthyologique des terrains crétacés du Nord de la France. Annales de la Société Géologique du Nord 31, 87–154.
- Leriche, M., 1905. Les poissons éocènes de la Belgique. Mémoires du Musée Royal d'Histoire Naturelle de Belgique 3(11), 49–228.
- Leriche, M., 1906. Contribution à l'étude des poissons fossiles du Nord de la France et des régions voisines. Mémoires de la Société Géologique du Nord 5(1), 1–430.
- Leriche, M., 1929. Les Poissons du Crétacé marin de la Belgique et du Limbourg hollandais (note préliminaire). Les résultats stratigraphiques de leur étude. Bulletin de la Société Belge de Géologie, de Paléontologie et d'Hydrologie 37(3) (1927), 199–299.
- Leriche, M., 1938. Contribution à l'étude des poissons fossiles des pays riverains de la Méditerranée américaine (Vénézuéla, Trinité, Antilles, Mexique). Mémoires de la Société Paléontologique Suisse 61(1), 1–42.
- Leske, N.G., 1778. Jacobi Theodori Klein naturalis dispositio echinodermatum. Leipzig, Ex Officina Gleditschiana, 279 pp.
- Lesueur, C.A., 1822. Description of a *Squalus*, of very large size, which was taken on the coast of New Jersey. Journal of the Academy of Natural Sciences of Philadelphia 2(2), 343–352.
- Lewy, Z., Cappetta, H., 1989. Senonian elasmobranch teeth from Israel. Biostratigraphic and paleoenvironmental implications. Neues Jahrbuch für Geologie und Paläontologie - Monatshefte H4, 212–222.
- Leymerie, A., 1851. Mémoire sur un nouveau type Pyrénéen, parallèle à la Craie proprement dite. Mémoires de la Société Géologique de France (2ème série) 4(3), 26 pp.
- Leymerie, A., 1877. Mémoire sur le type Garumien comprenant une description de la Montagne d'Ausseing, un aperçu des principaux gîtes du département de la Haute-Garonne et une notice sur la faune d'Auzas. Annales des Sciences Géologiques 9, 1–54.
- Leymerie, A., 1878. Description géologique et paléontologique des Pyrénées de la Haute-Garonne. Atlas, Édouard Privat, Toulouse, 52 pp.
- Leymerie, A., 1881. Description géologique et paléontologique des Pyrénées de la Haute-Garonne. Vol. 1, Édouard Privat, Toulouse, 1010 pp.
- Leymerie, A., Cotteau, G., 1856. Catalogue des Échinides fossiles des Pyrénées. Bulletin de la Société Géologique de France (2ème série) 13, 319–355.
- Lindsay, W., 1987. The acid technique in vertebrate palaeontology: A review. Geological Curator 4(7), 455–461.
- Lindsay, W., 1995. A review of the acid technique, in: Collins, C. (Ed.), The care and conservation of palaeontological material. Butterworth-Heinemann, Oxford, pp. 95–101.
- Lingham-Soliar, L., 1991. Predation in mosasaurs – a functional approach, in: Natural structures. Principles, Strategies, and Models in Architecture and Nature. Proceedings of the II International Symposium SFB 230, 6, 169–177.

- Lingham-Soliar, T., 1994. First record of mosasaurs from the Maastrichtian (Upper Cretaceous) of Zaire. *Paläontologische Zeitschrift* 68(1/2), 259–65.
- Link, H.F., 1790. Versuch einer Enttheilung der Fische nach den Zähnen. *Magazin für das Neueste aus der Physik und Naturgeschichte* Gotha 6, 28–38.
- Linnaeus, C., 1758. *Systema naturæ per regna tria naturæ, secundum classes, ordines, genera, species, cum characteribus, differentiis, synonymis, locis*. Tomus I. Editio decima, reformata. Laurentii Salvii, Holmiæ, 1–824.
- Loeblich, A.R. Jr., 1951. Coiling in the Heterohelicidae. *Contributions from the Cushman Foundation for Foraminiferal Research* 2(3), 106–110.
- López, G., 1993a. Aportaciones al conocimiento de la fauna de Bivalvos del Cretácico Superior de Álava y Navarra. Parte I. *Estudios del Museo de Ciencias Naturales de Álava* 8, 5–26.
- López, G., 1993b. Presencia de *Otostoma rugosa* Hoeninghaus en el Maastrichtiense de Álava. *Estudios del Museo de Ciencias Naturales de Álava* 8, 37–41.
- López, G., 1996. Afinidades paleobiogeográficas de los inocerámidos (Bivalvia) del Campaniense y Maastrichtiense de Álava y Navarra. *Estudios del Museo de Ciencias Naturales de Álava* 10–11 (1995–1996), 27–43.
- Lopez-Horgue, M.A., Baceta Caballero, J.I., Olive Davo, A., Niñerola Pla, S., Cerezo Arasti, A., 1996. Cartografía geológica de Navarra, escala 1:25.000 hoja 113–IV Olazti-Olazagutía, Memoria. Gobierno de Navarra, 94 pp.
- Lübke, A., Enax, J., Loza, K., Prymak, O., Gaengler, P., Fabritius, H.-O., Raabe, D., Epple, M., 2015. Dental lessons from past to present: ultrastructure and composition of teeth from plesiosaurs, dinosaurs, extinct and recent sharks. *The Royal Society of Chemistry RSC Advances* 5, 61612–61622.
- Luer, C.A., Blum, P.C., Gilbert, P.W., 1990. Rate of tooth replacement in the nurse shark, *Ginglymostoma cirratum*. *Copeia* 1990(1), 182–191.
- Lund, R., Bartholomew, P., Kemp, A., 1992. The composition of the dental hard tissues of fishes, in: Smith, P., Tchernov, E. (Eds), *Structure, Function, and Evolution of Teeth*. Freund Publishing House Ltd, London and Tel Aviv, pp. 35–72.
- Lundgren, B., 1891. Studier öfver fossilförande lösa block. 8. Om Hisingers *Serpula lituus*. *Geologiska Föreningens i Stockholm Förhandlingar* 13(2), 118–120.

M

- Machalski, M., Kennedy, W.J., Kin, A., 2004. Early Late Campanian ammonite fauna from Busko Zdrój (Nida Trough, southern Poland). *Acta Geologica Polonica* 54 (4), 447–471.
- Mackie, S.J., 1863. On a new species of *Hybodus* from the Lower Chalk. *The Geologist* 6, 241–246.
- Madsen, S.K., 1996. Some techniques and procedures for microvertebrate preparation, in: Cifelli, R.L. (Ed.), *Techniques for recovery and preparation of microvertebrate fossils*. Oklahoma Geological Survey Special Publication 96–4, 25–36.
- Maisey, J.G., 2012. What is an ‘elasmobranch’? The impact of palaeontology in understanding elasmobranch phylogeny and evolution. *Journal of Fish Biology* 80, 918–951.
- Maisey, J.G., Naylor, G.J.P., Ward, D.J., 2004. Mesozoic elasmobranchs, neoselachian phylogeny and the rise of modern elasmobranch diversity, in: Arratia, G., Tintori A. (Eds), *Mesozoic fishes 3 – systematics paleoenvironments and biodiversity*. Dr. Friedrich Pfeil, Munich, pp. 17–56.
- Mallada, L., 1904. Explicación del mapa geológico de España. *Sistemas Infracretáceo y Cretá-*

- ceo. Memorias de la Comisión del Mapa Geológico de España 5. M. Tello, Madrid, 519 pp.
- Mangin, J.Ph., 1955. L'Éocène inférieur des provinces de Burgos, d'Alava et de Navarre occidentale (Espagne). *Compte Rendus Hebdomadaires des Séances de l'Académie des Sciences* 241, 73–75.
- Mangin, J.Ph., 1958. Le nummulitique sud-Pyrénéen à l'ouest de l'Aragon. *Pirineos* 51–58, 656 pp.
- Mantell, G., 1822. The fossils of the South Downs; or illustrations of the Geology of Sussex. Lupton Relfe, London, 320 pp.
- Marck, W. von der, 1894. Vierter Nachtrag zu: Die fossilen Fische der westfälischen Kreide. *Palaeontographica* 41, 41–48.
- Mackie, S.J., 1863. On a new species of *Hybodus* from the Lower Chalk. *The Geologist* 6, 241–246.
- Marín, P., Márquez, G., Gallego, J.R., Permanyer, A., 2014. Characterization of asphaltic oil occurrences from the southeastern margin of the Basque-Cantabrian Basin, Spain. *Geologica Acta* 12(4), 327–342.
- Martin, L.D., Rothschild, B.M., 1989. Paleopathology and diving mosasaurs. *American Scientist* 77, 460–467.
- Martín Alafont, J.M., Ramírez del Pozo J., Portero, J.M., 1978. Memoria explicativa de la hoja nº 138 (La Puebla de Arganzón) del Mapa Geológico de España, segunda serie. E 1:50. 000. Instituto Geológico y Minero de España (IGME), Madrid, 44 pp.
- Martin-Chivelet, J., Berastegui, X. et al., 2002. Cretaceous, in: Gibbons, W., Moreno, T. (Eds), *The Geology of Spain*. The Geological Society, London, pp. 255–292.
- Martínez, R., Lamolda, M.A., Gorostidi, A., López, G., Santamaría, R., 1996. Bioestratigrafía integrada del Cretácico superior de la región Vasco-cantábrica. *Revista Española de Paleontología*, Número Extraordinario, 160–171.
- Martínez-Pérez, C., Dupret, V., Manzanares, E., Botella, H., 2010. New data on the Lower Devonian Chondrichthyan fauna from Celtiberia (Spain). *Journal of Vertebrate Paleontology* 30(5), 1622–1627.
- Martínez-Torres, L.M., Eguiluz, L., 2014. Dinámica cortical y pulsos termo-tectónicos alpinos en la cuenca vasco-cantábrica y Pirineo occidental, in: Bodego, A., Mendia, M., Aranburu, Apraiz, A. (Eds), *Geología de la Cuenca Vasco-Cantábrica*. Servicio Editorial de la Universidad del País Vasco, Bilbao, pp. 105–118.
- Martins, U.P., 1989. Sedimentary evolution of the shallow marine Late Cretaceous in the southern Basco-Cantabrian Basin (northern Spain), in: Wiedmann, J. (Ed.), *Cretaceous of the Western Tethys*. Proceedings of the 3rd International Cretaceous Symposium Tübingen, 1987. E. Schweizerbart'sche Verlagsbuchhandlung, Stuttgart, pp. 121–144.
- Massare, J.A., 1987. Tooth morphology and prey preference of Mesozoic marine reptiles. *Journal of Vertebrate Paleontology* 7, 121–137.
- Matheron, Ph., 1832. Observations sur les terrains tertiaires du Département des Bouches-du-Rhône, et Description des Coquilles fossiles inédites ou peu communes qu'ils renferment. *Annales des Sciences et de l'Industrie du Midi de la France* 3, 39–78.
- Matheron, Ph., 1842. Catalogue méthodique et descriptif des corps organisés fossiles du département des Bouches-du-Rhône, et lieux circonvoisins; précédé d'un Mémoire sur les terrains supérieurs au grès bigarré du S.E. de la France. *Répertoire des travaux de la Société de statistique de Marseille* 6, 81–341.
- Mathey, B., 1986. Les flysch du Crétacé supérieur des Pyrénées basques (France, Espagne). *Mémoires Géologiques de l'Université de Dijon* 12, 403 pp.

- May, P., Reser, P., Leiggi, P., 1994. Laboratory preparation, Macrovertebrate preparation, in: Leiggi, P., May, P. (Eds), *Vertebrate Paleontological Techniques*, Volume 1. Cambridge University Press, Cambridge, pp. 113–129.
- McKenna, M.C., 1962. Collecting small fossils by washing and screening: *Curator* 5, 221–235.
- McKenna, M.C., 1965. Collecting microvertebrate fossils by washing and screening, in: Kummel, B., Raup, D.M. (Eds), *Handbook of paleontological techniques*. W.H. Freeman and Co., New York, pp. 193–203.
- McKenna, M.C., Bleefeld, A.R., Mellett, J.S., 1994. Microvertebrate collecting: Large-scale wet sieving for fossil microvertebrates in the field, in: Leiggi, P., May, P. (Eds), *Vertebrate Paleontological Techniques*, volume 1. Cambridge University Press, Cambridge, UK, pp. 93–111.
- McLellan, J., 1988. Notes on fossil shark teeth from the Escondido Formation of Texas. Unpubl. report, 21 pp.
- McNeil, D.H., Wall, J.H., Eberth, D.A., 1995. Parasequences and foraminiferal distributions in the Campanian Foremost Formation of southern Alberta, in: Bell, J.S., Bird, T.D., Hillier, T.L., Greener, P.L. (Eds), *Proceedings of the Oil and Gas Forum '95 - Energy from Sediments*. Geological Survey of Canada, Open File 3058, 93–97.
- McNulty, C.L., Slaughter, B.H., 1972. The Cretaceous selachian genus, *Ptychotrygon* Jaekel 1894. *Eclogae geologicae Helvetiae* 65(3), 647–656.
- Meek, F.B., Hayden, F.V., 1861. Descriptions of new Lower Silurian, (Primordial), Jurassic, Cretaceous, and Tertiary Fossils, collected in Nebraska, by the Exploring Expedition under the command of Capt. Wm. F. Reynolds, U. S. Top. Engrs.; with some remarks on the rocks from which they were obtained. *Proceedings of the Academy of Natural Sciences of Philadelphia* 13, 415–447.
- Megías, A.G., 1988. La tectónica pirenaica en relación con la evolución alpina del margen noribérico. *Revista de la Sociedad Geológica de España* 1(3–4), 365–372.
- Metzger, C.A., Terry, D.O., Grandstaff, D.E., 2004. Effect of paleosol formation on rare earth element signatures in fossil bone, *Geology* 32, 467–500.
- Miake, Y., Aoba, T., Moreno, E.C., Shimoda, S., Prostack, K., Suga, S., 1991. Ultrastructural Studies on Crystal Growth of Enameloid Minerals in Elasmobranch and Teleost Fish. *Calcified Tissue International*, 48, 214–217.
- Mikhailov, N.P., 1951. Upper Cretaceous ammonites from the southern part of European Russia and their importance for zonal stratigraphy (Campanian, Maastrichtian)]. *Academy of Sciences of the USSR, Proceedings of the Institute of Geological Sciences* 129, *Geological Series* (No. 50), 143 pp. [In Russian].
- Miller, R.F., Cloutier, R., Turner, S., 2003. The oldest articulated chondrichthyan from the Early Devonian period. *Nature* 425(2), 501–504.
- Moberg, J.C., 1885. *Cephalopoderna i Sveriges Kritsystem, II Artsbeskrifning*. Sveriges Geologiska Undersökning C73, 1–64.
- Montes Santiago, M.J., Alonso Gavilán, G., Dabrio, C.J., 1989. La transgresión Ilerdense (calizas de Alveolinas) en la Cuenca de Villarcayo (Burgos). *Geogaceta* 6, 61–64.
- Morton, S.G., 1828. Description of the fossil shells which characterize the Atlantic Secondary Formation of New Jersey and Delaware; including four new species. *Journal of the Academy of Natural Sciences of Philadelphia* 6, 73–76.
- Morton, S.G., 1830. Synopsis of the Organic Remains of the Ferruginous Sand Formation of the

- United States, with Geological Remarks. The American Journal of Science and Arts 18, 243–250.
- Morton, S.G., 1834. Synopsis of the organic remains of the Cretaceous Group of the United States. Key & Biddle, Philadelphia, 103 pp.
- Motta, P.J., Tricas, T.C., Hueter, R.E., Summers, A.P., 1997. Feeding mechanism and functional morphology of the jaws of the lemon shark *Negaprion brevirostris* (Chondrichthyes, Carcharhinidae). The Journal of Experimental Biology 200, 2765–2780.
- Moyer, J.K., Riccio, M.L., Bemis, W.E., 2015. Development and Microstructure of Tooth Histotypes in the Blue Shark, *Prionace glauca* (Carcharhiniformes: Carcharhinidae) and the Great White Shark, *Carcharodon carcharias* (Lamniformes: Lamnidae). Journal of Morphology 276, 797–817.
- Müller, A., 1989. Selachier (Pisces: Neoselachii) aus dem Höheren Campanium (Oberkreide) Westfalens (Nordrhein-Westfalen, NW-Deutschland). Geologie und Paläontologie in Westfalen 14, 1–161.
- Müller, A., 1991. Fische aus dem Campan (Oberkreide) der Bohrung Metelen 1001 (Münsterland, NW-Deutschland). Facies 24, 129–134.
- Müller, A., 2014. Die Neoselachier der höheren Oberkreide (Campanium) des Münsterlandes, Eine Übersicht. Geologie und Paläontologie in Westfalen 85, 5–65.
- Müller, A.H., 1966. Mesozoic serpulids. Geologie, Berlin 15(9), 1053–1070.
- Müller, A., Diedrich, C.G., 1991. Selachier (Pisces, Chondrichthyes) aus dem Cenomanium von Ascheloh am Teutoburger Wald (Nordrhein-Westfalen, NW-Deutschland). Geologie und Paläontologie in Westfalen 20, 3–105.
- Müller, J., Henle, J., 1837. Gattungen der Haifische und Rochen nach einer von ihm mit Hrn. Henle unternommenen gemeinschaftlichen Arbeit über die Naturgeschichte der Knorpelfische. Bericht über die zur Bekanntmachung geeigneten Verhandlungen der Königlich Preussischen Akademie der Wissenschaften zu Berlin 2(1837), 111–118.
- Müller, J., Henle, J., 1838. On the generic characters of cartilaginous fishes, with descriptions of new genera. The Magazine of Natural History 2, 33–37 and 88–91.
- Müller, J., Henle, J., 1839. Systematische Beschreibung der Plagiostomen. Veit und Comp., Berlin (1838–1941), 29–102 (Part 2 published in 1839).
- Müller, A., Schöllmann, L., 1989. Neue Selachier (Neoselachii, Squalomorphii) aus dem Campanium Westfalens (NW-Deutschland). Neues Jahrbuch für Geologie und Paläontologie - Abhandlungen 178(1), 1–35.
- Musick, J.A., Harbin, M.M., Compagno, L.J.V., 2004. Historical zoogeography of the Selachii, in: Carrier, J.C., Musick, J.A., Heithaus, M.R. (Eds), Biology of Sharks and their Relatives. CRC Press, Boca Raton, FL, pp. 33–78.
- Mustafa, H.A., Case, G.R., Zalmout, I., 2002. A new selachian fauna from the Wadi Umm Ghudran Formation (Late Cretaceous) - Central Jordan. Neues Jahrbuch für Geologie und Paläontologie - Abhandlungen 226(3), 419–444.

N

- Nakkady, S.E., 1950. A new foraminiferal fauna from the Esna Shales and Upper Cretaceous Chalk of Egypt. Journal of Paleontology 24(6), 675–692.
- Nederbragt, A.J., 1991. Late Cretaceous biostratigraphy and development of Heterohelicidae (planktic foraminifera). Micropaleontology 37(4), 329–372.

- Nelson, J.S., 2006. *Fishes of the World*. John Wiley & Sons, Hoboken, 4^a ed., 601 pp.
- Nessov, L.A., Udovichenko, N.I., 1986. New findings of Cretaceous and Paleogene vertebrate remains of Soviet Middle Asia. *Voprosy Paleontologii* 9, 129–136 [in Russian].
- Neumann, C., 2000. Evidence of predation on Cretaceous sea stars from north-west Germany. *Lethaia* 33, 65–70.
- Newberry, J.S., 1885. Description of some gigantic placoderm fishes recently discovered in the Devonian of Ohio. *Transactions of the New York Academy of Sciences* 5, 25–28.
- Ngoc-Ho, N., 2003. European and Mediterranean Thalassinidea (Crustacea, Decapoda). *Zoosystema* 25(3), 439–555.
- Nilsson, S., 1827. *Petrificata Suecana Formationis Cretaceae, descripta et iconibus illustrata. Pars Prior, Vertebrata et Mollusca sistens*. Berling, Londini Gothorum, 29 pp.
- Nishida, K., 1990. Phylogeny of the suborder Myliobatoidei. *Memoirs of the Faculty of Fisheries, Hokkaido University* 37(1–2), 1–108.
- Noubhani, A., Cappetta, H., 1994. Révision des Rhombodontidae (Neoselachii, Batomorphii) des bassins à phosphate du Maroc. *Palaeovertebrata* 23(1–4), 1–49.
- Noubhani, A., Cappetta, H., 1997. Les Orectolobiformes, Carcharhiniformes et Myliobatiformes (Elasmobranchii, Neoselachii) des bassins à phosphate du Maroc (Maastrichtian-Lutétien basal). *Systématique, biostratigraphie, évolution et dynamique des faunes. Palaeo Ichthyologica* 8, 1–327.
- Núñez-Betelu, K., 1999. Preliminary palynological assessment of the vertebrate-rich Laño beds: age and paleoenvironment. *Estudios del Museo de Ciencias Naturales de Álava* 14(Número especial 1), 37–42.

0

- Odin, G.S., Morton, A.C., 1988. Authigenic green particles from marine environments, in: Chilingarian, G.V., Wolf, K.H. (Eds), *Diagenesis II. Developments in Sedimentology* 43. Elsevier, Amsterdam, pp. 213–264.
- Ogg, J.G., Hinnov, L.A., 2012. Cretaceous, in: Gradstein, F.M., Ogg, J.G., Schmitz, M., Ogg, G.M. (Eds), *The Geologic Time Scale 2012*. Elsevier, Oxford, pp. 793–853.
- Olsson, R.K., 1960. Foraminifera of latest Cretaceous and earliest Tertiary age in the New Jersey Coastal Plain. *Journal of Paleontology* 34(1), 1–58.
- Olsson, R.K., 1964. Late Cretaceous planktonic foraminifera from New Jersey and Delaware. *Micropaleontology* 10(2), 157–188.
- Oppel, M., 1811. *Die Ordnungen, Familien und Gattungen der Reptilien als Prodrom einer Naturgeschichte derselben*. Joseph Lindauer, München, 87 pp.
- Oppenheim, P., 1895. Beiträge zur Binnenfauna der provençalischen Kreide. *Palaeontographica* 42, 309–378.
- Ortuño, V.M., 1990. Estudio sistemático del género *Steropus* (sensu Jeannel, 1942) de la fauna Iberomauritánica (2^a parte). El género *Corax* (Coleoptera, Caraboidea, Pterostichidae). *Nova Acta Científica Compostelana (Biologia)* 1, 31–46.
- Owen, R., 1840–1845. *Odontography*. Bailliere, London, 2 vol., 655 pp, 150 pl.
- Özcan, E., 2007. Morphometric analysis of the genus *Omphalocyclus* from the Late Cretaceous of Turkey: new data on its stratigraphic distribution in Mediterranean Tethys and description of two new taxa. *Cretaceous Research* 28, 621–641.

P

- Paine, C. (Ed.), 1993. Standards in the museum care of geological collections. 1993. Museums & Galleries Commission, London, 1–57.
- Pajaud, D., Plaziat, J.-C., 1972. Brachiopodes Thanétien du synclinal sud-cantabrique au S-E de Vitoria (pays basque espagnol). Étude systématique et interprétation paléocéologique. Extrait du Bulletin de la Société d'Histoire Naturelle de Toulouse T 108(3–4), 446–473.
- Palacios, P., 1919. Los terrenos mesozoicos de Navarra. Est. Tipográfico Sucesores de Rivadeneyra (S.A.), Madrid, 159 pp.
- Páramo Fonseca, M.E., 1997. Les vertébrés marins du Turonien de la vallée supérieure du Magdalena, Colombie. Ph.D. dissertation, University of Poitiers, Poitiers, 174 pp.
- Pendás Fernández, F., Menéndez Casares, E., Roqueñi, N., 1994. Mapa geológico y memoria explicativa de la hoja nº 134 (Polientes) del Mapa Geológico de España, segunda serie. E 1:50000. Instituto Geológico y Minero de España, Madrid, 68 pp.
- Peng, J., Russell, A.P., Brinkman, D.B., 2001. Vertebrate microsite assemblages (exclusive of mammals) from the Foremost and Oldman formations of the Judith River Group (Campanian) of Southeastern Alberta: An Illustrated Guide. Natural History Occasional Paper 25. Curatorial Section / Provincial Museum of Alberta, Edmonton, Alberta, 54 pp.
- Pereda-Suberbiola, X., Astibia, H., Murelaga, X., Elorza, J.J., Gómez-Alday, J.J., 2000. Taphonomy of the Late Cretaceous dinosaur-bearing beds of the Laño Quarry (Iberian Peninsula). *Palaeogeography, Palaeoclimatology, Palaeoecology* 157, 247–275.
- Pereda-Suberbiola, X., Corral, J.C., Astibia, H., Badiola, A., Bardet, N., Berreteaga, A., Buffetaut, E., Buscalioni, A.D., Cappetta, H., Cavin, L., Díez Díaz, V., Gheerbrant, E., Murelaga, X., Ortega, F., Pérez-García, A., Poyato-Ariza, F., Rage, J.C., Sanz, J.L., Torices, A., 2015a. Continental and marine vertebrate assemblages from the Late Cretaceous of the Laño Quarry (Basque-Cantabrian Region, Iberian Peninsula): an update. *Journal of Iberian Geology* 41(1), 101–124.
- Pereda-Suberbiola, X., Pérez-García, A., Corral, J.C., Murelaga, X., Martín, G., Larrañaga, J., Bardet, B., Berreteaga, A., Company, J., 2015b. First dinosaur and turtle remains from the latest Cretaceous shallow marine deposits of Albaina (Laño quarry, Iberian Peninsula). *Comptes Rendus Palevol* 14, 471–482.
- Pessagno, E.A. Jr., 1967. Upper Cretaceous planktonic foraminifera from the western Gulf Coastal Plain. *Palaeontographica Americana* 5(37), 245–445.
- Picard, S., Lécuyer, C., Barrat, J.-A., Garcia, J.-P., Dromart, G., Sheppard, S.M.F., 2002. Rare earth element contents of Jurassic fish and reptile teeth and their potential relation to seawater composition (Anglo-Paris Basin, France and England). *Chemical Geology* 186(1–2), 1–16.
- Pictet, F.-J., Humbert, A., 1866. Nouvelles recherches sur les poissons fossiles du Mont Liban. Georg, Genève, 115 pp.
- Plaziat, J.-C., 1970a. La limite Crétacé-Tertiaire en Alava méridionale (Pays basque espagnol): le Rognacien n'y est pas l'équivalent continental du Danien. *Compte Rendu sommaire des Séances de la Société Géologique de France* 3, 77–78.
- Plaziat, J.-C., 1970b. Conséquences stratigraphiques de l'interstratification de Rognacien dans le Maestrichtien supérieur d'Alava (Espagne). *Comptes Rendus de l'Académie des Sciences, Paris* 270 (D), 2768–2771.
- Plaziat, J.-C., 1986. Influence respective de événements locaux (sédimentologiques, tectoniques)

- et globaux (climatiques variations du niveau des océans) sur la répartition et l'évolution des peuplements pyrénéens du début du Tertiaire. *Bulletin des centres de recherches exploration-production Elf-Aquitaine* 10(2), 467–476.
- Plaziat, J.-C., Toumarkine, M., Villate, J., 1975. L'âge des calcaires pélagiques et néritiques de la base du Tertiaire (Danien, Paléocène), Bassin basco-cantabrique et béarnais (Espagne, France). *Mise au point sur les faunes d'Échinides. Eclogae Geologicae Helvetiae* 68(3), 613–647.
- Pluchery, E., 1995. Cycles de dépôts du continent à l'océan. Les séries d'âge Maastrichtien supérieur à Eocène moyen de la marge basco-cantabrique et de son arrière-pays ibérique (Espagne du Nord). Ph.D. thesis, Université de Bourgogne, Dijon, 324 pp.
- Plummer, H.J., 1926. Foraminifera of the Midway formation in Texas. *University of Texas Bulletin* 2644, 1–206.
- Plummer, H.J., 1931. Some Cretaceous Foraminifera in Texas. *University of Texas Bulletin* 3101, 109–203.
- Plummer, T.W., Kinyua, A.M., Potts, R., 1994. Provenancing of hominid and mammalian fossils from Kanjera, Kenya, using ED-XRF. *Journal of Archaeological Science* 21, 553–563.
- Pojeta, J., Balanc, M., 1989. Uses of ultrasonic cleaners in paleontological laboratories, in: Feldmann, R., Chapman, R., Hannibal, J. (Eds), *Paleotechniques. The Paleontological Society Special Publication No. 4*, Department of Geological Sciences, The University of Tennessee, Knoxville, pp. 213–217.
- Portero, J.M., Ramírez del Pozo, J., 1979. Memoria explicativa de la hoja nº 170 (Haro) del Mapa Geológico de España, segunda serie. E 1:50 000. Madrid. 42 pp.
- Portero García, J.M., Carreras Suárez, F., Olmo Zamora, P. del, Ramírez del Pozo, J., 1978. Memoria explicativa de la hoja nº 113 (Salvatierra) del Mapa Geológico de España, segunda serie. E 1:50 000. IGME, Madrid, 33 pp.
- Poyato-Ariza, F.J., Fielitz, C., Wenz, S., 1999. Marine Actinopterygian fauna from the Upper Cretaceous of Albaina (Laño Quarry, northern Spain). *Estudios del Museo de Ciencias Naturales de Álava* 14(Número especial 1), 325–338.
- Prasad, G.V.R., Cappetta, H., 1993. Late Cretaceous selachians from India and the age of the Deccan Traps. *Palaeontology* 36, 231–248.
- Priem, F., 1897. Sur des dents d'Élasmobranches de divers gisements sénoniens (Villedieu, Meudon, Folx-les-Caves). *Bulletin de la Société Géologique de France, 2e série* 25, 40–56.
- Priem, F., 1898. Sur des pycnodontes et des squales du Crétacé supérieur du Bassin de Paris (Turonien, Sénonien, Montien inférieur). *Bulletin de la Société Géologique de France (3ème série)* 26, 229–243.
- Priem, F., 1908. Étude des poissons fossiles du Bassin parisien. *Annales de Paléontologie*, 1–144.
- Priem, F., 1914. Sur des vertébrés du Crétacé et de l'Éocène d'Égypte. *Bulletin de la Société Géologique de France (4ème série)* 14, 366–382.
- Pucéat, E., Lécuyer, C., Reisberg, L., 2005. Neodymium isotope evolution of NW Tethyan upper ocean waters throughout the Cretaceous. *Earth and Planetary Science Letters* 236, 705–720.
- Putzeys, J., 1846. *Prémices entomologiques. Mémoires de la Société Royale des Sciences de Liège* 2, 353–417.
- Pujalte, V., Baceta, J.I., Payros, A., Orue-Etxebarria X., 1993. Late Cretaceous-Middle Eocene sequence stratigraphy and facies of the SW and W Pyrenees. Pamplona and Basque Basins, Spain. *Field-Seminar. Universidad del País Vasco, Bilbao, Spain*, 113 pp.

- Pujalte, V., Robles, S., Orue-Etxebarria, X., Baceta, J.I., Payros, A., Larruzea, I.F., 2000a. Uppermost Cretaceous-Middle Eocene strata of the Basque-Cantabrian Region and western Pyrenees: a sequence stratigraphic perspective. *Revista de la Sociedad Geológica de España* 13(2), 191–211.
- Pujalte, V., Baceta, J.I., Payros, A., Orue-Etxebarria, X., Schmitz, B., 2000b. Upper Paleocene–lower Eocene strata of the western Pyrenees, Spain: A shelf-to-basin correlation. *GFF (Transactions of the Geological Society in Stockholm)* 122(1), 129–130.
- Pujalte, V., Baceta, J.I., Schmitz, B., 2015. A massive input of coarse-grained siliciclastics in the Pyrenean Basin during the PETM: the missing ingredient in a coeval abrupt change in hydrological regime. *Climate of the Past* 11, 1653–1672.

Q

- Quaas, A., 1902. Beitrag zur Kenntniss der Fauna der obersten Kreidebildungen in der libyischen Wüste (Overwegischichten und Blätterthone). *Palaeontographica (1846–1933)* 30(4), 153–336.

R

- Radig, F., 1963. Die Orbitoiden-Kreide am Nordrande der Mulde von Villarcayo (Prov. Burgos, Spanien) und ihre stratigraphische und paläogeographische Stellung. *Neues Jahrbuch für Geologie und Paläontologie - Abhandlungen* 117, 251–264.
- Radwanska, U., 1996. Tube-dwelling polychaetes from some Upper Cretaceous sequences of Poland. *Acta Geologica Polonica* 46(1–2), 61–80.
- Rafinesque, C.S., 1810. Caratteri di alcuni nuovi generi e nuove specie di animale e pinate della Sicilia, con varie osservazioni sopra i medesimi. Sanfilippo, Palermo: Part 1, 3–69; Part 2, 71–105.
- Ramírez del Pozo, J., 1971. Biostratigrafía y Microfacies del Jurásico y Cretácico del Norte de España (Región Cantábrica). *Memoria del Instituto Geológico y Minero de España* 78, 3 Vols., 357 pp.
- Ramírez del Pozo, J., 1973. Síntesis geológica de la provincia de Álava. *Institución Sancho el Sabio*. Vitoria, 158 pp.
- Ramírez del Pozo, J., del Olmo Zamora, P., 1978. Memoria explicativa de la hoja nº 112 (Vitoria) del Mapa Geológico de España, segunda serie. E 1:50 000. IGME, Madrid, 34 pp.
- Rat, P., 1988. The Basque-Cantabrian basin between the Iberian and European plates. Some facts but still many problems. *Revista de la Sociedad Geológica de España* 1(3–4), 328–348.
- Rebouças, J.C., Santos, R.D., 1956. Fauna ictiológica do fosfato de Pernambuco. *Divisão Geologia e Mineralogia, Boletim* 162, 1–29.
- Redtenbacher, A., 1873. Die Cephalopodenfauna der Gosauschichten in den nordöstlichen Alpen. *Abhandlungen der Geologischen Bundesanstalt in Wien* 5(5), 101 pp.
- Regan, C.T., 1906. Descriptions of new or little-known Fishes from the Coast of Natal. *Annals of the Natal Government Museum* 1, 1–6.
- Repelin, J., Parent, H., 1920. Monographie du genre *Lychnus*. *Mémoires de la Société géologique de France, Paléontologie* 53, 25 pp.
- Reuss, A.E., 1845. Die Versteinerungen der Böhmischen Kreideformation, mit Abbildungen der neuen oder weniger bekannten arten. A - Fische. Erste Abtheilung. Schweizerbart, Stuttgart, 58 pp.

- Reynard, B., Lécuyer, C., Grandjean, P., 1999. Crystal - chemical controls on rare-earth element concentrations in fossil biogenic apatites and implications for paleoenvironmental reconstructions. *Chemical Geology* 155, 233–241.
- Riba, O., 1956. La cuenca terciaria de Miranda-Treviño, con 1 mapa escala 1:50.000. Informe CIEPSA, Vitoria – Madrid [not seen].
- Riba, O., 1976. Tectogenèse et sédimentation: deux modèles de discordances syntectoniques pyrénéenes. *Bulletin du Bureau de Recherches Géologiques et Minières* 4, 383–401.
- Richter, M., Ward, D.J., 1990. Fish remains from the Santa Marta Formation (Late Cretaceous) of James Ross Island, Antarctica. *Antarctic Science* 2(1), 67–76.
- Risso, A., 1810. *Ichthyologie de Nice, ou histoire naturelle des poissons du département des Alpes Maritimes*. F. Schoell, Paris, 388 pp.
- Rixon, A.E., 1976. Fossil animal remains – their preparation and conservation. The Athlone Press, London, 304 pp.
- Robaszynski, F., Caron, M., 1995. Foraminifères planctoniques du Crétacé; commentaire de la zonation Europe-Méditerranée. *Bulletin de la Société Géologique de France* 166(6), 681–692.
- Robaszynski, F., Dhondt, A.V., Jagt, J.W.M., 2001. Cretaceous lithostratigraphic units (Belgium), in Bultynck, P., Dejonghe, L. (Eds), *Guide to a revised lithostratigraphic scale of Belgium*. *Geologica Belgica* 4(1–2), 121–134.
- Robles, S., 2014. Evolución geológica de la Cuenca Vasco-Cantábrica, in: Bodego, A., Mendia, M., Aranburu, Apraiz, A. (Eds), *Geología de la Cuenca Vasco-Cantábrica*. Servicio Editorial de la Universidad del País Vasco, Bilbao, pp. 9–103.
- Robles, S., Aranburu, A., Apraiz, A., 2014. La Cuenca Vasco-Cantábrica: génesis y evolución tectosedimentaria. *Enseñanza de las Ciencias de la Tierra* 22(2), 99–114.
- Roemer, F.A., 1841. *Die Versteinerungen des norddeutschen Kreidegebirges*. Hahn'schen Hofbuchhandlung, Hannover, 145 pp.
- Roemer, F., 1849. Texas, mit besonderer Rücksicht auf deutsche Auswanderung und die physischen Verhältnisse des Landes nach eigener Beobachtung geschildert. Adolf Marcus, Bonn, 464 pp.
- Roemer, F., 1852, *Die Kreidebildungen von Texas und ihre organischen Einschlüsse*. Adolph Marcus, Bonn, 100 pp.
- Rogers, R.R., Kidwell, S.M., 2000. Associations of vertebrate skeletal concentrations and discontinuity surfaces in terrestrial and shallow marine records: A test in the Cretaceous of Montana. *Journal of Geology* 108, 131–154.
- Rothschild, B.M., Martin, L.D., Schulp, A.S., 2005. Sharks eating mosasaurs, dead or alive? *Netherlands Journal of Geosciences / Geologie en Mijnbouw* 84(3), 335–340.
- Ruiz de Gaona, M., 1943. El piso Maestrichtiense en Olazagutía (Navarra). *Boletín de la Real Sociedad Española de Historia Natural* 41, 85–101.
- Rutot, A., 1875. Note sur l'extension de *Lamna elegans*, Ag. à travers les terrains crétacé et tertiaire. *Annales de la Société Géologique de Belgique, Mémoires* 2, 34–41.
- Rutzky, I.S., Evers, W.B., Maisey, J.G., Kellner, A.W.A., 1994. Chemical Preparation Techniques, in: Leiggi, P., May, P. (Eds), *Vertebrate Paleontological Techniques, Volume 1*. Cambridge University Press, Cambridge, pp. 155–186.
- Russell, D.A., 1967. Systematics and morphology of the American mosasaurs. *Bulletin of the Peabody Museum of Natural History* 23, 1–240.
- Russell D.A., 1975. A new species of *Globidens* from South Dakota, and a review of *Globidentine* Mosasaurs. *Fieldiana Geology* 33, 235–256.

S

- Samoilov, V.S., Benjamini, C., 1996. Geochemical features of Dinosaur Remains from the Gobi Desert, South Mongolia. *Palaios* 11, 519–531.
- Samoilov, V.S., Benjamini, C., Smirnova, E.V., 2001. Early diagenetic stabilization of trace elements in reptile bone as an indicator of Maastrichtian-Late Palaeocene climatic changes: evidence from the Narun Balak locality, the Gobi Desert, South Mongolia. *Sedimentary Geology* 143, 15–39.
- San Martín, D.M., 1986. Estudio Micropaleontológico de los Materiales del Senoniense de la Cuenca de Vitoria. Unpublished Bachelor's thesis, Universidad de Zaragoza, Zaragoza, 142 pp.
- San Martín, D.M., 1987. Biostratigrafía del Senoniense de la Cuenca de Vitoria. *Estudios del Instituto Alavés de la Naturaleza* 2, 7–27.
- Santamaría, R., 1995. Los Ammonoideos del Cenomaniense superior al Santoniense de la plataforma nord-castellana y la cuenca navarro-cántabra. Parte II. Sistemática: Acanthocerataceae. *Treballs del Museu de Geologia de Barcelona* 4, 15–131.
- Santamaría-Zabala, R., 1992. Los Ammonoideos del Cenomaniense superior al Santoniense de la plataforma Nord-Castellana y la Cuenca Navarro-Cántabra. Parte I. Biostratigrafía y Sistemática: Phylloceratina. Ammonitina (Desmocerataceae y Hoplitaceae) y Ancyloceratina. *Treballs del Museu de Geologia de Barcelona* 2, 171–268.
- Santamaría Zabala, R., 1996. Los ammonites del Campaniense de la provincia de Álava. Sistemática y biostratigrafía. *Estudios del Museo de Ciencias Naturales de Álava* 10–11 (1995–1996), 5–25.
- Santamaría, R., López, G., 1994. Aspectos sistemáticos y biostratigráficos de los ammonites e inocerámidos de la provincia de Álava. *Comunicaciones X Jornadas de Paleontología* 182–184.
- Santamaría, R., López, G., 1996. Aspectos biostratigráficos de los ammonites e inocerámidos (Bivalvia) del Albiense superior al Maastrichtiense de la provincia de Álava. *Revista Española de Paleontología Número extraordinario X Jornadas de Paleontología*, 148–159.
- Schlumberger, C., 1901. Première note sur les Orbitoïdes. *Bulletin de la Société Géologique de France (4ème série)* 1, 459–467.
- Schlüter, C., 1867. Beitrag zur Kenntniss der jüngsten Ammoneen Norddeutschlands. Verlag von A. Henry, Bonn, 36 pp.
- Schlüter, C., 1872. Cephalopoden der oberen deutschen Kreide. *Palaeontographica* 21 (1872–1976), 1–120.
- Schlüter, C., 1879. Neue und weniger gekannte Kreide- und Tertiär-Krebse des nördlichen Deutschlands. *Zeitschrift der deutschen geologischen Gesellschaft* 31, 586–615.
- Schluter, N., Diaz, M., Wiese, F., 2004. Response of irregular echinoid assemblages to environmental changes: a case study from the Lower/Middle Campanian of Cantabria (northern Spain) – preliminary data, in: Reich, M., Hagdorn, H., Reitner, J. (Eds), 3 Arbeitstreffen deutschsprachiger Echinodermenforscher. Universitätsverlag Göttingen, pp. 49–56.
- Schmitz, L., Thies, D., Kriwet, J., 2010. Two new lamniform sharks (*Leptostyrax stychi* sp. nov. and *Protolamna sarstedtensis* sp. nov.) from the Early Cretaceous of NW Germany. *Neues Jahrbuch für Geologie und Paläontologie - Abhandlungen* 257, 283–296.
- Schneider, C., Ladwig, J., 2013. Fische (Pisces Fische (Pisces), in: APH, Fossilien aus dem Campan von Hannover, 3rd ed. Arbeitskreis Paläontologie Hannover, pp. 257–270.
- Schrammen, A., 1901. Neue Kieselschwämme aus der oberen Kreide der Umgebung von

- Hannover und Hildesheim. Mitteilungen aus dem Roemer-Museum, Hildesheim 14, 1–26.
- Schrammen, A., 1910. Die Kieselspongien der oberen Kreide von Nordwestdeutschland, I Teil, Tetraxonia, Monaxonia und Silicea incert. sedis. *Palaeontographica*, Supplementband V, 1–175.
- Schubert, J.A., Wick, S.L., Lehman, T.M., 2016. An Upper Cretaceous (middle Campanian) marine chondrichthyan and osteichthyan fauna from the Rattlesnake Mountain sandstone member of the Aguja Formation in West Texas. *Cretaceous Research* 69 (for 2017), 6–33.
- Schultze, H.-P., 1993. Patterns of Diversity in the Skull of Jawed Fishes, in: Hanken, J., Brian K. Hall, B.K. (Eds), *The Skull, Volume 2 Patterns of Structural and Systematic Diversity*. University Of Chicago Press, Chicago, pp. 189–254.
- Schweizer, R., 1964. Die Elasmobranchier und Holocephalen aus den Nusplinger Plattenkalken. *Palaeontographica A* 123(123), 58–110.
- Schwimmer, D.R., Stewart, J.D., Williams, G.D., 1997. Scavenging by sharks of the genus *Squalicorax* in the Late Cretaceous of North America. *Palaios* 12, 71–83.
- Scovil, J., 1996. *Photographing Minerals, Fossils and Lapidary Materials*. Geoscience Press, Tucson AZ, 224 pp.
- Seeling, J., Colin J.-P., Fauth, G., 2004. Global Campanian (Upper Cretaceous) ostracod palaeobiogeography. *Palaeogeography, Palaeoclimatology, Palaeoecology* 213(3–4), 379–398.
- Seilacher, A., 1990. Taphonomy of fossil-lagerstätten, in: Brigs, D.E., Crowder, P.R. (Eds), *Palaeobiology. A synthesis*. Blackwell Science, Oxford, pp. 266–270.
- Sequeiros, L., 1988. La enseñanza de la paleontología en España en el siglo XIX: ¿modernidad o tradición? *Henares: Revista de geología* 2, 83–87.
- Seunes, J., 1890. Recherches géologiques sur les terrains secondaires et l'Eocene inferieur de la region sous-pyrénéene du sud-ouest de la France (Basses-Pyrenees et Landes). *Annales de Mines* 18, 209–458.
- Sharpe, D., 1853–1957. Description of the fossil remains of Mollusca found in the Chalk of England, Cephalopoda. The Palaeontographical Society, London, 68 pp. (1855, Part 2, pp. 27–35).
- Sheldon, R.P., 1981. Ancient marine phosphorites. *Annual review of Earth and Planetary Science* 9, 251–284.
- Shelton, S.Y., Chaney, D.S., 1994. An evaluation of adhesives and consolidants recommended for fossil vertebrates, in: Leiggi, P., May, P. (Eds), *Vertebrate paleontological techniques, Volume 1*. Cambridge University Press, Cambridge, pp. 35–45.
- Shimada, K., 1993. Preliminary report on the Upper Cretaceous shark, *Cretoxyrhina mantelli*, from western Kansas. *Geological Society of America Abstracts with Programs* 25, A–58.
- Shimada, K., 1997a. Paleoeological relationships of the Late Cretaceous lamniform shark *Cretoxyrhina mantelli* (Agassiz). *Journal of Paleontology* 71, 926–933.
- Shimada, K., 1997b. Skeletal anatomy of the Late Cretaceous Lamniform shark, *Cretoxyrhina mantelli*, from the Niobrara Chalk in Kansas. *Journal of Vertebrate Paleontology* 17, 642–652.
- Shimada, K., 1997c. Dentition of the Late Cretaceous Lamniform shark, *Cretoxyrhina mantelli*, from the Niobrara chalk of Kansas. *Journal of Vertebrate Paleontology* 17, 269–279.
- Shimada, K., Brereton, D., 2007. The Late Cretaceous Lamniform shark, *Serratolamna serrata* (Agassiz), from the Mooreville Chalk of Alabama. *Paludicola* 6(3), 105–110.
- Shimada, K., Hooks, G.E., 2004. Shark-bitten protostegid turtles from the Upper Cretaceous Mooreville Chalk, Alabama. *Journal of Paleontology* 78(1), 205–210.
- Shimada, K., Tsuihiji, T., Sato, T., Hasegawa, Y., 2010. A Remarkable Case of a Shark-Bitten

- Elasmosaurid Plesiosaur. *Journal of Vertebrate Paleontology* 30(2), 592–597.
- Signeux, J., 1959. Contributions à la stratigraphie et la paléontologie du Crétacé et du Nummulitique de la marge NW de la Péninsule Arabique. A: Poissons et reptiles marins. Notes et Mémoires sur le Moyen-Orient 7, 223–228.
- Simon, E., 2000. Upper Campanian brachiopods from the Mons Basin (Hainaut, Belgium): the brachiopod assemblage from the *Belemnitella mucronata* Zone. *Bulletin de l'Institut Royal des Sciences Naturelles de Belgique, Sciences de la Terre* 70, 129–160.
- Simpson, G.G., 1969. *La géographie de l'évolution*. Masson & Cie, Paris, 203 pp.
- Sinzow, J., 1899. Notizen über die Jura-, Kreide- und Neogen-Ablagerungen der Gouvernements Saratow, Simbirsk, Samara und Orenburg. *Ökonomische Buch- u. Steindruckerei, Odessa*, 106 pp.
- Siverson, M., 1989. Palaeospinacid selachians from the Late Cretaceous of the Kristianstad Basin, Skåne, Sweden. *Examensarbete i Geologi vid Lunds universitet. Historisk geologi och paleontologi* 30, 1–24.
- Siverson, M., 1992. Biology, dental morphology and taxonomy of lamniform sharks from the Campanian of the Kristianstad Basin, Sweden. *Palaeontology* 35, 519–554.
- Siverson, M., 1993. Late Cretaceous and Danian neoselachians from southern Sweden. *Lund Publications in Geology* 110. Lund University, Lund, Sweden, 28 pp.
- Siverson, M., 1995. Revision of the Danian Cow Sharks, Sand Tiger Sharks, and Goblin Sharks (Hexanchidae, Odontaspidae, and Mitsukurinidae) from Southern Sweden. *Journal of Vertebrate Paleontology* 15(1), 1–12.
- Siverson, M., 1996. Lamniform sharks of the mid Cretaceous Alinga Formation and Beedagong Claystone, Western Australia. *Palaeontology* 39(4), 813–849.
- Siverson, M., Lindgren, J., 2005. Late Cretaceous sharks *Cretoxyrhina* and *Cardabiodon* from Montana, USA. *Acta Palaeontologica Polonica* 50(2), 301–314.
- Siverson, M., Lindgren, J., Kelley, L.S., 2007. Anacoracid sharks from the Albian (Lower Cretaceous) Pawpaw Shale of Texas. *Palaeontology* 50(4), 939–950.
- Siverson, M., Lindgren, J., Newbrey, M.G., Cederström, P., Cook, T.D., 2015. Cenomanian–Campanian (Late Cretaceous) mid-palaeolatitude sharks of *Cretalamna appendiculata* type. *Acta Palaeontologica Polonica* 60(2), 339–384.
- Siverson, M., Cook, T.D., Cederström, P., Ryan, H.E., 2016. Early Campanian (Late Cretaceous) squatiniiform and synechodontiform selachians from the Åsen locality, Kristianstad Basin, Sweden, in: Kear, B.P., Lindgren, J., Hurum, J.H., Milán, J., Vajda, V. (Eds), *Mesozoic Biotas of Scandinavia and its Arctic Territories*. Geological Society, London, Special Publications 434, pp. 251–275.
- Siveter, D.J., 1990. Photography, in: Briggs, D.E.G., Crowther, P.R. (Eds), *Palaeobiology: A Synthesis*. Blackwell, Oxford, pp. 505–508.
- Slaughter, B.H., Springer, S., 1968. Replacement of rostral teeth in sawfishes and sawsharks. *Copeia* 1968(3), 499–506.
- Smith, A., 1828. Description of new, or imperfectly known objects of the animal kingdom found in the south of Africa. *South African Commercial Advertiser* 3(145), 2 [not seen].
- Smith, A., 1837. Revision of the groups included in the Linnean genus *Squalus*. *Proceedings of the Zoological Society of London* 5, 85–86.
- Smith, A.B., Gallelli, J., Jeffrey, C.H., Ernst, G., Ward, P.D., 1999. Late Cretaceous–Early Tertiary echinoids from northern Spain; implications for the Cretaceous–Tertiary extinction

- event. *Bulletin of the Natural History Museum, Geology Series* 55(2), 81–137.
- Smith, C.C., Pessagno, E.A., 1973. Planktonic foraminifera and stratigraphy of the Corsicana Formation (Maestrichtian) north-central Texas. *Cushman Foundation for Foraminiferal Research, Special Publication* 12, 1–68.
- Smith, A.G., Smith, D.G., Funnel, B.M., 1984. *Atlas of Mesozoic and Cenozoic Coastlines*. Cambridge University Press, Cambridge, 99 pp.
- Soler-Gijón, R., López-Martínez, N., 1998. Sharks and rays (chondrichthyes) from the Upper Cretaceous red beds of the southcentral Pyrenees (Lleida, Spain): indices of an India-Eurasia connection. *Palaeogeography, Palaeoclimatology, Palaeoecology* 141, 1–12.
- Sørensen, A.M., Finn Surlyk, F., Lindgren, J., 2013. Food resources and habitat selection of a diverse vertebrate fauna from the upper lower Campanian of the Kristianstad Basin, southern Sweden. *Cretaceous Research* 42, 85–92.
- Sornay, J., 1973. Sur les Inocérames du Maestrichtien de Madagascar et sur une espèce de la craie à *Baculites* du NW de la France. *Annales de Paléontologie* 59(1), 83–93.
- Sowerby, J., 1812–14. *The mineral conchology of Great Britain; or coloured figures and descriptions of those remains of testaceous animals or Shells, which have been preserved at various times and depths in the earth, vol. I*. Benjamin Meredith, London, 234 pp.
- Sowerby, J., 1818. *The mineral conchology of Great Britain; or coloured figures and descriptions of those remains of testaceous animals or shells, which have been preserved at various times and depths in the earth, vol. 2*. Arding and Merrett, London, 251 pp.
- Sowerby, J.D.C., 1825. *The mineral conchology of Great Britain; or Coloured figures and descriptions of those remains of testaceous animals or Shells, which have been preserved at various times and depths in the earth, vol. 5*. Richard Taylord, London, 168 pp.
- Sowerby, J.D.C., 1829. *The mineral conchology of Great Britain; or Coloured figures and descriptions of those remains of testaceous animals or Shells, which have been preserved at various times and depths in the earth, vol. 6*. Richard Taylord, London, 230 pp.
- Spielmann, J.A., Lucas, S.G., 2006. Late Cretaceous marine reptiles (Mosasauridae and Plesiosauria) from New Mexico and their biostratigraphic distribution. *New Mexico Museum of Natural History and Science Bulletin* 35, 217–221.
- Springer, S., 1961. Dynamics of the feedings mechanism of large galeoid sharks. *American Zoologist* 1, 183–185.
- Stephenson, L.W., 1941. The larger invertebrate fossils of the Navarro Group of Texas (exclusive of corals and crustaceans and exclusive of the fauna of the Escondido Formation). *The University of Texas Publication* 4101, 1–641.
- Stevens, J.D., 2005. Taxonomy and field techniques for identification and available regional guides, in: Musick, J.A, Bonfil, R. (Eds), *Management techniques for elasmobranch fisheries*, *FAO fisheries technical paper* 474, 15–44.
- Stoliczka, F., 1866. The fossil Cephalopoda of the Cretaceous rocks of Southern India, Ammonitidae with revision of the Nautilidae, etc. *Memoirs of the Geological Survey of India, Palaeontologia Indica* 1(10–13), 155–216.
- Stromer, S., 1917. *Ergebnisse der Forschungsreisen Prof. E. Stromers in den Wüsten Ägyptens. II. Wirbeltier-Reste der Baharije-Stufe (unterstes Cenoman). 4. Die Säge des Pristiden *Onchopristis numidus* Haug sp. und über die Sägen der Sägehaie*. *Abhandlungen der Königlich Bayerischen Akademie der Wissenschaften, Mathematisch - physikalische Klasse* 28(8), 1–28.
- Stromer, E., Weiler, W., 1930. *Ergebnisse der Forschungsreisen Prof. E. Stromers in den Wüsten*

- Ägyptens. VI. Beschreibung von Wirbeltier-Resten aus dem nubischen Sandsteine Oberägyptens und aus ägyptischen phosphaten nebst Bemerkungen über die Geologie der umgegend von Mahamid in Oberägypten. Abhandlungen der Bayerischen Akademie der Wissenschaften, Mathematisch-naturwissenschaftlichen Abteilung, Neue Funde 7, 1–42.
- Sugarman, P.J., Miller, K.G., Bukry, D., Feigenson, M.D., 1995. Uppermost Campanian–Maestrichtian strontium isotopic, biostratigraphic, and sequence stratigraphic framework of the New Jersey Coastal Plain. *Geological Society of America Bulletin* 107(1), 19–37.
- Surlyk, F., Sørensen, A.M., 2010. An early Campanian rocky shore at Ivö Klack, southern Sweden. *Cretaceous Research* 31, 567–576.
- Swen, K., Fraaije, R.H.B., van der Zwaan, G.J., 2001. Polymorphy and extinction of the Late Cretaceous burrowing shrimp *Protocallianassa faujasi* and first record of the genera *Coralianassa* and *Calliax* (Crustacea, Decapoda, Thalassinoidea) from the Cretaceous. *Contributions to Zoology* 70 (2), 85–98.
- Świerczewska-Gładysz, E., 2006. Late Cretaceous siliceous sponges from the Middle Vistula River Valley (Central Poland) and their palaeoecological significance. *Annales Societatis Geologorum Poloniae* 76, 227–296.
- Świerczewska-Gładysz, E., 2016. Early Campanian (Late Cretaceous) Pleromidae and Isoraphiniidae (lithistid Demospongiae) from the Łódź-Miechów Synclinorium (central and southern Poland): new data and taxonomic revision. *Papers in Palaeontology* 2(2), 189–233.

T

- Taverne, L., 1970. Les poissons fossiles et quelques dents de reptiles récoltés par C.R. Hoffmann dans le Crétacé supérieur de Vonso (Bas-Congo). Musée royal de l'Afrique Centrale – Tervuren (Belgique) – Annales – IN-8° – Sciences Géologiques, Série N° 70, 44 pp.
- Taylor, L.R., Compagno, L.J.V., Struhsaker, P.J., 1983. Megamouth – a new species, genus, and family of lamnoid shark (*Megachasma pelagios*, Family Megachasmidae) from the Hawaiian Islands. *Proceedings of the California Academy of Sciences* 43(8), 87–110.
- Taylor, S.R., McLennan, S.M., 1985. *The Continental Crust: Its Composition and Evolution*. Blackwell Scientific, Oxford, 312 pp.
- Thies, D., Müller, A., 1993. A neoselachian fauna (Vertebrata, Pisces) from the Late Cretaceous (Campanian) of Höver, near Hannover (NW Germany). *Paläontologische Zeitschrift* 67(1/2), 89–107.
- Tilev, N., 1951. Étude des Rosalines maestrichtiennes (genre *Globotruncana*) du Sud-Est de la Turquie (sondage de Ramandag). *Bulletin des laboratoires de Géologie, Minéralogie, Géophysique et du Musée géologique de l'Université de Lausanne* 103, 101 pp.
- Toombs, H.A., Rixon, A.E., 1959. The Use of Acids in the Preparation of Vertebrate Fossils. *Curator* 2(4), 304–312.
- Tricas, T.C., McCosker, J.E., 1984. Predatory behavior of the white shark (*Carcharodon carcharias*), with notes on its biology. *Proceedings of the California Academy of Science* 43, 221–238.
- Trueman, C.N., 1999. Rare earth element geochemistry and taphonomy of terrestrial vertebrate assemblages. *Palaios* 14, 555–568.
- Trueman, C.N., Benton, M.J., 1997. A geochemical method to trace the taphonomic history of reworked bones in sedimentary settings. *Geology* 25, 263–266.

- Trueman, C.N., Tuross, N., 2002. Trace metals in recent and fossil bone, in: Kohn, M.J., Hughes, J.J. (Eds), *Phosphates: geochemical, geobiological, and materials importance. Reviews in Mineralogy and Geochemistry* 48, 489–521.
- Trueman, C.N., Benton, M.J., Palmer, M.R., 2003. Geochemical taphonomy of shallow marine vertebrate assemblages. *Palaeogeography, Palaeoclimatology, Palaeoecology* 197, 151–169.
- Trueman, C.N.G., Field, J., Wroe, S., Charles, B., Dortch, J., 2005. Prolonged coexistence of humans and megafauna in Pleistocene Australia. *Proceedings of the National Academy of Sciences* 102, 8381–8385.
- Trueman, C.N., Behrensmeyer, A.K., Potts, R., Tuross, N., 2006. High-resolution records of location and stratigraphic provenance from the rare earth element composition of fossil bones. *Geochimica et Cosmochimica Acta* 70(17), 4343–4355.

U

- Uchupi, E., 1988. The Mesozoic–Cenozoic geologic evolution of Iberia. A tectonic link between Africa and Europe. *Revista de la Sociedad Geológica de España* 1(3–4), 257–294.
- Underwood, C.J., 2006. Diversification of Neoselachii (Chondrichthyes) during the Jurassic and Cretaceous. *Paleobiology* 32(2), 215–235.
- Underwood, C.J., Mitchell, S.F., 2000. *Serratolamna serrata* (Agassiz) (Pisces, Neoselachii) from the Maastrichtian (Late Cretaceous) of Jamaica. *Caribbean Journal of Earth Science* 34, 25–30.
- Underwood, C., Ward, D., 2008. Sharks of the Order Carcharhiniformes from the British Coniacian, Santonian and Campanian (Upper Cretaceous). *Palaeontology* 51(3), 509–536.
- Underwood, C.J., Mitchell, S.F., Veltkamp, K.J., 1999. Shark and ray teeth from the Hauterivian (Lower Cretaceous) of north-east England. *Palaeontology*, 42, 287–302.
- Uyeno, T., Hasegawa, Y., 1986. A new Cretaceous ganopristoid sawfish of the genus *Ischyrbiza* from Japan. *Bulletin of the National Sciences Museum, C (Geology and Paleontology)* 12, 67–72.

V

- Van Bakel, B.W.M., Guinot, D., Artal, P., Fraaije, R.H.B., Jagt, J.W.M., 2012. A revision of the Palaeocorystoidea and the phylogeny of raninoidian crabs (Crustacea, Decapoda, Brachyura, Podotremata). *Zootaxa* 3215(3215), 1–216.
- Van Sickle, W.A., Kominz, M.A., Miller, K.G., Browning, J.V., 2004. Late Cretaceous and Cenozoic sea-level estimates backstripping analysis of borehole data, onshore New Jersey. *Basin Research* 16, 451–465.
- Villas, E., Herrera, Z.A., 2001. Fotografía y paleontología. *Revista de la Asociación Española para la Enseñanza de las Ciencias de la Tierra* 9(2), 200–206.
- Vogler, J., 1941. Ober-Jura und Kreide von Misol (Niederländisch-Ostindien). *Palaeontographica - Supplementbände SIV Reihe/Abt 4* (1941), 243–293.
- von Buch, L., 1847. Über Ceratiten, besonders von denen, die in Kreidebildung sich finden. Bericht über die zur Bekanntmachung geeigneten Verhandlungen der Königlich Preussischen Akademie der Wissenschaften zu Berlin (Aus dem Jahre 1847), 214–223.
- von Buch, L., 1852. Monatsberichte über die Verhandlungen der Gesellschaft für Erdkunde zu Berlin IX, 54, t. 1 [not seen].

- von Hagenow, F., 1842. Monographie der Rügen'schen Kreide - Versteinerungen, III. Mollusken. Neues Jahrbuch für Mineralogie, Geognosie, Geologie und Petrefactenkunde (1842), 528–575.
- von Hauer, F., 1858. Ueber die Cephalopoden der Gosauschichten. Beiträge zur Palaontographie von Oesterreich 1, 7–14.
- von Schlotheim, E.F., 1813. Beiträge zur Naturgeschichte der Versteinerungen in geognostischer Hinsicht. Taschenbuch für die gesammte Mineralogie, mit Hinsicht auf die neuesten Entdeckungen, herausgegeben von C.C. Leonhard Bd. 7, 1–134.
- von Schlotheim, E.F., 1820. Die Petrefactenkunde auf ihrem jetzigen Standpunkte durch die Beschreibung seiner Sammlung versteineter und fossiler Überreste des Thier- und Pflanzenreichs der Vorwelt-erläutert. Becker'schen Buchhandlung, Gotha, 437 pp.
- Voorwijk, G.H., 1937. Foraminifera from the upper Cretaceous of La Habana, Cuba. Koninklijke Nederlandse Akademie van Wetenschappen, Proceedings of the Section of sciences 40(2), 190–198.
- Vullo, R., 2005. Selachians from the type Campanian area (Late Cretaceous), Charentes, western France. *Cretaceous Research* 26, 609–632.
- Vullo, R., Courville, P., 2014. Fish remains (Elasmobranchii, Actinopterygii) from the Late Cretaceous of the Benue Trough, Nigeria. *Journal of African Earth Sciences* 97, 194–206.

W

- Walaszczyk, I., Cobban, W.A., Harries, P.J., 2001. Inoceramids and inoceramid biostratigraphy of the Campanian and Maastrichtian of the United States Western Interior Basin. *Revue de Paléobiologie* 20, 117–234.
- Walaszczyk, I., Kennedy, W.J., Klinger, H.C., 2009. Cretaceous faunas from Zululand and Natal, South Africa. Systematic palaeontology and stratigraphical potential of the Upper Campanian-Maastrichtian Inoceramidae (Bivalvia). *African Natural History* 5(1), 49–132.
- Ward, D.J., 1988. *Hypotodus verticalis* (Agassiz 1843), *Hypotodus robustus* (Leriche 1921) and *Hypotodus heinzlini* (Casier 1967), Chondrichthyes, Lamniformes, junior synonyms of *Carcharias hopei* (Agassiz 1843). *Tertiary Research* 10(1), 1–12.
- Ward, P.D., Kennedy, W.J., 1993. Maastrichtian ammonites from the Biscay Region (France, Spain). *Memoir (The Paleontological Society)* 34, Supplement of the *Journal of Paleontology* 67(5), 58 pp.
- Welles, S.P., 1943. Elasmosaurid plesiosaurs with description of new material from California and Colorado. *Memoirs of the University of California* 13, 125–254.
- Welton, B.J., Farish, R.F., 1993. The collectors guide to fossil sharks and rays from the Cretaceous of Texas. Horton Printing Company, Dallas, 204 pp.
- Werner, C., 1989. Die Elasmobranchier-Fauna des Gebel Dist Member der Bahariya Formation (Obercenoman) der Oase Bahariya, Ägypten. *Palaeo Ichthyologica* 5, 1–112.
- Wetzel, W., 1930. Die Quiriquina-Schichten als Sediment und Paläontologischen Archiv. *Palaeontographica A* 73, 49–106, 5 figs., pls. 9–14.
- White, M.P., 1928. Some Index Foraminifera of the Tampico Embayment Area of Mexico. Part II. *Journal of Paleontology* 2(4), 280–317.
- White, E.I., Moy-Thomas, J.A., 1940. XLVIII.—Notes on the nomenclature of fossil fishes.—Part I. Homonyms A–C. *Annals and Magazine of Natural History* 5(30), 502–507.

- Whitfield, R.P. 1877. Preliminary report on the paleontology of the Black Hills, containing descriptions of new species of fossils from the Potsdam, Jurassic, and Cretaceous formations of the Black Hills of Dakota. U.S. Geographical and Geological Survey of the Rocky Mountain Region. Government Printing Office, Washington, 49 pp.
- Whitley, G.P., 1939. Taxonomic notes on sharks and rays. *Australian Journal of Zoology* 9(3), 227–262.
- Whitley, G.P., 1940. The fishes of Australia. Part 1. The sharks, rays, devilfish, and other primitive fishes of Australia and New Zealand. *Australian Zoology Handbooks*, Royal Zoological Society of New South Wales, Mosman, 280 pp.
- Wiedmann, J., 1960. Le Crétacé supérieur de l'Espagne et du Portugal et ses céphalopodes, in: Colloque sur le Crétacé Supérieur Français, *Comptes Rendus du Congrès des Sociétés Savantes de Paris et des Départements tenu à Dijon en 1959*. Gauthier-Villars, Paris, pp. 709–764.
- Wiedmann, J., 1962. Ammoniten aus der Vascogotischen Kreide (Nordspanien) I. Phylloceratina, Lytoceratina. *Palaeontographica A* 118(4–6), 119–237.
- Wiedmann, J., 1964. Le Crétacé supérieur de l'Espagne et du Portugal et ses Céphalopodes. *Estudios Geológicos* 20(1–2), 107–148.
- Wiedmann, J., 1979. Itinéraire géologique à travers le Crétacé moyen des chaînes Vascogotiques et Celtibériques (Espagne du Nord). *Cuadernos de Geología Ibérica* 5, 127–214.
- Wiedmann, J., 1988a. Ammonoid extinction and the “cretaceous-tertiary boundary event”, in: Wiedmann, J., Kullmann, J. (Eds), *Cephalopods - Present and Past*. Schweizerbart, Stuttgart, pp. 117–140.
- Wiedmann, J., 1988b. The Basque coastal sections of the K/T boundary – a key to understanding “mass extinction” in the fossil record. *Revista Española de Paleontología*, N° Extra (Palaeontology and Evolution: Extinction Events), 127–140.
- Wiedmann, J., Kauffman, E.G., 1978. Mid-Cretaceous biostratigraphy of Northern Spain. *Annales du Museum d'Histoire Naturelle de Nice* 4, 1–22.
- Wiedmann, J., Reitner, J., Engeser, T., Schwentke, W., 1983. Plattentektonik, Fazies und Subsidenzgeschichte des basko-kantabrischen Kontinentalrandes während Kreide und Alttertiär. *Zitteliana* 10, 207–244.
- Wiese, F., Brüning, J., Otto, A., 1996. First record of *Libycoceras ismaelis* (Zittel, 1885) (Cretaceous Ammonoidea) in Europe (Campanian of the Santander area, Cantabria, northern Spain). *Acta Geologica Polonica* 46(1–2), 105–116.
- Williamson, T.E., Lucas, S.G., 1992. Vertebrate Fauna from the Upper Cretaceous (Campanian) Pictured Cliffs Sandstone, Mesa Portales, New Mexico, in: Lucas, S.G., Kues, B.S., Williamson, T.E., Hunt, A.P. (Eds), *San Juan Basin IV*, New Mexico Geological Society Fall Field Conference Guidebook 43, pp. 26–29.
- Williston, S.W., 1897. Range and Distribution of the *Mosasaurus*. *Kansas University Quarterly* 6, 177–189.
- Williston, S.W., Moodie, R.L., 1917. *Ogmodirus martinii*, a new plesiosaur from the Cretaceous of Kansas. *Kansas University Science Bulletin* 10, 61–73.
- Wilmsen, M., Voigt, T., 2006. The middle–upper Cenomanian of Zilly (Sachsen-Anhalt, northern Germany) with remarks on the *Pycnodonte* Event. *Acta Geologica Polonica*, 56(1), 17–31.
- Wilmsen, M., Wiese, F., Ernst, G., 1996. Facies development, events and sedimentary sequences in the Albian to Maastrichtian of the Santander depositional area, northern Spain. *Mitteilungen*

- aus dem Geologisch-Paläontologischen Institut der Universität Hamburg 77, 337–367.
- Wilson, J., 1995. Conservation and processing – cleaning and mechanical preparation, in: Collins, C. (Ed.), *The Care and Conservation of Palaeontological Material*. Butterworth-Heinemann, Oxford, pp. 89–94.
- Wolberg, D.L., 1985. Selachians from the Late Cretaceous (Turonian) Atarque Sandstone Member, Tres Hermanos Formation, Sevilleta Grant, Socorro County, New Mexico. *New Mexico geology* 7(1), 1–7.
- Woodward, S., 1833. *An Outline of the Geology of Norfolk*. Longman and Co. London, Norwich, 60 pp.
- Woodward, A.S., 1888. On some Remains of *Squatina Cranei*, sp. nov., and the Mandible of *Belonostomus cinctus*, from the Chalk of Sussex, preserved in the Collection of Henry Willett, Esq., F.G.S., Brighton Museum. *Quarterly Journal of the Geological Society* 44, 144–148.
- Woodward, A.S., 1889. *Catalogue of the Fossil Fishes in the British Museum, Part 1*. British Museum of Natural History, London, 474 pp.
- Woodward, A.S., 1911. The fossil fishes of the English Chalk, Part 6. *The Palaeontographical Society, London*, 185–224.
- Wueringer, B.E., Squire, L., Collin, S.P., 2009. The biology of extinct and extant sawfish (Batoidea: Sclerorhynchidae and Pristidae). *Reviews in Fish Biology and Fisheries* 19, 445–464.

Z

- Zalmout, I.S., Mustafa, H., 2001. A selachian fauna from the Late Cretaceous of Jordan. *Abhath Al-Yarmouk, Basic Sciences and Engineering* 10(2B), 377–434.
- Zammit, M., Kear, B.P., 2011. Healed bite marks on a Cretaceous ichthyosaur. *Acta Palaeontologica Polonica* 56(4): 859–863.
- Zhelezko, V.I., 1988. Selachian zones of the Santonian and Campanian of South Urals and Mugodzhary, in: Chuvashov B.I. (Ed.), *Biostratigraphy and lithology of the Upper Paleozoic of Urals*. Ural collection of scientific papers. Urals Branch of USSR, Academy of Science Publication, Sverdlovsk, pp. 117–131 [in Russian].
- Zhelezko, V.I., 1990. Pisces (Selachii), in G.N. Papulov, V.I. Zhelezko, and A.P. Levina (Eds), *Upper Cretaceous deposits of southern post-Urals (region of the upper Tobol River)*. Uralian Branch of the Academy of Sciences of USSR, Sverdlovsk, 122–133 [in Russian].

SYSTEMATIC INDEX

A

Abathomphalus
mayaroensis 147, 182, 187
Acanthoscyllium 368, 379
Acrodus 92
Acrolamna 368
Adnetoscyllium
angloparisensis 239
Agerostrea
ungulata 180, 197
Alopiidae 69, 361
Alveolina 30
Amonotodon 365
Amphilectella
piriformis 121
Amphydonte (*A.*)
pyrenaicum 180, 197
Amphydonte (*Ceratostreon*)
pliciferum 121
sp. 135
Anacoracidae 74, 91, 164,
216, 257, 279, 304, 340,
356, 358, 359, 404
Anacorax 340
Anchosaurus. See *Onchosaurus*
Angolabatis 368, 383
Ankistrotrhynchus 368
Anomotodon 6, 221, 362,
363, 368, 419
hermani 221–222, **222**,

357, 360, 363, **398**,
400, 402, 419

plicatus 221
Archaeoglobigerina
cretacea 121, 135
Archaeolamna 368, 383
Archaeotriakis 75, 368
Argyrotheca
hirundo 123
Asteracanthus 92
Ataktobatis 326
variabilis 326–328, **327**,
407, 412, 413, 424

B

Baculites 187
alonsoi 144, 150
anceps 182, 183, 187, 197,
198, 203, 425
baculus 183
cf. *texanus* 135, **138**
grandis 183
sp. 134, 144, 149, 150
sp. 1 **136**
sp. 2 **136**
vaalsensis **26**
Behavites
subquadratus 149
Belemnellocamax
balsvikensis 220, 245

mammillatus 220, 244,
270
Belemnitella
mucronata 212, 222, 232,
245, 270, 278
Borodinopristis 368, 379
Bostrychoceras
polyplacum 241, 245
Bourgueticrinus
sp. 123, 134
Brachyrhizodus 368, 379
Brachyura 123

C

Callianassa 187
Callianassidae 120, **189**
Cantioscyllium 368
Carcharhinidae 89, 91
Carcharhiniformes 69, 75, 91,
241, 276, 288, 317, 356, 358,
369, 389, 404, 406, 424
Carcharias 225, 261, 284,
309, 344, 363, 368, 381,
419
aasenensis 226–227, **227**,
357, 360, 361, 363,
400, 419
adneti 227, 261–263, **262**,
357, 358, 360, 365,
398, 400, 401, 420

Bold numbers refer to illustrations; a page range indicates that a taxon is expressly described.

- aff. gracilis* 311–312, **312**,
 407, 412, 414, 424
gracilis 311, 312
beathi 162, 166, 197,
 284–286, 286, **287**,
 309–311, **312**, **344**,
 344–345, 405, 406,
 407, 409, 411, 412,
 413, 414, 423, 424
latus 226, 227
samhammeri 226, 227
 sp. 181, 286, **287**, 405, 412
 spp. 91
taurus 87, 225, 261, 284,
 286, 309, 344, 361, 365
Carcharodon 91
carcharias **79**, 83, 86, 391
Carinodens
fraasi 388
 cf. *Cataceramus*
balticus 121, **123**
Cataceramus?
glendivensis 182, 183, **184**
Cederstroemia 368
 Centrophoridae 75
Centrophoroides 368, 379
appendiculatus 394
Centrosymnus 368, 379
Ceratostreon
pliciferum 103
Cerithium 237
Cestracion pygmaeus. See *Parapalaeobates pygmaeus*
Cetorhinus maximus 69
Chiloscyllium 237, 315, **317**,
 329, 362, 363, 365, 368, 419
frequens 237, 240
 cf. *gaemersi* **239**, 239–240,
 356, 357, 360, 419
gaemersi 239, 241
 sp. 315–317, **317**, 407, 412
 cf. *vulloi* **239**, 240–241,
 356, 357, 360, 419
vulloi 240
Chiloscyllium greeni. See *Hemiscyllium hermani*
Chlamydoselachus 368, 383
Cicatricosisporites
aratus 175
Cirroceras
 sp. 149
Cladoselache 72
 Cladoselachiformes 72
Clausilia
 cf. *matheroni* 176
Columbusia 368
Contusotruncana
fornicata 121, 135
patelliformis 135
plicata 147
plummerae 121, 135
Conulidae 126
Conulus
dowillei 123
gigas 197
Corax 340
affinis 271
kaupii 218
pristodontus 6, 216, 258,
 279, 304, 340
Corax pristodontus. See *Squali-
 corax pristodontus*
Corbicula
 sp. 135
Coupatezia 297, 334
fallax 166, 188, **296**, 297,
 334, **335**, 405, 407,
 409, 412, 414, 423,
 424, 425
 sp. 409
woutersi 297, 334
 Craniida 123
Crassescyliorhinus 368
Cretacoranina
schloenbachi 144
 sp. 134
Cretalamna 228
Cretaplatyrhinoidis 368, 379
Cretascyllium 246
expansum 246
Cretascymnus 368, 379
Cretolamna 228, 263, 283,
 307, 363, 365, 368, 376,
 378, 381, 383, 390, 391,
 394, 408, 414, 419, 421
appendiculata 228, 232,
 270, 307, **308**, 358,
 365, 395, 406, 407,
 424, 425
 sp. aff. *Cretolamna appendi-
 culata* 283, **285**, 405,
 411, 412, 414
appendiculata lata 283, 307
*appendiculata var. pachyrhi-
 za* 270
borealis **228**, 228–232,
231, 234, 263–266,
265, 270, 357, 358,
 389, 360, 364, 390,
 394, 395, 400, 402,
 419, 420, 421, 422
hattini 232
sarcoportheta 232, **233**,
 233–234, **266**,
 266–271, **268**, 357,
 358, 360, 364, 365,
398, 400, 402, 419,
 420, 422
 sp. **127**
 spp. 359
Cretorectolobus 368
Cretoxyrhina 219, 359, 363,
 368, 378, 383, 419
mantelli **53**, 219–220,
220, 357, 359, 360,
 365, 394, 395, 400,
 402, 419, 421, 422
 Cretoxyrhinidae 74, 219,
 356, 358, 359
 Ctenacanthiformes 69, 72, 90

D

- Dalatiidae 75, 91
Dalpiazia 331, 353
stromeri 188, 331, **333**,
 407, 411, 412, 413,
 414, 424, 425
 Dasyatidae 71
Dasyatis
pastinaca **78**
Dasyatis fallax. See *Coupatezia*

fallax
 Dasyatoidea 295, 334, 404
 Dasyatoidei 92
 Decapoda 120
Diplodus 72
Discocyclus 29
Dissostoma
 sp. 176
Dughiella
 aff. *obtusa* 174

E

Echinocorys
 sp. 132, 143
subglobosa 134, 135
 Echinorhinidae 89
 Echinorhiniformes 69, 70,
 91, 369
Echinorhinus 368, 383
Enchodus 163
 sp. **181**, 398
Endocoste
 aff. *impressus* 196, 203
typica 183
Eoetmopterus 368, 379
Eostriatolamia 368
 Etmopteridae 75
Eubaculites
carinatus 187
ootacodensis 183
 cf. *vagina* 182, 183, **187**
vagina 183
Eupachydiscus
grossouwei 149
levyi 149
 cf. *Euspira*
 sp. **184**
Exogyra (E.)
overwegi 197
Extratriporopollenites
 sp. 175

F

Forresteria (*Harleites*)
 aff. *nicklesi* 103, **106**, 110
petrocoriensis 106

G

Galeocерdo 394
capellini **79**
cuvier 77, 82, 91, 406
Galeocorax 368
Galeola
basiplana 278
Galeorhinus 276, 368, 381
galeus 365
ginardoti **277**, 277–278,
 357, 358, 360, 365,
398, 400, 401
 sp. 278
unilateralis 278
Ganopristis 295, 331, **333**,
 353, 368, 383
leptodon 188, 295, **296**,
 331, **333**, 405, 407,
 409, 412, 414, 424, 425
Gansserina
gansseri 135, 147, 151, 258,
 261, 264, 266, 271,
 272, 275, 277, 356, 420
wiedenmayeri 135
Gaudryceras
 cf. *kaye* 135, **138**
Gauthierceras
margae 106
vascogoticum **106**
Gigantichthys. See *Oncho-*
saurus
Ginglymostoma
rugosum 288, 315
Ginglymostoma globidens.
 See *Chiloscyllium* cf. *vulloi*
Ginglymostoma lehneri.
 See *Plicatoscyllium lehneri*
Ginglymostoma rugosum.
 See *Plicatoscyllium lehneri*
 Ginglymostomatidae 74,
 164, 287, 314, 404
Globator
petrocoriensis 123
Globidens
dakotaensis 388
Globigerinelloides
multispina 135

prairiehillensis 121, 135
Globotruncana
aegyptiaca 121, 125, 135,
 147, 216, 219, 221, 222,
 226, 228, 233, 234,
 237, 239, 240, 241,
 243, 247, 249, 250,
 253, 355, 419
arca 121, 135
bulloides 121, 135
linneiana 121, 135
mariei 121, 135
orientalis 121
rosetta 135
ventricosa 135, 146
Globotruncanella
havanensis 121, 147
Globotruncanita
angulata 135
calcarata 147
elevata 146
insignis 121, 135
stuartiformis 135
Glomerula
gordialis 123
Glyptoxoceras
 cf. *retrosum* 149
 Goniasteridae 123
Gonioteuthis
granulataquadrata 222
quadrata gracilis 271
Goniotheutis
quadrata 276
Gryphaeostrea
vomer 121, **127**, 128
Gublerina
acuta 147
 Gymnuridae 71, 75

H

Hedbergella
bolmdelensis 121, 135
monmouthensis 121, 135
 Hemigaleidae 91
Hemipneustes 6
 cf. *pyrenaicus* 180
pyrenaicus 197

- striatoradiatus* **182**, 188, 197
Hemipristis
serra 86
Hemiscylliidae 236, 315, 356, 362
Hemiscyllium 236, 317, 329, 363, 368, 419
bermani 236–237, **239**, 356, 357, 360, 362, 419
Hemitissotia
lenticeratiformis **106**, 110 sp. 103, 110
turzoi 106, 110, 418
Heterodontidae 90, 92
Heterodontiformes 69, 70, 90, 369, 389, 406
Heterodontus 92, 368, 378, 381
Heterohelix
globulosa 121, 134, 135
labellosa 121
navarroensis 135
planata 121, 134, 135
Hexanchidae 87, 91
Hexanchiformes 69, 70, 369, 406
Hexanchus 368
Holectypidae 123
Homalodoriana
ficus 121
ramosa 121
Hoplitoplacenticerus
marroti **26**, 134, **136**, 144, 145, 147, 150, 151, 356
Hoploscaphites
constrictus 197, **198**, 203, 425
Hybodontidae 82
Hybodontiformes 69, 74, 90, 369
Hybodus 368, 378
dubrisiensis 243
Hyostissa
semiplana 121
Hypsobatidae 75
- |
Igdabatis 368
indicus 409
‘*Inoceramus*’
ianjonaensis 183
Interulobites
triangularis 175
Ischyrbiza 353, 368
cf. avonicola 333
iwakiensis 214
Isocrania
campaniensis 123
Isocrinus
sp. 123
Isuridae 91
Isurus
oxyrinchus **78**, **79**, 80, **86**
paucus 77
sp. 395
- J
? *Jaekelotodus* 368
- L
Lacazina 25, 25, 149
Laeviheterohelix
glabrans 135
Lamna
borealis 232
elegans 3, 4, **5**
nasus **76**, **88**, 394
sp. 180
Lamna (Odontaspis) bronni.
See *Odontaspis bronni*
Lamna serrata. See *Serratomamna khderii*
Lamniformes 69, 76, 89, 216, 257, 279, 304, 340, 356, 358, 369, 379, 389, 404, 406, 419, 424
Leiodon 212
anceps 388
Leptocharias 368, 379
Leptomaria 103
Lewyites
elegans 134, **136**
- Lissodus* 368
Litbothamnion
sp. **119**, 120
Lonchidion 368
Lucinidae **182**
Lychnus 6, 176
ellipticus **177**
giganteus 176
- M
Marsupites
testudinarius 147
Matonispurites
sp. 175
Megachasma pelagios 69
Melobesiae 29
Menabites (Bererella)
sp. **26**, 150
Menabites (Delawarella)
delawarensis 147, 149
Menuites
fresvillensis 187, 197, **198**, 203, 304, 307, 309, 310, 311, 313, 315, 317, 319, 322, 326, 328, 331, 333, 334, 335, 337, 340, 341, 345, 425
terminus 203
Meristodon 368
Meristodonoides 368
Mesostylus
faujasi 187, **189**
Metatissotia
ewaldi 103, **106**
Micraster
coranguinum 245
cortestudinarium 243
sp. **22**, 116, 123, 132
tercensis 6
Micropristis 368
Mitsukurina
owstoni 419
Mitsukurinidae 74, 76, 221, 356, 358, 362
Mobulidae 71
Mosasauridae 388, 398
Mosasaurinae **65**, 388, 397

Mosasaurinae indet. **65**,
388–392, **389, 398**
Mosasaurus 212, 401
 compressidens 388
 lemonnieri 398, 400, 401
Mustelus 92
Myledaphus 368
Myliobatidae 71, 75
Myliobatiformes 71, 295,
334, 369, 406, 424
Myliobatoidea 297, 334
Myliobatoidei 90

N

Nanocorax 369, 383
Naticidae **184**
Nautilus danicus 6
Neithea (*Neithea*)
 cf. *quadricostata* 180
 regularis 121
 sexcostata 135
 striatocostata 197
Neocrioceras (*Schlueteria*)
 riosi 149
Neovermilia
 ampullacea 123
Nostoceras (*B.*)
 polyplocum 143, 144, 147,
 150, 387
Nostoceras (*Euskadiceras*)
 euskadiense II 387
 unituberculatum 387
Nostoceras (*N.*)
 hyatti 147
Notidanodon 369, 383
Notidanoides 369

O

Odontaspidae 74, 163,
164, 225, 261, 284, 309,
344, 356, 358, 404
Odontaspis 312, 369
 bronni 188, 312–314, **313**,
 407, 412, 414, 424, 425
 ferox **88**
Offaster

pilula 222, 226, 243, 245, 252
Omphalocyclus
 macroporus 182
Onchopristis
 numidus 209, **211**
Onchosaurus 105, 207, 208,
349, 351, 353, 369, 418
 pharao 209, **210**, 211, 212,
 214, 350, 351, 352,
 353, 418
 radicalis 101, 110, **209**,
 208–212, **210, 211**,
 213, 349, 350, 351,
 352, 418
Onchosaurus manzadinensis.
 See *Dalpiazia stromeri*
Onchosaurus maroccanus.
 See *Dalpiazia stromeri*
Operculina 29
Orbitoides 6
 apiculata 182
 gensacicus 182
Orectolobiformes 69, 91,
236, 287, 314, 356, 369,
389, 404, 406, 424
Otodontidae 228, 263, 283,
307, 356, 359, 404
Otodus 91
 appendiculatus 228, 263,
 283, 307
 serratus 275, 283, 309
Otodus appendiculatus.
 See *Cretolamna appendi-*
 culata
Otodus serratus. See *Serrato-*
 lamna serrata
Otostoma
 ponticum 182, 184
 retzii 180, 182, 184, 197
 rugosa 197
 spp. 187
Owenirhynchia
 aff. *rubra* 135
Oxynotidae 75
Oxyrhina
 angustidens 234
 mantelli 219

P

Pachydiscus
 sp. 121, **123**
Pachydiscus (*P.*)
 armenicus 203
 cf. *bassae* 149
 haldemisi 135, **138**, 144,
 150, 151
 jacquoti 6, **198**, 203
 launayi 149
 neubergicus 196, **198**, 203
 oldhami 135, **138**, 144
 praecolligatus 149
 sp. 150
Palaeocarcharodon
 orientalis 86
Palaeogaleus 75, 289, **317**,
 318, 369, 381
 dahmanii 318
 faujasi **81**, 188, **289**,
 289–290, 317–318,
 319, 405, 407, 409,
 411, 412, 414, 424, 425
 havreensis 318
 navarroensis 318
 sp. 409
Palaeohypotodus bronni.
 See *Odontaspis bronni*
Palaeoscyllium 369, 379
Palaeospinacidae 74, 243,
356, 362
Palaeostoa
 hispanica 176
Palaeotriakis 369, 379
Palidiplospinax 74
Panopaea
 sp. 135
Paranomotodon 234, 236,
363, 369, 381, 419
 cf. *angustidens* **234**,
 234–236, 357, 359,
 360, 363, 419
Paraorthacodus 369
Parapalaeobates 248, 249,
363, 369, 419
 atlanticus 250
 cf. *glickmani* 250

- cf. pygmaeus* 248
pygmaeus 60, 248–250, 249, 357, 360, 363, 398, 400, 402, 419, 422
 Parapalacobatidae 248, 357
Paraphorosoides 369, 379
Pararhincodon 369, 381
Parasquatina 369, 379
Paratexanites
 serratmarginatus 106
Paratriakis 75, 271, 369
 sp. 409
Paratrygonorrhina
 amblysoda 409
Pastinachus 92
Patagiosites
 stobaei 278
Peroniceras
 cf. tridorsatum 106
 sp. 103
Phylloceras (Hypophylloceras)
 sp. 144, 150
Placenticerus
 bidorsatum 147, 149
 sp. 149
Placostegus
 sp. 123
Plagiostoma
 gigantea 103
Planoglobulina
 acervulinoides 147
 carseyae 121
Platychara
 caudata 174
 turbinata 174
 Platyrrhinidae 75
Plicatoscyllium 287, 314, 369, 381, 394
 derameei 287, 314
 lebneri 166, 188, 288, 289, 290, 314–315, 317, 405, 407, 409, 411, 412, 413, 414, 423, 424, 425
 minutum 288, 290, 315
Plicatoscyllium minutum.
 See *Plicatoscyllium lebneri*
- Plioplatecarpus*
 marshi 394
Polyacrodus 369, 381
 Potamotrygonidae 71
Prionace 83, 84
Prionocycloceras
 iberiense 103, 106
 turzoi 103, 106
 Pristidae 207
 Pristiformes 71, 76, 90
 Pristiophoriformes 69, 70, 76, 90, 406
 Pristoidei 71
Problematicum. See *Dalpiazia stromeri*
Proetmopterus 369, 379
Prognathodon 401
 cf. sectorius 388
 giganteus 388
 saturator 394
 sp. 398, 400
Probaploblepharus 241, 363, 365, 369, 419
 riegrafi 241–243, 242, 356, 357, 360, 362, 419
 Proscylliidae 91
Protexanites
 bourgeoisianus 103, 106, 110, 208, 418
Protolamna 272, 274, 369, 381
 acuta 274
 borodini 272, 272–275, 357, 358, 360, 398, 400, 402, 420
 roanokeensis 274
 sarstedtensis 274
 sokolovi 272, 274
Protoplatyrhina 369
 Pseudocoracidae 271
Pseudocorax 271, 369, 381
 affinis 272
 laevis 271–272, 272, 357, 358, 360, 400, 420
Pseudoguembelina
 hariaensis 147
Pseudoheterodontus 369
- Pseudohypolophus* 369, 379
Pseudophyllites
 cf. indra 149
 indra 135, 138, 197, 198, 203, 425
 sp. 144, 150
 Pseudoscanpanorhynchidae 272
Pseudoscylliorhinus 369, 379
Pseudotextularia
 nuttalli 121, 135
Pseudoxybeloceras (Parasolenoceras)
 phaleratum 144, 150
 Pteroscyliainae 74
Pteroscyllium 369
Pterotrigonia (Scabrotigonia)
 scabra 103
Ptychocorax 92
Ptychodus 92, 369
 triangularis 253
Ptychotrygon 253, 255, 363, 369, 419
 agujaensis 254
 blainensis 254
 boothi 254
 aff. P. cuspidata 254
 cuspidata 254, 255
 ellae 254
 eutawensis 254
 geyeri 253
 greybullensis 254
 henkeli 255
 ledouxii 254
 pustulata 253
 slaughteri 253, 254
 sp. 251, 253–255, 357, 360, 363, 400, 402, 419, 422
 striata 253
 triangularis 254, 255
 cf. P. vermiculata 255
 vermiculata 254, 255
 winni 255
 Ptychotrygonidae 253, 357
Pycnodonte 25, 27
 sp. 103, 132

- vesicularis* 114
Pycnodonte (*Phygraea*)
 sp. 25
vesicularis 27, 121
- R
- Racemiguembelina*
fructifera 147
- Radiolitidae 182, **184**
- Radotruncana*
calcarata 146
- Raja*
rhinobatos 250, 291, 318
- Raja fallax*. See *Coupatezia fallax*
- Rajidae 75
- Rajiformes 68, 71, 76, 89, 207, 208, 248, 291, 301, 318, 356, 369, 406, 414
- Rajiformes indet. 301
- Rajoidei 71, 92
- Rastellum* (*F.*)
macropterum 197
- Retusochara*
macrocarpa 174
- Rhincodon*
typus 70
- Rhinobatidae 76, 164, 250, 291, 318, 357, 363, 404
- Rhinobatiformes 71, 72, 76
- Rhinobatoidei 68, 71, 250, 291, 301, 318, 404, 424
- Rhinobatoidei incert.
 fam. 292, 326
- Rhinobatos* 92, 250, 291, 318, **324**, 363, 369, 383, 419
casieri 250–253, **251**, 324, 326, 357, 360, 363, 365, **398**, 400, 402, 419, 422
craddocki 324, 325
echavei 252, 291, **293**, 318–322, **320**, 405, 407, 409, 412, 413, 414, 424
 ‘*gonzalo*’ 324
grandis 325
bakelensis 325
halter 324, 325
ibericus 291–292, **293**, **322**, 322–326, 405, 407, 409, 411, 412, 413, 414, 424
incertus 324, 325
incidens 324
intermedius 325
kiestensi 325
ladoniaensis 325
latus 301, 325
lobatus 325
mariannae 325
maronita 325
obtusatus 325, 326
picteti 325
seruensis 252, 325
 ‘*sotoi*’ 325
 sp. 252, 325
tenuirostris 325
tesselatus 325, 326
uwulatus 252, 322, 325, 326
whitfieldi 325
- Rhinognathus*
lewisii 222
- Rhizocorallium*
 isp. 138, 142
- Rhombodontidae 75, 164, 297, 334, 404
- Rhombodus* 84, 163, 164, 192, 297, 334, 369
andriesi 188, 189, 300, 334–335, **336**, 407, 411, 412, 413, 414, 424, 425
binkhorsti 166, 188, 298, **299**, 300, 334, 335, **336**, 337, 404, 405, 406, 407, 409, 411, 412, 414, 423, 424, 425
ibericus 300
 sp. 298–301, **300**, 405, 412
 spp. 83
- Rhombopterygia* 369
- Rostellana*
 sp. 184
- Rostellaria*
 sp. 184
- Rostellariidae **184**
- Rotaliina* **136**
- Rotularia* (*Praerotularia*)
saxonica 123
- Rotularia* (*Rotularia*)
hisingeri 123
- Rugoglobigerina*
hexacamerata 135, 147
milamensis 135
rotundata 135, 147, 151, 258, 261, 264, 266, 271, 272, 275, 277, 356, 420
rugosa 121, 135
scotti 147
- S
- Saghalinites?*
 sp. **198**
- Scapanorhynchus* 6, 222, 362, 363, 369, 376, 378, 383, 419
minimus 225
perssoni 225
rapax 225
 aff. *raphiodon* 225
raphiodon 224
 cf. *texanus* **222**, 222–225, 357, 360, 363, 365, 366, **398**, 400, 402, 419
texanus 224, 225
- Scaphites*
hippocrepis 124, 149
hippocrepis III 149
- Scaphites* (*Scaphites*)
gibbus 121, **123**, 124, 144, 149, 150, 355
- Sclerorhynchidae 74, 90, 164, 207, 208, 295, 331, 404
- Sclerorhynchiformes 207
- Sclerorhynchoidei 71, 76, 90, 208, 253, 295, 331, 424
- Sclerorhynchus* 369
batavicus 333

- germaniae* 333
Sclerorhynchus batavicus.
 See *Ganopristis leptodon*
Sclerorhynchus leptodon.
 See *Ganopristis leptodon*
 Scyliorhinidae 74, 91, 241,
 356, 362
 Scyliorhininae 74
Scyliorhinus 369, 381
reyndersi 245
?riegrafi 241
Scyliorhinus reyndersi. See *Sy-
 nechodus aff. filipi*
Scylliogaleus 92
Scyllium
plagiosum 237, 315
vincenti 289, 317
Serratolamna 163, 275, 283,
 309, 369, 381, 408
khderii 272, 275–276, 357,
 358, 360, 400, 401, 420
serrata 49, 162, 166, 188,
 284, 285, 309, 310,
 405, 406, 407, 409,
 423, 411, 412, 414,
 424, 425
Serratolamnidae 164, 275,
 283, 404
Sigmoscyllium 369, 379
 Somniosidae 75
Sphenodus 369, 383
Sphyrna
tiburo 92
 Sphyrnidae 69
Spondylus
spinosus 22
truncatus 135
Squalicorax 216, 257, 279,
 304, 340, 359, 369, 376,
 378, 381, 383, 385, 390,
 391, 394, 408, 394
benguerirensis 281
falcatus 342
 ex gr. *kaupi* 127, 216,
 216–219, 258, 259,
 261, 357, 358, 389, 359,
 360, 364, 365, 366,
 390, 394, 395, 398,
 400, 401, 419, 420,
 421, 422
kaupi 163, 197, 218, 219,
 258, 280, 282, 304,
 305, 340–341, 341,
 342, 394, 395, 405,
 406, 407, 409, 423,
 411, 412, 414, 424, 425
lindstromi 218, 219, 258,
 342, 394
plicatus 219
 ex gr. *pristodontus* 219
pristodontus 7, 37, 48, 86,
 158, 162, 166, 188,
 197, 198, 218, 258,
 280, 280–281, 282,
 304–307, 306, 340,
 341–343, 343, 405,
 406, 407, 409, 411,
 412, 414, 424, 425
pristodontus-plicatus 218
 sp. 281–283, 282, 405, 412
 spp. 414
yangaensis 86, 281
 Squalidae 74, 90, 379
 Squaliformes 69, 70, 75, 90,
 91, 369, 379, 406
Squalus 369, 379, 383
ferox 312
galeus 277
ocellatus 236
 Squamata 388, 398
Squatigaleus 75
Squatina 246, 362, 363, 369,
 378, 381, 383
cranei 246
 cf. *hassei* 248
hassei 398, 400, 402
Squatina (C.)
hassei 244, 247–248, 419
Squatina (Cretascyllium)
hassei 357, 360, 365, 366
Squatina (*Squatina*)
squatina 246
 Squatinidae 246, 356, 362
 Squatiniformes 69, 70, 91,
 246, 356, 369, 406
Squatirhina 369, 379
Striatolamia
macrota 5
Strophodus
pygmaeus 248
Strophodus pygmaeus. See *Pa-
 rapalaeobates pygmaeus*
Submortonicerus
tenuicostulatum 149
 Symmoriiformes 72
 Synechodontiformes 243,
 356, 369
Synechodus 74, 243, 362,
 363, 365, 369, 378, 383, 419
faxensis 245, 246
 aff. *filipi* 243–246, 244,
 357, 360, 362, 419
filipi 243, 246
lerichei 243, 245
perssoni 244
turneri 245, 246
- T
 Terebratulida 123
Terebratulina
chrysalis 123
 Tetractinellida 121
Tetraporites
 sp. 175
Texasia
 sp. 106
Texatrygon 369
 Thalassinidea 187
Thalassinoides 120, 126
 isp. 120, 124
Thecidea
papillata 180
 Tissotidae 103
Tissotioides
haplophyllus 103, 106
hispanicus 106
Titanichthys. See *Onchosaurus*
 Torpediniformes 71, 72
Trachyscaphites
pulcherrimus 388
spiniger 151

- spiniger porchi* 135, **138**,
 150
spiniger spiniger 150
 Triakidae 74, 75, 92, 164,
 276, 289, 317, 358, 404
Tricolporopollenites
 sp. 175
Trochoceras
radius 183
Tylocidaris
ramondi 198
 sp. 123
- Tylosaurinae 401
Tylosaurus
 sp. 388, 398, 400
Tylostoma 103
- V**
Vascobatis 292, 317, 328, 329
albaitensis 292–295, **294**,
 328–329, **331**, 405,
 407, 409, 411, 412,
 413, 414, 424
- X**
 Xenacanthiformes 69, 72
Xenacanthus 72
- Y**
Youssoubatis 92
- 'Viviparus'*
cingulata 176
 Volutidae **184**

NATURA NIHIL AGIT FRUSTRA



Nature does nothing in vain | La naturaleza nada hace en vano

Aristotle, *Politics* I,3 (330 – 323 BC)



Photo: Nathalie Barber, 2011

J. Carmelo Corral was born in Vitoria-Gasteiz (Basque Country, Spain) in 1963. His curiosity about nature led him to discover fossils since teenage years. He gained his **BSc in Geology** from the Universidad del País Vasco – Euskal Herriko Unibertsitatea (UPV-EHU) in 1988, and after graduating he obtained a **Master's Degree in Museum Studies** in 1991 at the same university. He further obtained an **Official Master's Degree in Initiation to Research in Geology** at the University of Zaragoza in 2009.

Carmelo spent a five-month stay in the Sedgwick Museum (Department of Earth Sciences, University of Cambridge, UK) and then moved in mid-1992 to the Arabako Natur Zientzien Museoa – Museo de Ciencias Naturales de Álava (MCNA). Since then, he has lent her knowledge and expertise to this institution working as curator of the Palaeontology collection.

He has participated in several palaeontological field seasons organized by the Department of Stratigraphy and Palaeontology of the University of the Basque Country (UPV-EHU) and the MCNA, including the lower Miocene track site discovered near Salinas de Añana (Álava) (excavated during 1992, and 1993), the Upper Cretaceous fossil vertebrate beds in the Lajo Quarry (Treviño County, Burgos) (excavated during 1987, 1988, 1989, 1993, 1995, and 1997), and the Lower Cretaceous amber deposits in Peñacerrada (Álava) and Moeza (Treviño County, Burgos) (excavated during 1995, 1997, and 2006).

Through the years he has specialised in the preparation and conservation of paleontological and geological specimens, in addition to the curation and management of geological collections. His main current interest is the study of Upper Cretaceous marine ecosystems of the Basque-Cantabrian Region. He has given several popular talks on palaeontology and geology of the Basque-Cantabrian Region and has taught a hands-on training course for art restorers entitled "Materials and techniques for making moulds and replicas".

UNIVERSITY OF THE BASQUE COUNTRY



Universidad
del País Vasco

Euskal Herriko
Unibertsitatea